

UNIVERSAL
LIBRARY



141 040

UNIVERSAL
LIBRARY

IRON AND STEEL DIVISION

1944

TRANSACTIONS
OF THE
AMERICAN INSTITUTE OF MINING
AND METALLURGICAL ENGINEERS
(INCORPORATED)

Volume 158

IRON AND STEEL DIVISION
1944

PAPERS AND DISCUSSIONS PRESENTED BEFORE THE DIVISION AT THE MEETINGS
HELD AT CLEVELAND, APRIL 29-30, 1943; CHICAGO, OCT 16-20, 1943;
NEW YORK, FEB. 20-24, 1944

PUBLISHED BY THE INSTITUTE
AT THE OFFICE OF THE SECRETARY
29 WEST 39TH STREET
NEW YORK 18, N. Y.

Notice

This volume is the seventeenth of a series containing papers and discussions presented before the Iron and Steel Division of the American Institute of Mining and Metallurgical Engineers since its organization in 1928, one volume each year, as follows.

1928, Iron and Steel Technology in 1928 (later listed as Volume 80 of the TRANSACTIONS), 1929 (vol 84), 1930 (vol 90), 1931 (vol 95), 1932 (vol 100), 1933, 1934, 1935, 1936, 1937, 1938, 1939, 1940, 1941, 1942, 1943, and 1944, TRANSACTIONS of the American Institute of Mining and Metallurgical Engineers, Iron and Steel Division

This volume contains papers and discussions presented at the meetings at Cleveland, April 29-30, 1943, Chicago, Oct 16-20, 1943; New York, Feb 20-24, 1944

Papers on iron and steel subjects published by the Institute prior to 1928 are to be found in many volumes of the TRANSACTIONS of the Institute, in Vols 37 to 45, inclusive; 47, 50 and 51, 53, 56, 58, 62, 67 to 71, inclusive, 73 and 75 Vol 67 was devoted exclusively to iron and steel

Iron and steel papers published in the TRANSACTIONS before the year 1936 may be found by consulting the general indexes to Vols 1 to 35 (1871-1904), Vols 36 to 55 (1905-1916), Vols 56 to 72 (1917-1925), and Vols 73 to 117 (1926-1935).

COPYRIGHT, 1944, BY THE
AMERICAN INSTITUTE OF MINING AND METALLURGICAL ENGINEERS

PRINTED IN THE UNITED STATES OF AMERICA

FOREWORD

THIS volume, the one hundred and fifty-eighth of the regular Institute TRANSACTIONS, is the seventeenth devoted to technical papers and discussion presented at the fall and annual meetings of the Iron and Steel Division. The twenty-four papers in this volume cover a wide field—from iron-ore concentration and blast-furnace refractories, through the chemistry of the bessemer and open-hearth processes, to the more theoretical phases of structural changes in the solid state—and it is certain that at least one, and probably more, of these papers will be of lasting value to every member of the Division. Of special interest to all of us, regardless of our specialty, is Dr. James T. MacKenzie's fine Howe Memorial Lecture on gray cast iron, in which he shows what a valuable constituent graphite is when interspersed with a steel matrix.

The high quality of the papers in this volume is self-evident and the Division's Publications Committee under the chairmanship of E. S. Davenport and Carl M. Loeb, Jr., has worked conscientiously to ensure that our high standards were constantly maintained and that an author whose paper is published in this volume is sure that his work is new, important, and of lasting value.

This volume of TRANSACTIONS represents only the formal technical papers presented at the regular meetings of the Division, and does not include the proceedings of the three important conferences—open-hearth steel, blast furnace and raw materials, and electric-furnace steel—sponsored by Division standing committees. The published proceedings of these three groups, totaling 850 to 900 printed pages of up-to-the-minute data for operating men and metallurgists in the production field, are unique in technical society publications, and they have attained a world-wide fame for the value of their subject matter.

It is a pleasure for me to compliment the Institute, the Iron and Steel Division, and the three committees concerned for the fine reputation they have established and for the stimulation they have afforded to blast-furnace, open-hearth, and electric-furnace men everywhere to make a better product at a lower cost.

WILLIAM A. HAVEN, *Chairman*,
Iron and Steel Division.

A.I.M.E. OFFICERS AND DIRECTORS

For the year ending February 1945

PRESIDENT AND DIRECTOR
CHESTER A. FULTON, New York, N. Y.

PAST PRESIDENTS AND DIRECTORS
EUGENE MCAULIFFE, Omaha, Nebraska
C. H. MATHEWSON, New Haven, Conn.

TREASURER AND DIRECTOR
ANDREW FLETCHER, New York, N. Y.

VICE-PRESIDENTS AND DIRECTORS

JOHN L. CHRISTIE, Bridgeport, Conn.
ERLE V. DAVELER, New York, N. Y.
HARVEY S. MUDD, Los Angeles, Calif.

J. R. VAN PELT, JR., Chicago, Ill.
H. Y. WALKER, New York, N. Y.
L. E. YOUNG, Pittsburgh, Pa.

DIRECTORS

HOLCOMBE J. BROWN, Boston, Mass.
CHARLES CAMSELL, Ottawa, Ont., Canada
MILTON H. FIES, Birmingham, Ala.
C. A. GARNER, Jeddo, Pa.
WILLIAM B. HEROT, Washington, D. C.
CHARLES H. HERTY, JR., Bethlehem, Pa.
O. H. JOHNSON, Denver, Colo.
WILBER JUDSON, New York, N. Y.

J. C. KINNEAR, McGill, Nev.
RUSSELL B. PAUL, New York, N. Y.
WALLACE E. PRATT, New York, N. Y.
LEO F. REINARTZ, Middletown, Ohio
JOHN R. SUMAN, Houston, Texas
ROBERT W. THOMAS, Ray, Ariz.
FRANCIS A. THOMSON, Butte, Mont.
F. A. WARDLAW, JR., Salt Lake City, Utah
FELIX E. WORMSER, New York, N. Y.

SECRETARY

A. B. PARSONS, New York, N. Y.

DIVISION CHAIRMEN—Acting as Advisers to the Board

ARTHUR PHILLIPS (Institute of Metals), New Haven, Conn.
W. S. MORRIS (Petroleum), Kilgore, Texas
WILLIAM A. HAVEN (Iron and Steel), Cleveland, Ohio
A. W. GAUGER (Coal), State College, Pa.
A. C. CALLEN (Education), Bethlehem, Pa.
CHARLES H. BEHRE, JR. (Industrial Minerals), New York, N. Y.

STAFF IN NEW YORK

Assistant Secretaries
EDWARD H. ROBIE
CHESTER NARAMORE
FRANK T. SISCO
E. J. KENNEDY, JR.

Assistant Treasurer
H. A. MALONEY
Advertising Manager
"Mining and Metallurgy"
WHEELER SPACKMAN

CONTENTS

FOREWORD. By W. A. HAVEN	3
A.I.M.E. Officers and Directors	4
Iron and Steel Division Officers and Committees	7
Howe Lectures and Lecturers	10
Photograph of J. T. MacKenzie, Howe Lecturer.	12

PAPERS

Howe Lecture

Gray Iron—Steel Plus Graphite By J. T. MacKENZIE. (<i>Metals Technology</i> , June 1944) . .	13
---	----

Iron Ores and Blast Furnace Practice

Concentration of Iron Ores in the United States by T. B. COUNSELMAN. (<i>Metals Technology</i> , December 1943)	38
Selection of Blast-furnace Refractories By H. M. KRANER and E. B. SNYDER (<i>Metals Technology</i> , April 1944)	55
The Washing of Pittsburgh Coking Coals and Results Obtained on Blast Furnaces. by C. D. KING. (<i>Metals Technology</i> , September 1943)	67

Steelmaking

The Role of Basic Slags in the Elimination of Phosphorus from Steel. By RICHARD L. BARRETT and WILLIAM J. McCAUGHEY. (<i>Metals Technology</i> , April 1944) (With discussion) . .	87
The Relative Deoxidizing Power of Boron in Liquid Steel and the Elimination of Boron in the Open-hearth Process. By R. W. GURRY (<i>Metals Technology</i> , December 1943) (With discussion)	98
Manufacture and Properties of Killed Bessemer Steel. By E. C. WRIGHT. (<i>Metals Technology</i> , June 1944) (With discussion)	107

Hardenability

Effect of Quenching Temperature on the Results of the End-quench Hardenability Test. By CLARENCE E. JACKSON and ARTHUR L. CHRISTENSON. (<i>Metals Technology</i> , December 1943) (With discussion)	125
Effect of Sixteen Alloying Elements on Hardenability of Steel. By IRVIN R. KRAMER, ROBERT H. HAFNER and STEWART L. TOLEMAN. (<i>Metals Technology</i> , September 1943) (With discussion)	138
Effect of Some Elements on Hardenability. By WALTER CRAFTS and JOHN L. LAMONT (<i>Metals Technology</i> , January 1944) (With discussion)	157
Effect of Several Variables on the Hardenability of High-carbon Steels. By E. S. ROWLAND, J. WELCHNER and R. H. MARSHALL. (<i>Metals Technology</i> , January 1944) (With discussion) .	168

Mechanical Properties

Influence of Hydrogen on Mechanical Properties of Some Low-carbon Manganese-iron Alloys and on Hadfield Manganese Steel. By HERBERT H. UHLIG. (<i>Metals Technology</i> , June 1944) (With discussion)	183
---	-----

Aging and the Yield Point in Steel. By J. R. Low, JR., and M. GENSAMER (<i>Metals Technology</i> , December 1943) (With discussion)	207
Tensile Properties of Medium-carbon Low-alloy Cast Steels By H. A. SCHWARTZ and W. KENNETH BOCK (<i>Metals Technology</i> , August 1944) (With discussion)	250
Variables Affecting the Results of Notched-bar Impact Tests on Steels By CLARENCE E. JACKSON, MYRON A. PUGACZ and FRANK S. MCKENNA (<i>Metals Technology</i> , August 1944) (With discussion)	263
Conditions of Fracture of Steel By J. H. HOLLOMON and C. ZENER (With discussion)	283
The Notched-bar Impact Test By JOHN H. HOLLOMON (<i>Metals Technology</i> , April 1944) (With discussion)	298
Hardness Measurement as a Rapid Means for Determining Carbon Content of Carbon and Low-alloy Steels By K. L. CLARK and NICHOLAS KOWALL (<i>Metals Technology</i> , January 1944) (With discussion)	328
Fracture and Commminution of Brittle Solids (Abstract) by EUGENE F. PONCELET	333

Metallography

Influence of Various Elements upon the Position of the Eutectoid in the Iron-carbon (Carbide) System. By CARL L. SHAPIRO and JEROME STRAUSS (<i>Metals Technology</i> , December 1943) (With discussion)	335
Orientation in Low-carbon Deep-drawing Steel. By JAMES K. STANLEY. (<i>Metals Technology</i> , September 1943) (With discussion)	354
Recrystallization and Twin Relationships in Silicon Ferrite. By C. G. DUNN (<i>Metals Technology</i> , February 1944)	372
Precipitation and Reversion of Graphite in Low-carbon Low-alloy Steel in the Temperature Range 900° to 1300°F. By G. V. SMITH, R. F. MILLER and C. O. TARR (<i>Metals Technology</i> , June 1944) (With discussion)	387
The Bainite Reaction in Hypoeutectoid Steels By E. P. KLIER and TAYLOR LYMAN. (<i>Metals Technology</i> , June 1944) (With discussion)	394
<hr/>	
Contents of 1944 Institute of Metals Division Volume	423
INDEX	425

IRON AND STEEL DIVISION

Established as a Division February 22, 1928

(Bylaws published in the 1939 TRANSACTIONS Volume of the Division)

Officers and Committees for Year ending February 1945

W. A. HAVEN, *Chairman*, Cleveland, Ohio
H. W. GRAHAM, *Past Chairman*, Pittsburgh, Pa.
E. G. HILL, *Vice-Chairman*, Gary, Ind
G. M. YOCOM, *Vice-Chairman*, Wheeling, W. Va.
F. T. SISCO, *Secretary*, 29 W. 39th St., New York 18, N.Y.

PAST CHAIRMEN

RALPH H. SWEETSER, 1928
G. B. WATERHOUSE, 1929
W. J. MACKENZIE, 1930
F. M. BECKET, 1931
F. N. SPELLER, 1932

JOHN JOHNSTON, 1933
L. F. REINARTZ, 1934
A. B. KINZEL, 1935
C. E. WILLIAMS, 1936
FRANCIS B. FOLEY, 1937
J. T. MACKENZIE, 1938

J. HUNTER NEAD, 1939
FRANK T. SISCO, 1940
C. H. HERTY, JR., 1941
E. C. SMITH, 1942
H. W. GRAHAM, 1943

Executive Committee

1945
C. E. MACQUIGG, Columbus, Ohio
GILBERT SOLER, Canton, Ohio
T. S. WASHBURN, Indiana Harbor, Ind.

1946
WALTER CRAFTS, Niagara Falls, N.Y.
C. D. KING, Pittsburgh, Pa.
W. J. REAGAN, Warren, Ohio

1947
G. R. BROPHY, Bayonne, N.J.
H. J. FORSYTH, Buffalo, N.Y.
A. P. MILLER, E. Chicago, Ind.

Blast Furnace and Raw Materials

W. E. BREWSTER, *Chairman*
T. B. COUNSELMAN, *Vice-Chairman*
B. W. NORTON, *Vice-Chairman*
OWEN R. RICE, *Secretary*

A. J. BOYNTON
P. F. DOLAN
P. G. HARRISON
W. A. HAVEN
G. W. HEWITT

H. W. JOHNSON
T. L. JOSEPH
C. D. KING
R. A. LINDGREN
H. E. McDONNELL
J. C. MURRAY

J. H. SLATER
G. E. STEUDEL
H. A. STRAIN
H. M. STUBBLEFIELD
C. L. WYMAN

Open-hearth Steel

L. F. REINARTZ, *Chairman*
A. P. MILLER, *Vice-Chairman*
FRANK T. SISCO, *Secretary*

GEORGE S. BALDWIN
J. M. CAHILL
R. K. CLIFFORD
C. R. FONDERSMITH
H. M. GRIFFITH
C. H. HERTY, JR.
E. G. HILL

WILLIAM C. KITTO
L. A. LAMBING
E. L. RAMSEY
W. J. REAGAN
A. E. REINHARD
E. A. SCHWARTZ
C. E. SIMS

GILBERT SOLER
A. H. SOMMER
FRANCIS L. TOY
DON N. WATKINS
T. T. WATSON
M. F. YAROTSKY
W. H. YECKLEY

Bessemer Steel

H. C. DUNKLE
J. D. GOLD
H. W. GRAHAM
M. A. JONES

E. C. SMITH, *Chairman*
C. D. KING
E. E. MCGINLEY
R. E. PENROD

W. J. REAGAN
G. A. REINHARDT
A. W. THORNTON
G. M. YOCOM

Electric Furnace Steel**EXECUTIVE COMMITTEE**

C. W. BRIGGS
A. L. FEILD
T. J. McLOUGHLIN

H. W. McQUAID, *Chairman*
FRANK T. SISCO, *Secretary*
T. S. QUINN
W. J. REAGAN

C. A. SCHARSCHU
GILBERT SOLER
E. A. WALCHER

CONFERENCE COMMITTEE

SAMUEL ARNOLD, III
W. M. FARNSWORTH
K. L. FETTERS
R. H. FRANK
R. C. GOOD

C. W. BRIGGS, *Chairman*
W. J. REAGAN, *Vice-Chairman*
R. P. HEUER
JOHN JUPPENLATZ
ANDREW KAUL, III
C. C. LEVY
G. A. LILLIEQVIST

F. A. MELMOTH
H. E. PHELPS
FRED RIGGAN
J. F. ROBB
NORMAN STOTZ

Physical Chemistry of Steelmaking

R. S. ARCHER
JOHN CHIPMAN
G. R. FITTERER
J. J. GOLDEN
J. W. HALLEY

T. S. WASHBURN, *Chairman*
K. L. FETTERS, *Secretary*
C. H. HERTY, JR.
T. L. JOSEPH
B. M. LARSEN
J. S. MARSH

W. O. PHILBROOK
L. F. REINARTZ
C. E. SIMS
GILBERT SOLER
H. K. WORK

Metallography and Heat Treatment

WALTER CRAFTS
J. T. EASH
SAMUEL EPSTEIN

F. M. WALTERS, JR., *Chairman*
J. T. NORTON
HOWARD SCOTT

G. V. SMITH
G. A. TIMMONS
CYRIL WELLS

Mining and Metallurgy

R. H. ABORN

A. B. KINZEL, *Chairman*
R. E. CROCKETT
T. S. FULLER

G. M. YOCOM

Howe Memorial Lecture

E. C. BAIN

W. A. HAVEN, *Chairman*
A. V. DEFOREST
JOHN HOWE HALL

E. C. SMITH

Robert W. Hunt Medal and Prize

F. B. FOLEY

W. A. HAVEN, *Chairman*
J. HUNTER NEAD
H. A. STRAIN

C. E. WILLIAMS

J. E. Johnson, Jr. Award

O. E. CLARK

B. J. HARLAN, *Chairman*
P. V. MARTIN

T. L. JOSEPH

MembershipW. E. BREWSTER, *Chairman*

E. L. APPLEGATE
O. E. CLARK
P. F. DOLAN
R. M. GARRISON
H. L. GEIGER
J. L. GREGG

J. W. HALLEY
J. E. JACOBS
E. C. MILLER
J. C. MURRAY
R. M. PARKE

H. S. RAWDON
W. E. REMMERS
C. E. SIMS
J. N. STAPLETON
M. J. UDY
E. R. YOUNG

ProgramsK. L. FETTERS, *Chairman*

J. B. AUSTIN
GERHARD DERGE
H. B. EMERICK

W. O. PHILBROOK
GILBERT SOLER

MICHAEL TENENBAUM
FRANCIS L. TOY
F. M. WALTERS, JR.

PublicationsC. M. LOEB, JR., *Chairman*

L. S. BERGEN
EARNSHAW COOK

F. B. FOLEY

J. L. GREGG
B. M. LARSEN

NominatingH. W. GRAHAM, *Chairman*

JOHN JOHNSTON

J. T. MACKENZIE
J. HUNTER NEAD

L. F. REINARTZ

The Howe Memorial Lecture

THE Howe Memorial Lecture was authorized in April 1923, in memory of Henry Marion Howe, as an annual address to be delivered by invitation under the auspices of the Institute by an individual of recognized and outstanding attainment in the science and practice of iron and steel metallurgy or metallography, chosen by the Board of Directors upon recommendation of the Iron and Steel Division.

So far, only American metallurgists have been invited to deliver the Howe lecture. It is believed that this lecture would gain in importance and significance were it possible to include metallurgists from other countries, but the Institute has not yet been able to do this on account of lack of special funds to support this lectureship.

The titles of the lectures and the lecturers are as follows

- 1924 What is Steel? By Albert Sauveur.
- 1925 Austenite and Austenitic Steels. By John A. Mathews.
- 1926 Twenty-five Years of Metallography By William Campbell.
- 1927 Alloy Steels By Bradley Stoughton.
- 1928 Significance of the Simple Steel Analysis. By Henry D. Hibbard
- 1929 Studies of Hadfield's Manganese Steel with the High-power Microscope. By John Howe Hall.
- 1930 The Future of the American Iron and Steel Industry. By Zay Jeffries.
- 1931 On the Art of Metallography By Francis F. Lucas.
- 1932 On the Rates of Reactions in Solid Steel. By Edgar C. Bain
- 1933 Steelmaking Processes. By George B. Waterhouse.
- 1934 The Corrosion Problem with Respect to Iron and Steel. By Frank N. Speller
- 1935 Problems of Steel Melting By E. C. Smith.
- 1936 Correlation between Metallography and Mechanical Testing. By H. F. Moore.
- 1937 Progress in Improvement of Cast Iron and Use of Alloys in Iron. By Paul D. Merica
- 1938 On the Allotropy of Stainless Steels. By Frederick Mark Becket.
- 1939 Some Things We Don't Know about the Creep of Metals. By H. W. Gillett.
- 1940 Slag Control. By C. H. Herty, Jr.
- 1941 Some Complexities of Impact Strength By Alfred V. de Forest.
- 1942 Time as a Factor in the Making and Treating of Steel By John Johnston.
- 1943 The Development of Research and Quality Control in the Modern Steel Plant. By Leo F. Reinartz.
- 1944 Gray Iron—Steel Plus Graphite. By J. T. MacKenzie.



J. T. MACKENZIE

Henry Marion Howe Memorial Lecturer, 1944

Gray Iron—Steel Plus Graphite

By J. T. MacKENZIE,* MEMBER A.I.M.E.

(Henry Marion Howe Memorial Lecture†)

HENRY MARION HOWE, in whose memory we are gathered together, was one of the great thinkers who develop from time to time to whom is given the rare gift of synthesis. Analysis is given to few, but synthesis, the ability to show the relation of all parts to each other and thus to give a clear picture of the whole, is reserved for the very few. Analysis can be achieved by honesty, intelligence, and industry, but synthesis is only given to genius.

Professor Howe's crowning achievement is the picture of the whole iron-carbon series shown in Fig. 1, which places steel, malleable, gray iron, mottled and chilled irons in their proper relation to each other and shows the essential unity of the series. Perhaps his best statement of the case is found on page 90 of the *Metallography of Steel and Cast Iron* in these words: "Each member of the gray cast-iron series consists of the metallic matrix approximately equivalent to that member of the steel-white-cast-iron series to which it corresponds in percentage of combined carbon with its continuity broken up—by masses of graphite . . ." Apparently he had taken considerable interest in this idea around the turn of the century, for he refers to a discussion at the Franklin Institute in 1900 in which he said: "Though many others had probably conceived this relation between the steels and cast irons, it was here enunciated for the first time, so

far as I know. It was received with great incredulity."

The concept was explained in some detail in a paper on "The Constitution of Cast Iron" presented before the A.S.T.M. in 1902 when Professor Howe was retiring president of that young society. In the discussion Dr. Sauveur stated that he was "very well acquainted with Professor Howe's theory of the constitution of cast iron," and went on to say that while he "shared it to the fullest extent, some foundrymen . . . claim cast iron is a metal entirely different from steel . . . that steel and cast iron have very little in common, and that therefore the knowledge gained in the study of steel is of little or no value in the study of cast iron." Dr. Moldenke, in discussing the same paper, said he had been working on the same theory for 12 years but he laid no claim to publication.

Discussing the difference in the microstructure of the metallic matrix, Professor Howe pointed out that "such minor structural differences are indeed to be expected, because of the difference in the conditions under which these constituents are generated.

"One difference in these conditions is that the steel of most micrographs has been either forged or at least treated thermally in such a way as to give a new structure radically different from that which formed during the initial solidification, whereas the cast irons have not. Hence what we see in the steels is a transformation structure, but in the cast irons a solidification structure. By giving the cast

Manuscript received at the office of the Institute April 20, 1944. Issued as T.P. 1741 in *METALS TECHNOLOGY*, June 1944.

* Chief Metallurgist, American Cast Iron Pipe Co., Birmingham, Alabama.

† Presented at the New York Meeting, February 1944. Twenty-first Annual Lecture.

irons a suitable thermal treatment, they too can be given a transformation structure much closer to that of steel."

Today large tonnages of cast iron are

FORMATION OF GRAPHITE

The mechanism of the formation of graphite* has been studied by many metallurgists, but the most concise and

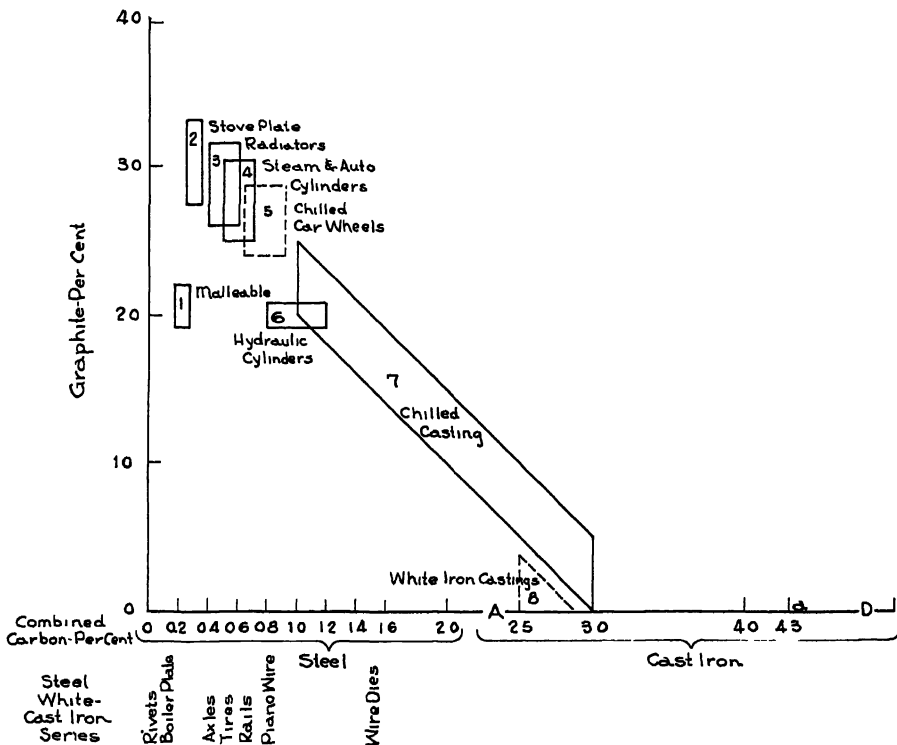


FIG. 1.—RELATION OF CAST-IRON FOUNDRY PRODUCTS TO THE STEEL-WHITE-CAST-IRON SERIES AS REGARDS THEIR CONTENT OF COMBINED CARBON AND OF GRAPHITE.
(Fig. 19, p. 87, *Metallography of Steel and Cast Iron*, by Howe)

heat-treated—some annealed, some normalized, some quenched and drawn. Two examples are shown in Fig. 2 coming out of commercial production. These are $3\frac{1}{2}$ -in. dia. bar stock of low total carbon (2.4 per cent). The as-cast structures show coarse pearlite and had a tensile strength of 39,000 lb. per sq. in. with a Brinell hardness number of 235 to 255. The structures after heat-treatment (normalized at 1700°F.) gave tensile strengths of 53,000 with a Brinell of 285—a great improvement due to transformation of the matrix, since the graphite was changed practically none at all by this treatment.

clearest statement of it was made by Alfred Boyles after a thorough investigation presented before this Institute in 1937. Boyles summed it up as follows:

1. Primary austenite freezes out in the form of dendrites, which continue to grow down to the eutectic temperature.
2. Crystallization of the eutectic liquid begins at centers which grow equally in all directions, forming a cell-like structure.
- 3 Segregation takes place in two stages: (a) between the primary dendrites and the liquid. (b) from the crystallization centers of the eutectic outward into the boundaries of the cells.

* "Gray iron," unless qualified, in this paper refers to normal hypoeutectic irons.

4 Constituents formed during the freezing of the eutectic occupy the interstices of the dendrites. The graphite flakes and the phosphide eutectic thus are restricted by the size and distribution of the dendrites

With this clear statement before us, we thought of the method used by Roll to obtain a space model of the graphite flakes. The method is shown in Fig. 3. It

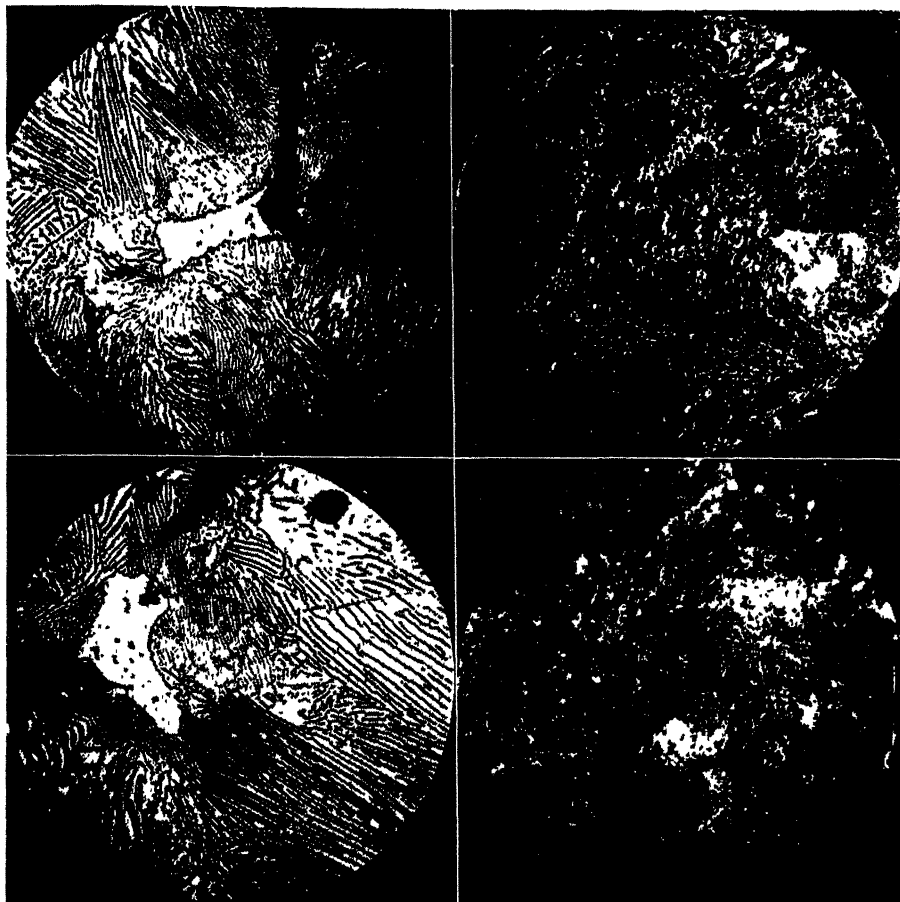


FIG. 2.—CAST IRON ETCHED WITH 2 PER CENT NITAL. $\times 875$

- a. Cast 9/15/43. As cast.
- b. Cast 9/15/43. Heat-treated.
- c. Cast 9/17/43. As cast.
- d. Cast 9/17/43. Heat-treated.

5 Graphite flakes do not begin to form until the eutectic begins to freeze. As soon as the eutectic is completely frozen, the flake structure essentially is complete. The flakes grow radially from the crystallization centers of the eutectic outward into the surrounding liquid, resulting in a "rosette" or "whorl" formation.

consists of firmly establishing the position of the specimen on the stage of the microscope, photographing and repolishing. Between polishings the specimen is measured accurately and when enough plates are obtained they are stacked with the

proper spacing between to give the three-dimensional picture as shown. A model can then be constructed of some plastic, as shown in Fig. 4. Roll seemed to think of the graphite only as flakes, but with

word "whorl" appears to be a better description than "rosette." Four more of these formations are shown in Figs. 6 and 7. Three "cuts" are shown as the conventional photographs in Fig. 8.



FIG. 3.—ROLL'S METHOD OF CONSTRUCTING A SPACE MODEL OF GRAPHITE FLAKES.



FIG. 4.—PLASTIC MODELS OF GRAPHITE FLAKES.



FIG. 5.—MODELS OF GRAPHITE WHORLS. $\times 150$.

Boyles' theory in mind we observed the relative position of the flakes and thus obtained the highly satisfactory confirmation of his theory, shown in Fig. 5. Boyles'

After constructing the individual flakes, we tried setting them up in their actual space relationships, with the results shown in Fig. 9, which gives views from both

sides and the top (standard inch included for scale). The magnification of the models is about 150. These are not all of the formations in this volume but enough are

typical of all of them. This phenomenon probably is the reason why cast iron does not have a porous structure, as is commonly supposed. Even Professor Howe



FIG. 6.—MODELS OF GRAPHITE WHORLS. SAME FLAKES FROM DIFFERENT ANGLES $\times 150$.

developed to show that the space relationships confirm Boyles' reasoning.

The formation of graphite is accompanied by the expansion. This has been shown by a number of investigators, notably Keep, West, and Turner, and was lately the subject of some very accurate tests by the National Bureau of Standards. Their curves for two bars cast from the same iron are shown in Fig. 10 and are

passed on this idea, saying: "The presence of this graphite skeleton offers to liquids a path of relatively easy passage."

As just shown in the space model, Fig. 9, the graphite flakes do not completely envelop the grains. Piwowarsky showed (Die Giesserei, 1929, p. 838) that cast iron becomes permeable only at a thickness that is governed by the greatest length of graphite flake. He concluded that the

flakes do not join each other and that, therefore, if the cast iron is of sufficiently great thickness with respect to the length of flake, there will be no permeability

porosity, as commonly understood, is due to flaws in the casting—never to the metal structure. Thousands of tests on cast-iron pipe and fittings have proved this beyond



FIG. 7.—MODELS OF GRAPHITE WHORLS. SAME FLAKES FROM DIFFERENT ANGLES. $\times 150$.

To prove it he tested three grades of iron with hydrogen at 45 lb. per sq. in. (3 atmospheres). His criterion of leakage was one cubic inch of hydrogen per square inch per week. The two soft irons, one a pig iron, showed leakage through 0.024 in. but not through 0.030 in. The high-test cast iron, with its smaller flakes, showed leakage through 0.020 in. but not through 0.024 in. A test on 0.118-in. (3 mm.) plates of all three at 2100 lb. per sq. in. (140 atmospheres) showed no leakage in any of them. From this, he concluded that

a doubt. Every leak is a flaw, sometimes a shrink, a blowhole, a cold run, or a sand or slag inclusion—but more often two or more of them together. One test 6-in. line was kept under gasoline pressure 233 days with all valves closed. The pressure, which was started at 800 lb. per sq. in., rose and fell in exact proportion to the temperature for the whole time. The temperature in the line varied from 42° to 85° with a corresponding change in pressure from 0 to 1690 lb. per sq. in. One week's chart is shown in Fig. 11. The lag is due to the

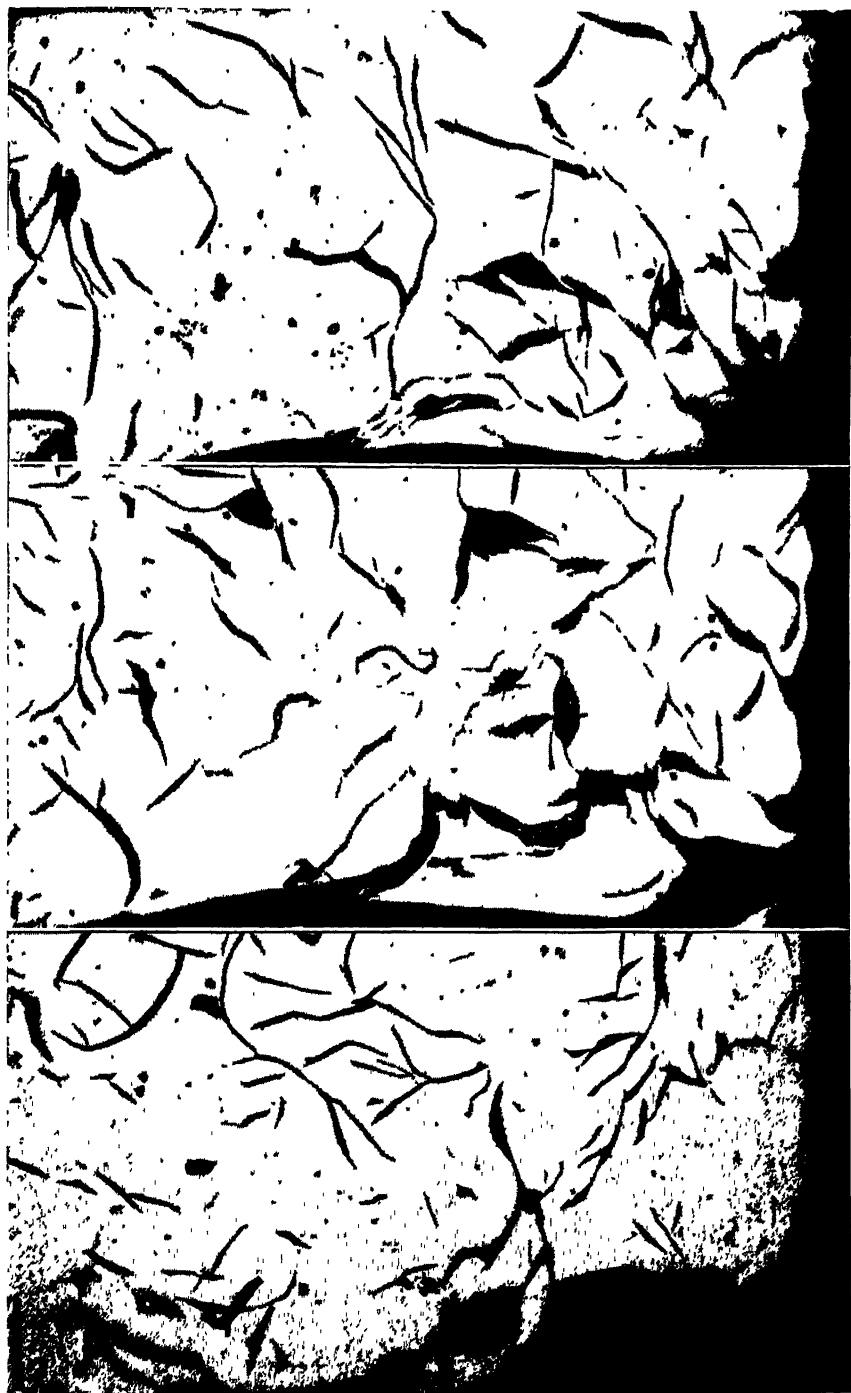


FIG. 8.—CUTS OF GRAPHITE-FLAKE MODELS $\times 100$
a, top; *b*, middle; *c*, bottom.

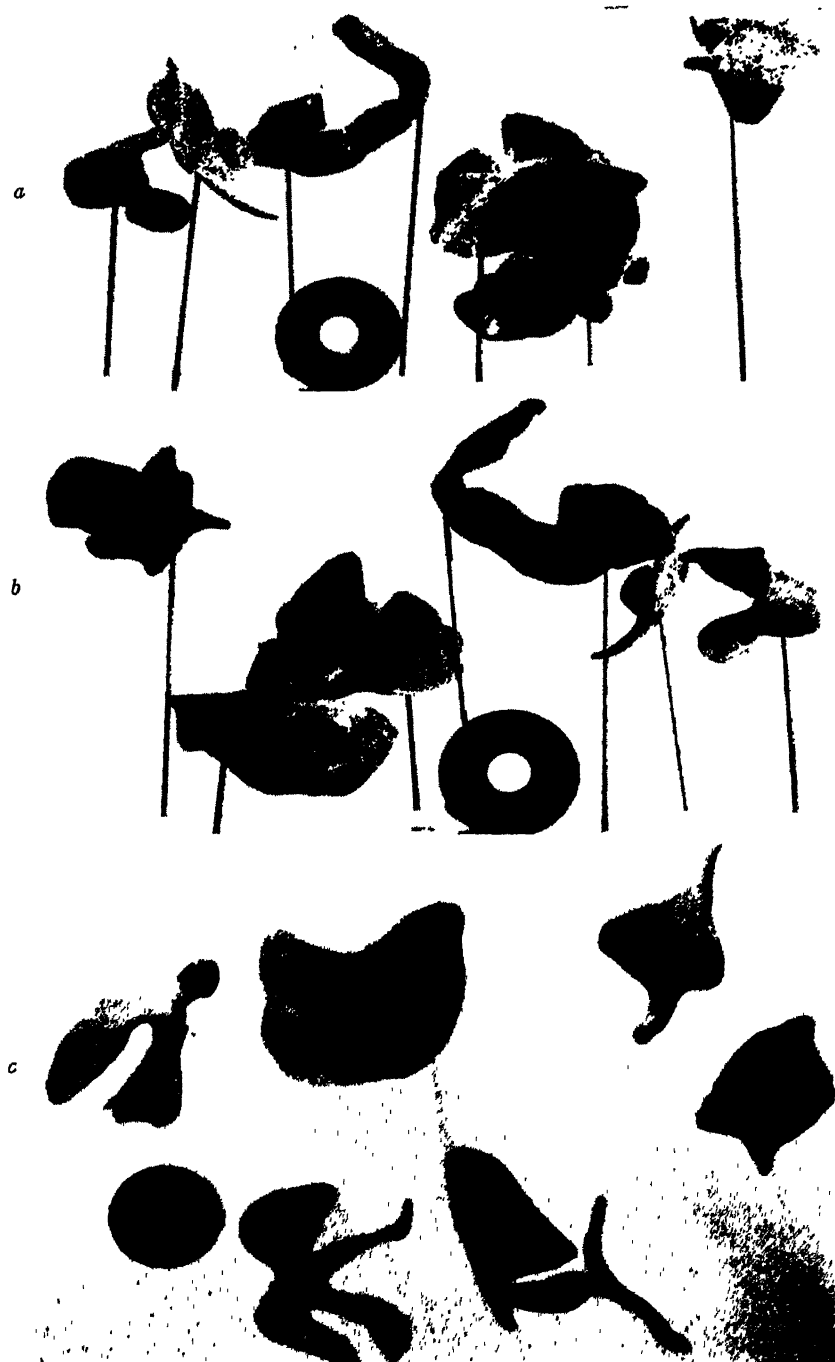


FIG. 9.—MODELS OF GRAPHITE FLAKES SET UP IN SPACE RELATIONSHIPS. $\times 150$.

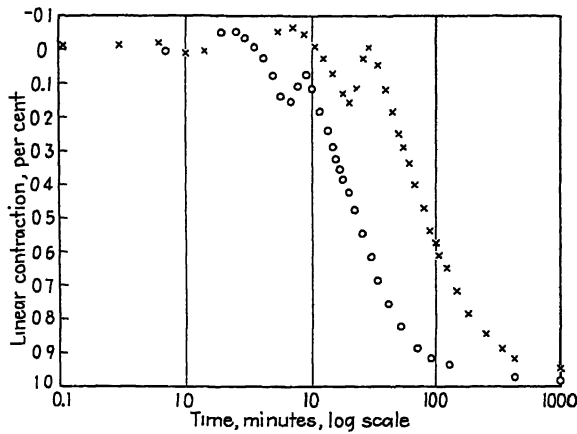


FIG. 10.—RELATIVE CHANGES OF LENGTH IN $\frac{3}{4}$ -INCH SQUARE BAR AND $1\frac{1}{2}$ -INCH SQUARE BAR, EACH CONTRACTING INDEPENDENTLY.

Curves supplied by Foundry Section, National Bureau of Standards (Fig. 82, Symposium on Cast Iron, 1933)

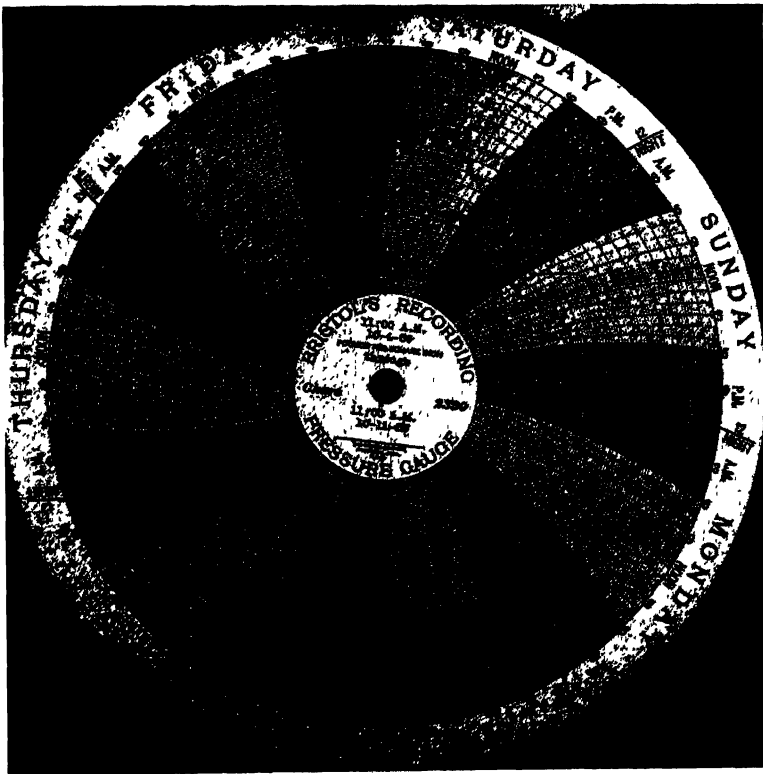


FIG. 11.—ONE WEEK'S CHART OF THE HIGH-PRESSURE GASOLINE TEST LINE AT ACIPCO
Outer record, temperature, deg. F. $\times 10$.
Inner record, pressure, lb. per sq. in.

fact that the thermometer was in the atmosphere but the pressure was that of the gasoline. Even a slight seepage through the whole surface of the line (100 ft. of

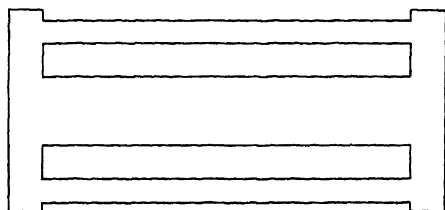


FIG. 12.—STRAIN LATTICE.

6-in. pipe of different classes with wall thicknesses varying from 0.30 to 0.45 in.) would have been evident from the temperature-pressure relation. The line was under water and no sign of gasoline was ever visible during the test.

This expansion on freezing, while it tends to reduce shrinkage, cannot entirely eliminate it, since the expansion of the first shell tends to enlarge the mold. The next layer to freeze also expands, producing a further expansion in the still plastic outer shell, so that the still liquid metal of the interior is not sufficient to fill the volume due to this extra expansion; and as there is still some liquid shrinkage to take place, a pipe must result unless the cavity is fed.

Again referring to Fig. 10, we see that contraction on freezing gives the same set of phenomena at 1130° that occur in steel at 725° . Thus cast iron is twice put in jeopardy for the same offense. At 1130° , though, cast iron has no tensile strength at all, while steel and cast iron have some strength at 725° . Thus, for thick and thin sections joined together the only "out" is the plasticity of the metal and some compressive strength. Assume two sizes of bars connected at both ends as in the familiar strain lattice of the Germans (Fig. 12). The small bars first freeze and expand. Now the small bar begins to contract but the large bar begins to expand, so that tensile stresses are set up

in the small bar and compressive stresses in the large one. The relative strength and plasticity of the two will determine what happens. But this is an exact analogy to

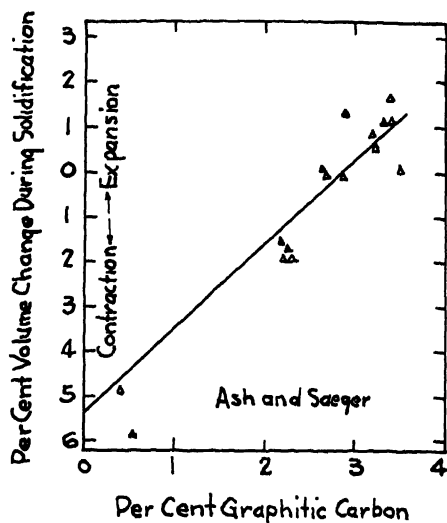


FIG. 13.—RELATIONS BETWEEN VOLUME CHANGE DURING SOLIDIFICATION OF SOME CAST IRONS AND THE GRAPHITIC CARBON CONTENT.

From Saeger and Ash: Amer. Foundrymen's Assn., 1932.

the performance of both iron and steel at the pearlite transformation point, so that it is not necessary to go into the many things that can happen. Fig. 13 shows the relation of volume change during solidification to the graphite content.

Another erroneous idea in connection with this expansion on freezing has been current in the literature for a long time. That is the idea that, as Professor Howe expressed it: "the generation of graphite is useful in the process because, occurring as it does during and immediately after solidification, it causes a sudden expansion, which both lessens the tendency of the castings to tear themselves into pieces during solidification and causes them to reproduce more accurately the shape of the pattern." As we have just seen, the first "advantage" is fully realized only in uniform sections (which the designers seem

to avoid whenever possible) but the ability to reproduce the shape of the pattern is solely a function of the fluidity of the metal, giving the word the foundry-

spaces it might not have sufficient fluidity to enter during the casting. The idea probably started from the exquisite detail of the cast-iron art ware of the first half

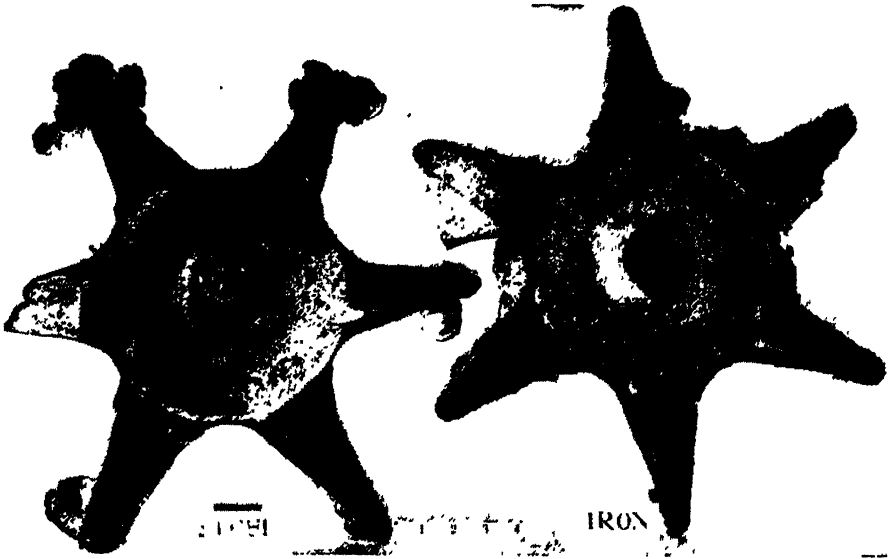


FIG. 14.—PATTERN CAST FROM STEEL AND GRAY IRON.

man's definition, not the physicist's. This may be mathematically expressed thus:

$$\text{Fluidity} = K \frac{T - FP}{FP - MT}$$

in which T = temperature of the metal,
 FP = freezing point of the metal,
 MT = temperature of the mold,
 K = a coefficient depending on the true fluidity, surface tension, mold friction, mold atmosphere, and the chemistry of the metal at that temperature in that atmosphere, etc.

It is obvious, since graphite does not begin to form until a considerable part of the metal has frozen, that the fluidity is, at that time, for all practical purposes, zero. The only exception might be a rigid mold, where there might be sufficient resistance to force the plastic metal into

of the nineteenth century, but having the misfortune of breaking one of those pieces awhile back, it was some secret satisfaction to find it white! Fig. 14 shows a pattern cast with steel and gray iron. Although the steel was not quite fluid enough to fill out one of the points, the detail of the other points is as sharp as the gray iron; in fact, the fins are quite a little more pronounced on the steel.

EFFECT OF GRAPHITE ON MECHANICAL PROPERTIES OF GRAY CAST IRON

Now, let us consider the effect of the graphite on the mechanical properties of gray cast iron. For more than a hundred years mathematicians and testing engineers have been interested in the performance of gray cast iron and especially in the discrepancy between bending strength as measured and that calculated from the tensile strength by the conventional beam

formulas. Tredgold, in 1823, seems to have been the first to make an extensive investigation of the strength of cast-iron beams and his calculations were recognized to

axis, for this particular beam, of 8 per cent toward the compression side—that is to say that there was 38 per cent more metal in tension than in compression at the

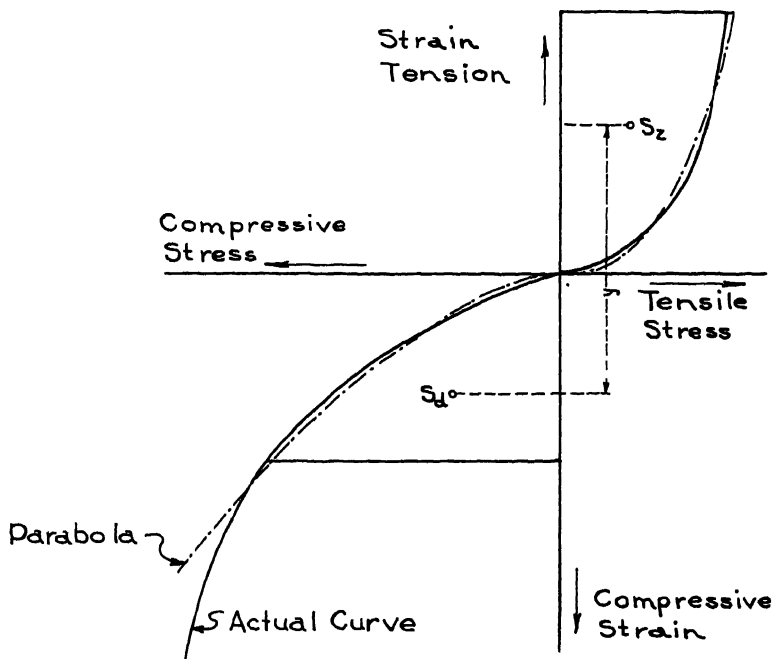


FIG. 15.—BACH'S STRESS-STRAIN DIAGRAM.
(Fig. 5, p. 301, Ed. 9 of his book.)

give results differing from tensile strength by Hodgkinson, the editor of the fourth edition of Tredgold's book, "The Strength of Cast Iron" (1842). Hodgkinson stated that this "arises principally from the supposition that the neutral line remains stationary during the flexure of the body."

The concept of the shifting of the neutral axis was used by St. Venant to reconcile the results of observations with the theory of elasticity in 1864 and beginning in 1888 Bach wrote a series of papers, later incorporated in his "Elastizität und Festigkeit," the first edition of which was published in 1889, in which some experimental and theoretical results were reconciled within 3 per cent. His calculations showed a displacement of the neutral

instant of fracture. Bach's curves are shown in Fig. 15.

W. J. Schlick and B. A. Moore made a study of this in *Bulletin* 127 of the Iowa Engineering Experiment Station, in 1936, in the course of a study on combined bending and tension, which is the foundation of the modern design of cast-iron pipe. Their method of analysis was essentially the same as that of Bach and consists in plotting the stress-strain curves for both tension and compression as in Fig. 15; locating the center of gravity of the tension side, then determining the area on the compression side, which, multiplied by the distance from the center line to its center of gravity, gives an amount equal to the same product on the tension side. Then

the difference between the distances of the tension and compression centers from the center line gives the displacement of the neutral axis. About the only use for the equations for stress strain is in this

suggested for cast iron, in all of which P indicates load (or stress); f , the strain, and c , a , b , q and n are constants of the particular material and conditions of loading. P_B is load (stress) at failure.

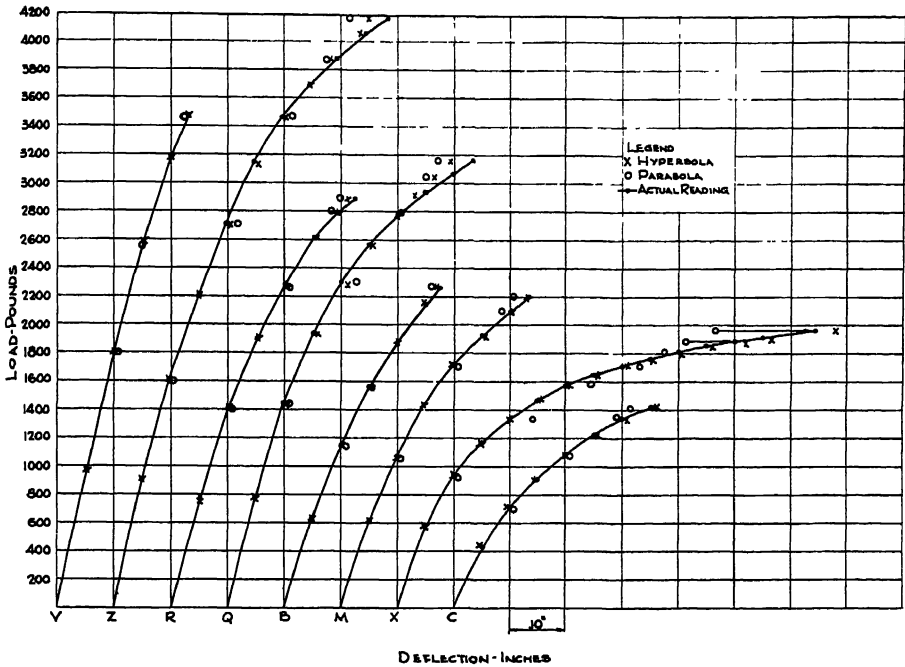


FIG. 16.—LOAD-DEFLECTION CURVES OF CAST IRONS OF DIFFERENT CHARACTERISTICS.

Test Bar	$f = CP^n$		$\frac{P}{f} = a - bP$		$P = C(100f)^n + q \sin 2\pi \frac{P}{P_B}$			
	$\frac{1}{100C}$	n	$\frac{a}{100}$	b	C	n	q at $\frac{1}{4}$ load	q at $\frac{3}{4}$ load
V	624	1.169	212	0.0171	286	0.797	81	76
Z	4,879	1.406	206	0.0267	488	0.553	287	283
R	2,844	1.424	180	0.0313	344	0.612	144	114
Q	6,881	1.544	185	0.0327	478	0.602	540	186
B	1,076	1.326	141	0.02475	245	0.669	102	60
M	3,118	1.490	150	0.0385	294	0.573	137	88
X	344,100	2.214	161	0.0686	414	0.361	237	186
C	2,452	1.554	108	0.0500	192	0.563	78	59

calculation and the calculation of resilience, the term applied to the area under the stress-strain curve of nonductile materials. Still, there is somewhat of a fascination about them to anyone interested in the behavior of the material.

Three general equations have been

Bach used the parabola $f = CP^n$, which he ascribes to Buelffinger in 1729 and which later was rediscovered by Hodgkinson. Gruebler in 1900 proposed a hyperbolic equation $P = f(a - bP)$, which has since been used by several investigators. It fits the actual curve much better than the

parabola. Meyersberg, in 1931, proposed the equation $P = Cf^n + q \sin 2\pi \frac{P}{P_B}$, which is the Bach parabola with a positive cor-

rection of 0.05-in. deflection of the standard 1.2×18 -in. test bar. The errors of the equations calculated as above are indicated. The Meyersberg equation, using the actual q

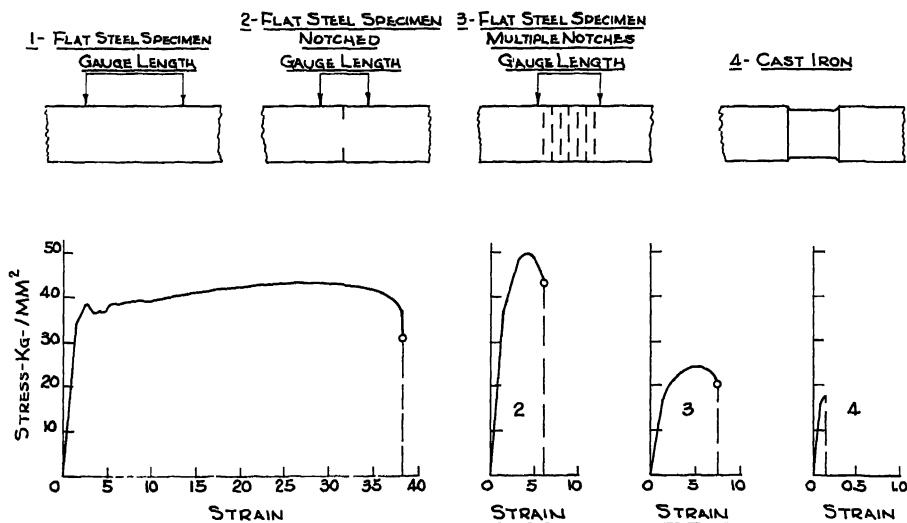


FIG. 17.—THUM'S EXPERIMENT.

rection for the curvature of the lower half of the curve and a negative correction for the upper half.

The parabola and hyperbola, determined by least squares, fit the actual curves very well until near the breaking point, where the deflection becomes increasingly greater than the load. The Meyersberg formula uses only the simultaneous equations for half load and breaking point (where the $\sin = 0$) for the first term, hence is exact at these points; the second term is then easily obtained from the difference between the first term and the data at the quarter and three-quarter points where the \sin is $+1$ and -1 , respectively.

Cast iron of widely differing characteristics are shown in Fig. 16. These were selected from the report of Subcommittee XV of Com. A3 of the American Society for Testing Materials, published in the *Proceedings* of 1933. The actual observed points are readings of the load at each

for the two halves of the curve (which fits it exactly at five points) agrees too closely to show a difference on these scales. No part of these curves is a straight line. Even the very stiff iron V shows curvature from the origin if a large enough scale is used.

Thum, of Darmstadt, became interested in why cast iron behaved as it did and made the simple experiment shown in Fig. 17. Naturally it would be most difficult to duplicate the pattern of graphite by any such means, but the change from the characteristic ductility shown in the first figure by the usual steel specimen is very good evidence that, in tension, the graphite acts as voids. Fig. 18 shows some further tests along this line in which steel with different patterns of "damage" is compared with six cast irons of different graphite contents. The original photographs are very poorly printed in the only available reference (Die Giesserei, 1929) but the reproductions here at least give

an idea of the relative graphite arrangement. Table 1 gives the analysis and some of the physical properties of these cast irons. Obviously, the increase in amount of graphite is the main feature of the series but its shape and distribution as well as the structure of the matrix cause upsets in the relative positions of the curves. No. 6, for example, is lower in graphite than No. 5, but it is also lower in combined carbon and phosphorus. (It is quite

same iron, same size, tested in direct tension and compression. His results for two quite different irons are plotted in Fig. 20. The endurance limits for the two irons were respectively 7 and 12 kg. per sq. mm. as conventionally calculated, so from the curves we obtain as correction factors:

$$\frac{6.3}{7} = 0.90 \quad \text{and} \quad \frac{11}{12} = 0.92$$

TABLE 1.—Data on Thum's Cast Irons

Data	1	2	3	4	5	6
Carbon, per cent.						
Total	3.22	2.94	3.35	3.30	3.77	3.30
Combined	1.37	1.39	0.85	0.86	0.85	0.70
Graphitic	1.85	1.55	2.50	2.44	2.92	2.60
Silicon, per cent.	1.15	2.00	1.46	1.80	1.85	2.60
Manganese, per cent.	0.91	1.07	0.97	0.90	0.63	0.80
Phosphorus, per cent.	0.39	0.22	0.40	0.50	0.08	0.50
Sulphur, per cent.	0.12	0.06	0.08	0.08	0.12	0.10
Tensile strength, kg. per sq. mm.	28.0	29.0	29.0	25.0	18.7	15.7
Modulus of rupture	47.5	41.0	53.5	53.5	38.8	37.8
Deflection, mm.	9.8	8.8	10.5	12.9	14.0	13.1
Brinell hardness number	241	266	220	227	190	187
Modulus of Elasticity in Tension, Thousands						
Stress, kg. per sq. mm.:						
0-2	1,380	1,250	1,160	1,145	895	750
8-10	1,350	1,230	1,060	895	665	538
Modulus of Elasticity in Compression, Thousands						
Stress, kg. per sq. mm.:						
0-2	1,450	1,450	1,400	1,155	888	765
8-10	1,350	1,290	1,340	1,144	890	1,000

probable that No. 5 was sampled or analyzed incorrectly, since the total carbon given is 0.23 per cent above the eutectic for that silicon and phosphorus. Incidentally, "combined carbons" are always doubtful, as MacPherran stated in his classic remark that "combined carbon is the sum of two errors.")

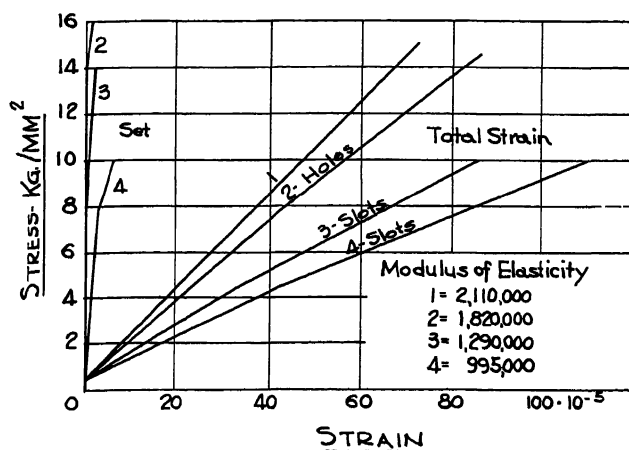
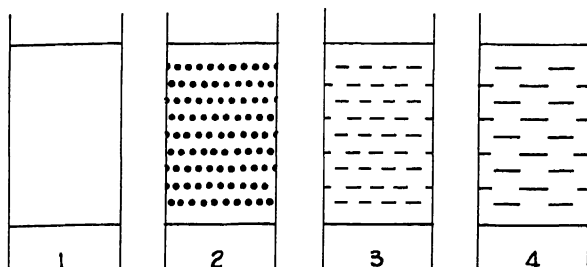
Thum was interested in the error of the usual beam calculations when applied to the rotating beam commonly used for the determination of the endurance limit. He therefore made some studies using the device shown in Fig. 19. This gave actual strain on both sides of the beam, which was converted to tensile or compressive stress by previous readings on bars of the

Considering the normal scatter of values obtained in endurance testing, these are not serious corrections, but if cast iron is to be used under dynamic tension and compression it should be remembered that such a factor is needed. In reversed bending, the factor does not apply, since the stress and strength calculations are mutually corrective.

Many investigators since Tredgold's time have studied the effect of the shape of the beam on the calculated strength. Thum, using the device shown above, determined the actual stress for the shapes shown in Fig. 21 and compared it with the modulus of rupture. This is undoubtedly the best set of tests available and

shows clearly the departure from the assumptions of the elastic theory; viz., homogeneity, isotropy, and elasticity. The shapes vary progressively in the way the rectangular bars have corroborated the results on shapes 2 and 3 of Thum's work. Using the rich fund of data contained in the Report of Subcommittee XV pre-

ARRANGEMENT OF NOTCHES

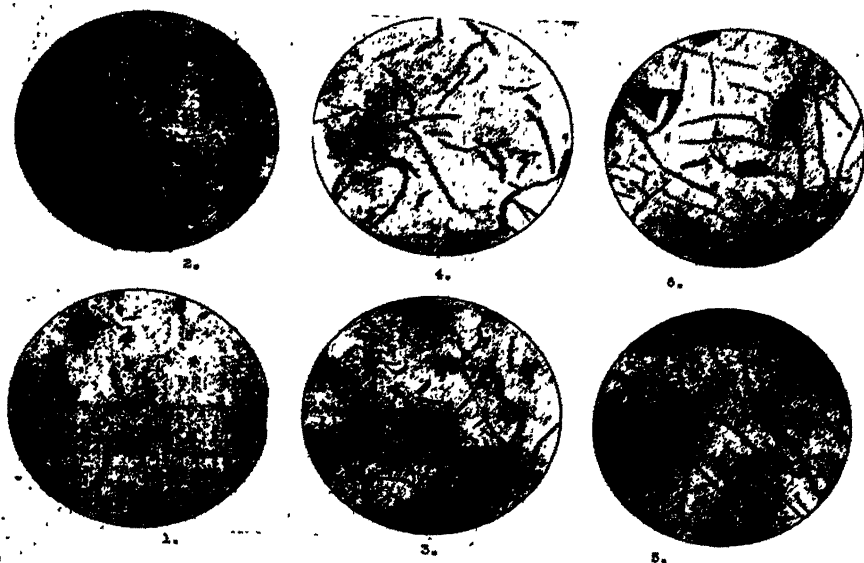


Steel

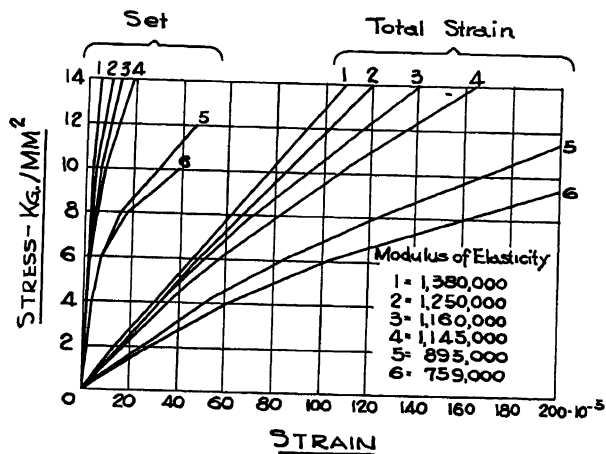
FIG. 18.—THUM'S COMPARISON.

metal is distributed about the center line and the departure from theoretical increases as the distance from the center line to the center of gravity of the half sections decreases. The difference in the performance of the strong, low-graphite No. 3 iron and the soft, high-graphite No. 5 is very small on the I-beam but quite noticeable on the other shapes. Bach's tests in the 1880's give substantially the same relations and many thousands of tests on round and square or

viously mentioned, there are illustrated in the next few figures some of the relations between graphite and the strength and stiffness of gray iron. Fig. 22 shows in capital letters the relation of tensile strength to graphite content for the 24 irons of the investigation and in small letters the ratio of the modulus of rupture to the tensile strength. (The identification letters of the original report have been used as a convenience to anyone wishing to refer to the other data on these irons.)



ARRANGEMENT OF GRAPHITE X 200



Cast Iron
FIG. 18.—(Continued.)

In the lower figure the "out of line" irons are *V*, hypereutectoid; *N*, austenite + martensite; *X*, austenite; *D*, hypereutectic with 2 per cent phosphorus; and

pronounced. A survey of the published results of the 10 years from 1922 to 1932 showed the results listed in Table 2.

Thus for as-cast transverse bars against

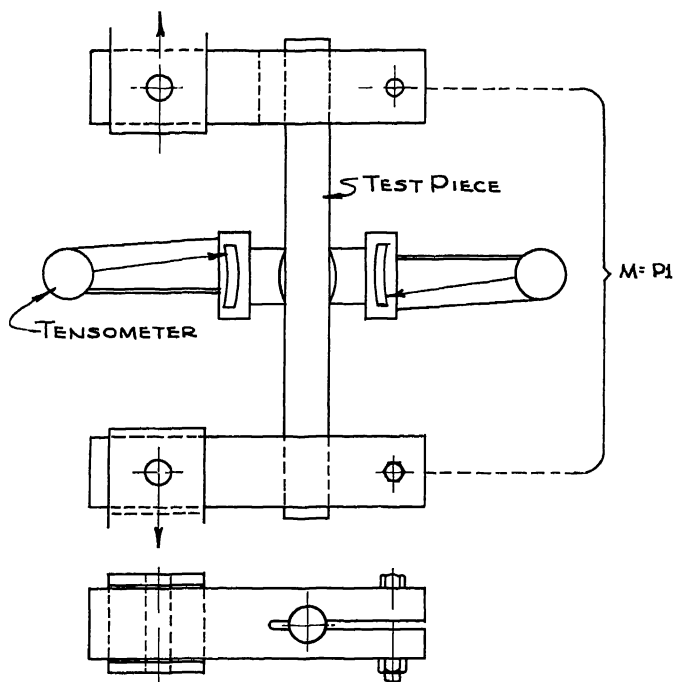


FIG. 19.—THUM'S DEVICE FOR MEASURING ACTUAL STRESS IN BENDING TEST.

U, hypereutectic with 3 per cent silicon. The upper figure shows that while the graphite reduces the bending strength, it does not reduce it proportionally, as the ratio rises owing to increasing displacement of the neutral axis. For example: at 51,000 tensile (iron *J*) the ratio is 1.9 and the modulus of rupture is 92,500, while at 20,000 tensile (iron *I*) the ratio is 2.45—a modulus of rupture of 49,000. Thus, for gray iron, an increase of 155 per cent in tensile strength is accompanied by only 90 per cent increase in bending strength.

These results are on machined transverse as well as tensile bars. Where the transverse is not machined, as in the usual comparisons, the decrease in ratio of modulus of rupture to tensile strength is even more

pronounced. A survey of the published results of the 10 years from 1922 to 1932 showed the results listed in Table 2.

TABLE 2.—*Ratios of Modulus of Rupture to Tensile Strength Published in Ten Years 1922-1932*

Tensile Strength	Number of Tests	Average Ratio
15,100-20,000	8	2.27
20,100-25,000	22	1.89
25,100-30,000 ^a	11	1.67
30,100-35,000	19	1.88
35,100-40,000	10	1.72
40,100-45,000	14	1.55
45,100-50,000	7	1.38
50,000+	5	1.26

^a The group of 11 tests between 25,100 and 30,000 averaged much higher phosphorus than the other groups

Obviously, as the graphite decreases in size and amount the surface is increasingly sensitive to stress raisers. Fig. 23 shows that the same thing is true for compressive strength (V , N , and D being farthest out of line) and Fig. 24 shows much the same pattern for the shear.

As a measure of the stiffness of cast iron, the somewhat misnamed "secant modulus of elasticity" has been used. This is simply a substitution of the load and deflection in the conventional beam formulas and, while it has very little relation to the true modulus of elasticity of the mathematicians, it is a very useful quantity. Fig. 25 shows how this quantity varies inversely with the graphite, the exceptional irons again being N , X , and U . The change in the values for the different degrees of loading gives a very good idea of the curvature of the bending curves. A direct quantity, long used in specifications for cast-iron pipe, and quite simple when using a standard bar, is the load at a certain deflection. This can be read directly while making a test and does not require an autographic or other recording of the

whole curve. Such a study is made in Fig. 26, which gives the loads at 0.15 and

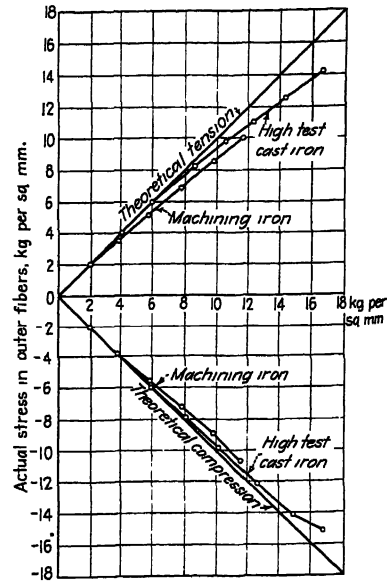
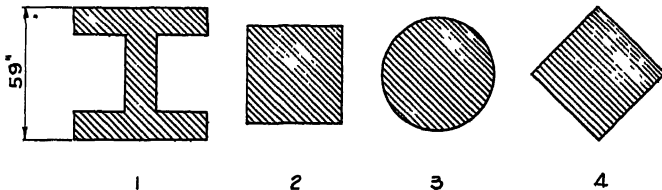


FIG. 20.—CALCULATED AND ACTUAL STRESS IN OUTER FIBERS IN BENDING TEST.

0.20-in. deflection of the 1.20×18 round bar. Again, N , X and U are farthest out



ACTUAL STRESS Kg/MM ²								
MATERIAL	5				3			
SHAPE	1	2	3	4	1	2	3	4
THEORETICAL								
4	40	38	40	36	39	39	39	40
8	73	70	70	66	76	74	75	75
12	101	98	94	92	110	107	107	104
16					142	138	138	133
Actual Bending Stress	192	195	186	202	295	288	298	290
Modulus of Rupture (Conventional)	314	353	371	484	475	497	555	640
Ratio $\frac{MB}{I}$	164	181	200	240	1.61	1.72	1.86	2.21
Displacement of the Neutral Axis in % of the depth.	38	33	26	23	3.5	19	15	16

FIG. 21.—EFFECT OF SHAPE ON BENDING STRENGTH.

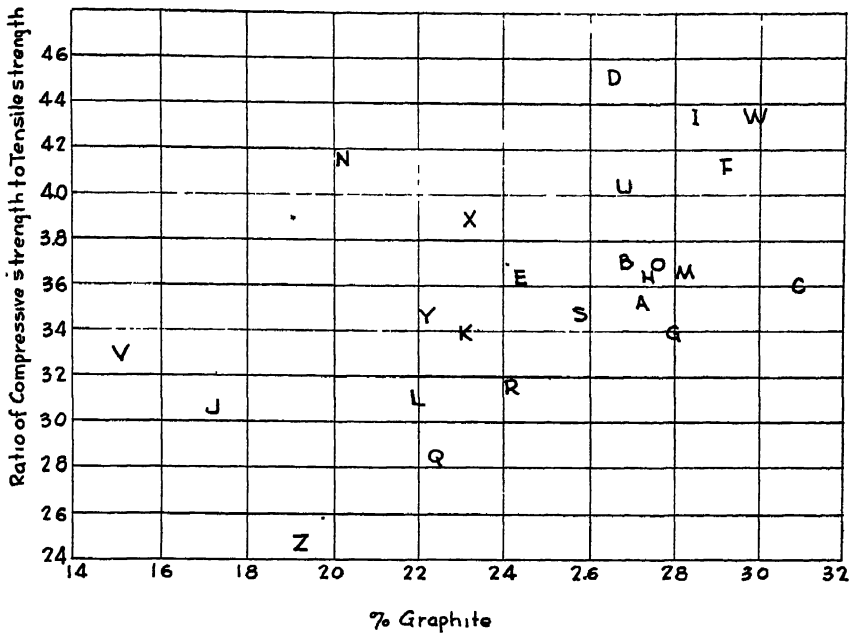


FIG. 23.—RELATION OF COMPRESSIVE: TENSILE RATIO TO GRAPHITE CONTENT.

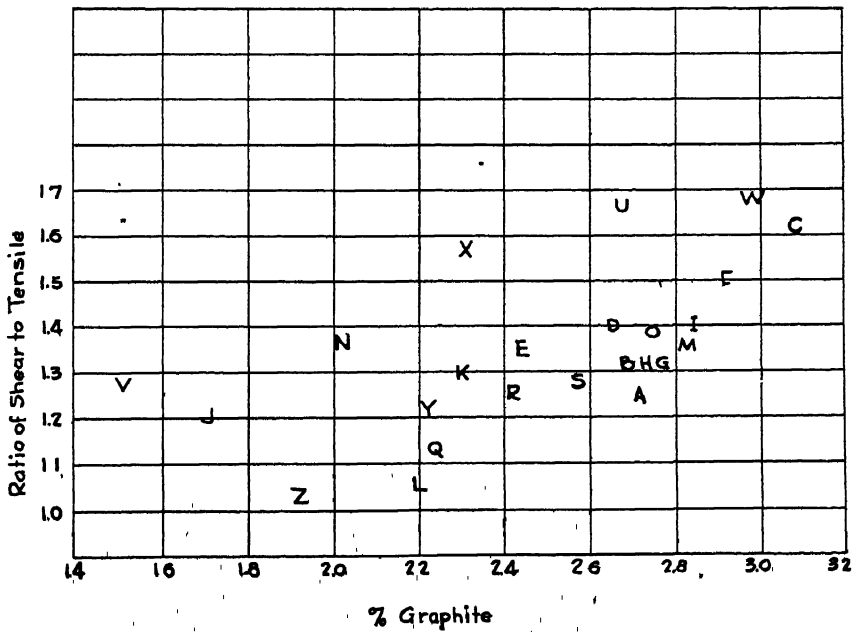


FIG. 24.—RELATION OF SHEAR: TENSILE RATIO TO GRAPHITE CONTENT.

elasticity. A typical case of a medium iron (2.9 per cent graphite) is given in Table 3.

A similar iron was loaded as follows:

LOADING NO.	SET, IN.
1	0 015
3	0 019
60	0 023
240	0 025
373	0 022

The bar showed little change after the third loading. If, however, the bar be loaded above the point previously stressed

from galling. As Mochel has pointed out, it does not gall when run on itself or on many other metals which are notorious for their galling tendencies. The graphite flakes also act as cushions against thermal shock and thus prevent crazing. Gray iron, therefore, is the only material that has been successfully used, at least on a large scale, for brake shoes or brake drum linings, which must absorb tremendous energy, convert it to heat, or noise, and

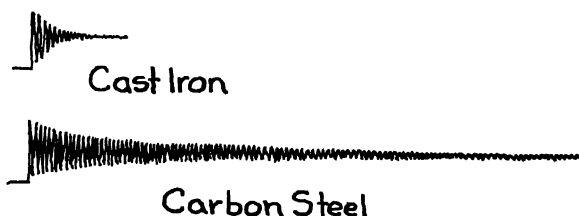


FIG. 29.—CURVES TAKEN WITH FÖEPPL-PERTZ DAMPING TESTER INDICATE DIFFERENCE BETWEEN INTERNAL DAMPING CAPACITY OF CAST IRON AND CARBON STEEL.

it behaves almost exactly like an unstressed bar from a little above that point. For the impact report, above cited, a study was made of the set of all of these irons at 20, 40, 60, and 80 per cent of the bending strength. Each bar was bent 25 times to the first load point, then 25 times to the second, and so forth. After the twenty-fifth loading to 80 per cent, the load was released and the bar was broken as in the usual test. On the first loading to each point, a bending curve was taken. Fig. 28 shows the comparative curves for Z and X when the set curves are assembled, as described in the report.

USEFUL FUNCTIONS OF GRAPHITE

Some of the more useful functions of the graphite are difficult to evaluate numerically. Because of the brittleness of the chip and the lubricating properties of the graphite, gray iron is easily machined. As Professor Boston has shown, it is the easiest ferrous material to machine at any given hardness level. The graphite undoubtedly is responsible for its freedom

still not "seize" the wheel or axle. This lack of galling tendency combined with the oil-retaining ability and the actual lubricating action of the graphite is also probably responsible for the excellent wear resistance of gray iron. These properties, not cheapness, are the reasons for the large use of gray iron by the automotive industry.

Another credit to gray iron is its almost complete insensibility to the notch effect. Prof. H. F. Moore showed that a specimen of cast iron with a radial hole which should have reduced the endurance limit 67 per cent actually reduced it only 13 per cent. Two other specimens tested with filleted grooves, which should have reduced the endurance limit 74 per cent, actually showed 0 and 8 per cent reduction. Prof. J. B. Kommers tested one soft cast iron with a square notch and got an increase of 500 lb. per sq. in. in the endurance limit.

The high damping capacity of gray iron is entirely due to the cushioning effect of the graphite. Damping capacity is closely related to the acoustic resistivity of the physicists and is mathematically expressed

as $u = \sqrt{Ep}$, where E is Young's modulus and p is density. Considerable work has been done on this property using the Foeppl-Pertz machine. Typical diagrams of gray iron and steel are shown in Fig. 29. The sound of a bar is that portion of the diagram reaching the ear. One of our wartime laboratory workers, a cellist by profession, became interested in the relation of pitch to stiffness and became able to predict, with considerable accuracy, the modulus of elasticity by the pitch of the tone given by the test bar, when struck by a hammer. Inasmuch as the modulus is an inverse function of the graphite, it is also an inverse function of the damping capacity. The Meehanite Research Institute, for example, in a tabulation of properties of its various grades, lists the relative values for Young's modulus and damping capacity (expressed as the energy dissipated in the first cycle of a torsion test at 20,000 lb. per sq. in.) as follows:

MODULUS OF ELASTICITY	DAMPING CAPACITY
23,000,000	21
21,000,000	24
19,000,000	25
17,500,000	28
15,000,000	30
12,000,000	32

Thus in many cases a softer iron—i.e., one with more graphite—would stand vibratory stresses better than a stronger iron.

Professor Howe said: "Graphite itself is source of weakness and brittleness. Its presence is sought rather for process than for product purposes." This was before the automobile had taught the value of gray iron in resistance to wear and galling and before autogenous welding had proved that strength and rigidity alone could not overcome vibration in heavy, high-speed machinery. I believe that were Professor Howe alive today he would be the first to recognize the value of the material, Steel plus Graphite.

Concentration of Iron Ores in the United States

By T. B. COUNSELMAN,* MEMBER A.I.M.E.

(Cleveland Meeting, April 1943; New York Meeting, February 1944)

PROBABLY the earliest concentration of iron ore in this country was carried on in the northeastern magnetite areas. Magnetic concentration was relatively simple and gave a concentrate that, after agglomeration, and in spite of being high in phosphorus because of the dry concentrating methods then in use, was satisfactory blast-furnace feed.

Production from the northeastern magnetite area languished after the discovery and development of the Lake Superior ores, where there was seemingly an unlimited tonnage of high-grade ore, first the Michigan ores, and subsequently the still larger deposits of Minnesota.

For years only the higher grade, direct shipping ores of the Lake Superior district were mined. Those of Michigan, and of the Vermilion Range in Minnesota, were hard ores and came principally from underground mines. The softer ores of the Mesabi came partly from underground mines, but mostly from the enormous deposits that could be worked by open-pit methods. The costs of ore from these open-pit deposits, even with the high initial cost of stripping, were so low that the underground mines of the Mesabi could hardly compete. The so-called Old Range ores, of Michigan and of the Vermilion Range of Minnesota, were hard and lumpy, and opened up the burden in the blast furnace, therefore making possible harder driving with greater output. Also, some of these ores were of such grade and physical

characteristics that they were suitable for charge ore in the open hearth. These ores, therefore, commanded a price premium, and could compete with the softer, finer, but cheaper, Mesabi ores. The big tonnage reserves, however, are on the Mesabi, and it is these big open-pit deposits that constitute our stock pile of iron ore, from which we are drawing so heavily during this war period.

On the western end of the Mesabi the ore was found to be high in silica, and not suitable as furnace feed. As early as 1902, attempts were made to concentrate this so-called wash ore and by 1910 the first washing plant was put into operation. The process was very simple, consisting essentially of a sizing and washing operation, with scalping screens, logwashers, and tables, which later were replaced by classifiers. Ore particles finer than 100 mesh were deliberately wasted, because these fines were undesirable in the furnace. Fortunately, these tailings were impounded, and already are being reworked.

Before long some of the low-grade ores began to require more elaborate treatment than the simple washing operation and, tables having been discarded because of their low capacity, in favor of classifiers, jigs were next introduced. These were able to discard coarser pieces of tailing than classifiers. Jigs are in active use today, various improvements having been made in their design and application. Various other machines and methods of concentration have been tried from time to time, and have in turn been discarded for more improved processes. The latest and most important process that has been

Manuscript received at the office of the Institute May 25, 1943. Printed in PROCEEDINGS of the Blast Furnace and Raw Materials Conference, A.I.M.E., 1943, and also issued as T.P. 1620 in METALS TECHNOLOGY, December 1943 and MINING TECHNOLOGY, January 1944.
*Manager, Industrial Division, The Dorr Company, Inc. Chicago, Illinois.

introduced is the heavy-media method of separation.

PRESENT RATES OF PRODUCTION

Concentration of the low-grade ores of the Lake Superior district has had a gradual but steady growth, up to the beginning of the present war. Table 1 shows the importance of concentrated ore compared with total shipments in 1942, and Table 2 shows the gradually increasing amount of concentrates over the last 10 years.

TABLE 1.—*Shipments from Lake Superior District in 1942*

	Gross Tons	Percentage of Total Shipments	Percentage of Minn. Shipments
U. S. shipments, rail and lake ^a	93,008,762	100.0	
Lake shipments only, United States and Canada ^a	92,085,324		
Total shipments from Minnesota (lake) ^b	73,566,179	79.1	100.0
Total concentrates (all Minnesota) ^{a,c}	17,961,746	19.3	24.4

^a Preliminary information from Lake Superior Iron Ore Association.

^b Preliminary information from *Skilling's Mining Review*.

^c Includes ore beneficiated by sintering or drying, but does not include ore which was merely crushed to make a better furnace feed.

TABLE 2.—*Concentrated Ore Compared with Total Lake Superior Shipments (U. S.)^a*

Year	Concentrated, Gross Tons	Total Shipments, Gross Tons	Percentage of Total Shipments Concentrated
1933	3,134,657	21,672,410	14.5
1934	3,440,041	22,063,824	15.6
1935	5,153,574	28,502,606	18.1
1936	7,764,501	45,251,250	17.2
1937	9,692,091	63,279,208	15.3
1938	2,826,444	19,549,909	14.4
1939	6,221,363	45,436,667	13.7
1940	9,207,681	63,948,846	14.4
1941	14,713,346	80,747,859	18.2
1942	17,961,746	93,008,762	19.3

^a Data from Mines Experiment Station, Mining Directory, 1942, and Lake Superior Mining Institute.

The significant point is the gradually increasing tonnage of concentrated ore shipped yearly. For instance, of the in-

creased tonnage shipped in 1942 over 1941 some 26 per cent was concentrated ore. For 1943, the schedule of total shipments is set at 100,000,000 tons. At the same rate, we can expect that concentrated ore shipments will be approximately 20,000,000 tons.

Most of the large bodies of direct shipping ore are already producing, and are almost at their peak capacity. Some additional direct shipping mines that have been idle will be brought back into production this year; some additional stripping is being done, but it will be difficult to get the desired increase in shipments unless production of concentrated ore is also increased. Additional plant facilities are already being provided.

These considerations are most significant and important, and will be referred to later.

Breaking down the 1942 shipments of concentrated ore, we have Table 3.

TABLE 3.—*Shipments of Concentrated Lake Superior Ore (U. S.) in 1942^a*

Method of Concentration	Gross Tons	Percentage of Total Concentrated Ore	Percentage of Total Shipments
Washing.....	15,469,163	86.2	16.6
Jigging.....	1,087,233	6.0	1.2
Heavy media.....	606,366 ^b	3.4	0.6
Total wet concentrates	17,162,762	95.6	18.4
Sintering.....	289,729	1.6	0.3
Drying.....	509,255	2.8	0.6
Total concentrates...	17,961,746	100.0	19.3

^a Data from Lake Superior Iron Ore Association.

^b Includes heavy-media tailing shipped as siliceous ore.

This shows that by far the most important method of concentration is still straight washing. Concentrate from heavy-media separation is increasing rapidly. This method of concentration was started in 1937 with a pilot plant, 7500 tons of concentrate was shipped in 1938, and the tonnage shipped each year is increasing

steadily. Jig concentrate has fallen off, however, from 1941 shipments.

LAKE SUPERIOR RESERVES

It is interesting to study the published figures of the ore reserves of the Lake Superior district. The latest available figures are as of May 1, 1941 (Table 4).

TABLE 4.—*Iron-ore Reserves of Lake Superior District, as of May 1, 1941**

Source	Direct Ore	Concentrates	Total
Open pit.....	592,425,000	117,520,000	709,945,000
Underground, Minnesota.....	429,975,000	56,264,000	486,239,000
Michigan, Wisconsin (mostly underground).....	141,325,000		141,325,000
Total.....	1,163,725,000	173,784,000	1,337,509,000

* Data from Mines Experiment Station.

NECESSITY FOR CONCENTRATING IRON ORE

The big stock piles of easily won ore, on which we are drawing so heavily at present, are the open-pit direct shipping ores. These can simply be loaded into cars and sent on their way. The present drain on this class of ore has necessitated the opening of many small pits, so as to have enough places in which to work. Many of these will be exhausted in two to five years, and then we will again be faced with the old problem of a herd of cattle eating its way toward the center of a haystack. There may be quite a lot of ore left, but it will be the remaining ore in a few large pits, and it will not be physically possible to get it out fast enough to maintain present rates of shipment.

Then we will have to turn to the underground ores. Ores in Michigan and Wisconsin are being produced at a rate of 15 to 17 million tons per year, and this rate cannot be increased materially. Some of the underground direct ore in Minnesota is being mined regularly, and production can be increased by operating additional mines. Underground mining, however, necessarily produces ore at a much slower rate than that at which open-pit ore can be loaded out. Also, underground ore is more costly

than open-pit ore, although cost is a secondary consideration under war conditions.

Tonnages of concentrate figured as reserve ore are based, of course, on present methods of concentration. If these methods can be improved to handle lower grade ores, reserves will increase at a tremendous rate.

It is easy to see from Table 4 that if the war continues five to six years, and shipment is at the 1943 rate of 100 million tons a year, the reserves of open-pit ore will be seriously depleted. We will also have bitten deeply into the reserves of underground and concentrating ore. True, we will probably be able to get through this war without too much trouble, even if it should last 10 years, but by that time we would pretty well have exhausted the open pits that are the present emergency stock piles. We ought to be wise enough to save some of this ore for future emergencies.

For all of these reasons the concentration of low-grade ores is assuming much more importance than ever before, and various companies have embarked on elaborate research programs, to develop method of treating ores of still lower grade.

CLASSES OF ORE

There are three general classes of ore on the Mesabi Range: direct shipping ore, wash and jig ore, and unaltered taconite.

Direct Shipping Ore

Direct shipping ore is the most important, commercially, at present, since the grade is satisfactory for blast-furnace feed,

and it needs no treatment other than possibly crushing to a limiting size. The reported tonnage of this class of ore on the

which preclude winter operation of wet concentrating plants. The buildings could be heated, but the wet concentrate cannot

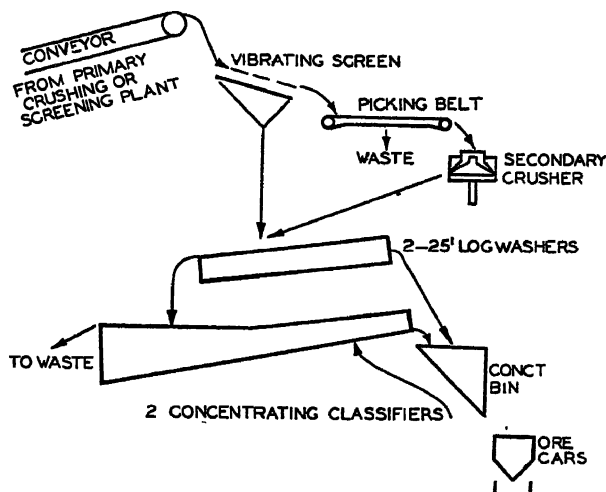


FIG. 1.—GENERALIZED FLOWSHEET FOR WASHING MESABI ORES.

Mesabi is a little under a billion tons, of both open-pit and underground ore.

Wash and Jig Ore

Wash and jig ore is the second class in importance, and is limited to ore that can be washed up to a satisfactory grade, or can be concentrated, by methods known and in satisfactory operation today. These methods include jigging, heavy-media separation, sintering and drying. The tonnage reserve for the Mesabi Range is reported as about 150,000 tons of concentrate, but a third of this is underground ore. It is usually considered not very feasible to treat this class of ore, because the already high mining cost must be multiplied by the ratio of concentration. This situation differs from the eastern magnetite practice, where underground ore is concentrated, or even from the growing practice of concentrating underground ore in the Birmingham district, in three important respects: (1) high royalty per ton in the Lake Superior district; (2) high rate of taxation; (3) climatic conditions,

which preclude winter operation of wet concentrating plants. The buildings could be heated, but the wet concentrate cannot

Unaltered Taconite

Unaltered taconite is the original formation of banded, ferruginous chert. Where it has been leached so that most of the silica has been dissolved and washed away, there are bodies of direct shipping ore. Where it has been partly leached, so that the silica has been more or less completely loosened from the particles of iron oxide, but has not been washed away, there are the wash ores; or, with less complete loosening of the silica particles, the jig ore, grading all the way to the hard unaltered taconite.

PRESENT METHODS OF CONCENTRATION

Washing

Fig. 1 shows a generalized flowsheet for straight washing of Mesabi ores. Usually there is a primary screening operation at about 6 in., the oversize going to the lean-

ore stock pile. This oversize consists principally of lumps of unaltered taconite, too low-grade to ship.

The undersize is conveyed to a vibrating screen, usually with openings of about $\frac{3}{4}$ in. up to 2 in. This screen is equipped with sprays to wash the oversize as clean as possible. This oversize may go direct to the shipping bin, may go direct to a secondary crusher, or may go to a picking belt for removal of waste. Frequently this hand-picking of waste (which goes to the lean-ore stock pile) cannot be shown to be a paying proposition, over a season. It does, however, help to keep down the silica when the shovel gets into banks of particularly lean ore.

The ore left on the picking belt may then go to the shipping bin, or may have to be crushed. If the latter, the vibrating screen usually has coarser openings, $1\frac{1}{4}$ to 2 in. The crusher is set to about $\frac{5}{8}$ in., more or less. The crusher product then joins the undersize from the vibrating screen and goes to a logwasher.

The coarse product from the logwasher goes to the shipping bin, being drained or rinsed on a vibrating screen at some plants. The logwasher overflow then goes to a classifier, the coarse product of which also goes to the shipping bin, while the overflow goes to waste. Formerly bowl classifiers were used for this step, but with the leaner wash ores now being encountered it was necessary to get a lower silica in the rake product, which is done by making a coarser classification, at 65 or 48 mesh, instead of 100 mesh. There has been some sacrifice of iron lost in the tailing, of course, but this is justified by the lower silica in the concentrate.

This typical flowsheet is varied to suit conditions at various plants. For instance, at many of the smaller plants, the picking belt, crusher, and logwasher are all omitted. The oversize from the vibrating screen goes direct to the shipping bin, and the undersize, sometimes as coarse as $1\frac{1}{2}$ -in. square

opening, goes direct to the classifier, these two being the only machines in the plant.

The vibrating screens are of several different kinds, each operator having his own preference. The secondary crushers are high-speed short heads, either Symons or Newhouse. The logwashers are 25 ft. long by 6 ft. wide, with two logs, and equipped with wash-water boxes underneath. They are made by several manufacturers. The classifiers are either Akins or Dorr, both specially built for this severe service, and equipped with wash boxes or underdeck sprays.

Typical metallurgical results of such a washing plant are given in Table 5. Such figures will vary with the grade and structure of the ore.

TABLE 5.—Results at Mesabi Range Washing Plant

	Fe, Per Cent	SiO ₂ , Per Cent	Loss on Ignition, Per Cent
Crude ore.....	45.42	28.61	
Concentrate.....	59.38	7.18	6.64
Tailing.....	15.00		
Weight recovery.....		69.4	
Iron unit recovery		90.7	
Moisture in concentrate....		7.97	

In Table 5 the iron analyses are given on the dry basis. After draining such as would be obtained in ore cars on the way to the docks, the concentrate contains 7.97 per cent moisture, hence the "natural iron" assay would be 54.65 per cent Fe, and the ore is sold on that basis. The reason is that a ton of this ore, as weighed and charged into the blast furnace, will contain 54.65 per cent Fe. This simplifies blast-furnace calculations.

Jigging

When the lean ore cannot be brought up to a satisfactory grade by straight washing, as described above, more elaborate treat-

ment is required. Many different methods have been tried but only two general methods have survived, of which jiggling is the older.

the jig feed. This is for the primary purpose of tightening up the bed, and secondarily to obtain greater recovery of the liberated particles of ore.

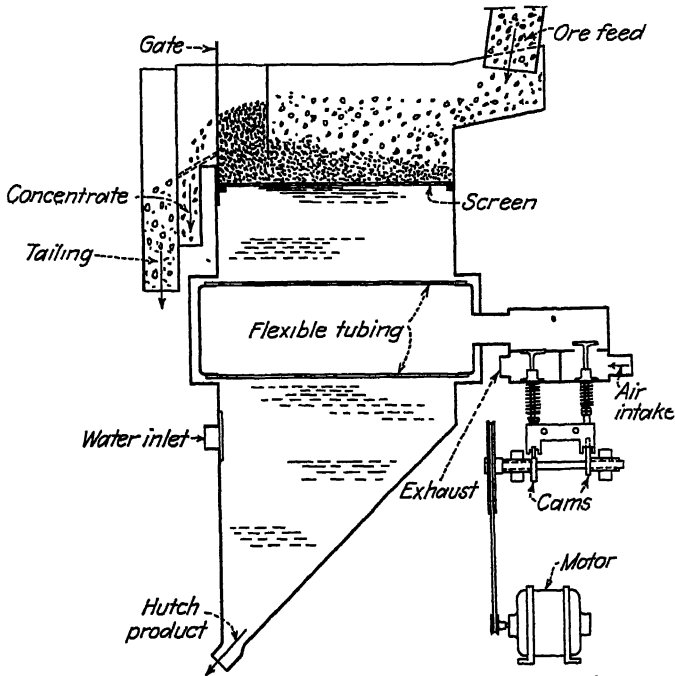


FIG. 2.—CONSET PNEUMATIC JIG.

There are certain broad requirements for jigs used on iron ore. In general, the concentrate product will be a very large percentage of the total feed, from one third to two thirds by weight. Standard types of jigs are not designed to meet this condition, since usually the heavy product is a much smaller proportion of the total feed. Therefore, standard types of jigs have had to be redesigned to meet iron-ore conditions.

In other types of work, jigs frequently are designed to treat a roughly sized feed, in two or more size ranges, usually delimited. Jigs of this type were the first ones tried on iron ore, and some are still in use, although their days appear to be numbered. In general, for iron-ore work, unsized feed has given better results, even to the extent of regrinding and returning middling to

Four general types of jigs are in use:

Harz-type Plunger Jigs.—An installation of McLanahan-Stone jigs is still in operation, the feed being prepared in two different sizes and going to two different batteries of jigs with appropriate stroke adjustments. This installation will be replaced before long, probably by a heavy-media sink-and-float installation.

Movable-sieve Jigs.—There is an installation of hancock jigs operating. Customarily the Hancock discharges its concentrate through the sieve, there being a ragging on the bed in most cases. For iron-ore work, long, controllable slots transversely across the bed have been provided, to discharge a greater tonnage of coarser material. Middlings are recrushed

and returned to the feed, to give a tight bed.

Movable-diaphragm Jigs.—Both Bendelari and Wood jigs have been used, where the plunger or diaphragm is directly under

at will. For instance, a sharp expansion of the tube with a slow collapse is readily obtained, and gives an excellent result, from which the jig derives its name, "Conset," meaning "constant settling."

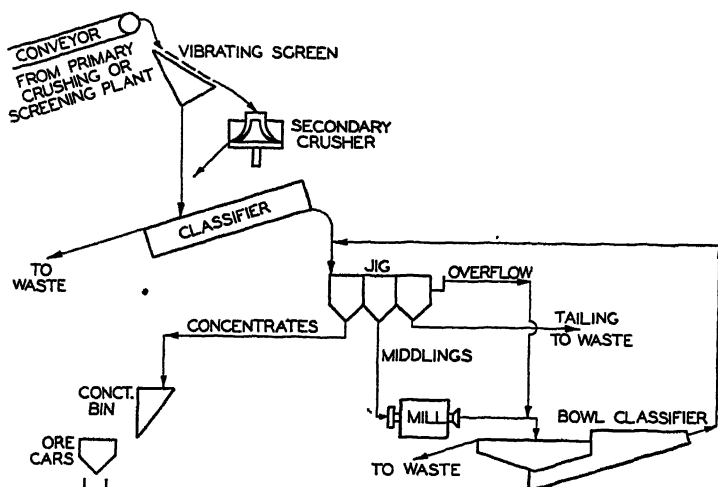


FIG. 3.—TYPICAL SIMPLIFIED FLOWSHEET OF CURRENT PRACTICE IN JIGGING MESABI IRON ORES.

the sieve and of substantially the same area. Results have been excellent in some cases. Redesign of the concentrate draw-off for iron-ore work has been found advantageous.

Air-operated Jigs.—The Baum type jig, where compressed air operates direct as the plunger, has not found its way into the iron-ore field. This type of jig is used extensively in coal preparation, but some of the inherent characteristics of this unit do not appear well suited for iron ore.

However, an air-operated jig has been designed for iron ore, and has given excellent results. In this machine a large rubber tube, something like an inner tube of a tire, is placed directly under each sieve of the multicompartiment jig. By means of a poppet-valve mechanism, air is alternately admitted to and withdrawn from this tube. The valve mechanism being motor-driven, by means of cams of varying shape, the number and length of stroke, and the characteristics of the stroke can be varied

Fig. 2 gives a conventionalized view of the mechanism of the Conset jig. Fig. 3 gives a typical flowsheet, with regrinding of the middling for maximum recovery. Table 6 gives some typical results.

TABLE 6.—Jigging Results on Mesabi Range

	Iron	SiO ₂ *	H ₂ O
Crude ore.....	40.00	37.50-39.50	7.30
Concentrate.....	57.50	12.00-14.00	5.00
Tailing.....	24.00	61.00-63.00	
Weight recovery....		48.00	
Iron-unit recovery...		69.00	

* Variations in silica analysis are caused by the varying hematite-limonite ratios in the ore.

Heavy-media Separation

The heavy-media process, which previously had been applied to zinc ore at Mascot, Tenn., was first introduced on the Cuyuna Range in 1937. Galena was used as a medium, but had many disadvantages. Since the treatment of the iron ore was a

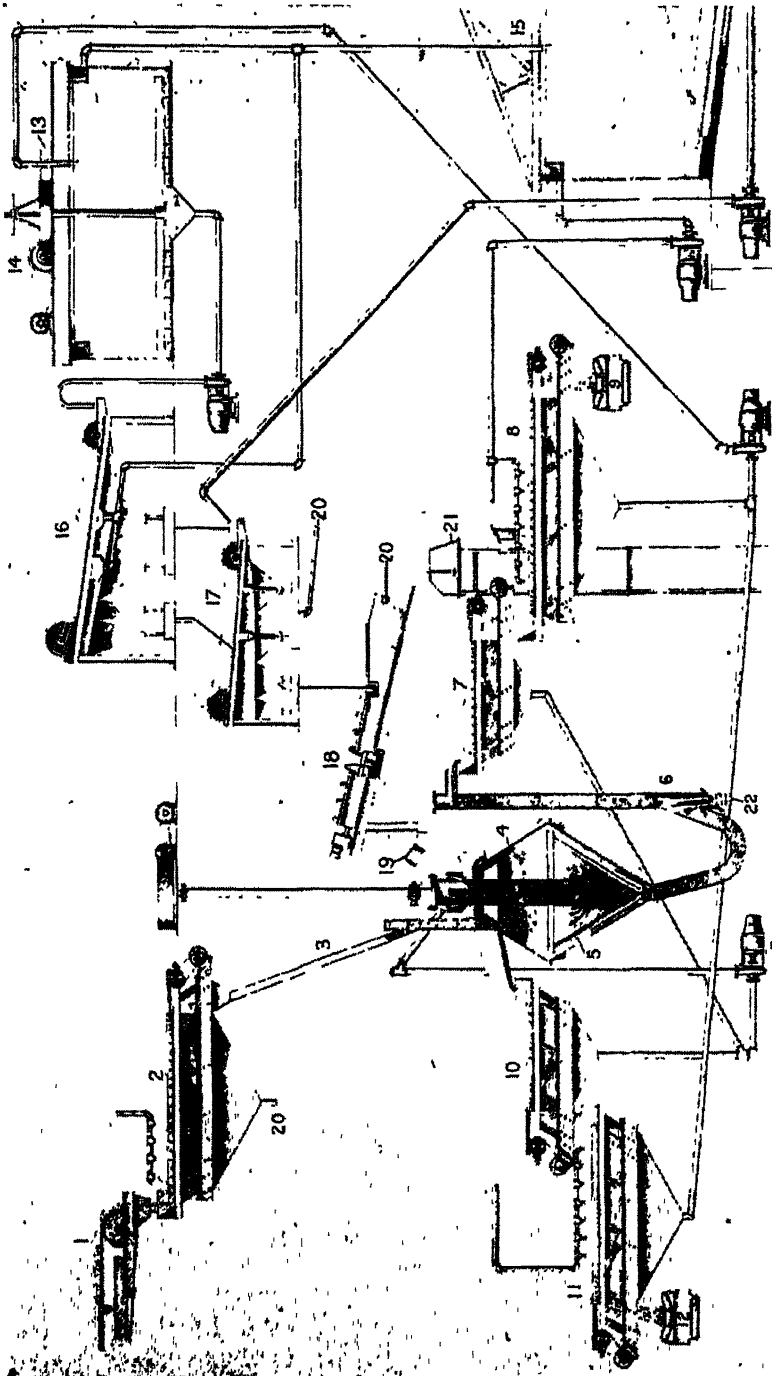


FIG. 4.—FLOWSHEET OF SINK-AND-FLOAT PLANT USING FERROSILICON.

- | | | |
|--------------------------------------|------------------------------------|--|
| 1. Crushed ore, washed and screened. | 12. Cone tailings. | 18. Reclaimed-medium supply. |
| 2. Rinsing and drainage screen. | 13. Magnetizer. | 19. Demagnetizer. |
| 3. Sized washed feed. | 14. Thickener. | 20. To jig plant or double classification. |
| 4. Cone separator. | 15. Clarification tank. | 21. Clear-up and new-medium elevator. |
| 5. Agitator. | 16. Roughing magnetic separator. | 22. High-pressure air |
| | 17. Scavenging magnetic separator. | |

one-pass proposition producing a finished concentrate and a final tailing, it became particularly important to clean the medium thoroughly. With a galena medium, this was complicated and costly, and required operations quite foreign to customary practice in the district. Degradation of particle size of the medium was serious, and caused trouble from viscosity.

The use of ferrosilicon as a medium was an outstanding development in the Lake Superior district. Cleaning is easy, and uses machines customary in the iron-ore industry. Ferrosilicon is hard and resists abrasion. Loss of medium is satisfactorily low, and contamination of the concentrate by the medium is not harmful. The desired high gravities, 3.20 to 3.40, can be obtained without difficulty. Therefore ferrosilicon is the only medium at present being used in the treatment of iron ore by heavy-media separation.

Fig. 4 gives a flowsheet of a typical plant. The crude ore is screened at $\frac{1}{4}$ in., de-watered, by using a longer, or a separate screen, and fed to the heavy-media cone. The gravity in the cone being between 3.20 and 3.40, as required for the ore being treated, tailing lighter than this gravity overflows the cone, while heavier pieces sink to the bottom, and are elevated by an air lift. Both tailing and concentrate go to (separate) drainage screens, the medium that drains off being returned direct to the cone. The products are then washed by sprays on washing screens, and discharged as clean products, to their respective destinations, tailing pile or shipping bin.

The medium washed from the two products is combined, magnetized to make the ferrosilicon particles stick together and sink more rapidly, and thickened in a special heavy-duty thickener. The overflow goes to a second thickener, to trap any escaping ferrosilicon, while the underflow goes to a magnetic separator. Two of these machines are used in series, to reject the fine particles of ore abraded off in the heavy-media cone

and in screening. If left in the medium, these particles, being lighter in gravity than ferrosilicon, would gradually contaminate the medium, and it would no longer be possible to maintain the desired gravities in the cone.

The concentrate of the magnetic separator goes to a densifier, a spiral screw, where the gravity of the mixture of ferrosilicon is brought up to about 3.80, higher than required in the cone, and thus the cone gravity is kept under control. The medium is demagnetized just before entering the cone, so that it will maintain a more uniform suspension.

Table 7 gives some typical results of this method of concentration. In this particular set of figures, the ore was first washed, to eliminate the slimes and fines under 100 mesh, then screened at $\frac{1}{4}$ in., the oversize going to heavy-media separation, the undersize to jigging. Latest practice is to treat the minus $\frac{1}{4}$ -in. material by double classification, which will be described later.

TABLE 7.—*Heavy-media Separation, with Jigging of Minus $\frac{1}{4}$ -inch*

	Heavy-media — $\frac{1}{4}$ + $\frac{1}{4}$		Jigging Minus $\frac{1}{4}$ -inch	
	Fe	SiO ₂	Fe	SiO ₂
Crude ore after washing and screen.....	53.18	18.32	51.49	19.72
Concentrate.....	59.88	8.76	56.29	13.05
Tailing.....	33.73	46.11	46.63	26.55
Weight recovery.....	74.4		50.5	
Iron-unit recovery.....	83.8		55.1	
Proportion of total concentrate produced.....	56.6		43.4	
Over-all weight recovery from unwashed crude ore	40.0			

Double Classification

Jigging of the minus $\frac{1}{4}$ -in. fraction of the ore is difficult, requires close operating attention, and is costly. This has been replaced in present practice by a system of double classification, which, while it gives

about the same metallurgical results as jigging, is simpler and less costly.

The minus $\frac{1}{4}$ -in. material is first classified, at a mesh varying from 100 up to 48, depending on the ore, the tailing of this step being rejected. The concentrate of this operation is then reclassified at a considerably coarser mesh of classification, and a final concentrate is made, of a grade about corresponding to the grade of the jig concentrate. The overflow of this second classification step is then screened on vibrating screens, to get the coarse particles of silica out of the circuit, these being rejected as tailing. Screening is carried out at 48 to 28 mesh, again depending on the ore. The screen undersize is returned to the primary classifier, establishing a rather large circulating load.

This second step of classification is not true classification at all, but rather a crude concentration step wherein the slightly heavier product is taken as a concentrate and the slightly lighter product, after screening, is recirculated. This method of separation gives rather poor metallurgical results, but is the best method available at the present time. Intensive work is under way to improve this method of treatment.

This minus $\frac{1}{4}$ -in. material cannot be treated economically by heavy-media separation, because the fine particles are trapped by the viscosity of the mixture in the cone and will not quickly separate into concentrate and tailing at the high tonnage rates being handled in the cone. A $7\frac{1}{2}$ -ft. diameter cone treats about 150 long tons of feed per hour. Material has been successfully treated down to 10 mesh, but so far anything finer than this has not been found commercially practicable. The commercial limit of size treated seems to be about $\frac{1}{4}$ in., possibly $\frac{3}{16}$ in., at the tonnage rates required in iron-ore operations. Since recoveries must be made in even finer sizes than 10 mesh, it appears more sensible to limit cone treatment to plus $\frac{1}{4}$ -in. material.

Tailing Re-treatment

Tailing retreatment divides itself into two parts: (1) re-treatment of material accumulated in tailing ponds; (2) treatment of material being currently sent to these tailing ponds.

Re-treatment of Tailing-pond Material.—

The only tailing treatment that is being carried out commercially today is re-treatment of tailing-pond material. When tailing is discharged into the ground from the tailing pipe or flume, a natural segregation immediately begins to take place. The heavier and coarser particles settle out first, fairly close to the point of discharge. The lighter and finer, and consequently the leaner, particles, flow farther from this point. The slimes and water flow farthest of all, of course, and where the tailing area is impounded the more or less clarified water is customarily recovered for re-use.

It is usually possible to re-treat, at a profit, the material that has settled out closest to the point where the tailing was initially discharged onto the ground, and certain such areas have been and are being reworked. Current discharge of tailing having been discontinued or transferred to another point and the enriched portion of the tailing being fairly dry it is mined by conventional methods and trucked or conveyed to the treatment plant. Following a trash screen, double classification as described above, is the usual method of treatment today.

Treatment of Current Concentrating-plant Tailing.—

Treatment of current concentrating-plant tailing has long been a matter of academic interest, and now is receiving intensive study. Certain basic principles are obvious. The iron values are free, in the relatively fine washing-plant tailing. This is not true, of course, of efficiently jigged or heavy-media tailing. The washing-plant tailing, however, will require no grinding. The large volume of water in the tailing must be brought under control. The slimes and paint rock contain no recoverable iron

particles and therefore should be discarded, as far as possible prior to concentration. This can be done by suitable hydroseparation.

Some commercial method of treatment of the coarse product from this hydroseparation step remains to be found. Various operations have been tried. Mechanical classification, hydraulic classification, possibly followed by tabling, and flotation, all have their advantages and disadvantages.

Treatment of the coarser tailing, from jig and heavy-media separation plants, and also of the lean ore removed by grizzlies or screens at the head of most plants, and including the large stock piles of such lean ore, require quite a different method of treatment. Further crushing and frequently fine grinding, will be required, and methods of treatment will be along parallel lines to those required for unaltered taconite.

Sintering

Sintering of fine ore and fine concentrate, at blast-furnace plants, is becoming more and more the accepted practice. Fine concentrate is often shipped separately. Merch ore is frequently screened at the blast-furnace plant, and the coarser feed to the blast furnaces increases their production.

The fine concentrate and the screened fines from the ore are then mixed with the dry and wet flue dust and sintered. The sinter, added to the coarser part of the ore, still further increases blast-furnace capacity.

Sintering at the blast-furnace plant works out very well, economically. The dry flue dust contains an excess of carbon, which therefore is provided in part, at no cost, to the fine ore, fine concentrate, or wet flue dust. Coke braize, for the additional carbon, is available as a by-product from the coke plant. Blast-furnace gas for ignition on the sintering machine is available.

At the head of the lakes, however, sintering is considerably more expensive. Carbon in the form of coke braize or anthracite culm must be shipped to the head of the lakes, unloaded, and transported to the sintering plant. Gas is not available for fuel, and oil must be used. This in turn must be transported long distances.

Sintering at the head of the lakes, therefore, only works out in certain cases. There are two main applications:

1. Where the concentrate produced is so uniformly and extremely fine that it cannot be transported without agglomeration, as when unaltered taconite is treated. Such an operation would be purely for the improvement of physical structure.

2. Where the ore is limonitic, containing water of crystallization in such amounts that its removal will raise the iron analysis of the ore to an acceptable grade. This operation is really a form of concentration.

Operations of the Mesabi Iron Co. at Babbitt furnished an example of the first case, but no such operation is being carried out at the head of the lakes at the present time.

The only sintering operation being carried on in the Lake Superior district at present is on the Cuyuna Range, where limonitic ores are being agglomerated. Typical results of such treatment are given

TABLE 9.—*Typical Results of Agglomeration of Limonitic Ores*

	Before Sintering	After Sintering
Iron analysis, per cent.....	41.59	55.62
Phosphorus analysis, per cent....	0.221	0.297
Manganese analysis, per cent....	1.95	2.92
Silica analysis, per cent.....	7.67	11.07
Loss on ignition, per cent.....	9.21	2.56*
Free moisture, per cent.....	18.80	1.01
Weight recovery.....		72.9

* Gain on ignition.

in Table 9. The analyses of other elements, besides iron, naturally increase also, when free and combined H_2O is removed, and the

silica analysis of the ore as mined must be low enough to make an acceptable sinter.

Drying

Sometimes ores contain considerable free moisture, and by the removal of a part of this moisture, without any attempt to remove combined moisture, the ore can be brought up to an acceptable grade. One such drying plant is in use on the Cuyuna Range. Only partial drying is feasible, of course, since enough moisture must be left in the ore to avoid excessive dusting in handling.

TREATMENT OF UNALTERED TACONITE

The Mesabi Iron Co. at Babbitt, years ago, treated unaltered magnetic taconite by fine grinding and magnetic concentration, followed by sintering. The problem of treating taconites has been studied over a period of years, and research is becoming much more intensive at the present time.

By far the bulk of the tonnage of potential reserves on the Mesabi Range consists of these unaltered taconites. This is a local name for banded ferruginous cherts, with alternate bands of varying width, of rather high-grade material, running 40 to 55 per cent or more in iron, and lower-grade material, running 8 to 15 per cent iron. These bands are reasonably sharp in gradation, but there are no pronounced and dependable cleavages between high-grade and low-grade bands. Thin sections, in general, show a gradual increase in iron oxide particles within a short distance, rather than the presence or absence of such iron oxide.

There are probably 40 billion, possibly 60 billion tons of such taconite, running on the average 25 to 35 per cent metallic iron. This taconite falls basically into two kinds; one where the iron is present in magnetic form as Fe_3O_4 , the other where it is nonmagnetic, as Fe_2O_3 or variations thereof, or carbonate. On the eastern end of the range, where the metamorphic effect

of the Duluth gabbro flow was more pronounced, the taconite is usually in the magnetic state. Toward the west, the nonmagnetic form predominates, with, of course, some intermingling of the two.

Of 40 billion tons of taconite, perhaps 5 to 10 billion tons is naturally in a magnetic condition. Such taconite offers no great problem in concentration. It must be ground to approximately 150 mesh, and concentrated by magnetic concentration. The final ratio of concentration will be about 2.5:1, or a 40 per cent weight recovery. With proper arrangement of the flowsheet, perhaps one third of the crude tonnage can be rejected, by magnetic separators, ahead of the grinding circuit, thus reducing the tonnage requiring fine grinding. Sintering (or other agglomeration) of the finely ground concentrate seems to be necessary. The entire problem becomes one of the cost of the material ready for shipment, although when the cheaper, higher-grade ores are pretty well exhausted cost will become a less important factor.

The nonmagnetic taconites offer a more involved problem. They need not, in general, be ground quite so fine, 100 mesh being generally fine enough, as against 150 mesh for the magnetic taconites farther east.

Two principal methods of attack are available. The taconite can be given a magnetic roast, and then concentrated magnetically, or flotation may be used. Either the silica or the iron oxide could be floated.

The magnetic roasting method was tried for several years in a pilot plant treating 10 tons per hour, and results obtained have been previously published.* In that test, jig tailing was being treated, and although this had a higher iron content than taconite, the principles involved were the same. The magnetic roast was carried out in a shaft furnace, developed at The Mines

* T. B. Counselman: Developments in the Concentrating of Minnesota Iron Ores. *Trans. A.I.M.E.* (1943) 153.

Experiment Station, University of Minnesota. Magnetic concentration was by conventional methods, which since then have been improved.

There are certain definite objections to this method of treatment. A reducing atmosphere is essential for a reducing roast. This can be obtained by: (1) natural gas, which must be cracked; (2) producer gas (or other artificial gas); (3) cracking oil to make a reducing gas.

There is no natural gas now available on the Mesabi Range. Producer gas can be made, but it is a rather expensive operation to make small quantities at each property. No coke oven or blast-furnace gas is available.

Cracking oil to produce gas is rather an expensive way of solving the problem. That actually was done for four years of the life of the pilot plant referred to above. During the fifth, and last, year, a producer-gas installation was made at the plant, and this, of course, introduced all the attendant problems of cleaning the gas, and so forth.

The magnetic roasting furnace required cooling water, and this resulted in the production of superheated steam. These heat units could be recovered only in a boiler plant, and such a boiler plant was not feasible at each operation.

Flotation, on the other hand, also has its problems. The requirement is a concentrate carrying less than 12 per cent silica. First attempts at flotation were to float the iron oxide. The material used as feed was washing-plant tailing, but the problem was about the same as with taconite.

After considerable experience had been acquired, and experiments made with a variety of reagents, it was not too difficult to float the iron oxide, with a fair iron-unit recovery, and a fair tailing. The iron analysis of the concentrate was fairly good, but the silica always ran 14 to 16 per cent, rather than 12 per cent or less. This condition still obtains, and so far as known at this writing, it has not proved possible

consistently to obtain a concentrate running 12 per cent or less in silica.

Lately tests have been made with the objective of floating the silica and depressing the iron oxide. No results of this work have been published to date, and details are being kept very secret.

Investigation of flotation methods of concentration are being actively carried on by several of the operating companies.

Possible treatment of the wall-rock and lower-grade ore bodies of the Michigan and Wisconsin Ranges is being given consideration. Off-grade ores from this area have been treated in the past, though no such operations are going on at present.

Heavy-media methods or jigging operations are indicated, since the ores are hard, and quite unlike the soft, easily washed, ores of the Mesabi Range. (Cuyuna ores, while soft, are not true wash ores, since the values persist pretty much through the complete size range.)

Very little research work on the Michigan and Wisconsin low-grade ores has been carried on to date, but this will have to be intensified shortly. As shown in Table 4, at the present production rate of 15 to 17 million tons a year, the Michigan reserves do not have too long a life ahead of them.

EASTERN MAGNETITES

In the states of New York, New Jersey, and Pennsylvania are important deposits of magnetite. These deposits are pretty well scattered, rather than lying in the characteristic "ranges" of the Lake Superior district. Some of these deposits carry important tonnage of titanium, copper, or other valuable constituents. Practically all require concentration, although some deposits contain lump ore, used as charge ore in open hearths, and many of the properties are concentrating on its production.

Probable ore reserves of this general area are estimated at from $\frac{1}{2}$ to $\frac{3}{4}$ billion tons of crude ore. The grade varies widely, from

27 to 60 per cent Fe or more, with a probable average of 45 to 50 per cent Fe.

Except for the charge, or lump, ore, these crude magnetites require concentration, to make them suitable for blast-furnace feed.

During 1942, total shipments from the eastern magnetite district amounted to about 3,200,000 long tons, and for 1943 the projected rate of production is double this amount.

TABLE 10.—*Iron-ore Enterprises in the Adirondacks**

Property	Operating Company	Ratio Ore Mined to Sinter Shipped	Iron in Sinter, Per Cent	Sinter to Be Shipped, Long Tons, per Year
Mineville (Witherbee Sherman).....	Republic Steel Corp.	1:7:1	66	775,000 ^b
Fisher Hill.....	Republic Steel Corp.	2:5:1	68	1,000,000
Lyon Mountain (Chateaugay).....	Republic Steel Corp.	3:1	68	400,000
Clifton mines.....	M. A. Hanna Co.	1:5:1	65	375,000
Benson mines.....	Jones and Laughlin Steel Corp.	3:1	64	1,000,000
MacIntyre mines.....	National Lead Co.	3:1	60	450,000 ^c

* From *Mining and Metallurgy* (October 1942).

^b Includes 150,000 tons lump ore at 60 to 62 per cent Fe.

^c In addition to 250,000 tons ilmenite concentrate at 48 per cent TiO₂.

Also, despite the fact that a fairly coarse grind, varying from 14 to 65 mesh, is sufficient to liberate the mineral, some form of agglomeration, usually sintering, is required.

Since the iron occurs in magnetic form, concentration is relatively simple and recoveries are high. For many years dry concentration was practiced at certain of the properties, with the attendant dust troubles, and the dry concentrate was undesirably high in phosphorus. These dry plants have now been replaced by wet plants, eliminating the dust nuisance, and producing concentrate with a considerably lower phosphorus content.

Better recoveries and lower silicas are obtained with wet concentration. All of the new plants now being built are wet plants.

The ratio of concentration varies from 1:2 or 1:3:1 up to 3:1, but because of the efficiency of magnetic concentration, the iron-unit recovery is high, about 90 per cent. The grade of concentrate is also high, 60 per cent to 68 or 69 per cent Fe, and at the higher analyses the silica is very low, 2 or 3 per cent and, with a low phosphorus, 0.030 per cent or under, this becomes a very desirable sinter.

Several new properties will come into production during 1943. These include Fisher Hill, Benson mines, Clifton mines and MacIntyre in New York state, and the Ringwood group of mines and the new McKinley ore body at Oxford, New Jersey.

While these are known as magnetite mines, at certain properties, such as Benson mines and Clifton mines, there is an important tonnage of nonmagnetic iron oxides, in parts of the deposits, which will have to be concentrated by gravity methods. Also, MacIntyre mines produce a substantial tonnage of ilmenite concentrate, and at Lebanon a copper concentrate is also produced.

Iron-ore enterprises in the Adirondack region are listed in Table 10.

Many of these eastern magnetite operations involve underground mining, and it is interesting to note that underground concentrating ore can compete successfully with direct shipping open-pit ore from Minnesota. There are several reasons why this is true:

1. Eastern magnetite ores do not have to carry nearly as heavy taxes as do Minnesota (or even Michigan) ores.

2. Eastern magnetite ores do not have to carry the heavy royalties to the fee owners imposed on Minnesota or Michigan ores.

is very low, in some cases phenomenally low.

7. The high-grade lumps, or sinter

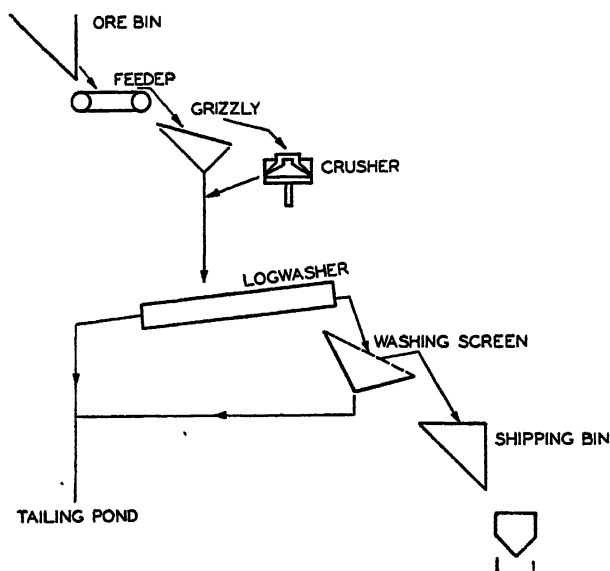


FIG. 5.—TYPICAL FLOWSHEET OF BROWN-ORE WASHER.

3. Uniform all-year rail transportation to Buffalo, Bethlehem, Cleveland, and Pittsburgh is possible in contrast to seasonal water transportation of Lake Superior ores. This reduces the size, and fixed charges, of treatment plants to produce a desired annual tonnage.

4. Because of the high iron content of eastern magnetite sinter and its negligible moisture content, a ton of this sinter is equivalent to nearly $1\frac{1}{2}$ tons of Lake Superior ores. For this reason the all-rail freight rates on eastern magnetite sinters are in many instances actually less, *per unit of iron*, than the combined rail and lake rates on Lake Superior ores.

5. The sinter is an ideal constituent of blast-furnace feed. In fact, the silica is so low that certain concentrates from this district may even be suitable for sponge iron processes.

6. The phosphorus in eastern magnetite sinters, when concentrated by wet methods

produced in such a way as to be hard and dense, is suitable for highly desirable charge ore.

8. It is the combination of all these advantages that makes commercially feasible the concentration of underground ores with such ratios as are shown in Table 10. It is primarily the radical reduction in phosphorus in the concentrate by modern wet methods of concentration that has led to renewed activity in this district, the opening of several new properties, and exploration for others.

BIRMINGHAM DISTRICT

Next to the Lake Superior district, the Birmingham district is the most important iron-ore-producing area in the country.

In general, there are two classes of ore—the brown ores and the red ores. The brown ores are limonitic, containing little if any lime. They occur in relatively small deposits, are mined by open-pit methods.

and nearly always must be concentrated. The red ores are oölitic, occur in flatly pitching veins and in general are mined by underground methods. Red ores are

Brown Ore

Most of the brown ore, probably 90 per cent, is concentrated. Standard practice involves a grizzly, a screen or trommel, and

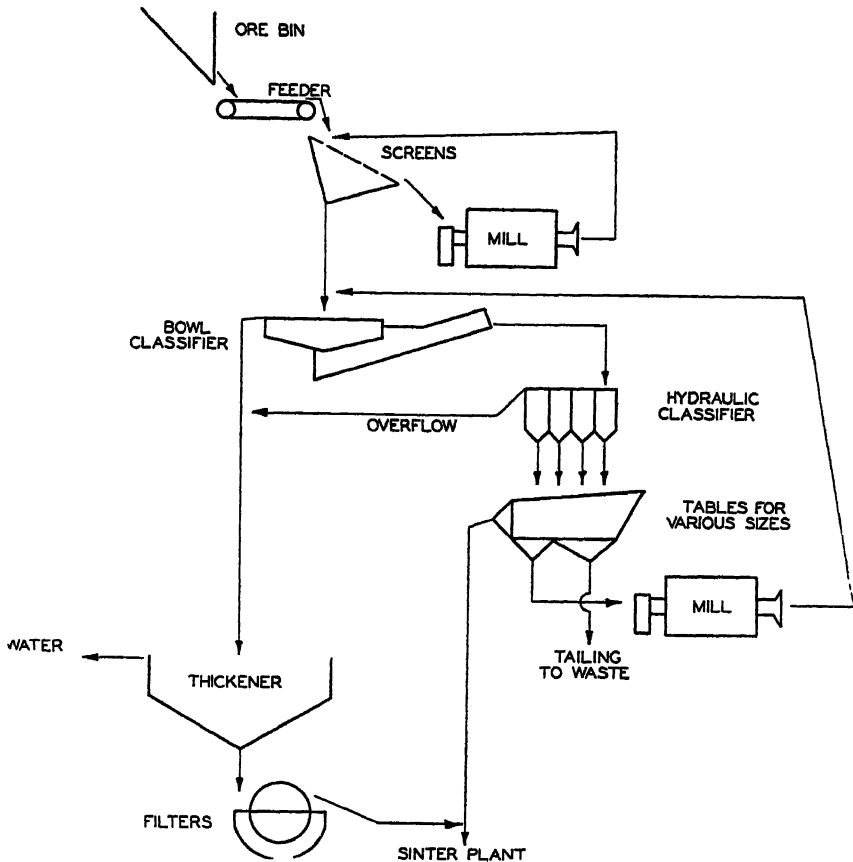


FIG. 6.—FLOWSHEET FOR CONCENTRATION OF RED ORE.

high in phosphorus and carry considerable lime, so that, while somewhat low in iron, they are self-fluxing. Most of the red ore mined to date has been direct shipping, but concentration of lower grade red ores, which has only recently been started, is becoming more important.

The relative importance of brown and red ores is shown by the shipments from Alabama in 1942, as follows: brown ore, 1,250,000 long tons; red ore, 8,250,000 long tons. Shipments scheduled for 1943 show slight increases for both kinds of ore.

logwashers. Jigs are used only to a limited extent, and then to recover fine ore from the tailing. The plants usually are temporary, easily moved, as each particular deposit is exhausted.

A typical flowsheet of a washing plant for brown ore is shown in Fig. 5. This does not represent any particular plant, and shows the best practice. Many small plants have less equipment than this requires, sometimes only a grizzly and a logwasher.

The tonnage of ore handled in brown-ore washers varies between extremely wide

limits, and no reliable data can be obtained as to the ratio of concentration or the iron content of the tailing. A typical analysis of brown-ore washed concentrate is as follows: iron, 45 to 51 per cent; insoluble, 18 to 10; CaO, none; manganese, 0.05 to 2.0; phosphorus, 0.2 to 1.0.

Red Ore

The bulk of the tonnage of red ore is direct shipping. Of the red ore mined in 1942, only about 300,000 tons was concentrated. In 1943 it is expected that about 800,000 tons of ore will be concentrated, from which will be produced about 480,000 tons of concentrate.

Toward the western end of Red Mountain, the red ore begins to fall off in grade. The lime-silica ratio decreases until the ore is no longer self-fluxing; it cannot be used direct in blast furnaces, and must be concentrated to be usable. Experimental work on the concentration of this ore was in progress over a number of years; a large-scale pilot plant was operated for some time, and now a full-scale plant treating some 2500 tons per day is in operation. A flowsheet of this operation is shown in Fig. 6.

The principle of concentration is, first of all, to save all the slimes. They contain the lime. Then the oolitic grains must be lightly ground, so as to crack off the conchoidal layers of iron oxide, without crushing the grain of sand at the center. These conchoidal layers having been cracked loose, the coarser material is then tabled, thus rejecting the silica grains. The table concentrate is then recombined with the thickened and filtered slimes, and sintered.

Table 11 shows typical results of concentration of red ore. Such results can be expected in 1943, and from further concentrating operations on red ore of this grade.

It is obvious that as time goes on it will be necessary to concentrate a larger and

larger tonnage of red ore. This has been the history of the great Mesabi Range, and there is no reason to hope that the deposits of Red Mountain will fare any differently. The probable tonnages for 1943 indicate that 5 to 6 per cent of the red ore moving to blast furnaces will be concentrate. In 1942, concentrate shipped from Minnesota was 24 per cent of total shipments, and since 1911 concentrates have been well over 6 per cent of total shipments from Minnesota.

TABLE 11.—*Typical Results of
Concentration of Red Ore
PER CENT*

	Fe	Insol- uble	CaO	P
Crude ore.....	34.5	29.0	10.0	0.35
Concentrate.....	47.5	14.0	7.5	0.36
Tailing.....	15.0	51.0	13.5	0.33
Weight recovery....		60.0		
Iron-unit recovery....		82.5		

Minnesota concentrates, as well as eastern magnetite concentrates, have had no difficulty in competing with direct shipping ores from the Lake Superior district. By the same token, red-ore concentrates should be able to compete with direct shipping red ores, and therefore with ores from other districts. Red-ore concentrate, for example, is sintered; therefore it has certain definite advantages over natural ores. True, some of the fine red ore is also sintered—nearly 1,500,000 tons of sinter was produced in Birmingham in 1942, from red-ore fines and red-ore concentrate. However, the same is true of Lake Superior ores, the finer portion of the ore being screened out and sintered at certain blast-furnace plants.

It will be found necessary in Alabama, as it is being found necessary in Minnesota, to concentrate the lower-grade ores in order to lengthen the life of the ore reserves.

The Selection of Blast-furnace Refractories

By HOBART M. KRANER,* MEMBER A.I.M.E., AND E. B. SNYDER†

(Chicago Meeting, October 1943)

THIS paper shows that volume stability, low porosity and decreased pyroplasticity are desirable for blast-furnace linings, particularly for the hearth. It shows further that a hot load test is a valuable means of testing the fusion or softening behavior of a refractory at operating temperatures. The effect of carbon monoxide on commercial blast-furnace refractories in their as-received condition and after refiring is reported, showing that many commercial blast-furnace refractories disintegrate badly but that refiring decreases the effect and certain special refractories are now available which are almost free of the tendency.

FACTORS AFFECTING CHOICE OF REFRACTORIES

If one were to depend entirely upon experience or trial in the selection of clay refractories, the solution of a problem would be a slow process. Furnace campaigns are so long and attended by so many variables that it is difficult to draw fine distinctions within a reasonable period of time in regard to the quality of refractories used. It could be said, of course, that if service results do not yield the proper information for intelligent choice, there is no difference in the quality of brick being considered, but this is not necessarily true.

Conventional ceramic tests are designed to give the ceramic engineer information

as to the refractoriness and firing temperature, which he in turn interprets in terms of volume stability, ability to withstand load at high temperature (pyroplasticity), permeability, chemical stability and resistance to the action of slag. In most refractory applications several of these factors are involved. In a particular instance, one requirement may be predominant, while in others some other factors may be of primary importance.

In this country, clay refractories are generally made from mixtures of plastic and flint fire clays. The process of firing a clay refractory is one of slowly melting the constituents, and during this operation its porosity is gradually reduced. The process is arrested, of course, in its incipient stages and the progress is determined by measuring slight changes in porosity, volume, bulk gravity, etc., that have taken place. Often the temperatures to which clay refractories are exposed in service are higher than those employed in their firing. However, if the manufacturer were to fire them at such high temperatures the brick would distort. Therefore it would be difficult for the manufacturer to fire all of his clay refractories to temperatures at which they are to be used, although in many cases it would be desirable from the user's point of view if he would do so. The porosity of clay refractories decreases by firing, to a minimum limit, after which a further increase in the temperature causes expansion in certain clay constituents and bloating in others. Both may occur in the same refractory containing two such clays.

Manuscript received at the office of the Institute Oct. 25, 1943. Issued as T.P. 1727 in METALS TECHNOLOGY, April 1944.

* Ceramic Engineer, Bethlehem Steel Co., Bethlehem, Pa.

† Bethlehem Steel Co., Bethlehem, Pa.

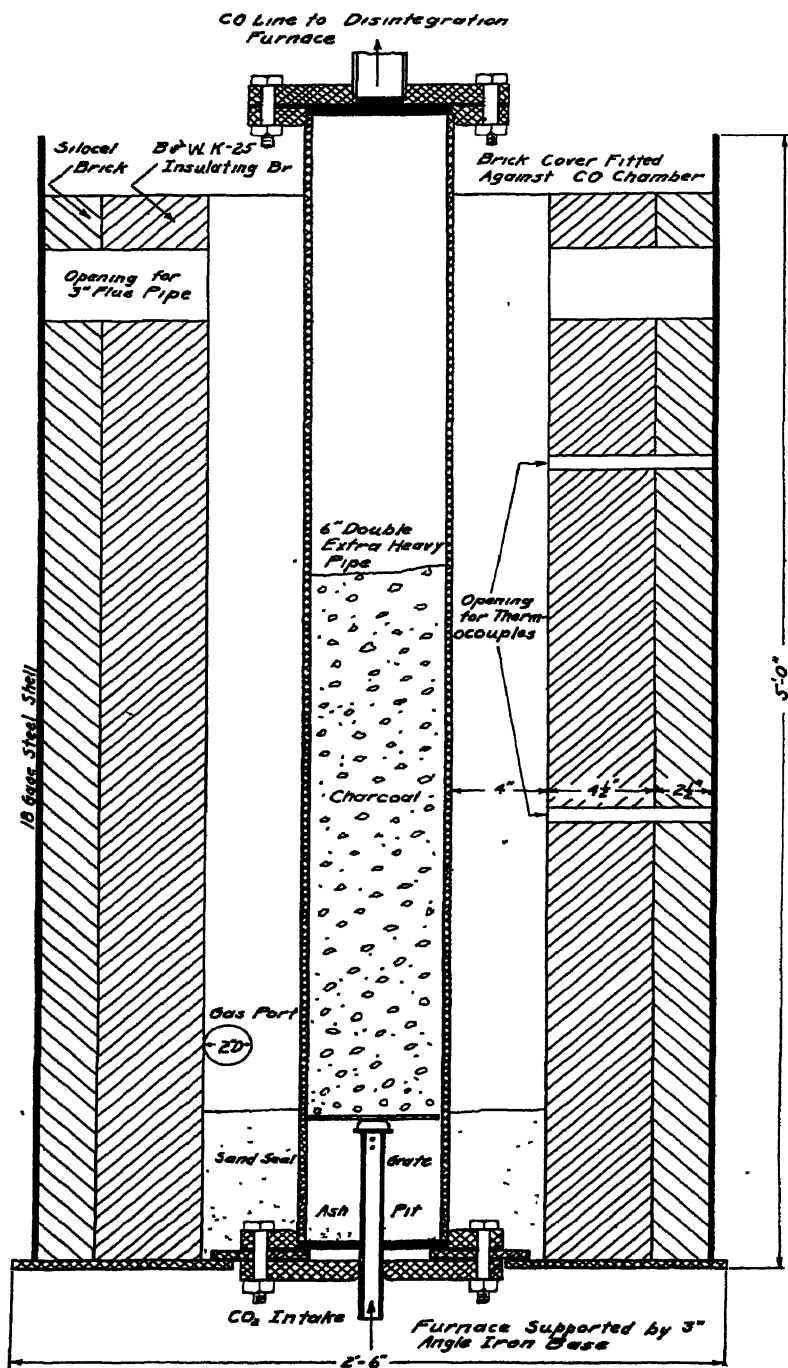


FIG. 1.—CO PRODUCER FURNACE.

REQUIREMENTS FOR VARIOUS APPLICATIONS

Volume stability through the temperature range in which a refractory is used

limits of utility, it is extremely illuminating in making careful studies to determine the reasons for the small variations in quality. The conventional hot load test terminates

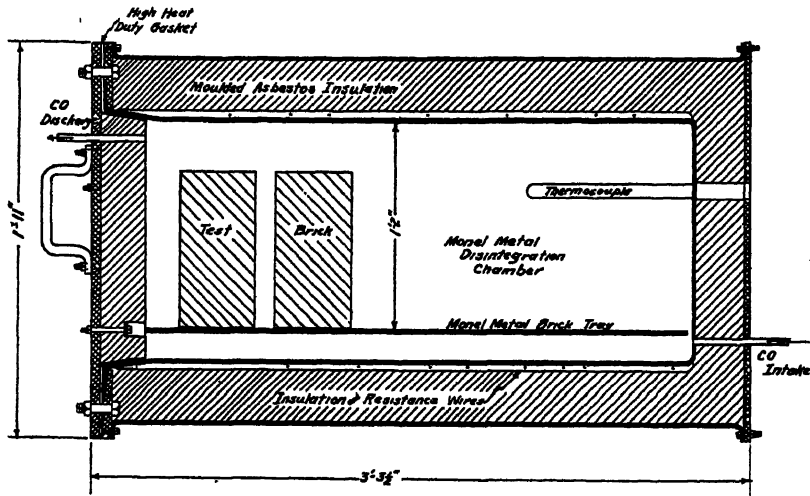


FIG. 2.—CO DISINTEGRATION FURNACE.

is generally considered desirable. However, in ladle linings a bloating clay is preferable because it eliminates joints and produces a lining that is virtually monolithic, free from crevices into which steel might penetrate. There are practically no cases where the reverse, shrinkage during use, would be acceptable.

Although the clay refractory consists largely of alumina and silica, the alkali content and certain other impurities such as lime, magnesia and iron oxide, are in large measure responsible for wide differences in refractoriness and load-bearing ability. Small changes in porosity may be used as a criterion, but the progress of fusion in a clay refractory is best determined by a load test in which the deformation is measured. Surprising as it may seem, this test shows greater differences in the characteristics of a refractory than do cone fusion temperatures or most other ceramic tests. Although the load test has been used primarily to determine the

by holding the brick under load for a short period of time at a prescribed temperature. A load test wherein the temperature is gradually increased to failure, the deformation being measured constantly during the process, provides more valuable information in regard to the temperature at which the failure occurs. It also shows quite readily where the brick becomes plastic and reveals small differences in quality of brick.

New ceramic tests and variations in the conventional older tests may be used to supplement experience and service tests in the selection of refractories for a particular service. It would be difficult to cover the philosophy of interpretation of ceramic test results by which many choices are made, but the following will serve to illustrate one approach to a problem.

COMPARISON OF REFRACTORIES

Because of the great length of the average blast-furnace campaign and the many

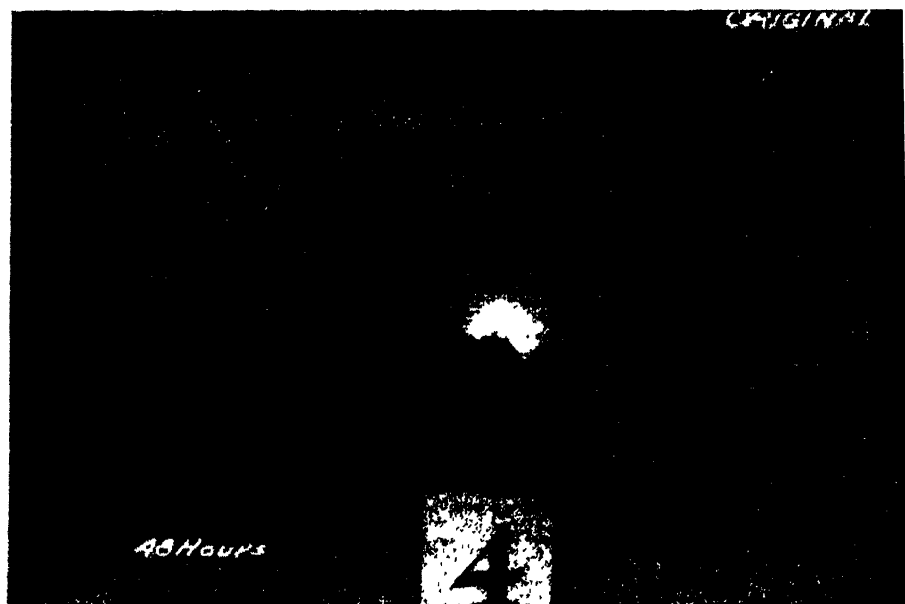


FIG. 3.—BRAND 4 BEFORE AND AFTER TREATMENT FOR 48 HOURS.

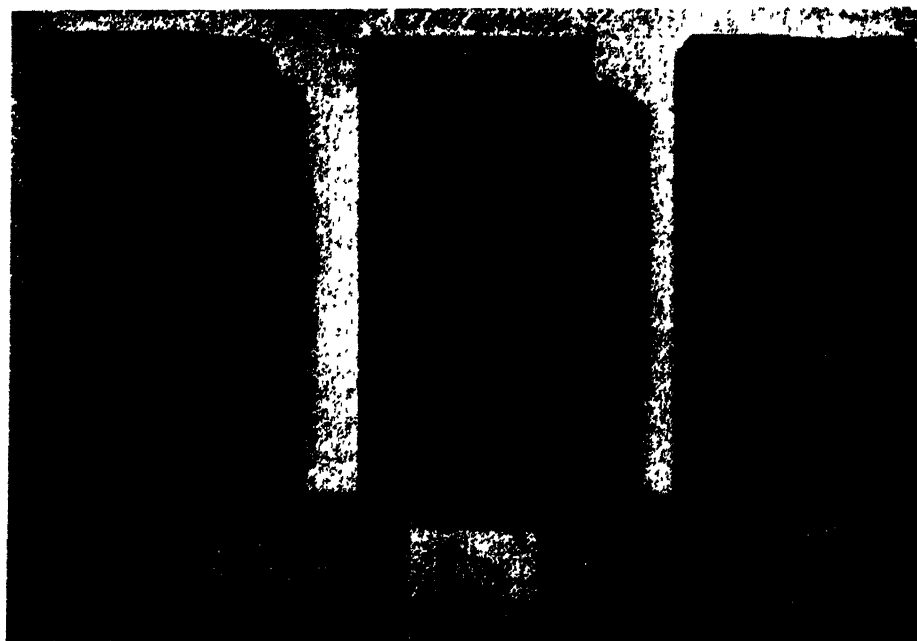


FIG. 4.—BRAND 8 BEFORE AND AFTER TREATMENT FOR 100 HOURS.



FIG. 5.—BRAND 8 BEFORE AND AFTER TREATMENT FOR 200 HOURS.

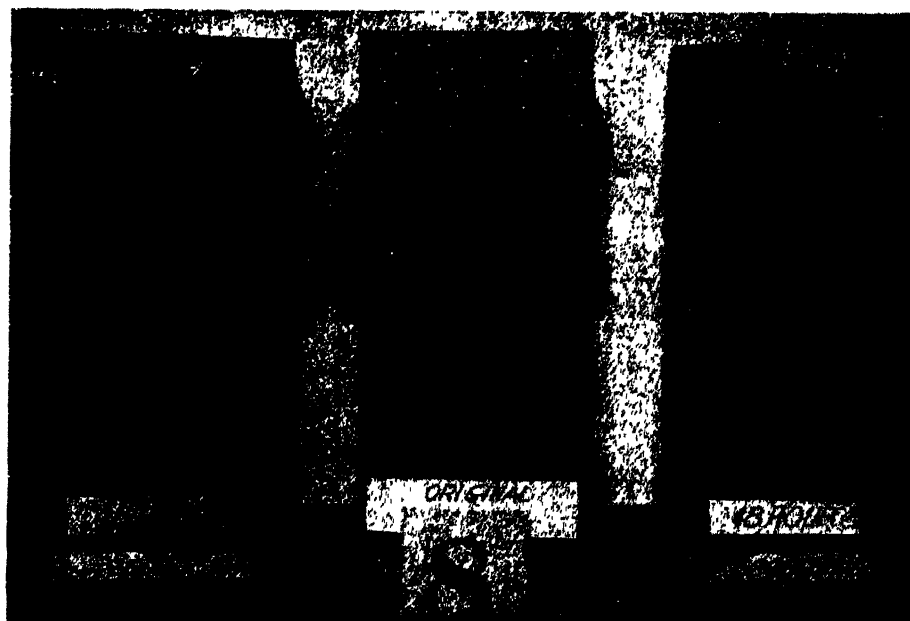


FIG. 6.—BRAND 8 REFIRED TO 2600°F.

produces extensive shrinkage, which causes bricks to loosen and float out.

Figs. 1 and 2 show the apparatus in which bricks are tested for resistance to carbon monoxide at the critical temperatures.

100-hr. test is insufficient as the basis for a definite opinion regarding the resistance of this refractory to carbon monoxide disintegration.

Hard firing of a blast-furnace refractory

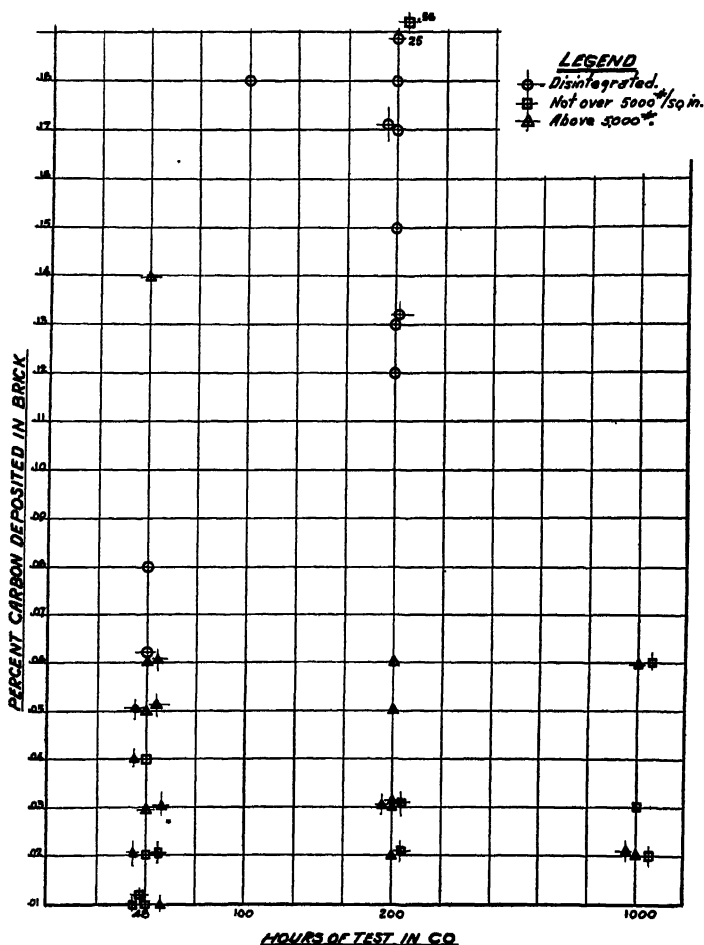


FIG. 10.—COLD-CRUSHING STRENGTH OF BRICK SUBJECTED TO CARBON MONOXIDE AT 485° TO 495°C.

Fig. 3 shows the result of treating brand No. 4 for 48 hr. in a carbon monoxide atmosphere. Further testing obviously was unnecessary with this refractory. Another refractory (brand 8) is shown in Fig. 4 (100 hr. in CO), and Fig. 5 (200 hr.). These pictures not only show the seriousness of this action but also reveal that a

decreases the probability of disintegration under these conditions by building up the mechanical strength of the brick, lowering its permeability and combining some of its iron oxide, so that it does not catalyze the reaction ($2\text{CO} \rightarrow \text{CO}_2 + \text{C}$) that is responsible for the phenomenon of carbon disintegration.

While hard firing decreases the tendency to disintegration, it does not entirely remove the danger, as will be seen by

Figs. 8 and 9 represent a summary of standard and special refractories subjected to the carbon monoxide tests.

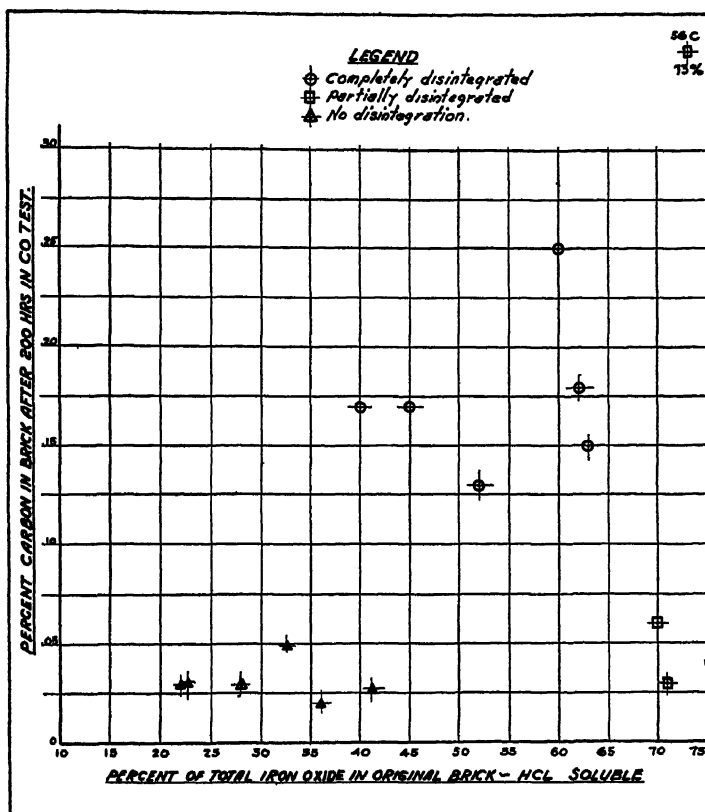


FIG. 11.—PLOT SHOWING RELATION BETWEEN "FREE" IRON IN BRICKS AND THEIR TENDENCY DEPOSIT CARBON AND DISINTEGRATE

Note that bricks of which the iron oxide content is more than 40 per cent C. causes partial disintegration, or tend to do so.

subsequent data. Carbon is deposited within the pores just as in the less well fired specimens, but a hard-fired brick is able to resist the disrupting forces to a greater extent. The apparent improvement is noted in Fig. 6 and Fig. 7. This represents brand No. 8 refired to 2600°F. and 2800°F., respectively. It will be remembered that brand No. 8 disintegrated completely in 200 hr. of test in the as-received condition, and that 2600° is not ample.

CARBON DEPOSITION

The amount of carbon necessary to cause disintegration of a refractory, in terms of the refractory weight, is very small. Fig. 10, for example, shows that as little as 0.01 per cent C. causes partial disintegration and that 0.06 per cent C. may cause complete destruction. Combining the iron oxide as a silicate by hard firing as indicated in Fig. 11 appears to retard carbon deposition. Refiring, as previously stated.

enables the brick to hold together during test but does not eliminate carbon deposition. Fig. 12 shows that many brands disintegrated with only small amounts of

used to study this reaction. Boats of these materials were held for 48 hr. at 485° to 495°C. in an atmosphere of carbon monoxide, with the results shown in Table 1.

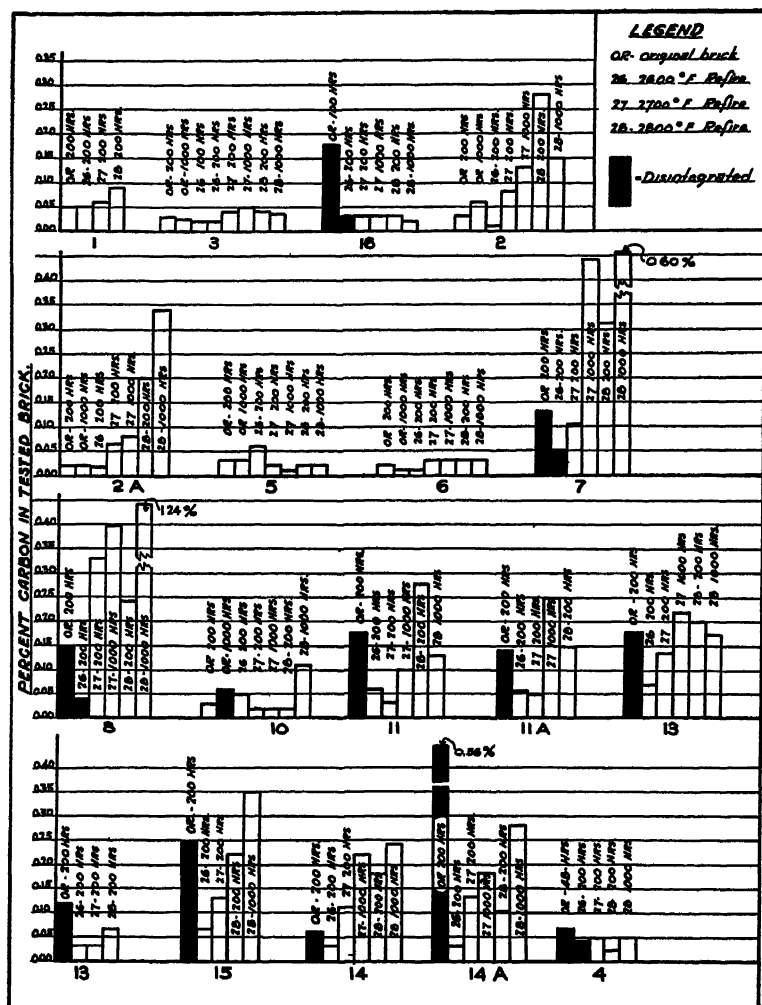


FIG. 12.—EFFECT OF REFIRING ON CARBON DEPOSITION.

carbon deposition before refiring. On subsequent refiring the same brick held together through the subsequent carbon monoxide testing, in which larger quantities of carbon were deposited.

In an effort to determine the causes of carbon deposition, various materials that might be found in a blast furnace were

Metallic iron and iron oxides strongly catalyzed the reaction. Metallic nickel was even more active.

Shrinkage due to pyroplasticity and ferrostatic pressure is a serious factor in the performance of hearth bricks.

Fig. 13 shows a hearth block that floated from the hearth of a furnace. It is one of

about a dozen that came from the furnace at the same time. They were vitrified and to some extent impregnated with metal. This is a frequent occurrence. Vitrification

the slag before the bricks were removed, as the reduction in volume was around 30 per cent of the original while the initial porosity was only about 20 per cent. Such



FIG. 13.—BLOCK THAT FLOATED FROM HEARTH OF FURNACE.

and widened joints in the hearth structure testify to the serious shrinkage in the

TABLE I.—*Carbon Deposition by Oxides and Other Materials in Carbon Monoxide at 485° to 495°C.*
LENGTH OF TEST, 48 HOURS

Material	Weight of Sample, Grams	Increased Weight after Test, Grams	Increased Weight, Per Cent
Fe.....	0.500	+ 5.170	1032
Fe ₂ O ₃	0.400	+10.470	2617
Fe ₃ O ₄	0.840	+16.990	2010
FeS.....	3.000	— 0.100	Negligible
Fe-SiO ₂ glass.....	1.000	0.000	Negligible
Pb.....	6.945	0.000	Negligible
PbS.....	2.195	— 0.350	—16
PbO.....	3.135	— 0.315	—10
Pb ₂ O ₃	2.220	— 0.205	—9
Zn.....	5.860	+ 0.080	Negligible
ZnO.....	0.980	+ 0.010	Negligible
ZnS.....	1.755	0.000	Negligible
Mn.....	7.610	+ 0.010	Negligible
MnO.....	1.440	— 0.165	—11
Ni.....	1.000	Overflowed	3000 or better
NiO.....	1.000	+ 1.270	13
TiO ₂	0.740	+ 0.005	Negligible
Al ₂ O ₃	1.195	— 0.005	Negligible

hearth. The length of the block had decreased 2 in., the width 1½ in. and the thickness about 1 in. Some of this decrease in size was due to the dissolving action of

vitrification obviously is ample evidence for greater refractoriness and volume stability being required for service in the hearth. Fig. 14 presents a schematic illustration of the fundamental concepts of the solution to this problem. The solid line represents the porosity-temperature relations of our present hearth bricks during their production. They are fired at a temperature represented by the solid vertical line *A*, which leaves them with a rather high porosity. Harder fire would reduce the porosity to the minimum point, but at this temperature the brick become pyroplastic and difficult to produce with most available firing equipment. Line *B* represents the operating temperature of the furnace hearth, and, as the standard brick is even softer at this temperature, it compresses under the ferostatic pressure of the liquid iron. A new brick whose properties are represented by the dotted line is available. It is less plastic at *B* and is more volume-stable than the standard product.

To illustrate this detail further, Fig. 15 shows the deformation characteristics of the two hearth blocks at elevated temperature and under a load of 25 lb. per

CONCLUSION

All of the foregoing test data show that if a knowledge of the requirements is

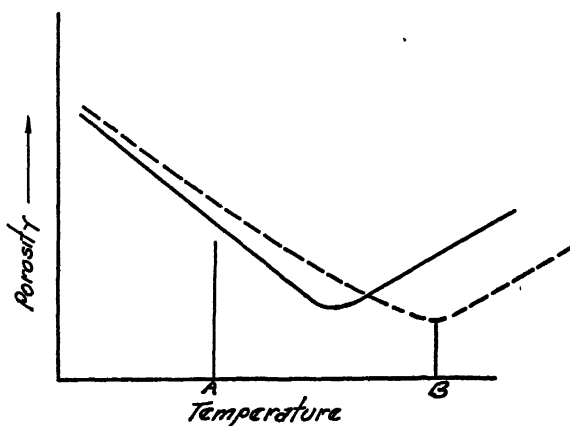


FIG. 14.—SCHEMATIC ILLUSTRATION OF FUNDAMENTAL CONCEPTS OF SOLUTION OF PROBLEM OF VITRIFICATION.

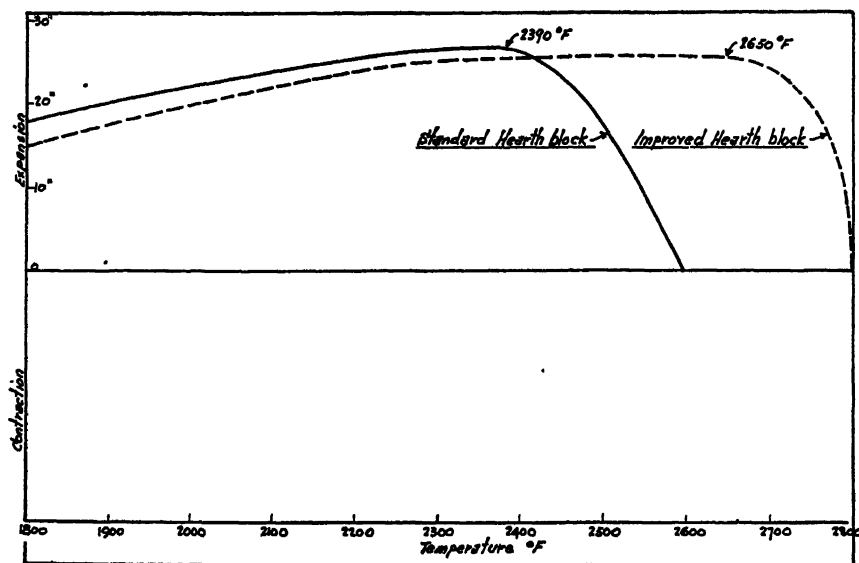


FIG. 15.—COMPARISON OF STANDARD AND IMPROVED BLAST-FURNACE HEARTH BLOCKS IN 25-POUND LOAD TEST.

sq. in. These clearly show why the standard blocks behave as they do, and why the improved block would have considerably greater volume stability in a furnace hearth.

available, it is possible to make intelligent selection of a clay refractory based on conventional and special tests that reveal particular characteristics of commercially available materials.

The Washing of Pittsburgh Coking Coals and Results Obtained on Blast Furnaces

By C. D. KING,* MEMBER A.I.M.E.

(Cleveland Meeting, April 1943)

THE key to maximum production of ingots for the war effort is maximum production of pig iron. For any given furnace and ore, the most important single influence on blast-furnace production is the quality of the furnace coke.

It is generally recognized that undoubtedly deterioration of Pittsburgh coking coals will be accelerated by the depletion of some of the better grades of coal; the extension of mine mechanization, with attendant degradation of coal quality; and the opening of new coal fields, some of which are known to be fairly high in sulphur. All of these factors, contributing as they do to higher ash and sulphur, and not infrequently to inferior quality of coke, made it desirable that an extensive study be undertaken to determine the effect of washing some coals that closely approximate the average chemical composition of coking coals to be expected in the future by the subsidiaries of the United States Steel Corporation in the Pittsburgh district. It was deemed advisable to study the improvement obtained by washing such coals and to determine the need for supplementing the existing coal washery at Clairton to assure continued maximum production of pig iron from presently available furnace stacks. The existence of

the coal washer at Clairton made it possible to conduct tests on coals used in raw form and on similar coals after washing.

This study covers an investigation of the quality of furnace coke as affected by washing coking coals, and is confined to the use of 100 per cent high-volatile Pittsburgh seam coals from Fayette and Greene Counties in the manufacture of furnace coke. It covers the improvement in chemical and physical properties as well as the degree of uniformity in coke obtained by washing these coals, and includes the effect on blast-furnace production and practice. The test period involved is four months; the plants, Clairton by-product coke plant, and the Carrie No. 1 and No. 2 blast furnaces at Rankin, Pa., Carnegie-Illinois Steel Corporation.

CLAIRTON BY-PRODUCT COKE PLANT AND COAL WASHER

The Clairton by-product coke plant carbonizes 30,800 net tons of coal daily in 22 batteries containing 1482 ovens. Three oven sizes are used, commonly known as wide, medium, and narrow types, recognizing the difference in oven width. These ovens also differ in height and length.

The present coal washer has a daily capacity of approximately 14,000 tons, leaving 16,800 tons to be carbonized in raw form. Washed coal is used on all the narrow ovens and on three of the six batteries with ovens of medium width, raw coals being used on all the remaining ovens. The customary arrangement is

Manuscript received at the office of the Institute May 18, 1943. Published also in the *Proceedings of the Blast Furnace and Raw Materials Committee, 1943* and issued as T.P. 1618 in *METALS TECHNOLOGY*, September 1943.
* Chairman Operating Committees, United States Steel Corporation of Delaware, Pittsburgh, Pa.

shown in Table 1, which also includes various oven dimensions.

The use of raw coal for approximately 55 per cent of the total Clairton output has in the past yielded satisfactory results, since relatively low-sulphur and low-ash coals were available for use in the raw state. Palmer and Gates coal, normally coals of moderately low sulphur-ash, have been carbonized in this form, whereas Colonial and Ronco, which are generally

set at 2-in. openings and the fine coal by-passing the crusher. The mixed crushed and fine coal is carried by conveying belts to the various coal bunkers serving the batteries, each bunker having a capacity of 4000 tons of coal. From the bunkers it is handled in the usual manner by larry cars to the ovens.

The Clairton by-product coke plant is unique in its use of 100 per cent high-volatile, Pittsburgh seam coals and also the fact that the coal is not pulverized prior

TABLE 1.—*Oven Dimensions and Normal Allocation of Raw and Washed Coals, Clairton By-product Coke Plant*

Type of oven.....	Koppers	Koppers-Becker Combination	
Number of batteries of each.....	12	6	4
Battery number or other designation...	Nos. 1-12, incl. (wide)	Nos. 13-18, incl. (medium)	Nos. 19-22, incl. (narrow)
Number of ovens per battery.....	64	61	87
Number of ovens.....	768	366	348
Oven dimensions:			
Width { Coke side.....	19 1/4"	18"	17 1/2"
{ Pusher side.....	17"	16"	15 1/2"
{ Average.....	18 1/4"	17"	16 1/2"
Length between doors.....	36' 6 1/2"	40' 4 1/2"	42' 6"
Height { Floor to roof.....	9' 10 3/8"	11' 8 1/2"	14' 0"
{ Coal charge.....	8' 10 3/8"	10' 8 1/2"	13' 0"
Capacities:			
Cubic feet.....	500	616	759
Coal charge per oven, net tons...	13.24	16.70	20.63
Coal charged per unit per day, net tons.....	12,700	8,200	9,900
Net coking time, hours.....	18.6	17 7/8	16.8
Coal carbonized.....	Raw Palmer	Batt. 13-15 Raw Gates	Batt. 16-18 Washed Colonial-Ronco
Coal analysis:			
Ash, per cent.....	8.70	8.25	8.91*
Sulphur, per cent.....	1.00	1.00	1.36*

*Prior to washing.

inferior, have been washed. The usual combination of Colonial and Ronco mixtures is 70 and 30 per cent, respectively, or in accordance with the mining schedules for these coals. In addition, the allocation of washed coals to some batteries and raw coals to others also recognized the location of the washer, which serves coal bunkers for only seven of the batteries.

Coking coals for the Clairton plant are shipped down the Monongahela River by barge, each barge holding about 900 tons. The coal is unloaded from barges into bins by clamshell buckets at four coal hoists, from which it passes over screens, the coarse coal being fed to roll crushers

to carbonization. Long experience at Clairton has shown that under existing conditions it is desirable to charge unpulverized coal to obtain maximum bulk density and, accordingly, maximum coke output.

By avoiding the fine crushing of coal, maximum bulk density is similarly obtained when employing washed coal. This practice also possesses the additional advantage of eliminating a considerable amount of slate as large pieces by the coarse coal launders and thereby avoids the more difficult fine launder elimination of this proportion as fine slate particles. The present coal washer, installed in 1931,

is the Rheolaveur type. The washer was built on the north end of the plant in order to utilize the capacity of the larger batteries as well as to permit the use of coal-handling facilities already available. After leaving the roll crushers at the coal hoists, the mixed coarse and fine coal is conveyed to three double-compartment blending bins, with a total capacity of 3000 tons. This arrangement permits the handling of three types of coal, Colonial,

COKE-PLANT TESTS

The study of the effect of washing Colonial and Ronco coals extended over a period of four months. The comparison was based on carbonizing washed Colonial-Ronco coals in the same battery used for coking Colonial-Ronco raw coals. This arrangement was considered advisable in order to eliminate any coke-plant variable other than the type of coals used. Since

TABLE 2.—Average of Control Data for Coal-washery Float-and-sink Test during the Four-months Washing Test, Clairton By-product Coke Plant

Coal	Size	Dry, Per Cent	Sieve, Per Cent	Float 1.55 Sp. Gr., Per Cent			Sink 1.55 Sp. Gr., Per Cent			Composite*	
				Total	Ash	Sulphur	Total	Ash	Sulphur	Ash	Sulphur
Raw.....	+ $\frac{3}{8}$ "		63.43	95.44	7.05	1.04	4.56	61.25	5.05	9.52	1.22
	$\frac{3}{8}$ "-20m.		26.09	96.15	5.72	1.07	3.85	59.67	7.49	7.80	1.32
	-20m.		10.48	93.49	6.11	1.06	6.51	60.79	11.93	9.67	1.77
	Over-all		100.00	95.42	6.60	1.05	4.58	60.83	6.61	9.09	1.31
Washed...	+ $\frac{3}{8}$ "		60.82	99.59	7.08	1.04	0.41	40.43	3.65	7.22	1.05
	$\frac{3}{8}$ "-20m.		25.14	99.24	5.86	1.04	0.76	36.70	4.36	6.09	1.06
	-20m.		14.04	96.70	5.83	1.04	3.30	53.68	11.93	7.41	1.40
	Over-all		100.00	99.10	6.60	1.04	0.90	46.45	8.04	6.96	1.10
Refuse....	+ $\frac{3}{8}$ "	96.63	47.30	5.01	17.66	1.78	94.99	65.59	5.48	63.18	5.29
	$\frac{3}{8}$ "-20m.		40.54	10.37	11.87	1.70	89.63	64.86	8.24	59.36	7.56
	-20m.		12.16	26.64	8.91	1.32	73.36	71.21	15.22	54.61	11.52
	Over-all	3.37	100.00	9.79	12.29	1.60	90.21	65.85	7.56	60.60	6.97

* Calculated from float-and-sink-test data.

Ronco, and any other coal received at Clairton if the first two are not available in quantity to utilize the full capacity of the washer. Variable-speed belt conveyors at the bottoms of the bins allow for adjustment in desired coal mixtures fed to the washing plant. Coals are screened to two sizes, plus and minus $\frac{3}{8}$ -in., prior to washing.

The washery was designed to yield a three-product separation; i.e., washed coal, middlings for boiler fuel, and refuse. Experience with coals received to date at Clairton has shown that under existing conditions it has not been economical to remove bone coal as middlings because of the small percentage present in raw coal. However, the provision for a middling product may prove highly desirable as insurance against adverse changes in sulphur and ash content of future coals.

Colonial-Ronco washed coal is customarily carbonized in batteries 19-22, and because these batteries were also provided with a spare coal bunker, arrangements were made to use this spare for storing Colonial-Ronco raw coals. Accordingly, 30 ovens in batteries 19 and 20 were charged with Colonial-Ronco unwashed coal and the remainder of the ovens in the same batteries were charged with Colonial-Ronco washed coal. The mixture of Colonial-Ronco coal was approximately 70 per cent of the former and 30 per cent of the latter.

Comparison of Analyses of Coals Used and Coke Produced

The high efficiency of the coal washer is indicated by the fact that in a two-product separation 96.63 per cent of the initial coal was recovered as a washed product; the refuse, or bank loss, being 3.37 per cent.

The refuse contained 4.91 per cent sulphur and 62.71 per cent ash. The plus $\frac{5}{16}$ -in. washed coal at 1.55 sp. gr. contained only 0.41 per cent sink and the $\frac{5}{16}$ in. to 20 mesh, 0.76 per cent. The refuse showed only 9.79 per cent float coal with an ash content of 12.29 per cent. Of the initial coal, less than 0.3 per cent was lost in the refuse. Detailed float-and-sink test data are shown in Table 2.

TABLE 3.—*Composite of Four-months Test Results Showing Effect of Coal Washing on Coal and Coke Analyses*
PER CENT

Proximate Analyses, Dry Basis	Unwashed Coals	Washed Coals	Effect of Washing
Moisture.....	3 93	7.27	+3 34
Sulphur.....	1 36	1.11	-0 25
Ash.....	8 91	7.12	-1 79
Volatile matter.....	32 49	32 97	+0 48
Fixed carbon.....	58.60	59 91	+1 31

Proximate Analyses, Dry Basis	Furnace Coke from		Effect of Washing
	Unwashed Coals	Washed Coals	
Moisture.....	2 95	2.88	
Sulphur.....	0 98	0.88	-0 10
Ash.....	11.87	10.36	-1.51
Volatile matter. . .	0 30	0.30	
Fixed carbon.....	87.83	89.34	+1 51
Available carbon (2.5 per cent moisture basis).....	83 02	84.58	+1.56

The results obtained by washing Colonial-Ronco coals for the four-months test period are shown in Table 3. The ash in the coal was reduced by 1.79 per cent and the sulphur 0.25 per cent; the fixed carbon increased by 1.31 per cent and the moisture 3.34 per cent. The sulphur content of 1.36 per cent in the initial coal was made up of 0.80 per cent organic sulphur, 0.54 per cent pyritic, and 0.02 per cent sulphate. Washing these coals resulted in the elimination of approximately 45 per cent of the pyritic sulphur. The furnace coke produced from washed coals was lower in ash than the coke from unwashed coals by 1.51 per cent, and the sulphur 0.10 per cent. The fixed

carbon was increased 1.51 per cent. Detailed data showing the results for each of the four months are shown in Table 5

The reduction of 1.51 per cent ash in furnace coke from washed coals does not fully account for the reduction of 1.71 per cent ash in coal by washing. The remainder of this ash difference will be found in the coke breeze produced from the respective coals, being approximately 20 per cent ash in coke breeze from unwashed coals and only 12 per cent in coke breeze from washed coals.

Comparison of Physical Properties of Coke Produced from Washed and Unwashed Coals

In addition to the beneficial effects obtained with respect to reduction of sulphur and ash in coal and coke by washing Colonial-Ronco coals, a marked improve-

TABLE 4.—*Composite of Four-months Tests Showing Effect of Coal Washing on Physical Properties of Coke*
PER CENT

Test	Furnace Coke from		Effect of Washing
	Unwashed Coals	Washed Coals	
Sieve Test			
On 3 in.	14.3	15 8	+ 1 5
Total on 2 in.	60.2	63 8	+ 3 6
Through 1 in.	2 4	1 7	- 0.7
Tumbler Test			
Strength	65.3	72 0	+ 6.7
Hardness	73 8	76 2	+ 2.4
Brittleness.	55 9	52 0	- 3 9
Fuel value	73 5	86 5	+13.0
Weight per cu. ft. (2.5 per cent moisture basis), lb.	31 61	31.41	- 0.20

ment in physical characteristics of the furnace coke was also derived. This is attributed to the greater tendency of coke made from raw coal to cross-fracture because of slate inclusions. Slate in coal over $\frac{3}{8}$ in. is relatively easy to eliminate, but its reduction is particularly desirable in sizes ranging from $\frac{3}{8}$ -in. to 20-mesh, since the number of incipient fractures caused by slate in coal is far greater in the smaller size than in the larger for equal percentages

of slate. It has, however, been Clairton's experience that under 20 mesh the disseminated ash, if not excessive, may actually improve the coke structure because of the increased physical strength it gives.

Because the large daily production of the Clairton coke plant serves many blast furnaces in the Pittsburgh and Youngstown districts, it was considered inadvisable to use the daily average analyses of coke pro-

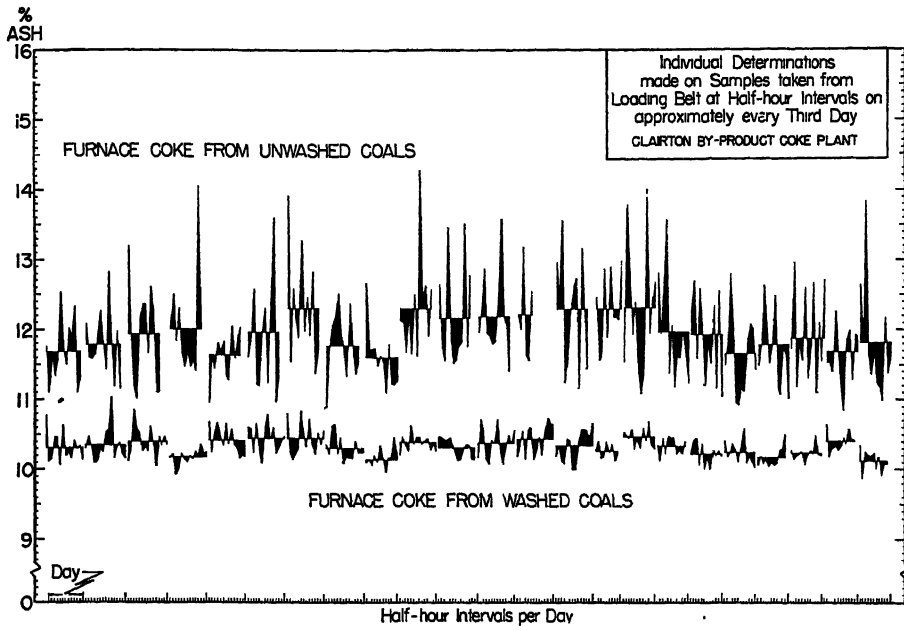


FIG. 1.—VARIATIONS IN ASH OF FURNACE COKE FROM WASHED AND UNWASHED COALS.

The physical tests of furnace coke produced during the four-months period are shown in Table 4. The physical tests relating to coke strength, hardness and brittleness, are conducted according to empirical methods developed at the Clairton by-product coke plant. These methods have proved reliable in determining the relative value of different cokes produced at that plant. Detailed data showing the results for each of the four months are shown in Table 5.

Variation in Sulphur and Ash Content of Furnace Coke

One of the most pronounced benefits obtained from washing Colonial-Ronco coals is the marked improvement in the uniformity of coke ash and sulphur content.

produced at this plant as the sole criterion of its regularity with respect to blast-furnace results at Carrie. Since the Carrie blast furnaces were not provided with facilities that made it feasible to obtain coke samples at the coke stock bins, arrangements were made to sample at the Clairton coke plant by obtaining samples of coke on the belt conveyors at 30-min. intervals during the day turn. Fig. 1 represents the variations in ash for the four months period for both types of coke. The days indicated represent approximately every third day for the entire four months and each day, in turn, is represented by from 8 to 14 samples. Since the half-hourly production of the Clairton plant on washed coals is equivalent to 200 tons, or a 6 to 8-hr. operation on a single Carrie blast furnace, this fre-

Analyses of Ash		51.76	53.80	52.78	6.28	54.14	53.46	53.83	6.38	52.26	54.18	53.22	5.53	53.83	53.30	53.30	53.38	+ 0.08
Silica.....		13.18	11.96	12.57	1.49	11.16	11.50	11.31	1.34	11.96	11.96	11.96	1.24	10.86	11.10	11.94	11.31	+ 0.63
Iron oxide.....		29.16	28.74	28.95	3.44	29.11	29.35	29.23	3.46	30.33	28.37	29.35	3.05	29.91	3.12	29.04	20.82	+ 0.73
Aluminum oxide.....		0.10	0.09	0.10	0.01	0.10	0.12	0.11	0.01	0.11	0.14	0.12	0.01	0.11	0.01	0.11	0.12	+ 0.01
Manganese oxide.....		2.64	2.60	2.67	0.32	2.37	2.33	2.35	0.28	2.24	2.24	2.24	0.23	2.29	2.11	2.56	2.23	+ 0.33
Calcium oxide.....		0.79	0.80	0.80	0.10	0.78	0.77	0.78	0.09	0.75	0.76	0.76	0.68	0.75	0.71	0.79	0.75	- 0.04
Magnesium oxide.....		0.27	0.25	0.26	0.031	0.26	0.23	0.23	0.030	0.29	0.27	0.28	0.029	0.25	0.25	0.25	0.27	+ 0.02
Phosphorus pentoxide.....																		
Physical Properties																		
Sieve test:																		
On 3 in.....		14.2	14.4	14.3		14.1	14.6	14.3		15.9	15.7	15.8		15.7	15.7	14.3	15.8	+ 1.5
Total on 2 in.....		60.8	59.9	60.4		59.9	59.9	59.9		63.6	63.7	63.6		64.1	64.2	60.2	63.8	+ 3.6
Through 1 in.....		2.3	2.4	2.4		2.4	2.6	2.5		1.7	1.7	1.7		1.7	1.7	2.4	1.7	- 0.7
Tumbler test:																		
Strength.....		65.8	65.9	65.8		65.4	64.2	64.9		72.9	70.3	71.6		72.4	72.4	65.3	72.0	+ 6.7
Hardness.....		74.0	74.1	74.0		73.0	73.3	73.6		76.0	76.1	76.0		76.3	76.3	73.8	76.2	+ 2.4
Brittleness.....		55.8	55.5	55.7		55.5	57.0	56.2		51.9	51.7	51.8		52.2	52.1	55.9	52.0	- 3.9
Fuel value.....		74	74	74		74	71	73		87	85	86		86	87	74	86	+ 12
Weight per cu. ft. (2.5 per cent moisture basis), lb.....		31.61		31.61						31.41		31.41				31.61	31.41	- 0.20

* Coke basis.

quency of sampling made it possible to study the magnitude of variations of coke during short intervals of time at Clairton.

The study of ash variability may prove of particular value in connection with the treatment of coals in the future, which are expected to be higher in ash and sulphur than the Colonial-Ronco coals used as a basis for this study. This is due to the well known fact that the frequency of slate particles of sufficient size to cause cross fracturing increases at a rate faster than

reduction in the range of ash variation is largely the result of removal by washing of varying amounts of segregated high-ash fractions in the coal, which otherwise are not leveled out and persist throughout the entire unloading and bunkering system when these coals are carbonized in raw form. Although Fig. 1 indicates a high degree of uniformity in ash content of coke produced from washed coals, it is believed that a further improvement could be expected if the blending-bin capacity of

TABLE 6.—*Amount and Variation of Ash and Sulphur in Coke*
PER CENT

Variation for Any Single Day Based on Periodic Daily Tests Using Half-hour Samples for Four-months Period	Furnace Coke Produced from					
	Unwashed Coal			Washed Coal		
	Maximum	Minimum	Range	Maximum	Minimum	Range
Ash.....	14 05	11.08	2.97	11 04	10 08	0.96
Sulphur	1.08	0 82	0 26	0 97	0 80	0 17

Variation Based on Daily Average Analysis for Every Day of the Four-months Period	Unwashed Coal		Washed Coal	
Average ash.....	11 87		10 36	
Average day to day variation in ash...	0.40		0 14	
Variations exceeding 0.30 per cent ash	50 00		9 50	
Variations exceeding 0.50 per cent ash	31.50		0 00	
Variations exceeding 1.00 per cent ash	6 70		0 00	

indicated by the rising total average ash content. Likewise, the frequency and severity of short-time irregularities become disproportionately worse where the change in ash content is not caused by change in composition of the coal seam, but rather is due to the inclusion in irregular amounts of extraneous material from bottom and roof of coal seams.

Fig. 1 shows a marked and important difference between coke produced from washed and unwashed Colonial-Ronco coals with respect to frequency and magnitude of short-period irregularities in ash content. Similar trends were observed in sulphur content of the respective cokes, but obviously of a smaller character. The

3000 tons per day were increased to more properly conform with the daily washing capacity of 14,000 tons.

Table 6 shows the amount and variation of ash and sulphur in coke. Based on half-hourly samples, as previously described, the greatest variation in ash content for any one day was 2.97 per cent for coke from unwashed coals, while that for washed coals was only 0.96 per cent and, similarly, the sulphur showed a variation of 0.26 per cent for unwashed coals and only 0.17 per cent for coke from washed coals. A review of the variation based on daily average samples for each day of the four-months test confirms the improved uniformity in coke resulting from washing coals. The

coke from unwashed coals shows considerably more severe and frequent variations than the coke from washed coals. For example, day to day variations in excess of 0.30 per cent ash occurred 50 per cent of the time for the former, as opposed to only 9.5 per cent of the time for the latter; and perhaps of greater importance is the fact that no day to day variations in excess of 0.50 per cent ash occurred in coke from washed coals, whereas such occurrences represented 31.5 per cent of the time on coke from unwashed coals.

Comparison of Coke Yields

Four tests were conducted to determine the difference in carbonizing capacity and coke yields when charging washed and unwashed coals. The coal content of 11 larry cars, each of both washed and unwashed coals, was weighed by discharging the coal from the cars into a truck, which later was weighed on the plant scales. Identical volumetric ring settings were maintained throughout the test and the amount of coal pulled back by the leveler bar in the oven was also weighed. The net coal charged per oven, determined in this manner, indicated that the coal-carbonizing capacity of the ovens was reduced approximately 1.0 per cent when washed coals were used. This is shown in Table 7.

TABLE 7.—*Effect of Coal Washing on Oven Carbonizing Capacity*

	Oven Capacities Batteries 19 to 22, Inclusive		Effect of Washing, Per Cent
	Unwashed Coals, Lb.	Washed Coals, Lb.	
Coal as received (31.46 per cent moisture).	41,997.8	41,558.7	- 1.05

While several tests were undertaken to determine accurately the total coke yield from both types of coals, in all cases coke

over 1 in. being considered furnace coke, this procedure was abandoned because it was impossible to accurately weigh the coal charged as allocated to the different ovens. As a matter of information, this test showed approximately equal total coke yields from washed and unwashed coal, 72.24 per cent and 72.26 per cent, respectively. Since it is well known that a higher total coke yield is obtained with higher-ash coals, it was necessary to disregard these tests and use Clairton's actual experience with washed and unwashed coals as the basis for coke yields. As will be noted in Table 8, a very marked increase was obtained in furnace coke from washed coals, in the order of 2.20 per cent, and the coke dust reduced by 2.90 per cent. However, as was to be expected, the total coke yield for washed coal is less by 0.69 per cent than when using unwashed coals. The increase in yield of furnace coke for washed coal more than offsets the decreased coal-carbonizing capacity resulting from the use of higher-moisture washed coals, and a net increase of approximately 3.0 per cent is obtained per day per battery in the production of furnace coke.

TABLE 8.—*Effect of Coal Washing on Coke Yields*
PER CENT

Coke	Yield per Net Ton of Coal Charged, Per Cent		Effect of Washing
	Unwashed Coals	Washed Coals	
Furnace coke (2.5 per cent moisture basis)	65.48	67.68	+2.20
Coke dust, as produced basis	8.29	5.39	-2.90
Quencher sump sludge	0.10	0.11	+0.01
Total coke.....	73.87	73.18	-0.69

Comparison of By-product Yields

Since the same by-product plant served the batteries that were concurrently used in the production of coke from washed and unwashed coals, it was not possible to

segregate the by-products and determine the yields obtained from the two coals. Therefore, the by-product yields were established by recognizing the amount of by-products lost with float coal in washery refuse, such calculated yields checking past experience at Clairton.

Because of the higher moisture content of washed coals, it is obvious that more oven gas is required for underfiring ovens than when using unwashed coals, and to determine the exact difference a special test was undertaken. Gas-metering facilities were installed on various batteries and, based on an eight-months test, it was determined that 9.0 per cent more fuel was required per ton of washed coal carbonized. The B.t.u. per pound of coal carbonized was 1219 for washed coal—an increase of 102 B.t.u. over that required for unwashed coal. This adversely affected the surplus coke gas available and is included in the determination of the by-product yields shown in Table 9.

TABLE 9.—*Comparison of By-product Yields from Washed and Unwashed Coals*

	Yield per Net Ton of Coal Charged		Effect of Washing
	Unwashed	Washed	
Tar (160,000 B.t.u. basis), gal.	10 460	10.760	+0.300
Gas (500 B.t.u. basis), M cu. ft.: Used at ovens....	4 584	4 997	+0 413
Surplus.....	6 981	6 911	-0 070
Total.....	11 565	11 908	+0.343
Ammonium sulphate (25 per cent NH ₃ basis), lb.	25 38	26.10	+0.72
Light oil (total), gal..	3.16	3 25	+0 09

Effect on Sulphur Content of By-product Coke-oven Gas

Of more than passing interest to steel producers is the fact that by-product coke-oven gas produced from washed coals contained approximately 20 per cent less sulphur than gas produced from unwashed coals, the figures being 0.454 and 0.563 lb.

H₂S per M cu. ft., respectively. By-product gas produced at the Clairton Works usually contains more sulphur than that found in similar gas produced elsewhere because of the sulphur content of the coals carbonized. As a result, in the production of steels with low sulphur specifications, special efforts are required through the agency of additional fluxes, manganese, and furnace time, when appreciable proportions of by-product coke-oven gas are used in melting. Therefore a reduction in the sulphur content of the gas would permit the attainment of the required specifications for sulphur in somewhat less melting time and with a reduction in fluxes, manganese, and other materials involved. Indirectly, this matter is important to blast-furnace operators, since it would allow a moderate increase in the permissible sulphur content of pig iron if the present steelmaking practices were retained.

Summary of Four-months Test

The four-months test performed at the Clairton by-product plant to determine the effect of washing coking coals indicated that a marked improvement can be expected in ash, sulphur, physical properties and uniformity of the coke so produced. Blast-furnace operators will readily concede that the use of such coke, as opposed to coke from unwashed coals, should help to improve blast-furnace operations, but only carefully controlled blast-furnace tests can indicate the magnitude of the expected improvement.

BLAST-FURNACE TESTS

In the determination of the relative effect of each type of coke on blast-furnace performance, two furnaces of identical physical dimensions were selected, each provided with similar stove and gas-washing facilities. For a long period prior to the test both furnaces had operated with coke from washed coals, with similar operating results and characteristics. The

furnaces chosen for the test were Carrie No. 1 and Carrie No. 2, at Rankin, Pa., Carnegie-Illinois Steel Corporation. The essential dimensions are given in Table 10.

TABLE 10.—*Dimensions of Carrie Blast Furnaces Used in Test of Coke from Washed and Unwashed Coals*

Hearth diameter.....	22 ft. 6 in.
Bosh diameter.....	25 ft. 11 in.
Stockline diameter...	18 ft. 3 in.
Large bell diameter...	13 ft. 3 in.
Bosh angle.....	81° 0'
Inwall batter.....	1 3/4 in.: 12 in.
Total height.....	92 ft. 0 in.
Hearth area.....	397.6 sq. ft.
Total volume.....	33,023 cu. ft.

The initial test comprehended a two-months operation using coke from unwashed coals on one furnace while the companion furnace was operated with coke from washed coals. Since it was recognized that every furnace has certain individual characteristics contributing to its operating efficiency, which may change from time to time, and that identical furnace size and design does not necessarily furnish a guarantee of duplicate performance, a second test of two months duration was considered essential for check purposes, during which the type of coke was interchanged between the furnaces. Between the two test periods, one month was allowed for the adjustment and stabilization of operating practice, and some special tests were also made during this interim for the determination of the amount of coke fines inherent in the two different types of coke used. The following illustrates the test program:

Period	No. 1 Furnace	No. 2 Furnace
July and Aug..	Coke from unwashed coals	Coke from washed coals
September ..	Change-over and special tests	
Oct. and Nov.	Coke from washed coals	Coke from unwashed coals

The immediate common objective with both types of coke was the production of standard basic iron of similar chemical composition and equal uniformity, the aim

being to produce iron containing 1.10 per cent silicon and 0.030 per cent sulphur, normal to Carrie's practice. The test was so arranged as to introduce no variable other than the type of coke. Since the sulphur content of the coke made from unwashed coals is higher than that from washed coals, similar sulphur content of iron from the two blast-furnace units could be accomplished only through a change in slag volume or slag composition.

The required magnitude of the change in slag volume could be readily determined in advance with accuracy from the prescribed sulphur specification as well as the expected sulphur content of the slag, whose composition and sulphur-carrying power corresponded to those normally produced at Carrie when using coke from washed coals. However, the average sulphur content of coke was not the only factor affecting the adjustment in slag volume. Prior experience with coke from washed coals having indicated a marked improvement in regularity of coke composition, it was anticipated that coke made from unwashed coals would show greater variation in sulphur as well as ash content; the resultant adverse effect on chemical composition of iron could be offset only by a further increase in slag volume. This additional slag volume could be obtained either by the use of gravel or a greater proportion of siliceous ore than normally employed when using coke from washed coals. Since this ore was similar in physical characteristics to the other ores, no additional variable was introduced by its use. The additional slag volume was, therefore, obtained by a combination of both practices; i.e., using some gravel and more siliceous ores.

The burdens of miscellaneous materials with metallic content, such as open-hearth slag, excess scrap or scale, were substantially the same on both furnaces throughout the test, and blowing rates were held as constant as practicable, being varied only

within the limits imposed by the quality of coke.

First Blast-furnace Test Period

During the first test period, July and August, the performance of No. 2 furnace, using coke from washed coals, was markedly superior to the companion furnace, the iron production being greater by 51.6 tons per day, or 6.7 per cent and the coke consumption correspondingly decreased

coke from washed coals was characterized by greater uniformity of iron analysis, as indicated by fewer offcasts in silicon and sulphur. Principal data for the first test period appear in Table II.

Second Blast-furnace Test Period

During the second test period, covering October and November, the type of coke used on the two furnaces was reversed,

TABLE II.—*Comparative Blast-furnace Performance and Practice Data for First Two-months Test Period*

	Furnace Coke from		Effect of Washing	
	Unwashed Coals	Washed Coals	Amount	Per Cent
	No. 1 Furnace	No. 2 Furnace		
Coke analysis (dry basis), per cent:				
Ash	11 89	10 40	-1.49	
Sulphur	0 99	0 89	-0.10	
Fixed carbon	87 81	89 30	+1.49	
Day to day variations exceeding 0.30 per cent ash in coke, per cent.	55.7	18 9	-36.8	
Iron production, net tons per day.	769 0	820 6	+51 6	+ 6 7
Net coke rate, lb. per ton iron	1,931	1,774	-157	- 8.1
Flux rate, lb. per ton iron.	987	764	-223	-22 6
Calculated slag volume, lb. per ton iron.	1,285	1,048	-237	-18 4
Air blown, cu ft. per min. (carbon basis)	53,422	53,522	+100	+ 0 2
Blast pressure, lb. per sq. in.	19 3	17 8	-1 5	
Average iron analysis, per cent:				
Silicon.	1 12	1 14	+0 02	
Sulphur	0 028	0 028	0 00	
Casts over 1.40 per cent silicon, per cent.	8 75	8 04	-0 71	
Casts under 0.85 per cent silicon, per cent.	9. 09	4 55	-4 54	
Casts over 0.040 per cent sulphur, per cent.	6 40	4 90	-1 50	

157 lb., or 8.1 per cent. Similarly, this furnace operated with 22.6 per cent less flux and with 18.4 per cent less slag volume. Throughout the test No. 1 furnace, using coke from unwashed coals, operated with higher blast pressures than the companion furnace and was more difficult to control, requiring more drastic counteraction against furnace swings for restoration of normal operating conditions.

While the average silicon and sulphur produced in the iron from the respective furnaces for the two-months period was closely similar, the furnace operating with

No. 1 operating with coke from washed coals and No. 2 with coke from unwashed coals. No. 1 furnace showed an improved performance over the companion furnace, producing 74.7 tons more iron per day, or 9.4 per cent, and using 139 lb. less coke per ton of iron, or 7.4 per cent. This furnace required 17.5 per cent less flux and operated with a 12 per cent lower slag volume. During this period the blowing rate on No. 1 furnace was increased approximately 2.7 per cent over the companion furnace, a blowing rate permitted by the improved quality of the coke.

The furnace operating with coke from washed coals also demonstrated a marked superiority with respect to regularity of iron analysis, since only 1.00 per cent of the casts for this period exceeded 1.40 per cent silicon as opposed to 9.19 per cent for the companion furnace. Similarly, only 2.70 per cent casts exceeded 0.040 per cent sulphur compared with 5.78 per cent for the other furnace. Table 12 shows the results obtained during the second test period.

improvement was obtained on coke produced from washed coals. The increase in wind rate of 2.2 per cent permitted by coke from washed coals when comparing the two periods was unaccompanied by a similar increase when comparing the two periods using coke from unwashed coals. The coke consumption decreased for both grades of coke used during the second period, but the magnitude of the change is not sufficient to account for the difference in production

TABLE 12.—*Comparative Blast-furnace Performance and Practice Data for Second Two-months Test Period*

	Furnace Coke from		Effect of Washing	
	Unwashed Coals	Washed Coals		
	No. 2 Furnace	No. 1 Furnace	Amount	Per Cent
Coke analysis (dry basis), per cent				
Ash	11 85	10 33	-1 52	
Sulphur	0 98	0 88	-0 10	
Fixed carbon	87 85	89 37	+1 52	
Day to day variations exceeding 0.30 per cent ash in coke, per cent.	43 4	0	-43.4	
Iron production, net tons per day.	793.5	868 2	+74 7	+ 9 4
Net coke rate, lb. per ton iron	1,887	1,748	-139	- 7 4
Flux rate, lb. per ton iron	1,003	827	-176	-17.5
Calculated slag volume, lb. per ton iron	1,287	1,132	-155	-12 0
Air blown, cu. ft. per min. (carbon basis).	53,301	54,721	+1,420	+ 2.7
Blast pressure, lb. per sq. in.	19 4	19 2	-0 2	
Average iron analysis, per cent:				
Silicon.	1 14	1 05	-0 09	
Sulphur	0.029	0 028	-0 001	
Casts over 1.40 per cent silicon, per cent	9 19	1.00	-8 19	
Casts under 0.85 per cent silicon, per cent	8.16	7 72	-0 44	
Casts over 0.040 per cent sulphur, per cent.	5 78	2 70	-3.08	

*Comparison of Furnace Performance
on Same Grade of Coke during the
Two Periods*

Of considerable interest is the effect of uniformity of coke quality on blast-furnace performance. This is illustrated by a comparison of the results obtained on the same grade of coke for the two test periods, as shown in Table 13. Pig-iron production using coke from unwashed coals increased 3.2 per cent during the second period, compared with the first period when using similar coke, whereas a 5.8 per cent

performance, particularly in view of the change in other related factors. The distribution of iron analysis also improved during the second period, the magnitude of the improvement being greater on coke from washed coals.

There are three distinct differences between the periods: (1) the use of equivalent amounts of sinter in the second period; (2) the lower atmospheric moisture content in the second period; (3) a major improvement in the regularity of coke produced from washed coals and a more mod-

erate improvement in coke produced from unwashed coals, as subsequently illustrated. The use of 4.6 per cent sinter in the burden of both furnaces during the second

statistical study of coke-ash variability for the two periods, based on differences in day to day average ash content of the respective cokes, reveals the pronounced

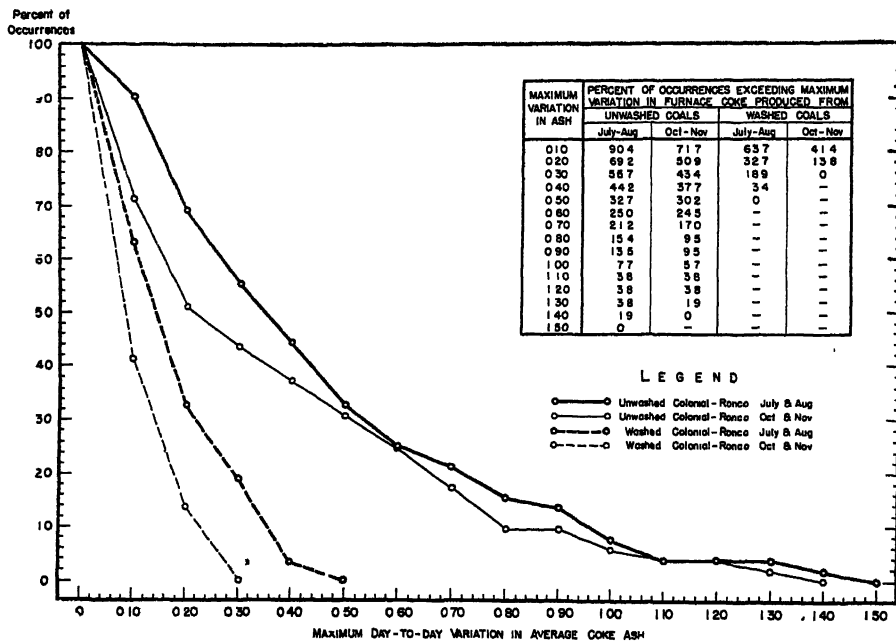


FIG. 2.—COMPARATIVE DAY TO DAY VARIATIONS IN AVERAGE DAILY ASH OF FURNACE COKE FROM WASHED AND UNWASHED COALS, CLAIRTON BY-PRODUCT COKE PLANT.

period could account for only a minor part of the relative improvement shown by both furnaces over the first period. While some operators may believe that some of the improvement is due to the lower atmospheric humidity during the second period, this does not explain the relatively greater improvement obtained during that period with coke from washed coals as opposed to coke from unwashed coals.

Since the differences in sinter charged and atmospheric humidity were common to the two grades of coke, it follows that by far the greater part of the general improvement in the second period must be credited to the greater uniformity of ash in coke produced from washed coals and the relatively moderate increase in uniformity of ash in the companion coke. A

improvement in ash uniformity of coke from washed coals over coke from unwashed coals and, of equal importance, shows improvement in uniformity of both grades of coke during the second test period. The data and graph shown in Fig. 2 demonstrate that the degree of improvement was far greater for coke from washed coals, as evidenced by the difference in number of occurrences exceeding a maximum day to day variation of 0.30 per cent coke ash. Occurrences exceeding this severity of variation decreased 12.3 per cent for coke from unwashed coals when comparing the second period with the first test period, whereas the improvement, on a similar basis, was 18.9 per cent for the coke from washed

coals; in fact, no such variations occurred in coke produced from washed coals.

The reduction in coke-ash variability logically not only explains the improved operating performance on both grades of coke during the October and November

coke discharge on a common conveyor for transfer to a common collecting bin. Since this arrangement did not permit separation of coke screenings produced at each unit during the test, both furnaces were operated on coke from washed coal during

TABLE 13.—*Comparison of Blast-furnace Performances*

	Coke from Unwashed Coals				Coke from Washed Coals			
	July, August	October, November	Difference		July, August	October, November	Difference	
			Amount	Per Cent			Amount	Per Cent
Coke analysis (dry basis), per cent:								
Ash.....	11 89	11 85	-0.04		10 40	10 33	-0.07	
Sulphur.....	0 99	0 98	-0.01		0.89	0.88	-0.01	
Fixed carbon.....	87 81	87 85	+0.04		89.30	89.37	+0.07	
Moisture.....	3 01	2 90	-0.11		2 90	2 86	-0.04	
Day to day variations exceeding 0.30 per cent ash in coke, per cent.....	55 7	43 4	-12 3		18.9	0	-18 9	
Sinter in ore and sinter burden, per cent.....	0	4 6	+4 6		0	4 6	+4.6	
Air blown, cu. ft. per min. (carbon basis).....	53,422	53,301	-121	-0.2	53,522	54,721	+1,199	+2 2
Blast temperature, deg. F.....	1,085	1,032	-53		1,116	1,080	-36	
Top temperature, deg. F.....	359	379	+20		414	388	-26	
Blast pressure, lb. per sq. in.....	19 3	19 4	+0.1		17.8	19 2	+1.4	
Moisture in air, grains per cu. ft.....	6 00	2.85	-3.15		6.00	2 85	-3.15	
Iron production, net tons per day.....	769 0	793 5	+24 5	+3 2	820 6	868 2	+47.6	+5 8
Net coke rate, lb. per ton iron.....	1,931	1,887	-44	-2 3	1,774	1,748	-26	-1 5
Flux rate, lb. per ton iron.....	987	1,003	+16	+1.6	704	827	+123	+17.6
Flue dust and sludge produced, lb. per ton.....	139	142	+3		158	123	-35	
Calculated slag volume, lb. per ton iron.....	1,285	1,287	+2	+0.2	1,048	1,132	+84	+8 0
Ratio bases to acids in slag.....	1.044	1.048	+0.004		1.024	1.035	+0.011	
Sulphur in slag, per cent.....	1.79	1.86	+0.07		1.81	1.83	+0.02	
Average iron analysis, per cent:								
Silicon.....	1.12	1.14	+0.02		1.14	1.05	-0.09	
Sulphur.....	0.028	0.029	+0.001		0.028	0.028	0	
Casts over 1.40 per cent silicon, per cent.....	8.75	9.19	+0.44		8.04	1.00	-7.04	
Casts under 0.85 per cent silicon, per cent.....	9.09	8.16	-0.93		4.55	7.72	+3.17	
Casts over 0.040 per cent sulphur, per cent.....	6.40	5.78	-0.62		4.90	2.70	-2.20	

period but may be interpreted as a primary factor in the greater magnitude of improvement in furnace performance on coke from washed coals in that period.

Determination of Coke Screenings

The coke-screening facilities at Carrie Nos. 1 and 2 blast furnaces are so arranged that the fines removed from the furnace

part of the interim period of September, and the coke screenings were determined. The total screenings recovered from both grades of coke at the blast furnaces during the four-months test period were known and the figure ascertained by the special test was used as a basis for determining the screenings produced from coke from washed coals. The screenings recovered

from coke from unwashed coals were obtained by difference. In all cases coke dust under $\frac{3}{4}$ in. was considered screenings. The essential data are shown in Table 14.

TABLE 14.—*Blast-furnace Coke Screenings Recovered at Carrie Blast Furnaces for Four-months Test Period*

	Furnace Coke from		Effect of Washing
	Unwashed Coals	Washed Coals	
Coke screenings:			
Per ton of coke, lb	59 3	42 5	— 16 8
Per ton of iron, lb	57 0	38 5	— 18 5
Coke required per ton of iron			Per Cent
Gross furnace coke	1,966	1,799	— 8 5
Net furnace coke.	1,909	1,760	— 7 8

Summary of Results at Blast Furnaces

Discussion of results obtained in the two separate periods confirms the need for duplicate checks such as were undertaken,

the year, therefore the composite of the four-months test, as shown in Table 15, represents a sound basis for evaluating the advantages of coke produced from washed coals. The following advantages were obtained by the use of such coke.

1. Daily iron production was increased 63.3 tons, or equivalent to 8.1 per cent.

2. Net furnace coke consumption was decreased 149 lb., or equal to 7.8 per cent.

3. Flux consumption was decreased 198 lb., or equal to 19.9 per cent, and slag volume was reduced 15.2 per cent.

4. A pronounced improvement was obtained in the regularity of pig-iron analysis.

In addition, an item of considerable importance is the fact that the increased yield of furnace coke of 3.0 per cent at the Clairton coke plant, combined with the subsequent reduction in coke requirements per ton of iron, means that less mined coal is required per ton of iron under such conditions than when using coke from

TABLE 15.—*Comparative Blast-furnace Performance and Practice Data for Composite Four-months Test Period*

	Furnace Coke from		Effect of Washing	
	Unwashed Coals	Washed Coals	Amount	Per Cent
Coke analysis (dry basis), per cent:				
Ash	11.87	10.36	— 1.51	
Sulphur	0.98	0.88	— 0.10	
Fixed carbon	87.83	89.34	+ 1.51	
Day to day variations exceeding 0.30 per cent ash in coke, per cent.	50.0	9.5	— 40.5	
Iron production, net tons per day	781.1	844.4	+ 63.3	+ 8.1
Net coke rate, lb. per ton iron	1,909	1,760	— 149	— 7.8
Flux rate, lb. per ton iron	995	797	— 198	— 19.9
Calculated slag volume, lb. per ton iron	1,286	1,091	— 195	— 15.2
Air blown, cu. ft. per min. (carbon basis)	53,362	54,129	+ 767	+ 1.4
Blast pressure, lb. per sq. in.	19.3	18.6	— 0.7	
Average iron analysis, per cent:				
Silicon	1.13	1.09	— 0.04	
Sulphur	0.029	0.028	— 0.001	
Casts over 1.40 per cent silicon, per cent.	8.97	4.45	— 4.52	
Casts under 0.85 per cent silicon, per cent.	8.63	6.17	— 2.46	
Casts over 0.040 per cent sulphur, per cent.	6.09	3.77	— 2.32	

and is indicative of differences in magnitude of benefits that may be obtained over an extended period. The periods involved reasonably approximate the average conditions that may obtain throughout

unwashed coals. In the former case 1,375 net tons of mined coal were required and in the latter 1,501, or a difference equal to 8.4 per cent less mined coal needed when using washed coals.

TABLE 16.—Comparative Blast-furnace Performance and Practice Data at Carrie Furnaces

	First Test Period July and August				Second Test Period October and November				Composite Test Period July, August, October and November			
	Coke from		Difference		Coke from		Difference		Coke from		Difference	
	Un- washed Coals	Washed Coals	Amount	Per Cent	Un- washed Coals	Washed Coals	Amount	Per Cent	Un- washed Coals	Washed Coals	Amount	Per Cent
Coke analysis (dry basis), per cent:												
Ash.....	11.80	10.40	-1.40		11.85	10.33	-1.52		11.87	10.36	-1.51	
Sulphur.....	0.99	0.89	-0.10		0.98	0.88	-0.10		0.98	0.88	-0.10	
Fixed carbon.....	87.81	89.30	+1.49		87.85	89.37	+1.52		87.83	89.34	+1.51	
Moisture.....	3.01	2.90	-0.11		2.90	2.86	-0.04		2.95	2.88	-0.07	
Day to day variations exceeding 0.30 ash, per cent.....	55.7	18.9	-36.8		43.4	0	-43.4		50.0	9.5	-40.5	
Burdens, lb. per ton iron:												
Group 3 ore.....	1,800	2,004	+204		2,744	2,840	+96		2,776	2,424	-352	
Group 7 ore.....	858	490	-368		507	398	-109		582	443	-139	
Beaver ore.....	959	972	+13		19	18	-1		486	481	-5	
Sintered fine dust.....	0	0	0		158	157	-1		80	80	0	
Pit under.....	26	20	-6		39	37	-2		33	31	-2	
Roll scale.....	51	51	0		57	53	-4		52	52	0	
Open-hearth slag.....	384	373	-11		349	405	+56		366	390	+24	
Excess scrap.....	5	2	-3		6	1	-5		5	5	0	
Gravel.....	43	4	-39		74	5	-69		58	4	-54	
Limestone.....	783	606	-177		749	618	-131		766	612	-154	
Dolomite.....	204	158	-46		254	209	-45		229	185	-44	
Production:												
Iron, net tons per day.....	769.0	820.6	+51.6	+6.7	793.5	868.2	+74.7	+9.4	781.1	844.4	+63.3	+8.1
Flue dust and sludge, lb. per ton iron.....	139	158	+19		142	123	-19		141	140	-1	
Consumption:												
Net coke, lb. per ton iron.....	1,931	1,774	-157	-8.1	1,887	1,748	-139	-7.4	1,909	1,760	-149	-7.8
Gross coke, lb. per ton iron.....	1,989	1,812	-177	-8.9	1,945	1,787	-158	-8.1	1,966	1,799	-167	-8.5
Flux, lb. per ton iron.....	987	764	-223	-22.6	1,003	827	-176	-17.5	995	797	-198	-19.9
Iron analysis, per cent:												
Silicon.....	1.12	1.14	+0.02		1.14	1.05	-0.09		1.13	1.09	-0.04	
Sulphur.....	0.028	0.028	0		0.029	0.028	-0.001		0.029	0.028	-0.001	
Cast iron.....	8.75	8.04	-0.71		9.19	1.00	-8.19		8.97	4.45	-4.52	
Cast iron.....	9.09	4.55	-4.54		8.16	7.72	-0.44		8.63	6.17	-2.46	
Cast iron.....	6.40	4.90	-1.50		5.78	2.70	-3.08		6.09	3.77	-2.32	
Slag:												
Analysis, per cent:												
Silica.....	34.80	34.34	-0.46		34.54	33.95	-0.59		34.67	34.15	-0.52	
Alumina.....	12.87	13.71	+0.84		12.93	13.79	+0.86		12.90	13.76	+0.86	
Lime.....	43.91	43.21	-0.70		43.51	43.73	+0.22		43.71	43.93	+0.22	
Magnesia.....	5.87	5.98	+0.11		6.22	6.70	+0.48		6.03	6.33	+0.30	
Sulphur.....	1.79	1.81	+0.02		1.86	1.83	-0.03		1.83	1.82	-0.01	
Ratio bases to acids.....	1.044	1.024	-0.020		1.048	1.035	-0.013		1.046	1.038	-0.008	
Calculated volume, lb. per ton iron.....	1,285	1,048	-237	-18.4	1,287	1,132	-155	-12.0	1,286	1,091	-195	-15.2
Practice:												
Air blown, cu. ft. per min. (carbon basis)	53,422	53,522	+100	+0.2	53,301	54,721	+1,420	+2.7	53,362	54,129	+767	+1.4
Blast pressure, lb. per sq. in.....	19.3	17.8	-1.5		19.4	19.2	-0.2		19.3	18.6	-0.7	
Blast temperature, deg. F.....	1,085	1,116	+31		1,032	1,080	+48		1,058	1,098	+40	
Top temperature, deg. F.....	359	414	+55		379	388	+9		368	402	+34	
Moisture in air, grains per cu. ft.	6.00	6.00	0		2.85	2.85	0		4.43	4.43	0	

The increase in production of iron and the reduction in coke rate shown in Table 15 can be attributed wholly to the improvement in quality of coke from washed coals.

improved production of iron and consumption of coke, but was also apparent in the improvement of the regularity of iron analysis, as shown by Figs. 3 and 4, repre-

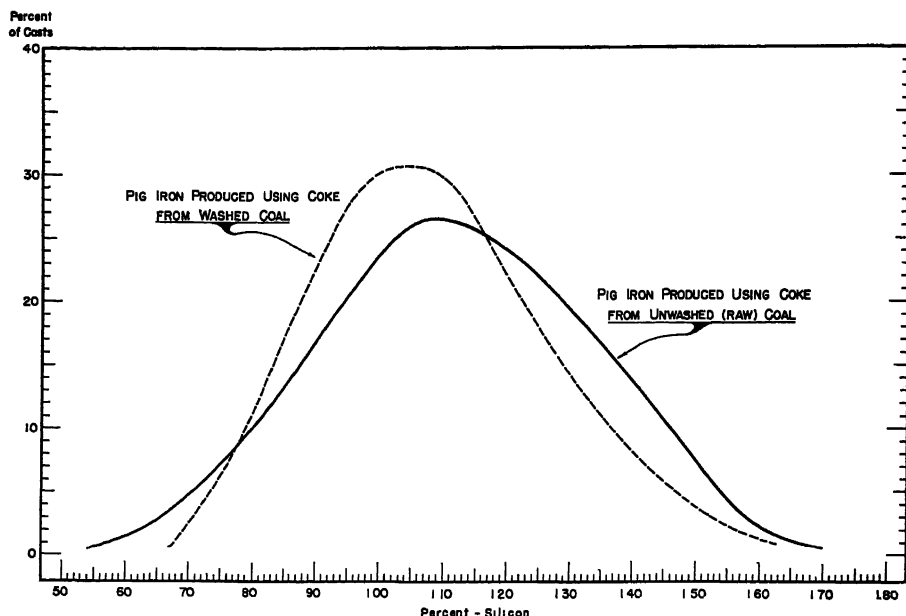


FIG. 3.—COMPARATIVE DISTRIBUTION OF SILICON IN PIG IRON PRODUCED USING FURNACE COKE FROM WASHED AND UNWASHED COALS, CARRIE FURNACES.

The decrease in amount and variability of ash and sulphur in coke and the improvement in physical coke quality, all of which permitted a reduction in flux consumption, slag volume and basicity, and marginal burden reserve, may be cited as major factors in decreasing the coke rate. The precise extent to which each of these factors contributed to the over-all result cannot be readily determined. No marked difference was noted in amount of flue dust produced, although we believe a more extended test would be required to determine accurately the true effect on that of several cokes tested. Complete data for the entire blast-furnace test period, including details relating to slag composition and burdens, appear in Table 16.

The effect of coke from washed coals on furnace operation was reflected not only in

senting distribution of silicon and sulphur analyses of the respective pig irons for the entire period. The fact that the average iron analysis over the entire test period was almost the same for all grades of coke, reflects creditably on the achievement of the blast-furnace operator charged with the responsibility of complying with the severely prescribed conditions under which the test was conducted.

Lower tuyere losses characterized operation with coke from washed coals and, further, the use of coke from washed coals permitted operation with a degree of freedom from irregularity impossible of attainment with coke from unwashed coals. It is difficult to convey adequately the importance of this factor by means of tabulations and graphs; nevertheless, the blast-furnace operator faced with various

production problems, many of which suddenly arise owing to unpredictable changes in raw materials, will regard this phase of the test as of the greatest significance.

CONCLUSION

The test was undertaken to determine on a practical plant scale the advantages accruing to blast-furnace operation by

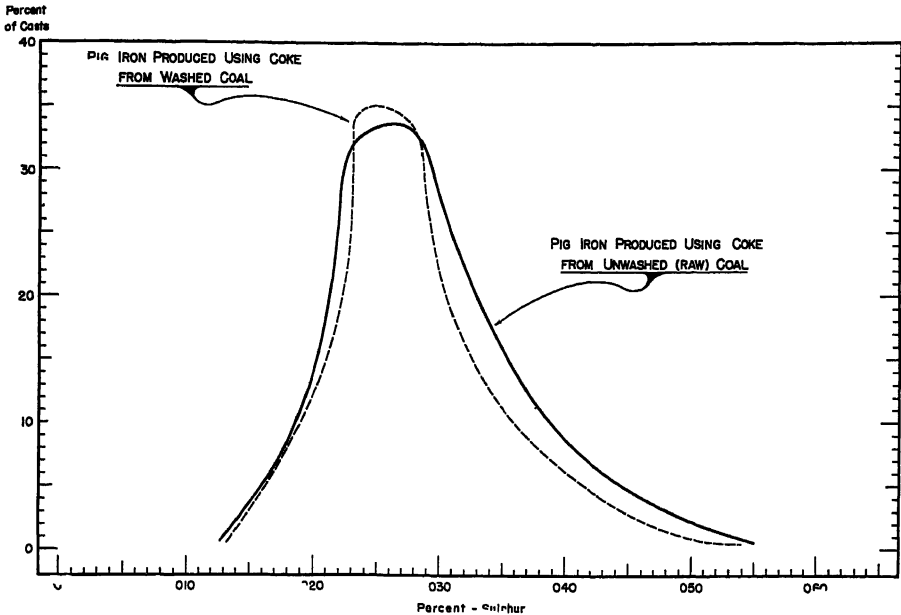


FIG. 4.—COMPARATIVE DISTRIBUTION OF SULPHUR IN PIG IRON PRODUCED USING FURNACE COKE FROM WASHED AND UNWASHED COALS, CARRIE FURNACES.

One word of caution appears to be in order. The benefits cited for washing the specific Pittsburgh seam coals under study do not apply to all coals or all conditions. While the test results closely agree with the blast-furnace operator's rule of thumb—that a decrease of 1.0 per cent in coke ash, above a certain minimum, permits an increase of 5.0 per cent in furnace production—the figures reported should not be applied without qualification to determine the desirability of washing metallurgical coals. The type of mining, the uniformity and grade of coal mined, the physical properties of coke, the degree of uniformity as well as amount of sulphur and ash, will all have a bearing on the magnitude of benefits to be derived from washing coals for furnace coke.

using coke produced from washed coals as compared with coke produced from unwashed coals. Since it was expected that the magnitude of these benefits would be pronounced, any unpredictable omissions or minor discrepancies that did result can well be disregarded in judging the value of washing the coals in question. In retrospect, we can recognize that detailed information might have been advantageously developed on some phases of this investigation to make this study a more truly technological effort, but we believe that these minor departures can have no bearing on the conclusions that follow from this investigation.

It is our belief that under the conditions outlined, the expected deterioration in quality of coking coals from the Pittsburgh

seam accelerated by extension of mine mechanization axiomatically involves coal washing, and that in some cases the potential advantages of mine mechanization cannot be fully realized without supplementing such practice with coal-washing facilities.

ACKNOWLEDGMENTS

The conduct of the test at the Clairton coke plant was under the direct supervision of Mr. D. P. Finney, Division Superintendent Coke Plant, Clairton Works, and the blast-furnace investigation at Carrie furnaces was the responsibility of Mr. C. P. Clingerman, Superintendent Blast Furnaces, Carrie Furnaces, Carnegie-Illinois

Steel Corporation. To them is due the credit for a truly fine accomplishment, since, thanks to their efforts, data permitting an unqualified conclusion on a problem of present-day importance was obtained.

We similarly wish to recognize the assistance of Mr. F. M. Becker, United States Steel Corporation of Delaware, who cooperated in many parts of the coke-plant test and was also responsible for the development of much of the data that appear in this report.

Appreciation is also expressed to various blast-furnace operators and other technologists of the subsidiary companies of United States Steel Corporation who assisted in various phases of this test.

The Role of Basic Slags in the Elimination of Phosphorus from Steel

BY RICHARD L. BARRETT* AND WILLIAM J. MCCAUGHEY,† MEMBER A.I.M.E.

(New York Meeting, February 1944)

FOR sixty years—in fact, ever since the inception of the basic steelmaking process—basic slags have been the subject of study by chemists, metallurgists and petrographers, with the purpose of providing a better understanding of the reactions between the slag and the metal during the refining process. The result of this work and of the researches of mineralogists and physical chemists into the chemistry of oxide systems is a considerable body of literature dealing not only with slags themselves but with equilibrium relationships in systems synthesized from pure components. Since any actual slag is a multicomponent system more complex than any yet worked out in the laboratory, a complete solution to the problem is still far away.

The writers have recently published a paper¹ which they believe sheds light on the role of the slag in the elimination of phosphorus and it is the purpose of the present paper to discuss the metallurgical applications of that work.

Since the pioneer investigations on the constitution of basic slags carried on by Stead and Risdale, Carnot and Richards, Hilgenstock and others in the 1880's, a considerable body of literature on this subject has appeared. Many of the more

important of these papers were summarized in the previous paper,¹ therefore they will not be reviewed here.

PETROGRAPHIC STUDY

The present writers have had occasion, over a period of years, to examine petrographically a great number of basic steel-making slags having a very wide range of chemical compositions and made under various conditions of operating practice. Although certain of these slags exhibit some unusual features, it is a remarkable fact that the great majority of mature slags show certain typical characteristics, which persist throughout the wide range of chemical compositions. The typical mature slag usually appears under the microscope to consist of two phases. The phase of primary crystallization is light colored and doubly refracting. If separated mechanically and subjected to chemical analysis, it is found to consist essentially of SiO_2 , CaO , and P_2O_5 . Sometimes, although not usually, two such silicate-phosphate phases are found. The other conspicuous phase is dark in color and optically isotropic, and occurs as the interstitial material between the grains of the light colored phase. This dark colored interstitial phase when analyzed is found to consist essentially of FeO , Fe_2O_3 , MnO , and MgO . In some slags high in iron oxide, particularly those from low-carbon heats, dicalcium ferrite is found. This phase is dark reddish brown in color and anisotropic.

Manuscript received at the office of the Institute Aug. 26, 1943. Issued as T.P. 1716 in METALS TECHNOLOGY, April 1944.

* Case School of Applied Science, Cleveland, Ohio.

† Ohio State University, Columbus, Ohio.

¹References are at the end of the paper.

If a slag of a given composition is compared with a synthetic preparation made from pure CaO , SiO_2 , and P_2O_5 in which these three components exist in the same ratio as in the slag, ordinarily we find that

believe that the study of the simplified three-component system would furnish a reliable guide to the complex multicomponent slag, at least as far as the reactions involving phosphorus are concerned.

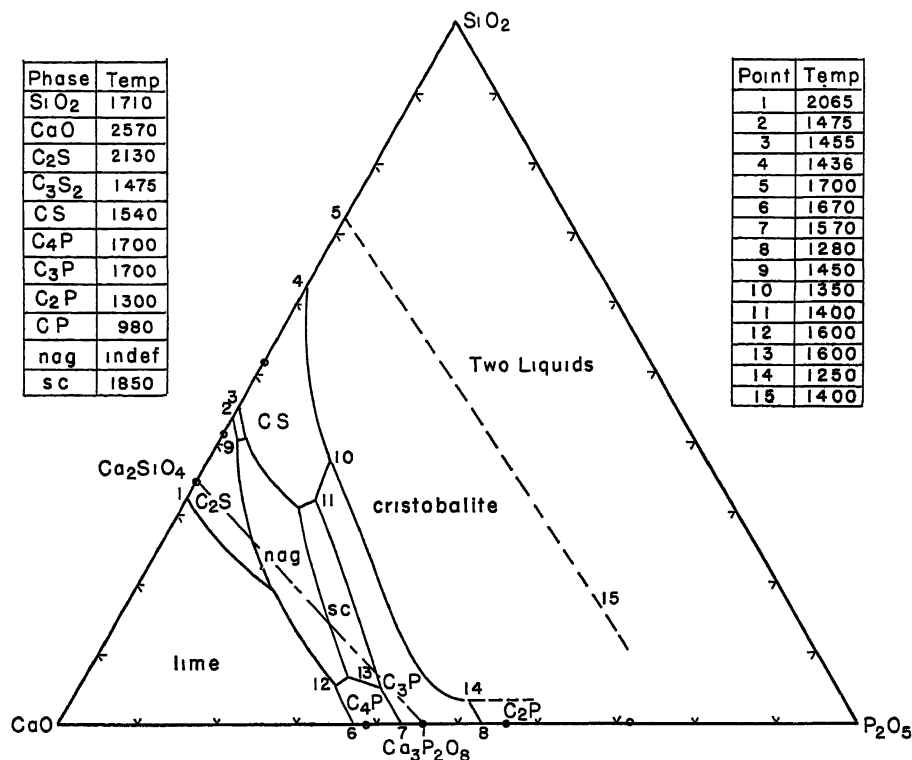


FIG. 1.—EQUILIBRIUM DIAGRAM FOR THE SYSTEM $\text{CaO-SiO}_2\text{-P}_2\text{O}_5$. TEMPERATURES ARE APPROXIMATE.

the phase of primary crystallization in the three-component melt can be identified as being the same as the light colored phase in the slag. It appears, then, that the equilibrium relationships in the mature slag follow very closely those in the pure system $\text{CaO-SiO}_2\text{-P}_2\text{O}_5$, and that the presence of FeO , Fe_2O_3 , MnO , and MgO , while it lowers the liquidus temperatures and may alter somewhat the form of the phase boundaries, does not essentially change conditions as far as the calcium silicophosphate reactions are concerned. This being the case, there is good reason to

Fig. 1 shows an equilibrium diagram for the greater part of the system $\text{CaO-SiO}_2\text{-P}_2\text{O}_5$, taken from the earlier paper.¹ This diagram presents a number of interesting aspects in connection with the study of basic slags. There are two ternary phases, which have compositions intermediate between those of dicalcium silicate and tricalcium phosphate. Since in basic slags CaO normally is present in sufficient amount to approximate or to exceed the orthosilicate ratio, this is the part of the diagram of principal interest in connection with the present problem. The light colored phases

found in basic slags of various types are dicalcium silicate, nagelschmidttite, silicocarnotite, tricalcium phosphate and tetracalcium phosphate. In the more acid portion of the equilibrium diagram, it is striking that cristobalite has a remarkably large field and that there is an extensive region of liquid immiscibility. It seems unlikely, however, that this part of the system applies to the slag problem, since R. A. Schoenlaub's work on the system $\text{CaMgSiO}_4\text{-CaMnSiO}_4\text{-CaFeSiO}_4$ indicates that where CaO is insufficient to equal the orthosilicate ratio, MgO , MnO , and FeO enter into combination with silica.

SOLID SOLUTION OF CALCIUM SILICATES AND PHOSPHATES

A number of years ago the writers, in the course of a petrographic examination of some basic open-hearth slags, noticed that the principal light colored phase had optical properties similar to those of beta dicalcium silicate except that the indices and birefringence were abnormally low. Some time later, A. T. Cape made the suggestion that the phosphorus in the slag might be carried in solid solution in the silicate phase, thus altering the optical properties of the latter. This suggestion was confirmed by H. C. Lee by a chemical analysis of dicalcium silicate from an open-hearth slag, which showed it to contain phosphorus. Since this phenomenon appeared to have an important bearing on the slag problem, the present writers made an investigation of the extent of solid solution between calcium silicates and phosphates, part of the result of which is shown in Fig. 2. This diagram shows the probable equilibrium conditions in the two-component system whose end members are dicalcium silicate and tricalcium phosphate. The two ternary phases, nagelschmidttite and silicocarnotite, whose fields of primary crystallization are shown in Fig. 1, have compositions that lie on this binary. Liquidus temperatures shown in this dia-

gram are approximate, since the temperatures are too high for accurate determination by available methods. In any case, in a slag the presence of additional components certainly lowers melting temperatures. The significant fact about the diagram is the great degree to which solid solution prevails in all four phases. Throughout three fourths of the range of compositions, only single phases exist. The extent to which each of these phases has variable composition may be defined by giving its homogeneity range, or the limits of composition within which only a single homogeneous crystal phase may exist.

Since slag analyses usually are expressed as oxides, the homogeneity range of these phases may be conveniently expressed in terms of the ratio $\text{P}_2\text{O}_5/\text{P}_2\text{O}_5 + \text{SiO}_2$ calculated by weight. As shown in Fig. 2, dicalcium silicate may contain up to 10 per cent P_2O_5 . The homogeneity ranges of the four phases, expressed in the form of the ratio $\text{P}_2\text{O}_5/\text{P}_2\text{O}_5 + \text{SiO}_2$, are as follows: dicalcium silicate from 0.0 to 0.27, nagelschmidttite from 0.31 to 0.58, silicocarnotite approximately from 0.71 to 0.80, and tricalcium phosphate approximately from 0.89 to 1.00. This extensive solid solution readily explains why in most mature slags only one light colored phase, which is composed of CaO , SiO_2 and P_2O_5 , appears. This solid solution appears to be of the substitution type with PO_4 groups substituting for SiO_4 groups, and vice versa. Solid solution in any of the phases in this system other than the four having the orthosilicate ratio is very limited in extent. It appears then that when there is enough CaO present to combine with all of the SiO_2 and P_2O_5 in the orthosilicate ratio these two components are almost completely interchangeable and the bonding between them and CaO is of a similar type regardless of the $\text{P}_2\text{O}_5/\text{P}_2\text{O}_5 + \text{SiO}_2$ ratio. This fact appears to be of major importance in the elimination of phosphorus from steel. Another significant feature of the diagram

is the sharp decline in liquidus temperatures as the ratio $P_2O_5/SiO_2 + P_2O_5$ increases. Where the prevailing practice involves the use of slags high in P_2O_5 , as in the Birming-

ham, Alabama, district for example, a lower temperature is effective in getting the lime and the silicate phase completely dissolved in the slag, and the lower working temperature probably is more favorable to long roof life than is the usual northern practice.

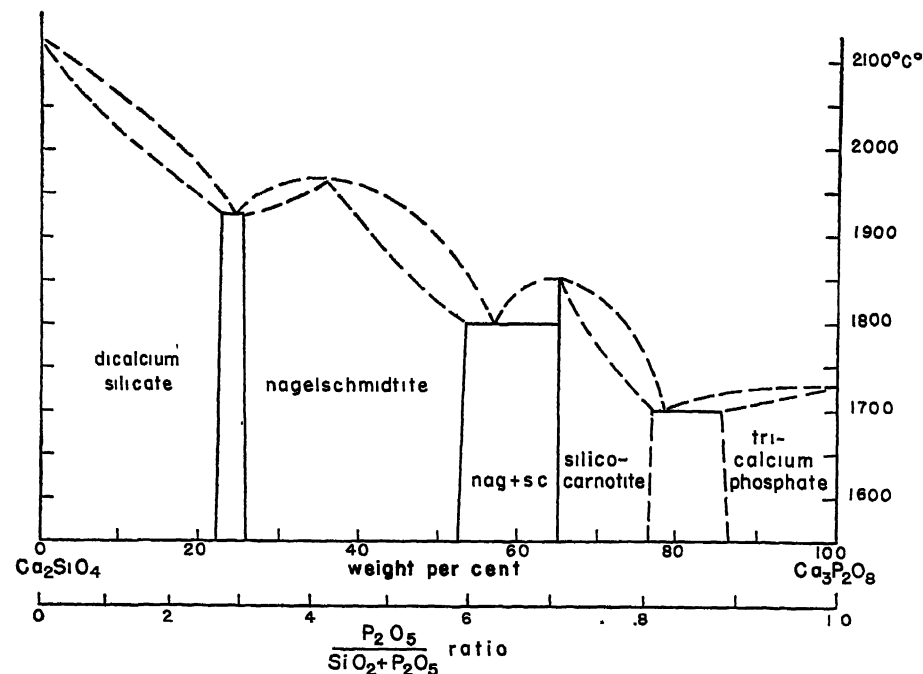


FIG. 2.—PROBABLE EQUILIBRIUM RELATIONSHIPS IN THE SYSTEM Ca_2SiO_4 - $Ca_3P_2O_8$. TEMPERATURES ARE APPROXIMATE.*

Extensive solid solution exists in all four solid phases.

ham, Alabama, district for example, a lower temperature is effective in getting the lime and the silicate phase completely dissolved in the slag, and the lower working temperature probably is more favorable to long roof life than is the usual northern practice.

Fig. 3 shows the compositions of a number of basic steelmaking slags plotted in terms of the three components CaO , SiO_2 and P_2O_5 . In this diagram all compositions

on the right side of the triangle and are represented within the diagram by triangular sectors. We may expect that the nature of the light colored phase to be found in each of these slags will depend upon which sector it lies within. Microscopic and X-ray study of the actual slags confirms this supposition.

MINERALOGICAL CONSTITUTION OF SLAG

The significance of the mineralogical constitution of the slag is clarified if the changes that take place during the progress of a typical open-hearth heat are traced. Furnaces in the Ohio Valley district operate on pig made from Lake Superior ore, the pig having a phosphorus content of

*Two recent papers^{1,2} present equilibrium diagrams for this system. They differ in certain respects from our diagram and from one another, but the points of difference do not materially affect the conclusions of this paper. Both of these interpretations, like our own, are admittedly diagrammatic and based upon incomplete data. There is rather general agreement among the three diagrams regarding the phases present and their solid solubility ranges.

around 0.2 per cent.* The resultant slag when in a mature condition has a P_2O_5/SiO_2 ratio between 0.10 and 0.25. In the early stages of the heat, however,

FeO , MnO , and MgO and relatively low in CaO . These meltdown slags fall largely within the system monticellite-glaucocroite-calcium fayalite ($CaMgSiO_4$ - Ca -

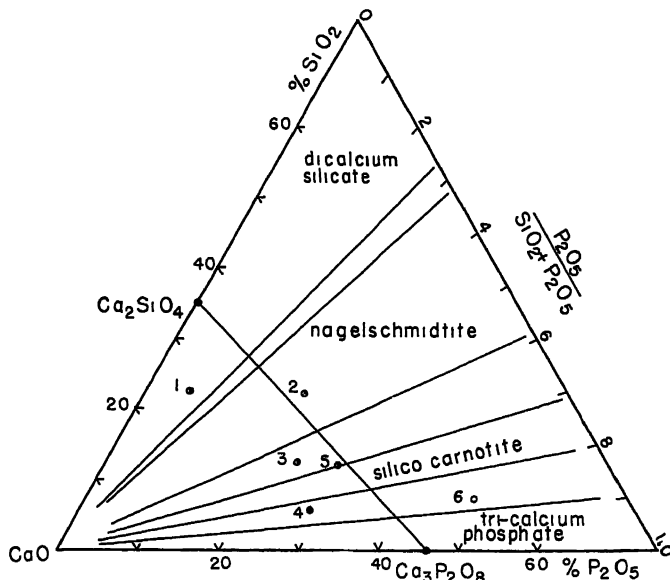


FIG. 3.—PROPORTIONS OF CaO , SiO_2 , AND P_2O_5 IN CERTAIN SLAGS AND THE LIMITING $P_2O_5/SiO_2 + P_2O_5$ RATIOS OF THE IMPORTANT SILICOPHOSPHATE PHASES.

No. 1. Typical open-hearth slag from the Mahoning Valley district. Light colored phase in this slag is dicalcium silicate.¹

No. 2. British open-hearth slag. Light colored phase is nagelschmidite.

No. 3. Open-hearth slag from the Birmingham district, Alabama, of which a photomicrograph is shown as Fig. 4. Light colored phases are nagelschmidite and silicocarnotite.

No. 4. German basic bessemer slag reported by Schneiderhöhn.⁴ Light colored phases tetra-calcium phosphate and silicocarnotite.

No. 5. Slag from same furnace as No. 4 but with sand added to converter to increase citrate solubility of slag. Light colored phase is silicocarnotite.

No. 6. Experimental electric-furnace slag of very high phosphorus content. Light colored phase is largely low-temperature form of tricalcium phosphate.

the slag has a composition quite different from that in the mature condition. This early slag is very fluid and is high in SiO_2 ,

* In many American mills the practice has arisen of charging open-hearth slag, particularly from low-carbon heats, into the blast furnace. The result is to increase the phosphorus content of the pig, the amount in present practice not usually exceeding 0.6 per cent. This is essentially a conservation measure and serves not only to recover iron from the open-hearth slag but to recover alloying agents that otherwise would be lost. Increased adoption of this practice would lead to the production of open-hearth slags of higher phosphorus content, perhaps approaching the type common in Europe.

$MnSiO_4$ - $CaFeSiO_4$). R. A. Schoenlaub has studied this system and has found that a continuous series of solid solutions exists between these end members; that the melting temperatures range from 1240° to $1500^\circ C.$ and that the solid solution of $Ca_3P_2O_8$ in this system varies between a maximum of 6 per cent and a minimum of 1 per cent.

The meltdown slag is sometimes referred to as a glaucocroite type, or a monticellite type. Since a complete series of solid solutions exists in this system, the use of one

or another of these terms may imply a distinction without a difference. The significant thing is that the iron and manganese oxides are combined with SiO_2 and CaO in the form of calcium fayalite (CaFeSiO_4) and glauchochroite (CaMnSiO_4). In this stage the slag is low in calcium oxide and is very fluid, and its temperature is considerably above the liquidus. During this stage the greater part of the limestone charged into the furnace is still in the solid state either underlying the bath on the bottom of the furnace or as large lumps of stone floating in the bath. The lime combines readily with silica from the slag to form dicalcium silicate, which, while it slowly goes into solution in the slag, at first forms a coating over the limestone lumps and prevents ready access of the slag to the mass of the lime. Many limestones, however, have a tendency to spall under these conditions, which causes continued exposure of fresh surfaces of the stone to the action of the slag. Limestones that are porous or do not exhibit a spalling tendency may become so heavily covered by this protective coating of dicalcium silicate that the progress of the heat is seriously retarded. This is one reason why limestones that may be satisfactory from the standpoint of chemical analysis may be unsuitable for open-hearth use. As the lime content of the liquid increases, the liquidus temperature is greatly raised, and although the temperature of the slag may be increasing it loses the high degree of superheat that it possessed during the meltdown stage.

The increase in CaO content of the slag causes a major change in its mineral constitution. Dicalcium silicate is formed, a considerable part of which may remain in the crystalline state for some time. The oxides of iron, manganese, and magnesium are no longer combined with silica and may be thought of as existing in an uncombined condition. It is during this stage that the

phosphorus content of the bath is most rapidly lowered.

REMOVAL OF PHOSPHORUS

The removal of phosphorus from the bath is the result of an oxidation reduction reaction:



It is a matter of common observation in the open hearth that the progress of this reaction is profoundly modified by variations in the composition of the slag. In all probability, the effect is a complex one and involves various factors. In pointing out the importance of slag constitution it is not implied that other factors such as viscosity may be ignored as negligible.

The increasing CaO content of the slag may be considered to affect the reaction between P and FeO in two ways. In the first place, by combining preferentially with silica, CaO releases FeO , which then is free to react with P . In the second place, by combining with one of the products of the reaction, P_2O_5 , CaO serves to promote progress of the reaction toward the right. It is customary to refer to the product of this combination of CaO with P_2O_5 as tricalcium phosphate, $\text{Ca}_3\text{P}_2\text{O}_8$. However, it is not necessary to suppose that tricalcium phosphate as such exists in the slag as a molecular species. As Fig. 2 shows, two ternary compounds, nagelschmidite and silicocarnotite, have compositions intermediate between dicalcium silicate and tricalcium phosphate. These two compounds, along with tricalcium phosphate itself, may be thought of as analogs of dicalcium silicate derived from it by the substitution of PO_4 groups for SiO_4 groups with the omission of one Ca ion for each such group substituted. Since dicalcium silicate itself can contain up to 10 per cent P_2O_5 in solid solution, it constitutes a stable compound of CaO , SiO_2 and P_2O_5 . As a matter of fact, since dicalcium silicate containing P_2O_5 does not invert to the low-

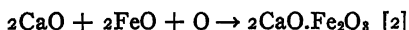
temperature form, it may be considered to be more stable than the pure compound.

Thus, insofar as the elimination of phosphorus is concerned, the important function of CaO is to promote formation of a stable compound containing P_2O_5 , which will not be readily reduced in contact with metallic iron and is relatively stable in such an environment.

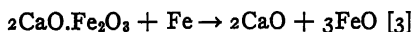
In the later stages of the heat, lime and iron ore are usually added, the former to control the basicity of the slag and the latter to increase the oxidation of the bath. In American practice it is customary to build up the CaO content of the slag to a considerable excess over the orthosilicate ratio.

An excess of CaO in the slag over that required to combine with the silica and the P_2O_5 is probably necessary in the basic process. The presence of this additional CaO with FeO provides a mechanism for the transfer of oxygen from the furnace atmosphere through the slag to the bath. Iron oxide can be preserved in the higher stage of oxidation even at high temperatures if the iron oxide is combined with the CaO to form ferrites, such as dicalcium ferrite ($2CaO.Fe_2O_3$). This compound is found frequently in well matured slags formed on low-carbon heats, such as open heats or ingot-iron heats.

The reaction calling for oxygen transfer is that taking place at the slag-atmosphere interface; i.e.,



The dicalcium ferrite so formed diffuses through the slag and at the slag-bath interface reaction 3 takes place:



Part of the FeO formed at the metal contact dissolves in the bath and oxidizes the metalloids molecularly dissolved in the bath as indicated by Eq. 1.

Reactions 2 and 3 take place in the slag and reaction 1 in the bath.

The increasing amounts of iron oxide found in the slag during the progress of the heat indicate that the reactions of oxidation of iron into slag exceeds the reduction of iron oxide in the bath by the metalloids.

In certain English and Canadian mills where ores higher in phosphorus are used, slags are produced having a $P_2O_5/P_2O_5 + SiO_2$ ratio of around 0.4 or 0.5. The development of these slags is similar to that just described except that when the CaO content approaches the orthosilicate ratio nagelschmidtite is produced. As previously pointed out, this phase may be thought of as an analog or substitution product of dicalcium silicate. Although it bears a striking resemblance to the latter, it can be readily distinguished by optical or X-ray methods. No. 2 on Fig. 3 represents such slag, and the material originally described by Nagelschmidt was separated from a slag of this type.

On the continent of Europe ores still higher in phosphorus are the rule and open-hearth slags having a $P_2O_5/P_2O_5 + SiO_2$ ratio of around 0.7 may be produced. As CaO goes into solution in these slags, silicocarnotite is produced. This is true also in the Birmingham, Alabama, district, although there the $P_2O_5/P_2O_5 + SiO_2$ ratio may be slightly lower and both nagelschmidtite and silicocarnotite may appear in the slag. Fig. 4 shows a photomicrograph of a thin section of an Alabama slag that shows both phases. The phases are readily distinguished by the pronounced difference in birefringence, which causes silicocarnotite to appear in the photograph as white and nagelschmidtite as medium gray.

Steel has been produced, at least experimentally, from ferrophosphorus, with a slag having a $P_2O_5/P_2O_5 + SiO_2$ ratio higher than 0.85. The light colored phase in this slag was principally the low-temperature form of tricalcium phosphate, which is the equivalent of the natural mineral whitlockite.

In the basic bessemer, or Thomas process, employed very largely in Europe, slags having a $P_2O_5/P_2O_5 + SiO_2$ ratio above 0.8 are produced as a routine matter. Higher



FIG. 4.—THIN SECTION OF REMELTED OPEN-HEARTH SLAG FROM BIRMINGHAM DISTRICT, ALABAMA (No. 3 IN FIG 3). ABOUT $\times 75$. CROSSED NICOLS.

Gray grains are nagelschmidtite, white grains silicocarnotite. Background is dark colored interstitial phase

CaO contents are employed there, causing the formation of tetracalcium phosphate. Slags so high in phosphorus can profitably be utilized as fertilizers, consequently the availability of the phosphorus for the use of plants is an important consideration. Available phosphorus usually is defined as the portion that can be dissolved in a 2 per cent citric acid solution. Since both whitlockite and tetracalcium phosphate have lower citrate solubilities than silicocarnotite, it is desirable to reduce the $P_2O_5/P_2O_5 + SiO_2$ ratio so that silicocarnotite is formed. This is done by adding sand to the converter. This is a matter of producing a salable by-product, however, rather than of steelmaking. From the foregoing evidence it would appear that steel can be produced just as successfully with slags having the higher $P_2O_5/P_2O_5 + SiO_2$ ratios.

There is, however, another consideration that is important where slags are to be sold as fertilizer. The common practice of

adding fluorspar to reduce the viscosity of the slag is disastrous to the utilization of phosphorus by plants. The presence of the fluorine ion causes the formation of apatite, which is a highly stable mineral with a low citrate solubility; consequently the use of fluorspar must be avoided if the availability of the phosphorus for plants is an important consideration.

Thomas, the father of the basic steel-making process, is supposed to have remarked that any amount of phosphorus would be removed from iron if the slag were made basic enough. Although other factors may be involved, it appears that the basis for this important fact is to be sought in the mineral constitution of the slag. The required condition is that a stable compound of CaO , SiO_2 and P_2O_5 shall be produced in the slag, the formation of which will promote the continued oxidation of phosphorus. This condition is attained when the CaO content of the slag approaches and exceeds the orthosilicate ratio. The particular compound formed depends upon the $P_2O_5/P_2O_5 + SiO_2$ ratio, as shown in Fig. 3. Dicalcium silicate, nagelschmidtite, silicocarnotite, and tricalcium phosphate all fulfill the required condition. Since the substitution of PO_4 for SiO_4 is confined for practical purposes to compounds having the orthosilicate ratio, the necessary conditions are attained only when the slag is sufficiently basic. In American practice it is usual to employ an "excess" of lime for reasons already discussed. In this connection, however, it should be noticed that CaO plays a part in the elimination of sulphur and in other phenomena not considered in this paper

REFERENCES

1. R. L. Barrett and W. J. McCaughey. The System $CaO-SiO_2-P_2O_5$. *Amer. Mineralogist* (1942) 27, 280.
2. G. Tromel *Stahl und Eisen* (1943) 63, 21
3. M. A. Bredig: *Amer. Mineralogist* (1943) 28, 594.
4. H. Schneiderhohn. *Stahl und Eisen* (1929) 49, 345.

DISCUSSION

(H K Work presiding)

M A BREDIG,* New York, N. Y.—The authors have presented an interesting review of the reaction mechanism by which phosphorus is eliminated from steel in basic slags. A somewhat different equilibrium diagram of the system $\text{CaO-SiO}_2\text{-P}_2\text{O}_5$ has recently been proposed by the writer. Since, in a sense, this new diagram is considerably simpler at the steel-melting temperatures—although, at lower temperatures, the new relationships between the solid phases are somewhat more complex—it is thought to be of sufficient interest to be briefly discussed.

In the temperature range above 1600°C . (2900°F), covered by the binary diagram, Fig. 2, only two solid phases, instead of four, are assumed by the writer to occur in equilibrium with the liquid phase (Fig. 5); namely, simply the high-temperature phases (alpha) of both components, tricalcium phosphate and dicalcium silicate. The phase called "nagelschmidtite" by Barrett and McCaughey, and previously considered as a ternary compound $7\text{CaO} \cdot 2\text{Si}_2\text{P}_2\text{O}_8$, was shown by the writer⁵ to be a solid solution of $\text{Ca}_3\text{P}_2\text{O}_8$ in a new hexagonal high-temperature form of Ca_2SiO_4 , which had not been known before, but lately was confirmed by K. T. Greene.⁶ The structure is one common to the high-temperature modifications of various compounds of the type $A_2\text{XO}_4$, such as Na_2SO_4 , K_2SO_4 , CaNaPO_4 , CaKPO_4 , and others.

Since even preparations as high in phosphate content as silicocarnotite, $5\text{CaO} \cdot \text{SiO}_2 \cdot \text{P}_2\text{O}_5$ (more than 70 weight per cent $\text{Ca}_3\text{P}_2\text{O}_8$), possess this simple hexagonal structure when quenched from above 1300°C . (2350°F .), the area of this new high-temperature form of dicalcium silicate (alpha) must, at the high temperatures, be extended across the concentration range of even silicocarnotite to an area in which alpha tricalcium phosphate is second phase. No ternary compounds can exist, therefore, in equilibrium with the liquid

in the system $\text{Ca}_2\text{SiO}_4\text{-Ca}_3\text{P}_2\text{O}_8$. In the diagram of the ternary system $\text{CaO-SiO}_2\text{-P}_2\text{O}_5$ (Fig. 1) the fields of primary solidification of "nagelschmidtite," of silicocarnotite and of " C_2S " (dicalcium silicate) are to be replaced by one single area (alpha C_2S) indicating the field of hexagonal, alpha, dicalcium silicate (solid solutions).

Silicocarnotite, as well as orthorhombic dicalcium silicate, actually is a product of transformation, in the solid state at lower temperatures, of the hexagonal phase. This lower temperature range is shown in Fig. 6. In accordance with recent data, some transformation temperatures are chosen somewhat different from the writer's previously published schematic diagram,^{5c} which, like Figs. 5 and 6, was not intended to give more than qualitative, or semiquantitative, information.

In Fig. 6 the existence of a dicalcium silicate phase (alpha prime) is indicated, which apparently was not recorded by the authors. In the range below 21 weight per cent $\text{Ca}_3\text{P}_2\text{O}_8$, they have reported one orthorhombic dicalcium silicate phase only, probably beta Ca_2SiO_4 , besides gamma, the lowest-temperature form. The additional phase alpha prime, isotypic with orthorhombic beta K_2SO_4 , and observed by the writer as well as by G. Trömel³ (phase K), appears to be so similar in its optical properties to the other, better known, orthorhombic beta form of dicalcium silicate that it can be identified by X-ray diffraction only.

The alpha prime phase is thought by the writer to be also represented by a preparation $23\text{CaO} \cdot \text{K}_2\text{O} \cdot 12\text{SiO}_2$, obtained by W. C. Taylor,⁷ who described its optical properties as very closely resembling those of beta dicalcium silicate. X-ray data indicate that the mineral merwinite, $3\text{CaO} \cdot \text{MgO} \cdot 2\text{SiO}_2$, may also simply be a solid solution of Mg_2SiO_4 in alpha prime dicalcium silicate.

The writer agrees with the authors in that the proposed modifications of the equilibrium diagrams—though of considerable importance—do not materially affect the conception of the process of elimination of phosphorus from steel, except that they permit one to think very simply in terms of essentially one solid phase only, in equilibrium with the liquid slag—namely, of hexagonal alpha dicalcium silicate.

⁷ W. C. Taylor: *Jnl. of Research*, Nat. Bur. Stds. (1941) 27, 311-323.

* Vanadium Corporation of America.

⁵ M. A. Bredig: (a) *Jnl. Amer. Chem. Soc.* (1941) 63, 2533; (b) *Jnl. Phys. Chem.* (1942) 46, 747-764; (c) *Amer. Mineralogist* (1943) 28, 594-601.

⁶ K. T. Greene: *Jnl. of Research*, Nat. Bur. Stds. R.P. 1570 (Jan. 1944).

in which numerous SiO_4 ions can be replaced by PO_4 ions. The complications, to the petrographer, or X-ray crystallographer, who observes three, or four, or even more, different

upon his idea of a structural analogy between some of the phases in this system and the high-temperature and low-temperature phases of K_2SO_4 . This in turn seems to be based upon the

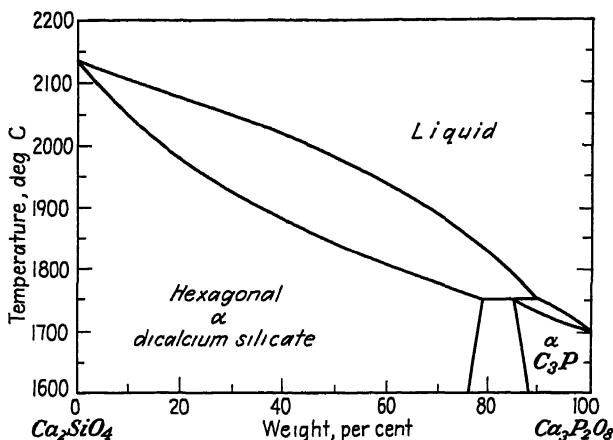


FIG. 5.

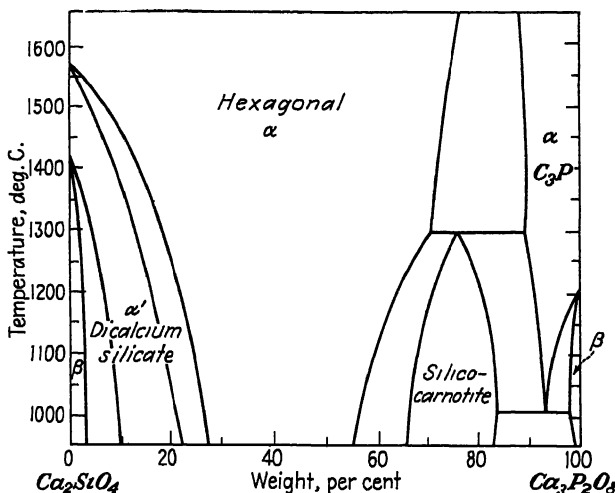


FIG. 6.

silicate-phosphate phases, depending on the composition of the slag, are solely due to the described transformations, in the solid state, at comparatively low temperatures during cooling

R. L. BARRETT AND W. J. MCCAUGHEY (authors' reply) —Bredig's interpretation of the equilibrium relationships in the system Ca_2SiO_4 - $\text{Ca}_3\text{P}_2\text{O}_8$ appears to rest primarily

evidence of X-ray powder diffraction patterns. In our opinion, this interpretation needs confirmation. At the same time, we do not wish to claim finality for our own interpretation, particularly with respect to the form of the liquidus.

One question of fact needs to be cleared up. We have not stated that beta Ca_2SiO_4 is orthorhombic, as Bredig says. Single crystals of this phase (with $\text{Ca}_3\text{P}_2\text{O}_8$ in solid solution)

have been obtained from casts of open-hearth slags. These single crystals are prismatic in form and have an extinction angle up to 7° from the axis of elongation, which would indicate that phase to be monoclinic.

In considering the application of this system to open-hearth slags, it must be kept in mind that the presence of additional components in the slag materially affects the equilibrium relationships. The presence of certain components often produces metastable conditions and structural compounds are formed that ordinarily are not present. For instance, in high-alumina systems containing SiO_2 and Na_2O , beta alumina is formed instead of corundum.

Similarly, in the system $\text{Li}_2\text{O} \cdot \text{Al}_2\text{O}_3 \cdot \text{SiO}_2$, gamma alumina crystallizes in octahedrons instead of the hexagonal corundum. A chemical analysis of the gamma alumina crystallizing from melts in system $\text{Li}_2\text{O} \cdot \text{Al}_2\text{O}_3 \cdot \text{SiO}_2$ contain only a small fraction of one per cent of Li_2O .

The phase equilibrium as worked out by us is in agreement essentially with phases identified in the examination of many open-hearth slags by X-ray and petrographic methods. This evidence leads us to believe that beta Ca_2SiO_4 , nagelschmidite and silicocarnotite all occur in the equilibrium associated with basic open-hearth steel slags.

The Relative Deoxidizing Power of Boron in Liquid Steel and the Elimination of Boron in the Open-hearth Process

By R. W. GURRY*

(New York Meeting, February 1944)

THERMODYNAMIC calculations indicate that boron is a better deoxidizer than silicon but probably is not quite as effective as aluminum. Boron should, therefore, be readily oxidized out of the open-hearth bath, which implies that it is not recovered in significant concentration from any scrap charged; also that, if added in the ladle, it tends to oxidize out during teeming unless protected by the presence of a better deoxidizing agent. These conclusions do not apply to liquid cast iron, in which the oxygen content is much lower than in liquid steel.

The possibility of conserving certain strategic alloying elements widely used in steelmaking, notably manganese, chromium and molybdenum, by the use of boron, which in small concentration appears to be extraordinarily effective in promoting hardenability, raises a question as to what extent any boron present in the scrap charged into the open hearth is oxidized out during melting and subsequent refining. This question is significant because the optimum concentration of boron in the finished steel, which is fairly critical, would be very difficult to attain if the boron in the charge were largely retained in the metal. Moreover, unless boron is substantially eliminated in the open-hearth process its use on a large scale would eventually make it impossible to produce boron-free steel

except by restricting the charge to virgin material.

There is at present, unfortunately, virtually no satisfactory direct evidence to provide an answer to this question; but there are indications from practice that boron is oxidized out in the open hearth in the production of medium or low-carbon steel, although it may be retained if the carbon content remains fairly high; that is, if the oxygen is kept fairly low.

In the absence of direct data, it is necessary to rely upon the indications of indirect evidence, the best approach now available being a thermodynamic calculation of the deoxidizing power of boron in liquid steel by the general method used so successfully by Chipman¹ in his study of the reactions in the open-hearth process. The thermal data for boron, upon which such a calculation must be based, are reasonably satisfactory; the only quantities not directly determined are the entropy of melting of boron, the activity coefficient of boron in liquid steel, and the activity coefficient of B_2O_3 in an open-hearth slag; but these values may be estimated with ample accuracy.

The results of this calculation, which is presented later, are given in Table I, together with corresponding data for other deoxidizing elements. This table shows the calculated residual content of oxygen in equilibrium with different residual concentrations of the deoxidizer in the metal;

Manuscript received at the office of the Institute July 16, 1943. Issued as T.P. 1641 in METALS TECHNOLOGY, December 1943.

* Research Laboratory, U. S. Steel Corporation, Kearny, New Jersey.

¹ References are at the end of the paper.

thus, for a given residual concentration of deoxidizer, the lower the residual oxygen content, the greater the deoxidizing power of the element in question. These data show beyond doubt that boron is a fairly effective deoxidizer for iron and should therefore be almost entirely removed during the open-hearth process; more specifically, the deoxidizing power of boron is greater than that of silicon, vanadium or titanium, and approaches that of zirconium or aluminum. This is not surprising when it is considered that boron and aluminum occupy adjacent positions in the third column of the periodic system. It should also be noted that the assumptions made in the calculations tend in general to yield too low a value for the deoxidizing power, hence the conclusions as stated above are probably conservative.

in the form of a complex alloy containing a good deoxidizer such as aluminum or calcium, the presence of these elements in relatively high concentration usually suffices to protect the boron, although the extent of this protection varies significantly with such conditions as the original oxygen content, the temperature of the liquid steel, and the composition of the deoxidizing alloy, so that the results obtained may be somewhat erratic. In any case the safest method is, as stated above, to be sure that the metal is well deoxidized before the boron is added, whether as ferroboron or as a complex alloy.

It is also evident from the calculations that borax (Rasorite) does not deoxidize steel except as it may act as a solvent for FeO, MnO and other oxides. If the slag contains a relatively large quantity of

TABLE 1.—*Deoxidizing Power of Boron and Other Elements at 1600°C. in Molten Iron in Contact with a Slag Composed of the Pure Oxide of the Element*

Deoxidizing Element, Per Cent by Weight in Iron	Residual Oxygen in Iron, Per Cent by Weight*						
	Boron		Aluminum	Zirconium	Titanium	Vanadium	Silicon
	$f = 0.10$	$f = 0.02$	$f = 0.68$	$f = 0.10$			$f = 0.02$
0.0005	0.0017	0.005	0.0006	0.0007	0.012	(0.4)	(0.3)
0.001	0.0011	0.003	0.0004	0.0005	0.008	0.25	0.19
0.005	0.0004	0.0011	0.00012	0.00023	0.004	0.09	0.09
0.01	0.00023	0.0007	0.00008	0.00016	0.0027	0.05	0.06
0.05	0.00008	0.00023	0.000026	0.00007	0.0012	0.019	0.027
0.1	0.00005	0.00014	0.000017	0.00005	0.0009	0.012	0.019
0.5	0.00002	0.00005	0.000006	0.000023	0.0004	0.004	0.009
1.0	0.00001	0.00003	0.000004	0.000016	0.00027	0.0025	0.006

* The symbol f represents the activity coefficient of the metal dissolved in liquid iron or steel relative to the liquid element at 1600°C. The value of f for aluminum is taken from Chipman¹ and that for silicon from Darken.²

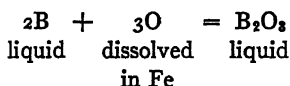
The relatively high affinity of boron for oxygen shown in Table 1 indicates that boron, unprotected, tends to oxidize out during teeming; hence, if "fading" is to be avoided, the boron must be protected by the addition of a more powerful deoxidizer, which means that preferably the steel should be thoroughly deoxidized before the boron is added. If the boron is introduced as ferroboron, the steel should first be deoxidized with aluminum or some other very powerful agent; if boron is added

borax, FeO or MnO may be so distributed between slag and metal that virtually all of these oxides go into the slag, to leave the metal low in oxygen; but this effect is quite different from the deoxidation of iron through removal of oxygen by reaction with boron to form B_2O_3 . On the other hand, a borate may be reduced to some slight extent by well-deoxidized liquid iron or steel, so as to introduce into the steel a very small, yet possibly significant, concentration of boron, the final boron and

oxygen contents being related by the equilibrium equation given in the next paragraph, provided that the slag is assumed to be B_2O_3 . It is readily seen that conditions are favorable for the introduction of a relatively large amount of boron when a borate is added to steel containing an appreciable residual concentration of aluminum or other good deoxidizer, or when a borate is added simultaneously with an amount of aluminum in excess of that necessary to deoxidize the steel. The amount of boron actually brought into the steel by such a process depends, in part, upon the degree to which the equilibrium is approached under operating conditions.

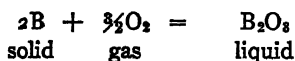
CALCULATIONS

The deoxidizing power of boron in liquid steel is most conveniently expressed in terms of the equilibrium constant K for the reaction:



No direct determination of this constant has been made but it may be evaluated with fair accuracy by a suitable combination of data for other reactions.

According to Southard,³ the free energy change at 1600°C. of the reaction



is

$$\Delta F^\circ_{1600} = -249000 \text{ cal.}$$

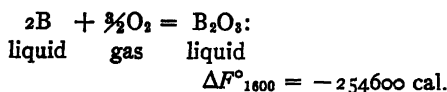
Neither the heat of melting nor the entropy of melting of boron (m.p. about 2300°C., or 2573° absolute) is known; but, judging from data on adjacent elements in the periodic table, the entropy change at the melting temperature cannot be very far from 4.0 entropy units, from which the heat of melting at the melting point is 10,300 cal. The free energy change per mol on melting is, therefore,

$$\Delta F^\circ = \Delta H^\circ - T\Delta S^\circ = 10300 - 4.0T$$

or

$$\Delta F^\circ_{1600} = 2810 \text{ cal. per mol}$$

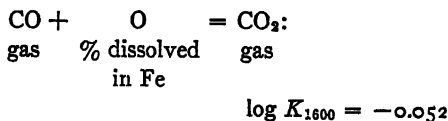
Hence, for the reaction



But since

$$\begin{aligned} \Delta F^\circ &= -2.3RT \log K \\ \log K_{1600} &= 29.71 \end{aligned}$$

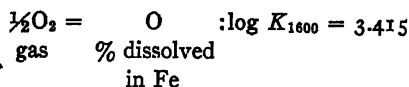
Marshall and Chipman⁴ give the following data: for the reaction



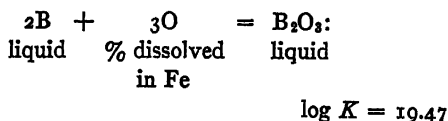
and for the reaction



Whence by subtraction



Hence, by combination with the data for the formation of B_2O_3 ,



or

$$K_{1600} = 3.0 \times 10^{19} = \frac{a_{B_2O_3}}{a_B^2 (\% O \text{ in Fe})^3}$$

where a_B and $a_{B_2O_3}$ are respectively the activity of boron and of its oxide.

It is now assumed that the activity of B_2O_3 is unity; that is, that the slag is pure B_2O_3 . This assumption yields a minimum

value for the deoxidizing power of boron, since in an open-hearth slag the B_2O_3 would normally be dissolved or combined with silica or other oxide, and its activity would be less than unity. On the basis of this assumption,

$$a_B(\% \text{ O in Fe})^3 = 3.3 \times 10^{-20}$$

But a_B is by definition equal to the product fN_B , where f is the activity coefficient relative to liquid boron and N_B is the mol fraction of boron in liquid steel. The mol fraction N_B may be expressed in percentage boron by means of the relation $N_B = 0.0516(\% \text{ B})$.

The value of f is not known exactly, but, judging from the value of the activity coefficient of other metals in liquid iron, as given in Table 1, it probably lies between 0.10 and 0.02. On the basis that $f = 0.10$, $a_B = 0.00516(\% \text{ B in Fe})$.

Therefore

$$(\% \text{ B in Fe})^2(\% \text{ O in Fe})^3 = 1.24 \times 10^{-18} \text{ or}$$

$$(\% \text{ O in Fe}) = \frac{1.07 \times 10^{-8}}{(\% \text{ B in Fe})^{3/2}}$$

If $f = 0.02$, $a_B = 0.0003(\% \text{ B in Fe})$ and $(\% \text{ B in Fe})^2(\% \text{ O in Fe})^3 = 3.1 \times 10^{-14}$ or

$$\% \text{ O in Fe} = \frac{3.1 \times 10^{-8}}{(\% \text{ B in Fe})^{3/2}}$$

From these two relations it is possible to calculate the concentration of oxygen and of boron in equilibrium with each other at 1600°C . in molten iron in contact with a boric oxide slag. This has been done with results listed in Table 1, from which, in spite of the uncertainty in the value of the activity coefficient, it is obvious that boron is an effective deoxidizer and tends to oxidize out of the metal during the open-hearth process and, if there is an appreciable increase in the oxygen content of the steel as it is being poured, during teeming of the ingots as well. This tendency is even more marked if the B_2O_3 formed dissolves in, or enters into combination with, some

other oxide. The results also suggest that boron added to the ladle or ingot mold may not be recovered in significant concentration unless the oxygen content of the steel is relatively low; that is, unless the steel has first been fairly well deoxidized. This, of course, implies that borax (Rasorite) does not react with the oxygen in liquid steel; however, at high concentration of borax in the slag some deoxidation probably will result from the solvent action of borax on FeO . Actually, the calculations indicate that, if equilibrium were attained with a pure B_2O_3 slag, a completely deoxidized liquid steel, even if it contained no excess of deoxidizing agent, would reduce boric oxide to the extent that the boron content of the steel would be of the order of 0.001 per cent; this final concentration would be larger if an excess of the deoxidizer were present, but smaller if the quantity of deoxidizer were insufficient for complete deoxidation.

DEOXIDIZING POWER OF SOME OTHER ELEMENTS

By combining the data for the oxidation of liquid aluminum⁶ with the data for the solution of liquid aluminum in iron,⁸ and with that for the solution of oxygen in iron (given above), we obtain the following relation between the residual oxygen and aluminum contents of iron that at 1600°C . is in equilibrium with a pure Al_2O_3 slag:

$$\% \text{ O} = \frac{3.56 \times 10^{-16}}{(\% \text{ Al})^{3/4}}$$

The same sources yield the following corresponding expressions at 1600°C . for titanium and vanadium, the oxides being pure TiO_2 and pure V_2O_5 , respectively.

$$\% \text{ O} = \frac{2.67 \times 10^{-4}}{(\% \text{ Ti})^{1/4}}$$

$$\% \text{ O} = \frac{2.52 \times 10^{-3}}{(\% \text{ V})^{1/4}}$$

The data for calculating the deoxidizing power of zirconium are incomplete; as with

boron, the entropy of fusion and the activity coefficient in iron are not available. The calculation was made from data on the oxidation of zirconium⁵ in the same manner as that for boron, using 5.0 as the entropy change during fusion of zirconium and 0.1 as the activity coefficient of zirconium in solution in iron, taking liquid zirconium as the standard state. The result, given below, expressing residual zirconium and oxygen contents in iron in contact with ZrO_2 , is very insensitive to the value chosen for the entropy change of fusion, since the melting point of zirconium, $1700^\circ C.$, is close to the temperature, $1600^\circ C.$, taken for the calculation.

$$\% O = \frac{1.62 \times 10^{-5}}{(\% Zr)^{1/2}}$$

Körber and Oelsen⁶ give the following relation between the oxygen and silicon contents of iron in equilibrium with pure SiO_2 at $1600^\circ C.$:

$$\% O = \frac{0.0060}{(\% Si)^{1/2}}$$

By means of these relations the concentration of oxygen in molten iron at $1600^\circ C.$ in equilibrium with any low percentage of the deoxidizing element, and with a slag composed of the pure oxide, can be calculated. This has been done for a series of concentrations of the deoxidizing element, with results, listed in Table 1, which indicate that the deoxidizing power of boron is greater than that of silicon, vanadium, or titanium and approaches that of aluminum or zirconium.

REFERENCES

1. J. Chipman: *Trans. Amer. Soc. Metals* (1934) 22, 385.
2. L. S. Darken: *Trans. A.I.M.E.* (1940) 140, 204.
3. Southard: *Jnl. Amer. Chem. Soc.* (1941) 63, 3147.
4. Marshall and Chipman: *Trans. Amer. Soc. Metals* (1942) 30, 695.
5. J. Chipman: *Trans. Amer. Soc. Metals* (1942) 30, 817.
6. Körber and Oelsen: *Mitt. Kaiser Wilhelm Inst.* (1933) 15, 271.

DISCUSSION

(H. K. Work presiding)

A. L. FIELD,* Baltimore, Md.—Although I have not had an opportunity to give careful study to the author's paper, I am of the opinion that some of the values given in Table 1 for the deoxidizing power do not agree with the indications of practical experience. I refer here particularly to the assigned values for the deoxidizing power of vanadium and titanium as related to that of silicon on the one hand and zirconium on the other. As a result of numerous observations on the relative recoveries of these elements when added in the form of ferroalloys, as well as on the relative rate of oxidation of these elements from a melt by means of an oxidizing slag, I have concluded that vanadium is a relatively weak deoxidizing element far removed from silicon; and, furthermore, that titanium does not exceed silicon in deoxidizing power as much as was indicated in the tabulation.

Another matter that causes me to question the practical utility of the calculated data contained in Table 1 is the failure of the author to take adequately into account the identity of the oxide formed in equilibrium with molten iron as a result of the deoxidizing process. Experiments which I made a number of years ago indicated that the oxide of vanadium in equilibrium with dissolved vanadium in steel was of the suboxide type containing a much smaller percentage of oxygen than is represented by the compound V_2O_5 . In addition, there are strong indications that the oxide in equilibrium with dissolved titanium in molten iron is certainly not TiO_2 , but is a lower oxide.

J. C. SOUTHEARD,† Niagara Falls, N. Y.—This paper shows convincingly that boron should be readily oxidized out of the open-hearth bath, and that its addition to steel should be preceded by thorough deoxidation. However, the remarks concerning the relative deoxidizing power of boron, aluminum, titanium and zirconium may be questioned.

There are at least two ways in which equilibrium concentrations of oxygen and de-

* Technical Director, Rustless Iron and Steel Corporation. † Titanium Alloy Manufacturing Company.

oxidizing elements can be determined. One is from the free energy of the supposed deoxidizing reaction as calculated from various thermal data; the other is by direct analysis of the steel in which the equilibrium has been "frozen" by sudden cooling of the melt. No general statement can be made as to which method is better.

The direct determination of equilibrium concentrations is sometimes very difficult, while errors in free energy values are magnified greatly by the logarithmic relation between the free energy and the equilibrium constant. Mr. Gurry appears to have used the direct experimental determinations of Körber and Oelsen for silicon while for the other deoxidizing elements he has chosen to use indirect thermal data, in spite of the existence of directly determined oxygen values for aluminum and titanium. The author is probably justified in this choice and we should very much appreciate his reasons for doing so.

In applying thermodynamic data, it is necessary first to postulate the correct reaction. The correct reaction can be selected by thermodynamic calculation when data are available. The elements aluminum, boron, and zirconium probably form only one oxide under steel-making conditions and there can be little question that correct reactions have been postulated. Titanium and vanadium, however, are known to form several oxides. Ti_2O_3 , for example, has been well established as an intermediate in the reduction of TiO_2 . The experimental data of Nasu⁷ on the hydrogen reduction of TiO_2 , combined with the data of Chipman (and others) on oxygen in liquid iron, indicates that Ti_2O_3 should be the principal oxide formed at the low oxygen concentrations encountered in killed steel. A comparison of the free energy of formation at 1600°C. will show that there is little difference between Ti_2O_3 , B_2O_3 and ZrO_2 , the values being approximately -83,600, -83,000 and -83,900 cal., respectively, on the basis of one gram-atom of oxygen. The free energy of Al_2O_3 on the same basis is only slightly higher, being -86,600 cal., while that of V_2O_5 is much lower. These free energy values apply to reactions between pure substances, each existing in a separate phase at one atmosphere pressure. Actual oxygen

concentrations in liquid iron can be computed from these values only when the activity of the various substances is known.

The activity of oxygen in liquid iron has been established, of course, by the work of Chipman, Vacher and others, but the activity of most of the deoxidizing elements has not been determined. Mr. Gurry has recognized this in regard to boron by giving two estimates of the activity coefficient. The activity coefficient selected for silicon gives good agreement between the direct measurements of Körber and Oelsen and the indirect thermal data.

The activity coefficient used for aluminum may be questioned. It was calculated from the distribution of aluminum between iron and silver, assuming that aluminum and silver form a perfect solution. Kelley⁸ was unable to calculate a reasonable heat of fusion for either aluminum or silver from the silver-aluminum diagram without assuming the existence of a silver-aluminum compound in the liquid phase. This indicates that the solution is far from perfect.

The activity coefficients for titanium, zirconium and vanadium are pure assumptions. Activity coefficients of titanium and aluminum could have been calculated from the existing thermal data and the directly determined values for residual oxygen of Wentrup and Hieber.⁹ However, their data indicate activity coefficients of the order of 0.001. This seems unreasonably low and should not be accepted unless confirmed by an independent method.

The values for residual oxygen given in Table I must therefore be considered as rough estimates, because of this high degree of uncertainty in activity coefficients. It should be emphasized that as far as existing thermodynamic data can say, boron, titanium and zirconium on an atomic basis are almost equally effective as deoxidizers.

N. F. TISDALE,* Pittsburgh, Pa.—This paper corroborates work on the use of boron performed by our company nearly eight years ago. We have developed a spectrographic method to determine small quantities of boron; also, there have been several chemical methods in use

⁸ Kelley: U. S. Bur. Mines *Bull.* 393; 7, 100.

⁹ Wentrup and Hieber: *Tech. Mitt.* Krupp (1935) No. 5, 47; No. 10, 115.

* Molybdenum Corporation of America.

⁷ Nasu: *Sci. Repts.*, Tohoku Imp. Univ. (1936) 25, 510.

long enough so that their accuracy is no longer questioned, and they too provide satisfactory analyses of small amounts of boron. By checking the residual boron as a carry-over from the open hearth, we have been unable to detect any boron in the steel, particularly when the carbon content of the heat was under 0.70 per cent. We have no data on heats over 0.70 carbon.

We also checked the fact that boron is carried over on remelt of cast iron containing boron and, while there is a slight loss in the remelting operation, there is a definite carry-over in cast-iron remelting.

We concur very heartily in having the steel thoroughly deoxidized before the addition of boron, otherwise there would be an excessive loss of boron due to oxidation. Factual evidence has been submitted elsewhere that boron can be uniformly distributed throughout heats of steel up to 250-ton quantities, provided that the precautions outlined by the author—namely, preceded by proper deoxidation—have been carried out.

I am sure that a number of steel men will be grateful to Mr. Gurry for his explanation of how borax, Rasorite or boric acid, essentially an oxide, perform deoxidation functions. It is certainly something to think about before rushing into a use of such reactions on a wide variety of steel.

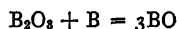
C. A. ZAPFFE,* Baltimore, Md.—This paper is an interesting contribution, but it may suffer from certain incorrect inferences. For example, should B_2O_3 be selected as the agent, and the only one, active at 1600°C . in contact with liquid iron? The oxide of iron is not regarded as Fe_2O_3 under these conditions, although that, too, is the common form at ordinary temperatures. True, the sesquioxide of boron may well be the stable form of boron oxide, even in contact with liquid Fe, in contrast to the more easily dissociated oxides of iron; but the monoxide of boron has not only been definitely shown to exist at the temperatures in question,¹⁰ but has been experimented with abroad.¹¹

* Assistant Technical Director, Rustless Iron and Steel Corporation.

¹⁰ R. S. Mulliken: The Isotope Effect in Band Spectra, I. *Phys. Rev.* (1925) 25, 119–138; II—The Spectrum of Boron Monoxide, *Ibid.*, 259–294.

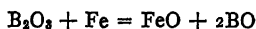
¹¹ E. Zintl, E. Morawietz, and E. Gastinger: Boron Monoxide. *Zisch. anorg. allg. Chem.* (1940) 245, 8–11.

Consequently, the complete picture of the Fe-O-B equilibrium may require modification similar to that which we found necessary for the Fe-O-Si system in which SiO apparently figures as well as SiO_2 .^{12,13} In that case, a given boron content may result in an oxygen pressure, or activity, which differs considerably from that calculated on the basis of B_2O_3 . Part of the dissolved B will be associated with dissolved O, expressible as dissolved BO. The total boron content will then include both the free and the associated forms of B and will not be properly accounted for by Gurry's activity coefficients. Similar error would result from calculations based on Fe_2O_3 , or MnO_2 , and is unwarranted until the species operative in that range of temperature and oxygen pressure is identified. The following reaction may then belong in the picture also, even if only until it is proved to be unimportant:



especially since the monoxide of boron is a gaseous form and the recovery of B is known to be difficult.

For liquid steel, of course, the foregoing equation can be modified to express the reduction of B_2O_3 by any of several constituents in the steel, including iron itself:



If one assumes, with Gurry, that a slag of B_2O_3 is pure B_2O_3 and may be expressed as having an activity of unity, then it must follow that:

$$K = [\text{FeO}][\text{BO}]^2$$

$$BO = \left(\frac{K}{[\text{FeO}]}\right)^{1/2} = K' \left(\frac{1}{[\text{FeO}]}\right)^{1/2}$$

whereupon the quantity of dissolved BO must increase as the FeO content of the metal decreases. This is analogous to the conclusion we found necessary to draw for SiO in the Fe-O-Si system.

Assuming the slag to be pure B_2O_3 , of course, introduces a definite error because it is not pure B_2O_3 . In calculations such as these it has been the custom to make that assumption

¹² C. A. Zapffe and C. E. Sims: Silicon-oxygen Equilibria in Liquid Iron. *Trans. A.I.M.E.* (1943) 154, 192.

¹³ C. A. Zapffe and C. E. Sims: Silicon Monoxide. *Iron Age* (1942) 149, 29–31, 34–39.

because contamination with the oxides of other metals is known to be slight; but the possibility of the slag being contaminated with other oxides of its own, such as the monoxide, has received scant consideration except in the case of iron oxide. Another fallibility lies in forgetting that a change in the activity of an equilibrium constituent from 0.001 to 0.002 per cent can be as significant as a change from 10 to 20 per cent, as far as the effect upon another constituent is concerned.

In regard to Gurry's remarks on the reduction of B from borates by residual Al, attention might be called to the interesting experiment of Zintl and his colleagues,¹¹ which showed that B attacks Al_2O_3 to form gaseous monoxide forms of both elements:



When ZrO_2 is used instead of Al_2O_3 , only BO sublimates, leaving a residue of ZrO, which apparently has a low vapor pressure even at high temperatures.

Because of the low atomic weight of boron (10.82), the latter figures in Table 1 scarcely concern melts having a "... low percentage of the deoxidizing element..." which Gurry in his closing paragraph rightly mentions as a restriction in making these calculations. A 1 per cent addition of B is actually a 5 per cent (atomic per cent) addition. In the Fe-O-Si system, the discrepancy between measured and calculated values becomes significant at Si contents considerably below 5 atomic per cent. In the Fe-O-C system, the measurable solubility of CO for comparable solutions has been established using vacuum-fusion analysis,¹⁴ which has a questionable efficacy with such alloys, and in any event certainly provides a minimum value.

Along the same line, Gurry's opening paragraph states that the "oxygen content" of cast iron is much lower than that of steel. We will agree that the oxygen pressure, or activity, is much lower in iron so diluted with roughly 20 atomic per cent of elements having a strong affinity for oxygen, but the matter of oxygen content should be left open. Because of their high affinity for oxygen, and for other reasons

which will not be discussed here, many of these alloying elements may increase the capacity of the bath for oxygen beyond a certain minimum that they first produce during deoxidation, when the bath does not as yet contain enough of their own species to make their dissolved oxide stable.

Such matters, of course, carry Gurry's article beyond its intended purpose. The principal point to be made is that the whole present understanding of residual oxygen, and the details of the deoxidation process itself, seem to require some revision now that we are applying physical chemistry to solutions that are not only no longer dilute but which contain residual elements that are highly associative with oxygen. Until at least the active species have been identified, and the laws of association in liquid steel understood, such calculations are exceedingly precarious. The argument is not against their being approximations, but against their being misleading through improper depiction of the deoxidation reaction.

R. W. GURRY (author's reply).—The foregoing comments, taken as a whole, seem to indicate that there should be some discussion of the mechanism of deoxidation and of the application of thermodynamics to deoxidation in order to clarify our concepts and bring us in a position properly to evaluate the indications of calculations such as those in the paper.

Let us consider, for example, the slow addition to a steel bath of an element that can form two oxides in that particular bath. Under equilibrium conditions at first only the higher oxide would form; then, when the activity of oxygen in the metal was reduced to the appropriate value the lower oxide would appear in turn. Under operating conditions, however, equilibrium does not prevail and both oxides are probably produced in the bath at the same time. If this is so, an adjustment toward equilibrium takes place immediately, either the higher or the lower oxide tending to disappear with the formation of the other, depending upon the amount of deoxidizing element originally added. The extent of this adjustment is controlled by flotation of the oxides but, at any rate, the metal finally must come essentially to equilibrium with one oxide phase of the deoxidizing element, neglecting

¹⁴ S. Marshall and J. Chipman: The Carbon-Oxygen Equilibrium in Liquid Iron. *Trans. Amer. Soc. for Metals* (1942) 30, 695-741; discussion 741-746.

for the moment the existence of a slag. When this situation is reached, the residual concentrations of the deoxidizing element and of oxygen in the metal are determinate, and if certain information is available the relationship between them can be computed.

As has been amply pointed out in the preceding comments, in order to calculate this relationship between residual concentrations of oxygen and deoxidizing element, it is necessary to know the composition of the final oxide phase that is in equilibrium with the metal. If this is a pure oxide of the deoxidizing element, we must know which one; if a solution of two or more oxides, we must know its composition and must have additional thermal information about the solution.

There seems to be little doubt that the oxide of titanium in equilibrium with steel up to saturation with oxygen at 1600°C . is Ti_2O_3 and not TiO_2 , as was inferred in the paper. The use of the lower oxide improves the calculated deoxidizing power of titanium and would give it a position in the vicinity of that shown in the paper by E. C. Wright (this volume, p. 107). If a lower oxide of boron than B_2O_3 is formed under the conditions considered, boron would be an even better deoxidizer than as shown in Table 1. However, this seems unlikely for two reasons: relatively little boron is lost in remelting cast iron as is pointed out by Mr. Tisdale; also if a lower oxide than B_2O_3 were stable, at least at any oxygen pressure corresponding to saturation of the steel with oxygen, B_2O_3 would react to completion with iron producing iron oxide and the lower boron oxide, a reaction which, as far as I know, has not been observed.

When two or more deoxidizing elements are added simultaneously to a steel bath, they compete for the oxygen, of course, the amount reacting with each depending upon the relative deoxidizing power of the elements, the concentration of each, the inherent rates of the several reactions, and the relative ability of the oxides to float out of the metal. When to these factors is added the additional uncertainty as to what combinations or solutions take place among

the oxides formed, it can be very difficult to gauge the true relative deoxidizing power of one element when several are present.

If we are satisfied that we know what oxide of the deoxidizing element is formed and are willing to restrict ourselves to consider the slag as being that pure oxide, an exact expression relating the final activity of the element and of oxygen in the metal can be derived from the appropriate data. All that is needed to convert this expression to an exact one in terms of percentages is a knowledge of the two activity coefficients as a function of concentration.

Thermodynamically, all questions regarding species in solution and laws of association in liquid steel are answered by a determination of the activity coefficient. In the paper the activity coefficients were taken to be those in pure iron and it was assumed that they remained constant; that is, that Henry's law was obeyed, over the concentration range covered. To do this seems reasonable when we consider that in the case of boron the composition of the metal solvent is altered by only about 5 atomic per cent in the worst case whereas the possible error in the estimated activity coefficient is admittedly at least a factor of five. Even for elements whose activity coefficients (in pure iron) are better known, the assumption that these coefficients remain constant is probably justified because of the very short range of concentration normally considered in the deoxidation of steel.

From a practical standpoint, it is doubtful whether a very precisely known activity coefficient would be advantageous when we consider the following difficulties, which are inherent in applying the calculated deoxidizing power of an element to actual deoxidation: the uncertainty of solution or combination of the oxide formed with other oxides, the influence of the slag present before the addition, and, where two or more elements are added simultaneously, the additional factors mentioned in a previous paragraph. The deoxidizing ability as calculated can serve as a guide, and a valuable one, to the operator, but in using it he should not forget its limitations.

The Manufacture and Properties of Killed Bessemer Steel

By E. C. WRIGHT,* MEMBER A.I.M.E.

(New York Meeting, February 1944)

THE bessemer process is nearly one hundred years old. William Kelly, the American inventor, was able to demonstrate that he had accomplished the pneumatic purification of molten pig iron as early as 1847; Henry Bessemer's English patent was granted in 1855. The application of this steelmaking process since then and the present position of bessemer steel are concisely discussed on pages 355 and 356 of the fifth edition of "The Making, Shaping and Treating of Steel."

The great expansion of the automotive, machine-tool, chemical and oil industries after 1910 opened up a large market for special steels, whereas the output of steel before that time was mainly for structural purposes. The need for building more blast-furnace capacity complementary to bessemer operations, combined with the availability of the necessary amounts of steel scrap, both contributed to the extension of open-hearth plants at the expense of bessemer capacity. The ability of the open-hearth furnaces to consume virtually all types of raw materials as far as phosphorus content is concerned, and the need for selecting low-phosphorus ores of rapidly decreasing sources for the bessemer, also played a part in the reduction of bessemer steelmaking operations and the increase in basic open-hearth plants. As a consequence, the proportion of bessemer steel made in this country decreased from 65.7 per cent

of the total in 1900 to 37.1 per cent in 1910, and only 6.8 per cent of the total in 1937.

The metallurgical concepts existent between 1910 and 1920 caused the writing of many specifications of very low phosphorus and sulphur content, which definitely barred bessemer steel from many commodities. Now sulphur is being added to many open-hearth and bessemer steels in amounts far exceeding the maximum sulphur content of good bessemer steel. Rephosphorizing is also widely practiced for several specific applications. Even today, the chemical-analysis limits of many important steel specifications have an arbitrary and archaic tinge. The old standard "0.30 to 0.60 per cent manganese" might be mentioned in this connection as similar to the rigid requirements for maximum sulphur and phosphorus that were established at least 25 years ago.

The literature is full of vague and complex discussions of the effects of nitrogen and oxygen where these elements existed in steel in amounts less than 0.02 per cent. Many failures have been attributed to these elements without reasonable proof on which to base the conclusion. Methods of determining oxygen in steel require such complicated equipment that only a few research laboratories have the required apparatus. Even so, the accuracy of oxygen determinations in steel has been only recently reproducible. Up to the present time, no one has succeeded in obtaining a sample of molten steel that accurately indicates the full oxygen content of the metal in the furnace or ladle because the molten sample

Manuscript received at the office of the Institute Nov. 15, 1943. Issued as T.P. 1692 in METALS TECHNOLOGY, June 1944.

* Assistant to President, National Tube Co., Pittsburgh, Pennsylvania.

takes up oxygen from the air in pouring. Past discussions of the oxygen content of steel have little quantitative foundation.

In the case of nitrogen it has lately been learned that many high-grade electric-furnace steels have considerable amounts of this element although generally lower than the 0.015 per cent nitrogen that is normal for bessemer steel. It has also lately become the vogue to add nitrogen to some open-hearth heats (up to 0.02 per cent), as these additions have been useful in regulating heat-treatment and grain-size control. Bessemer steel has been condemned frequently, and one may say erroneously, because of its higher nitrogen and phosphorus content.

In this present emergency, the time has arrived for a thorough survey of the characteristics of bessemer steel, especially in view of the shortage of high-grade scrap and the enormous demand for all kinds of steel. The gradual decrease in the manufacture of bessemer steel over the years can be traced to economic and technical factors. Neglecting the economic phases, which vary widely throughout the years, it is believed that the properties of the bessemer steel made in the United States have changed very little during the past 40 years. There have been no new installations of bessemer-steel plants since the last war except where bessemer equipment was installed in conjunction with duplex open-hearth melting. As a consequence, most of the bessemer-steel plants in the United States are obsolete, with small converting vessels and antiquated handling, mixing and teeming equipment. The fundamental methods of making bessemer steel have changed little, in spite of the great amount of work that has been done to develop instruments to control the blowing of the molten iron. During the same period very important improvements have been made in the construction and in operating practices on both basic open-hearth and electric melting furnaces.

STEELMAKING

After the first World War, the greatly increased demand for special steels—for gears, bearings, and other important automotive parts, for instance—caused a rapid expansion in the use of special alloy steels and a considerable increase in the amount of electric-furnace melting capacity, since it was found that open-hearth furnaces were not generally suited for the consistent manufacture of certain high-quality specialties. A trend to replace open-hearth steel with electric-furnace steel set in, as previously open-hearth steel displaced bessemer steel. This trend continues, as indicated by the enormous expansion in electric-furnace capacity during the present emergency.

About 1925 this situation led to a serious consideration of the fundamental physical chemical principles involved in the making of steel, particularly as related to basic open-hearth melting practice. During the past 20 years much valuable work has been done on such important features as slag control, oxidation of the open-hearth bath, and particularly the deoxidation of the open-hearth steel both in the furnace and in the ladle. Very illuminating information as to the effect of deoxidizing agents upon such vital properties of the steel as the hardenability, carburizing characteristics, properties at low temperatures, welding properties, grain size, was obtained in these investigations.

The most important principle encountered in these studies was that a control of the oxygen in the steel-melting bath and in the finished steel had a profound influence upon most of the important properties of the finished heat. This work enabled the production in basic open-hearth furnaces of an increased volume of high-grade carbon steels, and also alloy steels that could be consistently produced with definite grain-size control, hardenability, and so forth. Coincident with this im-

provement, the steels also exhibited more uniform forging characteristics, better yield and improved surface. It is the writer's opinion that much of the open-hearth steel made before 1920 was in many respects as lacking in uniformity as the bessemer steel produced before that date. In the National Tube Co. the improvement in quality of the open-hearth steel has caused an increased yield of product of at least 20 per cent in the past 15 years. The majority of the high-quality steels now made in the open hearth are fully killed steels treated with definite amounts of the proper deoxidizing agents such as silicon, aluminum, titanium and vanadium.

Most of the bessemer steel made in the United States has been of the undeoxidized or "open" type. These steels are usually termed rimmed, capped or semikilled. They are high in oxygen, freeze in the ingot mold with highly segregated center sections, have surface blowholes, and are extremely erratic in hardenability, grain size and susceptibility to strain-aging and low-temperature brittleness. Such steels generally are not suitable for forging, cold-forming or heat-treating operations.

The improvements in open-hearth furnace melting and control discussed above were a vital feature in the improvement of making seamless tubes. This difficult forging operation requires a billet of uniform density and forging characteristics. Satisfactory seamless tubes have never been produced with uniform practice from open-hearth steels of the rimmed or capped ingot type in the National Tube Co.

The physical chemical principles investigated in connection with open-hearth steel melting apply equally well to the processes involved in making bessemer steel. The only difference between the two methods is the rate at which the reactions occur. In the bessemer process the hot metal is oxidized by the air blown through the bath, and thereby removing practically all the silicon and manganese, and at the

time of the drop of the carbon flame above the converter, the carbon has reached the level of about 0.04 per cent. In the open-hearth furnace the oxidation of the carbon, silicon and manganese of the bath is accomplished slowly by means of the oxygen from scale on the melting scrap, the oxygen in the slag, and the iron ore added as charge ore or feed ore to the bath. The elimination of the silicon, manganese and carbon proceeds in a way similar to the reaction in the bessemer but at a much slower rate. This enables the melter to control the rate of elimination of carbon and to arrest the carbon drop at any desired level. However, in making a heat of low-carbon steel in the open-hearth furnace, where a tap carbon of 0.10 per cent may be the aim, the characteristics of such a bath with respect to the silicon, manganese and oxygen approach a point of chemical equilibrium similar to that existing in the blown metal at the end of the blow in the bessemer converter. The very low-carbon open-hearth bath may be treated with additions of ferrosilicon or spiegel in the furnace to partially deoxidize the FeO , and the molten metal may then be given further additions of silicon and aluminum in the ladle to thoroughly kill the heat. The manufacture of a forging-grade heat of low-carbon open-hearth steel generally follows this procedure.

Realizing that the physical chemical principles underlying the bessemer and open-hearth processes must be the same, the metallurgist naturally asked why bessemer steel could not be thoroughly deoxidized and finished in the same way as open-hearth steel. Following this line of reasoning, heats of blown bessemer metal were tapped into teeming ladles and treated with ferromanganese, ferrosilicon, aluminum and other deoxidizers much as open-hearth heats are treated. The results of such practice were in many ways inconsistent and a thoroughly killed steel of uniform characteristics was not produced

successfully in this manner. This was believed to be because either the blown bessemer-converter metal was overoxidized or the mixing of the deoxidizing reagents

silicon, carbon and manganese as representing the general agreement on these values at the present time. The curves are based on calculations from Chipman's data.

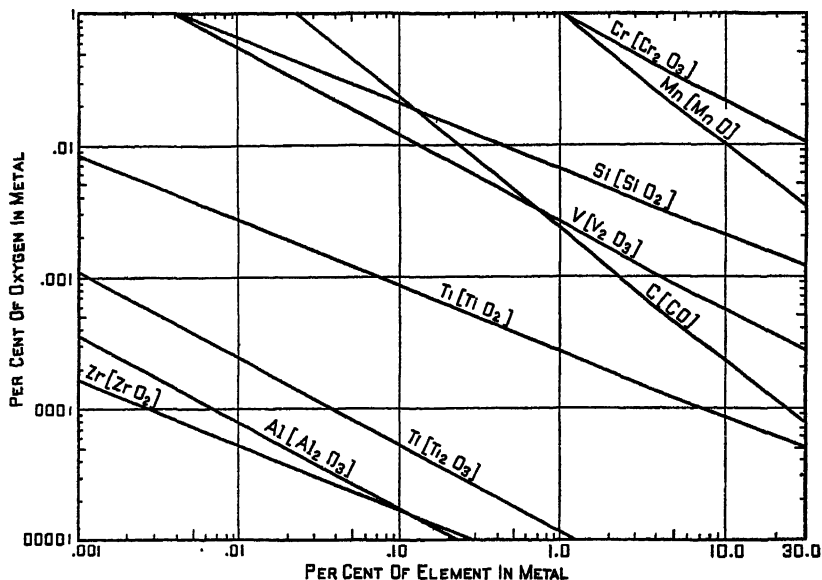


FIG. 1.—EQUILIBRIUM BETWEEN OXYGEN AND OTHER ELEMENTS IN LIQUID STEEL AT 1600°C.
[FeO] = 4.49 [O]

in the teeming ladle was not sufficiently uniform to develop a thorough deoxidation of the metal. Although theoretically 2 lb. of aluminum per ton should thoroughly deoxidize blown metal with 0.03 per cent carbon, additions of as much as 6 lb. of aluminum per ton would not effectively kill the heats in the ladle.

The splendid paper by John Chipman¹ on the physical chemistry of steel at 1600°C. (2910°F.) has done much to clarify this subject. The work of Larsen, Herty and others also has contributed greatly to an understanding of the equilibrium between oxygen in molten steel and such deoxidizing agents as carbon, manganese, silicon, aluminum, vanadium. Figs. 1 and 2 show the equilibrium proportions of oxygen in molten steel at 1600°C. (2910°F.) and 1700°C. (3060°F.) with aluminum,

The influence of temperature on these equilibria is extremely important. For example, carbon is a much more powerful deoxidizer than silicon or manganese at temperatures above 1600°C. (2910°F.) when the carbon content of the bath exceeds 0.10 per cent. The temperature of bessemer steel in the vessel generally exceeds 1600°C. (2910°F.). Recognizing this principle, attempts were made to deoxidize blown bessemer metal with additions of carbon and eliminate the oxygen in the bath as carbon gases instead of producing solid precipitated oxides such as SiO₂ and Al₂O₃, which remain to a considerable extent as inclusions in the steel bath.

The simplest and most thorough method of treating a blown converter bath with carbon is to add hot metal, which contains approximately 4 per cent carbon, as well as some manganese and silicon. The action

¹ References are at the end of the paper.

of such additions to fully blown bessemer heats gave a very thorough preliminary deoxidation, much like the "blocking" of an open-hearth bath by addition of

metal blown to 0.04 per cent carbon are treated with 1400 lb. of hot metal, added in each vessel after blowing, and then are poured into a 50-ton ladle. If no reac-

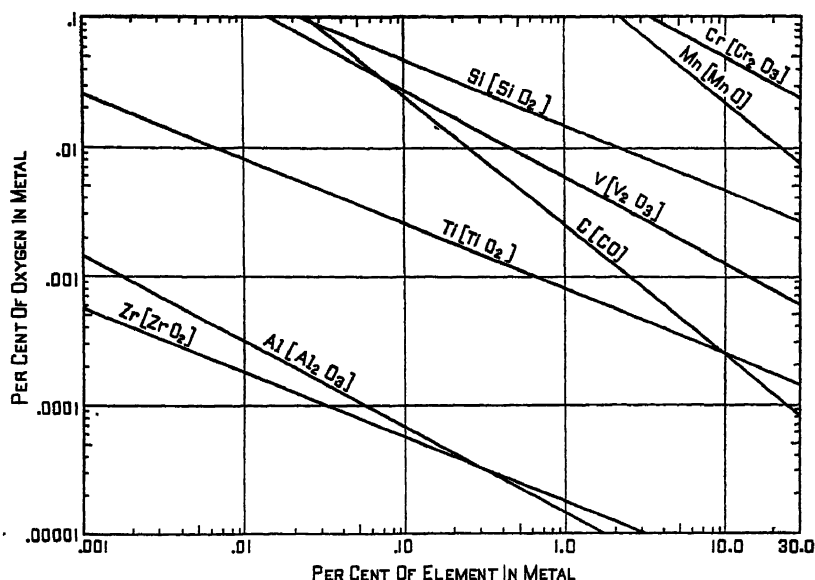


FIG. 2.—EQUILIBRIUM BETWEEN OXYGEN AND OTHER ELEMENTS IN LIQUID STEEL AT 1700°C.
[FeO] = 4.49 [O]

ferrosilicon or spiegel. To bessemer blows were added the proper amounts of hot metal as converter additions. The steel was then poured into a teeming ladle and treated with the required amounts of ferromanganese, ferrosilicon and aluminum to deoxidize the blocked heat, as in open-hearth practice. The bessemer heats so treated were found to be thoroughly killed and of good forging quality. They could be teemed into regular hot-top ingot molds, rolled into tube rounds and satisfactory seamless tubes with practices equaling results obtained on open-hearth steels.

A specific example of the methods* of "killing" or thoroughly deoxidizing a bessemer heat is offered by way of illustration. Two 25-ton blows of bessemer

tion occurred, the carbon content of this mixture would approximate 0.16 per cent. The mixing of the blown metal and hot metal in the vessel is almost instantaneous and the elimination from the metal of carbon and oxygen in the form of CO gas is extremely rapid. In fact, a large puff of flame over the mouth of the converter appears just after addition of the molten iron. In 100,000 lb. of blown metal containing 0.08 per cent oxygen, the amount of oxygen is approximately 80 lb.; 2800 lb. of hot metal with 4.25 per cent carbon and 1.5 per cent silicon contains 119 lb. of carbon and 42 lb. of silicon. The 80 lb. of oxygen should require 60 lb. of carbon for deoxidation. It is assumed that the finished steel contains 0.015 per cent oxygen, as thoroughly killed heats show this amount in several analyses. The oxygen removed is thus 65 lb., requiring 48 lb. of carbon. The

* The manufacture and application of the bessemer steels described are covered by United States Patent 2218458 and pending applications.

TABLE 1.—*Chemical Balance in a Killed Bessemer Heat*

Constituent	Blown Metal, 100,000 Lb.		Molten Pig, 2800 Lb.		Ferromanga- nese, 600 Lb.		Ferrosilicon, 500 Lb.		Final Heat, 103,900 Lb.		Addi- tion Effi- ciency, Per Cent
	Per Cent	Wt.	Per Cent	Wt.	Per Cent	Wt.	Per Cent	Wt.	Per Cent	Wt.	
Carbon.....	0.04	40	4.25	119	7.00	42			0.15	156	74.00
Silicon.....	0.008	8	1.50	42					0.21	218	74.50
Manganese.....	0.05	50	0.60	17	78.00	468	48.00	240	0.436	453	83.20
Oxygen 0.36 per cent FeO	0.08	80							0.015	15	

119 lb. of carbon in the 2800 lb. of hot metal is partly eliminated as CO gas and the carbon content of the resultant steel increased from approximately 0.04 to 0.12 per cent, indicating a carbon-oxygen equilibrium at 0.12 per cent carbon. This increase in carbon content of 0.08 per cent in 100,000 lb. of blown metal requires 80 lb. of carbon. Accordingly the 40 lb. of carbon has reacted with 53 lb. of oxygen. This result demonstrates that most of the oxygen in the blown metal is eliminated as CO. After this reaction, the steel may be treated in the usual manner with the proper additions of ferrosilicon, 1 to 3 lb. of aluminum per ton of steel, and sufficient ferromanganese for the final manganese content desired in the steel. The efficiency of the manganese and silicon additions to the ladle is as high as in open-hearth heats tapped at the 0.12 per cent carbon level. Table 1 shows the chemical balance between the additions in the example given.

A further indication of the effectiveness of the carbon deoxidation is found in inclusion ratings of thoroughly killed bessemer heats. The standard method of rating inclusions by means of microscopic examination of nine sample cuts taken from the top, middle and bottom of the first, middle and last ingot of several thoroughly killed bessemer heats reveals a cleanliness superior to that of open-hearth heats of the same carbon content, treated with the same deoxidizing reagents.

The carbon content of the steel may be raised to any level desired by increasing

the amount of hot metal used; satisfactory heats with carbon as high as 0.45 per cent and over 1 per cent manganese have been made. The addition of hot metal to open-hearth heats, instead of ferrosilicon or spiegel in the furnace, has also been successful. The higher temperature of the bessemer steel as compared with the usual temperature for open-hearth steel apparently makes the molten iron more effective as a deoxidizer in the bessemer heats.

PROPERTIES

It was soon found that the thoroughly deoxidized bessemer heats melted with this practice were fundamentally different from undeoxidized bessemer steel. Up to the present time over 300,000 tons (between 6,000 and 10,000 heats) of thoroughly deoxidized bessemer steel have been made with this procedure and converted into almost every size of seamless pipe. During the past five years the large tonnage of killed bessemer steel so made has been investigated to determine its properties in comparison with the old standard rimmed or capped bessemer steel, as well as with killed open-hearth steel. Many data concerning most of the important physical properties of steel have been obtained. The results of these tests are presented in order that the reader may compare and realize the fundamental difference exhibited by the thoroughly deoxidized bessemer steel in contrast with the erratic properties of bessemer steel formerly produced without this type of deoxidation.

The majority of bessemer steels made with this new practice for applications in seamless pipe have been produced to analyses aiming at 0.12 to 0.20 per cent

The striking features of these tests are the high yielding strength and tensile strength for the low carbon content and the high ratio of yield strength to tensile strength.

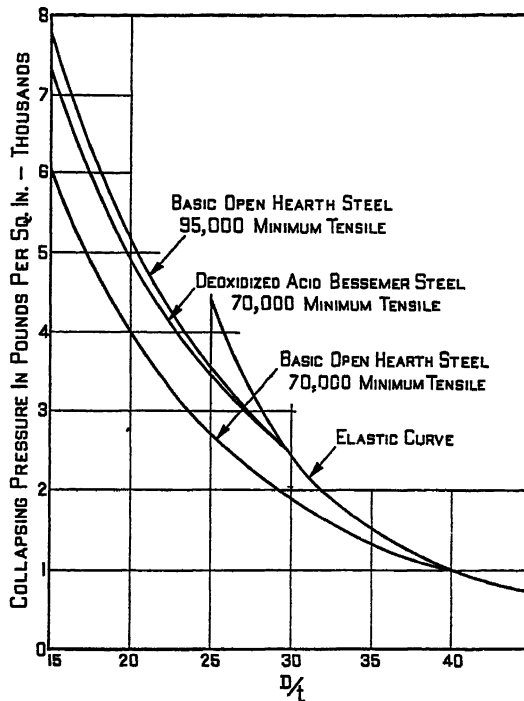


FIG. 3.—RESISTANCE TO EXTERNAL PRESSURE OF PIPE FOR SEVERAL GRADES OF STEEL.

carbon, 0.30 to 0.60 per cent manganese, 0.07 to 0.11 per cent phosphorus, 0.05 per cent maximum sulphur, and 0.15 to 0.30 per cent silicon. Tensile tests have been taken on every heat produced to this analysis. The average and minimum tensile properties for some 1800 tensile tests are as follows:

	Average	Minimum
Yield strength, 0.01 per cent set, lb. per sq. in.	53,020	43,400
Yield strength, 0.2 per cent set, lb. per sq. in.	55,000	45,000
Tensile strength, lb. per sq. in. .	75,000	66,000
Elongation in 2 in., per cent . . .	35	25

In addition, determination of elastic limit by the plotting of stress-strain diagrams has shown that steel of this composition has a uniformly high elastic limit, generally exceeding 95 per cent of the 0.2 per cent set yield strength. The ratio of the yield strength to the tensile strength has consistently been above 70 per cent. These two features of high elastic limit and high ratio of yield strength to tensile strength make these steels distinctly superior to open-hearth steel of the same tensile strength, as the latter generally exhibits a ratio of yield strength to tensile strength of about 62 per cent and a ratio of elastic limit to yield strength that may vary from 60 to 90 per cent. This is of particular advantage in pipe used for structural pur-

poses, such as tubular piling, drive pipe, and products subject to high pressures, such as line pipe. The greater stiffness resulting from the higher yield-strength ratio

considerably superior to the standard open-hearth steel casing of 70,000 lb. per sq. in. tensile strength, known as H-40 grade. Fig. 3 shows the collapse resistance of

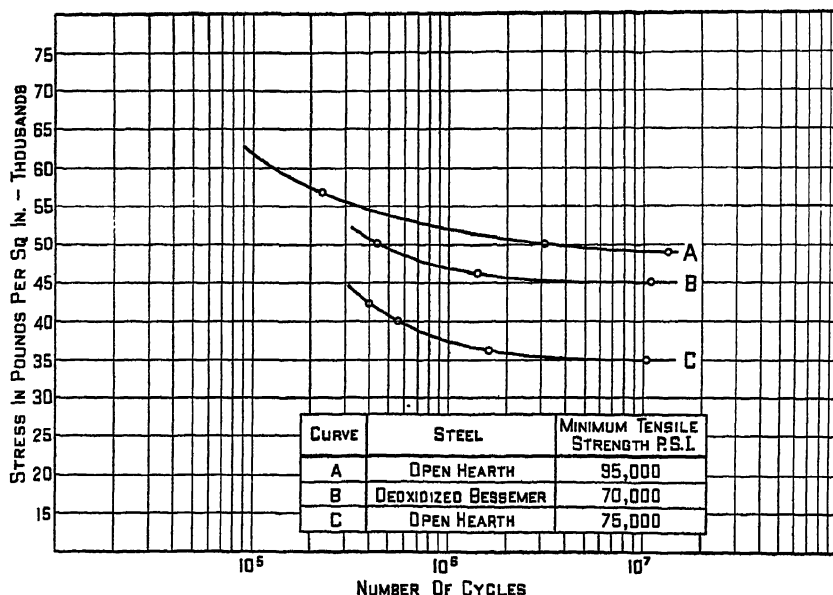


FIG. 4.—S-N CURVES FOR THREE GRADES OF PIPE STEEL.

has made this type of pipe extremely satisfactory for drive pipe, which is pounded into the ground much like piling, since it exhibits much less crushing and deformation in driving the sections, permitting the use of harder blows and faster driving.

Extensive investigations of the collapse resistance of pipe indicate clearly that the elastic limit, or proportional limit of the pipe steel is of prime importance in obtaining higher collapse resistance to external pressure. It is believed that the small content of phosphorus in this deoxidized bessemer steel is the main factor contributing to the high elastic ratios and high proportional limits. Collapse tests made on many sizes of pipe show that the collapse resistance of the low-carbon bessemer-steel casing is equivalent to the collapse resistance of open-hearth alloy-steel casing, designated as A.P.I. grade J-55, and con-

various sizes of casing for the H-40 and J-55 A.P.I. open-hearth grades compared with that of the killed bessemer-steel grade. The A.P.I. J-55 seamless grade is made from open-hearth steel with minimum yield strength of 55,000 lb. per sq. in. and minimum tensile strength of 95,000 lb. per sq. in. The ordinary analysis of this open-hearth steel for J-55 casing is of the order of 0.35 to 0.45 per cent carbon, 1.00 to 1.30 per cent manganese.

The fatigue properties of the killed bessemer steel are somewhat unusual in that the tests show a high endurance limit considerably above 50 per cent of the tensile strength of the material. Similar fatigue tests on open-hearth steels in the normalized state usually show endurance limits ranging from 45 to 50 per cent of the tensile strength. Fig. 4 shows fatigue tests on two types of open-hearth steel for

comparison with the endurance limit of the deoxidized bessemer steel. The superiority of the killed bessemer steel in this respect is quite evident.

with a carbon content of 0.12 to 0.40 per cent, show that ductility and toughness of this material are equal to open-hearth steel of similar hardness and tensile

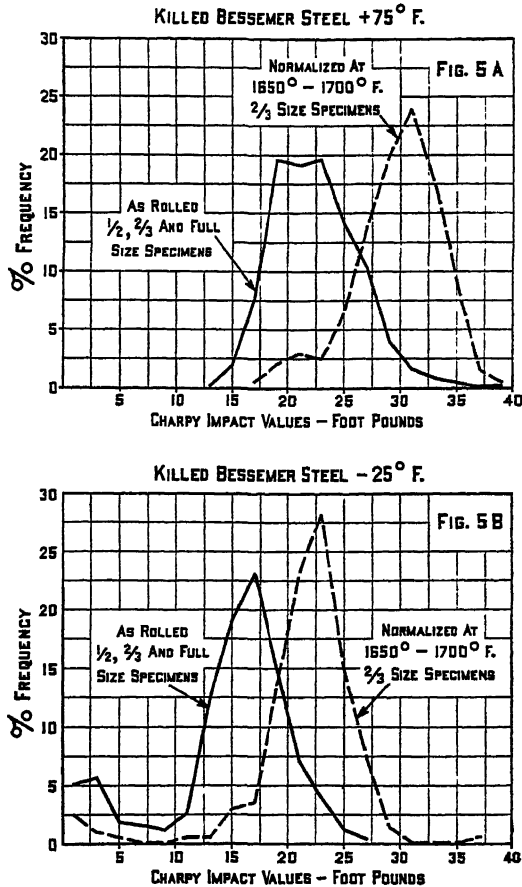


FIG. 5.—FREQUENCY DISTRIBUTION OF CHARPY IMPACT VALUES.

As stated previously, the bessemer steel described contains approximately 0.015 per cent nitrogen and from 0.06 to 0.11 per cent phosphorus. The sulphur is generally as low as in open-hearth steel, ranging from 0.020 to 0.050 per cent. Although many statements in the literature infer that both phosphorus and nitrogen tend to cause brittleness and lack of ductility in steel, thousands of tests on the thoroughly killed bessemer steel,

strength in spite of the presence of appreciable amounts of nitrogen and phosphorus.

The ductility of the killed bessemer steel as measured by percentage of elongation and reduction of area in tensile tests is normal in every respect. As shown in the average physical properties reported, the elongation in 2 in. is 35 per cent for an average tensile strength of 75,000 lb. per sq. in. The elongation on basic open-hearth steels of this tensile strength is in no way

superior. The reduction of area as determined on round tensile tests is well over 60 per cent for the thoroughly killed acid bessemer steel. Ductility determinations based on flattening tests on pipe and on bending tests also demonstrate that killed bessemer steel is in every way equal to basic open-hearth steel of the same hardness. In the early stages of the manufacture of the bessemer seamless pipe, every piece of material was subjected to flattening tests, as it was suspected that brittle specimens might be encountered. Several hundred thousand such flattening tests were made without revealing brittle failures and, moreover, the pipe made from the killed bessemer steel flattened to the same degree as open-hearth steel of equivalent hardness.

The toughness of the killed bessemer steel has been thoroughly explored by impact tests at both room temperature and minus 25°F. on every tenth heat produced. Up to the present time more than 5000 Charpy impact tests have been so made. The majority of these tests have been cut from pipe sections with a pipe-wall thickness less than the 0.394-in. width of the Charpy test piece. In many cases so-called half-size or two-thirds size Charpy impact tests have been necessary. The depth through the notch of the impact test was the same as that for the standard Charpy impact specimen. Fig. 5A shows the results of Charpy impact tests in both the hot-rolled state and normalized state of heats tested at 75°F., and Fig. 5B shows the results at minus 25°F. Tests at 32°F. and 0°F. fall between the limits exhibited by the two temperatures in the figures. The results are plotted as frequency distributions of several thousand tests at each temperature.

It should be emphasized that the majority of the Charpy impact tests were made on Charpy specimens two thirds the ordinary width and the impact value would be approximately 30 per cent

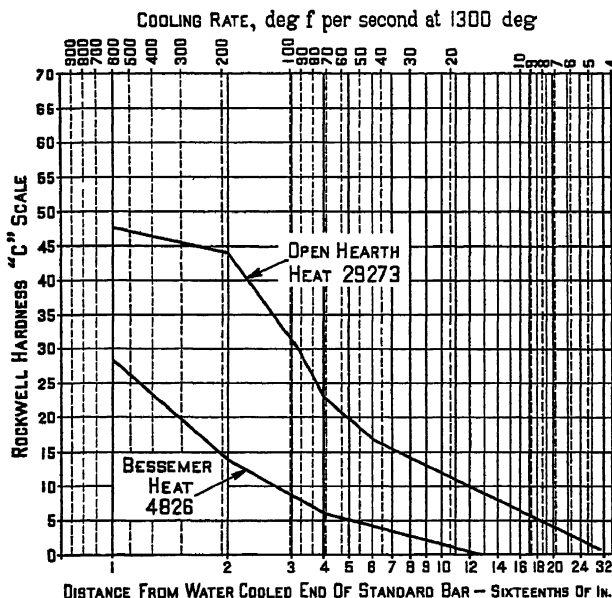
higher if made on full-width Charpy test pieces. The frequency distribution is similar to results obtained with fine-grained open-hearth steels of approximately 75,000 lb. per sq. in. tensile strength. These results clearly show that the fully killed bessemer steel is tough at temperatures at least as low as minus 25°F. A few tests made at minus 50°F. have also exhibited similar properties.

The excellent ductility and impact toughness exhibited by this bessemer steel, with carbon content between 0.12 and 0.40 per cent, show very definitely that phosphorus and nitrogen, even when present in considerable amounts, do not have a detrimental effect on these properties. It is concluded that the form in which the oxygen exists in the steel is probably the predominating factor in controlling toughness at subzero temperatures. It is well known that open-hearth steels in the semi-killed or coarse-grained state show very poor impact properties below 32°F. The material used at temperatures between minus 25° and minus 50°F., whether open-hearth or bessemer, must be fine-grained material, thoroughly treated with aluminum additions greater than 1½ lb. per ton of ingots.

Studies of the welding qualities of steels during recent years have emphasized that elements that impart high hardenability to the steel, such as carbon, manganese, chromium, and molybdenum, make welding more difficult as the percentage of these elements is increased in the steel. It has been found that standard hardenability tests similar to the Jominy end-quench test form an important index of the ease with which steel may be welded and also the degree of preheating necessary for safe welding procedure. An open-hearth steel of 75,000 lb. per sq. in. tensile strength must contain at least 0.30 per cent carbon and 1 per cent manganese. At the present time this represents about the optimum content of these two constituents that

may be safely welded without resorting to costly preheating and postheating operations. Even so, the Jominy hardenability of such an open-hearth steel is fairly high,

described herein contains less than 0.25 per cent carbon and less than 0.60 per cent manganese. The hardenability of the material adjacent to the weld is con-



STEEL ANALYSES AND QUENCHES

STEEL	C	Mn	P	S	Si	Ni	Cr	Mo	QUENCHING TEMPERATURE	BRAIN SIZE	HEAT NUMBER
BESSEMER	.18	.45	.09	.027	.21				1650° F	7-9	4826
OPEN HEARTH	.28	.87	.02	.025	.20				1650° F	6-7	28273

FIG. 6.—END-QUENCH TEST.

as the hardness adjacent to welds in open-hearth steel of 75,000 lb. per sq. in. tensile strength is apt to approach 45 Rockwell C. This may be readily determined by means of spot bead tests wherein the steel to be welded receives a spot deposit from the welding rod and is then sectioned and etched for hardness determinations. Such tests made on open-hearth steel of 75,000 lb. per sq. in. tensile strength have shown Rockwell hardness up to 45 on the C scale, whereas similar tests on the bessemer steel of 75,000 lb. per sq. in. tensile strength seldom develop Rockwell hardness exceeding 27 on the C scale. The bessemer steel of 75,000 lb. per sq. in. tensile strength

siderably less than with open-hearth steels of the same tensile strength.

This has been further verified through standard Jominy end-quench hardenability tests, and the comparison between the open-hearth and killed bessemer steel is shown in Fig. 6. The open-hearth steel shown has a lower tensile strength than the bessemer steel, and, even though it represents fine-grained quality, its hardenability is much greater than that of the killed bessemer steel. These results lead to the conclusion that for high-strength structures involving welding, the killed bessemer steel is superior to the grades of open-hearth

steels of similar tensile strength that are now available to the trade.

The properties of the killed bessemer steel at elevated temperatures have been

bessemer grades are strongly susceptible to increased strength and loss of ductility in the so-called blue-heat range between 400° and 600°F. In order to determine how

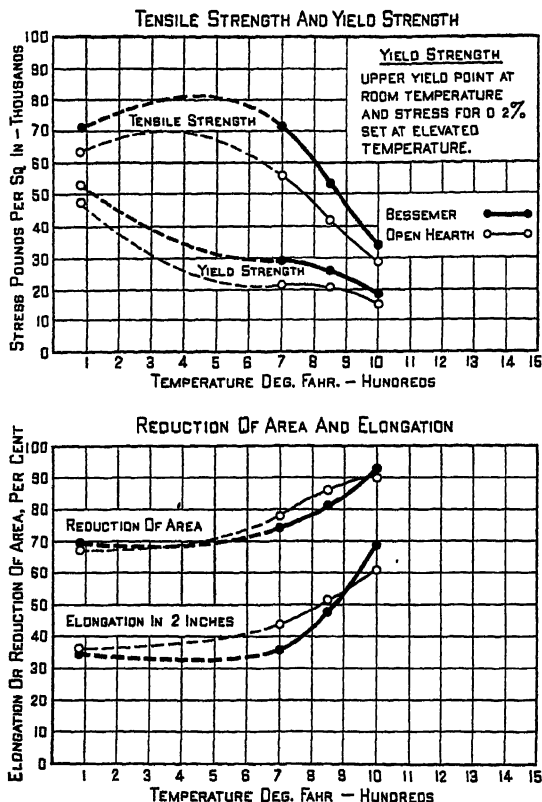


FIG. 7.—COMPARISON OF TENSILE PROPERTIES AT ELEVATED TEMPERATURE OF NORMALIZED OPEN-HEARTH AND BESSEMER CARBON STEEL (0.17 PER CENT C).

investigated at the United States Steel Corporation Research Laboratory by means of short-time tensile tests at elevated temperatures as well as long-time creep tests at 850° and 1000°F. In general, short-time high-temperature tests of killed bessemer steel and killed open-hearth steel, both in the fine-grained state, are similar with respect to tensile strength, yield strength, elongation, and reduction of area. The results of tests made on both types of steel are shown in Fig. 7.

It has long been known that undeoxidized steels of both open-hearth and

the thoroughly killed bessemer steel reacted in this temperature region in comparison with other steels, short-time high-temperature tensile tests have been made on the following types of steels:

- Undeoxidized capped bessemer steel
- Undeoxidized capped open-hearth steel
- Silicon-killed coarse-grained open-hearth steel
- Silicon-aluminum-killed fine-grained open-hearth steel
- Silicon-aluminum-killed fine-grained bessemer steel

Fig. 8 exhibits the results of these tests and shows that all the undeoxidized steels

are very susceptible to blue-heat brittleness in this temperature range, whereas both the fine-grained open-hearth and bessemer steels are practically free from this char-

acteristic of the fine-grained open-hearth steel approximated 6400 lb. per sq. in. at 850°F. compared with 10,200 lb. per sq. in. for the killed bessemer steel with correspond-

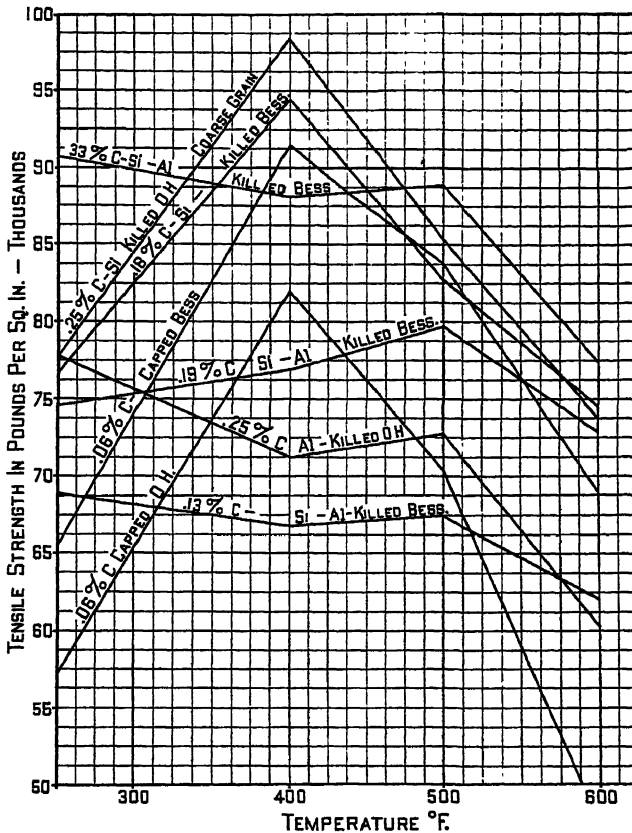


FIG. 8.—TENSILE STRENGTH OF STEELS AT BLUE-HEAT TEMPERATURES.

acteristic. It is therefore concluded that the fine-grained thoroughly killed bessemer steel, when made according to the practices given, is apt to be less susceptible to strain-hardening and effects of blue-heat brittleness than many steels used in the past.

Long-time creep tests were conducted at 850° and 1000°F. on fine-grained open-hearth steel and fine-grained silicon-aluminum-killed bessemer steel. Results of these tests show a definite superiority for the bessemer steel (Fig. 9). The creep limit

ing values at 1000°F. of 1500 lb. per sq. in. for the fine-grained open-hearth as against 3300 lb. per sq. in. for the bessemer steel.

It is believed that the superior creep resistance of the killed bessemer steel is largely due to its phosphorus content, as has been noted by numerous previous investigators, particularly Gillett,² Cross³ and their co-workers. It is well known that molybdenum increases the creep resistance of steels, and in order to determine whether phosphorus would supplement the effect of molybdenum, creep tests were made on

steels containing 0.50 per cent molybdenum and 0.10 per cent phosphorus. Here again the influence of phosphorus was verified; a low-phosphorus steel (0.02 per cent) con-

It has long been considered that ordinary bessemer steels, which in the past have been of the undeoxidized type, are extremely susceptible to work-hardening and

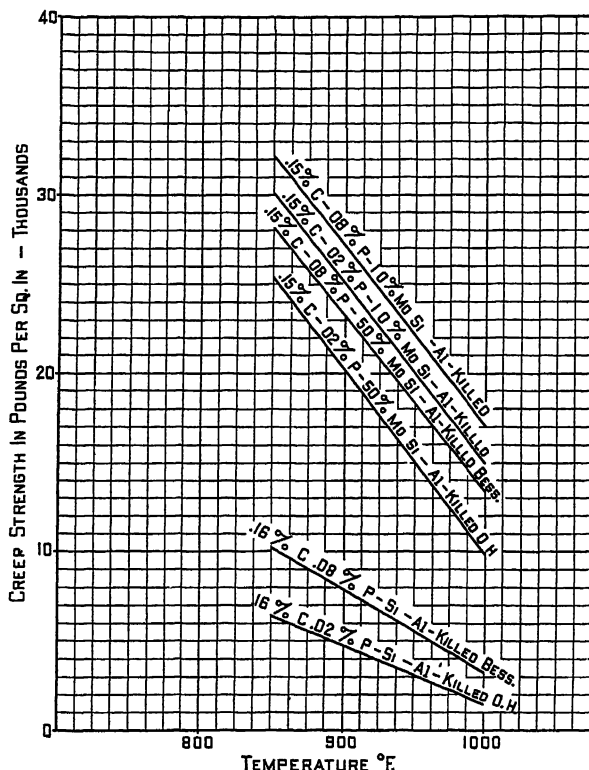


FIG. 9.—CREEP STRENGTH AT 850° TO 1000°F.
1 per cent elongation in 10,000 hours.

taining 0.50 per cent molybdenum exhibits a creep limit of 9,000 to 10,000 lb. per sq. in. at 1000°F. whereas a steel containing 0.10 per cent phosphorus and 0.50 per cent molybdenum showed a creep limit at 1000°F. of 13,000 lb. per sq. in. These results should indicate that bessemer steels treated with molybdenum would be considerably superior in high-temperature strength to molybdenum-bearing open-hearth steels used in the past, or open-hearth heats could be rephosphorized to level of 0.10 per cent in order to increase the high-temperature strength.

very sensitive to strain-aging. These properties can be readily determined by means of the strain-sensitivity test developed by Work⁴ of Jones and Laughlin Steel Corporation. This test consists in the drawing of a bar, previously forged, normalized, and machined with a tapered outside diameter, through a die in order to obtain a reduction in area along the bar length varying from 0 to 10 per cent. The bars after cold-drawing are tested in the as-strained state, while other bars are heated to temperatures in the region of 400° to 550°F. in order to develop a

strain-aged condition. The characteristics of the fine-grained killed bessemer steel were compared with those of several other types of carbon steel by means of this

viously. For both the open-hearth and bessemer steels, only the fine-grained fully deoxidized steels are free from strain-aging and blue-heat brittleness, and tough

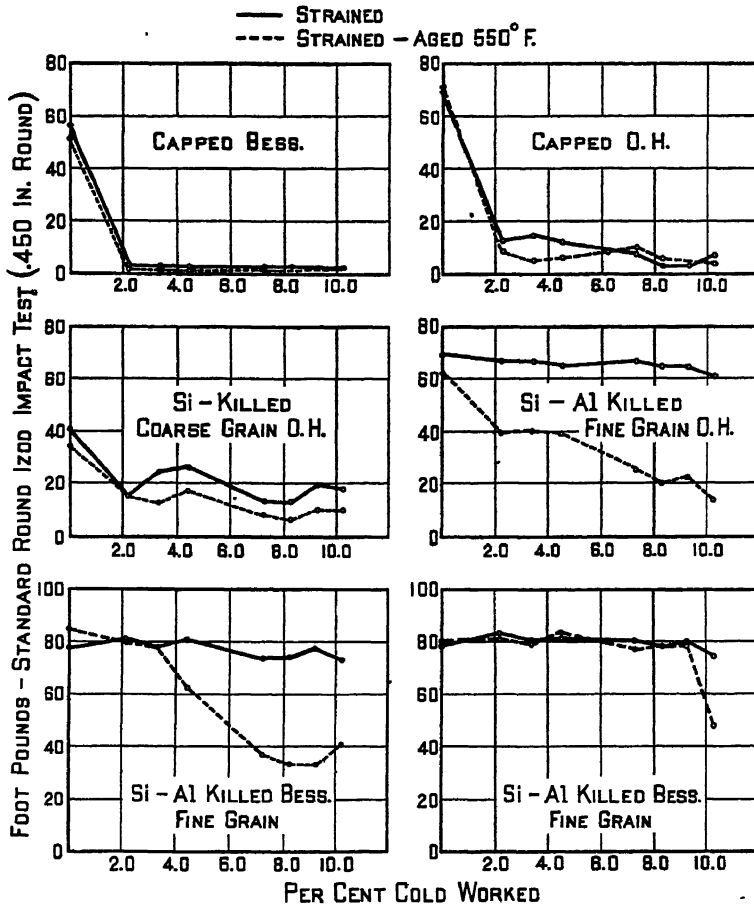


FIG. 10.—STRAIN SENSITIVITY.

strain-sensitivity' test. The results are shown in Fig. 10 for six different steels. The undeoxidized and partially deoxidized coarse-grained steels show a high strain sensitivity, while the fine-grained silicon-aluminum-killed open-hearth and bessemer steels are quite resistant to strain-aging effects.

These results coordinate closely with the high-temperature tensile tests and low-temperature impact tests given pre-

viously. Obviously the condition in which the oxygen exists in the steel has an important influence on these three characteristics. Apparently the aluminum treatment in the ladle precipitates or fixes the oxygen and possibly the nitrogen in the steel, thereby depressing their effect.

During the past few years T. Swinden⁵ and his associates in England, in numerous papers, have reported data on both coarse-

grained (semikilled or rimmed) and fine-grained (fully killed) bessemer steels, which fully corroborate the data presented in this paper regarding the freedom of fine-grained, fully killed bessemer steel from blue-heat brittleness, susceptibility to strain-aging, and low impact properties. Swinden's paper also points out the negligible effect of nitrogen, when under 0.018 per cent, on strain-aging embrittlement when the bessemer steel is in the fine-grained, fully deoxidized condition.

Previous reference has been made to the cleanliness and Jominy hardenability characteristics of the low-carbon killed bessemer steel. A survey of the carburizing properties of this material and investigation of specimens quenched after carburizing indicate that it compares very favorably in this respect with standard open-hearth carburizing steels of the 1020-X type, which normally contains 0.15 to 0.25 per cent carbon and 0.70 to 1.00 per cent manganese. McQuaid-Ehn tests on the fine-grained open-hearth steel compared with killed bessemer steel show that the latter is somewhat finer in grain size and possesses the same degree of normality as the corresponding open-hearth steel. A survey of quenched carburized specimens by Rockwell hardness tests and hydrochloric etch for detection of soft spots showed that the carburized bessemer steel was in general less affected by soft spots than the fine-grained 1020-X open-hearth steel after carburizing. In addition, the core strength of the bessemer steel is greater than that of the open-hearth steel. It is believed therefore that the low-carbon killed bessemer steels, because of their greater cleanliness and at least equally desirable carburizing characteristics, may have useful applications in this field.

Results of the investigations of the killed bessemer steel described are based on at least five years of testing on thousands of heats of steel. Except for the creep tests and the hardenability and carburizing studies,

the properties reported represent results on a large number of heats. There can be little doubt as to the uniformity of this type of bessemer steel compared with standard open-hearth grades.

A summary of the important conclusions drawn from the work is given below:

1. The yield strength and fatigue properties of killed bessemer steel are superior to those of open-hearth steel of the same tensile strength.

2. The ductility and toughness of the killed bessemer steel both at room and sub-zero temperature are equal to the ductility and toughness of open-hearth steel of the same tensile strength provided both steels are thoroughly killed with the same deoxidation practice.

3. The ease of welding and metallurgical effects adjacent to welds of the killed bessemer steel are better than for open-hearth steel of the same tensile strength.

4. The cleanliness and carburizing qualities of killed bessemer steel are equal to those of corresponding open-hearth grades.

5. The susceptibility to strain or strain-aging and the amount of blue-heat brittleness developed by killed bessemer steel is similar and approximately equal to the strain-aging or blue-heat brittleness of killed open-hearth steel of the same tensile strength, finished with the same deoxidation practice.

6. The creep strength of the fine-grained killed bessemer steel is higher than the creep strength of fine-grained open-hearth steel finished with the same deoxidation practice.

The development of the killed bessemer steel represents intensive work during the past five years among most of the metallurgists and steel-plant superintendents of the National Tube Co. Mr. P. F. Mumma, superintendent of steel plant at McKeesport, and Mr. W. B. Kennedy, chief metallurgist of the same plant; Messrs. J. E. Gould and J. D. Tyson, metallurgists at the Lorain plant of the National Tube

Co., and Mr. H. W. Hudson, assistant general superintendent of the National Tube Co. plant at Ellwood City, have all contributed greatly to the study of the properties of this type of steel as it has passed through operations under their supervision. The help and cooperation of these men greatly facilitated this development.

REFERENCES

1. J. Chipman: *Trans. Amer. Soc. for Metals*, 30, 817.
2. H. W. Gillett: Phosphorus as an Alloy Element in Steel. *Metals and Alloys* (1935) 6, 280-283, 307-310.
3. H. C. Cross and D. E. Krause: Phosphorus as an Alloying Element in Steels for Use at Elevated Temperatures. *Metals and Alloys* (1937) 8, 53-58.
4. H. W. Graham and H. K. Work: *Proc. Amer. Soc. Test. Mat.* (1939) 39, 571.
5. T. Swinden: *Jnl. Iron and Steel Inst.* (1936).
T. Swinden and F. B. Cawley: *Inst. of Marine Engrs.* (1939) 51, pt. 3, 99.

DISCUSSION

(W. O. Philbrook presiding)

C. E. SIMS,* Columbus, Ohio.—Discussions of bessemer steel usually start on the defensive, which is an inevitable result of the long-held popular conception that it is different in kind from steels made by other processes. Because it is made by a supposedly crude process, the inference is made that bessemer steel is somehow inferior. Yet, as the author points out, the physical chemical principles by which bessemer and open-hearth steels are made are the same.

It appears that the high light of this excellent paper is the evidence that any differences that were found in the comparison of bessemer and open-hearth steels can be adequately explained by known differences in chemical composition, notably of phosphorus and nitrogen. Bessemer steel has been suspected and accused of being inordinately high in oxygen content. In the light of our present knowledge of the physical chemistry of steelmaking, the deoxidation practice used on these steels should leave them with oxygen contents no higher than would be found in open-hearth steels of similar composition—composition including the deoxidizer. The data on inclusion count corroborates this expectation.

It would be appreciated if Mr. Wright would extend his discussion to include any observa-

tions as to inherent differences in the two groups of steels that could not be attributed to composition. That is the salient question at issue.

R. B. SOSMAN,* Kearny, N. J.—Mr. Sims' statement that the properties of a steel may be expected to depend only upon its composition should not go unchallenged, even though we interpret it broadly to mean that two steels should be identical in properties if they have the same composition and have been subjected to the same thermal history since solidification. The *distribution* of the minor constituents, especially the portion that is insoluble in the liquid metal, is known to influence the structure and hence the properties. In the bessemer vessel, oxygen is entering the metal direct from air by way of a very large and rapidly changing surface; in the open-hearth furnace oxygen is entering the metal from a liquid slag by way of a small and more stable surface. In the bessemer, liquid drops are in contact with a surrounding continuous gas phase; in the open hearth, gas bubbles are in contact with a surrounding continuous liquid phase. In the bessemer, concentrated nitrogen is reacting directly with liquid metal; in the open hearth, the metal is shut off from nitrogen except while the scrap is melting down, and even then is in contact with nitrogen greatly diluted with hydrocarbons, CO and CO₂. It would be surprising if the distribution of undissolved oxides and nitrides were to be found the same in steel made by the two processes, even though the percentages happened to be identical.

E. C. SMITH,† Cleveland, Ohio.—The common oil-country seamless material of England and Europe is bessemer steel, such as the Corby plant of Stewart and Lloyds makes in basic-lined vessels. It would be of interest to know what difference, if any, exists in the products of Europe and America, inasmuch as both are bessemer steels. The European steels are usually recarburized with pig iron when higher carbon products are involved.

H. B. EMERICK,‡ Pittsburgh, Pa.—The author and his associates merit high com-

* Research Laboratory, United States Steel Corporation.

† Chief Metallurgist, Republic Steel Corporation.

‡ Steel Works Metallurgist, Jones and Laughlin Steel Corporation.

* Battelle Memorial Institute.

mentation for the manner in which they have adapted liquid-iron recarburization of blown metal to the successful production of deoxidized bessemer steel for seamless piercing operations. The limited amount of experimental work carried on at Jones and Laughlin's Aliquippa works, using slight modifications of the procedure described, has largely confirmed the experience of the author with reference to the workability and physical properties of properly made bessemer seamless pipe.

In discussing the chemical specifications evolved for the grade employed in the manufacture of seamless pipe, the author refers to a carbon content of 0.12 to 0.20 per cent. No statement is made concerning the possibility of working to lower carbon limits, so as to permit use of the improved deoxidized bessemer steel for the more critical lapweld and butt-weld pipe applications. The last five years have seen highly important technological advances in the development of instrumental methods for controlling the end point and, consequently, the degree of oxidation of bessemer blown metal. These developments have contributed so significantly to improved uniformity of blown-metal oxidation that it is now possible to achieve a reasonably consistent and uniform deoxidation of the metal in the ladle. Many thousands of tons of low-carbon hot-topped bessemer steel, deoxidized in the ladle with aluminum, have been used successfully for a wide variety of structural bar, pipe and shape applications of a specialized nature. Such a steel possesses freedom from laminations, good impact resistance at low temperature, and a low degree of sensitivity to cold-work.

Rather extensive investigation into the physical properties of aluminum-killed bessemer steels in the lower carbon ranges has led us to attach considerable significance to the uniformity of inherent austenite grain size. It would be of interest to have the author comment on his experience in this connection. A statement of the residual metallic aluminum content typical for steel deoxidized in the manner described would also be of interest.

E. C. WRIGHT (author's reply).—The comments given by Mr. Sims are of interest in view of his previous excellent work on the characteristics of bessemer steel castings. I would

like to emphasize that the physical chemical principles by which bessemer and open-hearth steels are made are identical, and that the same physical chemical results may be obtained with either process by following the same procedure. The fact that bessemer operation is so much more rapid than the open-hearth process does not seem to alter the results. We are inclined to agree with Mr. Sims' opinion that the only difference between fully deoxidized basic and fully deoxidized acid bessemer steel is probably associated with the higher contents of nitrogen and phosphorus, which are not eliminated in the acid bessemer process.

Mr. Smith's comments do not relate exactly to the process discussed in this paper. The steel made at the Stewart and Lloyds plant is basic bessemer steel of rather high sulphur content and is not fully deoxidized by the procedures discussed. Most of the Corby steel is rimmed steel for pipe skelp or semikilled steel for extrusion or push-bench seamless-tube manufacture. It is believed that the type of steel made at Corby would not be adaptable to rotary piercing operations generally used in the United States for rolling seamless tubes.

Mr. Emerick's statements corroborate some of the findings in our work. We have purposely avoided making killed bessemer steel with carbon content below 0.12 per cent, since the carbon deoxidation was found to be so effective and the thoroughness of deoxidation with heats containing less than 0.12 per cent was considerably more erratic. It is our opinion that a steel bath with a content of 0.12 per cent carbon, whether open-hearth or bessemer, is fairly well deoxidized by the carbon content at that level, and final and complete deoxidation with silicon and aluminum is readily accomplished thereafter.

However, there is no question that killed bessemer-steel heats with carbon as low as 0.06 per cent can be made if sufficient amounts of silicon and aluminum added in a very thorough manner are used in finishing the heat. The inherent austenitic grain size as measured by McQuaid-Ehn tests show that all the heats are extremely fine grained. The order of the grain size is between 7 and 10. The residual aluminum content of the killed bessemer steel is generally between 0.025 and 0.05 per cent. This variation is dependent upon the efficiency of the aluminum addition.

The Effect of Quenching Temperature on the Results of the End-quench Hardenability Test

By CLARENCE E. JACKSON,* MEMBER, AND ARTHUR L. CHRISTENSON,* JUNIOR MEMBER A.I.M.E.

(Chicago Meeting, October 1943)

IN the establishment of the relationship between weldability and hardenability, two methods have been employed in correcting for the grain growth produced in the heat-affected zone: first, the hardenability calculated from chemical composition¹ may be corrected to the grain size observed in an actual weld,² or, second, a hardenability test may be made on the steel quenched from a temperature high enough to produce a grain size comparable to that found in the heat-affected zone.³ In order to obtain grain sizes in the end-quench hardenability bar comparable to those resulting in the base metal from the welding cycle, a quenching temperature of 2100°F. has been used. In studies of the end-quench hardenability specimen quenched from 2100°F. instead of from a lower temperature of 1700°F., it is important to ascertain the relative cooling rates for various distances along the bar. It is a question as to whether the cooling occurs at the same rate or whether there is any significant difference from the standard cooling-rate curve published by Jominy and confirmed by others.^{4,5} This

paper reports experimental evidence concerning the effect of quenching temperature on the cooling rates in the end-quench hardenability test.

The effect of quenching temperatures on cooling rates has been studied by a number of investigators.^{6,7} French has considered this effect from both theoretical and experimental aspects. In French's studies on complete quenching of spheres and rounds, an increase in the quenching temperature caused an increase in the cooling rate at 720°C. at the center of the specimen. The center cooling velocity also has been shown to be dependent upon the surface per unit volume for the type of specimens studied; the velocity of cooling increases with an increase in the surface per unit volume.

Three methods of indicating the rapidity of cooling of a body of metal during a quenching operation have been proposed:

1. The time it takes for the metal to cool from the quenching temperature to a temperature halfway between the quenching temperature and the temperature of the quenching medium (half-temperature time): Grossmann, Asimow and Urban⁷ justify the use of this criterion by the fact, that the half-temperature time includes the temperature and time of incubation as well as the zone of formation of pearlite and, further, the data so derived accord very closely with experimental values.

2. The time interval the metal remains in a given temperature range; for example,

This paper represents only the personal opinions of the authors and in no way reflects the official attitude of the U. S. Navy. Published with permission of Navy Department. Manuscript received at the office of the Institute July 12, 1943. Issued as T.P. 1647 in METALS TECHNOLOGY, December 1943.

* Division of Physical Metallurgy, Naval Research Laboratory, Anacostia Station, Washington, D. C.

¹ References are at the end of the paper.

1100° to 900°F.: A number of investigators have favored this criterion for indicating rate of cooling. The importance of the temperature interval 1100° to 900°F. is

bar have interpreted their data based upon the cooling rate at 1300°F. In fact, the commonly suggested form for reporting end quench hardenability data relates

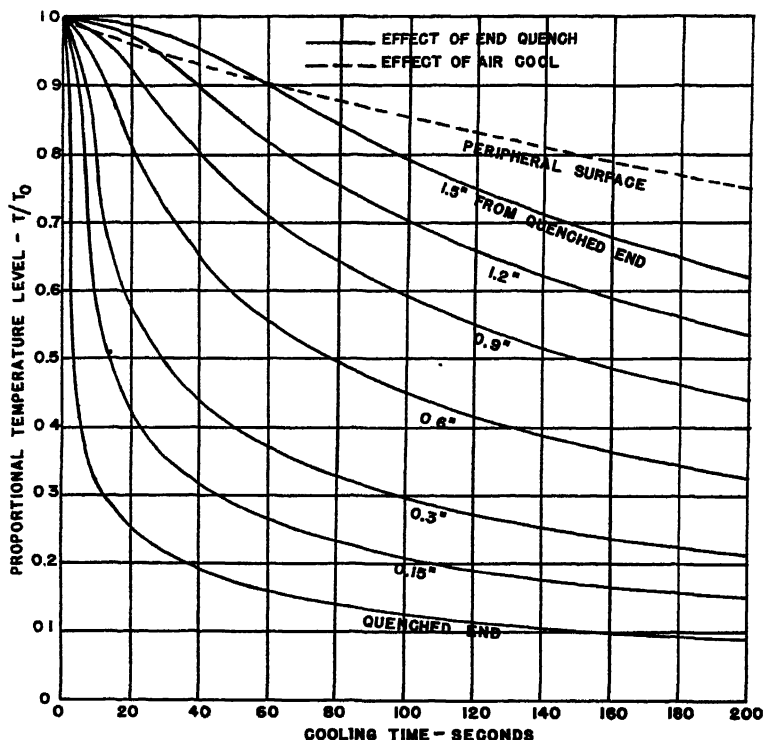


FIG. 1.—RELATION OF CALCULATED PROPORTIONAL TEMPERATURE LEVEL AND COOLING TIME FOR VARIOUS DISTANCES FROM QUENCHED END OF HARDENABILITY TEST BAR (Grossmann).

unquestioned for the plain carbon-manganese steels, but the critical range is usually lower for most alloy steels; for example, in S.A.E. X4130 the most critical temperature range is 900° to 600°F.; these temperature ranges are related to the isothermal transformation characteristics.

3. The instantaneous rate of cooling at a given temperature; for example, the number of degrees per second at 1300°F.: French,⁶ in his original work, reported cooling data based upon the instantaneous cooling rate at 1300°F. as an index of rate of cooling. Many of the investigators using the end-quench hardenability test

the distance from the quenched end to the cooling rate at 1300°F.

The effect of quenching temperature on rapidity of quench can be predicted from thermal calculations if two assumptions are made to simplify the mathematical analysis. These assumptions are that Newton's law of cooling is followed during the quenching operation and that the thermal constants of the metal are independent of temperature. Making use of these assumptions and Russell's tables,⁸ Asimow, Craig, and Grossmann⁹ have computed and drawn a chart (Fig. 1) showing the effect of air cool and end

quench on the cooling time at various distances from the quenched end along the surface of the end-quench hardenability bar. This chart was calculated assuming a "severity of quench factor" (Grossmann's H value) of 2.33 for the end quench and 0.022 for the air cool. The average thermal diffusivity was taken to be 0.009 sq. in. per second.

The effect of quenching temperature on the half-temperature time can readily be seen from the chart. The proportional temperature level $\frac{T}{T_e}$ (equal to $\frac{T - T_M}{T_e - T_M}$, where T_e is the quenching temperature and T_M the temperature of the quenching medium) will always be equal to 0.5 if T is the temperature halfway between the quenching temperature and the bath temperature. Therefore, it is expected that quenching temperature should have no effect on the half-temperature time.

The quantitative effect of the quenching temperature on the time interval that a given point on the end-quench hardenability bar remains in a given temperature range can also be obtained from Fig. 1. For example, with a quenching temperature (T_e) of 2100°F., and assuming the temperature of the water (T_M) as 100°F., the proportional temperature level at 100°F. will be

$$\frac{T}{T_e} = \frac{T - T_M}{T_e - T_M} = \frac{1100 - 100}{2100 - 100} = 0.5$$

From Fig. 1, this gives a cooling time of 29 sec. at 0.3 in. from the quenched end under the effect of the end quench only. If the effect of the air cool is also considered, the proportional temperature level $\frac{T}{T_e}$ will be the product of the effects of the end quench and air cool. By inspection (Fig. 1) a proportional temperature level of 0.5 will require a factor for the end quench of 0.53 and a factor of 0.95 for the air cool; this gives a cooling time of 25 sec. Likewise, at 900°F.

$$\frac{T}{T_e} = \frac{T - T_M}{T_e - T_M} = \frac{900 - 100}{2100 - 100} = 0.4$$

which from Fig. 1 gives a cooling time of 50 sec. for the end quench alone and a cooling time of 40 sec. with the effect of both the end quench and air cool. Thus it is seen that at 0.3 in. a bar quenched from 2100°F. will remain in the region of 1100° to 900°F. for approximately 25 from 40, or 15 sec. under the influence of both the end quench and air cool. Similarly, a bar quenched from 1700°F. will remain in the interval 1100° to 900°F. for approximately 9 sec. under the influence of both the end quench and air cool. At 0.3 in. distance, then, the bar quenched from 2100°F. will remain in the region 1100° to 900°F. roughly 1.7 times longer than if quenched from 1700°F. Calculations can thus be made showing the effect of quenching temperature on the time interval between 1100° and 900°F. for any distance along the end-quench hardenability bar. However, variations in quenching technique and composition of steel limit the use of such a calculated table, and of more immediate concern is the fact that the quenching temperature does have an effect and its direction is such as to give a less severe quench for higher quenching temperatures.

The mathematical equation for temperature distribution used as a basis for Fig. 1 cannot readily be used to calculate the effect of quenching temperature on the instantaneous rate of cooling at a given temperature. However, the equation is simplified if it is assumed that the end surface falls instantaneously to the temperature of the quenching medium (severity of quench factor is infinite) and that the effect of air cooling is negligible (Appendix 1). The relative cooling rates at various temperatures quenching from 1500°, 1700°, 1900° and 2100°F. have been calculated using this simplified equation and the results are shown in Table 1. It is to be expected that the results will apply only

in the region near the water-cooled end of the end-quench hardenability bar, although the calculations show a decrease in the

TABLE 1.—*Calculated Effect^a of Quenching Temperature on Cooling Rates at Any Given Distance*

Quenching Temperature, Deg. F.	Temperature at Which Cooling Rate is Measured		Ratio of Cooling Rate to 1700°F. Quench
	Deg. F.	Deg. C.	
1500	1300	704	1.229
	1200	649	1.283
	1100	593	1.308
	1000	538	1.318
	900	482	1.324
1700	1300	704	1
	1200	649	1
	1100	593	1
	1000	538	1
	900	482	1
1900	1300	704	0.795
	1200	649	0.786
	1100	593	0.781
	1000	538	0.780
	900	482	0.775
2100	1300	704	0.641
	1200	649	0.631
	1100	593	0.626
	1000	538	0.625
	900	482	0.622

^a See Appendix.

severity of quench as the quenching temperature increases. It is to be noted that, in the case of the ideal quench, the relative cooling rates for quenching from various temperatures are independent of the distance along the bar.

Since the transformation of steel occurs over a range of temperatures in the vicinity of the "knee" of the S-curve, the time the steel remains in this temperature range is probably the most useful indication of the severity of quench. The range 1100° to 900°F. has been used for many steels with considerable success. Some alloy steels with the minimum time of transformation occurring at a lower range require other temperature limits for the successful evaluation of quenching conditions.

TEST WORK

The relation of time and temperature for various distances along a standard end-quench hardenability test specimen was

determined for quenching temperatures ranging from 1500° to 2100°F. These measurements were made using stainless steel (18-8 type) and also low-carbon nickel-steel specimens.

Several end-quench hardenability specimens were made in duplicate or quadruplicate and quenched from various temperatures. In order to obtain a uniform grain size, this series of test bars was heated to 2100°F. to establish uniform grain size and then either quenched or transferred to a furnace at a lower temperature before final quenching. In this manner, a series was prepared with a uniform grain size quenched from a wide range of temperatures. If there is a practical difference in the cooling rates or in the length of time any portion of the test bar remains in the transformation range, the depth of hardening should be affected.

METHODS

In general, standard A.S.T.M. quenching equipment and procedure,¹¹ with the exception of quenching temperatures, were used in all end-quench hardenability tests. In order to obtain a more exact measurement of hardness changes, the Vickers hardness method was used in preference to the Rockwell hardness test.

The test specimens were 1-in. in diameter and 4 in. long, with a shoulder $\frac{1}{8}$ in. thick and $1\frac{1}{4}$ in. in diameter on one end, for supporting the specimens vertically in the quenching jig. For measurement of the quenching temperatures and cooling data, a platinum-platinum 10 per cent rhodium thermocouple (22 B. and S. gauge) was peened into a $\frac{1}{16}$ -in.-dia. hole $\frac{1}{8}$ in. deep along the side at a selected distance from the quenched end. The thermocouple leads were protected with a two-hole protection tube supported by a $\frac{3}{8}$ -in.-dia. rod threaded into the top end of the specimen.

Two methods for recording temperature and temperature changes were used. The first of these, a high-speed temperature

recorder, was used to obtain most of the data for the low-alloy nickel steel No. 63. Most of the data for the 18-8 specimens were obtained using a 35-mm. movie

wet-ground at 180° apart 0.025 in. in depth along the entire length of the specimen. The surfaces were further prepared by hand polishing through the various grades

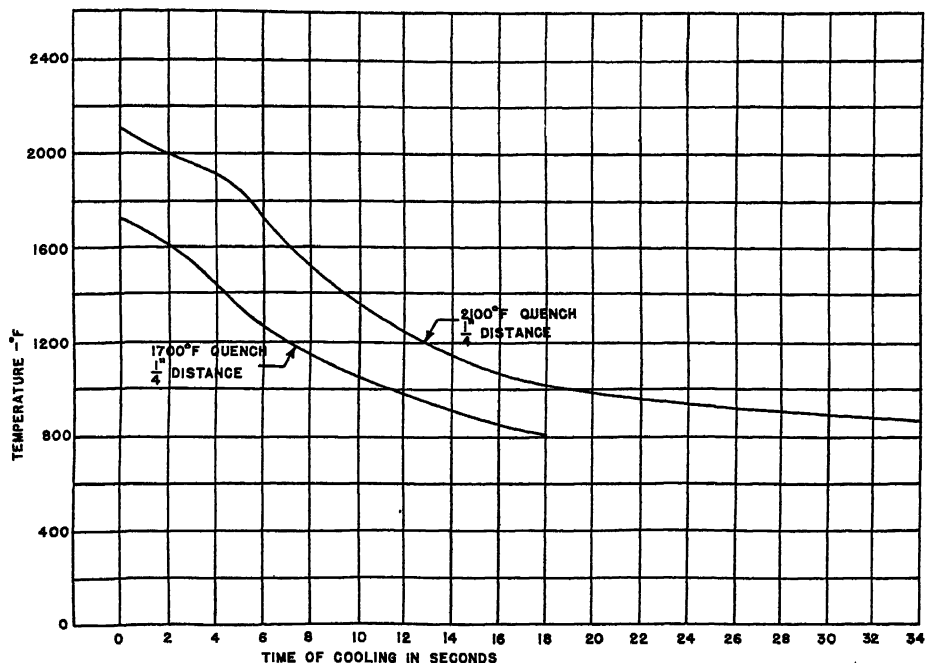


FIG. 2.—TIME-TEMPERATURE RELATION FOR ONE-FOURTH INCH DISTANCE ON END-QUENCH TEST BARS FROM LOW-ALLOY STEEL.

camera with 16 frames per second to photograph a millivoltmeter and stop watch. Although the measurements with the recorder were by far the more convenient to make, the measurements made by the camera and millivoltmeter were more easily reproduced.

The specimens were heated in a high-temperature controlled-atmosphere electric furnace with the specimen inserted in a carbon block to give further protection against decarburization. The specimens were maintained at the maximum temperature for at least 45 min. before quenching or transferring to a furnace at a lower temperature for 30 min. before quenching.

For the specimens on which a hardness survey was made, two flat surfaces were

of emery paper, finishing on 000. Vickers hardness measurements with a 10-kg. load were made at intervals of 0.025 and 0.050 in. along the ground surface for at least a distance sufficient to show a decrease in hardness commensurate with the carbon content and well below the hardness for 50 per cent martensite.

DATA OBTAINED IN THESE TESTS

Typical cooling curves for a distance of $\frac{1}{4}$ in. along the end-quench hardenability test bar for quenching temperatures of 2100° and 1700°F. are shown in Fig. 3 for stainless steel (18-8 type). The effect of quenching temperature upon the time to cool from 1100° to 900°F. for low-carbon nickel-steel specimens is shown in Fig.

4. Consistent results are much more difficult to obtain for steels with a phase transformation. from various temperatures is shown in Table 3. Typical end-quench hardenability curves are shown in Figs. 5 to 8.

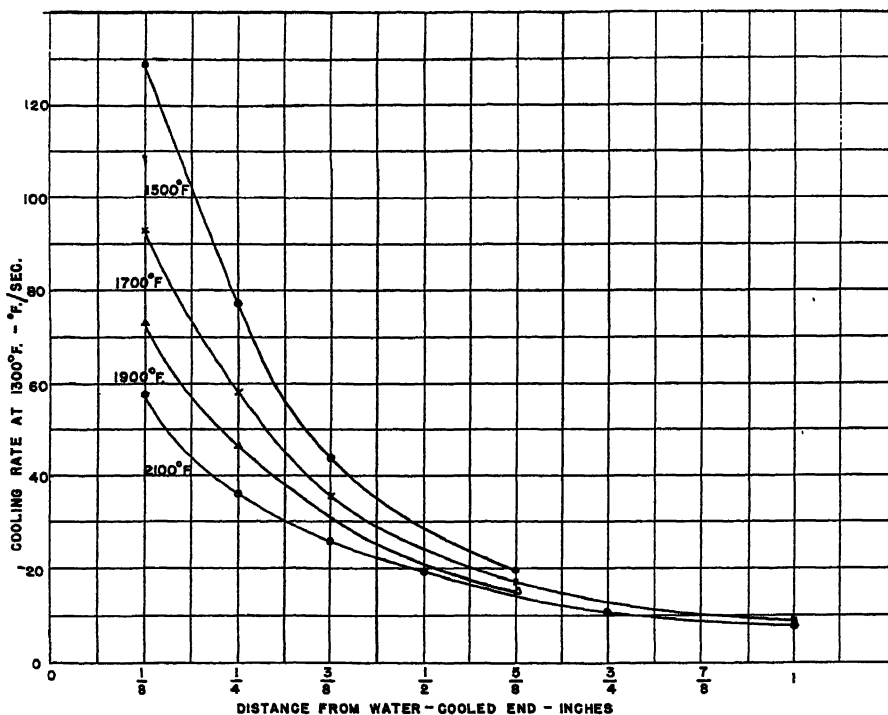


FIG. 3.—EFFECT OF QUENCHING TEMPERATURE ON COOLING RATE AT 1300°F. FOR END-QUENCH HARDENABILITY TEST SPECIMEN OF AUSTENITIC STAINLESS STEEL.

End-quench hardenability tests using a number of quenching temperatures were made on several steels, the chemical composition of which is given in Table 2. The

TABLE 2.—Chemical Composition

Steel No.	C	Mn	Si	S	P	Cr	Ni	Cu	Al
63	0.17	0.45	0.23	0.024	0.016		1.43		
175	0.36	0.88	0.22	0.028	0.012	0.10		0.09	0.001
180	0.20	0.42	0.05	0.032	0.012	0.04		0.05	
181	0.31	1.46	0.25	0.031	0.013	0.05	0.09	0.24	0.005
196	0.30	0.94	0.18	0.028	0.012	0.10		0.09	0.001
197	0.28	0.42	0.01	0.032	0.008	0.05	0.06	0.16	0.005
198	0.30	0.49	0.001	0.042	0.011	0.06	0.08	0.27	
199	0.23	0.38	0.16	0.037	0.010	0.04	0.09	0.09	0.002
200	0.30	0.65	0.19	0.037	0.012	0.06	0.02	0.15	
202	0.29	0.65	0.04	0.029	0.008	0.03	0.02	0.04	0.04
203	0.36	0.88	0.21	0.032	0.013	0.06	0.06	0.21	

analysis of the hardenability data obtained for a number of steels that were quenched

SUMMARY AND CONCLUSIONS

The data that are presented clearly establish the fact that the quenching temperature for the end-quench hardenability test bar is important, especially for steels of low hardenability. It is to be noted (Fig. 3) that the cooling rates follow closely the relative cooling rates predicted by the ideal quench (Table 1) at distances close to the end of the bar. The effect of quenching temperature beyond 1/2 in. is less important. This effect is not great for the narrow range of temperatures used in ordinary hardening, but is present and should not be neglected in comparative hardenability studies. The comparative end-quench test results re-

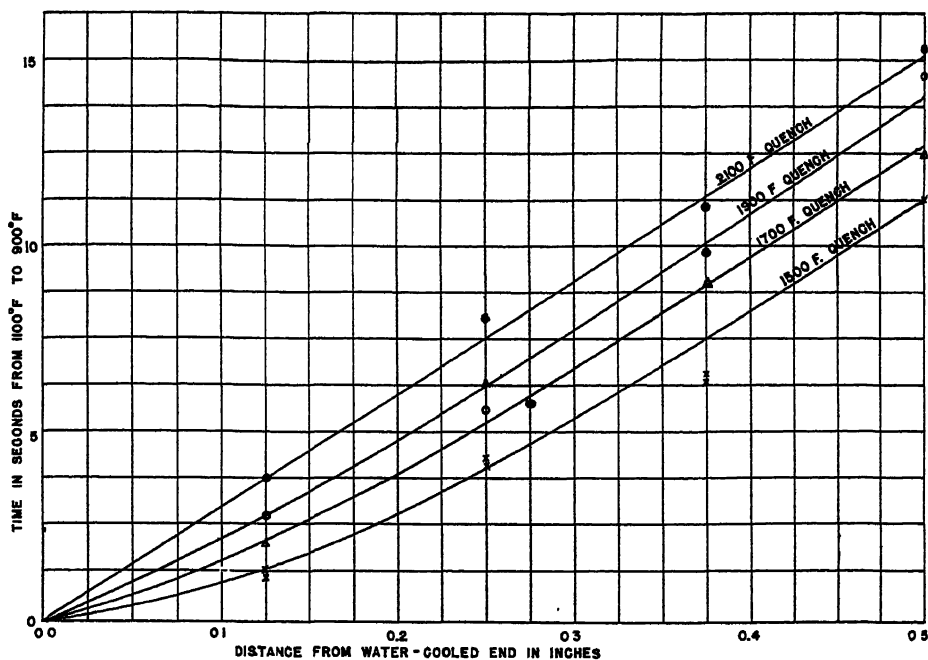


FIG. 4.—RELATION OF QUENCHING TEMPERATURE AND TIME TO COOL FROM 1100°F. TO 900°F. FOR END-QUENCH HARDENABILITY TEST ON LOW-ALLOY STEEL.

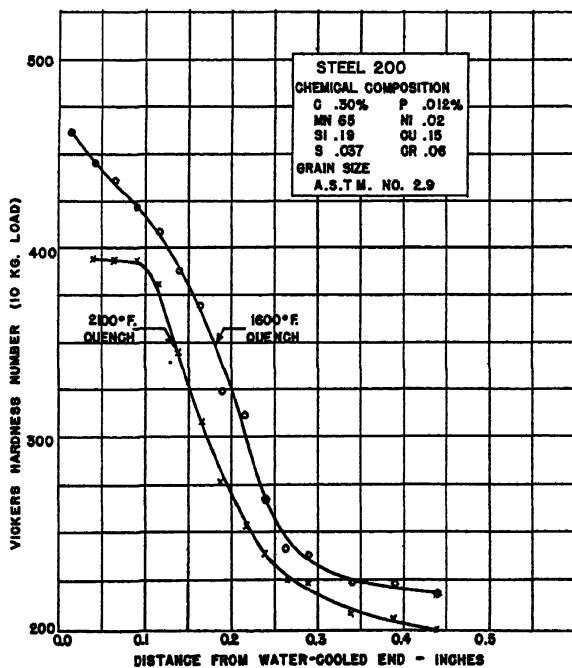


FIG. 5.—TYPICAL END-QUENCH HARDENABILITY CURVES.

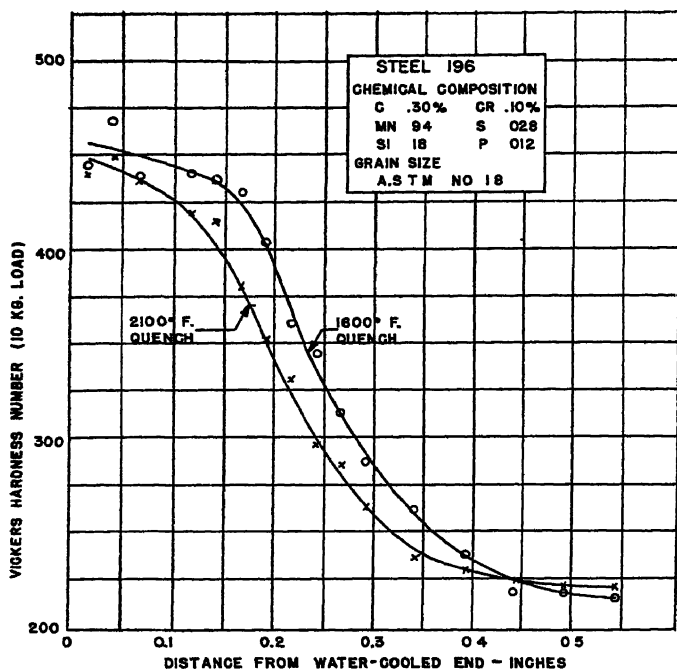


FIG. 6.—TYPICAL END-QUENCH HARDENABILITY CURVES.

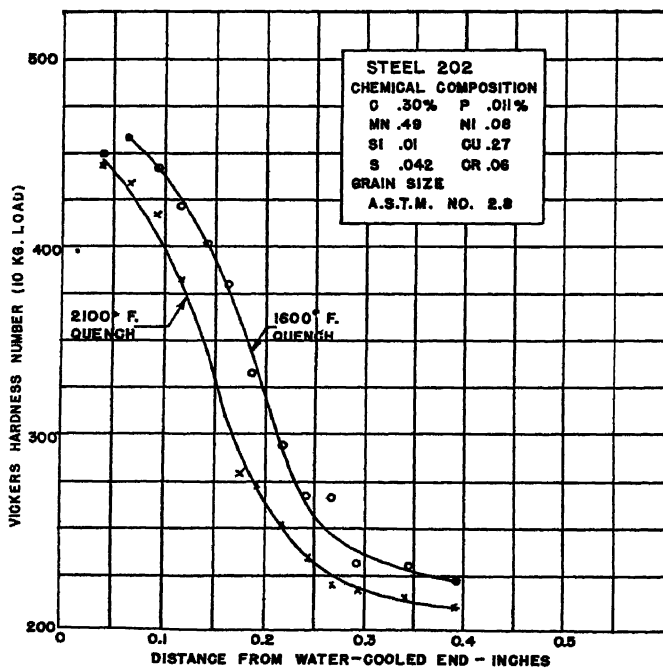


FIG. 7.—TYPICAL END-QUENCH HARDENABILITY CURVES.

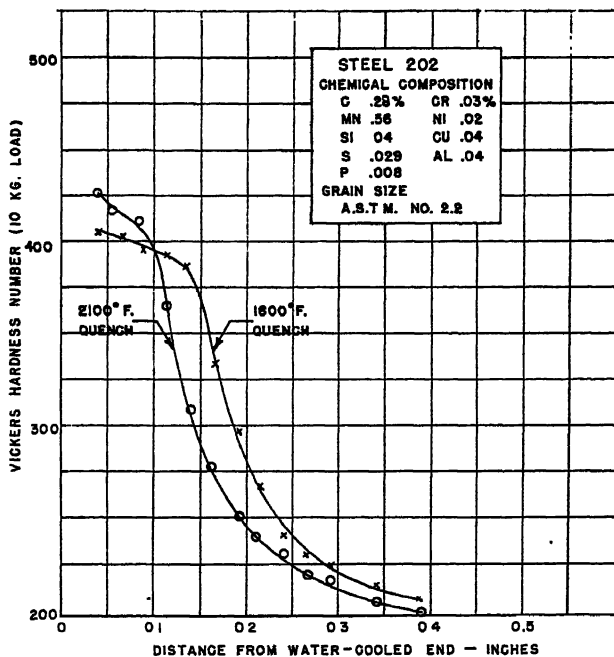


FIG. 8.—TYPICAL END-QUENCH HARDENABILITY CURVES.

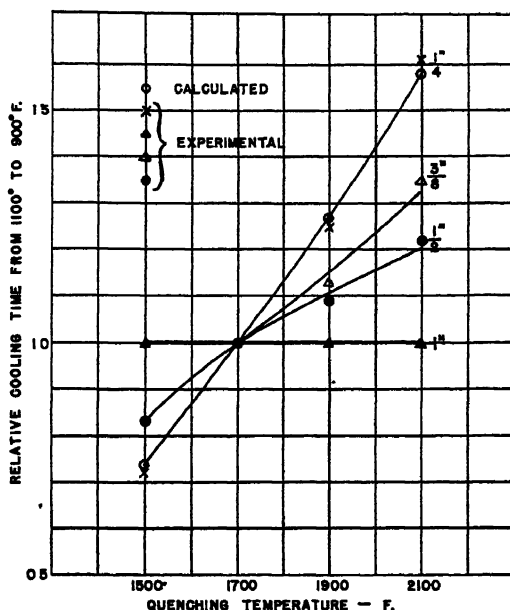


FIG. 9.—EFFECT OF QUENCHING TEMPERATURE ON RELATIVE TIME TO COOL FROM 1100° TO 900°F. FOR VARIOUS DISTANCES ALONG AN END-QUENCH TEST BAR.

Calculations were made assuming an ideal quench (infinite severity of end-quench factor and air cooling negligible).

TABLE 3.—Analysis of Hardenability Data

Steel No.	50 Per Cent Martensite Hardness	Quenching Temperature, Deg. F.	Grain Size No.	End-quench Hardenability Distance, In.	Ideal Diameter, In.
63	285	2100	1.7	0.21	1.70
		1700		0.27	1.95
		1700 ^a		0.21	1.70
175	375	2100	1.6	0.28	2.00
		1700		0.33	2.20
180	300	2100	1.8	0.10	1.20
		1700		0.12	1.30
181	350	2100	3.6	0.25	1.90
		1550		0.34	2.25
196	350	2100	1.8	0.19	1.60
		1600		0.23	1.80
197	345	2100	3.7	0.12	1.30
		1600		0.135	1.40
198	350	2100	2.8	0.135	1.40
		1600		0.18	1.60
199	330	2100	3.5	0.16	1.50
		1600		0.185	1.60
200	350	2100	2.9	0.14	1.40
		1600		0.18	1.55
202	340	2100	2.2	0.16	1.50
		1600		0.20	1.65
203	360	2100	4.1	0.21	1.70
		1600		0.25	1.90

^a Specimen heated to 1700°F. and quenched from this temperature.

ported in this paper were obtained on specimens that had undergone the same maximum austenitizing temperature that minimizes the effect of variations in the degree of carbide solution that ordinarily affect hardenability measurements.

The relation of quenching temperature and the time to cool from 1100° to 900°F. (Fig. 4) follows closely the effect of quenching temperature on the cooling rates at 1300°F. A marked effect of quenching temperature on the time to cool from 1100° to 900°F. is still noticeable at $\frac{1}{2}$ in. distance along the bar. It is doubtful that the relationship shown in Fig. 4 is valid for steels for other compositions, since the transformation range of steels varies considerably with composition.

Except in a few isolated instances, the quenching temperature had little effect on the hardenability of deep-hardening steels; because the half-hardness point for deeper hardening steels occurs at such a distance along the end-quench hardenability bar that there is little or no difference in the severity of quench for various

quenching temperatures. In an ideal quench of an infinite plate (severity of end-quench factor being infinite and air cooling negligible) the relative cooling rates when quenching from various temperatures are independent of distance from the surface of the plate. In the end-quench test, as the severity of end quench decreases in value and the air-cool factor increases, the relative cooling rates will depend upon the distance from the quenched end of the bar, and the quenching temperature will have less effect as the distance becomes greater.

This fact can be illustrated by Fig. 1, in which the severity of end-quench factor was taken to be 2.33 and the severity of air cool to be 0.022. By inspection from this chart, the ratio of cooling times between 1100° and 900°F. for a 2100° and 1700°F. quench with a bath temperature of 100°F. is found to be 1.7 at 0.3 in. and 1.1 at 0.9 in. Experimental verification of the lowering of the ratio of relative cooling times with respect to quenching temperature is shown on Fig. 9.

It is to be expected that the effect of quenching temperature on the end-quench test will assume its greatest importance in the quenching of low-hardening steels; however, the more nearly the quench of a section approaches the ideal quench of an infinite plate, the greater will be the effect of the quenching temperature on the cooling conditions. For instance, a severe quench of a heavy section of steel might approach an ideal quench for all practical purposes.

The increase of cooling rates with a decrease in quenching temperature should not always be expected when quenching other geometrical shapes. If a round, or sphere, is large enough to have as low a ratio of surface to volume as is characteristic of the end-quench bar, the quenching temperature should have the same qualitative effect on cooling rate, if the ratio of surface to volume is high, the effect of quenching temperature may be in the

opposite direction. In all cases, the effect of quenching temperature will depend on the size and shape of the quenched specimen and the severity of quench factor, which determines the amount of heat the coolant will remove from the surface of the quenched specimen.

ACKNOWLEDGMENT

The authors wish to acknowledge the assistance in test work given by E. C. Nelson and K. E. Fritz, of the Division of Physical Metallurgy, Naval Research Laboratory.

APPENDIX

The differential equation for the flow of heat in an infinite plate is

$$\frac{\partial T}{\partial t} = a \frac{\partial^2 T}{\partial x^2} \quad [1]$$

in which T is the temperature at time t at a distance x from the surface of an infinite plate and a is the thermal diffusivity constant.

The boundary conditions assumed are that: when $t = 0$ and $x = x$ then $T = T_q$ and when $t = 0$ and $x = 0$ then $T = T_M$ where T_q is the quenching temperature and T_M the temperature of the quenching medium. The values of the thermal constants are assumed to be independent of temperature.

A solution of Eq. 1 that fits the boundary conditions is:

$$T = A + Bx + C \frac{2}{\sqrt{\pi}} \int_{N=0}^N \frac{x}{2\sqrt{at}} e^{-N^2} dN$$

where $A = T_M$

$B = 0$

$C = T_q - T_M$

Thus

$$T = T_M + (T_q - T_M) \frac{2}{\sqrt{\pi}} \int_{N=0}^N \frac{x}{2\sqrt{at}} e^{-N^2} dN \quad [2]$$

Since x and t are two mutually independent variables, the instantaneous cooling rate,

which is $\frac{\partial T}{\partial t}$, can be found from

$$\frac{\partial T}{\partial t} = \frac{\partial T}{\partial N} \times \frac{\partial N}{\partial t} = Q$$

or

$$Q = (T_q - T_M) \frac{x(t)^{-3/2}}{2\sqrt{\pi a}} e^{-\frac{x^2}{4at}} \quad [3]$$

If $Q = Q_1$ when $x = x_1$, $t = t_1$, $T_q = T_{q1}$ and $Q = Q_2$ when $x = x_2$, $t = t_2$, $T_q = T_{q2}$ the instantaneous cooling-rate ratio at temperature T , quenching from T_{q1} and T_{q2} is:

$$\frac{Q_1}{Q_2} = \frac{T_{q1} - T_M}{T_{q2} - T_M} \times \frac{x_1}{x_2} \left(\frac{t_1}{t_2} \right)^{-3/2} \times e^{(N_2^2 - N_1^2)} \quad (4)$$

where

$$N_2 = \frac{x_2}{2\sqrt{at_2}} \quad \text{and} \quad N_1 = \frac{x_1}{2\sqrt{at_1}}$$

This equation has been evaluated for several quenching temperatures at several temperatures and the values are given in Table 1.

REFERENCES

1. M. A. Grossmann: Hardenability Calculated from Chemical Composition. *Trans. A.I.M.E.* (1942) 150, 227.
2. C. E. Jackson and G. G. Luther: Calculated Hardenability and Weldability of Carbon and Low-alloy Steels. (*Metals Technology*, Oct. 1942.)
3. A. B. Kinzel: The Specification of the Weldability of Steels. *Welding Jnl.* (1941) 20, 4838-4918.
4. W. E. Jominy and A. L. Boegehold: A Hardenability Test for Carburizing Steel. *Trans. Amer. Soc. Metals* (1938) 26, 574.
5. Hill: The End Quench Test: Reproducibility. *Trans. Amer. Soc. Metals* (1943) 31.
6. H. J. French: A Study of the Quenching of Steels. *Trans. Amer. Soc. Metals* (1930) 17, 646.
7. M. A. Grossmann, M. Asimow and S. F. Urban: Hardenability, Its Relation to Quenching and Some Quantitative Data. Hardenability of Alloys Steels, 124-190. Amer. Soc. Metals, 1939.
8. T. F. Russell: Some Mathematical Considerations on the Heating and Cooling of Steel. First Report of the Alloy Steels Research Committee. Iron and Steel Inst., Sec. IX, 149.
9. M. Asimow, W. F. Craig and M. A. Grossmann: Correlation between Jominy Test and Quenched Round Bars, S.A.E. *Jnl.* (1941) 48-49, 283.
10. A. Schack, H. Goldschmidt, and E. Partridge. *Industrial Heat Transfer*. New York, 1933. John Wiley and Sons.
11. A.S.T.M. Standards 1942; Part I, Metals, 1106-1113. A.S.T.M. Designation: A255-42 T.

DISCUSSION

(G. R. Brophy presiding)

W. CRAFTS, Niagara Falls, N. Y.—In quenching from the high temperature, the actual hardenability was less. I am not too sure, but I believe that that was after the steel quenched from 1600° to 1700° had been heated to a high temperature, so that the grain growth and other factors due to high temperature in the steel had been taken out of the comparison. I believe that the apparent hardenability usually increases in quenching from the high temperature as compared to a low temperature because of factors such as grain growth.

In the summary, there is a statement that it may not apply to other sections. I would appreciate very much a little clarification of that.

C. E. JACKSON (author's reply).—Commenting upon Dr. Crafts' first question: It is true that the measured hardenability probably will increase as the quenching temperature is increased, owing to the higher solution rate of the carbides and residuals. However, if two end-quench specimens are heated to 2100°F. to establish the same grain size and homogeneity, and one of the specimens is cooled to 1600°F., for example, and quenched from this lower temperature, that specimen will indicate greater hardenability than a specimen quenched directly from 2100°F.

Mr. Christenson, will you comment on the second question?

A. L. CHRISTENSON (author's reply).—In reference to the effect of quenching temperature for sizes other than the end-quench specimen, hardenability will depend upon the surface to volume ratio. With a high surface-to-volume ratio the higher quenching temperatures will produce a higher hardenability as measured. With a low surface-to-volume ratio, as with the end-quench bar, the measured hardenability will decrease as the quenching temperature increases. This is only the effect of quenching temperature on the cooling rates and does not take into consideration metallurgical effects of solution of carbides and residuals or changes in grain size.

R. D. STOUT,* Bethlehem, Pa.—I wonder whether the authors have tried correcting their hardenability curves with the data they have accumulated. They now know how to correct the cooling rate for the fact that the quenching temperature has been different. It might be interesting to try to correct the two curves that show the deeper hardening with a lower actual quenching temperature.

Also, have they any preference in treatment; that is, do they prefer to heat it at 2100° and then quench from 1700° or quench directly from 2100°? I ask that because in applying the Jominy test to welding they are, of course, making the rather arbitrary assumption that the cooling curve resembles the welding cooling curve along its full temperature-time relation. It may be that one temperature of quench has a preference over the other in matching that time-temperature relation in the two cases.

C. E. JACKSON.—We have few data to correct from one temperature to another, although in one particular set of data we found that the ideal diameters or the corrected hardenability agreed within themselves as well as the measured hardenability. As far as a preference for the low-temperature quench after the high-temperature treatment, it may be important that hardenability will be easier to measure and there will be a greater depth of hardening for the low-temperature quench.

We have not tried, as far as the welding cycle is concerned, to use the data from the lower temperature quench.

H. W. MCQUAID,† Cleveland, Ohio.—We ran a number of tests at 1400°, 1600°, 1800° and 2000° at 20 min., 60 min. and 3 hr. apiece. I was quite surprised to find that in some of these steels, in order to get maximum hardening, Jackson and Christenson had to go to 2000° for 3 hr; that the effect of temperature is very marked on some steels where there was difficulty in getting a carbide solution. I was surprised to find how well the low-temperature Jominys check with the high-temperature and the short-time connects with the long-time when maxi-

* Lehigh University.

† Republic Steel Corporation

mum hardenability is obtained. That is particularly true with the nickel steels.

At the usual temperature, 1550° for 20 min., the Jominy tests check very well with those at 2000° for 3 hr. I agree with the authors that the effect is relatively small between 1400° and 1700° , or, rather, between 1500° and 1700° , and that we should not be too quick to jump at the Jominy curve as being the final one unless they have pretty well convinced themselves that all their carbides are in solution and thoroughly diffused.

G. DEVRIES,* Washington, D. C.—The authors are to be congratulated for their interesting and timely paper. It might be pointed out, however, that if a bar of finite instead of infinite length is chosen for the condition of the ideal quench, the relative cooling rates at various temperatures are then dependent upon

the distance along the bar, even though air cooling is neglected. The flow of heat in a plate of finite thickness is like that of an end-quench bar of finite length and can be calculated from the tables of Russell.¹²

C. E. JACKSON and A. L. CHRISTENSON.—Mr. DeVries is correct in pointing out that in a finite bar the relative cooling rates when quenching from two different quenching temperatures are dependent upon the distance from the quenched end. In addition to this, the authors wish to emphasize that the relative difference in cooling rates when quenching end-quench specimens from different temperatures will have practical significance only at points close to the quenched end, and therefore will be most important in the quenching of low-hardening steels.

¹² T. F. Russell: Some Mathematical Considerations on the Heating and Cooling of Steel. First Report Alloy Steels Research Committee, Iron and Steel Inst. Sec. IX, 149.

* Assistant Metallurgist, National Bureau of Standards.

Effect of Sixteen Alloying Elements on Hardenability of Steel

BY IRVIN R. KRAMER,* JUNIOR MEMBER A.I.M.E., ROBERT H. HAFNER,* AND STEWART L. TOLEMAN*

(Chicago Meeting, October 1943)

In his paper on the calculation of hardenability from chemical composition, Grossmann¹ discussed the effect of most of the alloying elements used commercially. The purpose of the work reported in this paper was to determine the effect of several other elements on hardenability—arsenic, antimony, beryllium, cobalt, columbium, germanium, tellurium, tin, aluminum, and titanium—and to extend the range of composition of some of the elements studied by Grossmann—chromium, copper, manganese, molybdenum, nickel and silicon.

EXPERIMENTAL METHODS

To determine the effect on hardenability, suitable amounts of the alloying elements were added to experimental heats and the hardenability determined by means of end-quenched hardenability specimens.

The steels were melted in a high-frequency induction furnace with a basic crucible, using ingot iron as a base for some of the heats and S.A.E. 1015 for others. The alloying additions were made as ferroalloys or as metal, depending on the alloying element. Hundred-pound heats were split and poured into square, tapered, cast-iron ingot molds with hot tops. Aluminum was not used as a deoxidizer in most of the heats. The ingots were homogenized for 12 hr. at 1260°C. (2300°F.) and forged into rounds of 1½-in. diameter.

Published by permission of the Navy Department. Manuscript received at the office of the Institute July 14, 1943. Issued as T.P. 1636 in METALS TECHNOLOGY, September 1943.

* Division of Physical Metallurgy, Naval Research Laboratory, Anacostia Station, Washington, D. C.

¹ References are at the end of the paper.

These bars were normalized twice from 840°C. (1550°F.) before machining into Jominy bars.

The composition of the steels was deter-

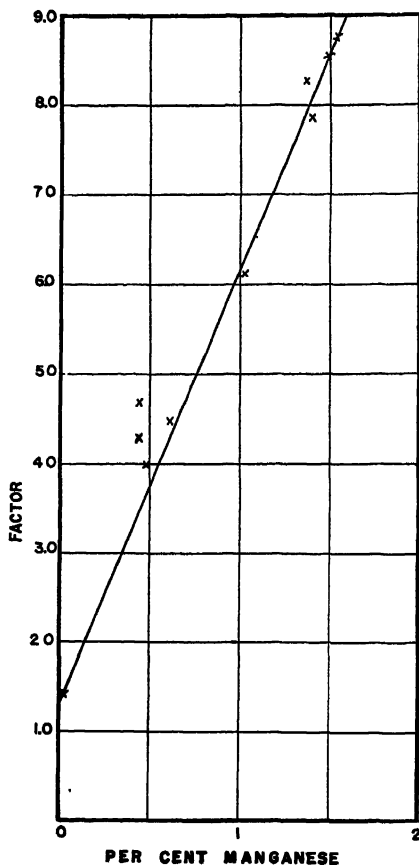


FIG. 1.—COMBINED MULTIPLYING FACTOR FOR MANGANESE AND SILICON VS. MANGANESE.

mined in most cases by samples taken from the end-quench hardenability specimen. As suggested by Crafts,³ acid-soluble

aluminum and titanium were determined instead of total aluminum and titanium.

The quenching apparatus and quenching

taken at appropriate positions on the Jominy test bars after electrolytic polishing and suitable etching.

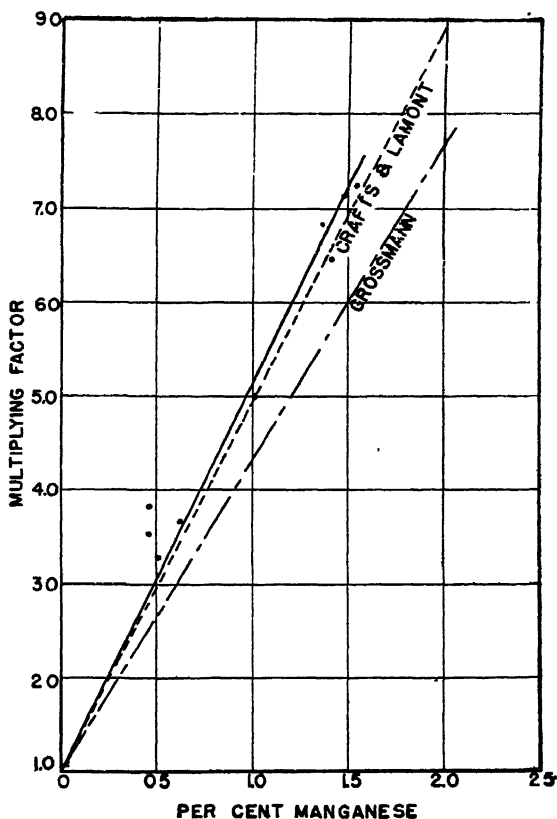


FIG. 2.—MULTIPLYING FACTOR FOR MANGANESE.

method were standard.⁸ The specimens were held at 840°C. (1550°F.) for 2 hr. in graphite blocks. After quenching, the specimens were wet-ground on two sides to a depth of 0.015 inches.

Hardness measurements were made with a diamond pyramid hardness testing machine. The indentations were spaced 0.05 in. apart, starting 0.025 in. from the quenched end. A 30-kg. load was used and both sides of the bar were measured. The 50 per cent martensite zone was determined from Fig. 29 of Grossmann's paper. The grain size was determined from an actual count of the grains on photographs

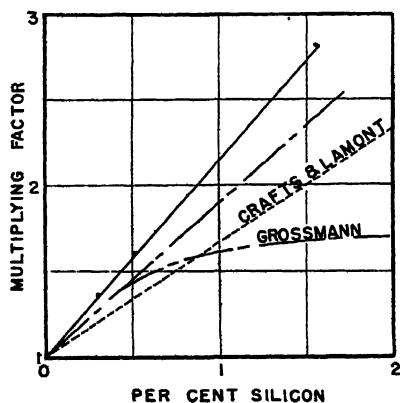


FIG. 3.—MULTIPLYING FACTOR FOR SILICON.

DETERMINATION OF MULTIPLYING FACTORS

The multiplying factors for manganese were obtained by computing the ratio of the experimental ideal critical diameter

to the ideal critical diameter as calculated from Grossmann's data on carbon, grain size, sulphur and phosphorus. These ratios, which also contain the factors for silicon

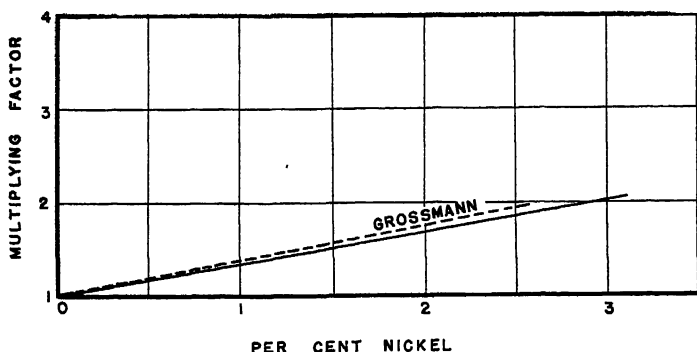


FIG. 4.—MULTIPLYING FACTOR FOR NICKEL.

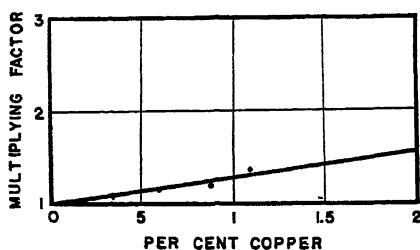


FIG. 5.—MULTIPLYING FACTOR FOR COPPER

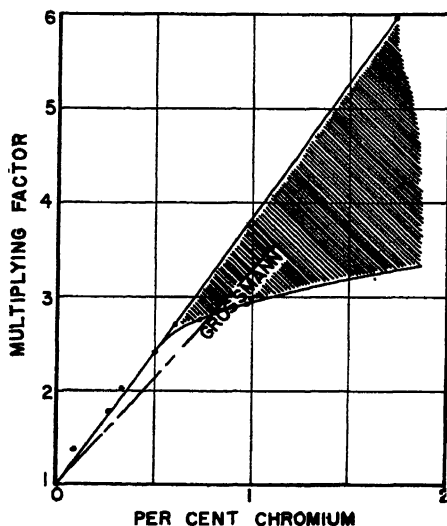


FIG. 6.—MULTIPLYING FACTOR FOR CHROMIUM.

and any undetermined impurities, as well as for manganese, were plotted as in Fig. 1. The intercept of a line drawn through these points gave the factor for the combined

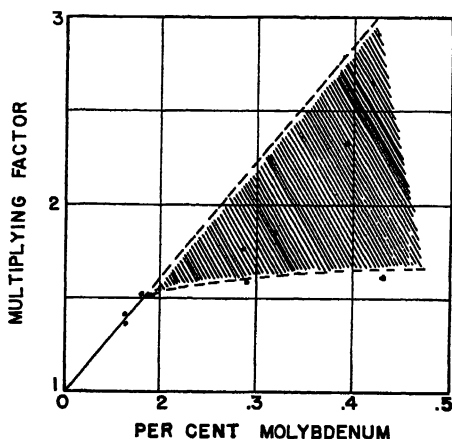


FIG. 7.—MULTIPLYING FACTOR FOR MOLYBDENUM.

effect of silicon and impurities, and dividing the ratios of Fig. 1 by this value gave the factors for the effect of manganese alone (Fig. 2).

The values obtained for manganese were then used in a similar manner to determine the multiplying factors for the other alloying elements. For nickel, copper, beryllium

and cobalt, the calculated hardenability factors did not extrapolate to unity for zero per cent alloying element. For nickel

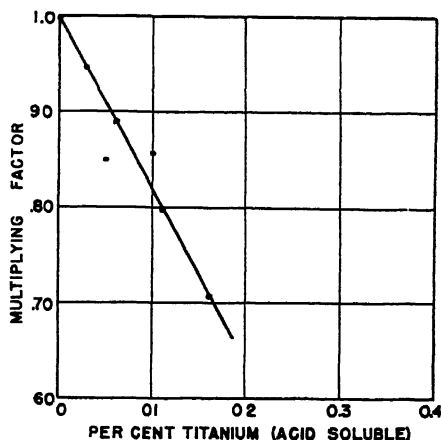


FIG. 8.—MULTIPLYING FACTOR FOR TITANIUM (ACID-SOLUBLE).

the unknown alloying elements together gave a factor of 1.20.

The factors for manganese (Fig. 2) are in agreement with those found by Crafts and Lamont and are higher than those

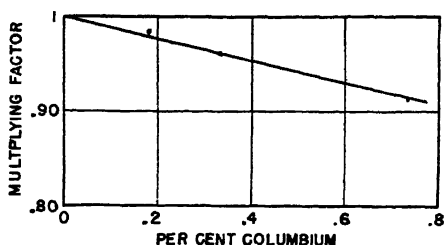


FIG. 9.—MULTIPLYING FACTOR FOR COLUMBIUM.

determined by Grossmann. Silicon (Fig. 3) was found to have a greater effect than reported by either Grossmann or Crafts and Lamont. Nickel (Fig. 4) and copper (Fig. 5) have about the same effect on hardenability as indicated by Grossmann, while chromium (Fig. 6) appears to have a somewhat greater effect. The curve for the chromium factors appears to depart

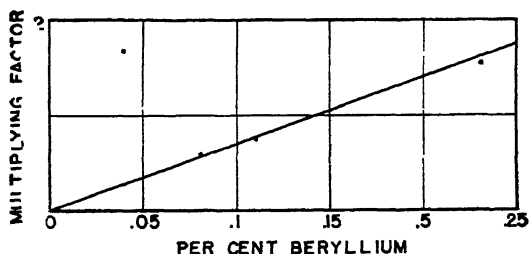


FIG. 10.—MULTIPLYING FACTOR FOR BERYLLIUM.

DATA

The composition of the steels as determined by chemical analysis is given in Table 1. Included in Table 2 are the observed Jominy distance, ideal critical diameter, the observed grain size, the ratio of the observed ideal critical diameter to the calculated ideal critical diameter for all of the elements except the one that was varied and the factors determined in this investigation. The factors for the various alloying elements are shown in Figs. 2 to 16, inclusive, and those of other investigators are given for comparison.

from linearity at about 0.5 per cent Cr; however, since a point at 1.73 per cent Cr falls on the extrapolated linear portion of the curve, the area between the two was shaded. It is believed that the lower curve is the more probable. As is to be expected of alloying elements forming stable carbides, the effect of molybdenum over 0.2 per cent (Fig. 7) is variable; below this amount the agreement with Grossmann is excellent. Titanium and columbium, the carbides of which are quite stable, decrease hardenability (Figs. 8 and 9). Beryllium has about the same effect on the hardenability as manganese (Fig. 10).

Arsenic and antimony (Figs. 11 and 12) behave in a similar manner; up to a certain percentage the hardenability increases but

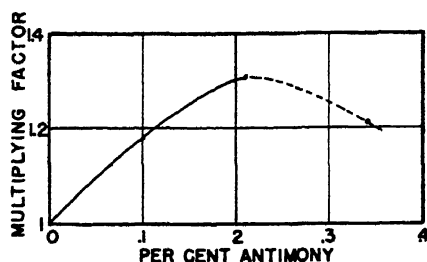


FIG. 11.—MULTIPLYING FACTOR FOR ANTIMONY.

with further additions of these elements, the hardenability decreases. Tellurium causes a marked decrease in hardenability (Fig. 13); 0.01 per cent has as much effect

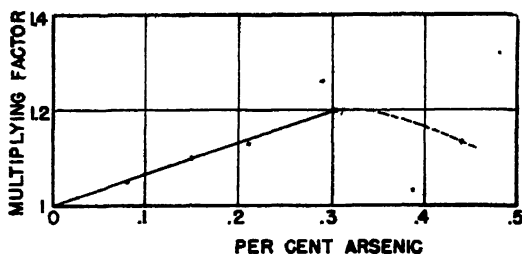


FIG. 12.—MULTIPLYING FACTOR FOR ARSENIC

in decreasing hardenability as 0.1 per cent sulphur. Although cobalt is known to decrease hardenability, no data for the effect of less than one per cent were found.

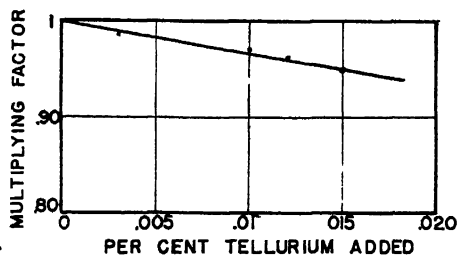


FIG. 13.—MULTIPLYING FACTOR FOR TELLURIUM.

However, even as little as 0.22 per cent decreases hardenability (Fig. 14).

The factors for aluminum show the same scattering observed by Crafts and Lamont

(Fig. 15), but the average curve is in close agreement with their results. The effect of tin (Fig. 16) on hardenability is

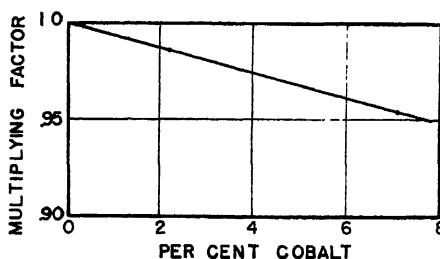


FIG. 14.—MULTIPLYING FACTOR FOR COBALT.

about the same as that of aluminum and silicon.

The rare element germanium, which occasionally is reported as present in

steel, was found to have no effect on hardenability.

DISCUSSION OF RESULTS

The effect of some elements is indeterminate because of the uncertainty that the method of chemical analysis employed determines, of the total amount present, the part that affects hardenability. It is known that aluminum can form oxides, sulphides, and nitrides. The ordinary chemical methods for "soluble" aluminum will separate the oxides, but it is not known whether the sulphides or nitrides as they exist in the steel are soluble in the acid. Experimental work on the analysis of sulphur⁴ has shown that the evolution method gives much lower results than the gravimetric method if the aluminum con-

TABLE I.—*Chemical Composition*
PER CENT

	C	Mn	Si	P	S	Ni	Cu	Cr	Mo	
GFE	0 39	<u>0.04</u>	0.34	0 004	0.031		0.10	0.009		
GV	0 41	<u>0.45</u>	0.28	0 027	0.027	0.01	0.11	0.082		
GFF	0 39	<u>0.45</u>	0 32	0.014	0.032		0.10	0 011		
CBA	0 31	<u>0.50</u>	0 30	0.014	0 033		0 19	0 062		
GAA	0 43	<u>0 63</u>	0.34	0 016	0 026		0.10	0.100		
GBH	0 56	<u>1.02</u>	0.26	0.016	0.034		0 20	0 044		
GBN	0 66	<u>1.36</u>	0 28	0 015	0.033		0.22	0 075		
GBM	0 59	<u>1.39</u>	0 30	0.015	0.033		0 22	0 075		
GBL	0 47	<u>1.47</u>	0.30	0 017	0.034		0.24	0 079		
GBK	0 40	<u>1.53</u>	0.31	0.017	0.034		0.24	0 079		
GJO	0 29	1.14	<u>0.32</u>	0.005	0 019	0 02	0 08	0 013	0 005	
GDK	0 39	1.07	<u>0.52</u>	0.013	0.031		0.13	0 031		
GDG	0 40	0 44	<u>1.04</u>	0.013	0.031		0 14	0.030		
GDM	0 38	1.02	<u>1.55</u>	0.013	0.031		0.13	0.031		
GAV	0.42	0 75	0.42	0 014	0.031		0 19	0 062	<u>0.02</u>	
GAU	0 43	0 74	0 39	0 014	0 031		0 19	0.062	<u>0.13</u>	
GLD	0.44	0 45	0 62	0.003	0 029		0.06	0 016	<u>0.16</u>	
GDB	0 39	0.50	0 32	0.014	0 031	0 10	0 19	0 060	<u>0.18</u>	
GLE	0 43	0 45	0 63	0 003	0 029		0 06	0.016	<u>0.37</u>	
GAW	0 41	0 76	0 45	0.014	0 031		0 19	0.064	<u>0.38</u>	
GDC	0 39	0 52	0 31	0.014	0.031	0 10	0 19	0.060	<u>0.44</u>	
GLG	0.40	0.45	0.63	0.003	0 029		0.06	0 016	<u>0.59</u>	
GAT	0 43	0.74	0.44	0.014	0.031		0.19	0 062	<u>0.66</u>	
GDD	0 37	0 51	0 29	0.014	0 031	0.10	0.19	0 060	<u>0.64</u>	
GKO	0 46	0 49	0 37	0.005	0.024	0.06	0 33	0 010		
GKP	0.45	0 49	0 36	0.005	0.024	0.06	<u>0.59</u>	0 010		
GKS	0 44	0 48	0 36	0.005	0 024	0 06	<u>0.86</u>	0 010		
GKT	0 41	0.48	0 36	0 005	0.021	0.06	1.08	0 010		
GKU	0 44	0 44	0 46	0 004	0.023	0.06	<u>1.66</u>	0 012		
GKV	0.44	0 43	0 46	0 004	0.023	0 06	<u>2.22</u>	0 012		
GKE	0 41	0 45	0 61	0 004	0 021	<u>0.31</u>	0 06	0.012		
GKG	0.40	0 44	0 63	0.004	0.021	<u>0.53</u>	0.06	0 012		
GKH	0 40	0 45	0 63	0.004	0.020	<u>0.76</u>	0 06	0 012		
GKJ	0 38	0 45	0 63	0.004	0 020	<u>0.93</u>	0 06	0 012		
GKK	0 39	0.39	0 72	0.005	0 022	<u>2.83</u>	0 06	0.012		
GKL	0 40	0 39	0.72	0 005	0 022	<u>2.72</u>	0 06	0 012		
GKM	0 41	0 39	0 72	0.004	0.024	<u>1.97</u>	0.06	0.012		
GKN	0 42	0 39	0 71	0 004	0.024	<u>1.49</u>	0.06	0 012		
GCK	0 40	1.16	0 21	0.014	0.034	0 10	0.18	<u>0.068</u>		
GLH	0 44	0 41	0 52	0.004	0.029		0.06	<u>0.22</u>		
GCH	0 34	0 46	0 29	0.013	0.034	0.10	0.17	<u>0.33</u>		
GLJ	0 43	0 39	0 53	0.004	0.029		0.06	<u>0.50</u>		
GCB	0.41	0 34	0 30	0.013	0 034	0 10	0.17	<u>0.59</u>		
GLK	0 43	0.43	0 53	0.004	0 029		0.06	<u>0.73</u>		
GLL	0.41	0 46	0.56	0.004	0.029		0.06	<u>0.96</u>		
GCC	0 41	0 35	0 26	0.012	0.033	0 10	0.17	<u>1.73</u>		
GAH	0.42	0 39	0.43	0.017	0.029		0.10	0.05		0.08 As
GAG	0.39	0 42	0.46	0 017	0.027		0.10	0.05		0.15 As
GJK	0.45	1.20	0 23	0.006	0.022		0.06	0.009		0.21 As
GJL	0 45	1.13	0.22	0.006	0.022		0 06	0.009		0.44 As
GFN	0 38	0.40	0.28	0.013	0.033	0.08	0 22	0.05	0.01	0.00 Be
GFO	0.37	0.41	0 29	0 013	0.033	0.08	0.22	0.05	0.01	0.08 Be
GFP	0.36	0 45	0.31	0.013	0.033	0.08	0.22	0 05	0.01	0.11 Be
GFS	0.37	0 45	0.31	0 013	0.033	0.08	0.22	0.05	0.01	0.23 Be

TABLE I.—(Continued)

	C	Mn	Si	P	S	Ni	Cu	Cr	Mo	
GAK	0.39	0.42	0.50	0.010	0.028		0.08	0.075		0.00 Sb
GAL	0.39	0.42	0.48	0.010	0.026		0.09	0.075		0.10 Sb
GAM	0.37	0.42	0.47	0.010	0.026		0.09	0.075		0.21 Sb
GAN	0.33	0.44	0.47	0.010	0.027		0.09	0.068		0.34 Sb
GJT	0.38	1.14	0.18	0.004	0.019	0.10	0.08	0.009		0.06 Cb
GJU	0.40	1.14	0.19	0.004	0.021	0.10	0.08	0.017		0.18 Cb
GJV	0.40	1.13	0.22	0.004	0.021	0.10	0.08	0.017		0.33 Cb
GJW	0.39	1.12	0.24	0.004	0.021	0.10	0.08	0.017		0.73 Cb
GDT	0.35	0.44	0.55	0.013	0.030	0.10	0.15	0.036		0.00 Co
GDU	0.35	0.44	0.52	0.013	0.032	0.10	0.14	0.033		0.22 Co
GDW	0.32	0.44	0.54	0.013	0.032	0.10	0.14	0.033		0.71 Co
GKA	0.40	1.08	0.24	0.006	0.023	0.02	0.08	0.010	0.005	0.003 Te ^a
GKC	0.40	1.06	0.25	0.006	0.023	0.02	0.08	0.010	0.005	0.010 Te ^a
GKD	0.40	1.08	0.26	0.006	0.023	0.02	0.08	0.010	0.005	0.015 Te ^a
GCU	0.43	0.46	0.29	0.015	0.034	1.17	0.17	0.04		0.003 Te ^a
GCX	0.39	0.46	0.29	0.015	0.034	1.18	0.17	0.04		0.012 Te ^a
GHA	0.31	1.13	0.22							0.00 Ge
GHB	0.29	1.12	0.22							0.59 Ge
GHC	0.28	1.13	0.22							0.106 Ge
GHD	0.27	1.17	0.20							0.165 Ge
GMO	0.38	1.08	0.30	0.006	0.016		0.06	0.052		0.03 Ti
GMP	0.39	1.04	0.37	0.006	0.016		0.06	0.052		0.05 Ti
GMR	0.39	1.09	0.39	0.006	0.016		0.06	0.052		0.10 Ti
GMS	0.37	1.11	0.40	0.006	0.016		0.06	0.052		0.16 Ti
GW	0.43	0.44	0.55	0.014	0.028		0.09	0.054		0.06 Ti
GX	0.42	0.44	0.54	0.014	0.028		0.09	0.054		0.11 Ti
GDP	0.31	0.48	0.54	0.013	0.028		0.14	0.05		0.03 Al
GMT	0.34	1.13	0.37	0.005	0.026		0.06	0.016		0.06 Al
GDS	0.28	0.48	0.54	0.013	0.028		0.14	0.05		0.06 Al
GMU	0.34	1.11	0.36	0.005	0.026		0.06	0.016		0.12 Al
GMW	0.30	1.10	0.38	0.005	0.028		0.06	0.018		0.19 Al
GME	0.44	1.09	0.50	0.005	0.030		0.06	0.016		0.02 Sn
GMG	0.42	1.09	0.50	0.005	0.030		0.06	0.016		0.06 Sn
GMH	0.41	1.05	0.51	0.005	0.030		0.06	0.016		0.11 Sn
GMJ	0.38	1.08	0.50	0.005	0.029		0.05	0.015		0.17 Sn

^a Added.

tent is high. The effect is not great, however, if the aluminum content is low. It is conceivable, therefore, that the acid-soluble aluminum may also contain some

diffraction examination of the insoluble residue showed the presence of titanium carbide as well as of titanium oxide. The question immediately arises as to whether

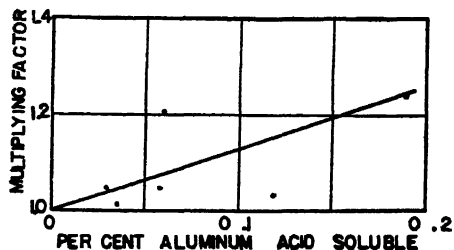


FIG. 15.—MULTIPLYING FACTOR FOR ALUMINUM (ACID-SOLUBLE).

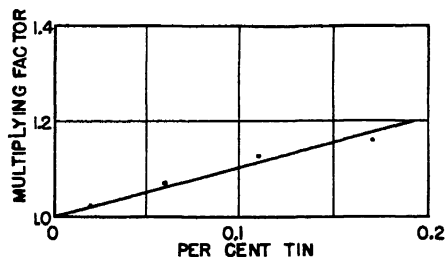


FIG. 16.—MULTIPLYING FACTOR FOR TIN.

aluminum other than that which contributes to hardenability.

The same question arises with the acid-soluble titanium determination. X-ray

this residue contains the titanium carbide that failed to dissolve in the austenite or the titanium carbide that may have precipitated upon air cooling or a mixture

TABLE 2.—Hardenability Data

	Percentage of Alloy	Grain Size	Jominy Distance	Ideal Diameter	$F_A \cdot F_x$	F_A
GFE	0 04 Mn	8 1	0 015	0 30	1.40	1 16
GV	0 45 Mn	6.2	0 16	1 50	4 65	3 84
GFF	0 45 Mn	6.1	0 10	1 15	4 24	3.51
GBA	0 50 Mn	5.9	0.11	1 20	3.97	3 28
GAA	0 63 Mn	4 5	0 20	1 70	4.45	3.68
GBH	1 02 Mn	4.7	0 35	2 40	6 05	5 00
GBN	1 36 Mn	5.8	0 68	3 50	8 25	6 81
GBM	1 39 Mn	5 8	0 50	3 20	7.81	6 48
GBL	1 47 Mn	5.5	0 60	3 30	8 55	7 06
GBK	1 53 Mn	5 2	0 59	3 20	8 74	7 23
GJO	0 32 Si	3 9	0 24	1 90	1 34	1.34
GDK	0 52 Si	5 5	0 32	2 27	1 53	1.53
GDG	1 04 Si	6 8	0 15	1 43	1 98	1 98
GDM	1 55 Si	9 3	0 50	2 95	2 82	2 82
GAV	0 02 Mo	7 8	0 16	1 49	1.00	1 00
GAU	0.13 Mo	10 0	0 18	1 60	1.37	1.37
GLD	0 16 Mo	6 4	0 25	1 95	1 53	1 53
GDB	0 18 Mo	6 2	0 26	2 00	1 53	1.53
GLE	0 37 Mo	6 1	0 31	2 20	1.76	1 76
GAW	0 38 Mo	11 2	0 23	1 85	1 58	1 58
GDC	0.44 Mo	6 0	0 30	2 19	1.85	1.85
GAT	0 59 Mo	7 0	0 42	2 65	2.32	2 32
GLG	0 66 Mo	10.7	0 30	2 19	1 82	1.82
GDD	0.64 Mo	6.6	0 50	2 95	2 65	2 65
GKO	0.33 Cu	6.1	0 19	1 65	1.50	1.07
GKP	0 39 Cu	6 2	0 20	1.70	1 61	1.15
GKS	0 86 Cu	6 0	0 21	1.75	1 65	1.18
GKT	1 08 Cu	5 9	0 25	1.95	1.87	1.34
GKU	1 66 Cu	6 2	0 27	2 05	2 06	1.47
GKV	2 22 Cu	5 8	0 33	2 32	2.26	1.62
GKE	0.31 Ni	6 1	0 18	1 60	1.36	1.13
GKG	0 53 Ni	6 5	0 19	1 65	1 40	1.17
GKH	0 76 Ni	6 6	0 22	1.80	1.57	1 31
GKJ	0 93 Ni	6 4	0 21	1 75	1 56	1.30
GKK	2.83 Ni	6 9	0 36	2 45	2.34	1 95
GKL	2 42 Ni	6 3	0 35	2 40	2.17	1 81
GKM	1 97 Ni	6 5	0 29	2.15	1 96	1 63
GKN	1.49 Ni	6.9	0 25	1 95	1.81	1.51
GCK	0 068 Cr	4.8	0.41	2 65	1.37	1.37
GLH	0 22 Cr	6 5	0 22	1.80	1 77	1 77
GCH	0 33 Cr	5 5	0 23	1.85	2 06	2.06
GLJ	0 50 Cr	6 8	0 33	2 28	2 40	2.40
GCB	0 59 Cr	5 4	0 33	2 28	2.70	2 70
GLK	0 73 Cr	6.5	0 45	2 75	2 72	2.72
GLL	0 96 Cr	6 6	0.53	3 03	2.93	2 93
GCC	1 73 Cr	6.0	1 30	4 80	5.94	5 94
GAH	0 08 As	3 2	0 17	1.55	1 05	1.05
GAG	0 15 As	3 9	0.17	1.55	1.10	1.10
GJK	0 21 As	4 3	0 33	2 28	1.13	1.13
GAE	0 29 As	4.1	0 15	1 44	1.26	1.26
GJL	0 44 As	5.0	0.27	2 05	1.23	1.23
GFN	0 00 Be	8 1	0 11	1 20	1.27	1.00
GFO	0 08 Be	5.8	0.21	1.75	1.59	1.28
GFP	0 11 Be	6 8	0.23	1 85	1.68	1.37
GFS	0 23 Be	5 8	0 35	2.40	2.19	1.77
GAK	0 00 Sb	6 0	0 11	1.20	1.00	1.00
GAL	0 10 Sb	4 7	0.18	1.60	1.18	1.18
GAM	0.21 Sb	6.1	0.16	1 50	1.31	1.31
GAN	0 34 Sb	5.1	0.16	1.50	1.21	1 21
GJT	0 06 Cb	7 3	0.19	1.65	1.006	1 006
GTU	0 18 Cb	7 5	0.17	1.54	0.984	0 984
GJV	0 33 Cb	8.7	0.15	1.42	0.960	0.960
GJW	0 73 Cb	9.4	0.12	1.27	0.912	0 912
GDT	0.00 Co	6 8	0 13	1 32	1 30	1.000
GDU	0 22 Co	6 4	0 15	1 43	1 28	0 985
GDW	0 71 Co	6.2	0 14	1.37	1.24	0 954

TABLE 2.—(Continued)

	Percentage of Alloy	Grain Size	Jominy Distance	Ideal Diameter	$F_A \cdot F_x$	F_A
GKA	0.003 Te ^a	8.9	0.16	1.50	1.05	0.990
GKC	0.010 Te ^a	8.6	0.15	1.44	1.03	0.970
GKD	0.015 Te ^a	8.8	0.15	1.44	1.01	0.950
GCU	0.003 Te ^a	7.9	0.18	1.60	1.19	0.985
G CX	0.012 Te ^a	7.9	0.16	1.50	1.16	0.960
GHA	0.00 Ge	5.6	0.24	1.90	1.00	1.00
GHB	0.059 Ge	5.5	0.23	1.85	1.00	1.00
GHC	0.106 Ge	5.5	0.23	1.85	1.00	1.00
GHD	0.165 Ge	5.6	0.23	1.85	1.00	1.00
GMO	0.03 Ti	7.8	0.15	1.43	0.945	0.945
GMP	0.05 Ti	7.2	0.17	1.52	0.849	0.849
GMR	0.10 Ti	9.1	0.14	1.37	0.857	0.857
GMS	0.16 Ti	8.5	0.11	1.20	0.707	0.707
GW	0.06 Ti	7.4	0.13	1.30	1.17	0.800
GX	0.11 Ti	7.1	0.11	1.18	1.05	0.799
GDP	0.03 Al	8.2	0.09	1.02	1.05	1.05
GMT	0.06 Al	9.0	0.14	1.38	1.05	1.05
GDS	0.06 Al	7.5	0.11	1.16	1.21	1.21
GMU	0.12 Al	8.3	0.14	1.38	1.03	1.03
GMW	0.19 Al	5.6	0.25	1.95	1.24	1.24
GME	0.02 Sn	8.1	0.21	1.71	1.02	1.02
GMG	0.06 Sn	7.2	0.25	1.95	1.07	1.07
GMH	0.11 Sn	6.6	0.27	2.02	1.12	1.12
GMJ	0.17 Sn	6.2	0.29	2.11	1.16	1.16

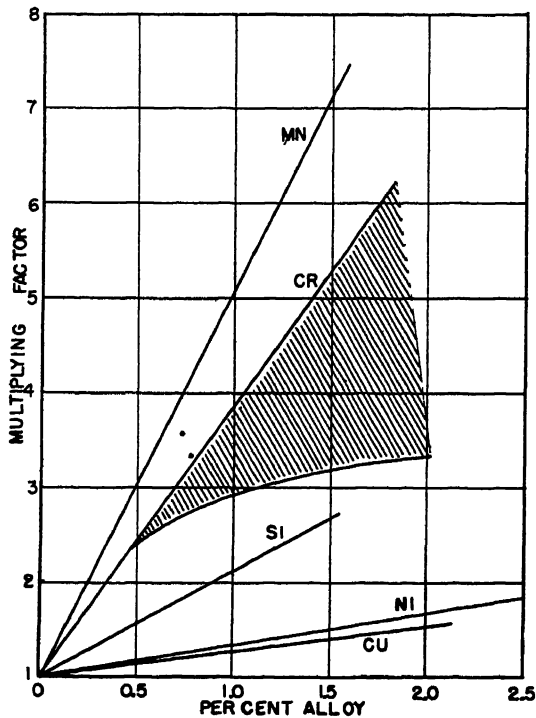
^a Added.

FIG. 17.—COMPARISON OF MULTIPLYING FACTORS FOR Mn, Cr, Si, Ni, Cu.

of both, since the chemical samples were taken from the upper end of the end-quench hardenability bar. It would be worth while to know how the proportion of insoluble

Of considerable interest is the number of different types of alloying elements that decrease hardenability; namely, cobalt, tellurium, columbium and titanium.

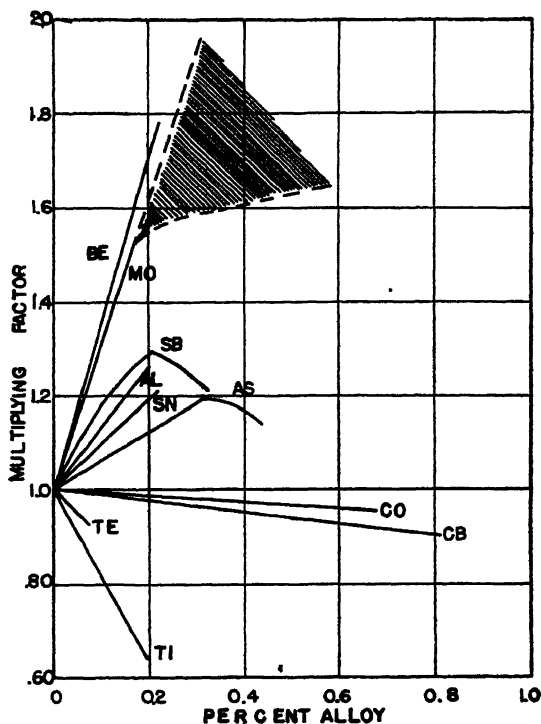


FIG. 18.—COMPARISON OF MULTIPLYING FACTORS FOR Be, Mo, Sb, Al, Sn, As, Co, Cb, Te, Ti.

titanium carbide changes with carbon content and the austenitizing temperature.

The effect of the elements that form stable carbides depends upon the austenitizing temperature and how completely such elements are in solution. The effect on hardenability is greater when the steels are held at a sufficiently high temperature and for a time long enough for the carbides to go into solution. When they are quenched from too low a temperature, the hardenability may be low either because the alloying elements have combined with carbon to decrease the alloy and carbon content available for hardenability or the undissolved carbides may act as nuclei for the transformation reaction.

The decrease of hardenability by cobalt may perhaps be associated with the fact that in the binary iron-cobalt system, cobalt raises the transformation temperature and decreases the hysteresis of the alpha-gamma transformation between heating and cooling.

While titanium and columbium both form stable carbides and nitrides, their individual effects on hardenability cannot be explained in the same manner. The decrease in hardenability due to the loss of available carbon by the formation of CbC or TiC is sufficient to account for the effect of columbium but not of titanium.

Tellurium, like sulphur, combines with manganese but its effect on hardenability

is far greater than can be attributed to the formation of manganese telluride.

SUMMARY

The effect on hardenability of nickel, chromium, molybdenum and copper is substantially that reported by Grossmann, while that of manganese agrees with the results of Crafts and Lamont. Silicon was found to have a greater effect than reported by either Grossmann or Crafts and Lamont. Beryllium, arsenic, antimony, tin and aluminum increase hardenability; cobalt, columbium, titanium and tellurium decrease it, while germanium has no effect.

ACKNOWLEDGMENTS

The authors wish to acknowledge their indebtedness to Mr. L. Singer for the analysis of the steels and to Mrs. R. B. DeAntonio for her assistance in the determination of the grain size; also to Dr. F. M. Walters, Jr., for his encouragement and suggestions.

REFERENCES

1. M. A. Grossmann: Hardenability Calculated from Chemical Composition. *Trans. A.I.M.E.* (1942) 150, 227-259.
2. W. Crafts and J. L. Lamont: The Effect of Silicon on Hardenability. *Trans. A.I.M.E.* (1943) 154, 386.
3. W. E. Jominy and A. L. Boegehold: Hardenability Test for Steels. *Trans. Amer. Soc. Metals* (1938) 26, 574-599.
4. L. Singer, Naval Research Laboratory, private communication.

DISCUSSION

(This discussion refers also to the paper by Crafts and Lamont, which begins on page 157)

(C. M. Loeb, Jr., presiding)

C. M. LOEB, JR.,* New York, N. Y.—A couple of years ago I attended a symposium on Caustic Embrittlement in Steel and one of the gentlemen who gave one of the 15 papers at that symposium made a statement that I think applies here. He said something like this: "Gentlemen, we have 15 papers on this

symposium on caustic embrittlement. I sincerely hope that next year there will be fewer. That will mean that we know something about caustic embrittlement."

I think we are about at the same stage in this interpretation of data as a result of work started by Grossmann, and I believe that the discussion, both oral and written, should be in some detail, so that we can all get more facts on which we could base ultimate conclusions. Are there any written discussions first, please?

G. F. COMSTOCK,* Niagara Falls, N. Y.—This paper is of so much practical interest, in view of the increasing use that is being made of the property of hardenability in alloy steels, that it is disappointing to find it so much condensed and lacking in detail. No doubt this is not the fault of the authors, however. An explanation of the meaning of the symbols *FA* and *FX* in Table 2 would be helpful, and it would seem that space might have been provided at the top of this table for self-explanatory headings of the sixth and seventh columns. It seems that in many instances *FX* must simply be unity, for in the Si, Mo, Cr, As, Sb, and Cb steel series, for instance, the values given in the two columns are identical. Some explanation for this, or for the values being different in other series of steels, seems to be called for.

It would also have been helpful if the total titanium contents of the titanium steels had been given, as presumably the titanium values in Table 1 are acid-soluble titanium, although they are not so marked. The reason for using acid-soluble titanium anyway is not entirely clear. Crafts and Lamont, who are referred to as authority for this practice, did not discuss titanium at all in the reference given. If titanium oxide alone were eliminated from consideration by basing the results on acid-soluble titanium only, as is true for aluminum, this procedure might be justified, but actually more or less of the carbide is also disregarded, and it is not clear why this should be done in studying hardenability any more than chromium or molybdenum carbides are disregarded. Just because titanium carbide

*Vice President, Climax Molybdenum Company.

*The Titanium Alloy Manufacturing Company.

happens to be less soluble in acid is no proof that it has no effect on hardenability

In our work with titanium steels it has not often been found that attempts to distinguish

authors and by Crafts and Lamont in the reference cited in the paper. Data obtained from specimens end-quenched from 1950°F. agreed very well with data obtained with

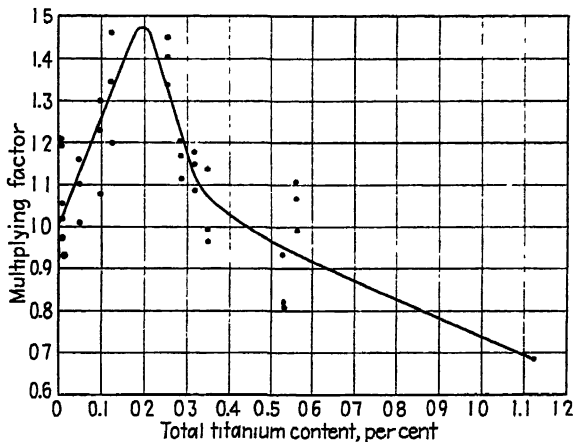


FIG. 19.—AVERAGE CURVE FOR ALL DATA ON HARDENABILITY FACTORS FOR TITANIUM, OMITTING DOUBTFUL POINTS.

between titanium carbide and titanium in solid solution, by analyzing for acid-soluble and insoluble titanium, have led to useful results. It seems that the carbide, if occurring in sufficiently fine particles, is sometimes partly soluble in acid. Possibly the presence of nitride, which exists in solid solution in the carbide, has also some effect on the solubility of the particles in acid. We have found that it leads to more consistent results in practice to base our investigations of the effects of titanium on the total titanium content of the steel. The error arising from the presence of titanium oxide has not appeared to be serious, since metallographic examination indicates that titanium oxide is not as apt to remain in the steel as alumina is, except perhaps in the higher alloy steels, where more than enough titanium is present to combine with all the carbon.

Our conclusions as to the effect of titanium on the hardenability of steel are quite different from the authors', and are as shown on the chart in Fig. 19. Each dot here represents the factor from one test. The steels used ranged from 0.23 to 0.40 per cent carbon, and from 0.62 to 1.69 per cent manganese. All the impurities revealed by the spectrograph were determined by analysis, and allowed for. The method of testing was the same as that used by the

1550°F. quenching, the differences in grain size being considered, of course.

Our results are based on total titanium, and the authors' curve might agree with the lower part of ours if their results could be plotted against total titanium too. But their failure to find any titanium factors above unity is not explained. It would seem that the soluble titanium should be more effective for promoting hardenability than the insoluble or carbide portion, if any difference is to be expected, yet these results apparently indicate the opposite. Our specimens, unlike those used by the authors, were not normalized twice, and were not held 2 hr. in graphite blocks before the end-quenching; but they were protected against scaling at the quenched end by our regular method, as described on p. 225 of *Metal Progress* for February 1943.

Perhaps the authors' failure to obtain any increase in hardenability from the titanium in their steels may have been due to the long soaking of the test specimens in graphite, resulting in combination of all the titanium with carbon near the surface where the hardness tests were made after quenching. The samples used for the chemical analyses may not have been affected in this way, or their "acid-soluble titanium" may have included

only the finer carbide particles. It is quite possible that this influence of the soaking in graphite may have affected only the titanium steels, because of the greater affinity of tita-

occasionally the scheme fails. The present paper, together with that of Crafts and Lamont⁵ and of Austin and coworkers⁶ have evidently aimed at improving on the accuracy

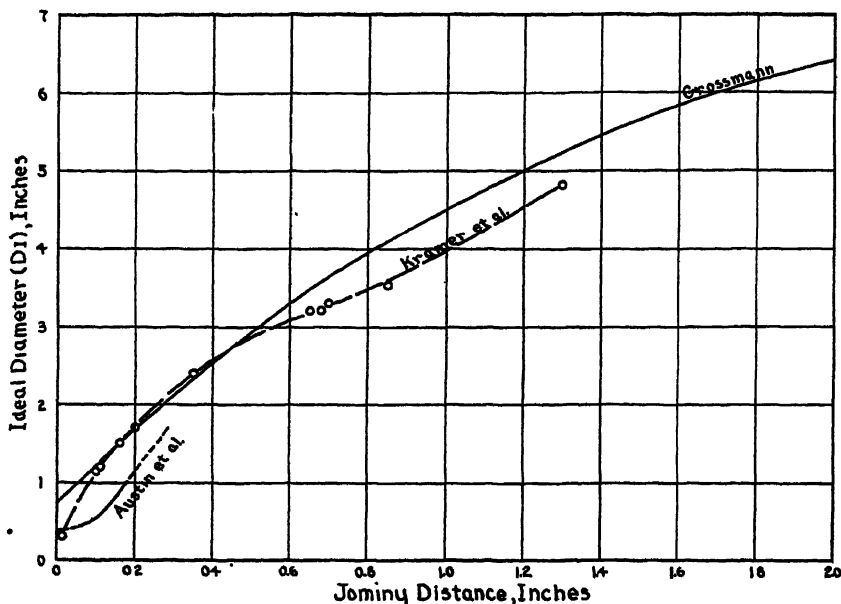


FIG. 20.—VARIATION IN BASIC RELATION, IDEAL DIAMETER VERSUS JOMINY DISTANCE.

nium, as compared with the other elements, for carbon. Or could it be possible that in the 12-hr. treatment at 2300°F. the titanium in the outside layers of the authors' samples, where the hardness tests were actually made, was largely oxidized? Our ingots were soaked only 4 hr. at 2200°F. before forging. The authors' views regarding these proposed explanations for the difference between their results and ours, or on any other explanation that they find preferable, would be appreciated.

G. R. BROPHY* and A. J. MILLER,* Bayonne, N. J.—The scheme proposed by Grossmann for the calculation of hardenability of steel from composition promises to be a valuable tool, but before the scheme can be applied broadly, accurate multiplying factors must be available. At present the scheme is practically successful and according to Grossmann "is accurate to 10 to 15 per cent in the great majority of cases." The inference is that

of the factors of a number of the elements, but, in the writers' opinions, have not succeeded because of. (1) the use of three different basic relations between Jominy distance and the ideal critical diameter; (2) different and, in some cases, wrong methods of choosing the Jominy distance to half hardness, and (3) the assumption of a linear relation between multiplying factor and element content.

In illustration of the first inaccuracy, the relations between ideal critical diameter and Jominy distance used by the investigators are shown in Fig. 20. Grossmann's original curve is the highest and falls as a simple convex curve. Austin, on a redetermination over a short distance at the lower end, found the curve to fall well below Grossmann's and to be concave. The probable accuracy of this was acknowledged by Grossmann, who believes that it is unimportant because it was only 10 per cent of the whole curve. Unfortunately, a large

* Metallurgist, The International Nickel Company, Inc., Research Laboratory.

⁵ This volume, page 157.

⁶ *Trans. Amer. Soc. Metals* (1943) 31.

number of shallow and medium hardening steels are included in this range and the range between the end of Austin's curve and the uncertain junction with Grossmann's curve. A

and, as might be expected, show a wide divergence as the manganese content decreases. It is interesting that the recalculated values using the authors' D_1 do not agree with the

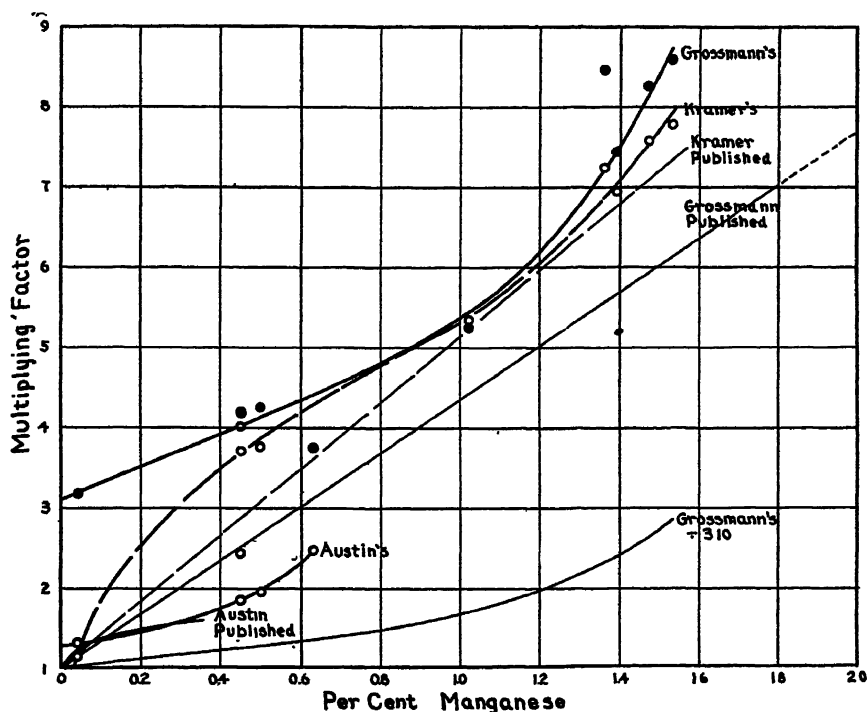


FIG. 21.—CALCULATED FACTORS ACCORDING TO THE SEVERAL JOMINY DISTANCE — D_1 RELATIONSHIPS.

large proportion of the steels of all the investigations are included within this uncertain range. The present authors have used a compromise relation shown in Fig. 21 which was constructed from the data contained in their Table 2. Beyond 0.35-in. Jominy distance, the curve, previously convex, becomes either linear or slightly concave as shown.

To illustrate the influence of these discrepancies, we have recalculated the authors' manganese series steels, using each of the D_1 relations mentioned and Grossmann's factors for each element as given. The factors for all the elements as listed in the authors' Table 1 (p. 143) except manganese were multiplied together and each D_1 divided by the product. The quotient then should be the manganese factor. This we believe to be the accepted procedure. The results are shown in Table 3,

authors' calculated manganese factors in most cases.

The recalculated factors are plotted in Fig. 21 together with the various published manganese factor curves. The curve labelled "Austin published" was calculated from his "Ideal Critical Diameter—Per Cent Manganese" relationship (Fig. 16 of the paper cited). Except at the very low manganese contents it agrees reasonably well with values calculated by the writers for the manganese series of Kramer and associates when employing Austin's ideal diameter versus Jominy distance curve. This suggests that if Austin had extended his work to include more highly alloyed steels he would have found also a concave factor curve. If the recalculated Grossmann curve be considered, the intercept on the D_1 axis indicates the presence of some undetermined element or

TABLE 3.—Variation of Determined Ideal Critical Diameter and Its Effect on Calculated Manganese Multiplying Factor

Steel	Composition, Per Cent										Grain Size	Jominy Distance	Ideal Critical Diameter According to: ^a			Prod. of Factors Except Mn ^b	Calculated Manganese Factor Using the Various Jominy Distances in Relationship of:			Kramer's Reported Man. Factor
						Cr	Ni	Cu	Mo	Grossmann			Austin	Kramer						
	C	Mn	Si	P	S															
GPE	0.39	0.04	0.34	0.004	0.031	0.01	0.10	0.009		8	0.015	0.84	0.36	0.30	3.18	1.31	1.14	1.16		
GV	0.41	0.45	0.28	0.027	0.027	0.01	0.11	0.082		6	0.16	0.55	0.90	0.30	4.14	2.31	4.00	3.84		
GPF	0.39	0.45	0.32	0.014	0.032	0.01	0.10	0.011		6	0.10	1.30	0.57	1.15	4.18	1.83	3.70	3.51		
GPA	0.31	0.50	0.30	0.014	0.033	0.01	0.10	0.062		5	0.11	1.35	0.62	1.20	4.22	1.94	3.75	3.28		
GAA	0.43	0.63	0.34	0.016	0.026	0.01	0.10	0.100		4	0.20	1.70	1.12	1.70	3.72	2.46	3.72	3.68		
GBH	0.56	1.02	0.26	0.016	0.034	0.01	0.20	0.044		4	0.35	2.35	2.40	2.40	5.33	5.33	5.00	5.00		
GBN	0.66	1.36	0.28	0.015	0.033	0.01	0.22	0.075		5	0.85	4.10	3.50	3.50	8.46	6.92	6.81	6.81		
GEM	0.59	1.39	0.30	0.015	0.033	0.01	0.22	0.075		5	0.65	3.43	3.20	3.20	7.41	6.92	6.48	6.48		
GBL	0.47	1.47	0.30	0.017	0.034	0.01	0.24	0.079		5	0.70	3.59	3.30	3.30	8.25	7.58	7.06	7.06		
GBK	0.40	1.53	0.31	0.017	0.034	0.01	0.24	0.079		5	0.68	3.53	3.20	3.20	8.59	7.78	7.23	7.23		

^a Fig. 20.^b Using Grossmann's factors.

elements that contribute to hardenability. Therefore these calculated factors should be divided by the intercept values. If this is done, the curve labeled "Grossmann +3" is developed. This shows a much too small manganese effect. Still when the authors' D_1 relation is used values well above Grossmann's published curve were obtained and a linear relation to composition is *not* indicated. The situation is quite confusing.

The second inaccuracy, the choice of Jominy distance, arises from the fact that the half-hardness point has been determined metallographically in some cases and in others from a measurement of the distance on a Jominy bar to a definite hardness, which was chosen from the carbon-steel half-hardness curve, in spite of the known fact that alloy steels have a higher 50 per cent martensite hardness at a given carbon level.

The third inaccuracy results from the original assumption of linear factor curves and the subsequent subjective construction of linear curves in spite of frequent contrary indications of the experimental data for some elements. The use of these inaccurate factors, which may be too small or too large, depending upon the true shape of the curve, causes an error in the determination of the factor for another element by the Grossmann method. It is believed this is the cause of the 10 to 15 per cent inaccuracy found, which in most cases is held so low only by the doubtful virtue of compensation. The inferred exceptional cases where greater inaccuracy results are those where compensation fails.

W. CRAFTS,* Niagara Falls, N. Y.—Although the question was directed toward Mr. Kramer, I should like to comment on Mr. Brophy's question. He questioned the accuracy of Grossmann's correlation between Jominy depth and ideal diameter near the water-quenched end of the Jominy specimen, and the effect of the discrepancy on the multiplying factors. It is felt that the ideal diameter in Grossmann's curve is somewhat on the high side but that the Austin curve is probably on the low side. In the work by Mr. Lamont and myself, this point was checked to a limited degree and it was considered that the error

* Union Carbide and Carbon Research Laboratories.

in using Grossmann's curve was too small to produce significant differences in the factors estimated from shallow-hardening steels. Inasmuch as most of our steels had hardenability beyond the questionable range, the Grossmann curve was not modified for determining multiplying factors.

It is believed that the nonlinear or S-shape tendency of some of the multiplying factors described by Mr. Brophy may be explained more reasonably by reference to the mode of transformation of the steel. For manganese and nickel we found a significant break in the multiplying factor at high alloy contents that corresponded with a change in the character of the nonmartensitic structure. Similarly, in high-chromium and molybdenum steels the factor derived from "half-martensite" hardness also broke to higher levels. This was found to result from the transition from pearlite to harder bainite in the nonmartensite portion of the structure as the alloy content was increased. The hardness of the nonmartensite portion of the structure at "half martensite" varies to such a degree, owing to the specific effects of the various elements, that the significance of factors based on "half-martensite" hardness is limited to some extent by the specific compositions that are tested.

It is believed that this is also true to a lesser degree in factors derived from microscopic determination of the "half-martensite" point. This is considered to be the probable major reason for the differences between the silicon and nickel factors determined by Messrs. Kramer, Hafner, and Toleman and those determined by Mr. Lamont and myself. The questionable significance of the "half-martensite" point and the difficulty of measuring it in nonpearlitic steels suggests that it might be more reasonable to base hardenability measurements on 100 per cent than on 50 per cent martensite.

The reliability of analysis and the significance of acid-soluble titanium are open to some question, and it would be appreciated if the total titanium analyses could be given. In our analyses it appeared that a large part of the titanium that had an effect on increasing hardenability and was presumed to be soluble in the austenite, was converted to an acid-insoluble carbide after transformation, so that the acid-soluble titanium figure repre-

sented less than the amount of titanium that was available to affect hardenability.

C. H. JUNG,*, Chicago, Ill.—I would like to comment a little about the use of the Jominy end-quench test as applied to cast steels. It is understood that the "critical hardness" of a steel is the hardness of an aggregate composed of 50 per cent martensite and 50 per cent fine pearlite. Many times in cast steels subjected to the end-quench test, it is found that some precipitated proeutectoid ferrite is present in the specimen in the region of apparent critical hardness. To what extent does the presence of this third microconstituent interfere with the relationship between carbon content and critical hardness (Grossmann's Fig. 29), and consequently with the correlation of Jominy distance with ideal critical diameter? I should be interested to know whether this ferrite separation has been encountered by other investigators in cast steels, and if it ever occurs in rolled or forged hypoeutectoid steels tested by the end-quench method.

I. R. KRAMER (author's reply).—Mr. Comstock has raised a great many questions concerning this paper, some of which are quite important because they have a definite fundamental bearing on the hardenability problem. The question of the use of acid-soluble titanium instead of total titanium and the correlation of acid-soluble titanium with hardenability arises from the difficulty in selecting a single parameter to express the hardenability of steels containing stable carbide-forming elements.

The question is more involved than the distinction between oxides and dissolved alloying element, which was made by Crafts and Lamont for aluminum. In the latter case the effect of using acid-soluble aluminum was simply to allow for the part of the alloying element that was tied up as oxides or sulphides, which played no role in the hardenabilities of the steels. With titanium, the problem is more involved, since titanium forms stable carbides, which are present at the austenitizing temperatures. This fact has been substantiated by Mr. Comstock himself in a paper presented before the American Society for Metals, entitled "Some Effects of Heat Treatment on Low Alloy Titanium Steels." These titanium

* Armour Research Foundation.

carbides act to lower the available titanium and carbon content of the steel and also act as nuclei for the transformation reaction on cooling.

method is reliable and gives reproducible results.

The amount of undissolved titanium carbides does not seem to be a simple function of the

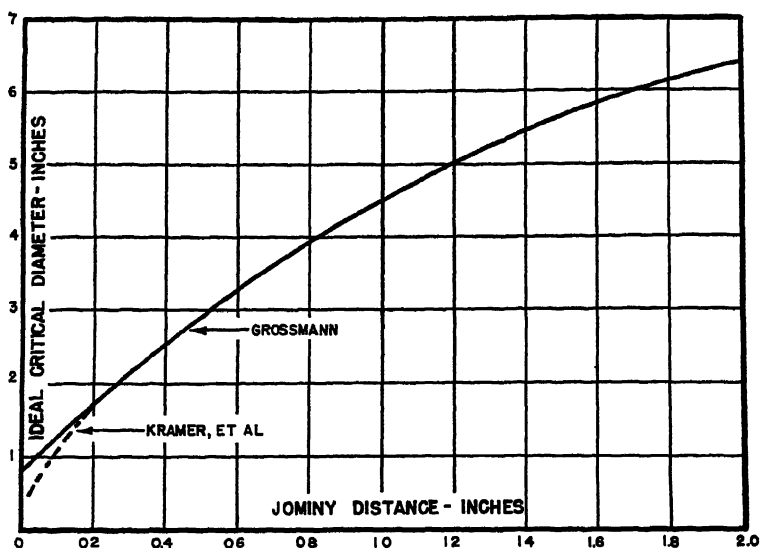


FIG. 22.

It therefore appears obvious that a single parameter cannot be used to express the hardenability factors of titanium steels in terms of chemical composition, since both the insoluble and soluble portions of titanium affect the hardenability in different ways. This same situation may very well apply to other alloying elements that form stable carbides; viz., chromium, molybdenum and vanadium, but much more work will have to be done before this problem is solved.

The necessity for a chemical analysis that can distinguish between titanium dissolved in the ferrite and combined titanium is therefore obvious. We find that 1:1 HCl in water or 1:1 H₂SO₄ in water will dissolve uncombined titanium but will not affect titanium carbide if care is taken to eliminate oxidizing agents. A variation from $\frac{1}{2}$ to 4 hr. in the length of time during which the insoluble residue was digested in the acid made no difference in the final determination. X-ray analysis of the residue showed the presence of TiC and a trace of TiO₂. It is therefore believed that this

final quenching temperature, especially in the vicinity of 1550°F., but it appears to be affected by the entire thermal history of the steel. The end-quench hardenability bars heat-treated by Comstock were normalized at 1650°F. before quenching from 1550°F. and probably contained less undissolved carbides than those heat-treated by the authors (Table 4). Our test bars were held for a total time of 6 hr. at 1550°F., which probably resulted in a more complete precipitation of titanium carbides. We have had an opportunity to obtain data on the effect of normalizing treatment on steels GMO and GX. When end-quench hardenability bars of these steels were normalized at 1650°F. instead of 1550°F., the titanium factor of steel GMO was raised from 0.95 to 1.0 and that of steel GX from 0.80 to 1.0. Therefore it is felt that the difference between the titanium carbide content of our steels and Comstock's steels may very well explain the differences in the hardenability factors.

It would be interesting to know the percentage of TiC that was present in the steels

investigated by Mr. Comstock, so that the results could be compared on this basis. The supposition that the decrease in hardenability with increasing titanium content may be due to decarburization or oxidation of the titanium during the 12-hr. homogenization treatment does not seem reasonable, since the *ingots* of 3-in. diameter and not the *test* pieces were homogenized in a controlled atmosphere furnace. After forging to 1½-in. diameter, the rounds were normalized before machining into test specimens. As to the statement that low hardenability might be due to the carburization of the test pieces, the specimens did not show any evidence of such carburization when examined under the microscope; in fact, the outer surface was very slightly decarburized.

The authors agree with Mr. Comstock that the brevity of this paper may have caused some inconveniences. Although the statement was made on page 144 of the test that acid-soluble titanium was determined and the caption of the titanium factor curve (Fig. 8) is so designated, it should also have been noted in Table 2. The factor F_A is, of course, the hardenability for the alloying element under study. Where the factor curve did not extrapolate to one for zero per cent alloying element, it was assumed that the undetermined alloying elements together gave a residual factor F_X . The factor F_X was divided into the factors $F_A \times F_X$ to obtain F_A . This procedure was based upon the assumption that the undetermined element remained constant in steels made from the same heat.

Messrs. Brophy and Miller have raised three questions for the purpose of clarifying some of the inconsistencies in the hardenability factors as determined by the several investigators. Unfortunately, their curves in Fig. 20 were based upon incorrectly reported values for Jominy distances in our Table 2. The corrections are as follows:

Correction of Table 2

Alloy	Jominy Distance	Alloy	Jominy Distance
GBH	0.31	GBL	0.62
GBN	0.68	GBK	0.58
GBM	0.58	GCC	1.15

The authors are inclined to agree with the statements given by Mr. Crafts that for the

most part the Jominy ideal critical diameter correlation curve proposed by Grossmann is correct. There has been, however, some evidence that the extreme lower end of the curve is too high. To correct this the authors have used a curve that was obtained by replotting the center portion of Grossmann's curve on a logarithmic scale to obtain a linear curve and extrapolating the lower end of the curve (Fig. 22).

TABLE 4.—Chemical Analysis of
Titanium-bearing Steels
PER CENT

Steel	Total Ti	Acid-soluble Ti	TiO ₂	Ti Combined as Carbide and/or Carbo-nitride
GMO	0.08	0.03		0.05
GMP	0.16	0.05		0.11
GMR	0.17	0.10	0.003	0.07
GMS	0.35	0.16	0.011	0.18

It is not at all surprising that the authors' calculated manganese factors do not agree with those recalculated by Messrs. Brophy and Miller using Grossmann's factors for all elements except manganese as given in Table 3. The authors in their calculations used Grossmann's data for carbon, grain size, sulphur and phosphorus, as stated on page 140, and their own derived factors for the other elements present.

The second source of inaccuracy referred to by Messrs. Brophy and Miller is in the choice of 50 per cent martensite on half-hardness as a criterion of hardenability. This we agree could be a possible source of error. However, for most steels used in this study, the Jominy curves dropped very sharply in the vicinity of the 50 per cent martensite zone. Error might be expected only when the transition from martensite to pearlite occurs over a considerable range. The authors have tested some 30 steels of varying carbon, nickel, titanium, chromium and molybdenum contents and have found that the 50 per cent martensite and half-hardness distances agree within ± 10 per cent. When the 50 per cent martensite zones were difficult to determine, it was felt that any disagreement in Jominy distance resulted from

inaccuracies of estimation rather than a real difference. Nevertheless, for high hardenability steel the choice of the proper hardenability parameter is still unanswered, for it must be remembered that Grossmann's definition for hardenability was chosen because of its ease of measurement rather than because it was a fundamental hardenability parameter. A hardenability distance measured to a point consisting of 50 per cent martensite and 50 per cent bainite certainly cannot be regarded as equivalent to a point consisting of 50 per cent martensite and 50 per cent ferrite plus pearlite.

The authors were not aware that Grossmann's original hypothesis required that the

factor curves be linear, as stated by Messrs. Brophy and Miller. In fact, Grossmann's factor curve for silicon and Craft's factor curves for manganese and nickel were curvilinear. It appears that in most cases the points are represented by a linear function as well as by any other curve. Perhaps when more data are available the form of the curves will change.

Mr. Junge's question on the effect of proeutectoid ferrite on the correlation between carbon content and critical hardness is covered in the reply to Messrs. Brophy and Miller. The precipitation of proeutectoid ferrite is nearly always encountered in rolled or forged hypoeutectoid steels at the critical hardness zone.

Effect of Some Elements on Hardenability

By WALTER CRAFTS,* MEMBER A.I.M.E., AND JOHN L. LAMONT*

(Chicago Meeting, October 1943)

AN investigation has been made of the multiplying factors for some of the more common alloying and deoxidizing elements for use in calculating hardenability of steel according to Grossmann's method.¹ The factors for manganese, silicon, and aluminum that were reported in an earlier communication² have been confirmed by microscopic determination of the half-martensite structure rather than on the basis of an empirically determined hardness corresponding to a half-martensite structure. Measurement of ideal critical diameter by microscopic examination was found to be necessary for other alloying elements, and multiplying factors for nickel, chromium, molybdenum, zirconium, vanadium, titanium, and boron have been determined. The nature and order of magnitude of the multiplying factors reflect the effect of the alloying elements on the structural character of the steel. Except for nickel and vanadium, the multiplying factors agree fairly well with previously published results. Good correlation between actual and calculated ideal critical diameters has been found in developing the multiplying factors and in checking the results against fairly simple steels. However, some discrepancies have suggested the need for a more thorough study of low-carbon and complex steels.

TESTING PROCEDURE

The investigation was conducted principally on steels made at the Union Car-

bide and Carbon Research Laboratories, Inc., in high-frequency induction furnaces using Armco iron and standard alloying materials. However, a few open-hearth steels were used in establishing the effect of nickel, and the hardenability factor for boron was based primarily on open-hearth steels. All bars were normalized prior to the machining of Jominy hardenability specimens. The Jominy test was carried out under conditions standard for the test.³ Austenitizing temperatures judged to be appropriate for the compositions of the steels were used.

Chemical analysis was determined on a sample taken adjacent to the Jominy specimen. Residual amounts of phosphorus, sulphur, nickel, chromium, molybdenum, and copper were determined on only one heat of each group made with the same materials during the same period. "Acid-soluble" aluminum and zirconium rather than total amounts were determined, as it is considered probable that the acid-soluble amount is more representative of the effective alloy. As tin was present to the extent of only 0.002 per cent, its effect was neglected. The method used to determine boron in the steels shown in Table 9* was developed by Galen Porter, Vincent Napoleon, and Thomas R. Cunningham, of the Union Carbide and Carbon Research Laboratories, Inc., and is a modification of J. Naftel's procedure for boron in soils

Manuscript received at the office of the Institute Oct. 8, 1943. Issued as T.P. 1657 in METALS TECHNOLOGY, January 1944.

* Research Metallurgist, Union Carbide and Carbon Research Laboratories, Inc., Niagara Falls, N. Y.

¹ References are at the end of the paper.

* Tables 1 to 9 have been deposited with the American Documentation Institute. To obtain them, write to the American Documentation Institute, Bibliofilm Service, 1719 N St., N. W., Washington, D. C., asking for Document No. 1804 and enclosing 50¢ for microfilm (images 1 in. high on standard 35-mm. motion-picture film) or \$1.50 for photostat (6 by 8 in.).

and plants.⁴ The procedure consists in dissolving the steel in phosphoric acid in a quartz flask equipped with a reflux condenser and subsequently separating the boron from the iron by cyclic distillation with methyl alcohol, the determination being finally completed colorimetrically in an electrophotometer.

For the estimation of actual grain size, a flat along the length of the Jominy specimen, which had been prepared for hardness measurements, was polished for microscopic examination. Actual grain size was estimated in the martensitic area of the microstructure. For specimens in which the martensitic grains were not outlined by a secondary structure, Vilella's⁵ reagent (5 c.c. HCl and 1 gram picric acid in 100 c.c. ethyl alcohol) was used to develop the outlines of the prior austenite grains.

To determine whether the hardness at 50 per cent martensite for steels containing different alloys could be estimated with a fair degree of accuracy from the hardness levels shown in Fig. 29 in Grossmann's paper, Jominy hardenability specimens of several different types of steel were submitted to microscopic examination along the surface prepared for grain-size estimation. It was observed that the hardness at 50 per cent martensite was influenced by alloying elements to a much greater degree than was indicated by Grossmann. The difference in hardness at 50 per cent martensite appeared to be due to the character of the nonmartensitic part of the structure, the nature of which is determined largely by the amount and type of alloying elements in the steel. In order, therefore, to determine hardenability factors based on 50 per cent martensite, it appeared essential that all hardenability samples be submitted to microscopic examination for estimation of the depth at which 50 per cent martensite occurred. Since carbon and alloys appeared to have interrelated effects on the hardness of

structures containing 50 per cent martensite, no simple hardness relation could be established with respect to alloy content.

In calculating the hardenability factors, the depth on the Jominy specimen corresponding to the 50 per cent martensite structure was converted to ideal diameter by the relation given in Fig. 28 of Grossmann's paper. In carrying out the necessary calculations, it was assumed that Grossmann's factors for carbon, grain size, phosphorus, sulphur, and copper were correct. Using these factors and those determined experimentally, the ideal critical diameter was calculated on the assumption that the elements shown accounted for all of the hardenability of the steel. The calculation was made according to the following formula:

$$[D_I (C \text{ and grain size})][1 + f(\% \text{ Mn})] \\ [1 + f(\% \text{ Si})][\text{etc.}] = D_I$$

The multiplying factor for a given element was determined as the ratio between the experimentally determined ideal critical diameter and the ideal critical diameter calculated from the other components of the composition.

Manganese

The multiplying factor for manganese was determined from the steels described in Table 1,* and is illustrated in Fig. 1. The points fall reasonably close to a straight line up to 1.70 per cent manganese. The line shown is the same as that previously determined² on the basis of "half hardness." Above 1.70 per cent manganese the rate of increase of the factor with higher manganese is greater. For convenience, the factor is shown as two straight lines rather than a curved line, but a curved line might represent the points equally well. The factor may be expressed as $[1 + (4.08)(\% \text{ Mn})]$ up to 1.70 per cent manganese, and as $[1 +$

(6.0)(% Mn - 0.55)] above 1.70 per cent manganese,"² and is consistent with the points established from microstructure. It was

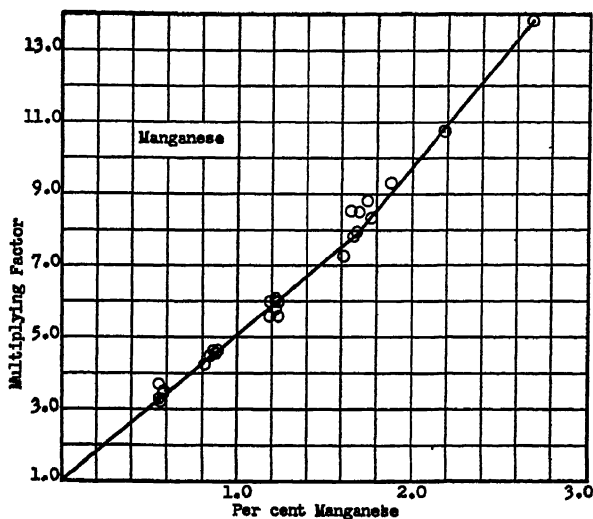


FIG. 1.—MULTIPLYING FACTOR FOR MANGANESE.

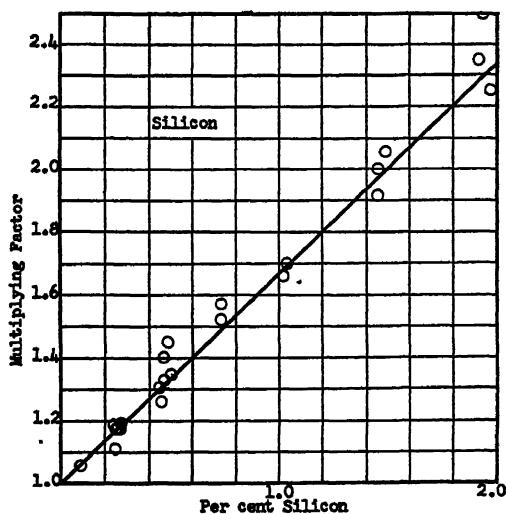


FIG. 2.—MULTIPLYING FACTOR FOR SILICON.

Silicon

The multiplying factor for silicon is based on the data in Table 1 and is shown in Fig. 2. The line is the same as that previously determined from "half hard-

observed that this agreement is more or less fortuitous, as the hardness determined at the points of half-martensite microstructure tended to be higher as the manganese increased and lower as the silicon increased. The greatest discrepancies

between half hardness derived from Fig. 29 in Grossmann's paper¹ and actual hardness at the point of half martensite would, therefore, be anticipated in high-man-

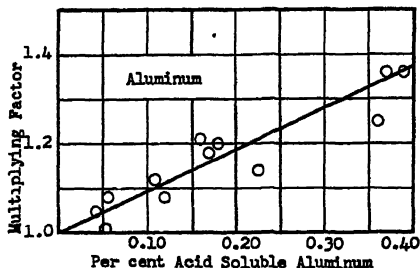


FIG. 3.—MULTIPLYING FACTOR FOR ACID-SOLUBLE ALUMINUM.

ganese, low-silicon or high-silicon, low-manganese steels. Inasmuch as the data would tolerate only a minor change, the

found for half hardness, although a tendency was observed for the hardness of the half-martensite structure to be lowered by aluminum. The multiplying factor is represented by the expression $[1 + (0.93)(\% \text{ Al})]$.

Nickel

As shown in Fig. 4 and Table 3, the multiplying factor for nickel becomes relatively higher above 3.20 per cent nickel. As for manganese, the nickel factor is represented as two intersecting straight lines rather than as a curved line, and may be expressed as $[1 + (0.74)(\% \text{ Ni})]$ up to 3.20 per cent nickel and as $[1 + (1.5)(\% \text{ Ni} - 1.63)]$ above 3.20 per cent nickel. The relatively higher factor in high-nickel steels appears to be the result of a tendency

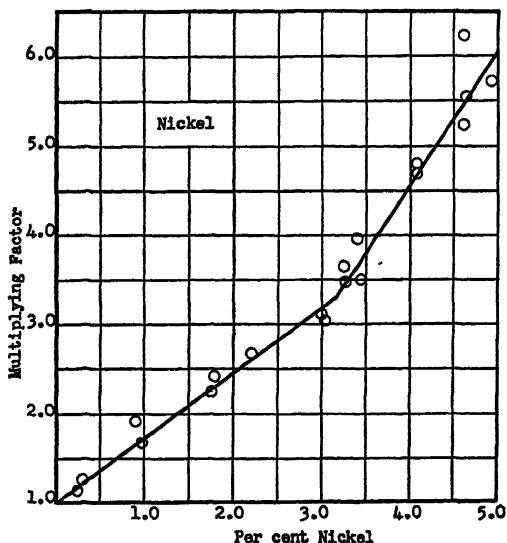


FIG. 4.—MULTIPLYING FACTOR FOR NICKEL.

previously established silicon factor was retained. It may be expressed as $[1 + (0.67)(\% \text{ Si})]$.

Aluminum

For aluminum, the multiplying factor, as shown in Fig. 3 and Table 2, based on half martensite, is also the same as that

to eliminate pearlite and bainite in the incompletely hardened locations, so that the structures consist mainly of martensite and ferrite.

This multiplying factor is somewhat higher than that suggested by Grossmann, and is of the same order as that shown by Edson.⁶ As in some of the steels containing

fairly large amounts of other alloys, it is somewhat difficult to establish the half-martensite point. In nickel steels, this is due in part to the acicular nature of the

Chromium

The multiplying factor for chromium is shown in Fig. 5. It was derived from the data given in Table 4. This chromium fac-

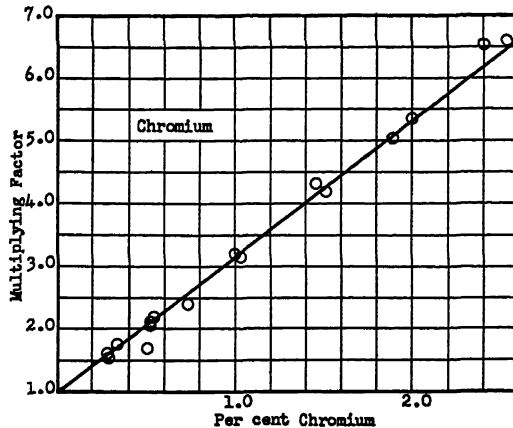


FIG. 5.—MULTIPLYING FACTOR FOR CHROMIUM.

ferrite and in part to heterogeneity. The more severely banded steels tend to have a lower factor but are within the range indicated by the points in Fig. 4.

tor is in close agreement with the upper border of Grossmann's chromium factor. However, no steels of relatively low hardenability were found to substantiate the

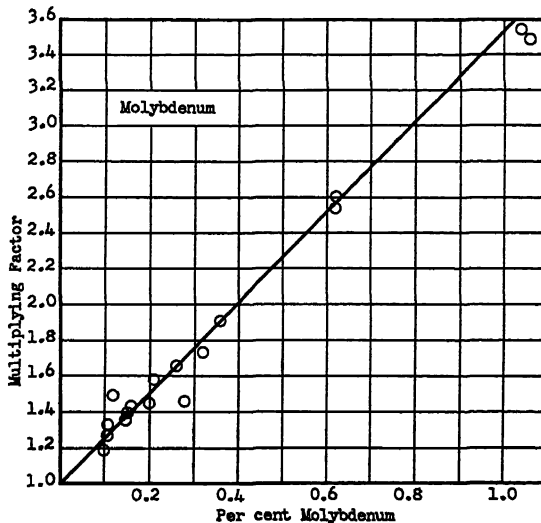


FIG. 6.—MULTIPLYING FACTOR FOR MOLYBDENUM.

Nickel appears to raise the hardness of the half-martensite structure slightly, but the trend has not been observed consistently.

shading indicated by Grossmann. The chromium factor may be expressed as $[1 + (2.16)(\% \text{ Cr})]$.

The structures of partially hardened high-chromium steels contain low-temperature bainite, which is readily distinguishable from martensite after a heavy

the same order as that given by Grossmann. The molybdenum steels were similar to those of the chromium series in that the presence of low-temperature

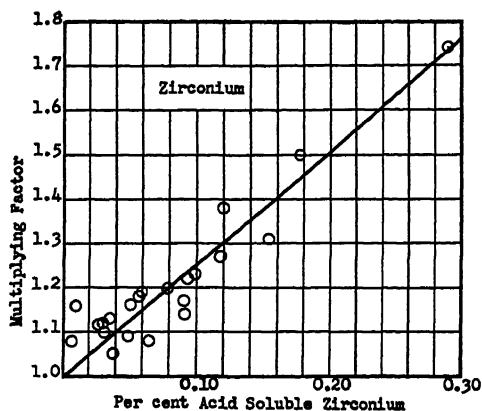


FIG. 7.—MULTIPLYING FACTOR FOR ACID-SOLUBLE ZIRCONIUM

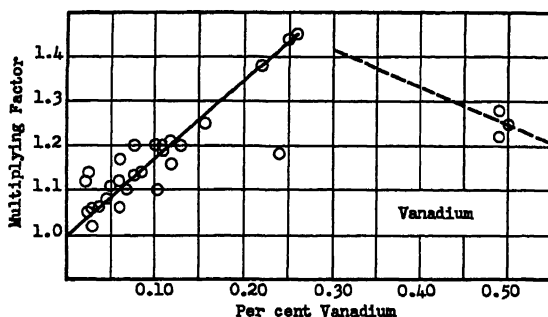


FIG. 8.—MULTIPLYING FACTOR FOR VANADIUM.

etch. The hardness of half-martensite structures containing this relatively hard nonmartensitic structure is much higher than is indicated by the vertical "feathers" in Fig. 29 of Grossmann's paper. If Grossmann's half-hardness values are used as an index of hardenability, the curve of the apparent factor increases rapidly with higher chromium content in the same way as the multiplying factors shown for manganese and nickel.

Molybdenum

As shown in Fig. 6 and Table 5, the multiplying factor for molybdenum is of

bainite caused a material increase in the hardness of the half-martensite structure. The molybdenum factor may be expressed as $[1 + (2.53)(\% \text{ Mo})]$.

Like the chromium steels, the high-molybdenum steels did not give relatively low hardenability that would require shading of the multiplying factor. However, as was indicated by Grossmann, some steels have been found to give lower hardenability than that indicated by calculation. The greatest discrepancies have been noted in steels containing less than 0.35 per cent carbon, particularly in those having a relatively large number of alloying ele-

ments. Examination of these steels has not suggested incomplete austenitization, as prolonged heating or relatively high quenching temperatures have not increased

multiplying factor, as shown in Fig. 7 and Table 6. The factor is the same as that of molybdenum, and may be expressed as $[1 + (2.53)(\% \text{ Zr})]$

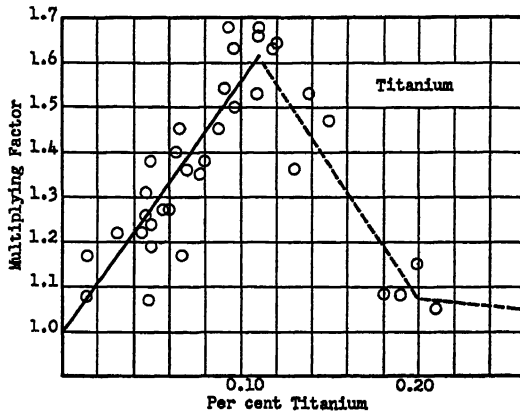


FIG. 9.—MULTIPLYING FACTOR FOR TITANIUM.

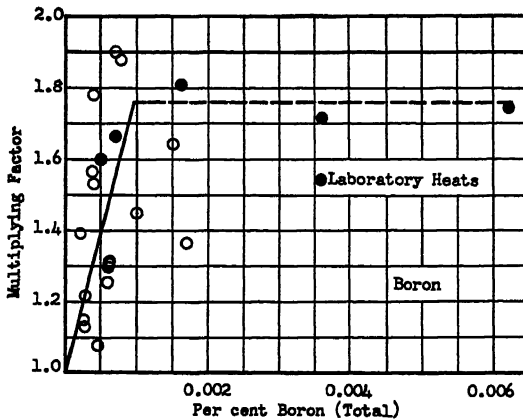


FIG. 10.—MULTIPLYING FACTOR FOR BORON (TOTAL).

the hardenability significantly. No satisfactory explanation of this behavior has been formulated, and it should be noted as a precaution that the hardenability factors developed in simple steels are not always realized in complex steels.

Zirconium

Zirconium, like some other "deoxidizing" elements, has a relatively high

Vanadium

The vanadium multiplying factor, as shown in Fig. 8 and Table 7, was found to increase in proportion to the vanadium content up to about 0.25 per cent, and to decrease at higher amounts. This tendency to lower hardenability is presumed to be due to the limited solubility of vanadium carbide and corresponding depletion of the

effective carbon in the austenite. Samples of many of the steels shown in Table 7 were quenched from 950°C. (1742°F.) as well as from 850°C. (1562°F.), but no significant differences in hardenability were observed.

Although the factors are different, Grossmann observed a similar tendency, but

hardenability with increase of vanadium is much higher in Grossmann's steel. This is notable, as it might be expected that up to the limit of solubility the vanadium that is in solid solution should give the same increase in hardenability regardless of the limit of carbide solubility. Inasmuch as both sets of steels gave the

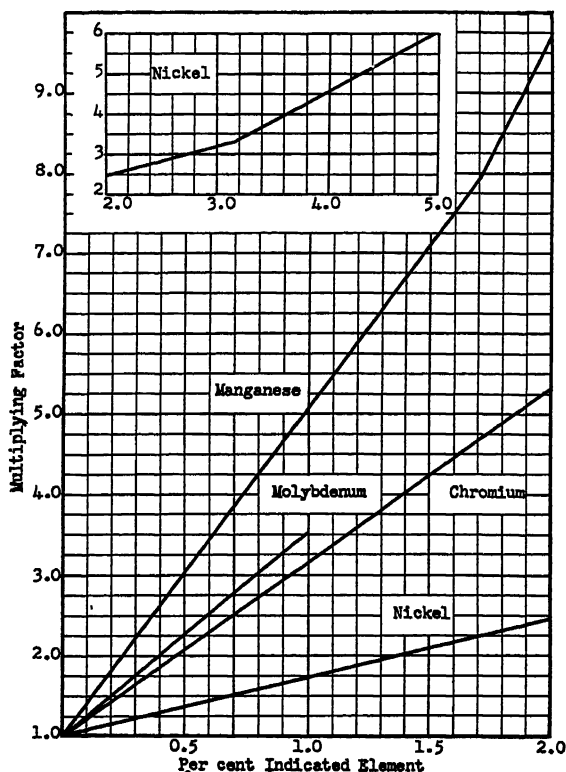


FIG. 11.—MULTIPLYING FACTORS FOR MANGANESE, NICKEL, CHROMIUM AND MOLYBDENUM

found a maximum effect of about the same magnitude at 0.04 per cent vanadium after quenching from 1500°F., and at about 0.10 per cent vanadium after quenching from 1750°F. It would appear that the limit of solubility of vanadium carbide in Grossmann's steel was greatly different from that found in this investigation. However, for small amounts of vanadium the multiplying factor or increment of

same maximum increase in hardenability, it might be reasoned that the increment of hardenability due to vanadium resulted from the tendency toward carbide insolubility, possibly from concentration at the grain boundaries. Up to 0.25 per cent the vanadium factor may be represented by $[1 + (1.73)(\% V)]$ but it is evident that additional work will be required to deter-

mine how the factor varies with steel composition or other qualities.

Titanium

The multiplying factor for titanium, given in Fig. 9 and Table 8, is similar to that of vanadium in that it reaches a

affect hardenability, but the results suggest that the amount of inactive titanium is rather small.

Boron

Because of the unusual behavior of boron, the multiplying factor was based

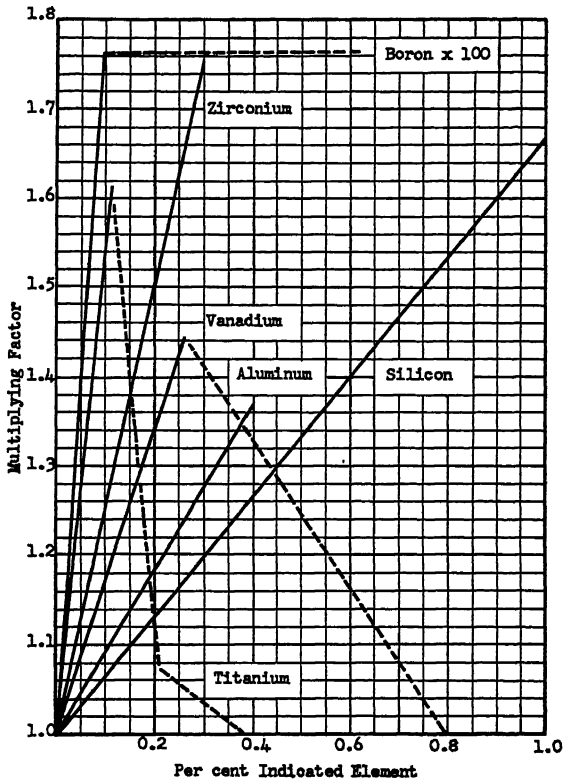


FIG. 12.—MULTIPLYING FACTORS FOR SILICON, ALUMINUM (ACID-SOLUBLE), ZIRCONIUM (ACID-SOLUBLE), VANADIUM, TITANIUM AND BORON (TOTAL).

maximum and then drops to lower values at higher titanium contents. It is possible that the maximum may shift in steels of other types. Up to 0.11 per cent titanium the multiplying factor may be expressed as $[1 + (5.58)(\% \text{ Ti})]$. The factor is based on analytical determinations of total titanium in the steel. It is reasonable to expect that part of the titanium may be isolated in stable compounds that do not

mainly on open-hearth steels. The open circles in Fig. 10 represent open-hearth steels and the closed circles represent induction-furnace laboratory heats. The boron was added either as ferrobore or as one of several complex addition alloys. All of the steels were made to have a fine inherent austenitic grain size except steel 195, which is not shown in Fig. 10. This steel contained 0.0005 per cent boron

but had relatively low hardenability. This result confirms other experience with coarse-grained steels and serves to emphasize that the multiplying factor shown in Fig. 10 is based on steels treated with sufficient deoxidizers to produce a fine inherent grain size as indicated by the McQuaid-Ehn test.

The multiplying factor increases in proportion to the boron content up to 1.76 at slightly less than 0.0010 per cent boron, and, as indicated by a limited number of experimental steels, the factor is maintained at that level up to at least about 0.006 per cent boron. The multiplying factor for boron up to slightly less than 0.0010 per cent may be expressed as $[1 + (790)(\% B)]$. It is presumed that the negligible effect of boron above 0.001 per cent results from the formation of insoluble iron boride. Unlike vanadium and titanium, the boron compound does not appear to abstract a constituent that affects hardenability, like carbon, so that the hardenability is not reduced by higher boron contents.

The effect of boron on hardenability did not appear to be affected by the alloy composition of the steel or by the manner of addition, except as the recovery of boron was affected. Sufficiently accurate data on the proportion of boron recovered from the addition agents were not available, so that representative figures cannot be given. It appeared, however, that the highest recoveries were obtained with complex addition agents containing vanadium. The only significant observation of a specific influence due to the composition of the steel was that the lower carbon steels (under 0.40 per cent carbon) tended to fall on the high side of the line and that higher carbon steels tended to give the lower results.

SUMMARY

Hardenability multiplying factors for the calculation of ideal critical diameter

according to Grossmann's principle have been found to be as follows:

ELEMENTS	MULTIPLYING FACTOR
Manganese (to 1.7%)	$1 + (4.8)(\% \text{ Mn})$
(Above 1.7%).	$1 + (6.0)(\% \text{ Mn} - 0.55)$
Silicon	$1 + (0.67)(\% \text{ Si})$
Aluminum	$1 + (0.93)(\% \text{ Al})$
Nickel (to 3.2%)	$1 + (0.74)(\% \text{ Ni})$
(Above 3.2%).	$1 + (1.5)(\% \text{ Ni} - 1.63)$
Chromium ..	$1 + (2.16)(\% \text{ Cr})$
Molybdenum	$1 + (2.53)(\% \text{ Mo})$
Zirconium .	$1 + (2.53)(\% \text{ Zr})$
Vanadium (to 0.25%) .	$1 + (1.73)(\% \text{ V})$
Titanium (to 0.11%) .	$1 + (5.58)(\% \text{ Ti})$
Boron (to 0.001%)	$1 + (790)(\% \text{ B})$

These factors are compared graphically in Figs. 11 and 12. It is of interest to note that the factors behave in a semiquantitative manner in proportion to the specific effect of the alloys on the constitution of steels. The austenite-forming elements, manganese and nickel, increase the factor in greater proportion as the amount is increased above a critical value. The magnitude of the respective factors, however, is quite different. The nickel factor is of the same order as those of the other ferrite-soluble elements, silicon and aluminum. The manganese factor, on the other hand, is similar to those of the carbide-forming elements. It is notable that the elements usually classed as deoxidizers—titanium, vanadium, and zirconium—increase hardenability in about the same proportion as the carbide-forming elements chromium and molybdenum. The boron factor is of a wholly different order and apparently increases hardenability by a special mechanism.

The consistent manner in which the alloys affect hardenability confirms strongly the validity of Grossmann's method of calculating ideal critical diameter. It should be emphasized, however, that the steels on which the factors are based are relatively simple types and that they are largely in

the range of 0.30 to 0.55 per cent carbon. Experience has shown that experimentally determined ideal critical diameter, especially in low-carbon and complex alloy steels, may be only a fraction of the ideal critical diameter calculated from multiplying factors. These discrepancies have not been analyzed sufficiently to define accurately the types of steel in which they may be expected.

ACKNOWLEDGEMENTS

The authors wish to acknowledge the generous assistance of the staff of the Union Carbide and Carbon Research Laboratories, Inc. in preparing, analyzing, and examining the steels used in this in-

vestigation. They also wish to thank those who contributed samples of open-hearth steels.

BIBLIOGRAPHY

1. M. A. Grossmann: *Trans. A. I. M. E.* (1942) **150**, 227.
2. W. Crafts and J. L. Lamont: *TRANS. A. I. M. E.* (1943) **154**, 386.
3. Soc. Automotive Engrs. Handbook (1943) 314.
4. J. Naftel: *Ind. and Eng. Chem., Anal. Ed.* (1939) **11**, 407.
5. J. R. VILELLA: *Metallographic Technique for Steel. Amer. Soc. for Metals Pub.* 1938.
6. A. P. Edson: Discussion of Ref. 1, *Trans. A. I. M. E.* (1942) **150**, 255.

DISCUSSION

(See page 148)

Effect of Several Variables on the Hardenability of High-carbon Steels

By E. S. ROWLAND,* JUNIOR MEMBER, J. WELCHNER,* MEMBER A.I.M.E., AND R. H. MARSHALL*

(New York Meeting, February 1944)

THIS paper presents results on an extension into the realm of high-carbon steels of some work recently published¹ on the effects of time at temperature, quenching temperature and prior structure on the hardenability of one 0.20 and four 0.40 per cent carbon alloy steels. It was shown at that time that unless the conditions of time, temperature and prior structure are substantially the same in performing the hardenability test as in conducting hardening of parts in production, the correlation of hardenability information with the

the quantitative variations produced on the hardenability of commercial high-carbon steels by changes in these factors of time, temperature and prior structure.

PROCEDURE

A plain carbon hypereutectoid steel, S.A.E. 52100 and Graph-Mo, a molybdenum-bearing high-carbon steel containing some graphite, were chosen for this investigation. The chemical analyses of these electric-furnace steels are given in Table I.

TABLE I.—*Chemical Analyses*
PER CENT

Code	Type	C	Gr. C	Mn	P	S	Si	Cr	Ni	Mo
A	Plain C	1.03		0.35	0.018	0.017	0.29	0.15	0.18	0.03
B	52100	1.01		0.34	0.021	0.015	0.28	1.44	0.36	0.02
C	Graph-Mo	1.47	0.20	0.39	0.017	0.018	0.75	0.10	0.15	0.24

hardness and properties of production parts is often not of satisfactory accuracy.

The general effects of these variables on the austenitic grain size, distribution of excess carbides and critical cooling rate have been known for many years and one or more have been investigated by Shepherd,^{2,3} Davenport and Bain,⁴ Digges,^{5,6} Digges and Jordan,⁷ Post and associates⁸ and Roberts and Mehl,⁹ to mention only a few. There has been no systematic investigation, however, into

The procedure used was exactly that reported previously,¹ hence the details will not be repeated here. Normalized (1650°F.) and spheroidized prior structures were utilized on all steels with hot-rolled and quenched (1600°F. oil) prior conditions added for the plain carbon steel. The end-quench test developed by Jominy¹⁰ was selected for use in this investigation and, with the noted exceptions, the American Society for Testing Materials standard procedure was followed.

The effect of time at temperature was examined at intervals of 0, 10 and 40 min. and 4 hr., and a few 16-hr. tests were run. Salt-bath heating of the specimens was employed to control and minimize the

Manuscript received at the office of the Institute Nov. 1, 1943. Issued as T.P. 1662 in METALS TECHNOLOGY, January 1944.

* The authors are associated with the Metallurgical Department, Steel and Tube Division, The Timken Roller Bearing Co., Canton, Ohio.

¹ References are at the end of the paper.

time necessary to reach temperature, a value previously determined to be 6 min. Quenching temperatures selected were 1450°F. for steel A, 1550°F. for steel B and 1500°F. for steel C.

The influence of varying quenching temperature on the hardenability of all three steels was investigated in 50°F. increments from 1450° to 1700°F. The specimens were heated in a Hump furnace, using closed-end metal tubes and spent carburizing compound for protection against decarburization. A constant time at temperature of 40 min. was maintained for all temperatures, after allowing the necessary time for the specimens to reach temperature (20 min.).

Shepherd fracture grain-size values were obtained on separate specimens after all conditions of testing (Table 2). All specimens were examined microscopically for decarburization and the effect found to be negligible up to 4 hr. in time and 1650°F. in temperature. At and beyond these values, the maximum depth of visible carbon depletion was sufficiently close to the 0.015-in. depth of flat for hardness determination that 0.030-in. depths were used. Separate tests without appreciable decarburization proved that results at these two depths were identical. All conditions were run in duplicate and the four sets of readings averaged. Results were not accepted unless all four readings for a given bar position were within 2 points Rockwell C. All hardenability curves were so drawn that the curve itself did not deviate from the plotted averages by more than 1 point Rockwell C.

PRESENTATION OF RESULTS

An analysis of all the hardenability data presented indicates that the reproducibility of results—that is, the experimental error—is not greater than $\frac{1}{2}$ in. at 60 Rockwell C or 0.020 in. at the 50 per cent martensite point. Hence, variations in hardenability equal to or greater than

these values will be considered as actual changes rather than due to errors in manipulation.

Steel A

The hardenability curves for this steel in four prior structures with time at temperature as a variable are shown in Fig. 1. Comparable information on the effect of temperature from spheroidized and normalized prior conditions is given in Fig. 2. An expected increase in hardenability with increase in both time and temperature is evident. As a means of more accurately assessing these results, the longitudinal flats on the specimens were polished, etched and the distance to 50 per cent martensite measured with a Brinell glass. The results for the time and temperature variables are shown in Figs. 3 and 4, respectively, and are substantially more accurate than measurements on the curves for such a shallow hardening steel. Note that the spheroidized prior structure produces a higher hardenability than the other three prior conditions at all time intervals (Fig. 3). With variation in quenching temperature (Fig. 4), however, the effects of the two prior structures also vary with temperature. Below about 1525°F., the spheroidized condition at 40 min. produces the higher hardenability but above this temperature the normalized has the greater value, except at 1700°F. where they again meet.

As a check on this method of testing, cylinders of 1-in. diameter were quenched in a brine spray and the depth to 50 per cent martensite was measured by the procedure reported by Barrow and Soler.¹¹ The data obtained under identical steel conditions with time as a variable are shown in Fig. 5 and illustrate the much superior sensitivity of the cylinder method over the end-quench test on such an extremely shallow hardening steel. Comparison of the curves of Figs. 3 and 5 shows, however, that the results are

definitely comparable and if accurate measurements of depth are made on the utilizing depth to 50 per cent martensite as a criterion of hardenability were ob-

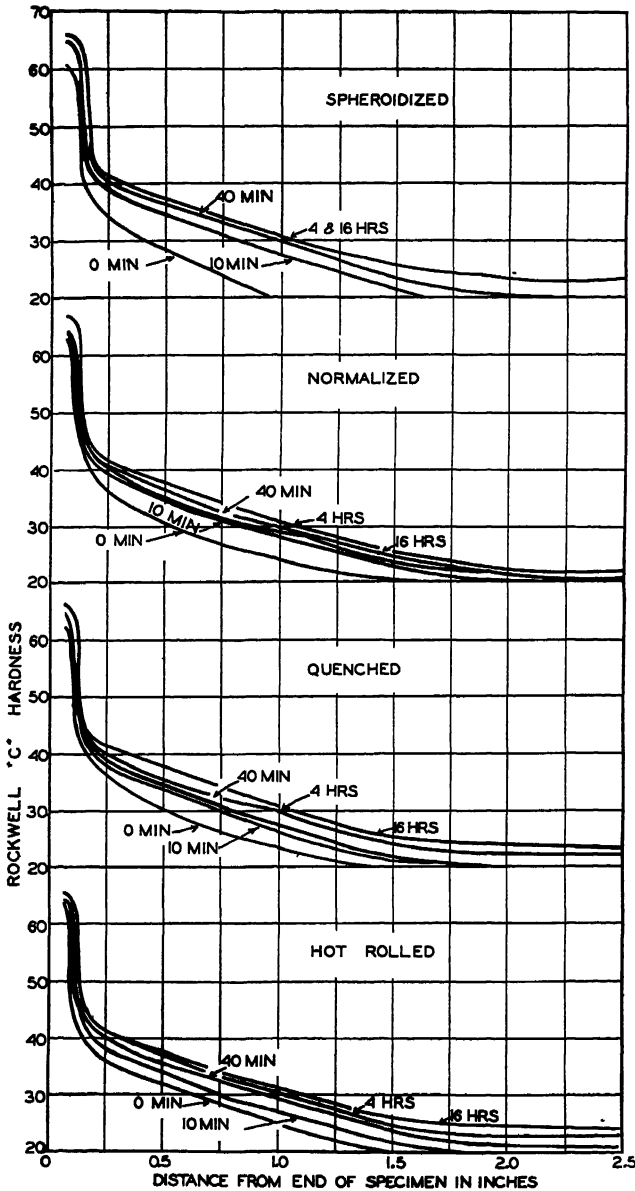


FIG. 1.—EFFECT OF TIME AT 1450°F. ON HARDENABILITY OF STEEL A.

end-quenched bar, a satisfactory interpretation of such data can be made. The end-quenched results presented herein

tained by the Brinell glass method. From a practical heat-treating standpoint, the hardenability variations shown for the

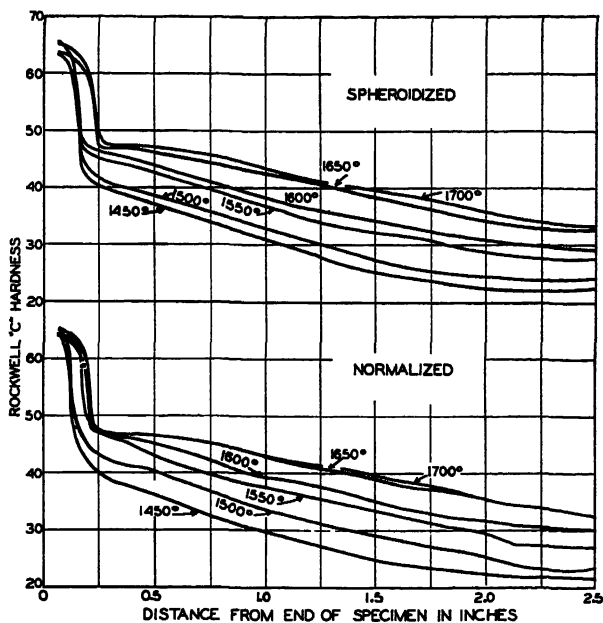


FIG. 2.—EFFECT OF QUENCHING TEMPERATURE ON HARDENABILITY OF STEEL A AFTER 40 MINUTES AT TEMPERATURE.

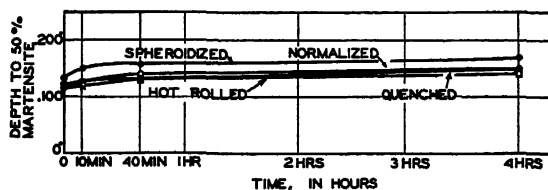


FIG. 3.—COMPOSITE EFFECT OF TIME AND PRIOR STRUCTURE ON HARDENABILITY OF STEEL A.

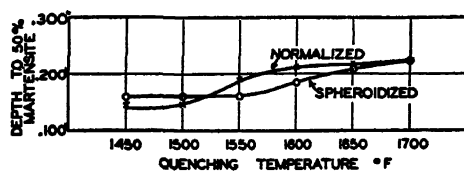


FIG. 4.—COMPOSITE EFFECT OF TEMPERATURE AND PRIOR STRUCTURE ON HARDENABILITY OF STEEL A.

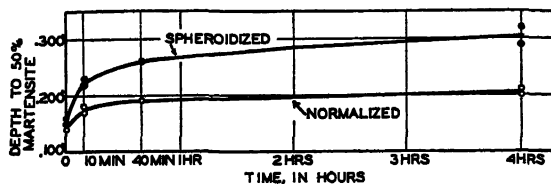


FIG. 5.—COMPOSITE EFFECT OF TIME AND PRIOR STRUCTURE ON HARDENABILITY OF STEEL A BY CYLINDER METHOD.

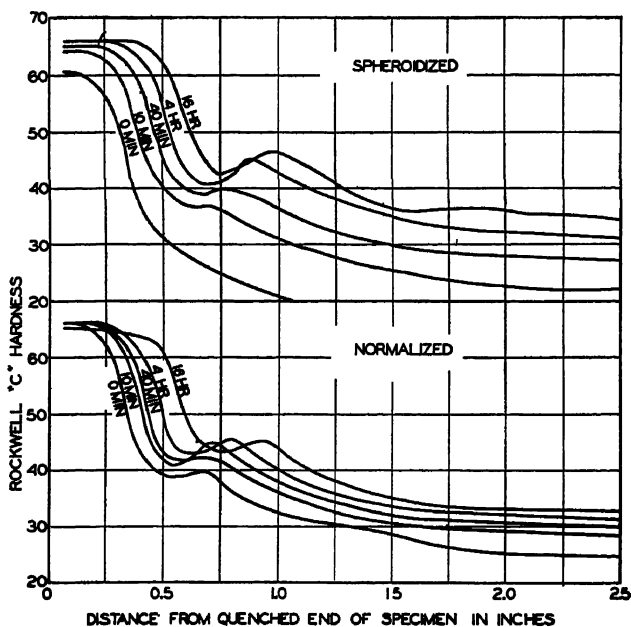


FIG. 6.—EFFECT OF TIME AT 1550°F. ON HARDENABILITY OF STEEL B.

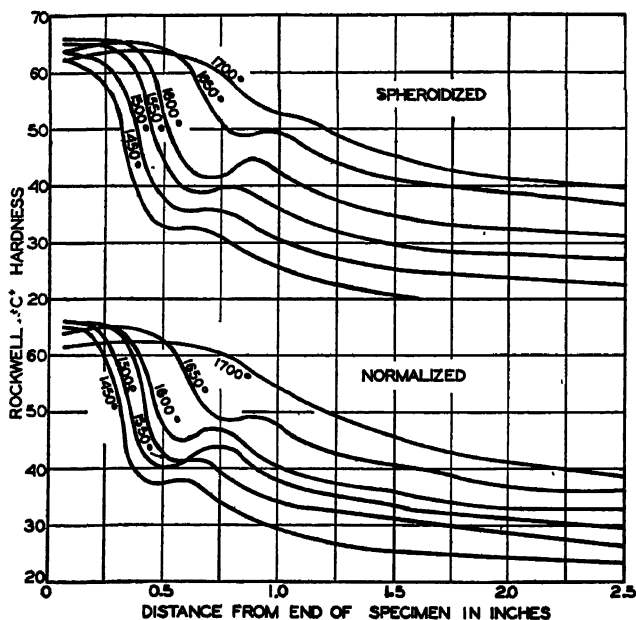


FIG. 7.—EFFECT OF QUENCHING TEMPERATURE ON HARDENABILITY OF STEEL B AFTER 40 MINUTES AT TEMPERATURE.

1 per cent carbon tool steel indicate clearly the necessity for control of the variables considered. The increase with time from a

between production and test results would seem to require substantially equal conditions in the steel just prior to quenching.

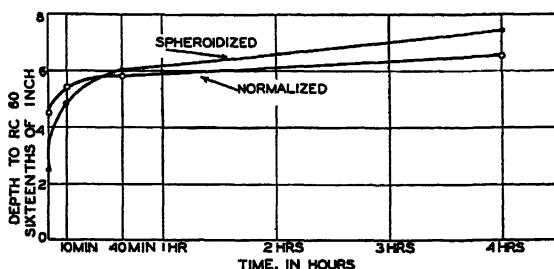


FIG. 8.—COMPOSITE EFFECT OF TIME AND PRIOR STRUCTURE ON HARDENABILITY OF STEEL B.

spheroidized prior condition is particularly important since the variation over a 40-min. interval is 0.120 in. (Fig. 5), a seemingly small change but an important one in many production applications.

Steel B

The effects of time and temperature for this analysis from both spheroidized and normalized prior structures are shown in Figs. 6 and 7, respectively, and the results are summarized, based on depth to 60 Rockwell C, in Figs. 8 and 9. Here again a continuous and expected increase in hardenability obtains with increase in both time and temperature but the percentage increase is very much greater than for the plain carbon steel.

With time as a variable, the normalized prior structure produces a higher hardenability up to about 40 min. at temperature, beyond which the spheroidized condition assumes superiority (Fig. 8). With variation in quenching temperature (Fig. 9), the spheroidized prior structure results in slightly higher hardenability except at the extreme values. These variations appear important from a practical standpoint, particularly the effect of time, since S.A.E. 52100 is normally production hardened from a spheroidized prior condition in continuous furnaces utilizing quite short times at temperature. Correlation

Steel C

The curves showing the effect of time at quenching temperature on the hardenability of steel C are given in Fig. 10 and those depicting the effect of quenching temperature in Fig. 11. In this case again, the hardenability is sufficiently low so that the depth to 50 per cent martensite is a more accurate indication of the very small hardenability variations. Conse-

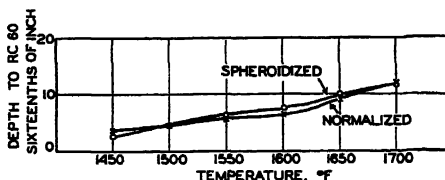


FIG. 9.—COMPOSITE EFFECT OF TEMPERATURE AND PRIOR STRUCTURE ON HARDENABILITY OF STEEL B.

quently, the summarizing curves for time and temperature (Figs. 12 and 13) are plotted on this basis. It is apparent that the hardenability variation with time is negligible from both prior structures and the total variation due to quenching temperature only slightly exceeds the experimental error.

DISCUSSION OF RESULTS

It must be stated at this point that the authors are more concerned with the

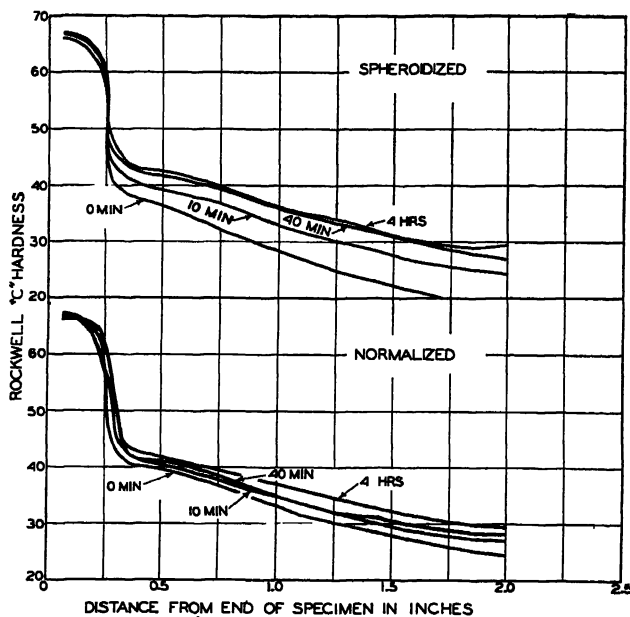


FIG. 10.—EFFECT OF TIME AT 1500°F ON HARDENABILITY OF STEEL C.

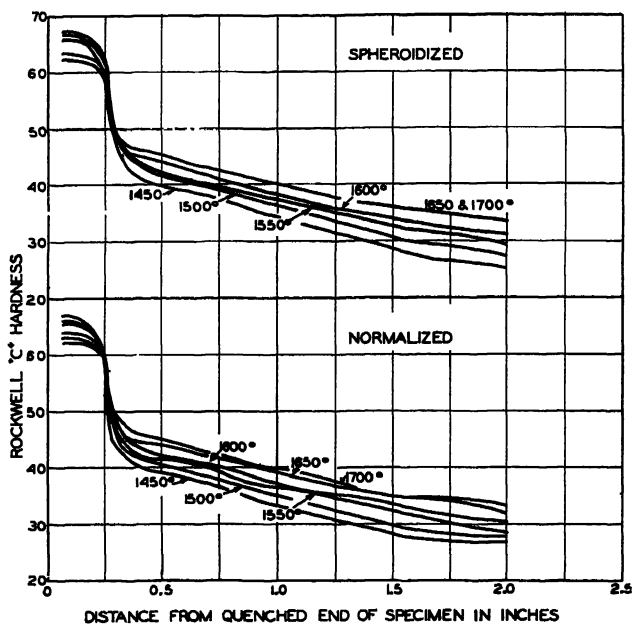


FIG. 11.—EFFECT OF QUENCHING TEMPERATURE ON HARDENABILITY OF STEEL C AFTER 40 MINUTES AT TEMPERATURE.

practical implications of the results presented above than in obtaining a satisfactory theoretical explanation for all the changes in hardenability produced by

known and accounts for the higher hardenability of steel B at short heating times resulting from normalized as compared with spheroidized prior structures, even though

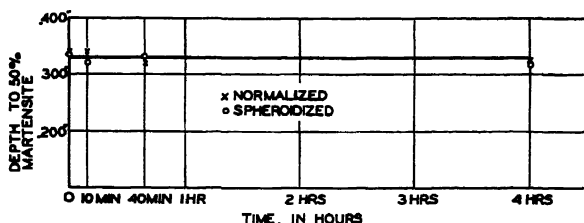


FIG. 12.—COMPOSITE EFFECTS OF TIME AND PRIOR STRUCTURE ON HARDENABILITY OF STEEL C

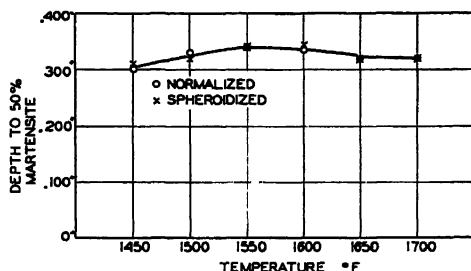


FIG. 13.—COMPOSITE EFFECTS OF TEMPERATURE AND PRIOR STRUCTURE ON HARDENABILITY OF STEEL C.

the variables mentioned. Some observations have been made in the course of this investigation, however, which throw some light upon the causes of these changes. Considerable additional experimental work is admittedly necessary for a thorough scientific explanation.

In a given high-carbon steel, it is believed that four factors control the hardenability obtained under a given set of conditions: (1) rate of carbon solution in the austenite, (2) concentration gradients of alloying elements, (3) grain size at the instant of quenching and (4) the exact number and distribution of nucleating carbides. All of these factors are interrelated and impossible of complete separation with the data at hand.

The faster rate of carbon solution from a fine lamellar prior structure, due to its high ratio of area to volume, is well

known and accounts for the higher hardenability of steel B at short heating times resulting from normalized as compared with spheroidized prior structures, even though the grain size is slightly coarser from the latter condition. With alloy carbides present, the greater resistance of these carbides toward solution causes this difference to persist for an appreciable time period (Fig. 8) while in steel A (Fig. 5) the solution rate from both prior structures is so rapid that the effect is overshadowed by other factors.

The part played by alloy concentration gradients in the austenite in limiting the hardenability is difficult to assess in these steels. Roberts and Mehl⁹ considered the effect of carbon concentration gradients on hardenability to be negligible. In previous work on lower carbon alloy steels,¹ it was shown, however, that hardenability increased with increasing time long after visible carbide had disappeared. It was presumed that this condition was caused by decrease in concentration gradients of

alloying elements in the austenite, and this reasoning extended to the present steels.

The factors of grain size and carbide nuclei must be considered together, since they are so closely interdependent. Increase in carbon solution brought about by increase in either time or temperature destroys carbide nuclei in the austenite. Such changes are almost universally accompanied by an increase in grain size, and one is tempted to conclude without direct experimental evidence that increase in grain size is the result of destruction of carbide nuclei. The very fact that differences in grain size exist as a result of heating from different prior structures supports the view that grain size is controlled by the nucleation existing in the austenite.

in steel B after the 10-min. time period from annealed and normalized prior structures, respectively. Figs. 16 and 17 reveal the changes in carbide condition after the 4-hr. time period. The greater loss of carbides from the annealed prior structure over this time interval is clearly evident, as well as the fact that the annealed shows definitely more carbide at 10 min. and slightly less at 4 hr. than the corresponding structures resulting from the normalized prior state. Beyond the short time period in which the effect of rate of carbon solution is the controlling factor, these changes in visible carbide condition very closely parallel the variations in grain size and hardenability. The hardenability differences produced by normalized and annealed prior structures at all time intervals are admittedly small, but the 40-min. time

TABLE 2.—Fracture Grain Size

Type Prior Cond.	Steel A Plain Carbon		Steel B S. A. E. 52100		Steel C Graph-Mo	
	Normalized	Annealed	Normalized	Annealed	Normalized	Annealed
Time at temperature						
0 min.	8½	7½	9	8½	8	8½
10 min.	7½	7	8½	8	8	8½
40 min.	7½	6½	7½	7	8½	8½
4 hr.	7½	6½	7	6½	8	8
Quench temperature, deg. F.						
1450	7½	6½	9	8	7	7½
1500	7½	6½	8½	8	7½	8
1550	5½	6	8	7½	7½	7½
1600	4½	4½	7½	6	7½	7
1650	4½	4	5½	4½	6½	6½
1700	4	3½	4	3½	6½	6½

In an attempt to evaluate the carbide nucleation conditions in the austenite just prior to quenching, the longitudinal flats of all end-quenched specimens were polished, etched and examined microscopically for relative number of visible carbides in the quenched structure. Without exception, it was found that in a given steel the prior structure that exhibited the higher hardenability under the same conditions of test contained fewer visible carbides in the quenched microstructure. Figs. 14 and 15 show the carbide condition

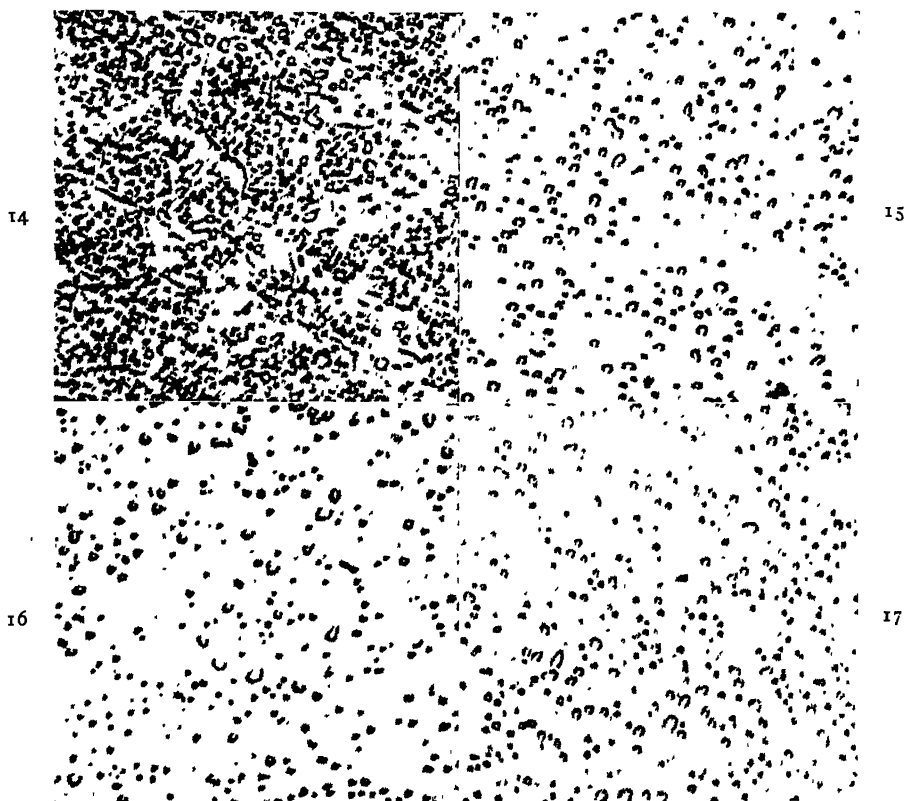
period was repeated on five heats of S. A. E. 52100 steel and, in every case, the annealed prior structure produced slightly higher hardenability and fewer carbides in the quenched microstructure.

Figs. 18 and 19 reveal the structures produced by 40 min. at 1450°F. for steel A from annealed and normalized prior structures, respectively. Analogous results, using a 1600°F. quenching temperature, are shown in Figs. 20 and 21. The reversal in carbide content with increase in temperature is coincident with the harden-

ability reversal (Fig. 4) and follows the grain-size variation extremely closely (Table 2).

Finally, the much larger and still

The foregoing are merely examples of the general observation that changes in visible carbide content with variation in the conditions studied closely parallel



FIGS. 14-17.—STEEL B. $\times 1000$.

Fig. 14. Ten minutes at 1550°F . from annealed condition.

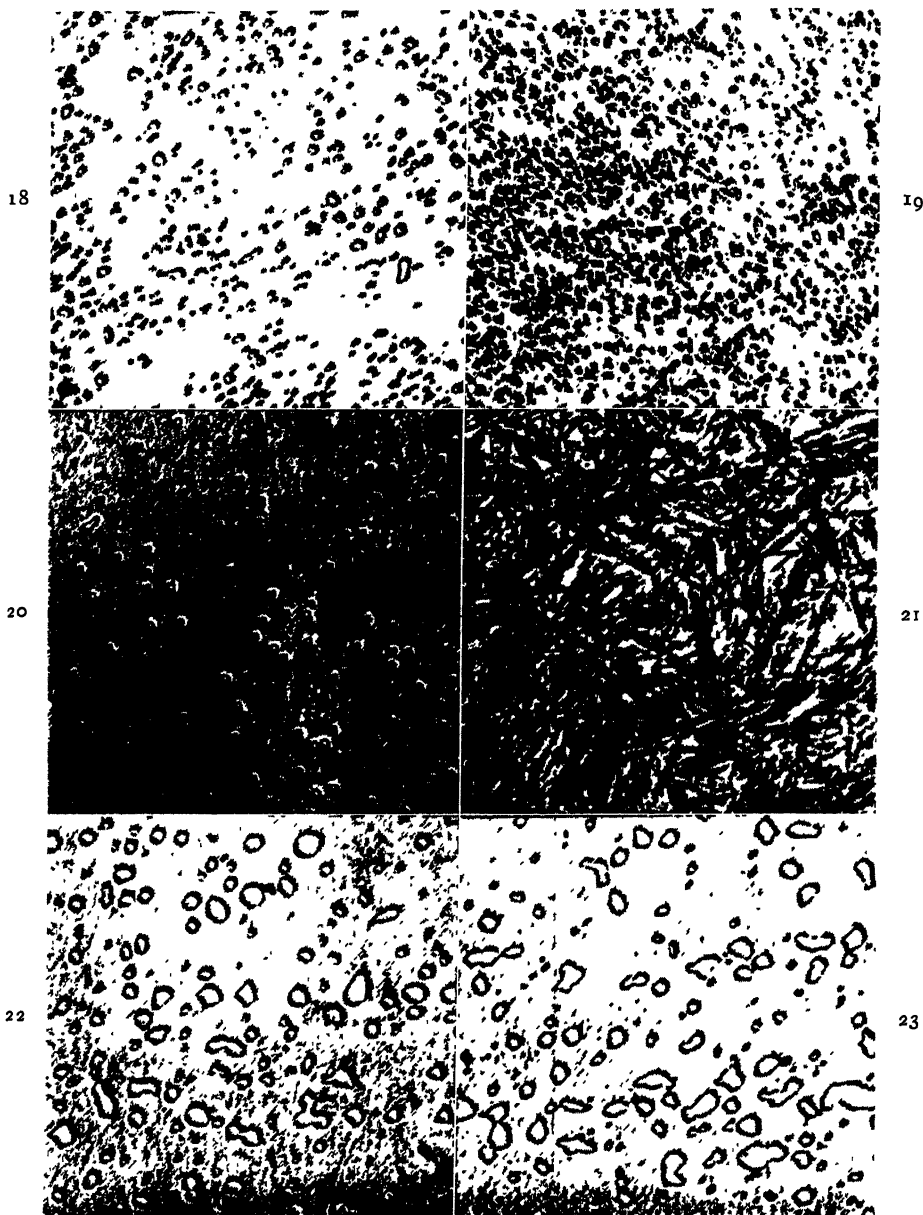
Fig. 15. Ten minutes at 1550°F . from normalized condition.

Fig. 16. Four hours at 1550°F . from annealed condition.

Fig. 17. Four hours at 1550°F from normalized condition.

numerous carbides in the quenched structures of steel C after 4 hr. at temperature from the annealed state and after 40 min. at 1700°F . from the normalized condition are shown in Figs. 22 and 23. This analysis showed little discernible variation in carbide content over the range of conditions studied, a parallel and surprisingly small grain-size variation and no significant hardenability change.

both the hardenability and grain-size variation. The conclusion is almost incapable that some definite relationship exists between the number and distribution of visible carbides and the corresponding number and distribution of submicroscopic carbide particles that actually act as nuclei for austenite decomposition on quenching. This generalization apparently does not extend to different analyses but

FIGS. 18-21.—STEEL A. $\times 1000$.Fig. 18. Forty minutes at 1450°F . from annealed conditionFig. 19. Forty minutes at 1450°F . from normalized conditionFig. 20. Forty minutes at 1600°F . from annealed condition.Fig. 21. Forty minutes at 1600°F . from normalized condition.FIGS. 22-23.—STEEL C. $\times 1000$.Fig. 22. Four hours at 1500°F . from annealed condition.Fig. 23. Forty minutes at 1700°F . from normalized condition.

does seem to be valid in a given type of steel.

SUMMARY AND CONCLUSIONS

The effects of time at temperature from zero minutes to 4 hr. and quenching temperatures from 1450° to 1700°F. on the end-quenched hardenability values were determined from both normalized and spheroidized prior structures. As a result of this work, the following general conclusions were reached:

1. From a practical heat-treating standpoint, it appears advisable to adjust the factors of time, temperature and prior structure in performing the hardenability test to those used in production treating of parts in order that the test information may be accurately applied. The exception seems to be those steels of such high carbon content that excessive carbide nucleation renders them insensitive to the variables considered.

2. The hardenability changes produced in a given analysis by variation in time, temperature and prior structure are predictable from a knowledge of the rate of carbon solution from the prior structure used, the grain size and the number and distribution of nucleating carbides. The additional factor of concentration gradients of alloying elements is probably of minor importance.

3. Microscopic evidence is presented to show that a definite relationship exists between the number and distribution of visible carbides in the quenched microstructure of a given hypereutectoid steel and the hardenability result, in that the conditions that produced the higher hardenability also caused fewer visible carbides in the microstructure. Such evidence points to the existence of a definite relationship in a given steel between the number and distribution of visible carbides and the corresponding number and distribution of submicroscopic carbides that may actually act as nuclei for austenite decomposition on quenching.

REFERENCES

1. Welchner, Rowland and Ubben: *Preprint No. 24*, Amer. Soc. Metals (1943).
2. Shepherd: *Trans. Amer. Soc. Steel Treat.* (1930) **17**, 90.
3. Shepherd: *Trans. Amer. Soc. Metals* (1934) **22**, 979.
4. Davenport and Bain: *Trans. Amer. Soc. Metals* (1934) **22**, 879.
5. Digges: *Trans. Amer. Soc. Metals* (1938), **26**, 408.
6. Digges: *Trans. Amer. Soc. Metals* (1940) **28**, 575.
7. Digges and Jordan: *Trans. Amer. Soc. Metals* (1935) **23**, 839.
8. Post, Greene and Fenstermacher: *Trans. Amer. Soc. Metals* (1942) **30**, 1202.
9. Roberts and Mehl: *Trans. A.I.M.E.* (1943) **154**, 318.
10. Jominy: Hardenability Symposium, Amer. Soc. Metals (1938) 68.
11. Barrow and Soler: *Preprint No. 13*, Amer. Soc. Metals (1942).

DISCUSSION

(Walter Crafts presiding)

E. S. DAVENPORT* and R. L. RICKETT,* Kearny, N. J.—One very interesting feature of this paper is the shape of the end-quench hardenability curves for S.A.E. 52100 shown in Figs. 6 and 7. Most of these curves exhibit a "shelf" or "hump" beginning $\frac{3}{8}$ to 1 in. from the quenched end of the specimen. We obtained a somewhat similar curve for NE 9650 and find that the rather unusual shape of this curve can be explained on the basis of the isothermal transformation diagram for this steel. It is very likely, we believe, that a similar relationship exists between the end-quench curves for S.A.E. 52100 and its isothermal transformation characteristics, even though the microstructure of this steel will be somewhat different from that of NE 9650.

The end-quench curve for NE 9650 is shown in Figure 24, in which the "shelf" begins about $1\frac{3}{16}$ in. from the quenched end. The isothermal transformation diagram for this steel is given in Fig. 25. The variation in hardness of the transformation product with decreasing temperature should be noted; upon isothermal transformation in the "intermediate" temperature range around 900°F. a softer product is formed than when transformation takes place at either a slightly higher or somewhat lower temperature. This anomalous drop in hardness is associated, in this steel, with the marked

* Research Laboratory, U. S. Steel Corporation.

A. S. T. M. TENTATIVE METHOD OF END-QUENCH TEST FOR HARDENABILITY OF STEEL (A 255 - 42 T)

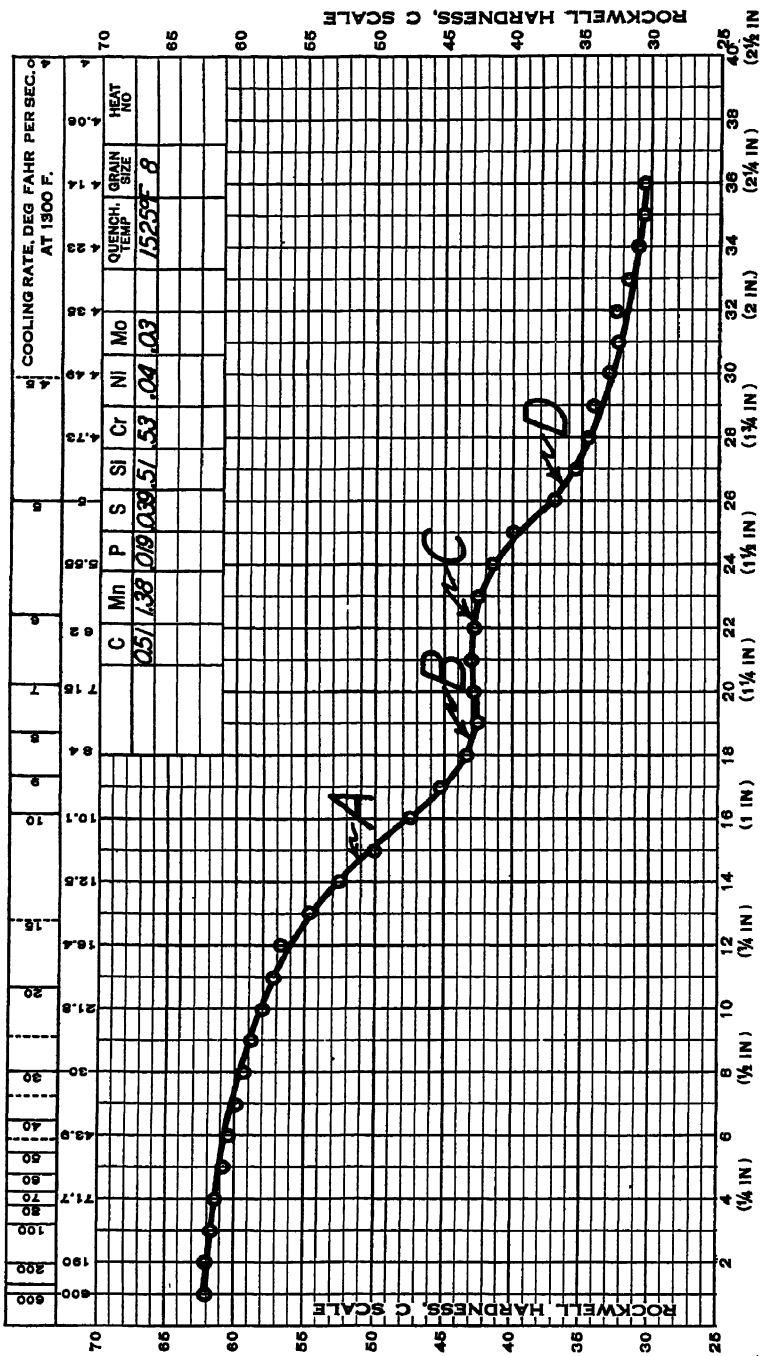


FIG. 24.—END-QUENCH HARDENABILITY OF NE 9650.

change in microstructure shown in Fig. 26. The isothermal transformation diagrams of a number of other steels, including S.A.E. 52100, show a drop in hardness in the intermediate

the region represented by the left-hand portion of the transformation diagram (Fig. 2). At *B*, the amount of this intermediate-temperature product is greater, and it is more "open" in

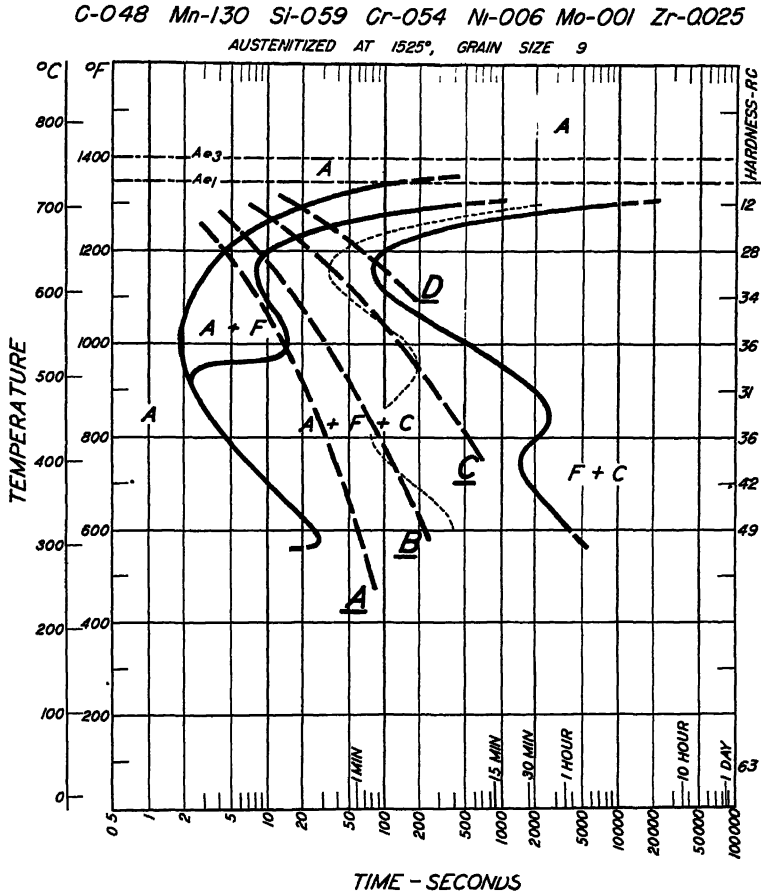


FIG. 25.—ISOTHERMAL TRANSFORMATION DIAGRAM NE 9650.

temperature range similar to that of NE 9650; hence it is to be expected that the end-quench curves of at least some of them should be like that of NE 9650.

Metallographic examination of the NE 9650 end-quench specimen revealed the microstructures that would be expected on the basis of the indications of the isothermal transformation diagram. Referring again to our Fig. 24, the microstructure at *A* consists of martensite and an intermediate-temperature transformation product, the latter formed on cooling through

structure, hence softer; fine pearlite begins to appear at this point in the bar. From *B* to *C* the intermediate-temperature transformation product decreases in amount, while fine pearlite, which is harder, increases. The softening from *C* to *D* is caused by a marked increase in amount of pearlite and decrease in martensite as the cooling rate of the specimen becomes slower, and transformation, consequently, takes place at higher temperatures. Martensite disappears completely at approximately the point marked *D*. In Fig. 25, lines *A*, *B*, *C*, and *D*

are drawn to represent schematically the cooling rate-transformation relationships for the corresponding points in Fig 24. These lines are not, however, the actual cooling curves for

E. S. ROWLAND, J. WELCHNER and R. H. MARSHALL (authors' reply) —The explanation given for the "shelf" or "hump" in some of the S.A.E. 52100 curves is indeed interesting

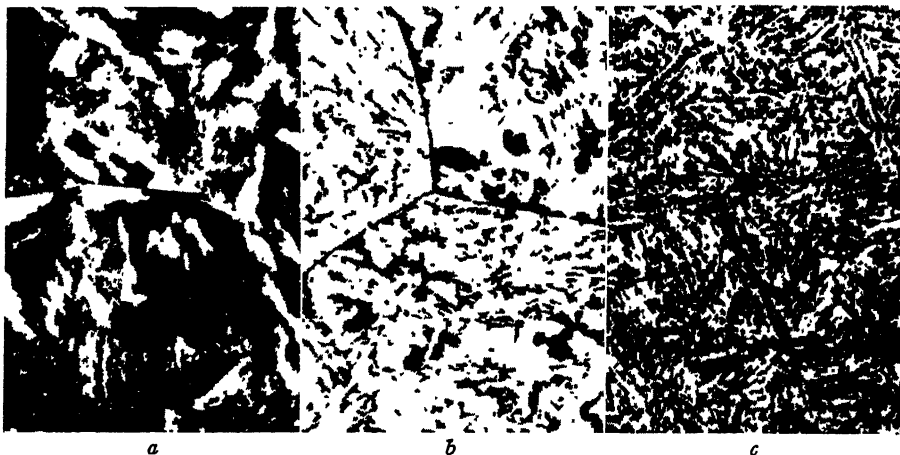


FIG. 26.—PRODUCTS OF ISOTHERMAL TRANSFORMATION IN NE 9650. $\times 2000$
a. 1000°F, R C 36 *b.* 900°F., R C.31. *c.* 800°F., R C.36.

these points on the end-quench specimen; such actual cooling curves would have to be superimposed on a cooling transformation diagram rather than on an isothermal transformation diagram, in order to represent quantitatively the transformation that actually occurs on cooling.

Another feature of the authors' end-quench curves for S.A.E. 52100, shown in Fig 7, is of interest. As the austenitizing temperature increases, the hardness at the quenched end of the bar increases to a maximum and then decreases. The initial increase in hardness is to be expected because of the greater amount of carbon taken into the austenite solid solution as the temperature increases. The drop in hardness on quenching from still higher temperatures suggests an increase in the amount of austenite retained at room temperature. Do the authors have any evidence to indicate that this is true?

and most plausible. Enough similarity appears to exist between the NE 9650 and the S.A.E. 52100 isothermal transformation curves to warrant drawing a parallel in their behavior during end-quenching. Lessening of the "hump" intensity with increasing quenching temperature once the maximum effect is displayed also can be attributed to the change in the isothermal transformation diagram, as progressively more carbon is taken into solution at the austenitizing temperature.

The interpretation suggested by Davenport and Rickett for the lowering of the quenched-end hardnesses of the S.A.E. 52100 curves with increasing quenching temperature beyond 1600°F is supported by a microscopic examination of the specimens. This steel, as well as steel C, shows an increasing amount of retained austenite as the austenitizing temperature is raised.

Influence of Hydrogen on Mechanical Properties of Some Low-carbon Manganese-iron Alloys and on Hadfield Manganese Steel

BY HERBERT H. UHLIG,* MEMBER A.I.M.E.

(New York Meeting, February 1944)

ALTHOUGH the mechanical properties of high-carbon manganese-iron alloys, particularly the Hadfield manganese steels, have been established, the literature discloses discrepancies in the reported properties for the low-carbon alloys. Hadfield^{1a} summarized the existing data up to 1927, including the investigations of Guillet, Arnold, Strauss, Burgess and Aston, and reported his own values for alloys containing for the most part from 0.06 to 0.15 per cent carbon. He noted:

From these comparisons it will be seen that while there is a broad and general agreement as to the character of the alloys at the different manganese percentages, there are disparities in individual cases, especially as regards the degree of toughness or brittleness displayed by an alloy with certain percentages and with particular types of treatment. These differences are not always readily explainable.^{1b}

His data showed that alloys containing 4 to 10 per cent manganese water-quenched from 1000°C. were brittle and hard with maximum brittleness at about 7 per cent. Slight improvement in ductility was obtained with compositions from 10 to 17 per cent manganese. Alloys containing up to 17 per cent manganese slowly cooled rather than quenched from 870°C., he found, were slightly improved in ductility with significant improvement in alloys analyzing 4.1 and 4.8 per cent manganese.

Manuscript received at the office of the Institute Nov. 27, 1943. Issued as T.P. 1701 in METALS TECHNOLOGY, June 1944.

* Research Metallurgist, General Electric Co., Schenectady, N. Y.

¹ References are at the end of the paper.

Recently Walters, Kramer and Loring² reported mechanical properties for alloys made up from electrolytic manganese and ingot iron and containing from 0.02 to 0.04 per cent carbon. They showed that a tempering treatment at 540°C. (1000°F.) for one hour significantly improved the ductility of compositions ranging from 6.7 to 20.7 per cent manganese. The differences of these compared with Hadfield's results they considered to originate in this tempering treatment plus the fact that Hadfield's alloys contained higher carbon and phosphorus (0.06 to 0.15 per cent C, 0.06 to 0.07 per cent P compared with 0.02 to 0.04 per cent C, <0.001 per cent P).

In this paper it is shown that of the low-carbon alloys (0.02 to 0.03 per cent) containing from 3.3 to 21.5 per cent manganese moderately or rapidly quenched from 1000°C. some are brittle or ductile, depending on presence or absence of hydrogen. Hydrogen is readily absorbed at high temperatures, and much of it is retained when the alloys are cooled to room temperature. The presence of hydrogen in the range of composition from 10 to 18 per cent manganese is a major factor in determining relative ductility. At 22 per cent manganese, and also at compositions below 10 per cent manganese, factors other than or in addition to hydrogen play a role. These are discussed. Also data are presented to show that hydrogen absorbed by the high-carbon alloys of Hadfield composition is without effect on their mechanical properties.

PREPARATION OF ALLOYS AND TEST SPECIMENS

All low-carbon melts were made in a 10-lb. basic-lined induction furnace using electrolytic manganese and hydrogen-fired electrolytic iron. These were poured into steel molds, except melt 10B, which was cast in sand. No silicon or other deoxidizer was added. The 1-in. diameter ingots were homogenized in air at 1050°C. for 1 to 2 hr., swaged to slightly over $\frac{1}{4}$ in., annealed in air at 1050°C. for one hour, then machined. The supplier's analyses of the electrolytic materials showed all impurities to be very low. The alloys can be considered, therefore, representative of relatively pure manganese-iron alloys. The Hadfield steels were of commercial origin. Chemical analyses are given in Table 1.

TABLE 1.—*Analyses of Manganese-iron Alloys*

Specimen	Mn, Per Cent	C, Per Cent
Electrolytic iron	0 0 ^a	0 005 ^a
Alloy 3	3 3	0 02
Alloy 6	6 3	0 02
Alloy 7	7 4	0 03
Alloy 10A	9 9	0 02
Alloy 10B	10 3	0 02
Alloy 12	11 6	0 02
Alloy 14	14 0	0 02
Alloy 18	17 6	0 02
Alloy 22	21 5	0 02
COMMERCIAL HADFIELD MANGANESE STEELS		
Alloy A	13 4	0 75
Alloy B	13 7	1 34
		Ni 3 0

^a Supplier's analysis.

The tensile specimens, 0.406-cm. (0.160-in.) diameter and 2.0-cm. (0.8-in.) gauge length, were machined from the annealed $\frac{1}{4}$ -in. rods. They were cleaned in boiling benzene and heat-treated in quartz tubes, either continually evacuated or containing slowly flowing hydrogen or nitrogen. The vacuum was produced by a Cenco Megavac pump. The hydrogen atmosphere was obtained using electrolytic hydrogen puri-

fied by passing over caustic soda, soda lime, and hot copper and finally was dried employing P_2O_5 and liquid air. Nitrogen when used was similarly purified. Specimens were cooled by water immersing the quartz tube in which they were contained, but without disturbing the gas atmosphere or vacuum inside the tube. This was preceded by a short air blast to lower the temperature of the quartz wall before immersion in water. All specimens after treatment were metallic bright except the vacuum-treated specimens, which usually acquired a superficial oxide film.

Temperatures given were automatically maintained within $\pm 3^\circ\text{C}$. ($\pm 5^\circ\text{F}$.) using Chromel-Alumel thermocouples in conjunction with photocell-potentiometric controllers. Absolute temperatures were based on frequent calibrations using an auxiliary platinum-rhodium thermocouple.

The small-size tensile specimens made possible a greater number of tests with the same material and facilitated heat-treatment. Comparisons of the 0.160-in. diameter with the standard specimen, 0.505-in. diameter and 2-in. gauge length, machined from both mild steel and a commercial 18-8, showed that properties obtained using the small size were comparable with those characteristic of the standard-size specimens. The order of differences expected for the manganese-iron alloys as effected by alpha and gamma phase can be estimated from data given in Table 2.

EFFECT OF FURNACE ATMOSPHERE ON DUCTILITY OF 14 PER CENT MANGANESE ALLOY

Heating in hydrogen compared with heating in vacuum had a striking effect on the ductility of some of the alloys. In Fig. 1 are shown two tensile specimens of low-carbon 14 per cent manganese iron. Both were treated simultaneously in hydrogen at 1000°C. (1830°F.) for 3 hr., followed by vacuum treatment at 1000°C. (1830°F.) for one hour. Specimen *b* was heated an

additional 15 min. in hydrogen at 1000°C. (1830°F.) before the mechanical test. Despite similar heat-treatment, differences in elongation and reduction of area are

Hydrogen-treated 14 per cent manganese-iron alloys, subsequently heated in air instead of in vacuum at 1000°C. (1830°F.) were ductile though oxidized, illustrating

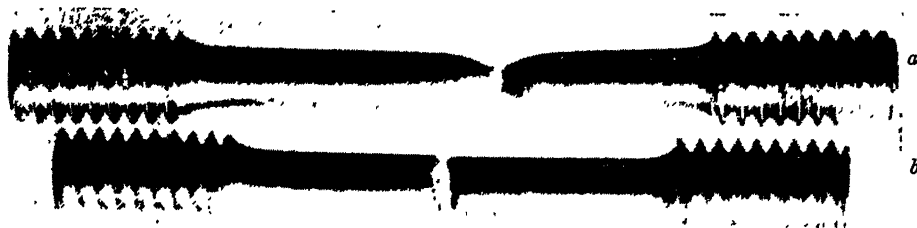


FIG. 1.—EFFECT OF HYDROGEN TREATMENT ON DUCTILITY OF 14 PER CENT MANGANESE-IRON ALLOY.
a. Quenched from 1000°C. in vacuum.
b. Quenched from 1000°C. in hydrogen

marked and arise because of the presence of hydrogen in one case and approximate absence in the other. Preliminary gas analyses of similar specimens showed that specimen *b* contains about 40 times more hydrogen than specimen *a*. Rate of cooling within a wide range did not alter the results. Specimens, for example, taken directly from (1) a hydrogen atmosphere at 1000°C. (1830°F.) or (2) an air atmosphere at 1000°C. (1830°F.), and rapidly quenched in water were respectively brittle in the first case and ductile in the second. Parallel water quenches of mild-steel specimens (0.18 per cent C) of the same size, on the other hand, produced martensite and were equally brittle whether heated previously in vacuum or hydrogen. A slower quench of the same steel in a quartz tube, as described for manganese-iron specimens, produced specimens equally ductile whether heated beforehand in hydrogen or vacuum. With larger mild-steel specimens, the effect of heating in hydrogen would be detected by reduced ductility,³ but the fact that embrittlement occurs in specimens of manganese-iron alloys 0.406 cm. (0.160 in.) in diameter, but not in 0.18 per cent C steel specimens of the same size, indicates how much more pronounced is hydrogen embrittlement in some of the manganese-iron series.

that hydrogen can rapidly escape despite an oxide coat. However, alloys heated in hydrogen at 1000°C. (1830°F.), then air-cooled in a 100°C. (210°F.) oven, were brittle, indicating that within this shorter time of cooling not sufficient hydrogen had

TABLE 2.—*Effect of Size of Tensile Specimens on Mechanical Properties*
VALUES AVERAGED FOR TWO SPECIMENS

Specimen Dimensions, In.		Tensile Strength, Lb per Sq. In. $\times 10^{-3}$	0.2 % Yield Strength, Lb per Sq. In. $\times 10^{-3}$	Elongation, Per Cent	Reduction of Area, Per Cent
Diameter	Gauge Length				
Mild Steel 0.18 Per Cent C.					
0 160	0 8	53 4	43 3	41	71
0 505	2 0	54 0	36 4	45	68 5
18-8 (17 3 Cr, 9 5 Ni, 0 10 C)					
0 160	0 8	95 9	45 6	73	80
0 505	2 0	91 3	39 5	64	74

escaped to avoid embrittlement. Hydrogen-treated specimens, heated subsequently in purified nitrogen at 1000°C. (1830°F.) for 15 min. to 5 hr. were ductile and did not significantly differ in properties compared with those treated in vacuum.

Specimens of manganese-iron alloys ranging from 12 to 22 per cent manganese treated in hydrogen at 1000°C. (1830°F.) remained brittle for at least 4 months when kept at room temperature. This was the

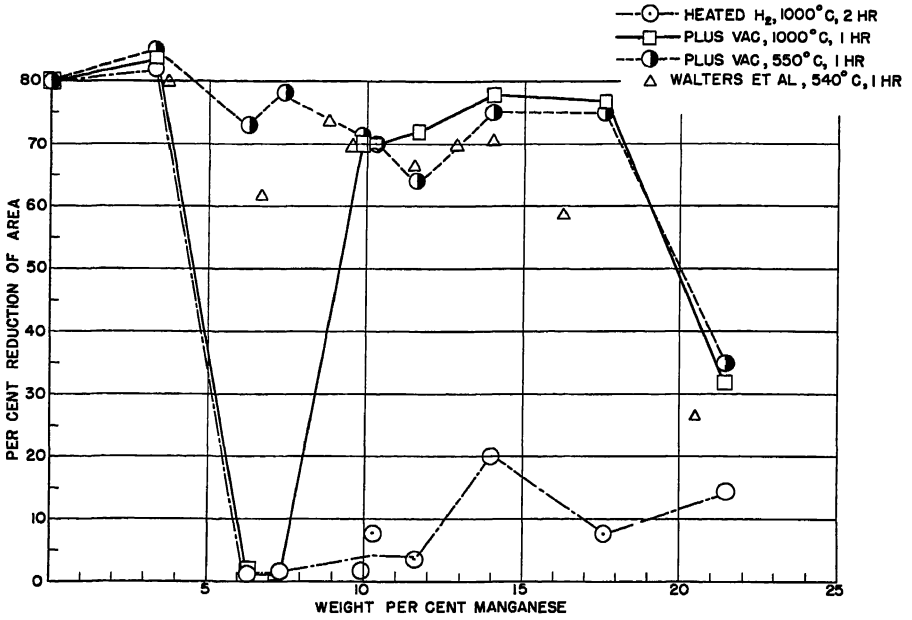


FIG. 2.—EFFECT OF HYDROGEN, VACUUM AND TEMPERING TREATMENTS ON REDUCTION OF AREA OF LOW-CARBON MANGANESE-IRON ALLOYS

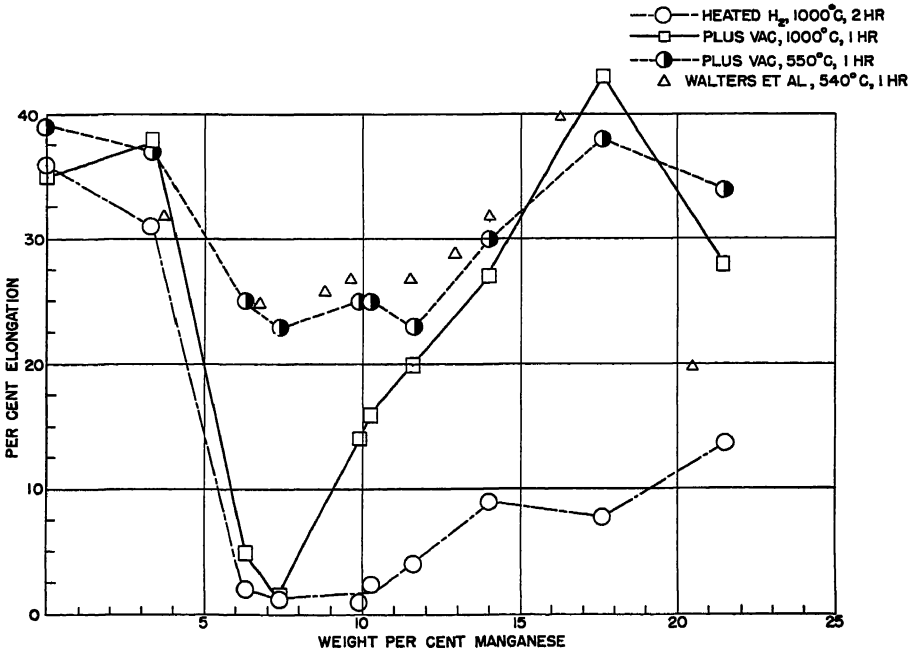


FIG. 3.—EFFECT OF HYDROGEN, VACUUM AND TEMPERING TREATMENTS ON ELONGATION OF LOW-CARBON MANGANESE-IRON ALLOYS.

maximum period of aging over which specimens were tested. Indications are that they remain brittle for a still longer period. Treatment at as low a temperature as 214°C. (415°F.) for 15 hr. in air, however, was found to restore ductility to a 14 per cent manganese-iron specimen previously heated in hydrogen at 1000°C. The values for reduction of area and elongation after the 214°C. (415°F.) air treatment were approximately four times corresponding values of specimens not heated in air.

EFFECT OF HYDROGEN ON REDUCTION OF AREA AND OTHER PROPERTIES

The effect of heat-treatment in hydrogen on the reduction of area and elongation of alloys ranging from electrolytic iron (heat-treated in hydrogen, swaged, and annealed before machining) to 21.5 per cent manganese is shown in Figs. 2 and 3. Tensile specimens of each composition were heated in hydrogen at 1000°C. (1830°F.) for 2 hr. and cooled inside a water-quenched quartz tube as previously described. Some specimens so treated were then heated at 1000°C. (1830°F.) for one hour in vacuum and similarly cooled. Some of the latter in turn were tempered at 550°C. (1020°F.) in an evacuated tube for one hour. No difference was observed between the alloys air-cooled or water-quenched from 550°C. (1020°F.).

Each point of Figs. 2 and 3 is an average for the most part of two or three specimens whose treatment was parallel. The reduction of area for electrolytic iron or for 3.3 per cent manganese iron is not affected by either hydrogen, vacuum or tempering treatments. At 6 to 7 per cent manganese, the reduction of area suddenly drops to a very low value whether the specimens are vacuum-treated or hydrogen-treated beforehand. At higher than 6 to 7 per cent manganese compositions, including 21.5 per cent manganese, the hydrogen-treated specimens are all relatively brittle. Vacuum-treated specimens, hence low in hydrogen,

display marked reduction of area for compositions above 7 per cent and including 17 per cent manganese composition, but at 21.5 per cent manganese there is again a falling off in ductility.

Curves representing elongation are similar to those for reduction of area, with some minor exceptions. Hydrogen treatment of alloy 3 reduces elongation to some extent, but this, as explained later, is ascribed to the more rapid cooling rate in hydrogen as compared with vacuum. It is observed that percentage of elongation for compositions from 7 to 17 per cent manganese, unlike reduction of area, rises steadily with manganese composition, but, like reduction of area, again decreases at 21.5 per cent manganese.

EFFECT OF TEMPERING

Specimens treated approximately in accordance with the tempering treatment of Walters, Kramer and Loring² show no great difference in reduction of area or elongation compared with the quenched low-hydrogen specimens, except the alloys containing from about 6 to 10 per cent manganese. For these the ductility is appreciably improved. As discussed later, the tempering treatment of 14 per cent manganese-iron composition at 550°C. (1020°F.) for one hour in air or vacuum was found sufficient to remove most hydrogen and restore ductility. The same probably is valid for other alloys of this series. It can be said, therefore, that whenever the one-hour tempering treatment of quenched low-carbon 12 to 22 per cent manganese-iron alloys produces appreciable improvement in ductility it does so by removal of hydrogen.

Data of Walters, Kramer and Loring for alloys tempered at 540°C. (1000°F.) for one hour are also given in Figs. 2 and 3. Their values for reduction of area at 7, 16 and 21 per cent manganese are lower than those of the present paper, but otherwise agreement is fair. A correction introduced for difference in size of tensile

specimens (Table 2) undoubtedly would bring the two sets of data into closer correspondence, in view of the fact that 16 to 22 per cent manganese are gamma

agreement. The tensile strengths for specimens so treated increase from a low value characteristic of pure iron to a maximum at approximately 12 per cent manganese,

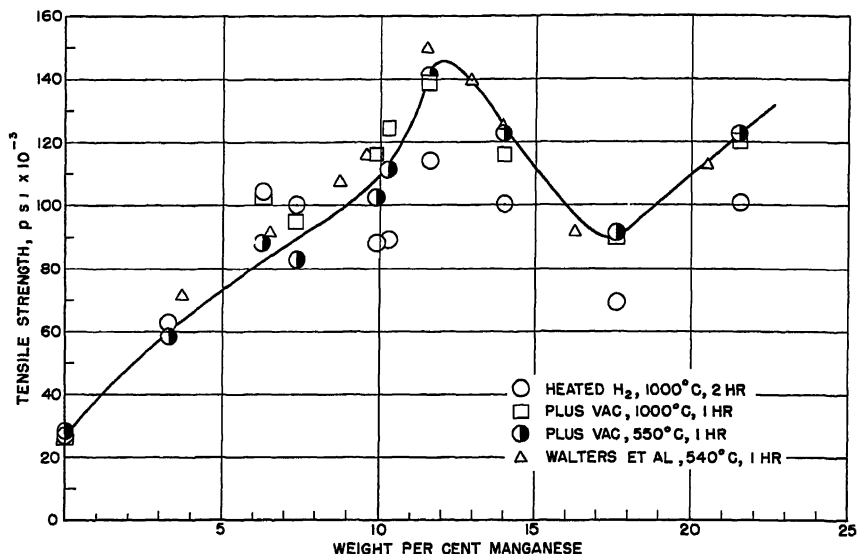


FIG. 4.—EFFECT OF HYDROGEN, VACUUM AND TEMPERING TREATMENTS ON TENSILE STRENGTH OF LOW-CARBON MANGANESE-IRON ALLOYS

and epsilon-phase alloys and 12 per cent or lower manganese compositions are, by and large, alpha-phase alloys. Hadfield's data, which show values for reduction of area and elongation all below 10 per cent for manganese compositions between 4 and 17 per cent, are not in agreement with the present data. As Walters, Kramer and Loring have already indicated, these disparities probably arise because of impurities in Hadfield's alloys.

TENSILE STRENGTHS OF LOW-CARBON ALLOYS

The effect of manganese on the tensile strengths of both hydrogen-treated and vacuum-treated specimens, and also tempered vacuum-treated specimens, is shown in Fig. 4. A curve connects points for the tempered specimens. Corresponding values reported by Walters, Kramer and Loring for similarly tempered alloys are in good

then undergo a minimum at about 17 per cent manganese before reaching a higher value at 21.5 per cent manganese.

Specimens vacuum-treated and consequently low in hydrogen follow the tensile strengths of tempered specimens. Values for hydrogen-treated specimens are coincident with values for other treatments at zero and 3.3 per cent manganese, lie above the curve at 6 to 7 per cent manganese and are uniformly below the curve at higher manganese contents.

In Table 3 are listed the averaged mechanical properties of low-carbon alloys subjected to various conditions of treatment. Yield strengths were found to be not as reproducible as tensile strengths, but it can be recognized that a definite maximum value is reached at about 6 to 12 per cent manganese.

In Table 3 are included data of some specimens tempered at 550°C. (1020°F.) for 24 hr. for comparison with specimens

Whenver properties are altered by heat-treatment at this intermediate temperature, 1 hr. appears to suffice.

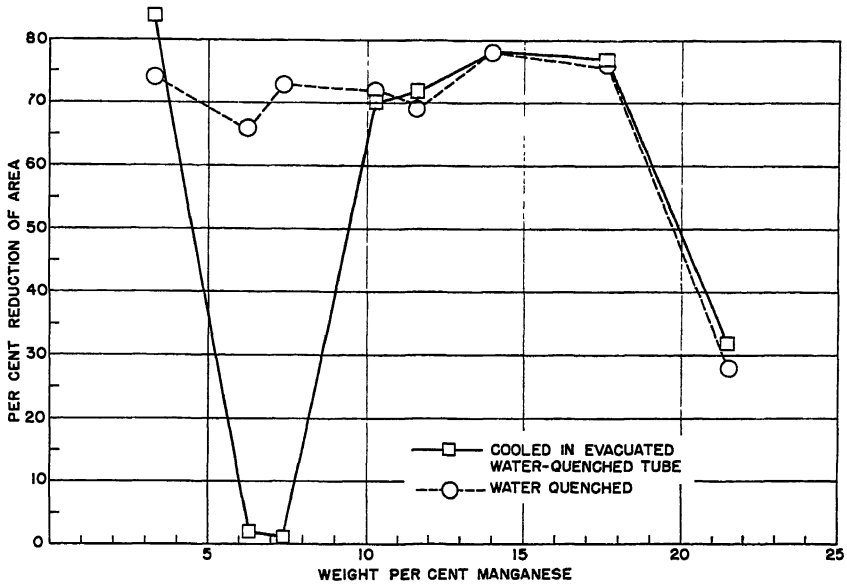


FIG. 5.—EFFECT OF COOLING RATE ON REDUCTION OF AREA OF VACUUM-TREATED LOW-CARBON MANGANESE-IRON ALLOYS.

TABLE 3.—Mechanical Properties of Manganese-iron Alloys

Alloy	Mn, Per Cent	Tensile Strength, Lb. per Sq. In. $\times 10^{-3}$						0.2 Per Cent Yield Strength, Lb. per Sq. In. $\times 10^{-3}$						Elongation Per Cent						Reduction Area, Per Cent					
		A ^a	B	C	D	E	F	A	B	C	D	E	F	A	B	C	D	E	F	A	B	C	D	E	F
Alloy 0	0 0	27	27	28				14.5	16	11				36 ^b	35 ^b	39 ^b				80 ^b	80 ^b	80 ^b			
3	3 3	63	60	58	53	84	58	46	46	42	36	79	39	31	38	37	41	17	38	82	84	85	83	74	84
6	6.3	104	103	88		109		99	101	80				2	5	25	12	1	2	73					
7	7.4	100	95		83	108	107	100	95	74	68	107	100	1	2	23	26	13	12	2	78	65	73	72	
10A	9 9	88	116	103			106	87	105	90				106	1	14	25		3	2	70	71			
10B	10 3	89	124	111	114	117	81	86	108	93	73	98	81	2	16	25	30	16	2	8	70	70	74	72	1
12	11 6	114	139	141		129	88	44	87	104				87	63	4	20	23	17	2	4	72	64	69	2
14	14 0	100	116	123		118	95	61	40	40		82	64	0	27	30		29	21	20	78	75	78	14	
17	17 6	69	90	91		88	87	58	04	77		71	63	8	43	38		44	41	8	77	75	76	70	
22	21 5	101	121	123		111	118	49	83	83		77	43	14	28	34		30	31	14	32	35	28	40	
Mild Steel.	0.4	55	51			120 ^c	52	42	33			108 ^c	38	37	39				8 ^c	32	72	75		28 ^c	46

^a Treatment A ... Heated H₂, 1000°C., 2 hours.

B ... A + vacuum, 1000°C., 1 hour.

C ... A + B + vacuum, 550°C., 1 hour.

D ... A + B + vacuum, 550°C., 24 hours.

E ... A + vacuum, 1000°C., 1 hour, water quenched.

F ... A + B + cathodic polarization, dil. H₂SO₄, 0.03 amp per sq. cm., 2 hours.

^b Approximate ^c Quenched from 1100°C.

tempered 1 hr. The longer-time tempering treatment produces no important changes in properties compared with 1-hr. treat-

Data are also given illustrating the effect of direct water quench from vacuum at 1000°C. (1830°F.) instead of the slower

quench inside a quartz tube. These are plotted in Fig. 5. The rapid quench reduces the ductility of alloy 3. The same mechanical properties within experimental variations of the test are obtained when the alloy is directly water-quenched from hydrogen, consequently the effect of rapid quench is not due to dissolved gas but to change in alloy structure. This is described later. The ductility of alloys 6 and 7, on the other hand, are increased by water quenching from 1000°C. (1830°F.), but the same treatment appears to produce no significant change in alloys containing more than 7 per cent manganese. *The difficulty that Hadfield experienced¹⁶ in checking Arnold's value for percentage of elongation using the same heat of 5.5 per cent manganese-iron alloy Arnold used can be explained by this critical effect of cooling rate on the ductility.*

The 0.18 per cent carbon steel is equally brittle, whether water-quenched from vacuum or hydrogen. The microstructure, as expected, reveals formation of martensite.

DISCUSSION OF RESULTS

To explain the effect or lack of effect of hydrogen, it was important to know the actual hydrogen content of the various specimens. Hydrogen analyses of the alloys were obtained by vacuum extraction of 5-gram samples, 0.38 cm. (0.15 in.) diameter, at 650° to 750°C. (1200° to 1380°F.), followed by analysis of the extracted gases. Preliminary values for several of the alloys are listed in Table 4.

Hydrogen, though small in quantity, was recovered from specimens previously treated in vacuum at 1000°C. as well as from those treated in hydrogen. This was not unexpected in view of the slow rate of hydrogen escape for the last portions combined with inherently better vacuum conditions in the analysis equipment than in the heat-treatment tube. Details of the analysis will be published later.

TABLE 4.—*Preliminary Hydrogen Analyses of Specimens Quenched in Quartz Tube*

Specimen	Mn, Per Cent	Wt Per Cent H ₂ × 10 ⁴	
		Heated H ₂ , 1000°C., 2 Hr.	Heated H ₂ , 1000°C., 2 Hr., Vacuum 1000°C., 1 Hr.
Electrolytic iron	0 0	0 23	
Alloy 3	3 3	0 98	
Alloy 6	6 3	1 3	0.49
Alloy 12	11 6	4 7	
Alloy 14	14 0	4 3	0 16
Alloy 17	17 6	5 5	
Alloy 22	21 5	6 0	

It is obvious from the analyses that relative lack of embrittlement of electrolytic iron and alloy 3 follows from the relatively small amount of hydrogen retained on quenching the small-diameter specimens. Quenched alloy 6 can be brittle despite a low hydrogen content. Alloys of higher manganese content retain appreciable quantities of gas and correspondingly are embrittled.

Rapidly water-quenching alloy 3 from hydrogen at 1000°C. (1830°F.) increased the amount of retained hydrogen from 0.98×10^{-4} to approximately 1.8×10^{-4} per cent. This amount, nevertheless, was insufficient to cause embrittlement. The elongation and reduction of area of specimens so quenched were reduced, it is true, from 31 and 82 per cent to 14 and 73 per cent, respectively, but the same change of properties was obtained when the alloy was water-quenched from vacuum at 1000°C. (1830°F.) (Table 3).

Why less hydrogen is retained by quenched pure iron and by alloys 3 and 6 is a point of interest that can more adequately receive explanation with further experiment. The results obtained by Baukloh and Müller⁴ indicate that hydrogen solubility in manganese-iron alloys at 1000°C. (1830°F.) does not vary with manganese content in a manner necessary to explain the slight retention of hydrogen by alloys containing less than 6 per cent

manganese. The effect of manganese to lower the $\gamma \rightarrow \alpha$ transformation temperature of iron is probably more closely related to the observed effects. It is known that the hydrogen-diffusion rate at comparable temperatures is lower in gamma iron than in alpha iron⁶ and the same order probably exists for gamma and alpha-phase manganese-iron alloys. The higher the transformation temperature, the higher is the temperature at which alpha phase appears, consequently hydrogen can diffuse out of the specimen with greater facility. This factor can plausibly account for the more rapid loss of hydrogen on cooling pure iron and alloys 3 and 6, all of which transform from gamma to alpha phase at temperatures sufficiently high for ready diffusion of hydrogen ($> 400^\circ\text{C}$). Higher manganese alloys transform at lower temperatures not favorable for rapid hydrogen diffusion.

THE 6 PER CENT MANGANESE COMPOSITION

The curious dip in reduction of area and elongation of manganese-iron alloys at about 6 to 7 per cent manganese, either quenched in a quartz tube in hydrogen or vacuum at 1000°C . (1830°F .), prompted an inquiry into the nature of this composition. Baukloh and Müller reported a discontinuity in hydrogen solubility at this manganese composition, the solubility at 1000°C . (1830°F .) being approximately 7.9×10^{-4} per cent at 7 per cent manganese but dropping off to approximately 5.4×10^{-4} per cent at either 4 or 8 per cent manganese. Our preliminary hydrogen analyses of vacuum-treated 6.3 per cent manganese alloy proved, however, that 1 hr. at 1000°C . (1830°F .) sufficed to reduce the hydrogen content to a low value (Table 4). This fact, together with experiments in which vacuum treatment at 1000°C . (1830°F .) was extended beyond the usual 1 hr. but with no resultant alteration of properties made it quite certain

that hydrogen was not the factor that accounted for the brittle nature of the quenched alloys.

Ductility, as reported earlier, was



FIG. 6.—BACK-REFLECTION X-RAY DIFFRACTION PATTERN OF 6.3 PER CENT MANGANESE—IRON ALLOY SHOWING EFFECT OF TEMPERING ON (211) ALPHA DOUBLET.

a. Quenched in evacuated tube.

b. Tempered 550°C . one hour.

acquired by the 6 to 7 per cent manganese alloys when the hydrogen-treated or vacuum-treated specimens were tempered at 550°C . (1020°F .) for about 1 hr. Any change in microstructure after this treatment compared with that of specimens quenched from 1000°C . (1830°F .) was not readily perceptible. X-ray patterns recorded body-centered cubic lines for the quenched as for the tempered alloys. An important difference appeared, however, in the breadth of the X-ray lines. The lines for the tempered alloy were sharp whereas those for the quenched alloy were more diffuse. A subsequent back-reflection pattern showed that the (211) alpha line was broad and diffuse for the quenched alloys but was split into a doublet for the tempered alloy. The X-ray photograms are reproduced in Fig. 6. These differences in X-ray structure have been previously described in the literature and are characteristic of alpha-phase manganese-iron alloys. When quenched, the alpha phase is in a metastable state, but when tempered it is in an equilibrium state. The brittle structure appears, therefore, to be no other than the alpha prime or super-saturated alpha phase reported by Öhman⁶ and recently described by Troiano and

McGuire.⁷ The latter authors report supersaturated alpha lines at compositions ranging from 3 to 15 per cent manganese. The marked effect of this metastable "phase" on ductility appears most pronounced in the composition range bordering 6 per cent manganese. A definite though smaller effect appears at 3.3 and 10 per cent manganese and still less or practically none at 11.6 per cent or higher manganese compositions.

The presence of this "phase" can explain the effect of rapid water quench compared with a slower quench in a quartz tube on the properties of alloys 3, 6, and 7 as shown in Fig. 5. Although a water quench decreases the ductility of alloy 3 and increases the ductility of alloys 6 and 7, the cause is probably the same because a still slower cooling rate applied to alloys 6 and 7 again renders them ductile. Elongation of alloy 3 happens to respond to a more rapid cooling rate than is characteristic of alloys 6 and 7. It is this effect of cooling on formation of a brittle alpha phase, therefore, that accounts for the reduced elongation of hydrogen-treated and cooled alloy 3 (Fig. 3). A further analysis of the brittle structure as influenced by cooling rate was not attempted.

THE 21.5 PER CENT MANGANESE COMPOSITION

The falling off of ductility at 21.5 per cent manganese for vacuum-treated or tempered specimens (Figs. 2 and 3) is related to a structural change differing from that which accounts for the properties of 6 to 7 per cent manganese alloys. Hydrogen analyses of Table 4 show that the quenched 21.5 per cent alloy retains approximately the same amount of hydrogen as does the 17.6 per cent alloy. Vacuum treatment of the 21.5 per cent alloy for 1 hr. at 1000°C. (1830°F.), however, fails to bring the ductility to as high a value as the 17.6 per cent alloy, nor does vacuum treatment for an additional hour alter

the properties. X-ray patterns of both alloys, quenched and cold-worked, furnished a clue. The approximate phase composition obtained from line intensities of wire specimens is given in Table 5. Heat-treatment was effected by passing an electric current through 0.051-cm. (20-mil) diameter wires of each alloy and recording temperatures with an optical pyrometer. A rapid quench was effected by interruption of the current.

TABLE 5.—Phase Composition of Alloys Containing 17.6 and 21.5 Per Cent Manganese

20-MIL WIRES, HEATED H₂, 1000°C, 4 MIN. FOLLOWED BY VACUUM, 1000°C., 2 MINUTES

Alloy	Mn, Per Cent	Quenched	Approximately 40 Per Cent Cold Reduction
17	17.6	$\gamma, \epsilon \left(\frac{\epsilon}{\gamma} = \text{approx } 4 \right)$	$\alpha, \epsilon (\alpha = \epsilon)$
22	21.5	$\gamma, \epsilon (\gamma = \epsilon)$	ϵ

α = body-centered cubic.
 γ = face-centered cubic.
 ϵ = hexagonal close packed.

It is apparent that whereas both alloys quenched from 1000°C. (1830°F.) in vacuum are composed of mixtures of gamma (face-centered cubic) and epsilon (hexagonal close-packed phases), cold-work transforms gamma phase of the 21.5 per cent alloy to epsilon but gamma phase and apparently some epsilon phase of the 17.6 per cent alloy are transformed to alpha (body-centered cubic). The greater ease of slippage in general of the body-centered cubic compared with the hexagonal close-packed polycrystalline metals accounts for the diminished ductility of the 21.5 per cent manganese alloy.

EFFECT OF TIME AND TEMPERATURE ON RECOVERY OF DUCTILITY

Specimens of 14.0 per cent manganese iron heated in hydrogen at 1000°C. (1830°F.) for 15 min., 1 hr., 2 hr., or 5 hr.

showed embrittlement to approximately the same extent. This was evidence that hydrogen diffuses very rapidly at 1000°C. (1830°F.). At lower temperatures a longer

atures. At 500°C. (930°F.), specimens are ductile, whether heated in hydrogen or vacuum. At 550°C. (1020°F.) and 600°C. (1110°F.), reduction of area of specimens

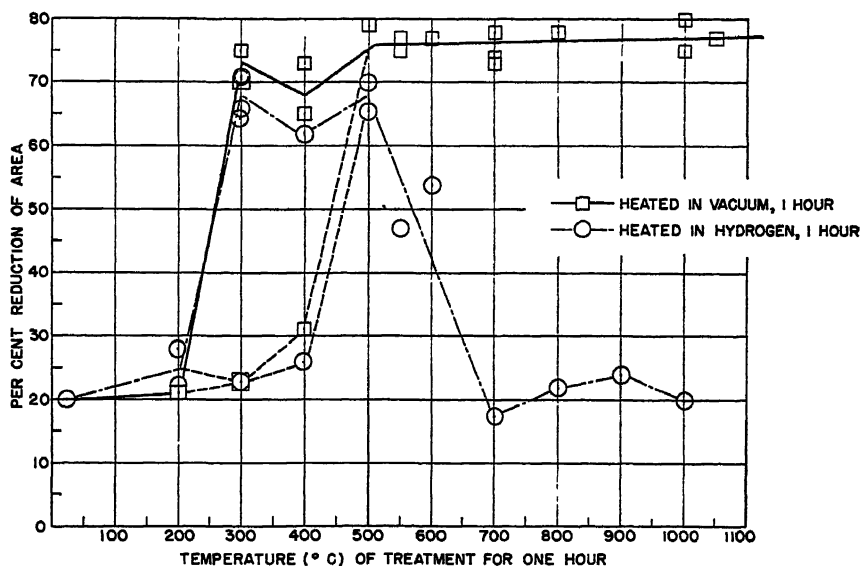


FIG. 7.—EFFECT OF ATMOSPHERE AND TEMPERATURE ON REGAIN OF DUCTILITY OF LOW-CARBON 14 PER CENT MANGANESE-IRON ALLOY.
Specimens previously heat-treated in hydrogen.

time for diffusion is expected and observed. This is illustrated by data plotted in Fig. 7 for reduction of area related to temperature at which specimens of 14.0 per cent manganese-iron alloy were held for 1 hr. in hydrogen or vacuum. All specimens were previously heated in hydrogen at 1000°C. (1830°F.) for 2 hr. and thereby were embrittled. Individual determinations, not averages, are recorded. At 200°C. (390°F.), specimens either heated in vacuum or hydrogen for 1 hr. remain embrittled. As mentioned earlier, treatment for longer times at this approximate temperature restores ductility in at least 15 hr. At 300°C. (570°F.) and 400°C. (750°F.) specimens behave erratically, sometimes becoming ductile, at other times not, whether in hydrogen or vacuum. The lower dashed lines of Fig. 7 trace the alternate behavior at these two temper-

atures. At 500°C. (930°F.), specimens are ductile, whether heated in hydrogen or vacuum. At 550°C. (1020°F.) and 600°C. (1110°F.), reduction of area of specimens

heated in hydrogen begins to decrease, whereas values for specimens heated in vacuum remain fairly constant at 75 per cent. At 700°C. (1290°F.) and higher, specimens heated in hydrogen remain embrittled. A number of dilatometer runs showed that this alloy heated to 500°C. (930°F.) is below the $\alpha \rightarrow \gamma$ transformation temperature range and that at approximately 625°C. (1160°F.) the alloy is completely converted to gamma phase. On cooling, the reverse transformation to epsilon phase begins at 175°C. (350°F.) with alpha phase appearing at a still lower temperature. X-ray data indicated that all three phases are present at room temperature. Extension data plotted with temperature are given in Fig. 8. Discontinuities in the slope of the extension curve, corresponding to phase transformations, were at the same temperature

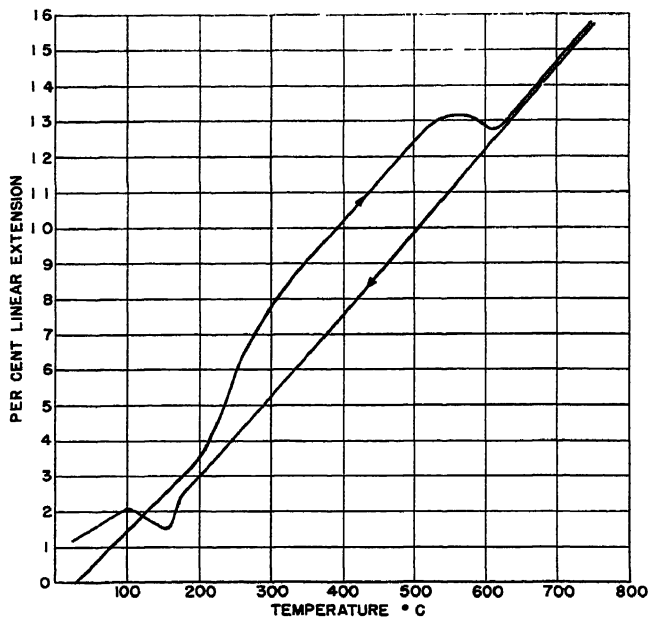


FIG. 8.—DILATOMETER CURVE FOR LOW-CARBON 14 PER CENT MANGANESE-IRON ALLOY.
Heating and cooling rate 140°C. per hour.

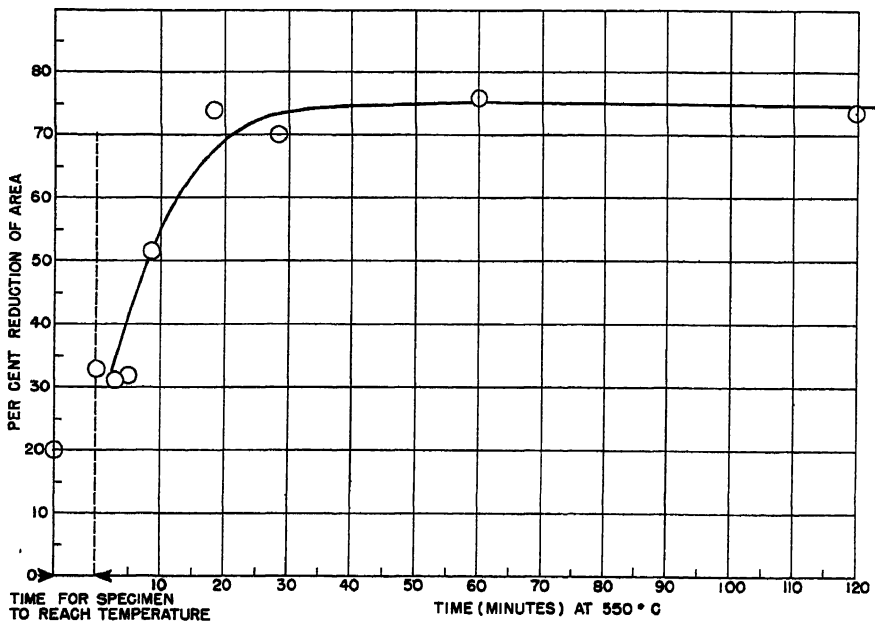


FIG. 9.—RELATION OF REDUCTION OF AREA TO TIME OF HEATING LOW-CARBON 14 PER CENT MANGANESE-IRON ALLOY AT 550°C. IN AIR.
Specimens previously heat-treated in hydrogen

whether the dilatometer specimen was heated and cooled in hydrogen or in vacuum. Any effect of hydrogen, therefore, on phase-transformation temperatures must be relatively small.

The respective temperatures for phase transformation in the 14 per cent manganese-iron alloy are related to its behavior when heated in hydrogen at various temperatures. Hydrogen is less soluble in the mixture of gamma and alpha phases at 500°C. (930°F.) than at temperatures above approximately 625°C. (1160°F.) at which the alloy is all gamma phase. This follows from the fact that the solubility of hydrogen is greater in gamma than in alpha phase^{4,8}. Furthermore, at 500°C. (930°F.) excess hydrogen retained on quenching from 1000°C. can readily escape via the alpha-phase portion of the lattice as compared with a lower rate of escape in gamma phase. Consequently, the alloy heated at 500°C. (930°F.) for 1 hr. in hydrogen or vacuum retains too little hydrogen to exhibit embrittlement at room temperature. At lower temperatures of heat-treatment in hydrogen or vacuum the rate of hydrogen escape is less and probably depends on several factors, including variable catalytic surface condition of the specimen with respect to combination of hydrogen atoms to form hydrogen gas. Hence these specimens may or may not be ductile after 1-hr. treatment, but undoubtedly would all be so if heated for somewhat longer times.

In Fig. 9, the relation is shown of reduction of area to time of heating 14.0 per cent manganese tensile specimens at 550°C. (1020°F.) in air. These specimens, too, were previously treated in hydrogen at 1000°C. (1830°F.) for 2 hr. The temperature was recorded by a thermocouple wired to the specimen. The time for the tensile specimen to reach 5°C. (9°F.) below the specified final temperature required 6½ min. after insertion into the air furnace. Time was recorded when the specimen

reached this temperature, indicated by the dotted vertical line of Fig. 9. The increase of ductility is erratic for short heating times, but within approximately 30 to 50 min. the specimens of 0.160-in. diameter lose sufficient hydrogen to reach their maximum ductility.

EFFECT OF DISSOLVED HYDROGEN ON HADFIELD MANGANESE STEELS

The properties of Hadfield manganese steels are sensitive to rate of quench, whereas the low-carbon manganese alloys above 7 per cent manganese are unaffected within a wide range of cooling rates. It was found that the usual procedure of quenching specimens inside a water-cooled quartz tube was too slow to obtain uniform and optimum properties of the high-carbon alloys. In all tests, therefore, a direct quench in water followed whatever treatment preceded. Tests were conducted soon after the quench.

The tensile specimens, ground to size, were of the same dimensions for Hadfield alloy A as those used for the low-carbon alloys. Specimens of this alloy quenched either from vacuum or hydrogen at 1000°C. (1830°F.) showed differences in mechanical properties only within the experimental variations of the test. The results averaged for two specimens are given in Table 6.

Further tests were conducted using a second commercial Hadfield alloy labeled B. This alloy, unlike alloy A, did not contain nickel. Tests were conducted initially with standard strip specimens of 2-in. gauge length and 0.412 cm. (0.162 in.) thick (Fig. 4, p. 134 of ref. 9). The results given in Table 6 show no significant effect of hydrogen on the mechanical properties.

The large tensile specimens became hot incidental to testing, however, with the possibility that some hydrogen escaped during the test. The thickness of sheet was too small to permit grinding of the small-diameter tensile specimens. It was con-

sidered best, therefore, to continue the tests with impact specimens. Impact values are known to be especially low for metals embrittled by hydrogen. A marked difference in impact value, for example, was observed for cylindrical specimens of low-carbon 14.0 per cent manganese-iron alloy

TABLE 6.—*Effect of Hydrogen on Tensile and Impact Properties of Hadfield Manganese Steels*

STEEL A

Specimens 0.8-in. Gauge Length, 0.160-in. Diameter. Averaged Results

Treatment	Tensile Strength, Lb. per Sq. in. $\times 10^{-3}$	0.2 Per Cent Yield Strength, Lb. per Sq. in. $\times 10^{-3}$	Elongation, Per Cent	Reduction of Area, Per Cent
H ₂ , 1000°C., 2¼ hr.	122	48	79	54
Vac., 1000°C., 2¼ hr.	126	54	83	59

STEEL B

Strip Specimens 2-in. Gauge Length, 0.162-in. Thickness. Averaged Results

H ₂ , 1000°C., 1 hr.	138	51	55	39
Vac., 1000°C., 1 hr.	143	49	52	39
Air, 1000°C., ¼ hr.	140	47	49	38

CHARPY IMPACT SPECIMENS 2.16 \times 0.394 \times 0.162 INCH

FT.-LB.

H ₂ , 1000°C., 15 min.	38	
H ₂ , 1000°C., 2 hr.	40	
<i>Effect of Aging</i>		
H ₂ , 1000°C., 1 hr.	40	Tested within few minutes
	36	Tested one day after treatment
	38	Tested 3 days after treatment
	37	Tested 6 days after treatment
	37	Tested 5 weeks after treatment
Vacuum, 1000°C., 1 hr.	41	
	38	
N ₂ , 1000°C., 1 hr.	36	
	38	
H ₂ , 1100°C., 1 hr.	37	
Vacuum, 1100°C., 1 hr.	37	

heat-treated in hydrogen, as compared with specimens heat-treated in vacuum.

The impact specimens of alloy B were ground to the dimensions of standard Charpy notched impact specimens (Fig. 2, p. 673 of ref. 9) except that the thickness was that of the rolled sheet, 0.412 cm. (.162 in.), and a V-notch was ground instead of a saw cut. Tests were conducted to illustrate the effect of heating in hydrogen or vacuum at 1000°C. (1830°F.) or 1100°C. (2010°F.) and in nitrogen at 1000°C. (1830°F.). A study of aging up to 5 weeks was made for specimens initially quenched from 1000°C. (1830°F.) in hydrogen. A rapid quench in fused nitrate-nitrite salt at 160°C. was compared with a water quench. The average value for all tests for all treatments was 38 ft.-lb. Data of Table 6 show that any variations from this mean were within the experimental fluctuations. The conclusion is that under the described conditions hydrogen retained on quenching has no measurable effect on impact or tensile properties of Hadfield manganese steels.

It is pertinent to note that lack of embrittlement is not due to deficiency of hydrogen absorption at high temperatures or absence of retained hydrogen at room temperature. Preliminary gas analyses showed that Hadfield steel A heated at 1000°C. (1830°F.) in hydrogen for 2 hr. and water-quenched contained 5.5×10^{-4} per cent H₂. This amount, which was without effect on Hadfield steel, was ample to cause embrittlement of the low-carbon alloys. Vacuum treatment of Hadfield steel at high temperatures was found to extract most of this dissolved hydrogen. A sample of Hadfield steel A heated in vacuum at 1000°C. (1830°F.) for 2 hr. analyzed only 0.09×10^{-4} per cent H₂. The lack of embrittlement of high-carbon 14 per cent manganese iron, and pronounced embrittlement of the low-carbon alloys, probably arises, therefore, from the less pronounced effect of dissolved hydrogen on totally gamma-phase alloys as compared with alpha and epsilon-phase alloys.

EFFECT OF CATHODIC HYDROGEN

It is of fundamental interest to know the comparative effect on metals of hydrogen introduced at room temperature as well

ductile, except the alloys analyzing 6 to 7 per cent manganese. The latter when quenched in this manner from 1000°C. (1830°F.) are inherently brittle, inde-

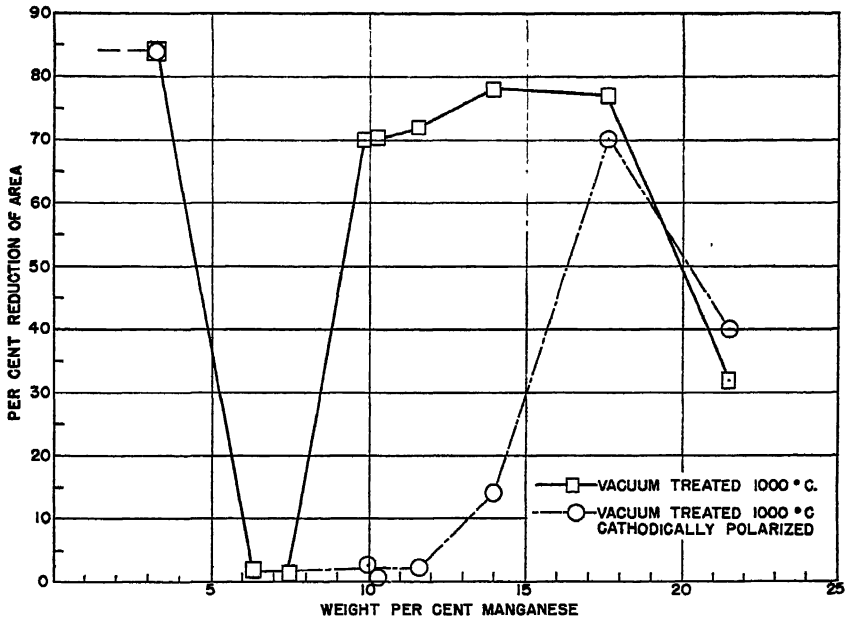


FIG. 10.—EFFECT OF EXPOSURE OF LOW-CARBON MANGANESE-IRON ALLOYS TO CATHODIC HYDROGEN IN DILUTE SULPHURIC ACID ON REDUCTION OF AREA.

as the effect of hydrogen retained by quenching. Hydrogen, in either case, is known to embrittle iron. The effect of manganese on the extent of embrittlement of iron by cathodic hydrogen apparently has not been investigated previously. The study is especially of interest because of the presence of one or more of the three common lattice types in quenched alloys containing up to 22 per cent manganese.

Specimens used were, as before, 0.406-cm. (0.160-in.) diameter and 2.0-cm. (0.8-in.) gauge length. These tensile specimens were first heated in hydrogen at 1000°C. (1830°F.) for 2 hr. followed by vacuum treatment at 1000°C. (1830°F.) for 1 hr. with the usual quench in a quartz tube. By application of this treatment they were relatively free of hydrogen and were

pendent of hydrogen content.

The tensile specimens were made cathode in pure dilute sulphuric acid employing platinum anodes. Current density was 0.03 amp. per sq. cm. (0.2 amp. per sq. in.) and time of electrolysis was for 2 hr. Tensile tests were conducted immediately after treatment, to avoid loss of hydrogen at room temperature.

Reduction of area plotted with manganese content is shown in Fig. 10. Mechanical properties are summarized in Table 3. The 3.3 per cent manganese alloy is unaffected by 2-hr. exposure to cathodic hydrogen. This is true also of the 17.6 and 21.5 per cent manganese alloys treated for 2 hr., or, as was done in later experiments, for a period as long as 23 hr. Compositions between 10 and 14 per cent

manganese, on the other hand, are severely embrittled. The alloys embrittled by cathodic hydrogen display in general lower tensile strength than control specimens heat-treated in vacuum.

Lack of embrittlement of the 3.3 per cent manganese alloy is not entirely unexpected in view of Körber and Ploum's experiments,¹⁰ which showed that pure iron does not absorb hydrogen when made cathode in a pure sulphuric acid solution. It is curious that the 17.6 and 21.5 per cent compositions are likewise unaffected, whereas intermediate compositions are embrittled. Preliminary hydrogen analyses made it clear that lack of response of these alloys to cathodic hydrogen resided in the relatively small amount of hydrogen that enters the lattice. Gas-analysis data are listed in Table 7.

TABLE 7.—*Preliminary Hydrogen Analyses of Alloys Exposed to Cathodic Hydrogen in Dilute Sulphuric Acid*

Alloy No.	Mn, Per Cent	Current Density, Amp. per Sq. Cm.	Time of Electrolysis, Hr.	Wt. Per Cent $H_2 \times 10^4$
3	3.3	0.03	2	0.89
14	14.0	0.03	2	3.5
18	17.6	0.03	2	0.74
22	21.5	0.03	3	0.48
Hadfield steel A.	13.4	0.05	5	0.29

Alloy 14 of Table 7, which is one of the compositions embrittled by cathodic hydrogen, contains, as expected, the largest quantity of gas. The expressed hydrogen content is more effective in causing embrittlement than the analysis indicates because the major portion of gas is localized at high concentration in a region near the specimen surface. A rim of relatively brittle metal surrounding a more ductile core can be seen in the fractured sections of tensile bars.

Hadfield steel is unaffected by exposure to cathodic hydrogen for a period as long as 5 hr. Here, too, practically no

hydrogen enters the lattice, allowing for a small amount originally present in the specimen. Addition of a trace of phosphorus dissolved in CS_2 to the sulphuric acid electrolyte, as was done by Körber and Ploum¹⁰ to increase absorption of cathodic hydrogen by iron, was found also to increase the amount of hydrogen absorbed by Hadfield steel. It was found that 1.0×10^{-4} per cent H_2 entered the alloy after 2-hr. electrolysis in sulphuric acid containing phosphorus at 0.05 amp. per sq. cm. (0.32 amp. per sq. in.). This amount, however, was insufficient to alter the mechanical properties of tensile specimens. It will be recalled that as much hydrogen as 5.5×10^{-4} per cent in Hadfield steel specimens quenched from high temperatures was also without effect.

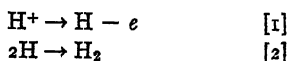
The tensile results obtained for alloy 7 point to the fact that this alloy, like alloys 3, 18 and 22, does not absorb cathodic hydrogen in pure sulphuric acid. Tensile specimens of alloy 7 quenched in a quartz tube are so embrittled that in test they tend to break at the threads. Hence the data of Table 3 for effect of cathodic hydrogen on this alloy are for specimens directly water-quenched from vacuum, and therefore initially more ductile. The mechanical properties are very nearly identical with those of specimens that have had parallel treatment but have not been exposed to cathodic hydrogen. Data that also indicate lack of cathodic hydrogen absorption were obtained for tempered specimens, which are more ductile than water-quenched vacuum-treated specimens. The properties of these, too, were unaffected after exposure to cathodic hydrogen for 2 hours.

Results for mild steel are included in Table 3. Unlike pure iron, the properties of this steel are altered by exposure to cathodic hydrogen in pure sulphuric acid. The tensile strength undergoes no appreciable change after 2-hr. treatment but the

elongation and reduction of area are decreased.

THEORY FOR THE CATHODIC HYDROGEN RESULTS

The fact that certain addition agents to the electrolyte are necessary before cathodic hydrogen enters the iron and some alloy lattices is proof that surface properties of the metals determine whether discharged hydrogen ions will escape as H_2 or become a constituent of the lattice. The reactions, somewhat simplified, which describe the situation at the cathode when a current flows are as follows:



The first reaction, in accordance with Faraday's law, proceeds as rapidly as the current flows. At the beginning of electrolysis, the second reaction may proceed rapidly on a clean metal surface, which catalyzes combination of hydrogen atoms, or it may be inhibited by additions such as phosphorus or arsenic, which act in no different sense than well-known surface catalyst poisons. Inhibition of reaction 2 will increase the effective surface concentration of hydrogen atoms on the cathode and thus increase the relative probability of their entrance into the metal lattice. This explains the immunity of pure iron to cathodic hydrogen and the embrittlement of mild steel. The latter contains small percentages of impurities, which contaminate the metal surface and partly destroy the property of iron to accelerate reaction 2. This particular mechanism is similar to one that recently has given plausible explanation for the effect of catalyst poisons on hydrogen overvoltage.¹¹

It is reasonable that 3 to 7 per cent manganese added to iron should have catalytic influence on the reaction $2H \rightarrow H_2$ not appreciably different from that of iron itself. Hence, as observed, only a small amount of cathodic hydrogen enters the

alloy lattice of low manganese composition. At higher manganese compositions, the over-all catalytic properties of the alloys may differ—or, alternately, the affinity of manganese for hydrogen may be greater than that of iron for hydrogen, so that more discharged hydrogen for this reason becomes part of the alloy lattice. One fact that bears relation to the second of these possibilities is the abnormally high solubility of hydrogen in manganese, the solubility exceeding that in iron, chromium, cobalt or nickel.¹² The effect of manganese on the entrance and concentration of cathodic hydrogen in the manganese-iron lattice appears to be confined to alloys of alpha phase or body-centered cubic lattice.

The b.c.c. lattice exists predominantly in quenched alloys containing up to 12 per cent manganese but constitutes only a small fraction of the 14 per cent Mn alloy structure. For the latter alloy, the face-centered cubic lattice (gamma phase) and hexagonal close-packed lattice (epsilon phase) are present in major amount. Fig. 10 shows that coincident with the predominance of these lattices at 14 per cent manganese the effect of exposure to cathodic hydrogen diminishes. In fact, when the alloys are virtually all gamma and epsilon phases, as occurs at 17.6 and 21.5 per cent manganese, cathodic hydrogen fails to enter the lattice in any significant amount and no embrittlement occurs.

The behavior of the manganese-alloy series is strong evidence that the lattice type plays a large part in determining whether or not cathodic hydrogen is absorbed. Further evidence of this is contained in the fact that commercial Hadfield steels, which are totally gamma phase, also fail to absorb appreciable cathodic hydrogen in pure dilute sulphuric acid (Table 7). Since the order of hydrogen solubility in these respective lattices would be expected to exert opposite to the

observed effect (hydrogen is more soluble in gamma than in alpha iron) it appears that other factors such as differing hydrogen-diffusion rates in the alloys and differing surface catalytic activity must enter into the explanation. Present evidence places less importance on the effect of lattice on catalysis and greater importance on the relatively low diffusion rate of hydrogen in the f.c.c. lattice at room temperature. This evidence is obtained from the experiment in which a catalyst poison added to sulphuric acid increased very little the cathodic hydrogen absorption by Hadfield steel, and is also evident in the fact that hydrogen at room temperature escapes extremely slowly from gamma-phase 18-8¹³ and from gamma-phase Hadfield steel.¹⁴

SUMMARY

Low-carbon manganese-iron alloys, containing 9 to 22 per cent manganese, hydrogen-treated at 1000°C. (1830°F.) and quenched are embrittled by retained hydrogen. This applies to large and small-size specimens. Small-size specimens of electrolytic iron, 0.406-cm. (0.160-in.) diameter, and 3.3 per cent manganese-iron alloy, on the other hand, are not embrittled because hydrogen dissolved at 1000°C. (1830°F.) for the most part is not retained, no matter how rapid the quench.

The alloys vacuum-treated at 1000°C. (1830°F.) and quenched in vacuum lose hydrogen. They are ductile, with the exception of alloys analyzing approximately 6 to 7 per cent manganese. The latter are brittle because of formation on quenching of a metastable alpha phase. The appearance of this "phase" is also evident in the properties of 3.3 and 10 per cent manganese compositions. The 21.5 per cent manganese alloy is less ductile than the expected value by extrapolation because with cold-work it practically completely transforms to brittle epsilon phase (hexagonal close packed).

Tempering at 550°C. (1020°F.) transforms the metastable or supersaturated alpha to equilibrium alpha phase and hence improves the ductility of alloys particularly of 3 to 10 per cent manganese composition. Any significant effect of this tempering treatment to improve the ductility of alloys containing from 12 to 22 per cent manganese is by removal of hydrogen.

The reduction of area and elongation of alloys containing 3.3, 6.3 and 7.4 per cent manganese, vacuum-treated and hence low in hydrogen, are dependent on rate of cooling. A rapid water quench instead of a slower quench in vacuum decreases the ductility of 3.3 per cent manganese but increases the ductility of 6 to 7 per cent manganese compositions and has no significant effect on the properties of higher manganese compositions. This effect of cooling rate explains in part the difficulties reported by Hadfield in his attempt to harmonize data for the low-carbon alloys.

The loss of hydrogen manifested by gain in ductility of the 14 per cent manganese alloy on heating in hydrogen or vacuum for 1 hr. at various temperatures can be interpreted on the basis of high diffusion rate of hydrogen in alpha phase and the high solubility of hydrogen in gamma phase.

Appreciable hydrogen is retained by the high-carbon 14 per cent manganese alloy (Hadfield manganese steel) on quenching from 1000°C. (1830°F.), but this has no effect on the tensile or impact properties in contrast to results obtained with the low-carbon 14 per cent manganese composition.

Exposure to cathodic hydrogen in a sulphuric acid electrolyte embrittles alloys containing 10 to 14 per cent manganese but has no effect on other alloys of the series, including Hadfield manganese steel. The reason was found to be lack of sufficient hydrogen absorption by the compositions not affected. Manganese in iron favors the

absorption of cathodic hydrogen in alpha-phase alloys. Alloys composed of gamma or epsilon phase, or both (low-carbon 17 to 22 per cent manganese and high-carbon 14 per cent manganese), as well as alpha-phase alloys containing less than approximately 8 per cent manganese, do not take up an appreciable amount of cathodic hydrogen in sulphuric acid. The reasons are related to differing surface catalytic activity with respect to the reaction $2H \rightarrow H_2$, to the appreciable affinity of manganese for hydrogen, and to the differing diffusion rates of hydrogen.

ACKNOWLEDGMENT

The author is indebted to Dr. John Naughton for the hydrogen analyses, to Dr. David Harker for the X-ray information, to Miss Catherine Ferguson for the many mechanical tests, and to Mrs. Constance Brodie for the dilatometer data.

REFERENCES

1. R. Hadfield: *Jnl. Inst. Metals* (1927) **115**, (a) 297; (b) 329; (c) 337.
2. F. Walters, I. Kramer and B. Loring: *Trans. A.I.M.E.* (1942) **150**, 401.
3. C. Zapffe and C. Sims: *Trans. A.I.M.E.* (1941) **145**, 225.
4. W. Baukloh and R. Müller: *Archiv Eisenhüttenwesen* (1938) **11**, 509.
5. W. Baukloh and H. Kayser: *Ztsch. Metallkunde* (1935) **27**, 281.
6. E. Ohman: *Ztsch. physik. Chem.* (1930) **B-8**, 81.
7. A. Troiano and F. McGuire: *Trans. Amer. Soc. Metals* (1943) **31**, 340.
8. A. Sieverts, G. Zapf and H. Moritz: *Ztsch. physik. Chem.* (1938) **A-183**, 19-37.
9. Metals Handbook, Amer. Soc. Metals (1939).
10. F. Korber and H. Ploum: *Mitt. K. W. I. Eisenforschung* (1932) **14**, 229.
11. A. Hickling and F. Salt: *Trans. Faraday Soc.* (1942) **38**, 474.
12. A. Sieverts and H. Moritz: *Ztsch. physik. Chem.* (1937) **A-180**, 249.
13. V. Holm and J. Thompson: *Jnl. Research, Nat. Bur. Stds.* (1941) **26**, 246.
14. Unpublished investigations of J. Naughton and H. Uhlig.

DISCUSSION

(F. B. Foley presiding)

R. E. CRAMER,* Urbana, Ill.—Mr. Uhlig says that "data are presented to show that

hydrogen absorbed by the high-carbon alloys of Hadfield composition is without effect on their mechanical properties." I would like to point out that these data are based on tests of small specimens of steel. It may well be doubted whether this conclusion would hold for a bar of steel of considerable cross section, say 2 in. in diameter or larger.

Judging from the results of our studies of the effect of hydrogen on the development of shatter cracks in railroad rails, we would be on the lookout for such internal cracks in all high-carbon alloy steels. However, it may be that the Hadfield austenitic steel used by Mr. Uhlig does not reject hydrogen at temperatures below a red heat, as the ferritic steels do, so such cracks would not develop. It will be interesting to keep on the lookout for further information on this subject.

F. C. KELLEY,* Schenectady, N. Y.—The General Electric Co. has been interested in the subject of hydrogen embrittlement of low-carbon steels, since copper brazing of this class of materials is carried out on a mass production scale. Over a period of about 25 years we have never found such materials to be embrittled by hydrogen except in certain cases where the trouble could be traced to some other cause.

The publication of Dr. Carl A. Zapffe's paper in *Metal Progress* in August 1942 led to an investigation of this subject by George Wright, of our works laboratory, and myself.

A steel of the following composition was selected and standard tensile-test specimens were machined from the material: carbon, 0.23 per cent; manganese, 0.48; phosphorus, low; sulphur, low; no alloy content. The results of tests on this steel are given in Table 8.

It was quite evident from these results that the steel had not been materially affected by the hydrogen treatment, for the specimens were tested immediately after quenching. They were hard, because of the formation of martensite perhaps, and had low ductility, but were physically virtually the same as the specimens treated in the closed tube.

It was then decided to select a more sensitive material, so Armco iron was chosen. The

* Special Research Associate Professor in Engineering Materials, University of Illinois.

* Research Laboratory, General Electric Company.

results of tests and the composition are given in Table 9.

The samples heated in hydrogen all showed an appreciable loss in ductility, but in no case could the material be classed as brittle.

ence between those samples pushed into the cooling chamber and those cooled with the furnace. These figures check with our observations over a long period of time. The ductility is too great to call the samples brittle and the

TABLE 8.—*Tests on Low-carbon Steel*

Material	Tensile Strength, Lb. per Sq. In.	Proportional Limit, Lb. per Sq. In.	Reduction of Area, Per Cent	Elongation, Per Cent
As received	68,000	41,900	38	59.8
Heated 2 hr. at 950°C. in hydrogen and water-quenched	179,000	69,900	3	5 2
Heated 2 hr. at 950°C. in a closed iron tube in air and water-quenched . . .	188,000	68,900	3	4 5

TABLE 9.—*Tests on Armco Iron*

Composition, Per Cent				
C, 0.03 per cent; Mn, 0.06; P, below 0.02; S, 0.041; Si, trace				
Material	Tensile Strength, Lb. per Sq. In.	Proportional Limit, Lb. per Sq. In.	Reduction of Area, Per Cent	Elongation, Per Cent
As received	41,900	15,700	46 5	78 7
Heated 2 hr. in hydrogen at 950°C. and water-quenched	52,400	38,700	19 0	46 2
Heated 2 hr. at 950°C. in closed iron tube in air and water-quenched	50,900	17,200	28.0	75 0
Heated 2 hr. at 950°C. in hydrogen, water-quenched, drawn 16 hr. at 200°C.	48,700	20,000	28 0	78 6
Heated 2 hr. at 1150°C. in hydrogen and water-quenched	48,900	15,400	16 5	31 2
Heated 2 hr. at 1150°C. in closed iron tube in air and water-quenched	49,400	15,900	27 5	65 6
Heated 2 hr. at 1150°C. in hydrogen, water-quenched and drawn at 200°C. for 16 hr.	47,200	21,700	37 5	78 0

TABLE 10.—*Tests on Copper-brazed Material*

Material	Tensile Strength, Lb. per Sq. In.	Proportional Limit, Lb. per Sq. In.	Reduction of Area, Per Cent	Elongation, Per Cent
Heated 2 hr. in hydrogen at 950°C. sample 1 pushed into cooler and sample 2 cooled with furnace:				
Sample 1	42,700	17,400	49 5	74.7
Sample 2	39,400	15,700	55 5	81 8
Heated 2 hr. in hydrogen at 1100°C. sample 3 pushed into cooler and sample 4 furnace-cooled				
Sample 3	42,400	24,400	51 0	77 3
Sample 4	39,700	19,900	54 5	80 2

In order to check our observations on materials that had been copper brazed, four additional samples were treated (Table 10). The physical properties of all four of these samples are just as good or a little better than the as-received material. There is little differ-

physical properties are too good to infer that they have been damaged by the hydrogen treatment.

Many Charpy impact specimens with both the keyhole and V-notch were also made and treated in hydrogen, and in no case did we have

an impact value below that of the standard sample in the as-received condition, and many of them showed values several times greater.

These findings check those of Dr Uhlig in regard to electrolytic iron. If any rifts were formed, the physical tests as well as microscopic examination failed to reveal them.

N. P. Goss, South Euclid, Ohio—The author has presented very interesting data showing how hydrogen affects the ductility of low-carbon Mn steels and the Hadfield Mn steels. That the H_2 does not embrittle the Hadfield steels is most interesting. Perhaps further experimental work will bring forth the answer. Anyone who reads Uhlig's paper will be impressed by the vast amount of further work it suggests.

In general the embrittlement of some of the low-carbon Mn alloys can be explained along the lines proposed by Zapffe and Sims, and the block structure theory which I have suggested. [See *A.I.M.E. Trans.* (1941) 145, 225, and discussion, 265.]

While line broadening has usually been taken to indicate lattice distortion, my own work strongly suggests that it is associated with smallness of crystallite size.

For example, drastically cold-rolled Mn steels exhibit X-ray patterns quite similar to the one shown in Fig. 6 of the author's paper. The hardness of cold-rolled Hadfield Mn steels closely approaches that of martensite. Surprisingly enough, tempering such steels at fairly high temperatures fails to sharpen the diffraction lines, and the hardness remains about the same. The results of this work will be reported some time in the future.

It would seem that the maximum hardness is associated with a limiting crystallite size, perhaps of the order of 10^{-6} cm. or smaller. Such particles have practically no capacity for further deformation, in that the slip planes are exhausted. When the forces of deformation are applied, they exceed the cleavage strength, with the result that failure or rupture occurs. In the case of alpha iron the (100) planes are the cleavage planes. Slip occurs on the (110) planes and when the forces required to induce further slip become large enough, cleavage occurs on the (100).

G. A. MOORE,* Columbus, Ohio.—Dr. Uhlig has presented a very satisfactory collection of new data on the embrittlement problem, in a manner that is especially timely and significant, in that it points out some of the ways that embrittlement of alloy steels may differ from that of pure iron or plain carbon steel. I can certainly see no reason to dispute his general conclusions. The attempt to relate embrittlement to hydrogen analysis is worthy, but perhaps premature, inasmuch as it will be brought out in the symposium on analysis that the methods, including vacuum extraction as used here, are subject to serious question in respect to absolute accuracy, and inasmuch as this method probably gives a different approximation for various alloy contents, especially where there is a change of phase. The use of analytical figures leads to certain involvements in the explanation of results, hence it is desirable to point out that the conclusions are actually independent of the analysis and these involved explanations.

Mention may be made to two previous technical papers,^{15,16} in which will be found references to the pertinent previous experimenters.

In regard to the question of the lack or reduction of embrittlement effect in the Mn-Fe alloys above 14 per cent and in Hadfield steel, it may be noted that there appears to be no record in the literature of even a single case of embrittlement of any metal having the gamma lattice. There can be little doubt that embrittlement is associated only with quantities of hydrogen over and above the portion that can be held in stable solid solution in the lattice at the existing temperature and pressure, and conversely that the small portion in true solution has no effect on the mechanical properties. In the references listed, this excess is regarded as existing as films of molecular hydrogen lying along imperfections or mosaic rifts within the grain structure and retained under a pressure of the order of thousands of atmospheres under embrittling conditions. An explanation in terms of a strained, distorted, or knotted lattice might be tenable under some circumstances, but, in any case, the pressure

* Battelle Memorial Institute.

¹⁵ G. A. Moore and D. P. Smith: Occlusion and Evolution of Hydrogen by Pure Iron. *Trans. A.I.M.E.* (1939) 135, 255-292.

¹⁶ C. A. Zapffe and G. A. Moore: A Micrographic Study of the Cleavage of Hydrogenized Ferrite. *Trans. A.I.M.E.* (1943) 154, 335-359.

term will appear, either in natural form or disguised as the stress necessary to produce the distorted condition.

As a first approximation, the pressure at a given temperature is:

$$P = ([H]'S)^2$$

where $[H]$ is the concentration of hydrogen in solution and S is the Sieverts' equilibrium solution at one atmosphere and the temperature of the experiment. (See Fig. 7 of ref. 16.) When part of the gas is in rift openings, H is decreased by:

$$[H] = (H_2)_{anal.} - (H_2)_{rift.} = (H_2)_{wt.} - \frac{Pv}{RT}$$

where the assumption of equal partition between the two states is probably close enough for rough calculations. The pressure necessary for embrittlement may be assumed equal to the normal yield strength, or about 4000 to 6000 atmospheres.

It is thus only necessary to note that the Sieverts' solubility in the gamma phase is about twice that in the alpha at 900°C. and that the ratio becomes larger with decreasing temperature until at 300°C. it is about 1×10^{-4} for gamma and immeasurably small for alpha. Thus, while the pressure over the alpha phase can easily run to 10,000 atmospheres and more at low temperature, that over the gamma phase is greatly decreased by the greater solubility and can hardly exceed the order of 1000 atmospheres under the most saturated conditions. Thus embrittlement of the gamma would appear to be impossible with any attainable hydrogen concentration.

The same pressure differential, of course, is basic to the differing diffusion and evolution rates of the two phases. However, if it should subsequently be shown that the slow rate of evolution from the gamma has led to a false analysis for alloys 18 and A, rather than to decreased hydrogen absorption, the basic fact of nonembrittlement of the gamma phase will remain unchallenged and logically explicable in terms of the pressure values.

The same reasoning applies to the case of 18-8 stainless steel. In the epsilon phase, the data on equilibrium solubility appear to be missing. However, it may be reasoned that,

since the dense FCC lattice dissolves more hydrogen than the open BCC lattice, the solubility is associated with the ability of that lattice to accept more free electrons. (Copper, silver, and gold, with the FCC lattice but an additional electron, have essentially zero absorptive capacity for hydrogen.) Since the HCP epsilon lattice can accept even more electrons from the hydrogen, the solubility is likely to be high in this lattice also; hence, the same reasoning will apply as for gamma.

With regard to the reasoning about pure iron and alloy 3, both alpha phase, it is apparent that embrittlement would occur if the hydrogen concentration were high enough and that the low analysis is basically correct. However, the Körber and Ploum experiment does not stand unopposed and the statement that pure iron does not absorb hydrogen is not strictly true in the sense in which it is applied in the paper. The degree of embrittlement of the purer irons is in fact quite sensitive to structure as well as to the amount of the poison-inhibitor elements and of carbon. The absorptive power in this range is in fact autocatalytically increased at high hydrogen pressures and hereditary between successive treatments. The embrittlement of relatively pure iron can become very severe (ref. 16) once it has a chance to get a start. It may therefore be expected that with other alloy samples, slightly less pure or less perfectly annealed, or with other treatments slightly more drastic in forcing hydrogen into the metal, embrittlement of the lower alloys will be encountered and entirely different analytical values may be obtained. The conclusion that alloy 3 cannot be embrittled is probably specific to the conditions used, as contrasted with the same conclusion for alloys 18, 22, and A, where the statement probably remains true for all treatments.

H. H. UHLIG (author's reply).—Although the present study did not extend to effect of formation of "flakes" or internal cracks, Dr. Cramer's point is well taken that on going to large cross sections of Hadfield manganese steel, such defects might be evident. However, there are reasons for believing that whatever the cross section of this particular alloy, neither embrittlement nor internal cracking would occur.

The first reason is based on analyses of hydrogen in specimens heated at 1000°C. in hydrogen and water-quenched. The value obtained is 5.5×10^{-4} wt. per cent as compared with Sievert's solubility value of 5.2×10^{-4} wt. per cent for iron at 1000°C. The close correspondence is evidence that very little of the hydrogen that dissolves at elevated temperatures escapes on quenching to room temperature, and, in fact, the diffusion rate is so low in this gamma-phase alloy that loss of hydrogen at room temperature is only very slight. Hence, the amount of retained hydrogen would be the same regardless of cross section, and any defects expected for large specimens would probably be apparent in small specimens. This is in contrast to the situation for a mild steel for which rapid loss of hydrogen on cooling accounts for very different over-all hydrogen analyses depending on the cross section of the steel.

The second reason centers on the relatively high solubility of hydrogen in austenitic steels and lack of $\gamma \rightarrow \alpha$ transformation on cooling. These facts combine to account for absence of the same high internal pressures of hydrogen as are generated on quenching low-alloy steels. Embrittlement does not take place, therefore, and "flaking" likewise should be absent. As an example of an austenitic steel, x8-8 is reported to be free of "flake" formation.¹⁷ Similarly, one would expect an austenitic steel of Hadfield composition of any cross section to be free of internal cracks caused specifically by hydrogen.

Mr. Kelley's data on Armco iron show that as the cross section is increased to $\frac{1}{2}$ in. the effect of hydrogen on ductility becomes noticeable. His mild-steel specimens, whether water-quenched from hydrogen or from air, are equally brittle, in agreement with results of the present investigation. Microscopic examination of our specimens proved that the embrittlement is accompanied by appearance of martensite.

One would not expect embrittlement or loss of ductility in a relatively pure iron of small cross section (approximately 0.160 in. or less) no matter how rapid the quench from high temperatures in hydrogen. The reason, as gas

analyses show, is that hydrogen escapes during cooling, allowing a remainder of gas insufficient to have an appreciable effect on the mechanical properties.

It will be interesting to have Dr. Goss' account of his reasons for believing that the X-ray pattern of Fig. 6 is associated with crystallite size rather than lattice distortion.

Dr. Moore's caution with regard to vacuum-extraction results for hydrogen in steels to some extent is justified. Work reported by Bennek and Klotzbach¹⁸ pointed out that the vacuum-extraction method gives low results as compared with a low-temperature fusion method employing tin. Our own work on gas analyses so far indicates results in the same direction. For that reason, we labelled our analyses "preliminary." We believe, however, that analyses of this kind, giving at least the order of magnitude of hydrogen involved, is far preferable to omitting analyses altogether. The vacuum-extraction results have given us added information about the effects of hydrogen in iron and in alloys with manganese, the conclusions from which, we believe, will be altered in only a minor way by future accepted techniques of analysis, whatever these may be.

Although Dr. Moore's argument regarding lack of embrittlement of gamma-phase alloys applies to hydrogen retained on quenching, a word of caution is necessary in the interpretation of his statement that no record exists for the hydrogen embrittlement of these alloys. Many metals of the face-centered cubic lattice, such as nickel, can be seriously embrittled by cathodic polarization. By this treatment, hydrogen in sufficient quantity is introduced into the lattice to cause the same type of embrittlement as occurs through quenching some of the carbon steels from high temperatures in hydrogen.

Our work on absorption of cathodic hydrogen by pure iron as affected by catalyst poisons confirms that of Körber and Ploum. It points to impurities adsorbed on or contained in the surface as the factors determining whether cathodic hydrogen is absorbed within the lattice or not. None of our results so far has shown any effect of so-called "structure" of pure iron.

¹⁷ W. Eilender, Y. Chih Chiu, and F. Willems: *Archiv Eisenhüttenwesen* (1940) 13, 309.

¹⁸ H. Bennek and G. Klotzbach: *Stahl und Eisen* (1941) 61, 597-606.

substantially constant load, the "lower yield point," and the amount of extension at this load the "yield-point elongation." With the initial sharp drop in load, local areas of deformed metal appear and grow over the surface until the entire specimen is deformed an amount equal to the strain in the first such localized region. When the entire specimen has been thus deformed, the load begins to rise again and proceeds along a normal load-extension curve. During the yield-point elongation the deformation is heterogeneous, deformed metal existing adjacent to undeformed metal, with the progress of deformation at any instant localized at the boundary between the deformed and undeformed metal. If the test is stopped before the entire specimen is strained "through the yield point," it is found that a portion of the specimen is reduced in thickness while the remainder still retains its initial dimensions. The phenomenon thus gives rise to irregularities in the surface, which were first observed by Piobert¹ and later by Lüders² and first studied in detail by Hartmann.³ The formations of these strain markings has been called the "Piobert effect," and the markings themselves have been called "Lüders' lines," "Hartmann lines," "stretcher strains," "worms" and other names.

In ordinary precipitation-hardening or "quench-aging" of the duralumin type, an alloy that exhibits decreasing solubility with decreasing temperature is heated to a sufficiently high temperature to dissolve some or all of the solute constituent and then cooled rapidly. It is then found that the physical, chemical and mechanical properties change with time. This change in properties with time has been termed "aging" or precipitation-hardening. In strain-aging, the tendency toward aging is produced not by solution annealing followed by quenching, but simply by straining the metal. Thereafter, the properties

of the metal change with time in a manner somewhat similar to that encountered in normal aging.

The yield-point effect and strain-aging have both been observed in other alloys, but not to the degree to which they are encountered in low-carbon steels. Both these phenomena have been the objects of numerous investigations and the literature dealing with them is extremely voluminous. Nevertheless, many questions still remain to be answered. While numerous hypotheses of the *mechanism* of the yield point have been proposed, these, for the most part, must still be classed as surmises which are yet to be substantiated by direct experimental evidence. Similarly, the mechanism by which strain-aging occurs remains to be explained. Presumably, this is a precipitation phenomenon in which a precipitation-hardening process is initiated by cold deformation, but whether by solution and reprecipitation or by a change in solid solubility resulting from plastic deformation, or by some other means, has never been demonstrated clearly.

With regard to the question of whether or not pure iron exhibits a yield point and strain-aging and which impurities commonly present in steels may be responsible for the two effects, the evidence is confused. In general it appears that the yield point is still observed in the purest iron yet produced while vacuum-melted electrolytic iron of a lesser degree of purity has a less marked yield point. Considerable evidence has accumulated to show that carbon, nitrogen and oxygen, individually or collectively, may be responsible for strain-aging. For the most part, however, this evidence is indirect and open to more than one interpretation. In the present work evidence is presented to support the view that pure iron should not exhibit either a yield point or strain-aging and, further, that carbon and nitrogen are primarily responsible for these two attributes of commercial steels, while oxygen is relatively unimportant.

¹ A review of the literature and a bibliography are at the end of the paper.

Having accomplished the elimination of aging and the yield point by purification, without the introduction of alloying elements, it became possible to ascertain which

for the wet hydrogen treatment itself increases the oxygen content of steel, and annealing under oxidizing conditions at the same temperature used in the wet hydrogen

TABLE 1.—*Ladle Analyses of Steels Used for Experiments with Wet Hydrogen Annealing*

Steel No.	Type	Sheet Thickness, In.	Analysis, Per Cent				
			C	Mn	P	S	Si
T.....	Rimmed	0 036	0.05	0.30	0 010	0.024	0 003
T-1.....	Killed*	0 036	0 05	0 30	0 007	0 022	0 005
T-2.....	Killed*	0.036	0 05	0.33	0.007	0 020	0.007
T-3.....	Rimmed	0 0365	0 08	0.38	0.008	0 020	0 007
T-4.....	Rimmed	0 0335	0 08	0 39	0 010	0.014	0 006
S-9.....	Killed*	0 033	0 08	0.33	0.006	0 032	0.002
Th-6.....	Rimmed	0.111	0 06	0.33	0.008	0 027	0 004
Th-1.....	Rimmed	0 0382	0 06	0.36	0 010	0.022	
C-3.....	Killed	0 035-0.036	0.10	0 53	0 010	0.029	0 005
C-2.....	Killed	0 035-0.037	0.23	0 48	0.010	0.025	0 005
C-1.....	Killed	0 036-0.037	0 36	0 67	0 010	0.030	0 13
Bessemer.....	Capped	0.042	0 07	0 40	0.088	0 028	0 028
S-2.....	Rimmed	0 035	0.05	0 37	0.01	0.015	0 004

* Aluminum-killed.

elements are responsible for these properties, by introducing different elements, one at a time, and observing which ones caused the return of aging and the yield point. This was done very carefully to preclude the possibility of introducing more than one element at a time. It was not necessary to study many of the elements, particularly the common metallic alloying elements, which have been found either to be without effect on yield point and aging behavior or to cause their disappearance. Phosphorus and sulphur are unaffected by the low-temperature wet hydrogen treatment and so, along with the metallic alloying elements, need not be considered as causes of these effects.

It has been established that the re-introduction of carbon and nitrogen, singly or together, causes the yield point and strain-aging to reappear. Very short times of carburizing and nitriding are necessary to accomplish this. The amounts of carbon and nitrogen necessary to cause aging and the yield point are less than the amounts that can be detected by chemical analysis, probably less than 0.001 per cent by weight. Oxygen in small amounts seems to have no effect on the yield point and strain-aging,

treatment caused no return of these properties. On the other hand, oxidizing annealing at 885° and 940°C., while causing too much grain coarsening to permit conclusions concerning its effect on the yield point, certainly causes a partial return of strain-aging capacity. It is concluded that in normal rimmed or killed steels of the grades used in deep-drawing applications, the yield point and strain-aging capacity are caused by the presence of carbon and nitrogen, both of which can cause these effects when present in amounts less than are always present in these steels.

MATERIALS AND METHODS

For the most part, the experiments to be described were conducted using low-carbon basic open-hearth sheets of deep-drawing quality. The major portion of the work was carried out on the first five steels of which analyses are shown in Table 1.

Changes in mechanical properties produced by annealing in wet hydrogen were determined by means of Rockwell hardness tests and tensile tests. All tensile tests were made with standard A.S.T.M. sheet specimens (2-in. gauge length) using Templin sheet grips. A Kenyon-Burns-

Young wedge extensometer was used in conjunction with an autographic recorder. All tensile tests, unless otherwise noted, were conducted with a speed of head movement of approximately 0.25 in. per minute. This was the highest speed at which it was possible to obtain accurate load-extension curves with the autographic equipment used.

The *lower yield-point* was calculated using the mean load prevailing during the yield-point elongation as estimated from the autographic curve.

The *yield-point elongation* was taken as the total elongation to the end of the yield point as recorded on the autographic curve.

The *tensile strength* was calculated from the maximum load observed on the indicating dial of the tensile machine.

The *uniform elongation* (i.e., elongation to the maximum load) was obtained by noting the point at which the indicated load began to decrease and simultaneously lifting the pin of the recorder momentarily. The reported values are not thought to be more accurate than plus or minus 1.0 per cent elongation in 2 inches.

The *total* or *bench elongation* values, which are reported simply as "elongation in 2 in." were obtained by fitting the fractured specimens back together and measuring the distance between two punch marks which originally had been 2 in. apart.

Throughout the discussion the term *yield strength* is used without defining any limiting permanent set. When so used, what is meant is the stress at which the autographic load-extension curve departs from a straight line. It has not been called the proportional limit because the sensitivity of the strain-measuring device used hardly justifies the use of this latter term.

As a measure of strain-aging, it was decided to use the percentage increase in yield strength caused by aging after straining. A tensile specimen was first strained 8 or 10 per cent and then unloaded and removed from the machine. The specimen

was aged for 3 hr. at 200°C. and reloaded in the tensile machine to fracture. The two autographic load-extension curves were superimposed to observe the amount by which the curve for the aged condition lay above the curve for the unaged. The time and temperature of aging following initial straining were kept constant at 3 hr. and 200°C. throughout the investigation. This time and temperature were chosen because the results of Davenport and Bain¹⁴ and Kenyon and Burns¹⁷ indicated that at this temperature a very marked increase in hardness is obtained, while the necessary time to produce the maximum effect is not unduly long. In addition, the curve of hardness against time at this temperature has a sufficiently flat maximum so that considerable variation from the specified time might be used without appreciably influencing the result. Most of the strain-aging tests were made using 10 per cent strain. This amount of strain was chosen as the least amount that would ensure uniform strain of the specimen; i.e., completely through the yield point.

The wet-hydrogen annealing furnace consisted of a 48-in. length of 2-in. i.d. steel tubing wound with Nichrome wire and surrounded by approximately 3 in. of Sil-O-Cel insulating powder over 30 in. of its length. Approximately 12 in. of the tube at the top was not heated, and this provided a cold zone into which the specimens could be raised at any time. The sheet tensile specimens to be treated were suspended from wires, which projected through a rubber stopper at the top of the furnace. These wires were used to raise and lower the specimens in the furnace and, by measurement of the amount of wire projecting, the specimens could be accurately located in the furnace so that the center of the reduced section was on a level with the end of the thermocouple protecting tube. The welded steel thermocouple-protecting tube, which also was inserted through the rubber stopper, was adjusted so that the end of the

tube was at the mid-point of the 3-in. uniform-temperature zone of the furnace. The furnace was arranged so that during heating and cooling dry tank hydrogen could be circulated, entering directly from the tank supply. When the furnace had reached the desired temperature, the dry hydrogen was turned off and hydrogen from the tank supply then flowed through a fritted glass dispersion tube, through water in a saturator, through a tube (heated to prevent condensation) to the furnace, through the furnace, through a second heated line to a condenser and finally to a flow meter. The wet hydrogen was allowed to flow through the system for about 15 min. before the specimens were lowered into the hot zone. Usually all of the specimens would be lowered into the hot zone at one time and then pulled up individually at the end of the desired time of treatment. The vapor pressure of water in the wet hydrogen was controlled by controlling the temperature of the saturator

CHANGES IN PROPERTIES AND COMPOSITION PRODUCED BY ANNEALING IN WET HYDROGEN

Annealing low-carbon sheets in wet hydrogen has been found to eliminate completely the yield-point elongation that is typical of these steels, to lower the yield-point stress to values less than have been reported previously even for the purest iron (fine-grained) and to eliminate all traces of both strain-aging and quench-aging. The principal changes in composition that have been observed are a marked lowering of the carbon and nitrogen contents while the oxygen content (as determined by vacuum-fusion methods) is unaffected or slightly increased. The only observable change in microstructure accompanying these changes is a disappearance of visible carbides and a decrease in the sharpness of the ferrite grain boundaries as developed by etching.

In the course of a great many treatments involving a large number of different heats

of steel, only two exceptions to these statements have been found. In attempting to treat a low-carbon bessemer steel by this method, no difficulty was encountered in eliminating strain-aging, but it was not found possible to eliminate completely the last traces of the yield point, even for times of annealing up to five times that required for open-hearth steel in the same sheet thickness. Annealing in wet hydrogen does, however, markedly lower the yield-point stress and the yield-point elongation. The other exception that was found was low-metalloid vitreous enameling sheet. No difficulty was encountered in eliminating strain-aging, but the original small amount of yield-point elongation was not substantially affected by the treatment.

The manner in which the yield-point elongation is eliminated by annealing in wet hydrogen is illustrated by the set of load-extension curves reproduced in Fig. 1. Curve 4 is typical of the results obtained by complete annealing in wet hydrogen. In the fully treated specimen, no drop in load or yield-point elongation occurs and the yield strength has been reduced from approximately 33,000 to 14,000 lb. per sq. in. The load-extension curve now is similar to the nonferrous materials that have a "normal" stress-strain curve. This elimination of the yield-point elongation means that the material no longer is capable of forming Lüders lines or of "fluting" when bent. A similar disappearance of the yield-point elongation occurs if the ferrite grain size is gradually increased in a series of specimens, as Edwards and Pfeil⁵⁷ and Andrew and Lee⁵⁸ have shown, but to eliminate it by this method requires the production of a very large grain size (six to eight grains per square millimeter in a sheet $\frac{1}{8}$ in. thick) whereas a specimen such as No. 4 in Fig. 1 will have a grain size of approximately 1000 grains per sq. mm. (A.S.T.M. No. 7). It is common practice to eliminate the yield-point elongation in low-carbon steels by temper rolling or

roller leveling. For rimmed steels, this elimination is only temporary, since these steels strain-age. While "nonaging" steels are being produced, they are necessarily killed steels and hence more expensive.

per inch. The specimens were carefully aligned using Robertson shackles in conjunction with Templin sheet grips in order that the true yield-point behavior might not be obscured by nonuniform

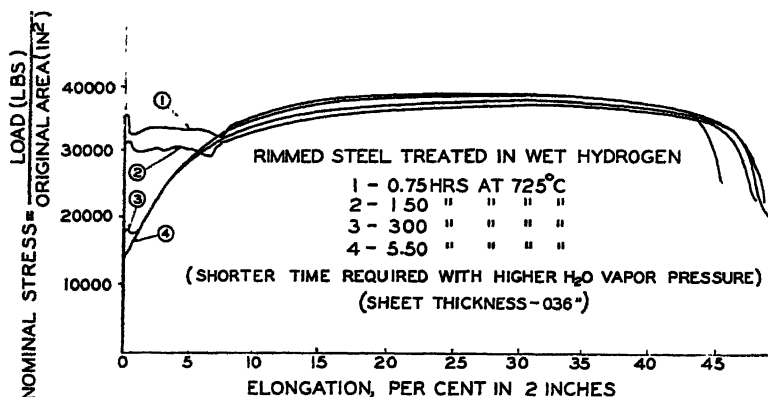


FIG. 1.—EFFECT OF WET HYDROGEN TREATMENT ON TENSILE PROPERTIES OF SHEET STEEL.

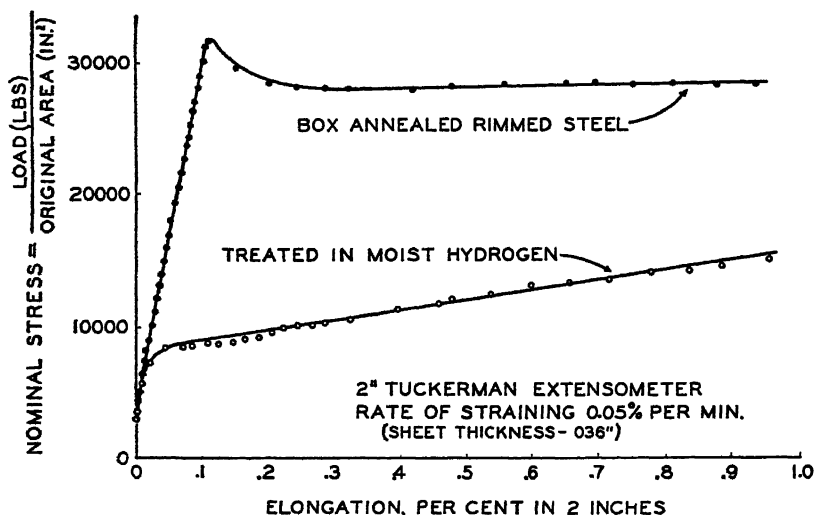


FIG. 2.—TYPICAL HIGH-SENSITIVITY STRESS-STRAIN CURVES FOR BOX-ANNEALED AND WET-HYDROGEN-TREATED SHEET STEEL.

In order to examine the yield-point behavior more closely, load-extension curves for a wet-hydrogen-treated specimen and a box-annealed specimen were made using Tuckerman optical strain gauges and a very slow rate of straining. The strain gauges have a sensitivity of 2×10^{-6} in.

loading. The curves obtained are reproduced in Fig. 2. The box-annealed specimen shows a drop at the yield point of about 3500 lb. per sq. in. and a yield-point elongation of 3.5 per cent. The wet-hydrogen-treated specimen has no drop in load on yielding and no flat portion to the curve,

although the slope of the curve up to 0.1 per cent extension is less than that above 0.1 per cent.

The effect of increasing time of annealing in wet hydrogen on both strain-aging and

Table 2 and Fig. 4, all the strain-aging measurements were made without applying any correction for relaxation. It was found without exception that the time of hydrogen treatment to remove strain-aging is

TABLE 2.—*Effect of Time of Annealing in Wet Hydrogen at 710°C.*

Steel T-3 (Rimmed). Partial Pressure H₂O, 216–218 mm. Hg. (29.5 volume per cent); 10 per cent strain; aged 3 hours at 200°C.

Annealing Time, Hr.	Hardness, Rockwell B	Lower Yield Point, Lb. per Sq. In.	Yield-point Elongation, Per Cent in 2 In.	Tensile Strength, ^a Lb. per Sq. In.	Uniform Elongation, ^a Per Cent in 2 In.	Bench Elongation, ^a Per Cent in 2 In.	Strain Aging, Per Cent
1	56	38,000	7.5	52,500			29.6
1.2	56	37,500	9.0	50,500	14	24.0	32.5
1.4	49	35,000	8.6	44,500	19	31.0	20.6
1.6	46	34,500	8.5	42,500	26	37.0	17.5
1.8	45	34,000	8.0	41,500	29	42.5	8.7
2.0	43	34,000	7.0	41,000	32	44.0	1.5
2.2	42	33,000	6.5	41,500	33	47.0	0.0
2.4	43	33,000	6.0	41,500	32	45.0	0.0
2.6	39	22,000	1.5	41,000	32	45.0	0.0
2.8	35	17,000	0.5	41,000	32	47.5	0.0
2.8	31	14,000	0.3	40,000	32	47.5	0.0
3.0	32	14,500	0.0	41,000	31	48.0	0.0
3.2	32	15,500	0.3	41,000	29	46.0	
3.4	32	14,500	0.0	39,000	32	46.5	
3.6	32	15,000	0.0	41,000	29	44.5	

^a As strain-aged.

the yield point is illustrated in the load-extension curves of Fig. 3. More data are given in Table 2, and summarized in Fig. 4.

In addition to numerous tests for strain-aging in which specimens were aged at 200°C., a number of fully treated specimens were strained 10 per cent in tension and aged at 25°C. for varying times up to 139 days (3332 hr.). None of these specimens showed any evidence of strain-aging or return of the yield point.

To obtain a correction to take into account the amount of relaxation of yield strength during the aging treatment, a number of specimens were treated with wet hydrogen for 5 hr., pulled, and aged in the same manner; then the amount of relaxation (expressed as decrease of yield strength after aging treatment) was measured. The total strain-aging (corrected for relaxation) seems to be independent of the amount of plastic deformation as long as the plastic deformation is uniform (see Table 3).

In the experiments summarized in

considerably shorter than that necessary to remove yield-point elongation. This is at once understandable if relaxation is taken

TABLE 3.—*Effect of Relaxation on the Apparent Amount of Strain-aging^a*

Amount of Straining, Per Cent in 2 In.	Amount of Aging, ^b Lb. per Sq. In.	Relaxation, ^c Lb. per Sq. In.	Total Aging Corrected for Relaxation, Lb. per Sq. In.
1	1,720		
5.1	5,830		
10	8,840	1,390	10,230
15	7,910	2,240	10,150
20	7,330	2,880	10,210
25	7,080	3,160	10,240

^a The steel used was T-2, killed; originally full hard temper.

^b The aging treatments were all 3 hr. at 200°C. The amount of aging was determined on specimens vacuum annealed 5 hr. at 700°C.

^c The amount of relaxation was determined on specimens treated with wet hydrogen 5 hr. at 700°C.

into consideration. Specimens that have been treated with hydrogen to the removal of strain-aging (without applying a correction for relaxation) really show an amount of strain-aging corresponding to the amount of relaxation. Thus, it is

reasonable to suggest that the times required to eliminate strain-aging and to eliminate the yield point are probably the same.

with time at room temperature as a measure of aging in sheets treated in hydrogen containing large amounts of water vapor. The specimens used were suspended in a

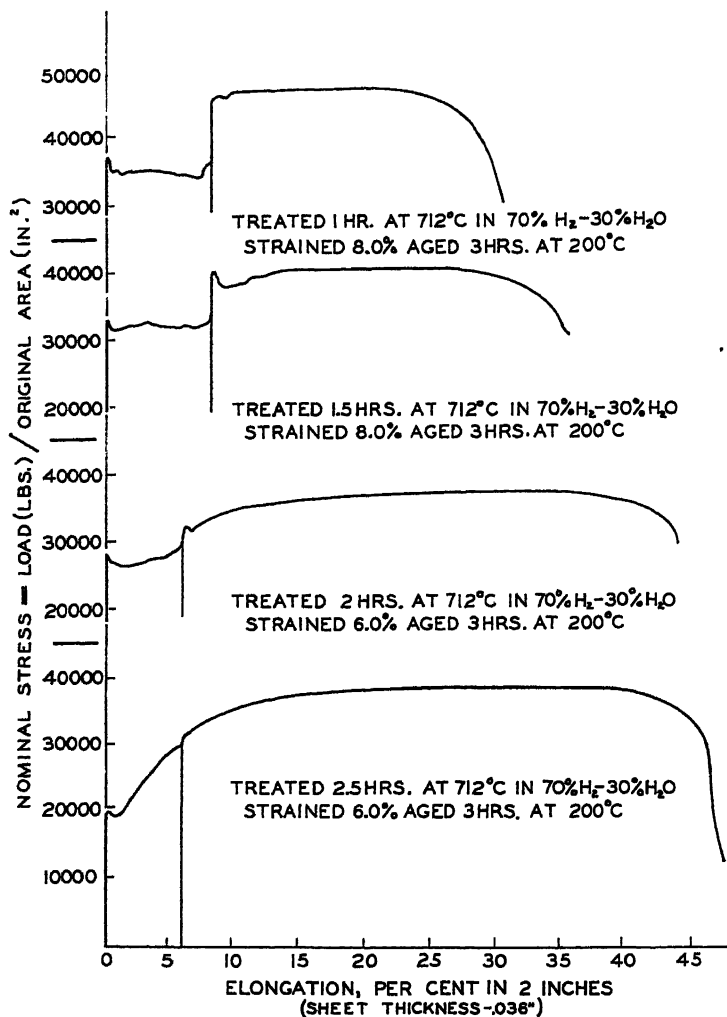


FIG. 3.—EFFECT OF TIME OF WET HYDROGEN TREATMENT ON TENSILE PROPERTIES OF SHEET STEEL, INCLUDING STRAIN-AGING.

Elimination of Quench-aging

Steels decarburized in fairly dry hydrogen have been shown to be free from aging after quenching.⁷⁶ Quench-aging experiments were carried out using change in hardness

silica tube and heated to 700° or 720°C . for $\frac{1}{2}$ hr. and then quenched into ice water directly from the furnace. The top end of the silica tube was closed with a rubber stopper provided with a gas outlet. The lower end of the silica tube was immersed 2

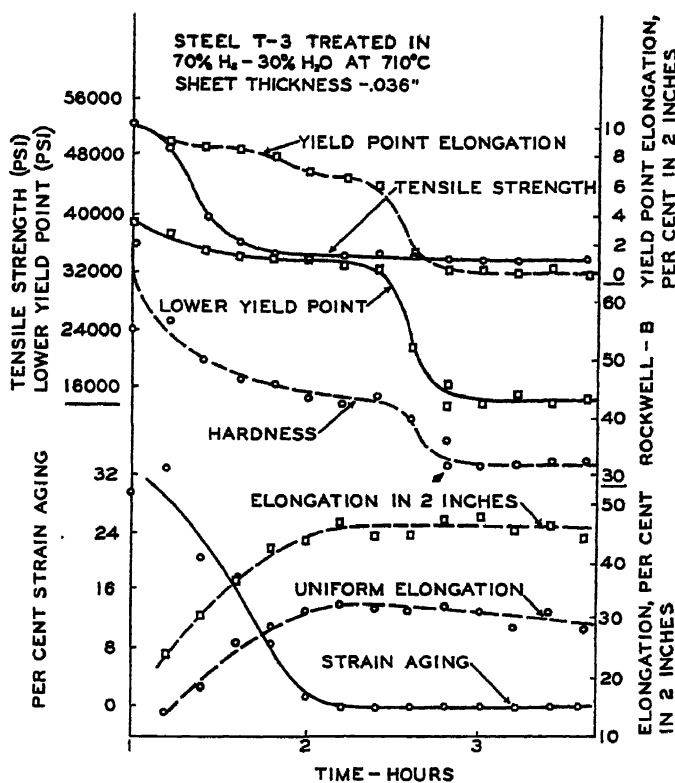


FIG. 4—EFFECT OF TIME OF WET HYDROGEN TREATMENT ON HARDNESS, TENSILE PROPERTIES AND STRAIN-AGING.

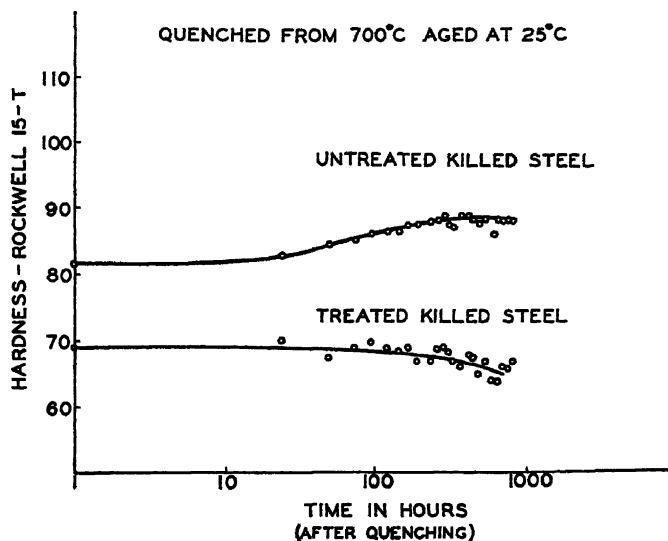


FIG. 5.—QUENCH-AGING IN WET-HYDROGEN-TREATED AND IN BOX-ANNEALED KILLED SHEET STEEL.

or 3 in. in the ice water, making a gas-tight system. During heating, tank hydrogen was circulated through the silica tube to prevent oxidation of the specimen. The

sheet were made using the T-15 scale of the superficial Rockwell, and on the 0.111-in. sheet using the B scale of the standard Rockwell. The results of these

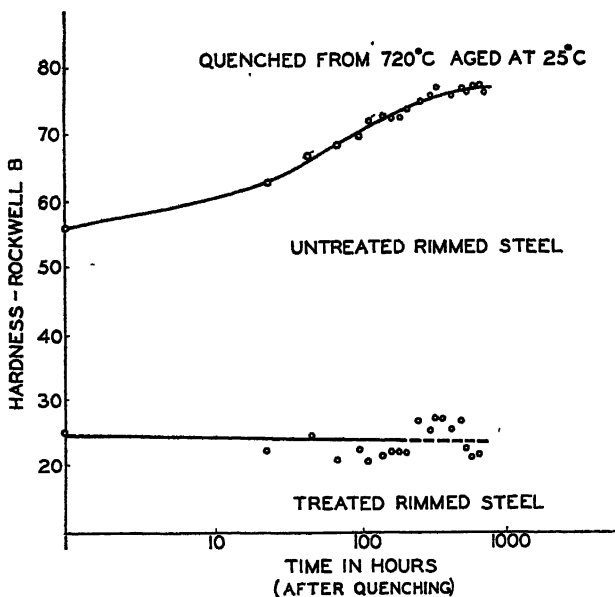


FIG. 6.—QUENCH-AGING IN WET-HYDROGEN-TREATED AND IN BOX-ANNEALED RIMMED SHEET STEEL.

first hardness readings were taken about one hour after quenching, and the specimens were then put in a constant-temperature room at 25°C., and taken out only long enough to make the hardness measurements for the remainder of the time of aging.

Two different steels were used. The first of these was an aluminum-killed 0.033-in. thick sheet, and the second was a 0.111-in. thick rimmed steel sheet. Analyses of the steels before treatment are given in Table 1, where they are listed as S-9 and Th-6. The untreated specimens were cut from the full-hard sheets as received, and the treated specimens were cut from 14 by 16-in. sheets that had been treated in wet hydrogen in a laboratory sheet-annealing furnace.

The 0.033-in. sheet was treated for 5 hr. and the 0.111-in. sheet was treated for 21 hr. Hardness readings on the 0.033-in.

aging experiments are shown in Figs. 5 and 6. While there is some scatter in the results of the hardness tests, particularly in the 0.033-in. material, which was somewhat bent as a result of quenching, there is clearly no increase in hardness on aging after quenching the wet-hydrogen-treated steels.

Changes in Composition Resulting from Annealing in Wet Hydrogen

In view of the fact that a review of the literature concerning the hydrogen purification of iron indicated that, at the temperature used, the wet hydrogen treatment might be expected to affect principally the carbon, nitrogen and oxygen contents of the steels used, no very careful check of changes in the other common impurities was made. The following analyses of the T steel before and after annealing in wet

hydrogen for 3 hr. at 725°C. also tend to support this view:

	Mn	P	S	Si
Steel T not treated...	0.30	0.010	0.024	0.003
Steel T hydrogen-treated to eliminate aging and the yield point.....	0.31	0.010	0.026	0.003

In view of the fact that wet hydrogen annealing has been used to introduce oxygen into iron, it is hardly likely that the hydrogen treatment as now carried out would reduce the oxygen content of the metal. As Krings and Kempkens⁷⁸ have

saturation limit, at which point FeO will begin to form on the surface. Since the speed with which the yield point and aging are eliminated increases with increasing water content of the gas mixture, it does not appear likely that these results are attained by the removal of oxygen from the steel. That the oxygen content is not reduced, but may even increase slightly, is evident from the results of vacuum-fusion analyses made on treated and untreated sheets and shown in Table 4.

Despite some scatter in the results, oxygen appears to increase rather than decrease as a result of the hydrogen treatment; the nitrogen content for the rimmed steel decreases as a result of the treatment,

TABLE 4.—Analyses of Treated and Untreated Sheets
PER CENT

Steel	Type	Condition	Mn	P	Si	N ^a	H ^b	O ^b
S-1	Rimmed	Treated	0.35	0.007	0.001	0.0006	0.00024	0.0235
		Not treated	0.37	0.008	0.002	0.0033	0.00026	0.0185
S-9	Killed	Treated	0.33	0.011	0.003	0.0039	0.00018	0.0113
		Not treated	0.35	0.008	0.005	0.0046	0.00026	0.0102

^a Wet method.

^b Vacuum fusion.

TABLE 5.—Effect of Time of Treatment on Properties and Analysis
Steel Th-6. Treated at 720°C. with 30 per cent water vapor. Sheet thickness, 0.111 inch.

Time of Treatment, Hr.	Rockwell B	Lower Yield Point, Lb. per Sq. In.	Yield-point Elongation, Per Cent in 2 In.	Tensile Strength, Lb. per Sq. In.	Uniform Elongation, Per Cent in 2 In.	Bench Elongation, Per Cent in 2 In.	Strain-aging, Per Cent	C, Per Cent	N, Per Cent
0 ^a	42	30,400	5.6	47,500	22.7	36	25.0	0.06	0.0036
8	33	29,700	6.2	40,300	27.5	44.5	15.0	0.0035	0.0012
9	33	29,000	6.3	39,600	25.5	47	14.5	0.0040	0.0017
10	32	25,600	4.0	38,800	31.2	49	5.5	0.0034	0.0012
11	30	21,300	1.5	38,400		50	0.0	0.0027	0.0014
12	30	17,900	0.6	38,800	31.6	51	0.0	0.0034	0.0014
13	26	15,200	0.2	38,800	30.1	50	0.0	0.0029	0.0014
13½	23	14,400	0.3	38,400	31.0	49	0.0	0.0038	0.0014
15	20	13,700	0.5	38,400	31.0	49.5	0.0	0.0031	0.0014

^a Vacuum annealed, 14½ hr., 730°C.

shown, at any given temperature and partial pressure of water there will be an equilibrium amount of oxygen in solid solution in alpha iron, the amount of oxygen in solution increasing as the partial pressure of water increases up to the

while that of the aluminum-killed steel is substantially unaffected. In every case the hydrogen content of these sheets both before and after treatment is negligibly small.

In an effort to fix more precise limits for the carbon and/or nitrogen content neces-

sary if a steel is to exhibit a yield point and strain-aging, a series of specimens was prepared in which all conditions were represented, varying from no hydrogen treatment through sufficient hydrogen treatment to eliminate completely both

properties from normal yield point and high percentage of strain-aging to no strain-aging and no yield point. *The nitrogen and carbon have been removed to the limit of chemical analysis before any appreciable reduction occurs in the yield point or in the*

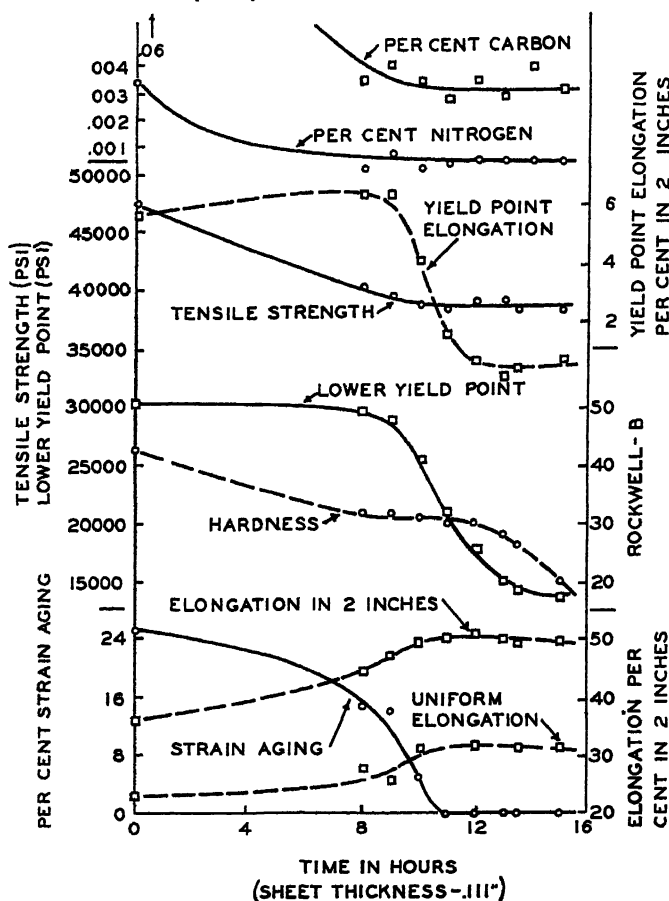


FIG. 7.—EFFECT OF TIME OF WET HYDROGEN TREATMENT ON CARBON AND NITROGEN ANALYSIS, TENSILE PROPERTIES AND STRAIN-AGING IN HEAVY-GAUGE SHEET STEEL (0.111-INCH THICK RIMMED STEEL).

strain-aging and yield point. Table 5 shows the mechanical properties together with the carbon and nitrogen analyses of this series of specimens. These results are also plotted in Fig. 7. All of these specimens were cut from a single sheet of the 0.111-in. thick, full-hard temper. rimmed steel. The specimens chosen have a full range of

degree of strain-aging. As far as the analyses shown are concerned, these two elements remain unchanged while a marked change is occurring in the yield point and strain-aging behavior.

Carbon analyses were carried out under the direction of Dr. J. B. Austin, in a special carbon-determination train in the United

States Steel Corporation Research Laboratory, Kearny, N. J. The apparatus used and the method of analysis were essentially the same as those described recently by Wooten and Guldner.⁷⁹ Nitrogen analyses were carried out in the chemical laboratory of the Homestead Steel Works of the Carnegie-Illinois Steel Corporation. The acid digestion and distillation method described in "Sampling and Analysis of Carbon Steels"⁸⁰ was used.

On the basis of these analyses, two possibilities suggest themselves. First, that the radical change in the yield point and strain-aging behavior is not a result of the loss of carbon or nitrogen during the hydrogen treatment, but results from some other change in composition which was not detected. Second, that despite the fact that the analyses reported here were obtained by means of high-precision analytical methods, the changes in carbon and nitrogen responsible for the marked change in mechanical and aging properties are so small as to escape detection. The latter possibility is believed to represent the true state of affairs. This belief is based on certain experiments to be described later, in which hydrogen-treated specimens were subjected to carburizing and nitriding treatments. In these experiments, it was found that either of these treatments caused a return of the yield point and strain-aging.

Changes in Microstructure Accompanying Hydrogen Treatment

In most of the hydrogen treatments carried out in the course of this investigation, the starting material was in the full-hard condition (cold-rolled 45 to 55 per cent). For this reason, recrystallization occurred during the treatment and obscured any other changes that might be taking place. However, some treatments were carried out with fully annealed sheets as the starting material. In addition, several series of specimens exhibiting

various degrees of strain-aging and the yield point were examined.

The first effect of the hydrogen treatment was to cause a complete disappearance of all visible carbides. This disappearance, however, took place before there was any marked reduction in the yield point or strain-aging. In etching for carbides, the nitrobenzol-nitric acid reagent described by Pilling⁸¹ was found to be a more satisfactory reagent than nital, picral or alkaline sodium picrate. In addition to outlining the carbides, this reagent imparted a pale but distinct color to the carbide particles, so that they could readily be distinguished. During disappearance of the yield point and strain-aging, the only apparent change was a decrease in the contrast between the grain boundaries and the grains themselves when nital (4 per cent) was used as an etchant. For example,

TABLE 6.—*Effect of Temperature of Wet Hydrogen Treatment on Grain Size*

Temperature of Hydrogen Treatment, Deg. C.	A.S.T.M. Grain Size No.	Approximate Grains per Sq. Mm.
710	7 to 8	1,526
750	7	1,024
800	5 to 6	384
850	4 to 5 and 1	96 and 16

if specimens treated for varying times were mounted and etched together, the specimens treated for the least time, and therefore still showing a yield point and strain-aging, would exhibit sharply defined grain boundaries, whereas the specimens that had been fully treated did not. In the latter case, considerably longer times of etching were required to develop the grain outlines. In examining the partially and fully treated specimens at high magnification (2000X), the difference in "sharpness" of the grain boundaries did not appear to result from the presence or absence of a second phase. No evidence for a grain-boundary network of a second phase was found.

The ferrite grain size resulting from annealing in wet hydrogen was found to be substantially the same as that obtained for the same materials by box annealing, using mill practice. This was true whether the starting material was full-hard cold-reduced sheets or sheets that had been box-annealed at the mill. Table 6 lists the grain sizes obtained at several temperatures where the time at each temperature was the minimum required for complete elimination of the yield point and strain-aging.

For most of the forming operations in which low-carbon sheets are used, the maximum grain size that may be tolerated without undue surface roughness is approximately A.S.T.M. No. 6. Since the optimum temperature range for the hydrogen treatment lies below $750^{\circ}\text{C}.$, this requirement is readily met.

Summary

The following changes are observed when low-carbon steel of the grades normally used for deep drawing is annealed in wet hydrogen:

1. The yield point that has been considered typical of steels containing large amounts of ferrite is completely eliminated and the stress for the beginning of plastic deformation is greatly reduced.

2. Both strain-aging and quench-aging are completely eliminated.

3. The carbon and nitrogen contents of rimmed steels so treated are markedly lowered. Carbon is believed to be less than 0.003 per cent and nitrogen less than 0.001 per cent after treatment.

4. With aluminum-killed steels, there is some evidence to indicate that the nitrogen content is unaffected by the treatment. The carbon content decreases as in rimmed steels.

5. Upon completion of the treatment, all traces of cementite have disappeared. The treatment appears to affect the etching characteristics of the steels, particularly

when nital is used as an etchant. As the treatment proceeds, it becomes more and more difficult to develop distinct ferrite grain boundaries.

FACTORS INFLUENCING THE EFFECTIVENESS OF THE WET HYDROGEN TREATMENT

After it had been demonstrated that annealing low-carbon sheets in wet hydrogen completely eliminated aging and the yield point, a number of experiments were undertaken to determine the most effective manner of carrying out the treatment. The factors that were examined with respect to their effect on the time required for treatment were: water content of the hydrogen, temperature of treatment, thickness of sheet, composition of sheet (principally carbon content), the initial condition of the sheet (cold-worked or annealed) and the flow rate of the gas mixture.

Influence of Moisture Content of Gas Mixture

The way in which various properties change as the time of treatment increases is illustrated in Figs. 8 and 9, which are typical. Fig. 8 is for $710^{\circ}\text{C}.$ with a partial pressure of water vapor of 216 mm. of mercury (30 per cent by volume); Fig. 9 is for the same temperature, but with a lower water-vapor content (10 per cent by volume). The curves for the various properties as a function of time are very similar in shape, but have been shifted to longer times at the lower water content. It should be noted that the values shown for tensile strength and bench elongation represent the material in the strain-aged condition. The tensile testing procedure was as follows: The specimen was strained to 8 per cent extension, taken out of the machine and aged 3 hr. at $200^{\circ}\text{C}.$, then tested to failure.

As the results in Table 7 show, the effect of increasing the water-vapor content of the gas mixture is most marked for the first few per cent added; at higher percentages slight variations in water

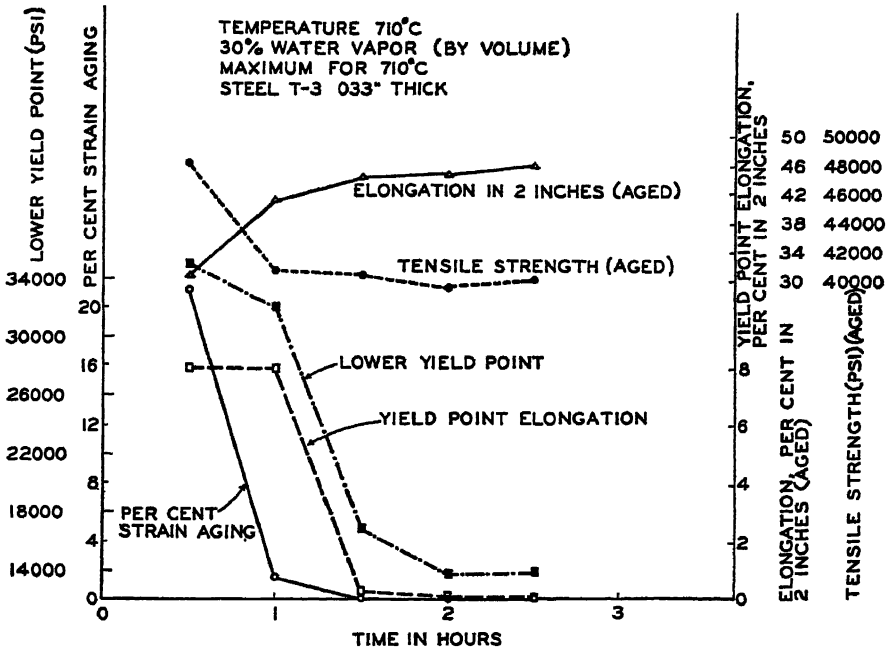


FIG. 8.—WET HYDROGEN TREATMENT WITH 30 PER CENT WATER VAPOR.

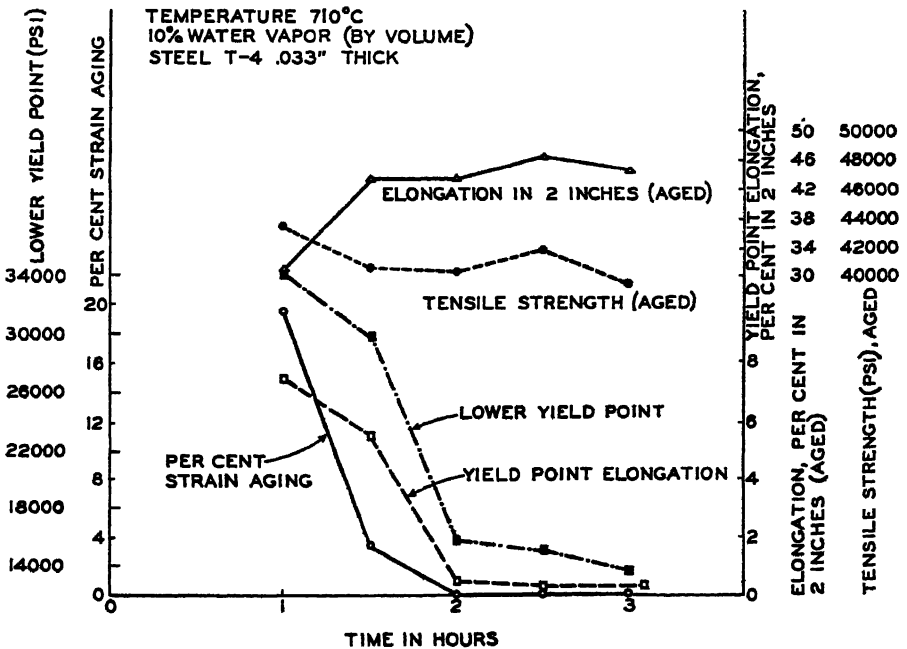


FIG. 9.—WET HYDROGEN TREATMENT WITH 10 PER CENT WATER VAPOR.

content do not affect the required time of treatment appreciably. For this reason, it was felt that carrying out an extensive series of experiments to obtain more precise data was not warranted. After these experiments had been concluded, all subsequent hydrogen treatments were made using the maximum possible amount of water for any given temperature. The partial pressures of water vapor used were chosen so as to be a few millimeters of mercury below the equilibrium value for the formation of oxide as interpolated from the data of Emmet and Schulz.⁸²

No determination was made of the water-vapor content of the tank hydrogen used, but, in the absence of any liquid water in the tank, this may safely be assumed to be extremely small. Since the tanks are

TABLE 7.—*Time Required for Elimination of Yield Point and Strain-aging Using Various Mixtures of Hydrogen and Water Vapor*

Temperature 710°C.; material, 0.0335 in. cold-reduced rimmed steel (T-4).

Volume Per Cent H ₂ O	Time to Eliminate Strain-aging, Hr.	Time to Eliminate Yield Point, Hr.
Tank hydrogen	20	140
4.7	2 5	3 0
7.5	2.0	2.5
21.0	1 5	2 0
39.1	1 5	1 5

filled at approximately 130 atmospheres pressure, the average water content would only be less than one thousandth of a per cent, even if saturated at room temperature. The times in Table 7 are those necessary for the complete elimination of all traces of strain-aging and the yield point, either of which may be markedly reduced in considerably shorter times. This is particularly true of the tank-hydrogen treatments.

Influence of Temperature

A preliminary investigation covering the range 680° to 850°C. indicated the

optimum temperature to be somewhere in the vicinity of 700° to 725°C. At 800°C and above the grain size obtained was greater than A.S.T.M. No. 6, and in addition, the treatment was not as effective in eliminating aging. No decision as to the effectiveness of the treatment as regards the yield-point elimination could be made, since the larger grain size in itself caused a partial elimination of the yield point. Following this preliminary survey of the effect of temperature, a second, more precise, series of experiments was made to

TABLE 8.—*Effect of Temperature on Time of Treatment in Wet Hydrogen*

Steel: Cold-reduced rimmed steel, T-3 Thickness, 0.0355 to 0.0375 in. Flow rate, 0.9 to 1.0 cu. ft. per hr. (furnace volume 0.11 cu ft.). Partial pressure of H₂O, maximum possible at each temperature without scaling (204 mm. at 670°C, 227 mm. at 740°C.).

Temperature, Deg. C.	Time to Eliminate Strain-aging, Hr.	Time to Eliminate Yield Point, Hr.
671	4 6	5.2
680	3 8	4 6
691	3 2	4 0
702	2 2	3.2
710	2 2	2.8
720	1 8	2.0
730	1 7	2 1
740	1 8	1.8
760	1 7 ^a	2 0 ^a
800	2 3 ^a	b
850	3 6 ^a	b

^a Estimated from approximate times obtained in preliminary experiments

^b True yield point obscured by large grain size

fix the optimum temperature more closely. In this series, specimens were treated for periods differing by 12 min., and the time to eliminate aging and the yield point was determined to the nearest 12-min. interval.

The experimental conditions for this series of experiments and the times necessary to eliminate completely aging and the yield point, as a function of temperature in the range 670° to 740°C. are shown in Fig. 10 and Table 8. The shape of these two curves strongly suggests two different types of reactions operating simultaneously, but

having temperature-rate coefficients of opposite sign.

Influence of Specimen Thickness

Tensile specimens were prepared from sheets varying in thickness from 0.0095 to

and the yield point are shown in Table 9. All treatments were carried out at 720°C. with the exception of the 0.033-in. thick which was treated at 710°C.

These results are plotted logarithmically in Fig. 11. The equation relating the time of

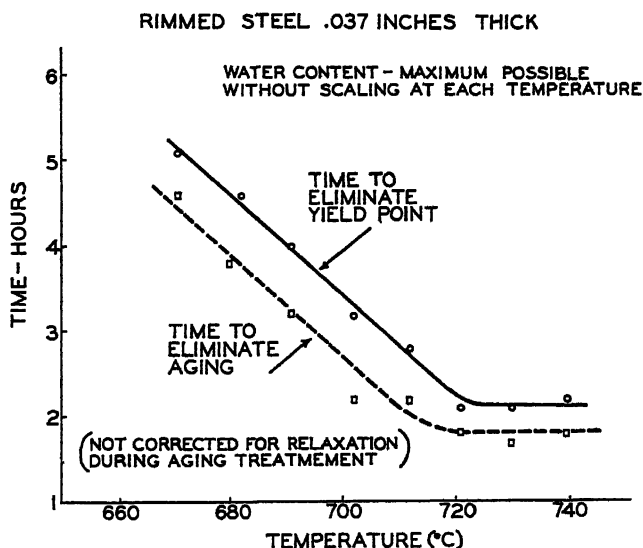


FIG. 10.—EFFECT OF TEMPERATURE OF WET HYDROGEN TREATMENT ON TIME OF TREATMENT.

0.111 in. and were treated for various lengths of time. All of the specimens were in the full-hard condition before treatment and all were rimmed steels containing less

treatment and the specimen thickness is $t = 1.4a^{1.5} \times 10^6$, where t is the time to eliminate the yield point in seconds and a is the specimen thickness in inches.

TABLE 9.—*Influence of Specimen Thickness on Time of Hydrogen Treatment*

Thickness, In.	Time to Eliminate Aging, Hr.	Time to Eliminate Yield Point, Hr.
0.0095	0.25	0.3
0.033	1.5	2.0
0.036	1.8	2.2
0.038	2.2	2.6
0.044	2.6	3.0
0.052	3.4	4.2
0.111	10.5	13.0

than 0.08 per cent carbon. The time interval between successive specimens for a given thickness varied from 5 min. for the 0.0095-in. series to 30 min. for the 0.111-in. series. The times to eliminate strain-aging

If the slow step in the process is assumed to be the diffusion of some element such as carbon to the surface of the specimen, and if it is assumed further that the yield point disappears when the mean concentration of carbon falls below some limiting value, the relationship between the thickness and time of treatment should be a parabolic one and the exponent should be 2 instead of 1.5; this is based on diffusion from a homogeneous single phase with no excess carbide present at the temperature of treatment. Since the solid solubility of carbon in alpha iron at this temperature (720°C.) is between 0.03 and 0.04 per cent^{82,84} most of the specimens probably contained some free carbides, which might

account for the exponent being smaller than the theoretical value of 2.0 for a diffusion process. This problem has not yet been treated mathematically.

steels after hydrogen treatment have slightly higher yield strength and tensile strength and lower elongation than the rimmed steels.

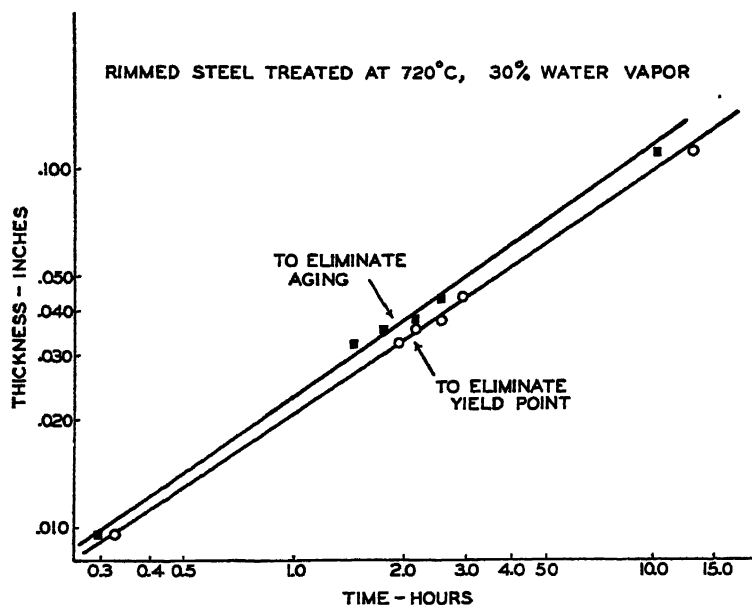


FIG. 11.—EFFECT OF TIME OF TREATMENT ON THICKNESS OF SHEET THAT MAY BE TREATED TO COMPLETION IN WET HYDROGEN.

Wet Hydrogen Treatment of Other Grades of Steel

In most of the experiments described low-carbon rimming-grade steels were used. The hydrogen treatment has also been applied successfully to low-carbon aluminum-killed steels and higher-carbon steels of open-hearth origin, and with partial success to a low-carbon bessemer steel containing considerably more nitrogen than is found in open-hearth steels.

With regard to the time required to eliminate aging and the yield point, both rimmed and killed steels in the low-carbon range were found to behave precisely the same. Steels T-1, T-2, T-3 and T-4 (see Table 1) were annealed in wet hydrogen for 3 hr. and then tested. The results of the strain-aging and tensile tests may be seen in Table 10. In general, the killed

Higher carbon steels may also be treated to eliminate strain-aging and the yield point, but the time required increases rapidly with increasing carbon content. This is shown in Table 11 for a series of steels of increasing carbon content.

Steels C-1, C-2 and C-3 were obtained in the form of full-hard, 3/4-in. wide, cold-rolled strip and steel TH-1 was full-hard sheet steel. Treatments were carried out in the vertical tube furnace with a partial pressure of water of 220 mm. and a flow rate of 2.0 cu. ft. per hr. Microscopic examination of the 0.23 and 0.36 carbon steels following treatment for various lengths of time indicate that the last traces of carbon have disappeared by the time the treatment is complete. The partially treated specimens have a decarburized surface layer, completely free from any carbides, that gradually

TABLE 10.—*Comparison of Hydrogen-treated Rimmed and Killed Steels*

Steel	Type	Hardness, Rockwell B	Yield-point Elongation, Per Cent in 2 in.	Uniform Elongation, Per Cent in 2 in.	Bench Elongation, Per Cent in 2 in.	Yield Point, Lb. per Sq. In.	Tensile Strength, Lb. per Sq. In.
T-1	Killed, strain-aged	36	Nil	31.5	40.5	17,100	44,800
T-1	Killed, not aged	35	Nil	31.5	44.0	17,400	45,000
T-2	Killed, strain-aged	38	Nil	33.0	42.0	16,300	44,500
T-2	Killed, not aged	36	Nil	31	44.0	16,600	45,000
T-3	Rimmed, strain-aged	32.5	0.5	32.3	41.0	16,200	40,900
T-3	Rimmed, not aged	28.0	0.5	33.0	46.0	14,800	41,000
T-4	Rimmed, strain-aged	29.0	Nil	33	47.0	14,200	39,600
T-4	Rimmed, not aged	25.5	Nil	33.5	47.0	12,900	39,500

moves in toward the center as the treatment proceeds.

In addition to these experiments with higher carbon steels, a bessemer steel of approximately the same analysis as the low-carbon rimming steels except for nitrogen and phosphorus was tested to determine the time required for the elimination of the yield point and strain-aging. This was a capped steel in sheets

per sq. in.), and even after this length of time, the material still shows a small amount of yield-point elongation, approximately 1 per cent. Open-hearth steel in the same gauge and carbon content requires only 3 hr. for complete elimination of the yield point. The time of treatment was gradually increased to 16 hr., with no further decrease in the stress at the lower yield point, and substantially no decrease in the yield-point elongation.

TABLE 11.—*Effect of Carbon Analysis on Time of Wet Hydrogen Treatment*
Partial pressure H₂O: 220 mm. Hg.

Steel	Carbon, Per Cent	Time to Elimi- nate Aging, Min.	Time to Elimi- nate Yield Point, Min.	Thickness, In.	Tem- per- ature, Deg. C.
Th-1	0.06	132 ± 6	156 ± 6	0.0382	720
C-3	0.10	135 ± 15	165 ± 15	0.035-0.036	730
C-2	0.23	225 ± 8	225 ± 8	0.035-0.037	730
C-1	0.36	360 ± 10	380 ± 10	0.036-0.037	730

0.042 in. thick. Treatments were carried out at 730°C. with a partial pressure of water vapor of 220 mm. and a flow rate of 2.0 cu. ft. per hr. Aging was eliminated in the bessemer material in approximately 160 min., which is substantially the same as that required for open-hearth steel in the same thickness (0.042 in.). The effect of the wet hydrogen treatment on the yield point of the Bessemer steel, however, is quite different. Six hours of treatment was required to reduce the yield-point stress to a constant level (22,000 lb.

Influence of Rate of Flow of Gas Mixture

This variable was not examined carefully over a wide range of flow rates, but certain qualitative observations indicate that some minimum flow rate must be exceeded in order that the treatment may proceed at its maximum rate. For example, when using the 2-in. i.d. tube furnace described on page 4, it was found that increasing the flow rate from 0.2 up to 1.0 cu. ft. per hr. decreased the time required, but no further decrease occurred if the flow rate was increased to 2.0 cu. ft. per hr. For this furnace, 1.0 cu. ft. per hr. corresponds to a linear flow rate of approximately 0.01 ft. per sec. For a rate of 0.001 ft. per sec. in a larger furnace there was no appreciable decrease in aging or the yield point up to 15 hr. When the flow rate was increased to approximately 0.01 ft. per sec., the time of treatment for complete elimination corresponded very closely to that found when treating tensile specimens in the smaller furnace.

*Effect of Heating in Air Following
Wet Hydrogen Treatment*

This experiment was carried out in order to determine whether or not annealing in air caused a return of either the yield point or aging, once they had been removed by treating in wet hydrogen. This question would be of considerable importance if it should be necessary to anneal sheets, or articles formed from them, at some time subsequent to the

by excessive scaling. The test data are listed in Table 12.

The same materials were normalized in air at 885 and 940°C., and it was found that some strain-aging will occur following either of these high-temperature treatments, although to a much smaller degree than in untreated sheets. The normalizing treatments were carried out by placing the specimens in an electric muffle furnace which was at temperature, holding at temperature for 15 min. and then removing

TABLE 12.—*Effect of Annealing in Air Following Wet Hydrogen Treatment*

Steel	Treatment	Yield Strength, Lb. per Sq. in.	As Strain-aged			
			Tensile Strength, Lb. per Sq. in.	Uniform Elongation, Per Cent in 2 in.	Bench Elongation, Per Cent in 2 in.	Strain-aging, Per Cent
T-3	Wet H ₂	13,850	41,100	31.5	47.0	0.0
T-4	Wet H ₂	13,850	39,800	33.2	47.0	0.0
T-3	Wet H ₂ followed by air anneal 3 hr. at 710°C. Furnace cool	17,350	39,800	26.5	35.7	0.0
T-4		16,600	39,600	28.2	37.5	0.0
T-3		20,050	41,100 ^a	29.5 ^a	39.5 ^a	
T-4		19,600	40,800 ^a	28.3 ^a	35.5 ^a	

^a Not strained and aged.

TABLE 13.—*Properties of Sheets Normalized at 885°C. and 940°C. Following Wet Hydrogen Treatment*

Steel	Treatment	Yield Strength, Lb. per Sq. in.	Tensile Strength, Lb. per Sq. in.	Yield-point Elongation, Per Cent in 2 in.	Strain-aging, Per Cent
T-3	Hydrogen treatment only	13,850	41,100	0.0	0.0
T-4		13,500	39,800	0.0	0.0
T-3		13,650	34,200	0.0	
T-4	Hydrogen-treated and normalized in air at 940°C.	11,100	33,000 ^a	0.0	6.8
T-3		20,500	37,300	0.0	
T-4	Hydrogen-treated and normalized in air at 885°C.	16,200	38,300 ^a	0.0	7.4

^a As strained 10 per cent and aged at 200°C. for 3 hours.

hydrogen treatment. In addition, Pfeil¹² has reported that annealing in air following wet hydrogen treatment causes a complete return of strain-aging. *No yield point, nor any evidence of strain-aging, was found following an anneal in air for 3 hr. at 710°C.* However, a slight increase in the yield strength occurred, and there was a marked drop in bench elongation, probably caused

and allowing to cool in still air. Irregularities occur in the early part of the stress-strain curves for the specimens normalized at 885°C., which might be interpreted as a tendency toward a return of the yield point, but there is no actual drop in the load nor elongation at constant load. For the specimens normalized at 940°C., no conclusion can be drawn regarding the

TABLE 14.—*Mechanical Properties of Sheet Treated with Wet Hydrogen and Cold-rolled*

Condition	Thickness, In.	Hardness, Rockwell B	0.2 Per Cent Yield Strength, Lb. per Sq. In.	Tensile Strength, Lb. per Sq. In.	Bench Elongation, Per Cent in 2 In.
As hydrogen-treated	0.132	15	13,100	37,500	53.0
Cold-rolled 25 per cent	0.100	66	45,400 ^a	46-47,000	19-20
Cold-rolled 50 per cent	0.067	78	56,400 ^b	60-64,000	9.5
Cold-rolled 72.5 per cent	0.037	85	74,500 ^b	76-77,000	3.0-3.5

^a Extension measured with Tuckerman strain gauge. Yield strength obtained by offset method.^b Extension measured with dial-gauge extensometer. Yield strength obtained by offset method.

yield point, since this treatment caused a ferrite grain size greater than No. 3, which would obscure any yield point that might be present. The grain size of the specimens normalized at 885°C. was No. 5 or No. 6.

The results of the mechanical tests on specimens so treated are shown in Table 13, together with results on the same steels after hydrogen treatment only. The low elongation of the two specimens normalized at 940°C. may be related to their extremely large grain size.

Mechanical Properties of Hydrogen-treated Sheets after Cold-rolling and after Cold-rolling and Annealing in Air

The effect of cold-work on the mechanical properties of hydrogen-treated steel is of interest, since this material is intended for use in various cold-forming operations. For this reason, strips cut from a 0.132-in. hydrogen-treated rimmed steel sheet were cold-rolled 25, 50 and 72.5 per cent and then tested for hardness, 0.2 per cent yield strength, tensile strength, and bench elongation. The results of these tests are shown in Table 14, and it will be noted that they are substantially the same as those to be expected for untreated steels after the same amounts of cold reduction following hot-rolling or box annealing.

The effect of cold reduction followed by ordinary annealing on the properties of hydrogen-treated sheets, particularly aging and the yield point, is of interest, since it might prove more economical to carry out the hydrogen treatment before cold

reduction rather than afterward. For this reason, several of the strips that had been cold-reduced 72.5 per cent were annealed in a small electric furnace (no atmosphere control) for 3 hr. at 700°C. and furnace cooled. Five specimens were made into a small pack to prevent excessive oxidation and the three inside specimens of the pack were tested. The results of these tests are shown in Table 15.

TABLE 15.—*Effect of Cold Reduction Followed by Ordinary Annealing on the Properties of Hydrogen-treated Sheets*

Lower Yield Point, Lb. per Sq. In.	Yield- point Elongation, Per Cent in 2 In.	Tensile Strength, Lb. per Sq. In.	Uni- form Elongation, Per Cent in 2 In.	Bench Elongation, Per Cent in 2 In.	Aging, Per Cent, 10 Per Cent Strain 3 Hr. 200°C.
19,250	1.0	35,000	27.7	46.0	0
20,250	1.4	35,400	28.7	45.0	0
21,150	1.6	36,900	30.1	46.5	0

Comparing these results with those given in Table 14 for the hydrogen-treated sheet before cold-rolling or annealing, it will be noted that the yield point has been raised and there is now a definite but small amount of yield-point elongation. However, neither the yield point nor the yield-point elongation are as high as those obtained with untreated box-annealed sheets. The tensile strength is slightly lower than that of the original sheet, as is the uniform elongation. While the bench elongation is considerably under that

of the original 0.132-in. sheet, it is, nevertheless, normal for the hydrogen-treated sheets in this thickness (0.037 in.). Cold-rolling followed by annealing has not caused any return of the susceptibility to strain-aging, which was removed by the hydrogen treatment.

Treatment with Wet Hydrogen Containing Nitrogen

Altenberger³⁰ reports that in the production of nonaging steel by annealing in tank hydrogen, the amount of nitrogen in the hydrogen must be kept below a certain minimum value, which amounts to about 0.004 per cent at 700°C., in order that the process shall be effective. To determine whether or not this same restriction applies when wet hydrogen is used, the wet hydrogen treatment was carried out by using hydrogen to which approximately 10 per cent by volume of nitrogen was added.

The material used in this experiment was steel No. T-3. In the earlier experiments the partial pressure of water used was approximately 220 mm. To avoid oxidation in this particular series because of reduced partial pressure of hydrogen, the partial pressure of water was reduced to about 170 mm. For this reason, it might be expected that the times to eliminate aging and the yield point would be increased slightly. The results of a series of treatments for different lengths of time are shown below. *The presence*

time required. The slight increase in the time required to eliminate the yield point might be explained simply on the basis of the dilution effect of the nitrogen. This result does not necessarily conflict with Altenburger's, which applies to annealing in tank hydrogen, since there is some reason to believe³⁵ that the presence of traces of oxygen or water prevent any reaction between molecular nitrogen and iron.

Summary

The following variables have been examined with regard to their influence on the effectiveness of the wet hydrogen treatment in eliminating the yield point and aging:

1. *Moisture Content.*—The time required for treatment decreases as the moisture content increases. This decrease is most marked as the moisture content is increased from zero up to 5 per cent, but a further slow decrease is observed as the partial pressure of water is raised up to the maximum permissible without oxidation. The treatment is ineffective if any oxide forms on the specimen surface.

2. *Temperature.*—The time required for the treatment goes through a minimum at approximately 730°C. The optimum temperature range appears to be 720° to 740°C. The effect of temperature was examined over the range 670° to 850°C.

3. *Specimen Thickness.*—The relationship between sheet thickness and time for complete elimination of the yield point and aging for rimmed steels under 0.08 per cent carbon is given by the equation:

$$t = 1.4a^{1.5} \times 10^6$$

where

t = time in seconds

a = sheet thickness in inches

4. *Composition of Steel.*—Rimmed and killed steels in the same carbon range appear to be very similar with regard to the effect of hydrogen treatment. Increasing the carbon content increases the time required, but does not affect the

	Wet H ₂ with 10 Per Cent N ₂ , Hr.	Wet H ₂ without N ₂ , Hr.
Aging eliminated.....	1.8	1.8
Yield point eliminated...	2.6	2.2

of even large amounts of nitrogen in the hydrogen used for the wet hydrogen treatment has no very profound effect on the length of

properties of the treated steels. Increasing the nitrogen content (e.g., bessemer steel) does not increase the time to eliminate aging. The time for virtual elimination of the yield point for the one bessemer steel examined was considerably longer than that for low-carbon open-hearth steels; the last trace of a yield point was not eliminated.

5. *Rate of Gas Flow.*—The influence of flow rate on the process was not evaluated precisely, but some evidence was obtained to indicate that the flow rate must be maintained above 0.01 ft. per sec. if the time of treatment is to be a minimum.

6. *Heating in Air Following the Wet Hydrogen Treatment.*—Annealing in air at approximately 700°C. does not cause a return of the yield point or aging. Some reduction in elongation was observed, but this may have been due to the loss of metal as a result of excessive scaling.

Heating for short periods of time at either 885° or 940°C. in air, followed by cooling in air, caused slight return of aging, but no return of the yield point.

7. *Cold-rolling Followed by Heating in Air.* Severe cold-rolling followed by "pack" annealing in air did not bring about any reappearance of strain-aging, but a small yield point was observed after this treatment.

8. *Nitrogen in the Wet Hydrogen.*—The presence of molecular nitrogen up to 10 per cent by volume does not increase the time required to eliminate aging and only slightly increases the time to eliminate the yield point. This latter effect may be due to the reduced partial pressure of hydrogen and water vapor.

EXPERIMENTS TO DETERMINE THE IMPURITIES THAT CAUSE STRAIN- AGING AND THE YIELD POINT IN LOW-CARBON STEELS

The general plan of these experiments was based on the assumption that strain-aging and yield point are the result of the

presence in ordinary low-carbon steels of some impurity or impurities as yet unidentified. Presumably, annealing in wet hydrogen removes these impurities and thereby renders the steel free from strain-aging and the typical yield-point behavior.

The present investigation had an advantage over those previously carried out in that the wet hydrogen treatment provides a fine-grained material in which the yield point and strain-aging are absent. It was planned, therefore, to determine which of the commonly suspected elements is responsible for aging or the yield point by putting carbon, nitrogen and oxygen back into hydrogen-treated sheets and determining whether or not aging and the yield point reappear, arranging the experiment to ensure the introduction of only one element at a time.

The starting material for these experiments was hydrogen-treated, 0.036 by 14 by 16-in. sheets. Each of these sheets yielded approximately 38 tensile specimens, each identified as to position in the particular sheet. Every third one of these specimens was then tested for aging and the yield point, and in this way the properties of the material immediately adjacent to the specimens used for carburizing, nitriding, or oxidizing were known. None of the specimens tested "as treated" were found to exhibit any evidence for strain-aging or a yield point, so it may safely be assumed that the specimens immediately adjacent to them were also free from either of these effects. The 14 by 16-in. sheets before treatment were in the cold-reduced, full-hard condition. The steel used is labeled No. S₂ in Table 1. The sheets were hydrogen-treated for 5 hr. at 720°C. in wet hydrogen, which constituted an "over-treatment," since the minimum time for this grade and thickness was approximately 3 hours.

The general scheme for the introduction of the three elements (O, C, N) singly was as follows:

1. *Oxygen*.—Tank hydrogen mixed with sufficient water vapor to cause scaling was passed through a furnace containing the specimens to be oxidized. The oxidized specimens were then vacuum-annealed for sufficient time to allow diffusion from the oxide layer into the specimen.

2. *Carbon*.—Purified hydrogen (O_2 , H_2O free) was bubbled through a high-purity hydrocarbon (normal heptane), and the mixture passed through a furnace containing the specimens to be carburized.

3. *Nitrogen*.—Mixtures of dried ammonia and purified hydrogen were used to introduce nitrogen into the hydrogen-treated sheets. The amount of ammonia in this gas mixture was maintained at a low enough value so that no nitride was formed on the surface (approximately 5 per cent by volume).

Oxidation of Wet-hydrogen-treated Specimens

Although the results of the vacuum-fusion analyses of wet-hydrogen-treated

sheets indicate that oxygen is not one of the elements removed by the hydrogen treatment, several oxidation experiments were carried out. Specimens cut from a hydrogen-treated sheet were oxidized at $720^\circ C$. (the temperature of the original hydrogen treatment) in wet hydrogen, and some of them were then vacuum-annealed for 24 hr. at three different temperatures: 720° , 805° , and $940^\circ C$. In every case oxide was still present on the surface following the vacuum anneal, so that the specimen may be assumed to have been saturated with oxygen at the particular annealing temperature. The mechanical properties of these specimens are shown in Table 16, together with the test results for specimens immediately adjacent to them in the original hydrogen-treated sheets.

Oxidation at $720^\circ C$. does not cause a return of either the yield point or aging. In some cases, there appears to be a decrease in the bench elongation as a result of the oxidation treatment, but this

TABLE 16.—*Mechanical Properties of Hydrogen-treated Sheets after Oxidation*

Oxidation Time at $720^\circ C$. ^a	Vacuum Anneal, Time and Temperature	Lower Yield Point, Lb. per Sq. In.	Yield-point Elongation, Per Cent in 2 In.	Tensile Strength, Lb. per Sq. In.	Uniform Elongation, Per Cent in 2 In.	Bench Elongation, Per Cent in 2 In.	Strain-aging, Per Cent
None	None	11,700	0.0	38,600	31.0	50.1	0.0
20 min.	24 hr. } $720^\circ C$.	10,400	0.0	36,800	29.5	43.0	0.0
None	None	12,800	0.0	38,500	31.0	49.0	0.0
30 min.	24 hr. } $720^\circ C$.	11,100	0.0	37,000	31.5	47.0	0.0
45 min.	24 hr. } $720^\circ C$.	11,200	0.0	36,400	32.5	45.5	0.0
None	None	11,600	0.0	38,800	31.0	49.0	0.0
60 min.	24 hr. } $720^\circ C$.	10,400	0.0	36,900	33.5	49.0	0.0
None	None	12,650	0.0	39,200	32.7	49.0	0.0
3 hr. ^b	24 hr. } $940^\circ C$.	9,700	0.0	30,300	20.4	24.0	1.7
None	None	15,000	0.0	39,000	31.3	47.5	0.0
3 hr. ^b	24 hr. } $940^\circ C$.	9,200	0.0	29,000	15.3	19.5	
None	None	11,700	0.0	39,100	31.5	46.0	0.0
3 hr.	None	14,600	0.5	38,400	28.3	46.5	
None	None	12,800	0.0	39,100	31.0	45.5	0.0
3 hr.	24 hr. } $805^\circ C$.	10,500	0.0	35,600	29.0	46.5	0.0
None	None	14,000	0.0	39,400	31.0	44.5	0.0
3 hr.	None	13,900	0.5	39,400		43.0	0.0
None	None	14,100	0.0	39,900	29.8	44.5	0.0
3 hr.	24 hr. } $805^\circ C$.	10,500	0.0	35,600	30.0	45.0	
None	24 hr. } $940^\circ C$.	10,200	0.0	32,000	28.0	38.0	1.7

^a Oxidized in mixture of water vapor and tank hydrogen.

^b Extremely coarse grain.

is not consistently true. Annealing at 805°C. after oxidation at 720°C. did not cause a return of the yield point or aging, and the bench elongation was unaffected. Annealing at 940°C. resulted in a very coarse ferrite grain size, so that all of the mechanical properties were markedly affected; however, there is no evidence of any yield point and only slight evidence of aging after 10 per cent strain. This slight aging is without significance, however, since there is also some indication of aging if hydrogen-treated specimens are annealed at this temperature without prior oxidation (cf. the last specimen in Table 16.)

asbestos and activated alumina brought about a definite return of the yield point. To determine whether this return of the yield point was due to the presence of small traces of impurities (such as hydrocarbons) in the gas after it had passed through the purification train, some of the wet-hydrogen-treated specimens were annealed in hydrogen obtained by diffusion through palladium. *No reappearance of the yield point was observed in the wet-hydrogen-treated sheet after 48 hr. annealing at 700°C. in hydrogen so purified* (see Table 17). It was concluded therefore that the appearance of the yield point originally noted was a result of impurities in the tank

TABLE 17.—*Experiments with the Carburizing Furnace*

Treatment	48 Hours Annealing at 700°C. in Hydrogen Obtained by Diffusion through Palladium		5 Hours Annealing at 700°C. in Tank Hydrogen Using the Purification Train: Liquid Nitrogen Trap → Platinized Asbestos → Activated Alumina	
	Not Strain-aged	Strained 10 Per Cent, Aged 3 Hr. at 200°C.	Not Strain-aged	Strained 10 Per Cent, Aged 3 Hr. at 200°C.
Lower yield point, lb. per sq. in.....	10,750	13,000	16,050	15,650
Yield-point elongation, per cent.....	0	0	0.5	0.5
Uniform elongation, per cent.....	35.0	33.0	31.0	31.2
Bench elongation, per cent.....	52.0	48.5	43.0	43.5
Tensile strength, lb. per sq. in.....	36,500	37,000	37,500	37,000
Strain-aging, per cent.....		0		0

Carburization of Wet-hydrogen-treated Specimens

In the carburizing experiments, the carburizing atmosphere was prepared and passed into a porcelain tube furnace through an all-glass system with no stop-cocks or rubber connections, except where the tank hydrogen entered. It was first necessary to ascertain that the purified hydrogen used to carry the hydrocarbon vapor was sufficiently pure so that no return of the yield point or aging occurred if wet-hydrogen-treated specimens were annealed in this carrier hydrogen alone. It was found that annealing wet-hydrogen-treated specimens in tank hydrogen purified only by passing through hot platinized

hydrogen, which were not eliminated by the platinized asbestos and the activated alumina, presumably hydrocarbons.

The purification train was then changed by introducing into the line a liquid nitrogen trap between the hydrogen tank and the platinized asbestos. With this arrangement, it was found that for all practical purposes the reappearance of the yield point was avoided. The return of the yield point (after 5 hr. annealing at 700°C.) was of such a small magnitude that any effect of the carbon in the carburizing experiments should be readily recognized. The final gas-purification train was: Tank hydrogen → activated charcoal in liquid nitrogen → platinized asbestos → activated alumina → heptane saturator → furnace.

The carburizing agent used was liquid normal heptane of high purity (Eastman). The normal heptane saturator was held at 25°C., at which temperature the vapor pressure is 46 mm. of mercury. The results are shown in Table 18.

It was found that at a carburizing temperature of 700°C. one minute in the carburizing atmosphere was enough for the wet-hydrogen-treated specimens to par-

properties of the specimen seem to be independent of the time of carburization. Under the conditions of the experiment, this limiting carburizing time appears to be $2\frac{1}{2}$ to 5 min. at 700°C.

Vacuum Annealing of Carburized Specimens

Specimens that had been carburized for 15 min. and for 3 hr. were vacuum-annealed at 700°C. for 15 hr. to determine

TABLE 18.—*Carburizing Experiments*
Temperature of carburizing furnace 700°C.
Temperature of normal heptane saturator 25°C.

Carburizing Time, Min.	Lower Yield Point, Lb. per Sq. In.	Yield-point Elongation, Per Cent	Uniform Elongation, Per Cent*	Bench Elongation, Per Cent*	Tensile Strength, Lb. per Sq. In.	Strain-aging, Per Cent
1	20,150	1.5	29.9	42.0	40,500	3.0
2.5	31,200	5.8	26.1	37.5	45,200	14.5
5	35,400	5.5	22.9	31.5	52,000*	22.9
5	35,200	0.0	22.0	31.0	51,000*	18.9
15	35,000	5.6	22.6	31.5	53,000*	23.5
15	34,500	0.7	22.0	29.5	51,200*	19.2
60	37,400	4.7	21.1	29.0	53,800*	13.1
120	35,800	4.7	21.3	30.5	53,000*	14.2
180	30,100	5.5	19.8	29.0	43,500*	21.6

* As strain-aged; strained 10 per cent, aged 3 hr. at 200°C.

tially regain their yield-point and strain-aging properties. It has already been pointed out that during a blank run wet-hydrogen-treated specimens annealed 5 hr. at 700°C. in the same train without the normal heptane saturator showed only a very small yield point and no strain-aging. In the carburizing experiments, the duration of run was much shorter. Any difference found in the carburized specimen must be due to the introduction of the normal heptane saturator and, therefore, to the presence of normal heptane in the gas. Thus, it can be safely concluded that carbon is one of the elements that are responsible for the yield-point and strain-aging phenomena in mild steel sheets.

The data indicate a limiting carburizing time. Below the limiting carburizing time the yield-point and strain-aging properties of the specimen are functions of the carburizing time (both increase with increasing time). Above the limiting carburizing time, the yield-point and strain-aging

the effects of homogenization. They are compared with specimens as carburized in

TABLE 19.—*Comparison of Mechanical Properties of Carburized Specimens with and without Vacuum Annealing*

Treatment.....	As Carburized 3 Hr.	Carburized 3 Hr. Vacuum-annealed 24 Hr., 700°C.	As Carburized 15 Min.	Carburized 15 Min. Vacuum-annealed 24 Hr., 700°C.
Lower yield point, lb. per sq. in....	30,100	32,000	35,000	30,000
Yield-point elongation, per cent	5.5	5.7	5.6	5.6
Total elongation, per cent*.....	28.9	31.2	31.5	33.8
Bench elongation, per cent*.....	29.0	32.5	31.5	34.0
Tensile strength, lb. per sq. in.*..	43,500	45,500	53,000	44,600
Strain-aging, per cent*.....	21.6	19.5	23.5	8.3

* As strain-aged; strained 10 per cent, aged 3 hr. at 200°C.

Table 19. Vacuum annealing of the specimen carburized for only 15 min. caused a

reduction in the yield-point stress and the amount of strain-aging, which were extraordinarily high before vacuum annealing. Neither of these effects is noted for the specimen carburized 3 hr. These effects in the specimens carburized only 15 min. are presumed to be caused by inward diffusion of carbon during the vacuum annealing, resulting in an average carbon content lower than the original carbon in the surface layers.

Nitriding of Wet-hydrogen-treated Specimens

Nitriding was done in the same apparatus used for carburizing, after a slight modification. The train used was as follows: Tank hydrogen → activated charcoal and liquid N_2 trap → hot platinized asbestos → activated alumina → liquid ammonia saturator → nitriding furnace. Pure liquid ammonia was introduced into the saturator from a side connection by the condensation, in the saturator, of dried ammonia vapor supplied from a cylinder. After enough ammonia was condensed in the saturator to last for a run, the side connection was cut off. The temperature of the liquid ammonia saturator was kept constant at -75°C . by the use of a mixture of acetone and dry ice. The temperature of the nitriding furnace was held at 500°C . These experimental conditions were so chosen that there was no danger of iron nitrides being formed in the sheet during the nitriding run at 500°C .⁸⁶

Before nitriding a few blank runs were made without any liquid ammonia in the saturator. It was found necessary to reactivate the charcoal from time to time to avoid introducing a yield point; when this was taken care of, the purification train was satisfactory.

The results of the nitriding experiments are given in Table 20.

As for carburizing, there seems to be a limiting time beyond which further nitriding produces no change in properties. At

500°C . this limiting time seems to be about 2 hr. Probably this can be explained on the assumption that after a certain time of nitriding the specimen has attained an equilibrium solid solution concentration

TABLE 20.—*Results of Nitriding Experiments*

Temperature of liquid ammonia saturator, -75°C .

Temperature of nitriding furnace, 500°C .

Time of Nitriding, Min.	Lower Yield Point, Lb. per Sq. In.	Yield-point Elongation, Per Cent in 2 In.	Per Cent Strain-aging ^a	Tensile Strength (as Strain-aged), Lb. per Sq. In.	Total Elongation (as Strain-aged), Per Cent in 2 In.
5	17,000	0	3 35	40,000	36 2
10	18,380	0 25	5 20	41,000	35 6
15	19,700	0 80	6 40	42,000	34 7
15	20,000	0 70	4 85	43,100	35 5
15	20,350	1 20	8 58	43,200	30 6
20	20,500	1 20	8 54	41,600	31 4
25	21,100	1 50		42,500	
40	20,300	1 20	9 10	41,600	41 4
50	22,200	1 70	11 40	43,000	36 9
60	25,050	4 70	13 10	45,600	29 0
120	30,500	3 75	16 47	47,000	24 7
180	29,450	4 50	15 70	49,000	17 2
480	31,780	4 40	16 74	50,700	22 7

^a Strained 10 per cent, aged 3 hours at 200°C .

TABLE 21.—*Mechanical Properties of Nitrided and Vacuum-annealed Specimens*

Time of Nitriding, Min.	Lower Yield Point, Lb. per Sq. In.	Yield-point Elongation, Per Cent in 2 In.	Strain-aging, Per Cent ^a	Tensile Strength (as Strain-aged), Lb. per Sq. In.	Total Elongation (as Strain-aged), Per Cent in 2 In.
1	24,350	3 30	2 93	38,180	45 5
2 5	24,830	3 60	3 09	38,410	44 3
5	26,240	5 25	10 16	38,820	42 6
15	29,000	5 25	16 00	41,900	33 3
20	28,000	5 30	15 98	41,450	32 3
60	29,400	4 50	20 60	48,600	28 5
180	30,500	4 00	19 13	51,600	28 0
480	30,000	4 30	17 51	49,900	22 3

^a Strained 10 per cent, aged 3 hr. at 200°C .

corresponding to the furnace atmosphere and furnace temperature; further nitriding will produce no change in the nitrogen concentration of the specimen.

Vacuum Annealing of Nitrided Specimens

Specimens that had been nitrided for various lengths of time were also annealed in vacuum for 24 hr. at 550°C. Mechanical properties of these specimens are given in Table 21. Vacuum annealing causes an increase in the effects of nitriding that may be explained as resulting from homogenization.

Annealing in purified hydrogen causes about the same effects, as may be seen from the data collected in Table 22.

tivity are available to indicate precisely the amount of either nitrogen or carbon that will cause strain-aging or the yield point, but it is believed that the presence of either element in amounts of the order of 0.001 per cent by weight is sufficient for both these phenomena to be fully developed. This belief is based in part on the extremely short times of carburizing or nitriding required and in part on analyses of wet-hydrogen-treated specimens in which the yield point and aging have just been eliminated. Another reason for be-

TABLE 22.—Comparison of Mechanical Properties of Nitrided Specimens Subjected to Different Annealing Treatments

Treatment	Lower Yield Point, Lb. per Sq. In.	Yield-point Elongation, Per Cent in 2 In.	Strain-aging, ^a Per Cent	Tensile Strength (Aged), Lb. per Sq. In.	Total Elongation (Aged), Per Cent in 2 In.
Nitrided 1 hr. as nitrided.	25,050	4 70	13.10	45,600	29.0
Nitrided 1 hr. Vacuum-annealed 550°C., 24 hr. .	29,400	4 50	20.60	48,600	28 5
Nitrided 1 hr. Vacuum-annealed 550°C. 24 hr., then cooled down slowly at 7° per hr.	28,630	4.60	17.42	49,500	18 4
Nitrided 1 hr. Annealed in pure hydrogen, 550°C., 24 hr.	29,650	4 60	17.66	49,000	21.8
Nitrided 1 hr. Annealed in pure hydrogen, 550°C., 24 hr.	29,000	5 40	17.05		

^a Strained 10 per cent, aged 3 hr. at 200°C.

Discussion and Summary

It is believed that these experiments, in which both the yield point and strain-aging were produced in a material previously free from either effect, by the introduction of carbon or nitrogen, conclusively demonstrate that these two elements are responsible for these phenomena as commonly observed in steels. The role of oxygen has not been completely clarified, since all of the materials used for carburizing or nitriding undoubtedly contained oxygen as a result of the wet hydrogen treatment. However, from the results of the oxidation experiments, it might be concluded that oxygen *per se* does not cause strain-aging, although it may have a secondary influence on the amounts of carbon or nitrogen required.

No analytical methods of sufficient sensi-

lieving that such extremely small amounts of carbon may be responsible for these effects is the fact that if hydrogen-treated specimens are annealed for a relatively short time in tank hydrogen from which the water and oxygen have been removed, the yield point and aging reappear. This reappearance is believed to be caused by the presence of hydrocarbon vapors in the tank hydrogen caused by contact of the commercial hydrogen with oil during the time it was being compressed. The amount of hydrocarbon vapor present in such tank hydrogen must be extremely small, but it is nevertheless sufficient to cause a complete return of the yield point and strain-aging. In the absence of accurate analyses following carburizing and nitriding, it is not possible to decide which of the two elements has the greater effect.

CONCLUSIONS

The important results of the experiments on the elimination of aging and the yield point by wet hydrogen treatment, and those on the causes of these two effects, are summarized below:

1. The yield point, strain-aging and quench-aging may all be eliminated from low-carbon steels by annealing for relatively short times in wet hydrogen at temperatures in the neighborhood of 700°C.

2. The time required for complete elimination of the yield point and aging increases as the thickness of the metal or its initial carbon content is increased. This time is decreased as the temperature of treatment increases up to approximately 740°C., as the water vapor content of the gas is increased, or as the flow rate past the surface of the metal is increased.

3. The elimination of the yield point and aging results from the removal of carbon or nitrogen or both and if either is reintroduced by carburizing or nitriding, both the yield point and aging reappear.

4. The presence of either carbon or nitrogen in amounts not greater than 0.003 per cent is sufficient to cause both the yield point and aging in iron, and it is believed that considerably smaller amounts of either element are capable of producing these effects.

5. Oxygen *per se* does not cause aging or the yield point in deep-drawing steels, although it may have a minor influence on the effects of carbon and nitrogen. The effects of oxygen are not completely known.

ACKNOWLEDGMENT

The results reported in this paper are part of those obtained from a cooperative research project on the general subject of the drawability of steel sheets, supported by the Carnegie-Illinois Steel Corporation in the Metals Research Laboratory of Carnegie Institute of Technology, and conducted by the Carnegie-Illinois Steel

Corporation Graduate Fellow in Metallurgical Engineering. So many employees of both organizations made valuable contributions to the work that it is impossible to acknowledge their assistance as individuals.

APPENDIX—REVIEW OF LITERATURE
THE YIELD POINT

In general, annealed plain carbon steels exhibit the maximum yield-point elongation in the range 0.05 to 0.10 per cent carbon. Fritsche⁴ reproduces load-extension curves for steels varying from 0.11 to 1.45 per cent carbon, in which a yield point is exhibited up to about 0.70 per cent carbon only. The yield point in higher carbon steels, however, depends on the microstructure as well as the carbon content.⁵ A plain carbon eutectoid steel does not exhibit a yield point when isothermally transformed to give pearlite, but does if the same material is spheroidized. As Ludwik and Scheu⁶ have shown, decreasing the carbon to that normally found in electrolytic iron decreases the yield-point effect markedly. However, Cleaves and Hiegel⁷ recently published load-extension curves for high-purity iron (99.99 per cent Fe), which definitely show a yield point including not only a level portion but in some cases a definite drop in load. The authors state that this high-purity iron in general showed a more pronounced yield point than did vacuum melted electrolytic iron. The high-purity iron contained approximately 0.001 per cent or less of carbon, 0.0001 to 0.0005 per cent of nitrogen and 0.001 to 0.004 per cent of oxygen. The grain size was approximately 45 grains per millimeter squared. Adcock and Bristow⁸ prepared an iron of almost equal purity and found no evidence for a yield point, but this result can probably be attributed to excessive grain size; photomicrographs in the paper indicate a very large grain size. Edwards, Phillips and Jones⁹ made up a large number of different low carbon alloys and found that certain of these did not exhibit a yield point. Additions of 0.21 per cent titanium or 6.10 per cent chromium sufficed to eliminate the yield point where the carbon was less than 0.025 per cent, but an alloy containing the same amount of titanium with 0.085 per cent carbon was found to possess a marked yield point. A third

alloy, containing 0.095 per cent carbon with 1.08 per cent titanium, had no marked yield point, although it did strain-age slightly. This dependence on carbon content of the alloy content necessary to suppress the yield point led these investigators to conclude tentatively that the yield point and strain-aging are not attributes of pure iron, but are due to the presence of carbon.

With regard to the effect of nitrogen, both Kuroda¹⁰ and MacGregor and Hensel¹¹ report that flow lines are more marked (i.e., greater yield-point elongation) in steels containing higher nitrogen (bessemer) than in those of lower nitrogen content (open-hearth).

Recently, Edwards, Phillips and Liu¹² have reported some experiments in which low-carbon steel was annealed in wet hydrogen at 950°C., cold-worked and then recrystallized to obtain a fine grain size. Steel so treated did not show a yield point if tested at extremely slow speeds, but if the speed of testing was increased to a point approaching normal testing speeds, a small yield point was observed.

Numerous hypotheses, or theories of the yield point have been put forward from time to time, but as yet none of these has been substantiated conclusively by experimental evidence. The more important explanations have been:

1. That carbon (or some other element) is rejected at the grain boundaries on cooling to form a honeycomb structure made up of hard Fe_3C cell walls filled with ductile ferrite. The honeycomb structure supports the load to a point above the yield strength of ferrite, and when the former is finally broken, the specimen flows under a reduced load or without an increase in load.

2. Since certain precipitation-hardening alloys, when tested at elevated temperatures, exhibit irregularities in the stress-strain curve somewhat similar to those encountered at the yield point in iron, it has been suggested that the yield point might be in some way connected with precipitation occurring within the ferrite.

3. Since single crystals of iron have considerable variation of elastic modulus with changing crystallographic direction, it has been suggested that certain of the crystals in a randomly oriented aggregate, owing to the constraints placed upon them by their neighbors, may store up sufficient elastic strain energy

so that when general flow begins it proceeds for some time without an increase in external load.

Dalby,¹³ who obtained some of the earliest accurate autographic load-extension curves for steel, suggested that a yield point would be expected in a material such as mild steel, which is "assumed to be an alloy of iron constructed of iron aggregates of large size through which is distributed a network of crystalline structure." The load-extension diagram of such a material should then be the resultant of two materials, one of which carries the load until elastic failure occurs and the other then deforming for a time under substantially constant load. Dalby also suggested that the load-extension diagram of chemically pure iron should be the same as that of copper. This network or honeycomb theory has been put forward numerous times in more specific form since it was suggested by Dalby in 1912. Nadai¹⁴ believed the yield point arose from a rupture of some grain-boundary material enveloping the ferrite grains. He suggested that a metastable condition arises in which the soft ferrite grains are loaded above their true flow limit because of the hindering effect of the "Zwischensubstanz" in the grain structure and the drop in load at the yield point results from the partial rupture of the grain-boundary envelopes. As evidence for this he cites the fact that Fry's reagent shows increased attack at the grain boundaries in flowed material (this has been recently confirmed by Adcock and Jenkins¹⁵) and the fact that as the grain surface area increases (with finer grain size) the effect becomes more pronounced. Ludwik¹⁶ also believed this type of mechanism would account for the yield point in mild steel and cites Scheu's observation that fractured cementite "veins" are observed in mild steel that has yielded, and also the fact that in low-carbon steels there is a tendency for the cementite to collect at the grain boundaries. He does not believe this will explain the presence of a yield point in electrolytic iron, however, and suggests that here the mechanism may be somewhat different (cf. Ludwik and Scheu's hypothesis below). Kuroda¹⁰ is another adherent of this theory and has conducted numerous experiments to prove it, none of which can be considered conclusive. He believes the grain-boundary material to be cementite in the form of envelopes completely

surrounding the grains, which provide a "honeycomb" that must be ruptured before the ferrite can flow. Fritsche⁴ suggests that the yield point arises because of the rupture of pearlite lamellae in a structure consisting of ferrite and pearlite, but this explanation will not account for the fact that the greatest yield point is observed in the neighborhood of 0.05 to 0.10 per cent carbon, where the fraction of the volume occupied by pearlite is extremely small, nor for a yield point in spheroidized high-carbon steels.

Some support for the "honeycomb" hypothesis is to be found in the observations of Morgan, Steckler and Schwarz.⁵⁴ These authors find that if a low-carbon steel specimen is very slowly dissolved in ammonium persulphate without rapid gas evolution, it is possible to preserve a honeycomb type of residue, which appears to have been present at the original grain boundaries. This network is not observed if the specimen is cold-worked before solution. Electron and X-ray examination of the residue indicates that it may be either iron carbide or a hydrate of iron. Benedicks⁵⁵ has recently attempted to show theoretically that impurities should tend to collect near grain boundaries, which would thus lead to a honeycomb of harder material even in the absence of a second phase. Ljunggren,⁵⁶ in a very carefully conducted series of experiments with ruled gratings, has attempted to prove Benedick's hypothesis of "molecular enrichment" near the grain boundaries resulting in an increase in hardness. For normal low-carbon steels these experiments failed to reveal any region of higher hardness except where a microscopically visible constituent (e.g., cementite) existed. For steels that had been annealed in oxygen-free nitrogen at 1000°C., there appeared to be some evidence for envelopes of a harder region near the grain boundaries. The nitrogen anneal had caused an increase in nitrogen content from 0.007 to 0.010 per cent.

Fell⁵⁷ objects to the grain-boundary theory, first because of lack of conclusive proof, and, second, because in several materials where such a boundary layer is known to exist (e.g., gold containing traces of lead or bismuth) the metal is rendered extremely fragile. He believes that the presence of a cementite honeycomb would render low-carbon steels completely unwork-

able. Fell believes the yield point is characteristic of pure iron and results from the body-centered cubic lattice and the multiplicity of possible slip systems. This multiplicity of slip systems, together with small grain size, makes it possible for deformation to take place along the planes of maximum shear just as though the metal were isotropic even on a microscopic scale. Takaba and Okuda⁵⁸ also attribute the yield point to the high "flowability" of the iron crystals that arises from the multiplicity of possible slip systems.

Without specifying precisely the nature of the solute, Ludwik and Scheu⁶ proposed that ferrite may be supersaturated with respect to "gases" and that any disturbance of the lattice will lead to precipitation of the solute and hardening. In slowly cooled ferrite (e.g., very low-carbon steel or electrolytic iron) the only "disturbed" lattice is that in the immediate vicinity of the grain boundaries, which leads to a harder grain-boundary network. Quenching such a material prevents any precipitation even at the grain boundaries and thereby suppresses the yield point; subsequent aging would cause precipitation and a reappearance of the yield point. They suggest that cold-work causes a disappearance of the yield point by solution of any precipitate present and aging of cold-worked irons allows reprecipitation in the "disturbed" regions with the reappearance of the yield point. Kuntze and Sachs⁵⁹ would modify this hypothesis only to the extent of specifying carbon as the specific element which goes in and out of solution. Epstein²⁸ has suggested that elastic straining causes "foreign matter" to go into solution, which increases the elastic strength above the "equilibrium value" of the yield point. When the metal finally does yield, a weak "disturbed" state ensues, and flow takes place under a reduced load until equilibrium is established, possibly by precipitation.

Andrew and Lee⁵⁸ believe that yielding in steel produces regions of austenite at the grain boundaries and slip planes, which immediately decompose to small crystals of ferrite. This then explains why iron does not deform to fracture at the yield, since the small alpha crystals have a strengthening effect that accounts for the subsequent rise in the load-extension curve. They make no effort to account for the upper yield point or the hetero-

geneous nature of the initial flow in materials with a yield point.

Orowan¹⁰ has recently observed a type of deformation in single crystals of zinc and cadmium, which differs from the usual mechanisms of slip, twinning or flexure gliding. In certain single crystals where the basal slip plane is nearly parallel to the stress axis in tension or compression, a "kink" type of deformation was observed, which appeared to depend on the direction of maximum shear stress in the crystal and not on the maximum resolved shear stress. He suggests that such a mechanism might account for the formation of flow lines in steel which generally take approximately the direction of maximum shear stress in the specimens without regard to crystal orientation.

Recently, Edwards, Phillips and Liu²⁷ have succeeded in producing yield points in nickel, silver and copper age hardening alloys by combinations of quenching, straining and aging. These experiments, together with the fact that iron purified in moist hydrogen exhibits little or no yield point, and the fact that a yield point may be produced in such a material by straining and aging, leads them to conclude that the yield point arises from the precipitation of a solute element on certain planes of slip within the crystals.

STRAIN-AGING

Iron free from strain-aging has been prepared by a number of different methods: Pfeil,¹² Dean, Day and Gregg,¹³ Davenport and Bain¹⁴ and Altenburger³⁰ have all found that hydrogen purification of low-carbon steels or electrolytic iron eliminates strain-aging. Dean, Day and Gregg¹³ and Sauveur¹⁶ have observed strain-aging effects in electrolytic iron, but the first-named authors found that these effects could be eliminated by vacuum melting. Commercial materials almost completely free of strain-aging have been prepared by thorough deoxidation and the use of small additions of aluminum, titanium, vanadium or zirconium,^{15,17,18} The "nonaging" character of the commercial materials is generally improved by heat-treatment involving either very slow cooling¹⁷ or quenching followed by tempering at a high temperature.¹⁹

Four general methods have been used to

attack the problem of determining which element (or elements) causes strain-aging in low-carbon steel.

1. The first method has been to make up low-carbon steels having varying amounts of the particular element being studied (usually carbon, nitrogen or oxygen) and then determine whether this tendency to strain-age varies as the element is varied. A variation of this same method has also been used in which a large number of steels have been examined for aging characteristics, analyzed very completely, and then attempts made to correlate the results of the aging tests with the various elements present, aging then being attributed to the element that showed the best correlation. These investigations have yielded inconclusive or incomplete results, since all of the materials used exhibited strain-aging and the impurity responsible for aging had to be inferred from the observed variations in the magnitude of the aging effect. The principal investigations of this type were those of Eilender, Cornelius and Knuppel²⁴ and Eilender, Cornelius and Menzen.²⁵

2. The second method of study has been to make certain additions to the steel (principally "deoxidizers") and from the effect of these additions on strain-aging the impurity responsible has been inferred. This method has been entirely successful in eliminating strain-aging by the use of various additions coupled (in some cases) with special heat-treatments. It suffers, however, from the fact that the result is obtained by means of an addition agent which may affect more than one of the impurities present or which may alloy with the iron, thereby changing the nature of the material being studied. This general method has been applied principally by Edwards, Phillips and Jones,⁹ Davenport and Bain,¹⁴ Altenburger,¹⁵ Wilder¹⁹ and Daniloff, Mehl and Herty.²³

3. A third method is to purify the steel in moist hydrogen at high temperatures for a sufficient length of time to eliminate the strain aging, and by following the changes occurring by analysis, determine the particular element responsible. Using this method, Pfeil¹² concluded that both carbon and oxygen could cause strain-aging; however, nitrogen was not considered and the treatments were carried out in such a manner that this particular element might have been affected.

1. The general method of adding a single element to a high-purity iron and noting its effect on the aging behavior has also been used. Dean, Day and Gregg¹³ and Altenburger¹⁵ have added nitrogen to purified irons and found that strain-aging occurred in materials that were free from strain-aging before nitriding. Davenport and Bain¹⁴ found that vacuum-melted electrolytic iron melted under pure iron oxide showed strain-aging. Presumably, the vacuum-melted electrolytic iron used was free from strain-aging before oxidation, but this is not definitely stated. Wilder¹⁹ found that vacuum-melted and hydrogen-purified iron (Wemco) exhibited considerable strain-aging after annealing in oxygen at various temperatures and quenching. The fact that the specimens were quenched before straining, and the fact that the purified material aged without oxidation, leave his conclusion that oxygen was responsible for strain-aging open to question.

HYDROGEN PURIFICATION

Early investigators disagree as to the effect of hydrogen annealing on carbon content; thus Forquignon,³⁵ Cely,³⁶ Ledebur³⁷ and Charpy and Bonnerat^{38,39} report that the carbon content of steel or cast iron is definitely lowered, while Heyn,⁴⁰ Wust and Geiger,⁴¹ Wust and Sudhoff⁴² and Emmons⁴³ failed to note any decarburization. Numerous investigations, principally those of Campbell,⁴⁴ Schmitz,⁴⁵ Austin,^{46,47} Baukloh⁴⁸⁻⁵³ and others⁵⁴⁻⁵⁸ have definitely established the decarburizing power of hydrogen. The addition of water vapor markedly increases the rate of decarburization as shown by Campbell,⁴⁴ Campbell, Ross and Fink,⁵⁴ Sykes,⁵⁹ Austin⁴⁷ and Bramley.⁵⁹ Sykes⁵⁹ work on the effect of water vapor on hydrogen-methane carburizing suggests that the increased decarburizing power of wet hydrogen should be relatively more marked at lower temperatures, although this has not been studied. Bramley and Allen⁵⁹ in the course of a careful study of the carburization and decarburization of steel by various gases found that the extent of decarburization for a fixed time (20 hr.) and a fixed temperature (1000°C.) increased if the water content of a hydrogen-water vapor mixture was increased. They examined the effect of water-vapor content over the range 0 to 15 per cent by volume and their results

indicate that while increasing water-vapor content continuously increases the decarburizing power of the gas mixture, increasing the water-vapor content is more effective at low concentrations than at high. They were of the opinion that any increase in water content above about 15 per cent would not cause any appreciable increase in the decarburizing power of the gas. Ciocchina⁶⁶ found that the addition of small amounts of oxygen greatly increased the decarburizing power of hydrogen.

Increasing the temperature of decarburization increases the rate, the greatest increase being noted between 700°C. and 950°C. according to Campbell,⁴⁴ Austin⁴⁶ and Johansson and Von Seth.⁵⁸

The presence of alloys in the steels being decarburized influences the rate of decarburization. Campbell⁴⁴ found that large amounts of manganese (12 per cent) decreased the rate of decarburization in wet hydrogen, as did silicon (3.5 per cent). Johansson and Von Seth⁵⁸ on the other hand found that up to 2 per cent of manganese, nickel and tungsten did not influence the rate, but that approximately the same amount of silicon increased it. More recently Baukloh and his associates^{50,53} have reported that silicon, tungsten, molybdenum, manganese, chromium, copper and tin all decrease the rate of decarburization. Averbukh and Chufarov⁵⁹ found that silicon transformer sheets are more readily decarburized in dry than in wet hydrogen.

Hydrogen annealing is reported to remove nitrogen from steel by Despretz,⁷⁰ Edwards,⁷¹ Mehl and Briggs,⁷² Altenburger^{15,30} and others.⁷³⁻⁷⁵ The influence of water vapor does not appear to have been investigated.

With regard to the effect of hydrogen annealing on the other common impurities, Ciocchina⁶⁶ has observed desulphurization at temperatures as low as 600°C. It appears that phosphorus may be removed by hydrogen annealing, but only at 1200°C. or higher is the rate appreciable;⁴⁸ no decrease is observed after several weeks at 950°C.^{13,54}

As to the effect of hydrogen annealing on properties, Pfeil¹² found that by decarburizing in wet hydrogen at 950°C. he was able to eliminate strain-aging when the carbon content was reduced below 0.003 per cent. This required about five weeks for a ½-in. round bar. Altenburger^{15,30} has reported the elimination of

strain-aging as indicated by a lack of increase in tensile strength in the "blue-brittle" range of temperature by annealing in tank hydrogen. He observed no increase in tensile strength at 400°F. for low-carbon sheets that had been annealed at 750°C. for as little as 6 hr. On the other hand, Edwards, Walters and Jones²² failed to note any decrease in strain-aging after annealing in moist hydrogen at 950°C.

Bates¹⁶ found that quench-aging could be suppressed in a 0.026 per cent carbon basic bessemer steel by annealing a 0.2 in. round bar for 12 hr at 950°C. in wet hydrogen. The carbon content after this treatment was 0.008 to 0.012 per cent. Davenport and Bain¹⁴ also report a substantial reduction in quench-aging in electrolytic iron by hydrogen purification.

BIBLIOGRAPHY

1. Piobert, Morin and Didion: Memorial de l'Artillerie (1842) 5, 505.
2. W. Lüders: Concerning the Elastic Behaviour of Steel and Iron Specimens and the Molecular Movement Observed in Bending Such Specimens. *Dingler's Polytechnisches Jnl.* (1860) 155, 18.
3. L. Hartmann: The Distribution of Deformation in Metals Subjected to Stress. *Compt. rend.* (1894) 118, 520.
4. J. Fritzsche: The Resistance to Flow in Bending of Steel Girders and Columns. *Der Stahlbau* (1938) 11, 54.
5. M. Gensamer, E. B. Pearsall, W. S. Pellini and J. R. Low, Jr.: The Tensile Properties of Pearlite, Bainite and Spheroidite. *Trans. Amer. Soc. Metals* (1942) 30, 983.
6. P. Ludwik and R. Scheu: The Yield Point of Electrolytic Iron and Mild Steel. *Ber. Fachausschusse Ver. deut. Eisenhüttenleute* (1925) 5, 1-7.
7. H. E. Cleaves and J. M. Hiegel: Properties of High Purity Iron. *Jnl. of Research, Nat. Bur. Stds.* (1942) 28, 643.
8. F. Adcock and C. Bristow: Iron of High Purity. *Proc. Royal Soc.* (1936) A-153, 172.
9. C. A. Edwards, D. L. Phillips and H. N. Jones: The Influence of Some Special Elements on the Strain-Aging and Yield Point Characteristics of Low-Carbon Steels. *Jnl. Iron and Steel Inst.* (1940) 142, 199.
10. M. Kuroda: Origin of the Yield Point in Mild Steel. *Sci. Papers, Inst. Physical Chemical Research (Tokyo)* (1938) 34, 1528-1633.
11. C. W. MacGregor and F. R. Hensel: The Influence of Nitrogen in Mild Steel on the Ability to Develop Flow Layers. *Jnl. of Rheology* (1932) 3, 37.
12. L. B. Pfeil: The Change in Tensile Strength due to Aging of Cold-drawn Iron and Steel. *Jnl. Iron and Steel Inst.* (1928) 118, 167-194.
13. Dean, Day and Gregg: Relation of Nitrogen to Blue-heat Phenomenon in Iron and Dispersion-hardening in the System Iron-nitrogen. *Trans. A.I.M.E.* (1929) 84, 446.
14. E. S. Davenport and E. C. Bain: The Aging of Steel. *Trans. Amer. Soc. Metals* (1935) 23, 1047.
15. C. L. Altenburger: Improving the Drawability of Steel by Controlling Nitrogen. *Metal Progress* (June 1940) 639.
16. A. Sauveur: Steel at Elevated Temperatures. *Trans. Amer. Soc. Steel Treat.* (1930) 17, 410.
17. A. Hayes and R. O. Griffiths: Non-Aging Iron and Steel for Deep Drawing. *Metals and Alloys* (1934) 5, 110.
18. G. G. Neuendorff: Izett Steels. *Metals and Alloys* (1932) 3, 61-68.
19. A. B. Wilder: The Influence of Oxygen on the Aging of Iron and Steel. *Metals and Alloys* (1938) 9, 145-148.
20. E. L. Dupuy: Experimental Investigation of the Mechanical Properties of Steels at High Temperatures. *Jnl. Iron and Steel Inst.* (1921) 104, 91.
21. A. Sauveur and D. C. Lee: Influence of Strain and of Heat on the Hardness of Iron and Steel. *Jnl. Iron and Steel Inst.* (1925) 112, 323-329.
22. C. A. Edwards, H. N. Jones and B. Walters: A Study of Strain-Age Hardening of Mild Steel. *Jnl. Iron and Steel Inst.* (1939) 139, 341.
23. B. N. Daniloff, R. F. Mehl and C. H. Herty, Jr.: The Influence of Deoxidation on the Aging of Mild Steels. *Trans. Amer. Soc. Metals* (1936) 24, 595.
24. W. Eilender, H. Cornelius and H. Knuppel: Effect of Nitrogen and Oxygen on Mechanical Aging of Steel. *Archiv Eisenhüttenwesen* (1935) 8, 507-509.
25. W. Eilender, H. Cornelius and P. Menzen: The Influence of Impurities in Mild Steel on the Changes which Occur in Mechanical Properties in the Blue-brittle Region. *Archiv Eisenhüttenwesen* (1940) 14, 217-221.
26. W. Koster: Nitrogen in Commercial Iron. *Archiv Eisenhüttenwesen* (1930) 3, 637-655.
27. L. R. Van Wert: Some Notes on Blue Brittleness. *Trans. A.I.M.E.* (1931) 95, 230.
28. S. Epstein: Embrittlement of Hot-galvanized Structural Steel. *Proc. Amer. Soc. Test. Mat.* (1932) 32, 293.
29. A. Sauveur: Notes on the Aging of Metals and Alloys. *Trans. Amer. Soc. Steel Treat.* (1934) 22, 97-113.
30. C. L. Altenburger: United States Patent 2271242 (Jan. 27, 1942).
31. W. Oertel and A. Schepers: Properties of Killed and Rimmed Steels. *Stahl und Eisen* (1931) 51, 710-715.
32. P. Oberhoffer, H. Hochstein and W. Hessenbruch: Discussion *Archiv Eisenhüttenwesen* (1929) 2, 725-738.
33. E. Gumlich: The Dependence of the Magnetic Properties, the Specific Resistance and the Density of Iron Alloys on the Chemical Composition and Thermal Treatment. *Wiss. Abh. der*

- physikal. tech. Reichsanstalt (1918) 4, 267-480.
34. P. Goerens: The Effect of Aging Cold-deformed Low-carbon Steel and 3 Per Cent Nickel Steel. *Ztsch. Ver. Deut. Ing.* (1924) 4.
 35. M. Porquignon: Researches on Malleable Iron and on the Annealing of Steels. *Ann. Chimie et Physique* (1881) 23, 433.
 36. L. Cely: The Purification of Pig Iron, Steel and Iron by Hydrogen. *Stahl und Eisen* (1883) 3, 306.
 37. A. Ledebur: On the Properties of Cast Iron Annealed in Charcoal. *Stahl und Eisen* (1886) 6, 373-777.
 38. G. Charpy and S. Bonnerat: On the Reactions that Accompany the Osmosis of Hydrogen through Iron. *Compt. rend.* (1913) 156, 394.
 39. G. Charpy and S. Bonnerat: On the Permeability of Iron for Hydrogen. *Compt. rend.* (1912) 154, 594.
 40. E. Heyn: Iron and Hydrogen. *Metallographist* (1903) 6, 39.
 41. F. Wüst and G. Geiger: Contribution to the Knowledge Concerning the Two Forms of Carbon in Iron. *Stahl und Eisen* (1905) 25, 1134.
 42. F. Wüst and E. Sudhoff: The Action of Hydrogen and Nitrogen on Graphitic Iron at Various Temperatures. *Metallurgie* (1910) 7, 261.
 43. J. V. Emmons: The Surface Decarbonization of Tool Steels. *Trans. A.I.M.E.* (1914) 50, 405.
 44. E. D. Campbell: On the Decarburization of Steel with Hydrogen. *Jnl. Iron and Steel Inst.* (1919) 100, 407.
 45. F. Schmitz: The Chemical Action of Gases on Iron and Their Combination with Nonmetals at High Temperatures. *Stahl und Eisen* (1919) 39, 373, 406.
 46. C. R. Austin: Hydrogen Decarburization of Carbon Steels with Consideration on Related Phenomena. *Jnl. Iron and Steel Inst.* (1922) 105, 93.
 47. C. R. Austin: A Study of Effect of Water Vapor on Surface Decarburization of Steel by Hydrogen with Certain Developments in Gas Purification. *Trans. Amer. Soc. Steel Treat.* (1934) 24, 31-58.
 48. W. Baukloh and B. Knapp: The Progress of the Reaction between Hydrogen and Carbon in Iron. *Archiv Eisenhüttenwesen* (1939) 12, 405-411; Iron and Steel Inst., *Carnegie Schol. Mem.* (1938) 21, 149-164.
 49. W. Baukloh: The Action of Hydrogen on Metals. *Chemische Fabrik* (1938) 449-455.
 50. W. Baukloh and W. Kronenfels: Hydrogen Decarburization of Pure Fe-C Alloys and Alloy Steels. *Archiv Eisenhüttenwesen* (1937) 11, 145-156.
 51. W. Baukloh and F. Springorum: Hydrogen Permeability and Decarburization of Cast Iron. *Metallwirtschaft* (1937) 16, 446-449.
 52. W. Baukloh: Formation of the Outer Layer during Annealing of Fe-C Alloys in Hydrogen. *Archiv Eisenhüttenwesen* (1936) 10, 217-219.
 53. W. Baukloh and H. Guthmann: Decarburization of Some Alloy Steels by Hydrogen. *Archiv Eisenhüttenwesen* (1935/36) 9, 201-202.
 54. E. D. Campbell, W. L. Fink and J. F. Ross: The Iron-Carbon Equilibrium in Dry Hydrogen at 950° C. *Jnl. Iron and Steel Inst.* (1923) 108, 173.
 55. C. A. Edwards and L. B. Pfeil: The Production of Large Crystals by Annealing Strained Iron. *Jnl. Iron and Steel Inst.* (1924) 109, 127.
 56. Gelsenkirchener-Bergwerk A. G. German Patent No. 413,622 (1925).
 57. C. A. Edwards and L. B. Pfeil: The Tensile Properties of Single Iron Crystals and the Influence of Crystal Size on the Tensile Properties of Iron. *Jnl. Iron and Steel Inst.* (1925) 112, 79.
 58. A. Johansson and R. von Seth: The Carburization and Decarburization of Iron and Some Investigations on the Surface Decarburization of Steel. *Jnl. Iron and Steel Inst.* (1926) 114, 295.
 59. W. P. Sykes: Carburizing Iron by Mixtures of Hydrogen and Methane. *Trans. Amer. Soc. Steel Treat.* (1927) 12, 737.
 60. E. H. Schulz and W. Hulsbruch: Concerning the Surface Decarburization of Carbon Steels. *Archiv Eisenhüttenwesen* (1927) 1, 225.
 61. Siemens-Halske British Patent 314439 (1928) and United States Patent 1821407, process of decarburizing iron or steel.
 62. S. Westberg: British Patent 317180 (Aug. 15, 1929), method of refining metals and alloys.
 63. J. Ciocchina: The Decarburization and Desulphurization of Steels and Pig Iron by Means of Hydrogen. *Stahl und Eisen* (1931) 51, 1024-1026.
 64. D. H. Rowland and C. Upthegrove: Grain Size and its Influence on Surface Decarburization of Steel. *Trans. Amer. Soc. Metals* (1936) 24, 96.
 65. J. Ciocchina: The Chemical Behavior of Hydrogen at High Temperatures; Decarburization, Deoxidation and Desulphurization of Steels. *Chim. et Ind.* (1936) 36, 261-269.
 66. F. Bartscheres: French Patent 817471 (Sept. 3, 1937).
 67. L. Jacque: Action of Hydrogen on Carbides of Iron and Chromium. *Compt. rend.* (1938) 206, 1900-1902.
 68. T. Mochida: On Decarburization of Steel by Wet and Dry Hydrogen. *Tetsu to Hagané* (1941) 27, 260-266 April, 1925. (In Japanese.)
 69. C. I. Chufarov: Kinetics of Decarburization of Transformer Steel by Annealing in Hydrogen. *Metallurg* (1939) 14, 48-61. Abstracted in *Chim. et Ind.*, 43, 126.
 70. C. Despretz: Observations on the Changes in the Physical Properties of Metals under the Combined Action of Ammoniacal Gas and Heat. *Ann. Chim. et Phys.* (1829) 42, 122.
 71. C. Edwards: British Patent 3333 (July 13, 1882).
 72. R. F. Mehl and C. W. Briggs: Discussion of Aging in Low Carbon Steels. *Trans. Amer. Soc. Metals* (1932) 19, 478.
 73. G. Englehardt and C. Wagner: Kinetics of the Nitriding Reaction: NH_3 (g)

- N. dissolved in $-Fe) 3/2H_2$. *Ztsch. Physik. Chem.* (1932) B18, 369-379.
74. S. Brunauer, M. E. Jefferson, P. H. Emmet and S. B. Hendricks: Equilibria in the Iron-nitrogen System. *Jnl. Amer. Chem. Soc.*, 53, 1778-1786.
 75. E. Lehrer: The Equilibrium, Iron-Hydrogen-Ammonia. *Ztsch. Elektrochemie* (1930) 36, 383-392, 460-473.
 76. A. A. Bates: Aging Low-Carbon Steels. *Trans. Amer. Soc. Metals* (1932) 19, 467.
 77. R. L. Kenyon and R. S. Burns: Aging in Iron and Steel. *Amer. Soc. Metals Symposium on Precipitation Hardening*, Chicago, October 1939.
 78. W. Krings and J. Kempkens: Solubility of Oxygen in Solid Iron. *Ztsch. anorg. allgem. Chem.* (1929) 183, 225-250; (1930) 190, 313-320.
 79. L. A. Wooten and W. G. Guldner: Microdetermination of Carbon in Low Carbon Iron and Steel. *Ind. and Eng. Chem., Anal. Ed.* (1942) 14, 835.
 80. Sampling and Analysis of Carbon and Alloy Steels. Chemists, United States Steel Corporation. New York, 1938. Reinhold.
 81. N. B. Pilling: Micrographic Detection of Carbides in Ferrous Alloys. *Trans. A.I.M.E.* (1924) 70, 254.
 82. P. H. Emmett and J. F. Schultz: Gaseous Thermal Diffusion. *Jnl. Amer. Chem. Soc.* (1933) 55, 1376-1389.
 83. J. H. Whiteley: Survey of the Iron-Carbon Diagram near Zero Carbon. *Jnl. Iron and Steel Inst.* (1936) 133, 377.
 84. B. Jones and N. Gray: Martensitic Grains in Rapidly Cooled Ingot Iron and Mild Steel. *Jnl. Iron and Steel Inst.* (1938) 137, 327.
 85. H. H. Gray and M. B. Thompson: The Action of Molecular Nitrogen on Highly Purified Iron. *Jnl. Phys. Chem.* (1932) 36, 889-908.
 86. S. Brunauer, M. E. Jefferson, P. H. Emmett and S. B. Hendricks: Equilibrium in the System Iron-Nitrogen. *Jnl. Amer. Chem. Soc.* (1931).
 87. C. A. Edwards, D. L. Phillips and Y. H. Liu: The Yield-Point in Steel. *Jnl. Iron and Steel Inst., Advance Copy* (1943).
 88. J. H. Andrew and H. Lee: The Work Hardening and Aging of Steel. *Jnl. Iron and Steel Inst.* (1942) 145, 153.
 89. A. Bramley and K. F. Allen: The Loss of Carbon from Iron and Steel when Heated in Decarburizing Gases. *Engineering* (1932) 131, 92-94.
 90. W. E. Dalby: Load-Extension Diagrams Taken With an Optical Load-Extension Indicator. *Proc. Royal Soc.* (1913) A-88, 281.
 91. A. Nadai: Concerning Flow Surfaces Arising in Solid Bodies when Loaded. *Ztsch. tech. Physik* (1924) 5, 371.
 92. F. Adcock and C. H. M. Jenkins: Inter-crystalline Cracking in Boiler Plates—IV, Strain-Etch Markings in Boiler-Plate Material of Acid Open Hearth Origin. *Jnl. Iron and Steel Inst.* (1941) 143, 133.
 93. P. Ludwik: The Flow Limit and Cold and Warm Brittleness. *Ztsch. Ver. deut. Ing.* (1926) 70, 379.
 94. R. Morgan, S. Steckler and E. B. Schwartz: An X-Ray Diffraction Study of Grain Boundary Inclusions in Steel. *Jnl. Franklin Inst.* (1940) 229, 191-199.
 95. C. Benedicks: Capillarity of Metal Grains: Its Influence on Their Growth and Its Importance in Steel. *Chim. et Ind.* (1939) 41, 434; see also *Kolloid Ztsch.* (1940) 91, 229.
 96. B. O. W. L. Ljunggren: Method of Sclero-Grating Employed for the Study of Grain Boundaries and of Nitrided Cases; Grain Structure Revealed by Cutting. *Jnl. Iron and Steel Inst.* (1940) 142, 277.
 97. E. W. Fell: 'Yielding' Phenomena in Iron, Steel, Aluminum Alloys and Other Metals under Stress. *Iron and Steel Inst., Carnegie Schol. Mem.* (1937) 26, 123.
 98. I. Takaba and K. Okuda: The Important Properties and a Theory of Flow Figures. *Archiv Eisenhüttenwesen* (1928) 1, 511.
 99. W. Kuntze and G. Sachs: The Yield Point of Steel. *Ztsch. Ver. deut. Ing.* (1928) 72, 1011.
 100. E. Orowan: A Type of Plastic Deformation New in Metals. *Nature* (1942) 149, 643.

DISCUSSION

(Anson Hayes presiding)

G. F. COMSTOCK,* Niagara Falls, N. Y.—In this very interesting paper, the author has described only one of several methods that can be used for eliminating the yield point and strain-aging of steel. One of the other methods is to add titanium to the steel, so that it contains at least $4\frac{1}{2}$ times as much titanium as carbon. This was described first by Edwards and his co-workers in England several years ago, in a paper referred to by the author.⁹ It was also mentioned in considerable detail in a paper presented to the American Society for Testing Materials last June. In that paper it was shown that steel of this kind with at least $4\frac{1}{2}$ times as much titanium as carbon, in the form of annealed bars, had a yield strength of about 18,000 lb. per sq. in., tensile strength of about 47,000 and about 32 per cent elongation. These are practically the same properties as the author has mentioned for the hydrogen-treated steel.

Since that paper was written, the steel has been made under commercial conditions at several steel plants, and in sheets temper-rolled 1 per cent, and aged at least five weeks, it was found that the yield point was definitely eliminated. The properties in sheet form were

* Titanium Alloy Manufacturing Company

about 37,000 lb. per sq. in. yield strength, 51,000 lb. tensile, 32 per cent elongation, and Rockwell B hardness about 40. This steel contained 0.045 per cent carbon and 0.33 per cent titanium. That gives a titanium-carbon ratio of about 7, which is probably higher than necessary. The grain size was about six to seven on the A.S.T.M. scale. This steel had a Rockwell B hardness of about 50.

The disadvantage of the titanium method over the hydrogen method is that an excess of titanium must be used in order to be sure to have enough, and that excess titanium gives slightly greater hardness than the hydrogen treatment. However, this steel has been subjected to deep-drawing tests and, in spite of the slightly increased hardness, it shows excellent drawing quality as well as complete elimination of strain-aging.

MEMBER.—Would any of the other carbide formers act as titanium does?

G. F. COMSTOCK.—We know that chromium will give a somewhat similar effect, decreasing the yield point elongation, but in our chromium steel the yield point was not entirely eliminated. Columbium would probably be as effective as titanium, but we have not tried it.

J. R. Low, JR.—There might be one point—that with the titanium addition a killed steel is necessarily obtained, is it not?

G. F. COMSTOCK.—Yes.

J. R. Low, JR.—The hydrogen treatment is applicable to either rimmed or killed steels.

S. EPSTEIN,* Bethlehem, Pa.—When the yield point is eliminated, is aging also eliminated, and is quench-aging eliminated to the same degree as strain-aging? Can any conclusions be drawn from the work as to possible differences between the effects of carbon and nitrogen—for example, whether carbon may have a greater effect on quench-aging and nitrogen a greater effect on strain-aging?

J. R. Low, JR. and M. GENSAMER (authors' reply).—In answer to Mr. Epstein's question, the following data may give some indication of the relative effects of carbon and nitrogen

as far as quench-aging is concerned. One hydrogen-treated rimmed-steel specimen was carburized for one hour at 700°C., and a second was nitrided for 8 hr. at 500°C. The carburizing and nitriding procedures used were those described in the paper. The carburized specimen was then heated to 700°C in a vacuum and quenched into ice water. The nitrided specimen was heated to 580°C. and similarly quenched. Specimens were then aged at 100°C. Table 23 shows that under these conditions there is a marked increase in hardness, due to aging, in the carburized specimen and virtually no increase in hardness of the nitrided specimen.

TABLE 23.—*Quench-aging of Hydrogen-treated Steels after Carburizing and after Nitriding*

Aging Time at 100°C., Min.	Rockwell 15-T	
	Carburized	Nitrided
Before quench	82 5	73 4
As quenched	79 3	71 8
10	78 5	71 4
60	86 5	72 4
120	87 4	73 1
240	87 0	73 8
480	87 6	73 6
1200	86 7	73 5

The results will hardly serve as a means of judging the relative effectiveness of carbon and nitrogen in producing quench age-hardening since the amounts of carbon and nitrogen introduced are not known. It is, however, known that the carburizing and nitriding procedures used will cause a complete return of both the yield point and strain-aging.

A. HAYES,* Middletown, Ohio.—Did you try the experiment of reheating that steel after hydrogen treatment to temperatures of, say, 1200° or 1300°, and quench from that temperature? I am interested in whether or not with such treatment strain-aging would return.

J. R. Low, JR.—We did not try that experiment precisely.

A. HAYES.—What I would like to know is if this material was reheated in the absence

* Research and Development Department, Bethlehem Steel Company.

* Director, Research Laboratories, American Rolling Mill Company.

of oxygen, carbon, and nitrogen and then quenched from a high enough temperature to dissociate and redissolve some of the aluminum nitride, would strain-aging return?

M. GENSAMER.—We did reheat some specimens that had not been intentionally scaled in as good a vacuum as we could make. Of course, that is not a vacuum. I do not think we can answer the question until we know better how to produce an atmosphere that does not contain oxygen. We had a pretty good vacuum, using a three-stage diffusion pump, but still it is not a vacuum.

A. HAYES.—It has been known for some time that material exhibits a definite yield-point elongation and is essentially free from strain-aging when stabilized by suitable annealing and slow enough cooling from the annealing temperature. Would the elongation at the yield point reappear in the presence of aluminum nitride, which probably would be present with residual aluminum?

J. R. LOW, JR.—I am afraid we cannot answer that.

C. A. ZAPFFE,* Baltimore, Md.—This paper is a challenging one, but so capably written there seems little else to say.

One pertinent question might be raised, however, in regard to the mechanism by which these nonmetallics are removed from the steel. If they leave by atomic diffusion and quiet surface reactions, the change in the material will follow from its chemical change; but if the impurities react internally and erupt their way to the surface as insoluble gases, an important structural effect may be imposed on the material quite apart from that produced mechanically.

Under the conditions of ammonia synthesis and hydrogenation processes, the marked decarburization of mild steels seems definitely to be of the latter type. In fact, decarburization with hydrogen in general shows two marked features that lead to that conclusion: (1) the purification progresses inward as a sharply delineated zone of pearlite-free ferrite, with no indication of a diffusion gradient of carbon; and, (2) until the purification is completed,

the material is badly embrittled by the intergranular accumulation of compressed gases.¹⁰¹

In other words, the evidence seems clear that the facile H atom enters the metal and reacts with the nonmetallic to form an insoluble gas, which subsequently explodes its way back to the surface. The evidence also seems clear that some type of *surface within the grain* first receives this insoluble product, before it migrates to the grain boundary. The case seems general for precipitates of insoluble phases. This internal surface for every precipitate studied so far is crystallographic in disposition and usually comprises the same planar systems that operate during mechanical deformation. Consequently, the treatment used by these authors may operate in some such subtle way to change those mechanical properties, which are sensitive to the inherited internal structure of the grain. That subject may seem academic, and probably is unsolvable on the basis of our present knowledge. However, it calls attention to the fact that the authors' claim to having " . . . accomplished the elimination of aging and the yield point by purification, without the introduction of alloying elements . . . " is not strictly true, since in every case they introduced the two gaseous elements, hydrogen and oxygen.

Furthermore, they introduced them uniquely, in that they were in equilibrium quantities at that elevated temperature. That calls attention to some effect that the hydrogen-oxygen system itself might cause. At room temperature, the ratio of H_2O/H_2 drops to such a small value that practically all H_2O that might remain in the minute seats of precipitation would tend to react with the contiguous Fe lattice to form a tiny film of iron oxide on those surfaces that later may be called upon for mechanical deformation.

The H_2 liberated from the entrapped H_2O would add to the original H_2 . Although outright embrittlement from this hydrogen seems to have no place in the present picture, some effect from subcritical pressures of precipitated H_2 might obtain. Once again this reasoning carries us beyond a practical conclusion because of the lack of specific information on these unobservable facts.

* Assistant Technical Director, Rustless Iron and Steel Corporation.

¹⁰¹ C. A. Zapffe: Boiler Embrittlement. *Trans. Amer. Soc. Mech. Engrs.* (Feb. 1944).

Some exception might be taken to the conclusion drawn on page 234 regarding the anneal in tank hydrogen. The greater partial pressure of hydrogen in that test would considerably change the metal as an Fe-H alloy, possibly accounting for the effects noted. A repetition of the experiment using electrolytic hydrogen could decide the point simply.

J. R. LOW, JR. and M. GENSAMER.—Dr. Zapffe's suggestion that the changes in properties resulting from the wet hydrogen treatment may not necessarily be due to changes in carbon and nitrogen content is an interesting one, but the authors do not know of anything in their experimental results that would lend support to this point of view. The "sharply delineated zone of pearlite (or cementite) free ferrite," which is cited as evidence for hydrogen penetration and "internal decarburization" is not peculiar to hydrogen decarburization but to temperatures of decarburization below that at which the steel is completely austenitic. Certainly for temperatures below the A_{c1} such a zone is to be expected unless the rate of solution of carbon at the cementite-ferrite interfaces within the steel is very much slower than the rate of carbon removal by diffusion to the surface and reaction there. If this rate of solution of carbon is equal to or greater than the rate of removal, the observed carbon gradient in the region affected by decarburization is limited to the solubility of carbon in alpha iron; i.e., approximately 0.03 to 0.04 per cent for these low temperatures. This explanation seems a much more plausible one than that which Dr. Zapffe has suggested. Further, if decarburization with wet hydrogen is carried out at temperatures where the steel is completely austenitic, then, as Wells and Rhines¹⁰³ have shown, the carbon gradient is a gradual one and of the type that would be expected if the mechanism of decarburization is diffusion to the surface and reaction with the decarburizing gas.

Regarding Dr. Zapffe's second point, that embrittlement results from partial hydrogen purification, we can only say that no such embrittlement has been observed. This was true in all of the great number of partial

purification treatments carried out. In general, the tendency is in the opposite direction. For example, the elongation in the tensile test tends to increase slightly all through the treatment, as may be seen in Fig. 1. This behavior was observed whether purification was carried out in hydrogen containing large amounts of water vapor or in tank hydrogen, to which no water had been added.

Dr. Zapffe takes exception to the statement that "aging and the yield point are eliminated without the introduction of alloying elements" on the ground that hydrogen and oxygen are both introduced by this treatment. If hydrogen is introduced into the sheet during the treatment it is not present for any great length of time following the treatment, since no permanent increase in hydrogen content is to be noted in the vacuum-fusion analyses reported in Table 4. The changes in properties are permanent, however, and do not vary with elapsed time after treatment.

The increase in oxygen content reported in this same table is not thought to be of any significance as far as the observed changes in properties are concerned, since these same changes may be produced by using hydrogen of much lower water content; e.g., tank hydrogen. The only difference is in the time of treatment required to produce the desired effects. It is to be expected that treatment in tank hydrogen would reduce the oxygen content rather than increase it.

Dr. Zapffe's suggestion regarding the conclusion reached on page 234 is ruled out by the series of experiments described on page 235, on which that conclusion is based. Briefly, if treated specimens are annealed in tank hydrogen free from water vapor and oxygen, the yield point and aging slowly reappear. Annealing in tank hydrogen *not* purified by the removal of oxygen and water vapor does *not* cause a reappearance of the aging and the yield point. In each case the partial pressure of hydrogen will be substantially the same, so that there appears to be no reason for attributing the effect noted to a difference in hydrogen content.

R. W. E. LETTER and J. WINLOCK,* Philadelphia, Pa.—The experiments described by

¹⁰³ F. N. Rhines and C. Wells: The Influence of Microstructure upon the Process of Diffusion in Solid Metals. *Trans. Amer. Soc. for Metals* (1939) 27, 648.

*Edward G. Budd Manufacturing Company.

Low and Gensamer were well conceived and well carried out. The paper makes a most significant advance in a more complete knowledge of this phenomenon. With so much done

point to tensile strength. This ratio averaged 0.45 for killed steel and 0.55 for good temper-passed rimmed steel. In the wet-hydrogen-treated steel described in this paper the ratio

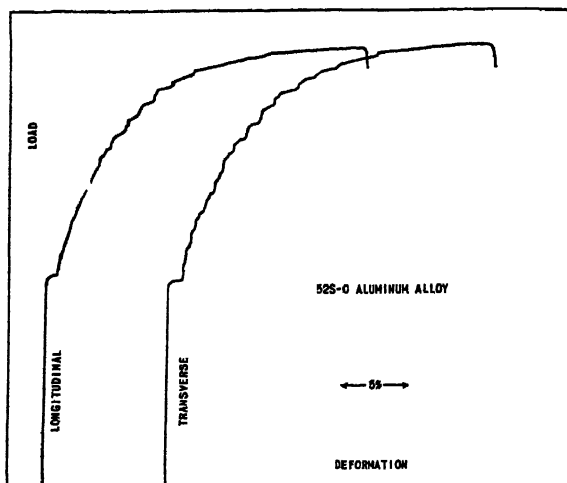


FIG. 12.

to show that carbon and nitrogen are responsible for aging and yield-point elongation, it should be possible to find an economical way to eliminate them.

It appears to us that the cost of the wet hydrogen treatment used in this research would be very high. The next big job is to find a way to lower the carbon and nitrogen content by changes in open-hearth practice with a moderate increase in cost.

The authors have made no attempt to explain the mechanism of the yield-point behavior, but their finding should pave the way toward a more complete understanding of this baffling subject.

The nonaging killed steels we used for difficult drawing operation in the two years prior to the war were entirely and permanently free of yield-point elongation after the proper light "temper" pass. In addition, the drawing quality appeared to be definitely superior to a good grade of rimmed steel even though the percentage elongation in a standard 2-in. gauge-length specimen is 1 to 2 points lower in the killed steel. We attribute the superiority of killed steel largely to the lower ratio of yield

has dropped to an average of 0.37 and the percentage elongation is at least the equal of the best grade of rimmed steel. Therefore we predict unusually good drawing quality for steel treated in this way.

Photomicrographs of typical longitudinal and transverse cross sections, preferably at 100 diameters, would be interesting. We have found that the grain-size count is in itself not too reliable a criterion of surface roughness after deep drawing. Fairly large grain in the order of A.S.T.M. No. 5 and No. 6 may be tolerated in grains elongated in longitudinal and transverse direction, as is typical in aluminum-killed steel. However, in rimmed steel where the grain is equiaxed, A.S.T.M. No. 7 is about the maximum size tolerated and even No. 8 size may draw coarse if there are a few scattered larger grains near the surface.

Effect of cold reduction followed by ordinary annealing (700°C.) on the properties of hydrogen-treated sheets, Table 15, is interesting. The yield-point elongation has returned to a moderate degree. It is still small enough to be very easily eliminated by roller leveling. We note also a pronounced increase in yield point

and a somewhat smaller decrease in tensile strength. The resultant increase in elastic ratio to about 0.55 throws this steel into the drawing quality class of a good grade of unhydrogen-treated freshly temper-passed rimmed steel. It would be very interesting to have a statement from the authors as to the reason for these changes. The low tensile strength is normally indicative of very large grain size. If that is true, the yield-point elongation of 1.0 to 1.6 per cent must be considered fairly large.

In the summary and in the conclusions the authors list results of the wet hydrogen treatment. Complete elimination of the yield point is claimed but data in Table 5 shows only a marked reduction of yield-point elongation to a value of approximately $\frac{1}{20}$ of the original. Do the authors feel that a longer time in the wet hydrogen would completely remove the yield-point elongation?

It may be of interest to the authors that a short time ago, in drawing some stampings of the aluminum alloy 52S-O (Aluminum Company of America symbols), we found definite and well-marked stretcher strains. The chemical analysis of this alloy as given in the publications of the Aluminum Company of America is 2.5 per cent magnesium; 0.25 per cent chromium; and the remainder aluminum.

We found that the stretcher strains in this alloy could be prevented from occurring by passing the sheets through staggered rolls ("roller leveling") prior to deep drawing in the usual manner.

Tensile specimens cut from the sheets in directions parallel and transverse to the directions of rolling produced load-deformation curves as shown in Fig. 12 when strained at a head speed of 0.125 in. per min. The reason these curves show only a "lower" yield point and no upper yield point was probably because of the unusual sensitivity of these phenomena to stress concentrations as described by us elsewhere* and because of the relatively small yield-point elongation. We have since found that the upper yield point is increasingly difficult to obtain as the yield-point elongation

decreases below about 2.5 per cent at normal testing speed. That the alloy does possess an upper yield point is undoubted, because a yield-point elongation can occur only if the material has an "upper" yield point, regardless of whether the load-deformation curve shows it or not.

In Fig. 12 the irregularities in the curve after the yield-point elongation has been completed may be due to a phenomenon similar to stretcher-strain formation. At each one of these irregularities local deformation starts at a stress concentration (usually at a fillet) and the heterogeneous flow travels across the test piece like a "wave" and at some 50° to the axis of the test piece. As the wave reaches the opposite end, the load moves higher and another "flow" band moves across the piece. Annealed low-carbon steel behaves in an identical manner when deformed in the 200° to 300°C. temperature range.

This same type of heterogeneous flow occurs well beyond the yield point in Hadfield manganese steel and in the borderline alloys of austenitic stainless steel, 18-8 type.

We are of the opinion that heterogeneous flow beyond the yield point is caused by a two-stage hardening process. The first stage is the normal work-hardening process and the second is a very slightly delayed precipitation-hardening process. This explanation is unquestionably true for low-carbon steel tested at 200° to 300°C. For the 52S-O aluminum alloy the cause may be the same. In the austenitic alloys the cause of the delayed hardening may well be a slightly delayed phase change or fast precipitation-hardening following the phase change.

J. R. Low, Jr. and M. GENSAMER.—The reappearance of a small yield point when wet-hydrogen-treated sheet is cold-rolled and then annealed has not been explained. The authors are of the opinion, however, that the presence of a yield point, and perhaps to some extent strain-aging as well, depends not only on the amount of carbon or nitrogen present but also on the manner in which these impurities are distributed. For example, the addition of certain carbide and nitride-forming elements such as titanium, vanadium, columbium and chromium to low-carbon irons will serve to eliminate

* J. Winlock and R. Leiter: Some Factors Affecting the Plastic Deformation of Sheet and Strip Steel and their Relations to the Deep Drawing Process. *Trans. Amer. Soc. Metals*, 25, 163.

to yield point when added in amounts that appear to depend upon the carbon content.^{103,104}

Further, quenching low-carbon irons from temperatures somewhat below the A_c , also serves to eliminate the yield point, although it does reappear upon aging following the quenching treatment.¹⁰⁵⁻¹⁰⁷ These facts, together with the well-known effect of grain size on the yield-point phenomenon, make it appear likely that cementite at the grain boundaries or at the boundary surfaces of some smaller crystal-line unit is responsible for the occurrence of the upper yield point and Lüders-line formation.

It may be then, that the wet hydrogen treatment eliminates the yield point by the preferential removal of carbon from these boundary regions without complete decarburization. Upon cold-rolling and recrystallization, a redistribution of the carbon takes place in such a manner as to produce a structure capable of exhibiting the small yield point reported in Table 15. The grain size of these specimens after annealing was A.S.T.M. Nos. 5 to 7, so that the small yield-point elongation reported must be considered as being well below that present in these steels before hydrogen treatment.

As Leiter and Winlock point out, a discrepancy exists between the claim made in the conclusions of the paper that the yield point is completely eliminated by wet hydrogen treatment and the data of Table 5, wherein a small yield-point elongation of some 0.5 per cent in 2 in. is reported. Experience with other sheet thicknesses indicates that a longer treatment of these specimens would undoubtedly have eliminated the last traces of the yield point. We have generally considered the yield point to be eliminated for all practical

purposes when the yield-point elongation is reduced to the value mentioned above, provided that at the same time the stress for the beginning of flow was reduced to a value of approximately 12,000 to 14,000 lb. per sq. in. when treating rimmed steels. This practice was followed throughout the paper in determining the times necessary to eliminate the yield point.

On the other hand, in preparing material free from aging and the yield point for the carburizing and nitriding experiments, it was necessary to know that the last trace of the yield point had been eliminated. In this case 0.036-in. sheets were treated for 5 hr. instead of 3 hr., which according to the above criterion would have "eliminated" the yield point. Sheets "overtreated" in this manner have no yield-point elongation and the stress for the beginning of flow and the tensile strength are somewhat lower. Test results on specimens of this type are included in Table 16, where it will be noted that all of the eight specimens that were not oxidized or vacuum-annealed following wet hydrogen treatment have zero yield-point elongation.

The load-extension curves for 52S-O aluminum alloy-sheet specimens which Leiter and Winlock have included in their discussion are of considerable interest because of the many points of similarity between the behavior of this material and that observed in low-carbon steels exhibiting a yield point. Similar irregularities in the load-extension curves for other aluminum alloys have been observed; e.g., in 17S-O and 24S-O. In the latter materials, however, the Lüders lines that are formed at each irregularity are not propagated over the surface of the specimen. The sudden localized shear which leads to the Lüders line is followed by an increase in load accompanied by what appears to be a period of elastic deformation. When the load has increased sufficiently, another Lüders line of the same character as the first suddenly appears at some other point, accompanied by a second drop in the load. This process continues until finally, in the latter stages of deformation, the formation of one of the Lüders lines causes fracture. Thus, in these materials a large portion of the deformation might be described as a series of upper yield points. Since the Lüders lines formed are not propagated, no lower yield-point elongation of any great magnitude is observed.

¹⁰³ C. A. Edwards, D. L. Phillips, H. N. Jones: The Influence of Some Special Elements on the Strain-Aging and Yield Point Characteristics of Low Carbon Steels. *Jnl., Iron and Steel Inst.* (1940) 142, 199.

¹⁰⁴ G. F. Comstock: Amer. Soc. Test. Mat. Preprint No. 27 (1943).

¹⁰⁵ M. Kuroda: Origin of the Yield Point in Mild Steel. *Sci. Papers Inst. Phys. Chem. Research, Tokyo* (1938) 34, 1528-1633.

¹⁰⁶ P. Ludwik and R. Scheu: The Yield Point of Electrolytic Iron and Mild Steel. *Ber. Fachauschüsse des Ver. deut. Eisenhüttenleute* (1925) 5, 1-7.

¹⁰⁷ J. Hurford: Unpublished Senior Thesis, Department of Metallurgy, Carnegie Institute of Technology (1943).

We are in complete agreement with the view held by Leiter and Winlock that any material capable of forming Lüders lines must possess an upper yield point even though it is not observed in the autographic load-extension curve for a 2-in. specimen of the standard shape. The series of events that results in a load-extension curve having an upper and lower yield point and a marked yield-point elongation, we believe to be somewhat as follows. As the load is gradually increased the stress in some region of the test piece finally reaches such a value (usually at the fillet or a machining scratch) that the true upper yield-point stress is exceeded locally and the material fails elastically by shearing along the plane of maximum shear stress. As a result of this local plastic deformation, a Lüders line is formed. The change in section at the boundary of the Lüders line then acts as a mild stress raiser, which serves to raise the stress above the true upper yield point of the unstrained material in this region. This material then yields and

the boundary moves farther along the specimen, with no increase in the load applied until the entire specimen has been strained "through the yield point" and the particular structure leading to the phenomenon of an upper yield point has been destroyed. After the entire reduced section of the specimen has been deformed, an amount equal to the deformation occurring in the first Lüders line the yield-point elongation ends and the material then strain-hardens uniformly and the load-extension curve rises. If this picture of the mechanism of deformation is correct, the initial yield point in steels and the irregular load-extension curves of the aluminum alloys are different aspects of the same phenomenon. A lower yield point with appreciable yield-point elongation will be observed, however, only in materials in which the stress-raising effect of the Lüders line and the strain-hardening characteristics of the material are such that the Lüders line is propagated.

Tensile Properties of Medium-carbon Low-alloy Cast Steels

By H. A. SCHWARTZ* AND W. KENNETH BOCK,* MEMBERS A.I.M.E.

(New York Meeting, February 1944)

IN this paper it is shown that when the tensile strength of a given steel in various states of heat-treatment is plotted against its elongation, a straight line results. The equation of this straight line can be computed with considerable accuracy from its chemical composition. The appropriate equations are given.

The logarithm of the slope of the tensile-strength locus is shown to be proportional to the cumulative effect of the total alloy addition and the position of the line to be directly proportional to the cumulative effect of the alloy content.

It is further pointed out that heat-treatment is more effective than composition in determining yield ratio. The latter enters mainly by its effect on hardenability, which is briefly discussed. Reduction of area and Brinell number are given some incidental attention.

The data are applicable only to steels that have been normalized and/or quenched. The steels, if normalized, may or may not have been tempered. If quenched they must have been tempered at or above 400°C. (750°F.).

INTRODUCTION

Cast steels vary in composition and frequently are used in various states of heat-treatment. It is obviously important

to be able to predict the compositions that might accompany specific engineering properties by suitable selection of heat-treatments. For cast steels, which are of necessity produced heat by heat in accordance with the particular requirements of the castings to be poured, there has been, happily, much less tendency to standardization than for rolled products, whose destination is not necessarily known when particular ingots are made or rolled. It is of distinct advantage to the steel foundrymen to be able to make steel of given properties, using alloys that can be recovered from scrap, or most conveniently or cheaply bought, rather than a particular formula adopted in the interest of standardization.

The heat-treatment appropriate to securing a given result in a given steel is well known to be closely related to composition. For example, molybdenum steels are not much softened by tempering except at rather high temperatures. Highly alloyed steels are "air-hardening," and on cooling in air behave like carbon steels that have been quenched. With these matters, we do not concern ourselves in this paper, although we recognize their importance.

The entire picture evidently will be very complex and can be brought within accurate understanding only if our knowledge of test results can be coordinated in terms of general principles.

Manuscript received at the office of the Institute Oct. 19, 1943. Issued as T.P. 1719 in METALS TECHNOLOGY, August 1944.

* Respectively Manager of Research and former Engineer of Tests in the Research

Laboratory of the National Malleable and Steel Castings Co., Cleveland, Ohio. (Mr Bock is now in the Corps of Engineers, U. S. A.)

PRELIMINARY CONSIDERATIONS

Very many curves plotting the mechanical properties of a given steel against heat-treatment have been published. If the tensile strength for each heat-treatment is plotted against the corresponding elongation, the locus invariably is very nearly a straight line, even though the initial graphs were curved. This investigation thus begins with the postulate, since confirmed, that the relation under discussion is always rectilinear.

A study of the data for rather "pure steels"¹ leads to the conclusion that the logarithm of the slope of such lines is proportional to the carbon content. This was again found to be substantially true for other alloying elements, though some future comment will be necessary.

We are thus led to the much simplified problem of determining the coefficients correlating the logarithm of the slope of the tensile strength-elongation locus and its intercept on the strength ordinate as functions of chemical composition, a task that, though laborious, has presented no insuperable difficulties.

We are aware of the data of Janitzky and Baeyerztz,² which seem to indicate a curvilinear relationship. Either the present observations do not completely confirm theirs, or the discrepancy arises because in the present work account is taken of differences of composition.

The linear relation of tensile strength and Brinell number is well known. Indeed, many metallurgists estimate tensile strength by taking 500 times the Brinell number. Modifications of this relation with composition were noted and recorded. Our ideas of system in relation to yield strength and reduction of area were not found on earlier records but developed as the work progressed, and will be discussed later in the paper. There seemed some need of drawing hardenability into

the picture, and in that field we attempted to correlate our work with that of Grossmann³ as far as possible.

In interpreting test data, some recognition must be taken of the reproducibility of results. A study of the agreement of duplicate tests on metal cast from the same heat and heat-treated together, often attached to the same feeder, showed that for quenched and tempered steels having tensile strengths of about 110,000 lb. per sq. in. and elongations of about 17 per cent, the standard deviations of the test results, whether carried on by the company's Inspection and Test Department at the plant or in the Research Laboratory, are of the order of magnitude of 4000 lb. per sq. in. for ultimate strength, 3000 lb. per sq. in. for yield strength and 2 per cent for elongation. Since this result is largely independent of the testing machine or operator, and since the Research Laboratory machine is never in error by more than 0.15 per cent, these uncertainties are believed to be related to undetected variations in the test coupons themselves.

SCOPE OF THE INVESTIGATION

The matter reported here is actually only a part of an investigation covering many other properties, which was initiated in an attempt to find any existing correlations between the several observed phenomena.

It was realized in the beginning that for the investigation to have value the steels would have to be made by commercial processes, and preferably by a variety of processes. An extension of the present work, still in progress, deals with finishing techniques. In the present investigation no recognition is given to differences in processes, and no need for such recognition has developed.

The decision to use commercial heats limited the steels generally to compositions required by the trade. Only a few special heats were made. Any program of special steels was further handicapped by the

¹ References are at the end of the paper.

inability to obtain the necessary alloys when the use of all such material was severely restricted.

Since it was felt necessary to demonstrate in each case the rectilinearity of the tensile strength-elongation relation, about 40 heat-treatments, representing various combinations of normalizing, quenching, tempering and aging, were included. The assumption of rectilinearity was graphically justified in each case except for fully annealed steel and quenched steel tempered below 400°C. (750°F.). The latter *invariably* fell on the high side of the straight line, the former often fell below. The conclusions, therefore, are definitely limited in scope to exclude these heat-treatments, which commercially is not much of a handicap.

Logically, heats should have been made with various concentrations of each of the six or seven important elements while all the others were held constant, but the cost and time of such a procedure would be prohibitive. The present report is based on 25 heats whose composition was selected as judiciously as practicable from the available possibilities. This number is admittedly smaller than might be wished, but since about a ton of coupons was cast from each heat, and since the preparation and testing of specimens, metallographic and chemical confirmation, occupied more than three years (many properties not reported here were studied), it was impracticable to do more. The statistical treatment of the data upon which this paper is based occupied the computer about six months. Statistical criteria and methods must be relied upon in evaluating and interpreting the data, because of their great bulk. These are quite standardized and explained in numerous well-known texts. Under these circumstances, the reader is asked to balance the completeness and accuracy with which each heat was studied against the relatively small number of heats before criticizing the work too severely.

EXPERIMENTAL PROCEDURE

The experimental technique involved nothing unusual and may be dismissed with few words. The present investigation covers 25 heats made mostly at the National Malleable and Steel Castings Co. plant at Cicero, Ill., but partly also at the plant at Sharon, Pa. Most of the steel is acid electric metal deoxidized with calcium silicide and aluminum. A few of the Sharon heats are basic open hearth. Three heats were Ti killed instead of Al killed. Where about 2 lb. of Al was used per ton, the Al recovered in the metallic state ranged from 0.003 to 0.046 per cent, but almost always from 0.010 to 0.022 per cent. Not all the heats were analyzed. One Ti-killed heat contained 0.0065 per cent soluble Ti and 0.0049 per cent insoluble, believed to be titanic oxide. All the heats contained approximately 0.035 per cent each of sulphur and phosphorus. None of these analyses form part of the conclusions and they are offered only as descriptive of the conditions of the experiments.

The composition of the heats was determined largely by commercial considerations, but covered as well selected a range of composition as was available to us. All of them were analyzed in the Research Laboratory for all the elements of interest in the investigation.

From each heat about 150 coupons of the usual "keel-block" type were cast. These were either cast to about 1-in. diameter or rough-turned to that size before heat-treating. After heat-treating the specimens were machined to the familiar threaded-end 0.505-in. diameter form. According to the custom in this laboratory, the diameter near the middle of the gauge length was made 0.001 to 0.002 in. smaller than the ends. The data are calculated with reference to the minimum diameter, which was held within 0.001 in. to rarely 0.002 in. of the desired 0.505 in. All specimens were filed and polished to eliminate tool marks.

Any specimens showing defects externally were discarded and replaced by others. All tests were made in duplicate and in the relatively unusual case of disagreement close inspection of the fracture was made to detect a cause. If successful, the result was discarded and the specimen replaced by another. In the few cases where such examination was inconclusive, a third specimen was broken and some judgment used as to whether to take the average of three, or of the two most nearly alike. It may be well to state in passing that two heats that consistently showed flaws of the subsurface, blowhole type were discarded and replaced by others of similar composition.

A stress-strain diagram was plotted for each case, with a Berry gauge. A yield point was recorded if, at any load, strain increased "without significant increase in stress"; otherwise a yield strength corresponding to a 0.1 per cent offset was recorded.

After the specimens had been broken, the threaded end was sawed off the connecting broken part of the gauge length, the sawcut was filed and polished and a Brinell impression made at the axis of the specimen using a (1-cm.) Carboly ball.

In the portion of the work underlying this paper there were about 40 heat-treatments for each melt. It seems a waste of space to enumerate them in detail. They represent normalizing from 900°C. (1650°F.) and/or from 820°C. (1500°F.), either untempered or tempered, at a series of temperatures beginning with 400°C. (750°F.) and advancing by 100°C. (180°F.) steps to the last permissible interval below the known Ac_1 point; also, quenching from 900° or 820°C. in the latter case, sometimes after preliminary normalizing at 900°C. followed by a variety of quenches as before, but terminating at the first step above Ac_1 . Quenching was always in oil and in many heats also in water. It is known that in all cases tempering was continued (gen-

erally 2 hr.) until constancy of properties was obtained. Typical heat-treatments were followed by aging at 200°C. (400°F.). All heat-treatments were in air in a "Hump" electric furnace fitted with a Leeds and Northrup-G. E. control panel and recorder controller. Fluctuations on the chart were held to less than 5°C. Decarburization was eliminated as a variable by the amount of metal, nearly $\frac{1}{4}$ in., removed after heat-treating.

Additional small specimens approximating $\frac{3}{4}$ -in. cubes were normalized and quenched and then tempered at successively higher temperatures to determine the lowest indentation hardness obtainable on each one of the several steels.

Jominy hardness curves were obtained on each steel. The steel was normalized

TABLE 1.—Analyses of Heats
PER CENT

Heat No.	C	Si	Mn	Ni	Cr	Mo	V	Cu
1	0.31	0.44	0.71	3.35	0.02	0.03	0.00	0.07
2	0.33	0.37	1.20	0.65	0.02	0.02	0.00	0.10
3	0.38	0.43	1.43	0.01	0.03	0.02	0.00	0.10
4	0.24	0.30	0.74	0.03	0.02	0.39	0.00	0.05
5	0.36	0.32	0.73	1.67	0.54	0.26	0.00	0.04
6	0.25	0.28	0.81	1.37	0.02	0.10	0.09	0.07
7	0.32	0.41	0.81	0.00	0.08	0.04	0.00	0.10
8	0.23	0.38	0.74	0.81	0.27	0.22	0.00	0.03
9	0.35	0.34	1.18	0.02	0.03	0.02	0.00	0.10
10	0.40	0.39	0.67	0.22	1.44	0.47	0.15	0.12
11	0.395	0.89	0.46	1.00	0.04	0.27	0.00	0.02
12	0.365	0.42	1.20	0.68	0.05	0.28	0.00	0.06
13	0.385	0.48	0.74	0.16	1.12	0.33	0.00	0.09
14	0.40	0.51	0.58	0.12	1.12	0.08	0.13	0.11
15	0.39	0.38	1.50	0.09	0.06	0.41	0.00	0.12
16	0.355	0.42	1.34	1.33	0.33	0.10	0.00	0.12
17	0.395	0.52	1.51	0.08	0.16	0.21	0.09	0.25
18	0.38	0.45	1.34	0.04	0.07	0.03	0.00	0.03
19	0.355	0.44	1.26	0.07	0.11	0.11	0.00	0.64
20	0.32	0.29	1.30	0.00	0.03	0.30	0.09	0.05
21	0.325	0.47	1.41	0.06	0.38	0.11	0.00	0.02
22	0.39	0.39	1.60	0.12	0.05	0.34	0.00	0.81
23	0.52	0.58	0.83	0.01	0.02	0.06	0.00	0.10
24	0.44	0.65	0.88	0.02	0.02	0.49	0.00	0.35
25	0.42	0.40	0.75	0.03	0.01	0.16	0.00	0.11

preceding this test, because in some no "green" material remained when this stage was reached. This may be open to criticism, since many, but not all, castings are quenched without previous normalizing. The specimens were $\frac{3}{8}$ -in. diameter, enclosed in a shell 1 in. in exterior diameter. The bottom of the shell was $\frac{1}{16}$ in. thick and thermal contact was maintained

with the end of the specimen by the introduction of a little Rose metal. The procedure has been employed by Focke at the Diamond Chain Co.,¹ we think, and has

the tensile strength-elongation relation and the tensile strength-Brinell number relation may be summarized in a graph similar to Fig. 1. Even the reproduction of 25 such

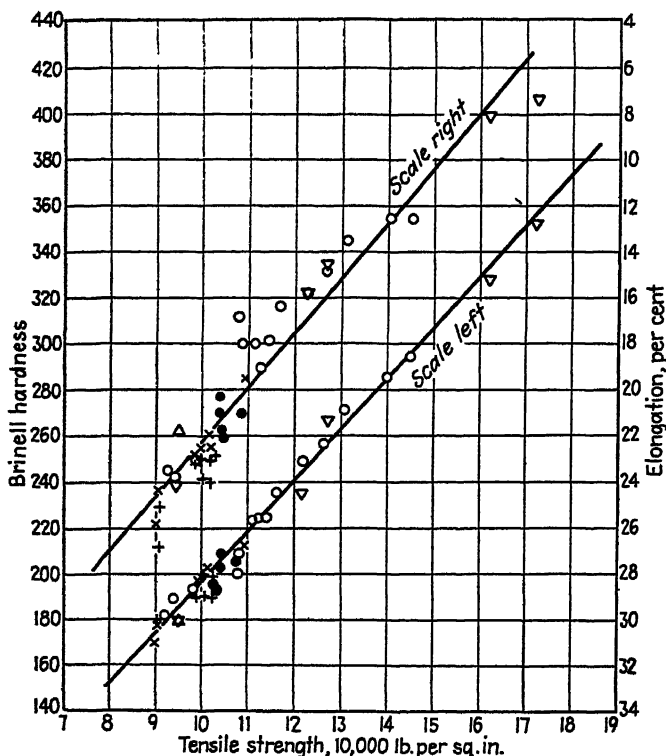


FIG. 1.—RELATION OF TENSILE STRENGTH TO BRINELL NUMBER AND ELONGATION OF A SINGLE STEEL IN VARIOUS STAGES OF HEAT-TREATMENT.

The vertical cross represents a normalizing treatment from 900°C. (1650°F).

The diagonal, or St. Andrew's cross, represents a normalizing treatment from 820°C. (1500°F).

The open circles represent quenching and tempering treatments, the quenching being in oil from either 900° or 820°C.

The solid circles represent heat-treatments that terminate in a draw at a temperature just above the A_1 point of the present steel.

The triangle pointing up represents full annealing, and the triangle pointing down, quenching.

been found in our laboratory to give results identical with the use of a full-sized specimen.

EXPERIMENTAL DATA

The analyses of the several heats are assembled in Table 1.

The test data comprise records of some 10,000 observations, which, unfortunately, cannot be included here. For each steel

figures seems avoidable, for, at least for the purpose of discussion of the three properties now in question, the trend line of each array of observations can be described, corresponding to a single steel, by record of its slope (a for elongation, x for Brinell number) and its intercept on the tensile strength or Brinell number (b and y , respectively.) This is done in Table 2. For the Brinell number, the

scatter is so small that trend lines can be determined by inspection; for elongation, they are the lines of regression of elongation on tensile strength as computed by least squares.

TABLE 2.—*Trend Lines*

Heat No.	<i>a</i>	<i>b</i>	$\pi \times 10^4$	γ
1	2 20	20 2	500	-0.3750
2	3 67	16 5	441	+1 3700
3	4 80	14 8	458	+1 3200
4	4 64	14 0	463	+0 6383
5	1 80	21 0	480	+0 4000
6	3 77	16 7	454	+0 8280
7	4 22	15 2	500	+0 2500
8	3 66	16 1	461	+1 0850
9	3 77	16 0	421	+1 7270
10	1 87	21 5	484	+0 4580
11	2 49	18 0	500	-0 5000
12	2 65	19 2	429	+1 2500
13	1 84	21 3	458	+1 0200
14	2 14	20 5	455	+1 0000
15	1 64	22 0	471	+0 2900
16	2 27	20 8	452	+0 8300
17	2 45	19 4	432	+1 5600
18	3 57	16 7	493	+0 2100
19	1 91	21 6	491	+0 0300
20	2 06	21 6	500	+0 2500
21	2 14	21 2	475	+0 2500
22	1 76	20 4	453	+0 8800
23	1 87	21 2	515	-0 3300
24	1 38	22 9	500	-0 7000
25	2 23	18 7	483	+0 5100

The minimum Brinell numbers for the several steels are recorded in Table 3.

TABLE 3.—*Brinell Numbers and Elongation*

Steel No.	Minimum Brinell	Elongation at 400° Tempering, Per Cent
1	187	9.3
2	165	16.5
3	175	10.8
4	151	18.3
5	197	5.5
6	156	20.8
7	156	21.3
8	148	16.0
9	158	16.5
10	207	1.3
11	194	3.5
12	197	13.0
13	194	5.3
14	197	7.3
15	187	0.5
16	207	3.5
17	201	5.3
18	179	14.0
19	197	7.0
20	187	11.5
21	192	10.3
22	229	0.8
23	187	6.0
24	217	3.0
25	172	8.0

The average elongation corresponding to quenching followed by a 400°C. (750°F.)

tempering process—which, be it remembered, was always found to be rather closely on the appropriate trend line—has been picked out of the records and listed in Table 3.

The Jominy curves for the 25 heats are shown in Fig. 2.

EVALUATION OF DATA

If the preliminary observations are correct, the slope *a* of the line of regression of elongation on tensile strength should be represented by such an equation as:

$$\log a = \alpha + \beta C + \gamma \text{Si} + \delta \text{Mn} + \epsilon \text{Ni} + \zeta \text{Cr} + \eta \text{Mo} + \theta \text{V} + \iota \text{Cu} \quad [1]$$

and the intercept of the line (prolonged) on the line of zero elongation *b* by an equation of similar form. The values of the Greek letter coefficients would be expected to differ in the two equations. Tables 1 and 2 give 25 values of log *a* and *b* accompanied by a similar number of

TABLE 4.—*Coefficients*

	Log <i>a</i>	<i>b</i>	<i>T</i> ₀	<i>E</i> ₀
Constant	1.25262	5.18479	3 7798	50 467461
C.....	-0 01665	0.23237	+0 0679	-0 627065
Si . . .	0 00053	-0.00172	+0 0102	-0 081446
Mn . . .	-0.00096	0.02501	+0 0159	-0 073307
Ni . . .	-0 00094	0.01632	+0 0047	-0 037237
Cr . . .	-0 00055	0.01633	+0 0095	-0 047877
Mo . . .	-0 00505	0 07174	+0.0196	-0.200159
V . . .	-0.00064	0.04259	+0.0119	0.075156
Cu . . .	-0 00114	0.01841	+0.0066	-0.031304

values of the concentrations of the eight elements. The chemical symbols in Eq. 1 represent the concentrations of the respective elements. Having 25 equations in nine unknowns, the problem is "over-determined" and, by least squares, the values can be calculated of the Greek letter coefficients that will make the best fit, considering all 25 steels. These coefficients are assembled in Table 4. The standard error of fit for log *a* is 0.0745 and for *b* is 1.431, the units of measurement being 0.01 per cent for concentration, 10,000 lb. per sq. in. for tensile strength and 1 per cent for elongation.

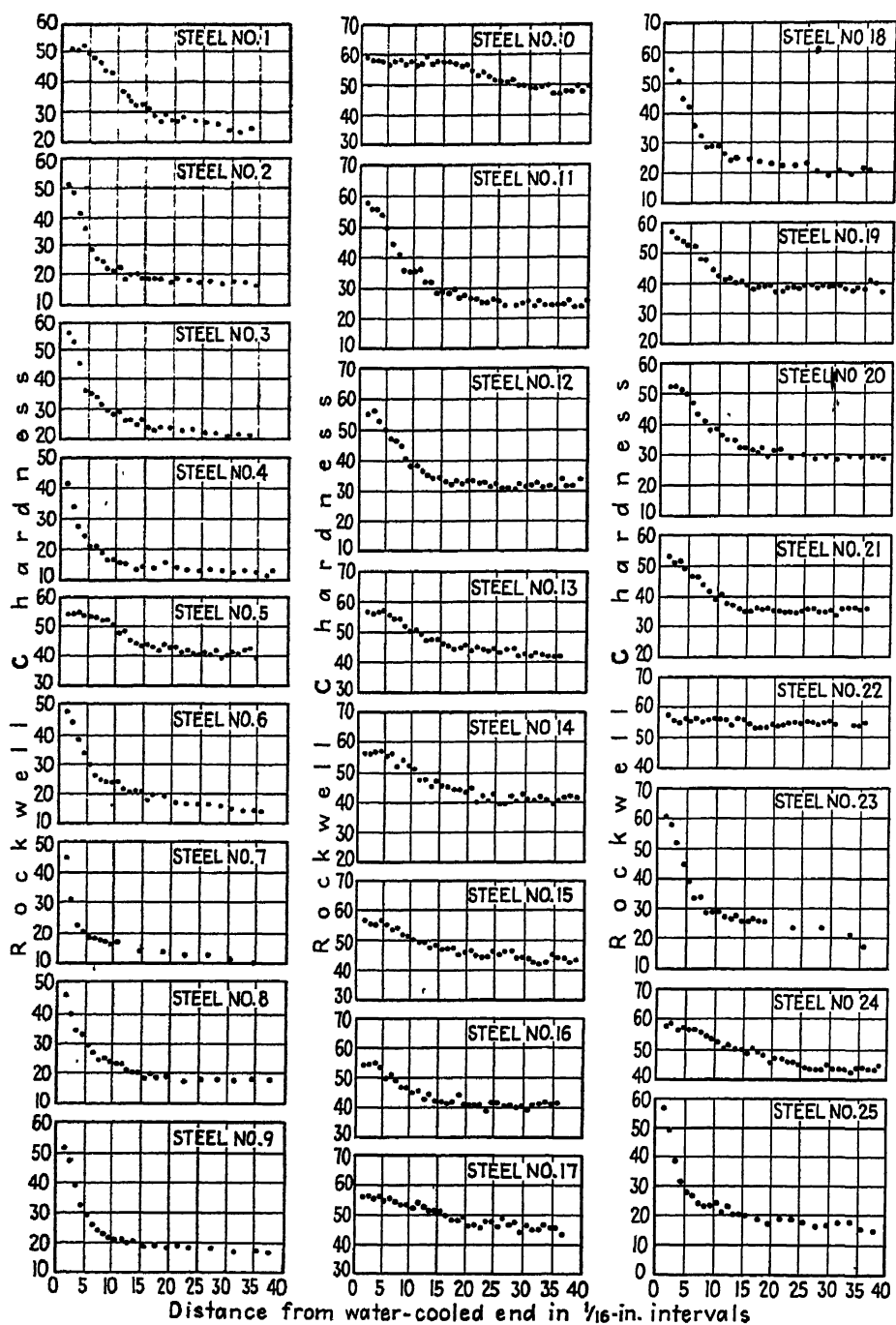


FIG. 2.—JOMINY CURVES OF THE TWENTY-FIVE STEELS.

From the values of x and y in Table 2, the tensile strength T in units of 10,000 lb. per sq. in., corresponding to a given Brinell number B , follows from

$$T = Bx + y \quad [2]$$

Using the data of Table 2, the minimum tensile strength T_0 of each steel is calculable and related to composition by least-squares calculation, as before. The appropriate coefficients are also included in Table 4. The standard error of fit of calculated and observed values of T_0 is 3060 lb. per sq. inch.

Setting these values of T_0 for T in Eq. 2 along with the corresponding values of a and b will yield the maximum obtainable elongation.

Again, by the usual least-squares method of elongation, E_0 of specimens quenched and tempered at 400°C. (750°F.) has been expressed in terms of composition by an equation of the form of Eq. 1, and the proper coefficients included in Table 4. The standard error of fit is 2.03 per cent.

Our study of yield points and yield strengths and of reduction of area has not yet advanced to the point where we wish to correlate them quantitatively with chemical compositions; therefore this paper will not be burdened with numerical data on this subject.

DISCUSSION OF OBSERVATIONS

It is plain that using equations of the form of Eq. 1, and the data of Table 4, the parameters a and b of the locus of the tensile strength-elongation relation of any steel can be calculated easily from its composition and its equation can be expressed in the form

$$E = a(b - T) \quad [3]$$

From the data of that table, T_0 , the minimum attainable tensile strength, also can be calculated. Substituting T_0 for T in

Eq. 3, the maximum elongation (E_{\max}) will be obtained:

$$E_{\max} = a(b - T_0) \quad [4]$$

From Table 4 and an equation having the form of Eq. 1, E_0 , the minimum elongation obtainable by tempering at not less than 400°C., can be calculated. Suitable substitution yields a value for the maximum tensile strength T_{400} to which an equation of the form of Eq. 3 would apply for a given steel.

Needless to say, this gives complete knowledge of the obtainable properties within our self-imposed limits of heat-treatment; which, incidentally, cover pretty much the entire commercially desirable range.

There is a generally accepted opinion that nickel concentrations greater than about 2 per cent are not useful. We were led to consider the possibility that the effect of that metal on $\log a$ and b might not be linear as postulated. Plotting the difference between the observed values of these parameters and the calculated value neglecting nickel against the concentration of that element did not suggest any need for a correction of that type. A similar investigation with regard to chromium and manganese, the only other elements studied in considerable concentration, corroborated this conclusion. It is to be remembered that this statement is made from the relatively practical viewpoint of predicting the properties of commercial steels and that the program followed was not suited to an investigation of purely academic interest into the effects of very low concentrations of alloys.

If the coefficients for calculating $\log a$ and b from composition were in the same ratio for all elements, there would be no choice, as far as attainable combinations of elongation and tensile strength are concerned, between various types of alloys; in fact, no alloy steel would produce any

result not attainable by a plain carbon steel. This is exclusive of considerations like hardenability, which determine how deeply steels will harden, or their casting

significance. The practical significance of the correlation of $\log a$ and b is that there is but a limited possibility of altering the relation of tensile strength to elongation by

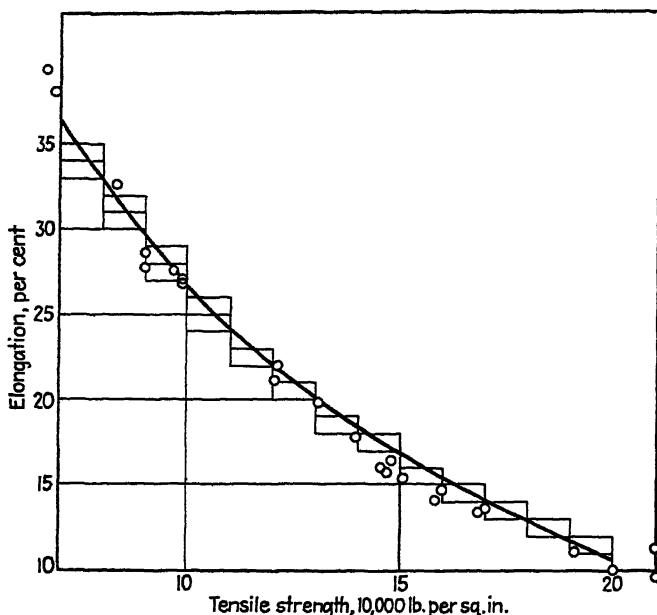


FIG. 3.—FIRST APPROXIMATION OF THE BEST ATTAINABLE COMBINATION OF TENSILE STRENGTH AND ELONGATION.

Circles are points of closest approach of the observed loci to the curve.

characteristics. Molybdenum and carbon do have coefficients almost exactly in the same ratio, and substitute for one another in constant proportion as far as the properties under discussion are concerned. It is, of course, much easier to produce the properties associated with drastic quench in molybdenum steels than in carbon steels in sections of considerable thickness. Nickel and copper present such similarities of constants as to suggest a considerable degree of interchangeability.

The various constants of Table 4 do not seem to be merely unrelated empirical values but often possess a high degree of correlation. The correlation coefficient of $\log a$ and b is -0.975 . The correlation coefficient of x and y is -0.92 . Both of these have a very high degree of statistical

selection of alloys. Even a and y in the table have a correlation coefficient of 0.66 , which is highly significant statistically. Had it been assumed that the relation of a and b did not depend on any particular choice of alloys, then by least squares from Table 4:

$$\log a = 1.52 - 0.0588b \quad [5]$$

It can be shown that this equation represents a family of straight lines tangent to the locus of

$$E = 1.954 - 0.0588T \quad [6]$$

T being in units of $10,000$ lb. per sq. in., as elsewhere in this paper. This locus is shown in Fig. 3 and represents the best attainable combination of properties by limitless choice of composition and heat-

treatment subject to the fallacious assumption that the combinations do not depend upon the particular alloys selected. It furnishes, however, a useful first approximation of what is attainable.*

It was the authors' hope to examine their data on hardenability in the light of Grossmann's, but certain difficulties were encountered. In this investigation there was a somewhat greater range of grain sizes, and there were difficulties in deciding what constituted the "half hardness." Vaguenesses also arose with very hardenable steels containing much chromium.

Metallographically there is no region in which the structure of our steels contained only martensite and troostite; ferrite was always present. To establish the conditions under which the Jominy tests of this investigation were equivalent to Grossmann's "ideal critical diameter," it was found empirically that a half hardness value should be selected about one Rockwell C number higher than Grossmann's maximum assumption for his alloy steel of equal carbon content; also, the lower boundary of his effect of chromium should be selected. With these assumptions, no systematic variations were found from calculated values that suggested any revision of the factors for particular elements. The writers were not, however, able to bring about an agreement within 15 per cent between calculated and observed values.

So far we have not been able to bring about an entirely satisfactory understanding of yield strengths (yield points), although we have established certain principles and qualitative relations as a basis for further mathematical treatment, which should be of interest in the present connection.

In brief, we find that any steel within the range of our studies may have either

* Can Janitzky and Baeyeritz' curved loci be similar approximations to a series of straight lines or are they comparable to our observations on material tempered below 400°C.?

a yield point or a yield strength. The result depends upon the type of heat-treatment; hence, to some extent, but not completely, on the Brinell number. The transition value of this property when a change is made from one type of plastic deformation to another is not perfectly sharp and apparently bears some relation to composition.

The yield ratio of a steel apparently is determined much more by the type of heat-treatment than by the composition, and is but little affected whether there is a yield strength or a yield point.

On the first 18 of the present series of steels it was found that either the yield point or yield strength (Y) was related to the tensile strength T , both in units of 10,000 lb. per sq. in., by

$$Y = -3.39 + 1.06222T \quad [7]$$

if the steels were limited to oil-quenched steels tempered at and above 500°C. Lower tempering temperatures and more drastic quenches raise the value of Y for a given value of T . There seems to be no doubt that hardenability must be drawn into these considerations, for evidently, in imagination at least, a steel might have a composition rendering it fully hard as the result of air quenching, or completely unhardened by the most drastic quenching.

However, normalized and tempered steels all seem to conform rather well to

$$Y = -1.66 + 0.83993T \quad [8]$$

Untempered steels cannot be nearly so well coordinated, perhaps for the hardenability reasons just given. Their yield strength (YS) when they have no yield point, is not identical with the latter (YP) if it exists, for equal tensile strength. Empirically, the relations are

$$YP = 0.35 + 0.62658T \quad [9]$$

and

$$YS = 0.18 + 0.54637T \quad [10]$$

Quite similar equations can be developed for the ratio of elongation to reduction of area. It may be assumed that the proper complete treatment of the properties of a steel here enumerated will consist of:

1. The correlation of tensile strength and elongation in terms of composition.
2. The correlation of tensile strength and Brinell number in terms of composition.
3. The determination of maxima and minima for the above in terms of composition.
4. The relation of yield strengths or points to tensile strength in terms of heat-treatment and hardenability.

5. The relation of reduction of area in terms of heat-treatment and hardenability.

Having completed well over half this task and recorded substantial progress in the remainder, we do not wish to deprive other steel-foundry metallurgists of the useful information obtained, while we delve into the final stages.

CONCLUSION

It has been shown that within the limits of composition and heat-treatment recorded in the body of this paper, the combinations of tensile strength and elongation obtainable from a given steel by variations in heat-treatment fall upon a straight line whose length, position and direction can be calculated with considerable accuracy from the chemical composition.

It has also been shown that similar statements may be made regarding Brinell number and tensile strength.

Reasons have been given for believing that the yield ratio of a steel can be expressed in terms of its heat-treatment and hardenability; also that similar statements may be made regarding the ratio of elongation to reduction of area.

It is hoped that this relationship will be useful in determining the chemical composition best suited to obtain a given mechanical result.

None of the data and conclusions of this paper involve anything but expected values. They include no tolerances that would make them applicable to the formulation of specifications without further knowledge of the reproducibility of results under operating conditions.

ACKNOWLEDGMENTS

So many employees of the National Malleable and Steel Castings Co. have participated in this investigation that it is practically impossible to enumerate them all. The metallurgical staffs of the Cicero and Sharon plants, and many employees of the laboratory, have contributed material and effort most generously.

We wish especially to express our thanks to Mr. Charles H. McCrea, President, for authorizing and encouraging publication; to Mr. J. O. Houze (retired), formerly manager of the company's Cicero plant, for suggesting that an investigation of this type would yield useful returns, and to Mr. Charles H. Junge, formerly of the Research Department, for the work on hardenability.

REFERENCES

1. F. T. Sisco: Alloys of Iron and Carbon—Properties. Alloys of Iron Monographs, 2. New York, 1937. McGraw-Hill Book Co.
2. E. J. Janitzky and M. Baeyer: The Marked Similarity in Tensile Properties of Several Heat Treated SAE Steels. Metals Handbook (1939) 515. Amer. Soc. Metals.
3. M. A. Grossmann: Hardenability Calculated from Chemical Composition. *Trans. A.I.M.E.* (1942) 150, 229.
4. A. E. Focke: Hardenability of Steel. *Iron Age* (Sept. 3, 1942) 58.

ADDENDA

Further evaluation of the original data, carried on since the paper was written, has developed certain additional points of interest.

The standard error of fit in log a and b recorded on page 255 involve uncertainties in E for a given T , which depend upon whether or not the error from both variables can be additive. The deviation of the

individual values of $\log a$ and b in Table 2 from those calculated from Tables 1 and 4 were compared and found to have a correlation coefficient of minus 0.93. High values

The resemblance of the coefficient of e_b above to that of b in Eq. 5 suggests that the remaining discrepancies are due to unaccounted-for causes, similar in char-

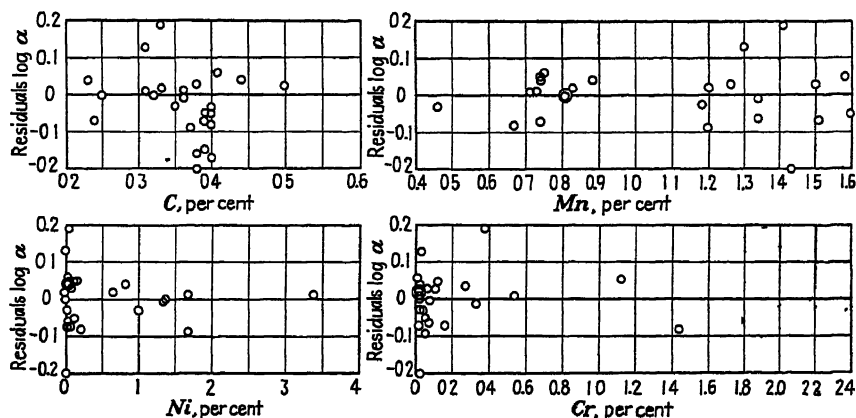


FIG. 4.

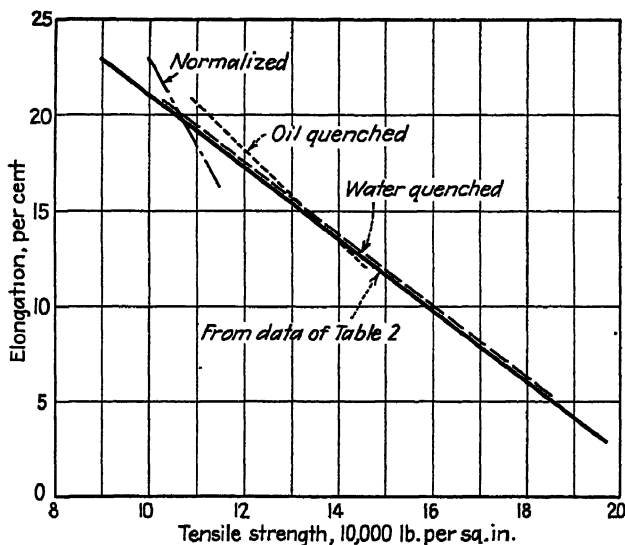


FIG. 5.

of $\log a$ thus very systematically accompany low values of b and the two sources of error compensate to a large extent.

The two residuals $e_{\log a}$ and e_b are related by the equation

$$e_{\log a} = 0.00029 - 0.0485e_b \quad [11]$$

acter to those controlling the general relationships here studied.

In confirmation of the validity of the assumption that $\log a$ (not a) is calculable by taking the sum of the effects of the several elements, Fig. 4 has been prepared. The residuals in $\log a$, comparing computed

with observed values, are plotted against content of the four elements present in a considerable range of concentrations in the series of steels. The array of points form random patterns around a horizontal line and indicate no tendency to a slope or curvature. This is evidence that for these elements, the logarithmic function satisfactorily represents the change of σ with concentration.

The postulate that the relation of elongation to tensile strength is independent of the type of heat-treatment is actually only a simplifying assumption, justified by the fact that the errors introduced are almost always insignificant in magnitude as compared with the precision of observation, and also of little engineering importance.

If one is more concerned with fundamental principles than practical applications, separate trend lines for normalized and tempered, oil-quenched and tempered and water-quenched and tempered steel may be computed. These fall frequently into some such relation as shown in Fig. 5. The two types of quenching treatments have similar trend lines, the slopes differing in the direction shown, and the normalized steels having a much steeper trend. Since the range of tensile strength realizable by normalizing and tempering is, however, usually relatively short, the errors in elongation introduced by the assumption of a common trend are seldom great.

Separate constants might be computed for each type of cooling and predictions based on an assumed type of heat-treat-

ment. The result would be some improvement in precision at the expense of greater labor in computation.

DISCUSSION

(*F. B. Foley presiding*)

N. A. ZIEGLER,* Chicago, Ill.—This paper is of a considerable interest to us because its authors use about the same line of attack in studying properties of cast steels as we do in our work. In general, the present results check quite well with ours and there is only one point I would like to bring up. The present paper does not give any data on impact resistance, and yet it is known that, depending on heat-treatment, its values may be quite different even though the tensile strength and hardness are the same. This is particularly true regarding thermally sluggish steels with suppressed transformations.

For example, No. 10 (Table 1) is definitely an air-hardening steel. If it is normalized from over 1600°F. and drawn at about 1250°F., its tensile strength will be well over 100,000 lb. per sq. in. with an elongation of about 25 per cent and hardness of 200 to 250 Brinell. At the same time, its impact resistance will be of the order of 20 ft.-lb. Charpy (keyhole notch). If, on the other hand, the same steel is heated to the austenitic state—i.e., to about 1600°F.—cooled to about 1350°F. and permitted to transform, its tensile strength, elongation and hardness may be very much the same as in the normalized and drawn condition, but its impact resistance will be quite low. This is true of all steels that have a tendency to air-harden; i.e., possess suppressed transformations with relatively slow cooling rates, such as annealing or even normalizing.

* Research Metallurgist, Crane Company.

Variables Affecting the Results of Notched-bar Impact Tests on Steels

BY CLARENCE E. JACKSON,* MEMBER A.I.M.E., MYRON A. PUGACZ,* JUNIOR MEMBER,
AND FRANK S. MCKENNA*

(New York Meeting, February 1944)

THE notched-bar impact test has proved worth while in certain applications as a test for control of the quality or the heat-treatment of steel. In view of the serious thought that even so simple a test as the tensile test has evoked during the past years, it is not surprising that the notched-bar impact test should have inspired much experimental work. The correlation of the great number of data has not been successful, although steady progress has been made toward a better understanding of this test. Progress has been made, especially, in the isolation of the effects of the many variables that control the results. The stress system imposed on a specimen with a notch is so complicated and unpredictable that no simple evaluation of the test has been possible. Because of this uncertainty, many engineers hesitate to use the notched-bar impact test, and this attitude may well continue until a better understanding of the effects of the variables in the test are available.

Without doubt, any additional data that may be presented should be accompanied by as complete a description of the details of test as possible, so that it may be added to the general fund of information

that is to serve as the basis for the theory of the notched-bar impact test. The many factors that may control the test results have been pointed out repeatedly. The importance of the effect of the type and dimensions of the specimen has been recognized.

Most of the work reported by American investigators has been limited to small-size (Charpy) specimens tested as a simple beam; two types of notches (Fig. 1) have been commonly used. Considerable data have also been presented by many investigators using a small specimen tested as a cantilever beam; this commonly being called the Izod test. Here, however, a shear component of stress makes the stress system even more complex than that present in the simple beam type of test, hence a critical analysis is difficult. Much work has also been reported by investigators using the tension type of specimen.

A second variable that must be controlled is the testing temperature. An indication that the tests were performed at room temperature is not sufficient, since in many steels a variation of a few degrees in the actual testing temperature may be sufficient to give an entirely different range of results. Other factors, such as the composition and condition of the material being tested and the speed of test, should also be considered.

Many investigators have contributed data and theoretical discussions on the problems encountered in notched-bar test-

This paper represents only the personal opinions of the authors and in no way reflects the official attitude of the U. S. Navy. Manuscript received at the office of the Institute Dec. 20, 1943. Published by permission of the Navy Department. Issued as T.P. 1668 in METALS TECHNOLOGY, August 1944.

* Division of Physical Metallurgy, Naval Research Laboratory, Anacostia Station, Washington, D. C.

ing; notably, Moser,¹ Greaves and Jones,² Maurer and Mailander,³ followed by the more recent work of Hoyt,⁴ McAdam and Clyne,⁵ Gillett⁶ and Rosenberg.⁷ An ex-

type with a length of 160 mm. and fracture across a section 15 by 30 mm., a specimen considerably larger than that commonly used in this country. The method of

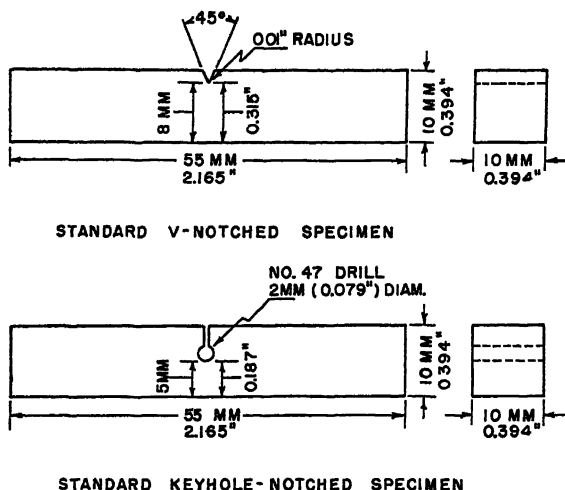


FIG. 1.—TYPES OF SPECIMENS.
Breadth was varied for many tests; e.g., 5 mm. for $\frac{1}{2}$ breadth.

tensive treatise is presented in Gmelins Handbuch der Anorganischen Chemie,⁸ while The Manchester Association of Engineers devoted much of its 1937-38 session to an extensive discussion of notched-bar impact testing.⁹

In general, the investigators agree that the total energy absorbed by a notched-bar specimen during test is due not only to the resistance to fracture but also to the resistance to deformation. The exact relationship and the relative importance of these two factors in any particular test is often obscure and exact correlation is difficult. Fortunately, however, the exact relationship may not be necessary for an evaluation of the test values encountered in notched-bar testing.

It has been suggested by Moser¹ that the volume of metal that is strained in the rupture of a test specimen is a function of the total energy absorption. Moser's specimen was of a keyhole-notched Charpy

measuring the volume of strained metal was that of observing the Hartmann or flow lines appearing on the side of a polished specimen and did not take into account the fact that the metal next to the fracture undergoes considerably more strain or deformation than the area farther away from the fracture. Also, it has been mentioned frequently that the volume deformation cannot be measured with any degree of accuracy by surface deformation, since at the surface all normal components of stress must vanish, and at a point near the surface a metal cannot resist deformation in the same way as at a point farther from the surface.

The present discussion is an outgrowth of the information on the notched-bar test accumulated from the studies of various types of test pieces that have been used in the determination of the quality of weldable steels. The complete picture of the relationship of the effects of many of the variables of notched-bar behavior

¹ References are at the end of the paper.

in testing plain carbon and low-alloy steels is not simple. Additional data are presented in the following study, however, in the hope that future investigators will be aided in this intriguing search for a more complete evaluation of notched-bar behavior.

TEST SPECIMENS

The majority of test specimens were standard keyhole or V-notched Charpy specimens (Fig. 1) with modifications of breadth. The notches in the V-notched type of specimens were milled with two

TABLE 1.—*Composition of Steels Investigated*
PER CENT

Specimen No.	C	Mn	Si	Ni	Cu	Mo	V	Cr	S	P	Al	Ti
1	0.17	0.41	0.17	1.97	0.28	0.002	0.001		0.007	0.032	0.04	
2	0.25	0.43	0.20						0.028	0.014		
5	0.21	0.38	0.003						0.026	0.013		
6	0.27	0.47	0.002	2.08	1.02	0.004	0.005		0.017	0.045	0.05	
9	0.24	0.48	0.23	0.59	1.01		0.003		0.011	0.027	0.01	
10	0.27	0.74	0.21						0.029	0.017		
11	0.29	1.06	0.25						0.002	0.017	0.003	
18	0.22	0.47	0.18			0.50			0.015	0.009		
20	0.24	0.46	0.001						0.051	0.022		
22	0.18	1.40	0.21				0.12		0.020	0.017		
27	0.06	0.35	0.002	1.95	0.94				0.020	0.088		0.005
29	0.028	0.19		2.08					0.044	0.002		
30	0.09	0.72	0.047	0.96	1.34	0.11			0.023	0.050		
31	0.24	0.74	0.012	0.76	1.48	0.16						
32	0.12	0.75	0.48					0.34	0.023	0.014		
33	0.11	0.38	0.19			0.51		5.85	0.005	0.015		
37	0.28	0.68	0.20	2.5					0.019	0.030		
51(1c)	0.19	0.51	0.054						0.017	0.033		
52(2c)	0.19	0.41	0.14						0.011	0.040		
53(3c)	0.43	0.79	0.27						0.041	0.041		
54(4c)	0.25	0.47	0.003						0.029	0.011		
56(6c)	0.12	0.41	0.030						0.022	0.035		
57	0.25	0.47	0.003						0.029	0.011	0.001	
58	0.50	0.58	0.005						0.046	0.016	0.001	
59	0.42	0.64	0.002						0.050	0.024	0.006	
60	0.50	0.41	0.003						0.047	0.021	0.004	
61	0.54	0.82	0.28						0.030	0.024	0.01	
63	0.17	0.46	0.23	1.43					0.024	0.016		
72	0.13	0.73	0.27	0.20	0.47				0.023	0.086		
82	0.36	0.83	0.28	1.67		0.33		0.79	0.021	0.027	0.03	
A	0.21	0.89	0.22						0.020	0.015		
B	0.18	0.90	0.24						0.029	0.014		
C	0.27	0.90	0.18						0.030	0.016		
D	0.39	0.80	0.19						0.020	0.021		
E	0.15	0.44	0.19	3.39					0.029	0.012		
F	0.12	0.40	0.31			0.48		2.02	0.011	0.014		
G	0.13	0.51	0.15			0.48		5.53	0.007	0.022		
H	0.05	0.46	0.34	8.98				17.51	0.009	0.011		

MATERIALS

The chemical composition of the plain carbon and low-alloy steel plates used in this investigation is given in Table 1. All materials were commercial hot-rolled steels $\frac{1}{2}$ in. thick, with commercial tolerances, and were tested either in the as-rolled or in the normalized condition, with specimens cut, unless otherwise specified, longitudinally to the direction of rolling. Details of the test specimens are given with each series of data.

machine cuts with automatic feed, using a special form of milling cutter designed so that it could be resharpened without changing the outline of the cutting tooth. The contour of the notch in the specimens was checked frequently microscopically at 100 diameters magnification, to maintain the dimension of the notch to within a thousandth of an inch.

EQUIPMENT FOR TESTING

An Amsler pendulum machine was used for breaking the notched bars in impact

loading. All tests were run using the full energy capacity of the pendulum (220 ft-lb.) with a striking velocity of 17.4 ft. per second.

This statement is true only for certain brittle steels and for a limited range of breadth of specimens. Many low-carbon and low-alloy steels with high energy-

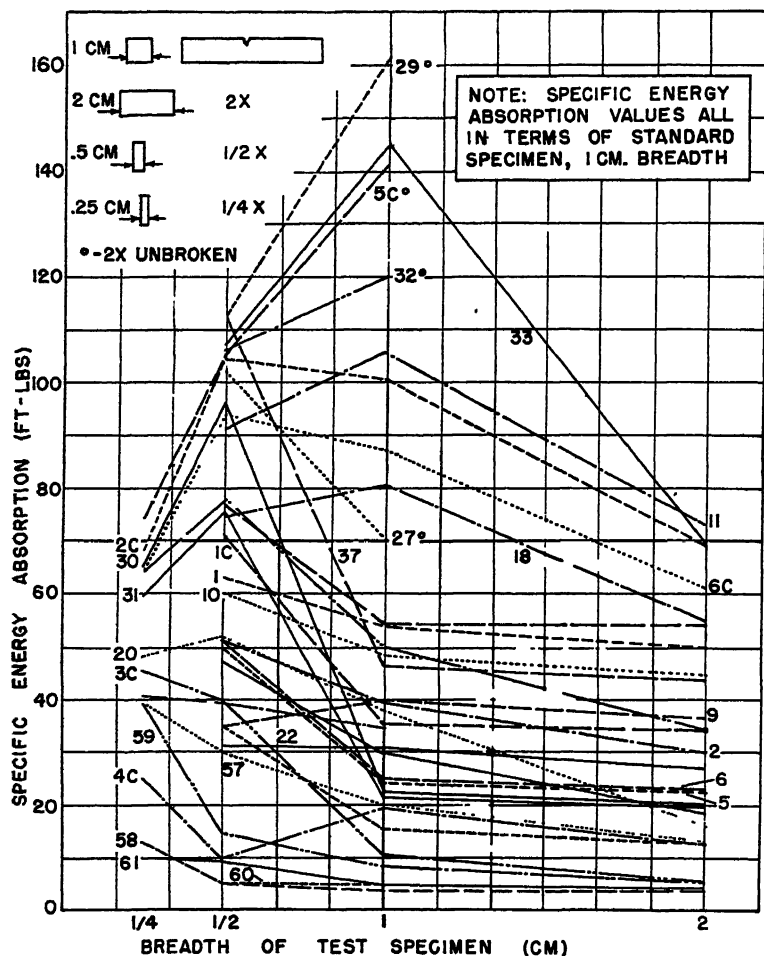


FIG. 2.—EFFECT OF BREADTH OF SPECIMEN ON ABSORPTION OF SPECIFIC ENERGY FOR CHARPY V-NOTCHED BAR.

All values in terms of standard specimen of 1-cm. breadth.

TESTS AND DATA

Effect of Breadth of Specimen

It has been stated repeatedly^{4,5} that the general effect of increase in breadth of the notched-bar impact specimen is to reduce the specific notched-bar value.

absorbing capacity require additional consideration. The data for different breadths of specimen for 27 low-alloy and carbon steels are plotted in Fig. 2. All specific energy-absorption values are based on a standard section of 10 by 10 mm. (0.394 in.) with a notch 2 mm. (0.079 in.) deep.

The relation of decreasing energy absorption per unit area with increasing breadth is applicable only to the more brittle steels with standard notched-bar values lower

A similar behavior is to be noted for specimens with the keyhole type of notch, as shown in Fig. 3. Additional data represented by the steels A to H, which have

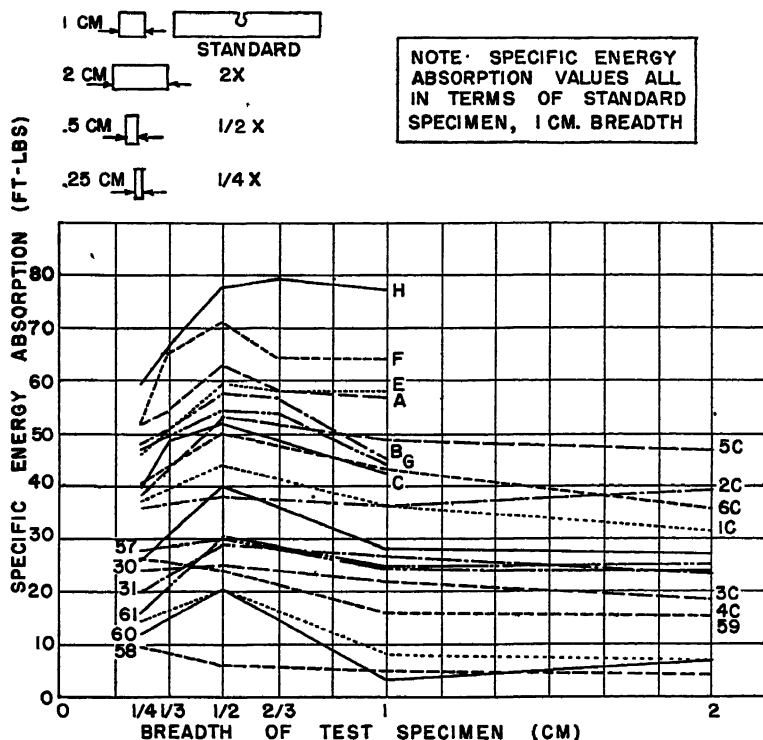


FIG. 3.—EFFECT OF BREADTH OF SPECIMEN ON ABSORPTION OF SPECIFIC ENERGY FOR CHARPY KEYHOLE-NOTCHED BAR.

All values in terms of standard specimen of 1-cm. breadth.

than about 60 ft-lb. In the tougher and more ductile steels the relation of resistance to deformation and resistance to fracture is such as to give a lower specific energy absorption for the narrow specimens. Probably the reason for this is that the initial deformation shifts the sectional mass of the specimen so that the area in which initial fracture must occur is reduced. On the other hand, the rigidity of wide specimens apparently is sufficient to retain the sharpness of the notch. The exact balance between resistance to deformation and resistance to fracture will always determine the behavior of the test specimen.

been presented by Habart and Herge¹⁰ are also included.

It is interesting to note that in these specimens with higher energy absorption the maximum specific energy absorption occurs with approximately a square fracture section; i.e., in the keyhole notched bar with one-half breadth and in the V-notched bar type of specimen with one-half to standard breadth.

Effect of Radius of Notch

The total energy absorbed in a notched-bar failure depends upon the energy absorbed in the deformation of the test

specimen together with the energy necessary to overcome the cohesive strength of the material. The relative importance of these two factors for a given material

a section 10 mm. (0.394 in.) square and a length of 55 mm. (2.165 in.) were notched to a depth of 2 mm. (0.079 in.) with a standard Charpy-type V-notch and with

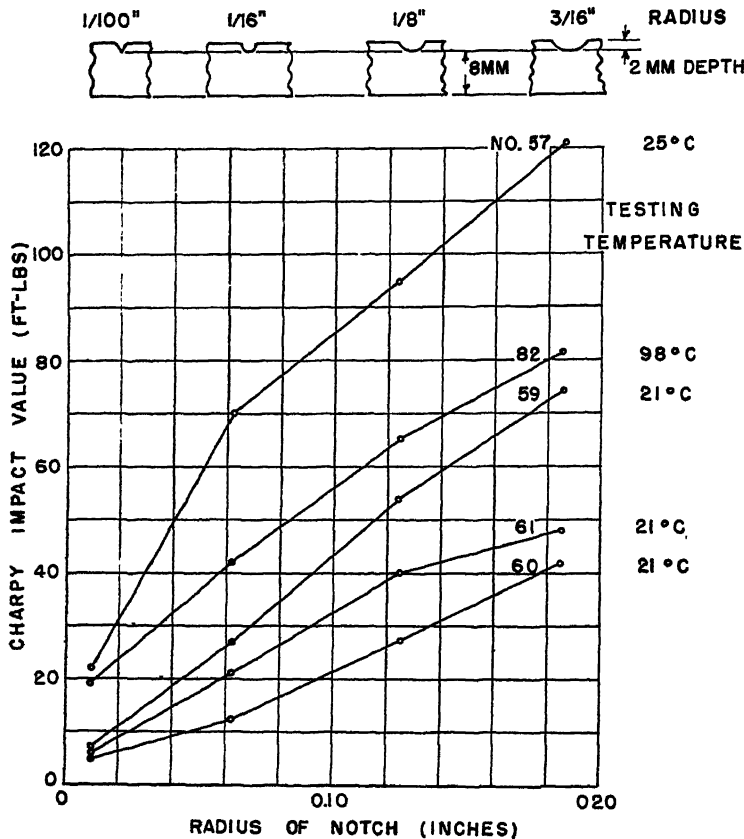


FIG. 4.—EFFECT OF NOTCH RADIUS ON CHARPY IMPACT VALUE.

depends much upon the geometry of the test specimen. In the notched-bar test, it is possible to change the relation of the resistance to fracture and the resistance to deformation by varying the radius of the notch. A sharper notch causes a greater tendency for brittle failure whereas an increase in the radius of the notch gives greater deformation with less tendency toward brittle behavior.

The effect of increasing the radius of the notch in similar notched bars is given for a number of steels in Fig. 4. Specimens with

milling cutters of $\frac{1}{16}$, $\frac{1}{8}$ and $\frac{3}{16}$ -in. radii. As the radius of the notch increases, the energy required to fracture the test specimen is increased.

Comparison of Keyhole and V-notch Specimens

The uncertain relation between the behavior of the V-notch and keyhole type of specimens is often mentioned. A comparison of these behaviors can be made only when variables such as temperature of test or width of specimen are considered.

The effect of type of notch and breadth of specimen on Charpy notched-bar values

cided increase in sensitivity is shown for the V-notched type.

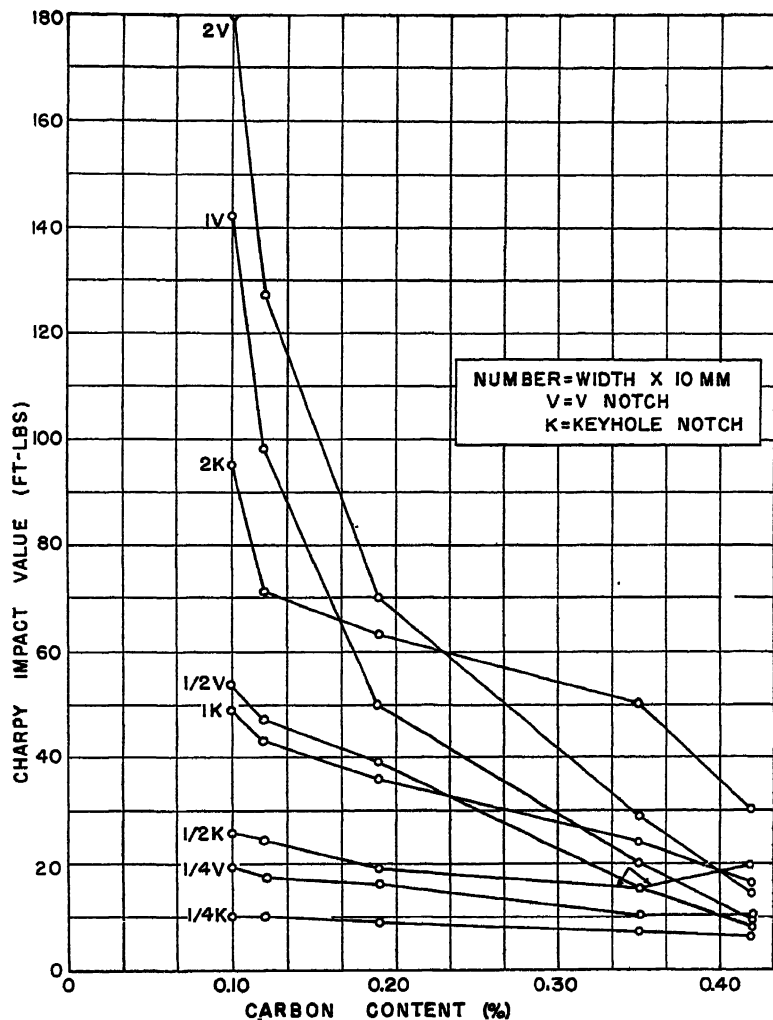


FIG. 5.—EFFECT OF TYPE OF NOTCH AND WIDTH OF SPECIMEN ON CHARPY IMPACT VALUE OF A SERIES OF PLAIN CARBON STEELS.

(temperature of test 70°F.) is shown in Fig. 5 for a series of hot-rolled plain carbon steels. Here again the sensitivity of the V-notched specimens is evident. These data also throw doubt on the validity of the results of subsize specimens, although in a comparison of the values for $\frac{1}{2}$ -width V-notched and keyhole specimens a de-

Effect of Temperature of Test

Of the variables that affect the relationship between resistance to plastic deformation and resistance to fracture, the one of primary importance is the effect of testing temperature. For some steels the effect of breadth of specimens becomes of

greatest importance in tests at room temperature (Fig. 6). It is generally agreed that reduction in testing temperature has very minor effect on resistance to fracture.

room temperature to temperatures below room temperature and, second, the area of low energy absorption just below the A_1 transformation temperature. The ap-

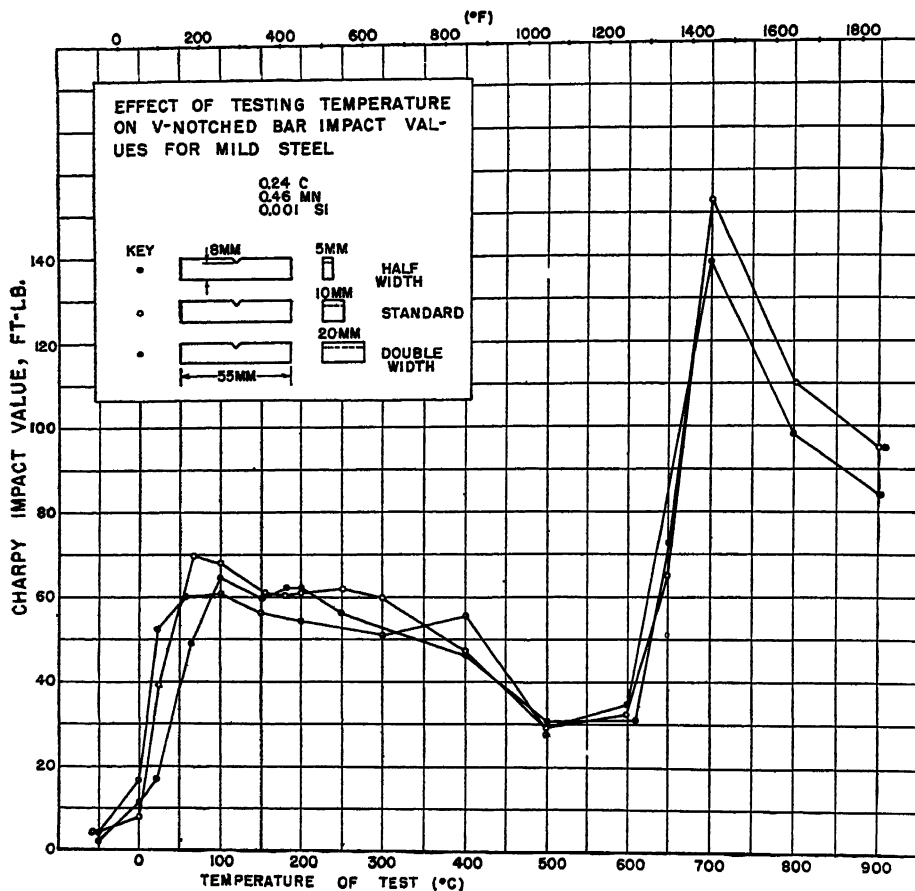


FIG. 6.—EFFECT OF TESTING TEMPERATURE ON V-NOTCHED BAR IMPACT VALUES FOR MILD STEEL.

However, for many steels, the resistance to deformation, and hence the total energy absorption, is greatly affected by a decrease in testing temperatures. Low-carbon steels are especially sensitive to the influence of low testing temperature. Two areas of increased brittleness are to be noted (Fig. 6): first, the area of rapid transition from high to low energy absorption as the temperature is decreased from just above

pearance of standard and double-width specimens for various testing temperatures is shown in Fig. 7 to be very similar, except those tested at room temperature.

The effect of temperature of test on the results for standard V-notched and keyhole specimens from a low-alloy high-tensile steel is shown in Fig. 8. The increased sensitivity of the V type of notch is shown by the steeper low-temperature drop and

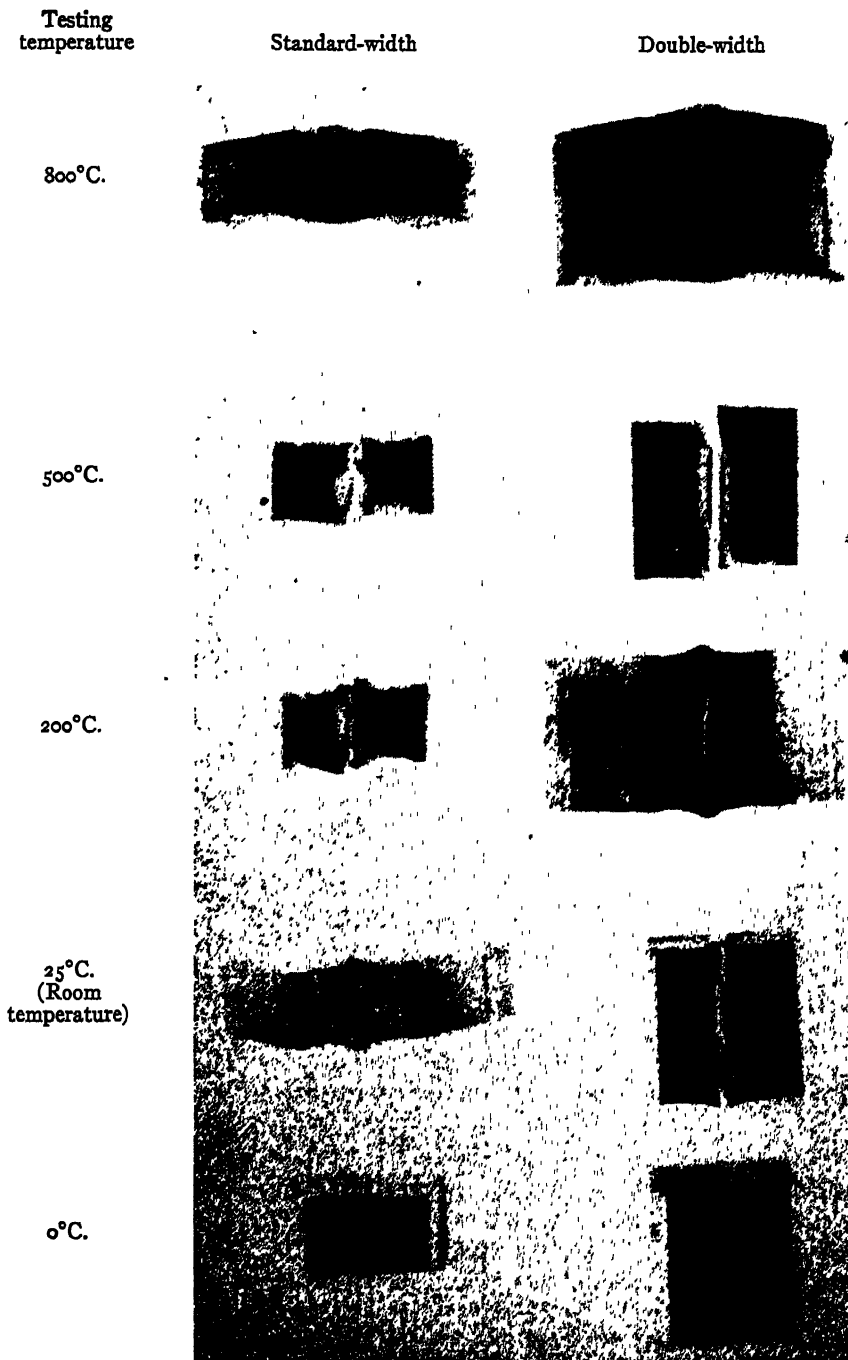


FIG. 7.—EFFECT OF BREADTH OF SPECIMEN ON TYPE OF FRACTURE FOR VARIOUS TEMPERATURES.

the wider range of values. It is difficult to obtain reproducible values for the V-notched-bar impact specimens for tests performed on many steels in the transition

bend machine is reported by Petrenko.¹¹ The results for these materials show some scatter, although the data when replotted (Fig. 9) indicate that there is little differ-

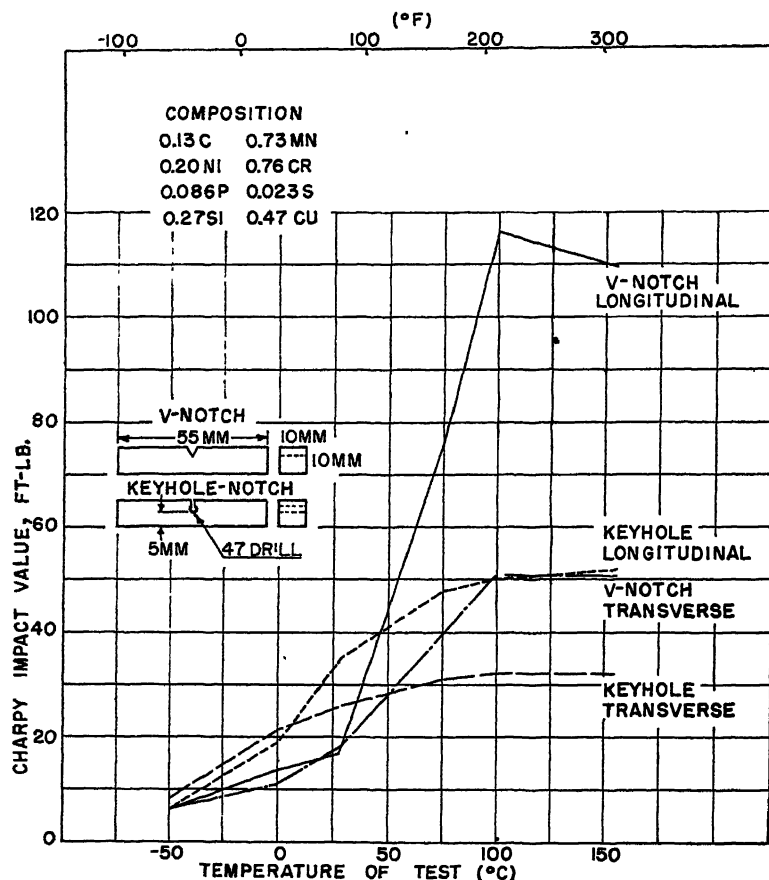


FIG. 8.—EFFECT OF TYPE OF NOTCH AND DIRECTION OF ROLLING ON STANDARD CHARPY NOTCHED-BAR VALUE FOR MAYARI-R STEEL.

zone, whereas, below and above this zone consistent results are to be expected. On the other hand, the keyhole notched-bar specimen is insensitive and the results even in the transition zone are consistent.

Effect of Speed of Test

A comparison of the energy absorbed by notched bars from nine ferrous materials broken in an impact machine (striking velocity 12.44 ft. per sec.) and in a slow-

ence between the energy absorbed by notched-bar specimens tested in either machine. Recently, in a discussion of tensile impact behavior, Brown and Vincent¹² have pointed out that changing the rate of strain from static condition to over 800 in. per in. per sec. has little effect on the total energy absorbed. These data are reproduced in Fig. 10.

A study of the effect of speed of test was carried out on the group of steels used

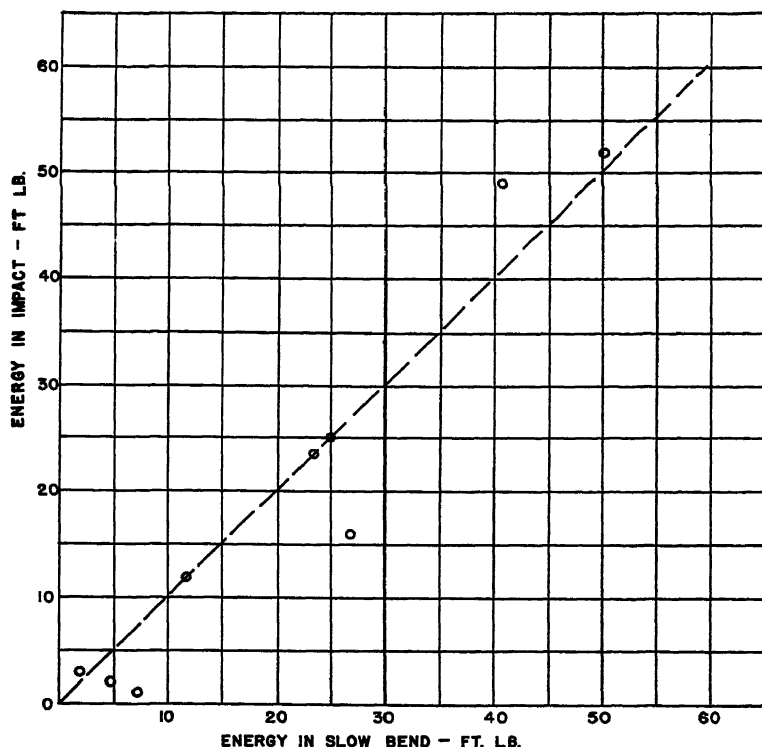


FIG. 9.—RELATION OF ENERGY ABSORBED BY NOTCHED-BAR SPECIMENS TESTED IN IMPACT AND SLOW BEND. (*Petrenko.*)

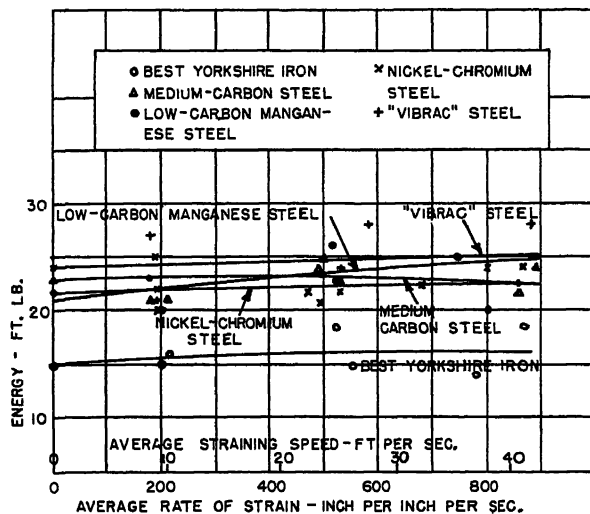


FIG. 10.—ENERGY ABSORBED IN FRACTURE OF TENSILE IMPACT SPECIMENS AT VARIOUS RATES OF STRAIN (*Brown and Vincent.*)

in the present investigation. Specimens were broken in the impact machine and a similar group was tested in a jig (identical with that of the impact machine) at a

for three steels (composition not reported) can be plotted from the data presented by Moser.¹ Although the work-hardening is not quantitatively evaluated, the relation

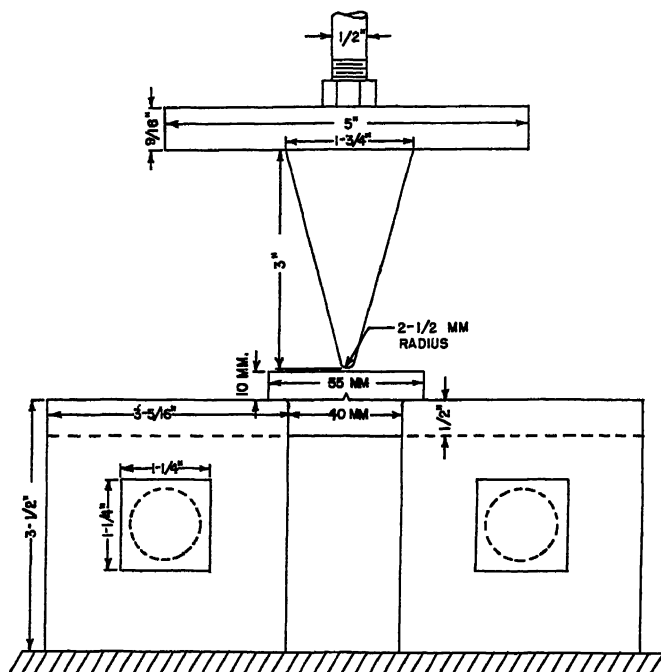


FIG. 11.—DIAGRAM OF JIG FOR TESTING SLOW-BEND SPECIMENS.

slow rate, using a tensile testing machine (Fig. 11). A stress-strain curve was made in order that the area under the curve might be measured with a planimeter and converted to energy units. In general, the energy absorption in the slow bend and impact loading are in good agreement in homogeneous materials (Fig. 12). However, a decided increase in energy absorption in the impact method compared with the slow-bend method was noted in a number of commercial-quality nonhomogeneous materials containing laminations or having fibrous breaks.

Resistance to Deformation of Notched-bar Specimen

The relationship between the volume of deformed metal and the energy absorption

of volume of deformed metal and the energy absorption is found to be approximately linear for each material (Fig. 13).

In the present study a great many specimens were examined in order to observe the deformation and flow of metal in the vicinity of the fracture. A surface normal to the notch was prepared on half of each specimen and surveyed using Vickers pyramidal diamond indentations with a 10-kg. load. Indentations were made 0.05 in. apart in rows perpendicular to the length of the specimen. These rows were spaced every 0.03 in. and were staggered (Fig. 14). Enough indentations were made so that the last several rows had approximately the same average hardness. This average hardness value was assumed to be that of the unstrained metal.

Typical data from the hardness survey are given in Fig. 14. An examination of the data in most cases reveals an illuminating picture of the progress of fracture. In the

tween the energy absorbed during fracture and the amount of work-hardening. The average hardness of the unstrained metal was subtracted from the average hardness

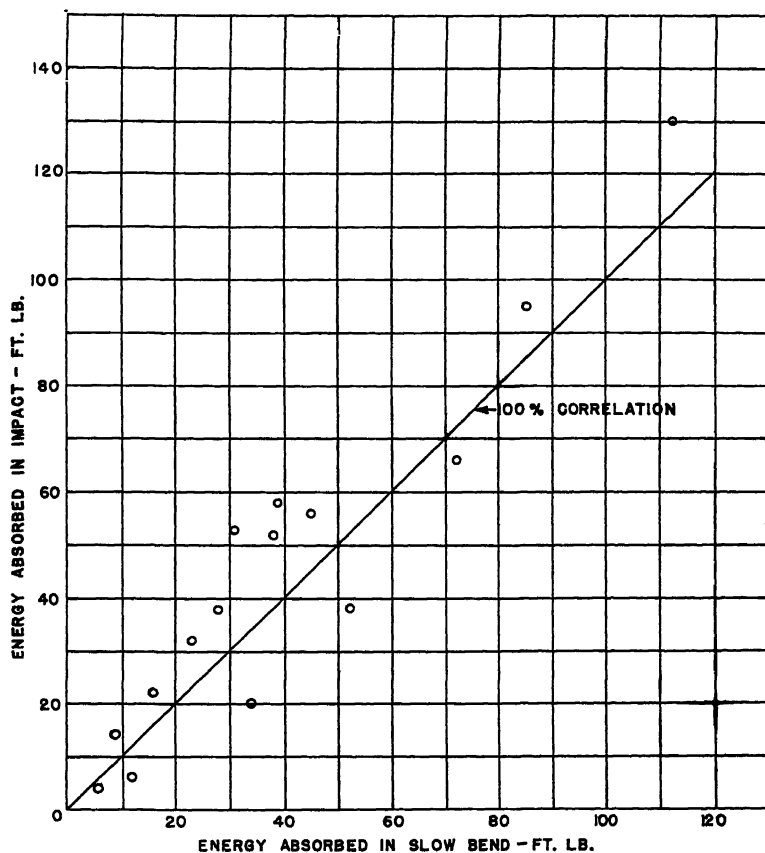


FIG. 12.—RELATION OF ENERGY ABSORBED BY NOTCHED-BAR SPECIMENS TESTED IN IMPACT AND SLOW BEND.

shallow notched specimens there are two areas, one above and one below the neutral axis, which show a higher hardness, indicating simple beam behavior during fracture. In the deep-notch or keyhole-notched specimens this type of deformation has not been found. Fracture is caused mainly by the punching action of the nose of the pendulum hammer on the area between the nose of the hammer and the notch.

An interesting correlation was noted be-

between the energy absorbed during fracture and the amount of work-hardening. The area surveyed was measured from a photograph at 3 diameters magnification, using a planimeter. Since only half of the specimen was surveyed, this value was doubled and converted to the volume it represented. A work-hardening value was obtained by multiplying the volume of the metal surveyed in cubic inches by the average hard-

ness increase in Vickers hardness numbers for that volume. It should be noted that this value remains a constant for each

specimens; it is expected that other types will give a different relationship between energy absorption and work-hardening.

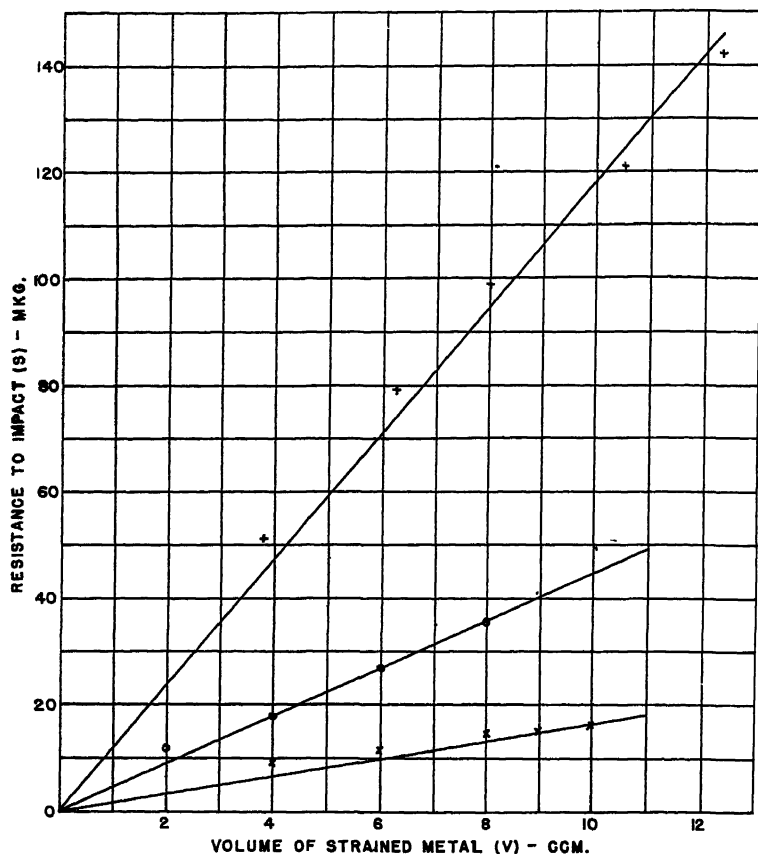


FIG. 13.—RELATION OF VOLUME OF STRAINED METAL AND AMOUNT OF ENERGY ABSORPTION FOR THREE STEELS OF VARYING TOUGHNESS. (*Moser.*)

specimen, regardless of the amount of unstrained metal included in the survey, as long as none of the strained metal is excluded.

The amount of work-hardening was determined for 18 specimens of two different carbon steels with a variety of breadths and notch conditions (Table 2) and plotted against the energy absorbed in foot-pounds (Fig. 15). The linear relation gives a fundamental basis for the behavior of the metal in various test

SUMMARY AND CONCLUSIONS

A number of conclusions may be drawn from this study:

1. Doubling the breadth of a standard (1 cm.) notched-bar impact specimen broken at room temperature causes a decrease in specific energy absorption for most of the steels studied. A further decrease in absorption of specific energy is expected from specimens of greater breadth.

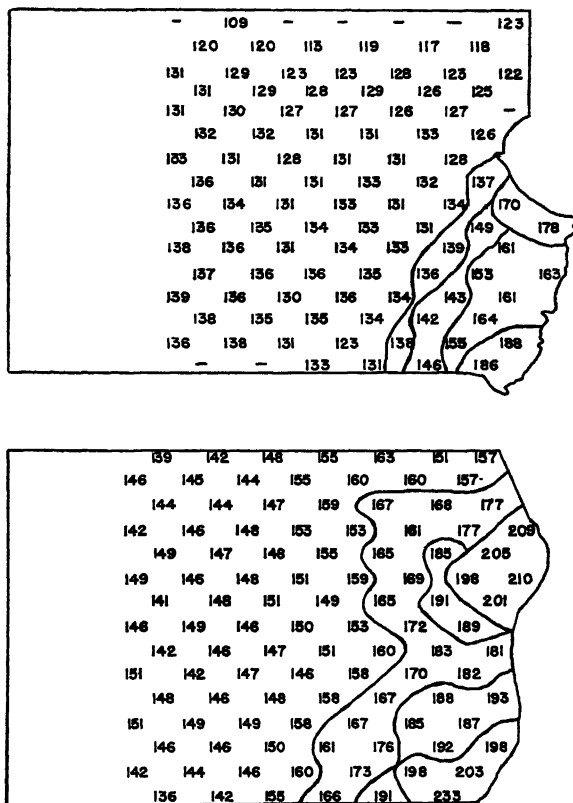


FIG. 14.—HARDNESS SURVEY OF TYPICAL KEYHOLE AND V-NOTCHED BAR SPECIMENS.

TABLE 2.—Summary of Data

Steel No.	Notched-bar Impact Value, Ft.-lb.	Type of Notch	Depth of Notch, Mm.	Breadth of Specimen, Cm.	Volume of Metal Surveyed, Cu. in.	Average Hardness Increase, Per Cent	Work-hardening*
61	4	Keyhole	5	1	0.141	2.0	0.28
61	4.5	Vee	2	0.5	0.048	0.8	0.04
61	21	$\frac{1}{16}$ " Rad.	2	1	0.082	5.4	0.44
61	37	$\frac{1}{8}$ " Rad.	2	1	0.066	14.6	0.96
61	40	$\frac{3}{16}$ " Rad.	2	1	0.137	6.3	0.86
61	48	$\frac{1}{2}$ " Rad.	2	1	0.129	7.5	0.97
57	5	Vee	2	1	0.055	2.5	0.14
57	7	Keyhole	5	0.5	0.048	8.3	0.40
57	15	Vee	2	0.5	0.068	8.0	0.54
57	15	Keyhole	5	1	0.096	3.8	0.36
57	15	Keyhole	5	1	0.112	4.8	0.54
57	20	Vee	2	1	0.077	5.0	0.38
57	20	Vee	2	1	0.107	9.2	0.98
57	29	Vee	2	2	0.234	1.3	0.31
57	50	Keyhole	5	2	0.266	3.9	0.99
57	54	$\frac{1}{16}$ " Rad.	2	1	0.077	16.6	1.28
57	70	$\frac{1}{8}$ " Rad.	2	1	0.139	12.3	1.71
57	95	$\frac{3}{16}$ " Rad.	2	1	0.115	20.3	2.34
57	110	$\frac{1}{2}$ " Rad.	2	1	0.130	20.8	2.70
57	121	$\frac{3}{16}$ " Rad.	2	1	0.105	25.0	2.62

* Volume of metal surveyed (cu. in.) multiplied by average hardness increase (Vickers hardness number).

2. The V-notched Charpy test specimen is preferred to the keyhole-notched specimen for the range of steels studied, since the sensitivity of the test is increased and

deduced from observations on a number of types of notched-bar impact specimens and under a variety of test conditions for two plain carbon steels. Other types of steel

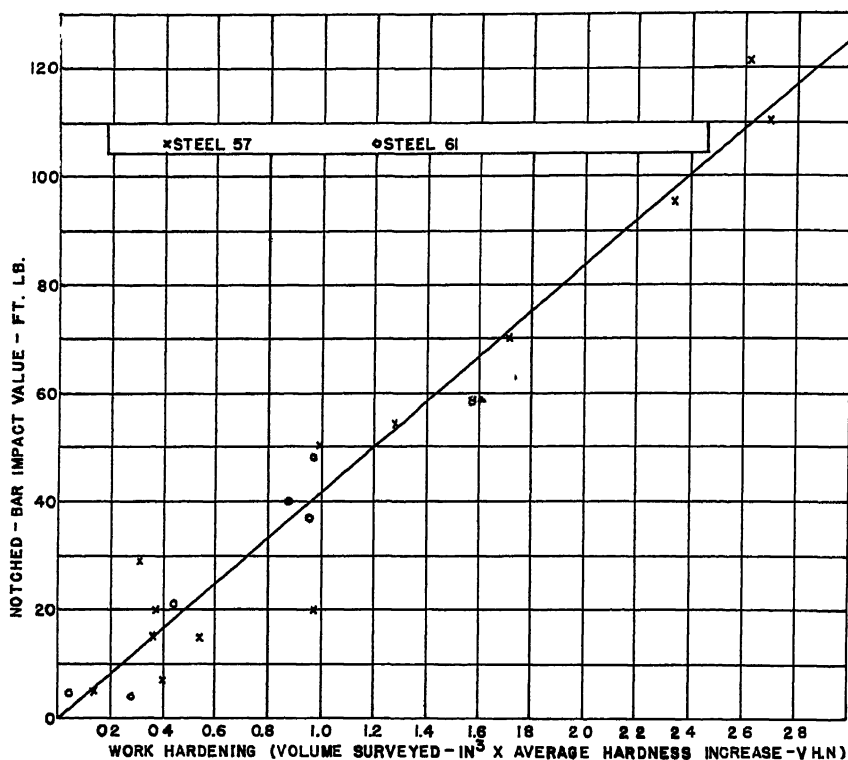


FIG. 15.—RELATION OF ENERGY ABSORPTION AND WORK-HARDENING FOR NOTCHED-BAR IMPACT SPECIMENS OF TWO PLAIN CARBON STEELS.

the test specimen is strained as a simple beam.

4. Testing temperature is one of the important variables that affects the specific-energy absorption of a notched-bar specimen broken in impact. For specimens tested at various temperatures, the effect of breadth is greatest for the steel studied in the range of temperatures from just above to below room temperature.

5. In general, the energy absorption in the slow bend and in impact loading are in good agreement for homogeneous steels.

6. A linear relation between energy absorption and work-hardening has been

undoubtedly will show a relationship between work-hardening and energy absorption, although the slope of the curve will vary.

The quantitative evaluation of the effect of changes in test specimen for a given steel will require a clearer understanding of the relationship of resistance to deformation and of resistance to fracture under all conditions of restraint and test. Further investigation should be made to determine whether the energy absorption of test specimens subjected to tensile, impact, bending, or torsion forces, either singly or in combination, follows the rule that the

total energy absorbed depends upon the total work-hardening. From a practical standpoint it may be possible that the relationship between work-hardening and energy absorption is a fundamental constant for each steel; this would be useful in the general solution of the behavior of mechanical test specimens.

REFERENCES

1. M. Moser: A New Method of Interpreting Notched-bar Impact Test Results. *Trans. Amer. Soc. Metals* (1925) 7, 297-320.
2. R. H. Greaves and J. A. Jones: The Effect of Temperature on the Behavior of Iron and Steel in the Notched-Bar Impact Test. *Jnl. Iron and Steel Inst.* (1925) 112, 123-165.
3. Von E. Maurer and R. Mailander: Zur Frage der Blausprodigkeit. *Stahl und Eisen* (1925) 45, 409-423.
4. S. L. Hoyt: Notched-Bar Testing. *Metals and Alloys* (1936) 7, 5-7, 39-43, 102-106, 140-142.
5. D. J. McAdam, Jr. and R. W. Clyne: The Theory of Impact Testing. *Proc. Amer. Soc. Test. Mat.* (1938) 38, pt. II, 112.
6. H. W. Gillett: Impact Resistance and Tensile Properties of Metals at Subatmospheric Temperatures. *Amer. Soc. Test. Mat.* (1941).
7. S. J. Rosenberg: Effect of Low Temperatures on the Properties of Aircraft Materials. *Jnl. of Research, Nat. Bur. Stds.* (1940) 25, 673-701.
8. Prüfung der Kerbschlagzähigkeit. Gmelins Handbuch der Anorganischen Chemie (1939) 8 Auflage system Nummer 59, Eisen Teil C-Lieferung 2.
9. Notched-Bar Impact Testing Discussion. *Trans. Manchester Assoc. Engrs.* (1937-38) 37-230.
10. H. Habart and W. J. Herge: Sub-size Charpy Relationships at Sub-Zero Temperatures. *Proc. Amer. Soc. Test. Mat.* (1939) 39, 649-658.
11. S. N. Petrenko: Comparative Slow Bend and Impact Notched Bar Tests on Some Metals. *Nat. Bur. Stds. Tech. Paper No.* 289.
12. A. F. C. Brown and N. D. G. Vincent: The Relationship between Stress and Strain in the Tensile Impact Test. *Proc. Inst. Mech. Engrs.* (1941) 145, 126-134.

DISCUSSION

(F. G. Tatnall presiding)

F. G. TATNALL,* Eddystone, Pa.—Why was the keyhole notch established?

Has consideration been given to the matter of taking into account the energy necessary to throw the specimen by the pendulum of the

impact machine? A great deal of energy is so expended which appears in the total impact value reported for the test. Is it not much better to drop the pendulum from increasing heights until incipient fracture occurs?

Then there is the matter of threshold energy value—that critical temperature at which a ductile material suddenly becomes brittle. That is a most important function of the impact test. A buzz saw will explode if operated at very low temperature; a rail will crack under impact. A great many things will happen at very low temperature. That should be emphasized.

The next thing is the matter of the slow bend. It has been said time and again that explosion patterns can be reproduced qualitatively but not quantitatively by a static test on the structure instead of an impact test. We can thus find out how failure progresses through the structure.

Colonel Zornig, of the Watertown Arsenal, tells me that the quickest way to differentiate between brittle and ductile fracture is to see whether it is shiny or dull.

Next is the matter of the double-width bar. Mr. Riegel, of Caterpillar Tractor, tells me that this is a good test for notch brittleness. If the double-width bar absorbs twice the energy of the single-width bar in impact, it is not notch brittle. Finally, I do not think that specific energy was clearly defined in this paper.

F. S. MCKENNA (author's reply).—In order to compare the energy absorbed by specimens of various breadths, use was made of the term "specific energy." This may be defined as the energy absorbed by a specimen multiplied by the ratio of the breadth of a standard specimen (10 mm.) to the breadth of the second specimen. Thus, in comparison, the following multiplying factors were used:

BREADTH	FACTOR
Standard.	1
Double	$\frac{1}{2}$
Half	2
Quarter	4

Such an analysis was used for the results shown in Figs. 2, 3 and 6.

The keyhole specimen has found favor because it is easier to machine than the V-notched type. The data obtained with the key-hole specimen are in general quite reproducible.

* Baldwin Locomotive Works.

The V-notched specimen, on the other hand, is a much more sensitive test piece, although it is somewhat more troublesome to prepare. The V-notched specimen has a decided advantage in the fact that a larger area is tested.

We agree that considerable information can be obtained regarding the notched-bar characteristics by using both single and double-breadth specimens. This information, however, is useful only in the area of rapid transition from high to low energy absorption as the temperature is decreased from just above room temperature to temperatures below room temperature in what is often called the threshold energy area.

F. H. ALLISON, JR.,* Pittsburgh, Pa.—It would be interesting to know whether there are any available data on triple-width specimens, and whether there exists a linear relationship between the values obtained on single, double, and triple widths. A few results from our laboratory gave less than double the impact value on double-width specimens, but gave larger values on triple-width specimens. Examples are given below, each value being the average of six tests.

Izod Ft.-lb.

SINGLE	DOUBLE	TRIPLE
6 0	8 0	14 0
9 0	11 0	20 0
10 0	12 5	20 0

F. S. McKENNA.—I think that the work on triple-breadth specimens is largely limited by the capacity of standard testing machines. The linear relationship between breadth of specimen and energy absorption does drop off considerably for some steels for double-breadth specimens, in fact, a steel might have 10 ft.-lb. absorption in single breadth and only 5 or 6 ft.-lb. for a double-breadth specimen. In other words, a double-breadth specimen may break with less energy than a single breadth. It would be very interesting to see some more information on triple-breadth specimens.

J. H. HOLLOMON,† Watertown, Mass.—I should like to comment on the difficulty of obtaining reproducible notch conditions. We

have done a little work on this problem and are doing more. Certainly the sharp cracks, or scratches, in the specimen can be removed, and, at least for very ductile material, this improves the reproducibility of the impact test. However, on stronger metals, it is somewhat questionable whether the reproducibility is improved by polishing the bottom of the notch with a small wire and with fine alumina. Dr. Gensamer suggested this procedure earlier and we use it as more or less standard practice. We polish the bottom of notch and examine it to see that the scratches are removed.

The next point that I would like to bring out is the effect of radius of notch. The problem is extremely complicated. As the bar is made wider, the metal at the base of the notch is more and more constrained; that is to say, as the bar is made wider the shoulder of the bar is more operative in preventing deformation at the base of the notch, so that the transverse constraint becomes greater. The effect of increasing the width of the bar is greatest when the width of the bar is small compared with the radius of the notch. For the standard Charpy specimen 1 cm. wide and 0.01-in. radius of notch, doubling the bar should not change the temperature of brittle failure. When a bar is made wider, of course, more material deforms, and the energy required for fracture increases.

When Moser, who made the first experiments, changed the width of the bar, he obtained brittle failures and decreases of energy. The relative behavior of specimens of various widths depends entirely on what type of specimen is being used and how large the radius is. The smaller the radius, the less effect there should be from the changing width of the bar, the larger the radius, the greater the effect of changing the width of the bar.

N. A. ZIEGLER,* Chicago, Ill.—In discussing the relative merits of Charpy and Izod tests, one factor is somewhat overlooked; that is, the nature of the machine marks in the notch. In preparing a Charpy bar, a hole is drilled and the machine marks are transverse to the notch. In an Izod bar, the notch is machined with a cutter and the machine marks are longitudinal. A few years ago, in some Russian articles by Davidenkoff et al., it was pointed

* Metallurgist, United Engineering and Foundry Company.

† Captain, Ordnance Department, Watertown Arsenal.

* Crane Company.

out that this condition may have some effect on the test results

F. G. TATNALL.—How about the throwing of the broken specimen? Did anybody ever evaluate that? This matter comes up frequently in all discussions of impact when people are procuring equipment. There ought to be some evaluation of it.

G. L. COX,* Watertown, Mass.—I do not think that the differences in the preparation of the Charpy specimen have nearly as much to do in the final result as the variation in the material or the susceptibility of the material to what is going to happen to it at the particular strain rate or temperature. Captain Hollomon mentioned our program for evaluating these differences in typical steels at several yield-strength levels. He mentioned that in the high-strength material (of the order of 150,000 lb. per sq. in.) the difference is practically nothing, and that is a fact. There seems to be no difference whether the specimen contains very bad scratches at the base of the notch or is polished smooth. In the lower strength material (such as 75,000 lb. per sq. in.) the difference is more significant. There is some indication of a larger spread in the unpolished specimen. However, this spread is still of the order of a very much lower magnitude than variations in the material itself, such as laminations, etc.

By way of a summary, what I mean is that if the material gives a high level of impact value, it is not going to be significantly changed from that by the condition of the notch as obtained in the usual method of preparing specimens. I think that probably too much emphasis has been placed on the inadequacy of the ordinary impact specimens. There are people in this room who have had a lot of experience in testing materials for notched-bar impact properties, and I do not think that many of them polish their specimens, and probably some have already established that it is in the main unnecessary to go to this extra trouble. This is one of those things that are very nice to know the magnitude of, but I feel that it is a lot less to worry about than the heat-treatment or other metallurgical condition of the material.

M. GENSAMER,* Pittsburgh, Pa.—Colonel Cox is perfectly right in that most of the time it does not make much difference whether the notch is ground or an ordinary machined notch is used, but occasionally it makes a good bit of difference. It does not with ordinary heat-treated steel but I have run into some cases, especially with some of the harder stainless steels, where it makes a great deal of difference. So you have to use discretion and be careful about the preparation of notch if it is important, and you have to find out by experience whether it is important or not.

F. M. WALTERS, JR.,† Washington, D. C.—The chairman has raised a question and has gotten no answer to it. I think he is the only one who has even the beginnings of information on it. I wish he would tell us about the error due to throwing the specimen.

F. G. TATNALL.—Some work has been done in plastics on the energy loss in throwing of the specimen. I seem to recall that the throwing of the specimen absorbed from 50 to 60 per cent of the impact energy reported. This appeared in a paper in *Modern Plastics*, by Dr. Nason, of the Monsanto Chemical Co., about three months ago. In other words, it makes you begin to question the values obtained by these impact tests which are so carefully reported.

It has been proposed in the *Plastics* discussions that impact testing be done on the basis of successively releasing the pendulum from increasing heights until incipient fracture is observed or just enough to break the bar. It means that we will have to try some such way if we want to get real, precise impact values. Impact by projectiles fired from rifles has been used for obtaining high-speed impact values. Notched-bar testing may be carried out as a static bend test plotting a stress-strain curve for qualitative study instead of employing a pendulum impact machine.

H. SCOTT, Pittsburgh, Pa.—May I make the comment that perhaps the point here is that we are dealing with an extremely brittle material. We are considering now degrees of

* Lieutenant Colonel, Ordnance Department, Watertown Arsenal.

* Carnegie Institute of Technology.

† Naval Research Laboratory.

brittleness in plastics, whereas in steels and other metals it is only necessary to know whether or not they are brittle by this test. Thus in metals the error due to throwing the specimen is a small percentage of the total value and something that we can afford to neglect. Captain Hollomon remarked also that it does not make much difference whether it is 2 or 4 ft-lb when a metal is brittle.

There is another side of this problem, already introduced by Colonel Cox, concerning fundamentals. The impact test is considerably more complex than the tensile test and we do not understand all the phenomena of tensile rupture. We can hardly expect then to explain fully the impact test. Once tensile rupture is understood, however, interpretation of the impact test should not be too difficult.

Conditions of Fracture of Steel

By J. H. HOLLOMON* AND C. ZENER,† JUNIOR MEMBERS A.I.M.E.

(Chicago Meeting, October 1943)

It is commonly recognized that a given material may be described as ductile or brittle only with reference to the conditions of test. Thus under the usual test conditions quartz is brittle, but under high pressures it is ductile. Salts that are brittle at room temperature become ductile at elevated temperatures. Pitch, brittle with respect to rapid loads, flows at low rates of loading. Pearlitic steel, ductile under the usual conditions of test, may be embrittled under the proper conditions of combined stresses, temperature, and rate of loading.

EARLIER INVESTIGATIONS

A clear analysis of the conditions necessary for plastic flow and for fracture was first given by Ludwik,¹ who introduced two types of stress, the "flow stress" and the "stress at fracture." These stresses may refer to tensile or to shear stresses, or, in fact, to any type of stress. Ludwik considered these two stresses to be independent of one another, functions of the conditions of test and of the prior history of the material. For the purpose of analysis, both a flow stress and a stress at fracture can be envisaged as functions of strain over the entire range from zero to infinite strain. Thus, the material is brittle if the stress at fracture is less than the flow stress and ductile if the reverse is true.

According to Ludwik's analysis, the problem of determining the effects of combined stresses, of temperature and of strain

rate upon the behavior of metals reduces to a problem of determining the effect of these variables upon the flow stress and upon the stress at fracture. In the present paper, methods are described for determining the effects of two of these variables, temperature and strain rate, and examples are given of the dependence of flow stress and stress at fracture, upon these two variables. The effect of combined stresses will be discussed in a succeeding paper.

The flow stress may be determined from a load-diameter curve. Load-diameter curves were obtained over a wide range of temperature and over the limited range of strain rates obtainable with the lever-type Riehle machine used. The curves were then converted to an extremely wide range of strain rate by making use of the equivalence of the effects of changes in strain rate and changes in temperature, previously proposed² and demonstrated³ by the authors. According to this principle of equivalence, strain rate $\dot{\epsilon}$ and temperature T affect the flow stress only through a single parameter $\dot{\phi}$ of the form:

$$\dot{\phi} = \dot{\epsilon} e^{Q/RT} \quad [1]$$

In this equation, R is the gas constant (2 cal. per gram mol per deg. C.), and Q is a heat of activation, which varies from material to material, and may depend upon the strain, but not upon the strain rate or the temperature. There is associated with every value of $\dot{\phi}$ a flow-stress curve. Combinations of strain rate and of temperature that give the same $\dot{\phi}$ have the same flow-stress curve. Therefore, merely by changing the temperature of test, the effect of changing the strain rate may be obtained. Thus, under isothermal conditions, the material will behave the same at

The statements or opinions in this article are those of the authors and do not necessarily express the views of the Ordnance Department. Manuscript received at the Office of the Institute Nov. 26, 1943.

* Captain, Ordnance Department, U. S. Army, Watertown Arsenal, Watertown, Massachusetts.

† Senior Physicist, Watertown Arsenal, Watertown, Massachusetts.

¹ References are at the end of the paper.

the temperature T , and strain rate ϵ , as at room temperature T_r and an equivalent strain rate defined by the following equation:

$$\text{Equivalent strain rate} = \epsilon e^{Q/RT} / e^{Q/RT_r} \quad [2]$$

Since a lowering of temperature by 50°C . is equivalent to an increase of strain rate of at least 1000 fold, the principle of equivalence furnishes a tool for finding the effects of very high strain rate upon the flow stress. For each material, preliminary tests over a range of strain rates must be made in order to determine the heat of activation Q , which relates quantitatively the effects of strain rate and temperature. The precise manner in which the stress S varies with the parameter p appears to be given by the following equation:

$$S \sim p^r \quad [3]$$

where the exponent r is some small number.

A small variation in material results in a larger variation in fracture strength than in the flow stress. It is, therefore, more difficult to establish the equivalence principle for the stress at fracture than for the flow stress. In the analysis of this paper, it will be assumed that the same equivalence holds for both types of stresses. The stress at fracture is not obtainable as a function of strain by a single tensile test as is the flow stress. Such a test gives only the stress necessary for fracture at one value of the strain; namely, the final strain. It does not show how the stress at fracture varies with deformation, or what is the stress at fracture of the undeformed material.

By a technique first used by Kuntze,⁴ McAdam⁵ has attempted to measure the effect of deformation and combined stress on the fracture strength. McAdam measured the tensile properties of several metals notched at various depths and angles. The amount of deformation before fracture and the stress distribution thus were varied.

As pointed out by Sachs,⁶ the analysis

made by Kuntze and used by McAdam of the stresses at the base of sharp notches is open to question. Furthermore, Kuntze and McAdam have assumed that the fracture stress can be obtained by dividing the final or breaking load by the final area. This method of determining the fracture stress tacitly assumes that the stress across the notched section is uniform. This assumption has little basis in fact and becomes less and less valid as the deformation before fracture becomes small. In the light of these objections to the notched-bar method of obtaining the effect of prior deformation on the fracture strength, another technique has been used in the present study. Certain classes of steels are brittle at the temperature of liquid nitrogen. For these steels, the effect of a prior deformation upon stress at fracture was found by first deforming a set of specimens by various amounts at room temperature, then lowering the temperature to that of liquid nitrogen and pulling to fracture.

MATERIALS

The steel used in this investigation was the same as that previously described.³ Small specimens ($\frac{5}{8}$ -in. rounds) were machined from a large centrifugal casting of the approximate composition: C, 0.25 per cent; S, 0.02; P, 0.01; Si, 0.4; Cr, 0.5; Mo, 0.5; V, 0.1. These were heat-treated in two groups: one group was air-cooled and the other water-quenched after holding at 900°C . for one hour. After this treatment, specimens from each group were tempered to two yield strengths: approximately 100,000 lb. per sq. in. and 130,000 lb. per sq. in. (at a strain of 0.01 and at a strain rate of 10^{-4} sec.⁻¹ at room temperature).

This steel was of such hardenability that the $\frac{5}{8}$ -in. rounds transformed completely to martensite upon water quenching and upon air quenching transformed to pearlite and proeutectoid ferrite. The

subsequent tempering resulted in slight spheroidization of the carbide lamellae in the air-cooled specimens and in a structure having spheroids of carbide embedded

EXPERIMENTAL TECHNIQUE

The method of automatically recording the information necessary for the calculation of stress-strain curves over a range



FIG. 1



FIG. 2

FIGS. 1 AND 2.—TEMPERED STEEL AT 100,000 POUNDS PER SQUARE INCH YIELD STRENGTH (AT STRAIN OF 0.01). $\times 1000$, NITAL ETCH.

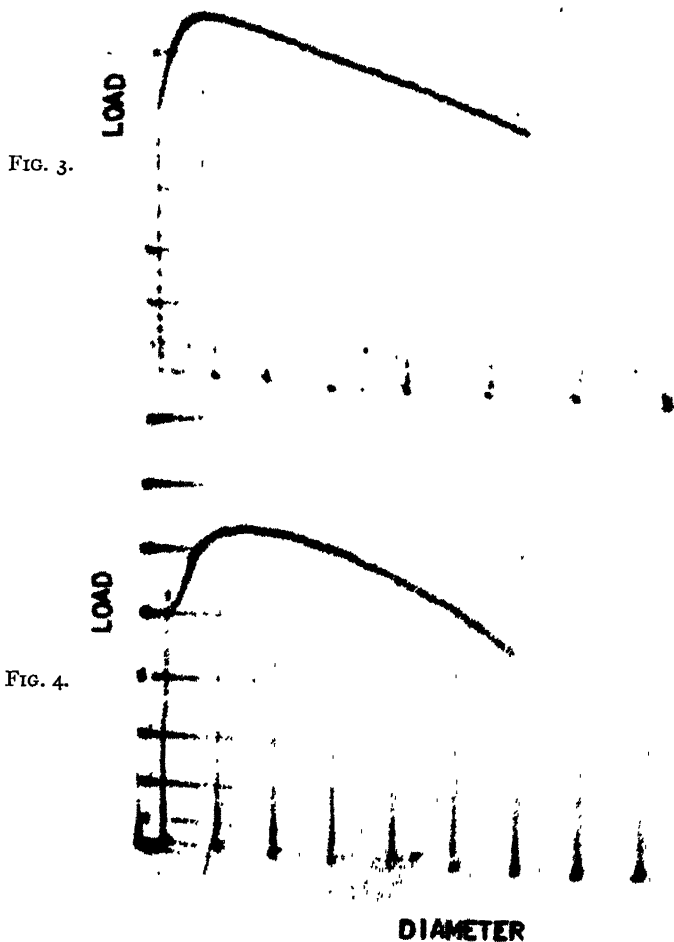
Fig. 1, pearlitic; Fig. 2, martensitic.

in a matrix of ferrite in the water-quenched specimens. Typical photomicrographs of the specimens heat-treated to 100,000 lb. per sq. in. yield strength are presented as Figs. 1 and 2.

of temperature and strain rates has been discussed in detail in a previous paper.³ Briefly reviewed, this method consists in the conversion of the diameter changes and of the load into elastic strains in certain

elastic elements, and then into changes in resistance of elastic strain gauges attached to these elements. The changes in resistance are converted, by an electric circuit,

thereby gives a permanent record of the load-diameter curve. Load-diameter curves were obtained in this manner at various strain rates and at temperatures down to



FIGS. 3 AND 4.—TYPICAL LOAD DIAMETER CURVES.
Fig. 3, room temperature; Fig. 4, minus 130°C .

into a deflection of the beam on the screen of a cathode-ray oscillograph, the horizontal axis corresponding to diameter changes, the vertical axis to load. A time photograph of the oscillograph screen

-190°C . (typical examples are presented as Figs. 3 and 4). At the very low temperatures, (below -70°C .), it was not feasible to vary the strain rate. At these lower temperatures, an uncertainty in tempera-

ture of a few degrees centigrade is reflected in changes of mechanical properties large compared with the possible variation that can be obtained by the range of strain rates possible in the Riehle type machine that was used. The actual strain rates referred to in this paper have been arbitrarily taken to be the head speed of the Riehle machine divided by the uniform gauge length of the specimen (1.4 in.). Since the strain rate varies as plastic deformation, and local necking occurs, these values are used only for purposes of comparison.

RESULTS AND DISCUSSION

Tempered Pearlitic Steel

The results of the experiments on the specimens that were air-cooled and tempered to approximately 100,000 lb. per sq. in. yield strength are presented in

yield and fracture strengths are plotted in Fig. 5 as a function of the logarithm of the equivalent strain rate. The value of r in Eq. 3 for the yield strength is 0.008. As the equivalent strain rate is increased, the fracture strength increases very slowly at first and then decreases sharply. At an equivalent strain rate of about 10^{17} sec.⁻¹, the yield strength becomes equal to the fracture strength, and the ductility as measured by the reduction of area is consequently equal to zero. Since the sharp decrease in fracture strength occurs in the same range of equivalent strain rate as the decrease in reduction of area, it is inferred that the two effects are related.

Since the steel whose properties are described in Table 1 breaks with very little reduction of area at $-190^{\circ}\text{C}.$, the effect of prior deformation may be determined by deforming specimens by various

TABLE 1.—*Tempered Pearlite*
YIELD STRENGTH, 100,000 POUNDS PER SQUARE INCH

Deoxidation			Steelmaking, Electric Furnace				Heat-treatment. $\frac{1}{2}$ Rounds Air-cooled from 1625°F. Drawn at 1265°F. for 3 Hr. Air-cooled						
			Forming, Centrifugal Casting										
Temperature, Deg. C.	Strain Rate $\times 10^4$	Type of S-S Curve ^a	Yield Strength at Plastic Strain		Tensile Strength		Fracture Stress	Strain			E_p , ^c Lb per Sq. In.	R. A., Per Cent	Type of Fracture ^d
			of 0.001 ^b	of 0.01 or L. Y. P.	Load Orig. Area	Load Act. Area		to T. S.	to F. S.	at Y. P. E.			
20	2.2	R	96	100.5	114.4	131.5	191	0.14	0.756		100	53.0	C.P.
20	18	R	99	103.0	121.0	136.0	194	0.13	0.706		100	50.8	C.P.
-11	84	R	101	105.0	122.0	136.0	197	0.12	0.734		100	52.0	C.P.
-60	2.2	?	106	110.0	130.0	158.0	201.5	0.19	0.622	<0.01	105	46.4	Trans.
-66	84	D	109	114.0	131.0	160.0	203.5	0.20	0.648	<0.01	110	47.2	Trans.
-130	84	D	122	126.0	138.0	152.0	204.0	0.12	0.58	<0.01	110	43.0	Trans.
-170	84	D	159	159.0	163.8	184.5	225.0	0.12	0.524	0.02	110	40.1	Trans.
-190	18	D	176.7	176.7			194.7	0.075	?			7.0	T.-C.

^a R, rounded—no drop in load at yield. D, drop in load at yield. All stresses 1000 lb. per sq. inch.

^b By the method employed. Difficult to determine accurately.

^c E_p is the slope of the strain-hardening curve.

^d See Fig. 8.

Table 1. The constant Q was determined from the yield-strength values of the tests performed at several strain rates at the three highest temperatures. Using this value of the heat of activation (10,000 cal. per gram cal.), the logarithms of the

amounts at room temperature and then breaking them at $-190^{\circ}\text{C}.$ The effect of prior deformation on the fracture stress of the specimens broken at $-190^{\circ}\text{C}.$ is plotted in Fig. 6. With increasing deformation, the stress necessary for fracture

increases markedly for this pearlitic steel. This increase in fracture strength with increasing deformation can be at least qualitatively interpreted by the micro-

to be primarily associated with the carbide lamellae. The reorientation of these carbide lamellae during deformation results in a smaller effective cross section of cracks

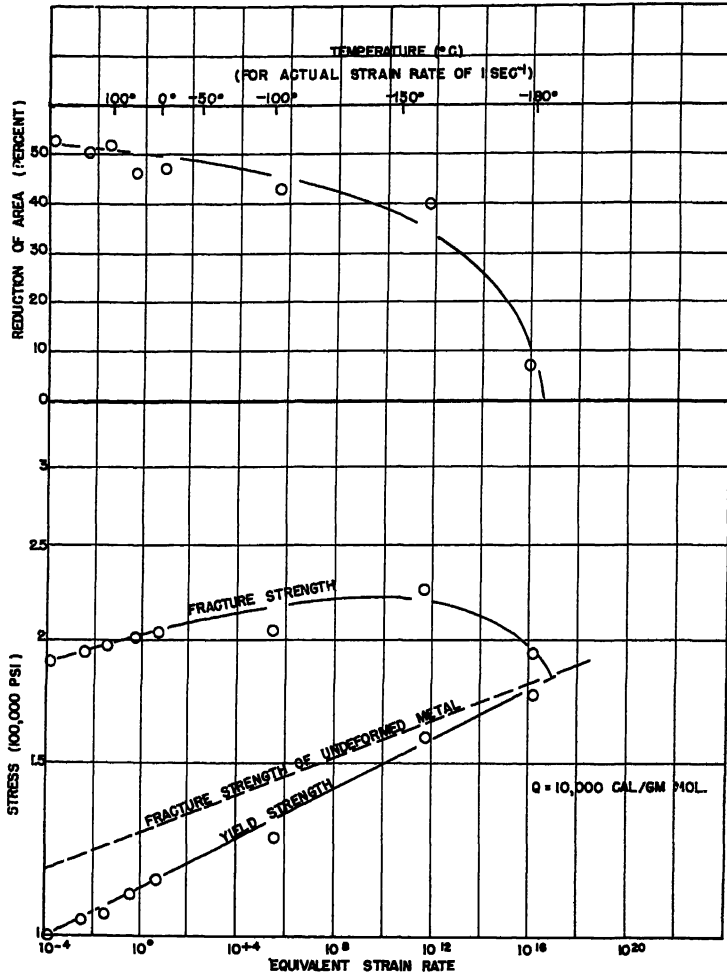


FIG. 5.—TENSILE PROPERTIES OF A PEARLITIC STEEL AS FUNCTION OF STRAIN RATE AND OF TEMPERATURE.
Yield strength, 100,000 lb. per sq. inch.

scopic crack concept suggested in a previous paper.² It was postulated that the fracture strength of metals in tension was determined by the average dimension of some inhomogeneity (crack) in a plane perpendicular to the applied stress. For a pearlitic material, the cracks are assumed

perpendicular to the direction of applied stress and therefore to an increase in fracture stress. The concept of reorientation of microscopic cracks has already² been used successfully in interpreting the effect of a pre-twist upon lowering the fracture strength in tension.

In the experiment just described, the fracture strength was measured as a function of deformation at a very high equivalent strain rate. It would be difficult to separate experimentally the effects upon fracture strength of deformation and of equivalent strain rate. Until evidence to the contrary is obtained, therefore, it is better to make the reasonable assumption that these two effects of deformation and of equivalent strain rate are independent and therefore additive. Using this assumption, the fracture strength of the undeformed metal may be obtained as a function of the equivalent strain rate in the following manner: For each value of the equivalent strain rate, the reduction of area may be obtained from Fig. 5, and its effect in increasing the fracture strength determined from Fig. 6. The fracture strength of the undeformed metal is then determined as a function of equivalent strain rate alone by subtracting from the observed fracture stress the increase in stress brought about by deformation. The variation of the fracture strength of the undeformed steel with equivalent strain rate is plotted as the dashed line in Fig. 5. The logarithm of the

fracture strength of the undeformed metal (actually at a strain of 0.01) increases

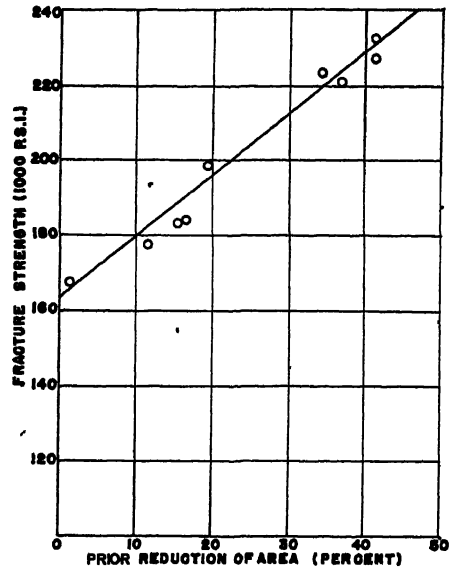


FIG. 6.—EFFECT OF PRIOR DEFORMATION ON FRACTURE STRESS AT MINUS 190°C., AIR-COOLED STEEL.

linearly with the logarithm of the equivalent strain rate but less rapidly than the

TABLE 2.—Tempered Pearlite
YIELD STRENGTH, 130,000 POUNDS PER SQUARE INCH

Deoxidation: Vanadium			Steelmaking: Electric Furnace:					Heat Treatment: 1625°F. Air-cooled. Drawn at 1115°F. 5/16-in. Rounds					
			Forming: Centrifugal Casting										
Tem- perature, Deg. C.	Strain Rate X 10 ⁴	Type of S-S Curve ^a	Yield Strength at .1astic Strain		Tensile Strength		Fracture Stress	Strain ^c			R. ^e , Lb per Sq. In.	R. A., Per Cent	Type of Fracture ^d
			of 0.001 ^b	of 0.01 or L.Y.P.	Load Orig. Area	Load Act. Area		to T. S.	to F. S.	at Y.P.E.			
20	2.2	R	119.0	128.5	145.4	162.5	207.0	0.115	0.622		100.0	45.4	Trans.
20	18	R	123.0	131.0	141.0	157.0	204.0	0.105	0.536		110.0	41.5	Trans.
20	84	R	124.0	132.0	143.0	158.5	210.0	0.115	0.572		110.0	43.6	Trans.
-12	84	R	125.0	134.5	144.6	162.0	213.0	0.115	0.552		110.0	42.2	Trans.
-65	2.2	R	131.0	139.5	151.0	169.5	217.0	0.115	0.532		115.0	41.3	Trans.
-65	84	R	134.0	141.0	155.0	171.0	219.5	0.110	0.524		115.0	40.8	Trans.
-97	84	R	137.0	145.0	158.2	173.0	221.0	0.09	0.505		115.0	37.5	Trans.
-140	84	R	160.5	165.5			173.5					4.2	T.-C.
-170	84	R	180.0	180.0			180.0	0				0	T.-C.

^a R, rounded—no drop in load at yield. All stresses 1000 lb. per sq. inch.

^b By the method employed. Difficult to determine accurately.

^c E_p is the slope of the strain-hardening curve.

^d See Fig. 2.

yield strength (also at a strain 0.01). Brittle failure occurs when the yield strength becomes equal to the fracture strength of the undeformed metal.

examples of which are to be found in the literature.² After the maximum load is reached, the stress (load divided by actual area) is a linear function of the strain

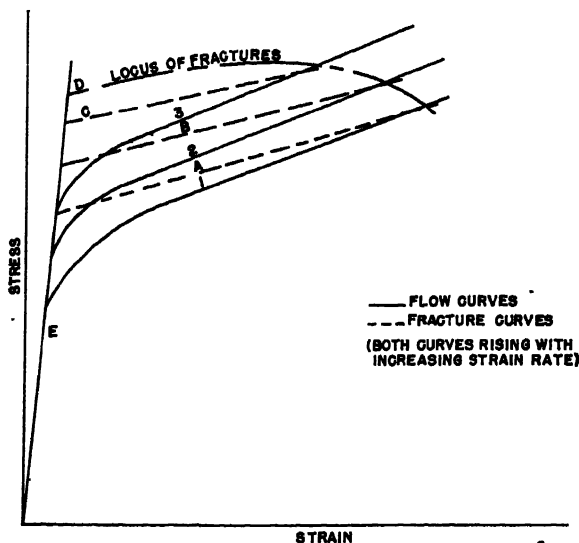


FIG. 7.—EFFECT OF INCREASING STRAIN RATE OR DECREASING TEMPERATURE ON TENSILE PROPERTIES OF A PEARLITIC STEEL.

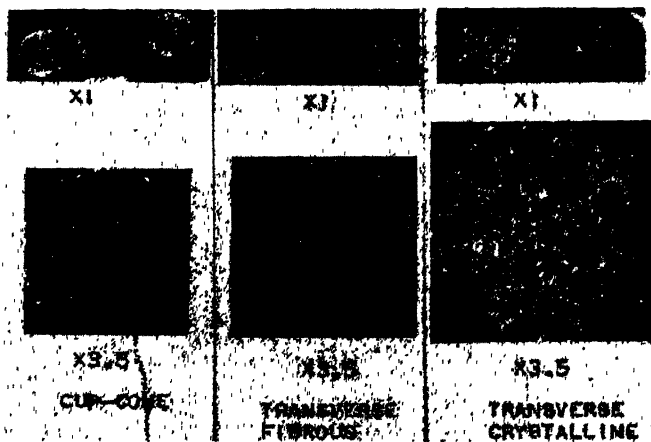


FIG. 8.—TYPES OF FRACTURES OF TEMPERED PEARLITIC STEEL AT VARIOUS TEMPERATURES OR STRAIN RATES.

A schematic representation of the effect of strain rate on the tensile properties of a pearlitic steel is presented as Fig. 7. Curve 1 is the typical stress-strain curve, many

(logarithm of the ratio of the original area to the actual area). The slope of this portion of the stress-strain curve is referred to as the strain-hardening modulus. Curve

B is the fracture strength curve which rises with reduction of area in accordance with Fig. 5. As the strain rate is increased, the flow (1, 2, 3) and the fracture-strength

increased, the fracture strength first increases and then decreases and the ductility decreases continuously (locus of fractures). As the equivalent strain rate increases, the

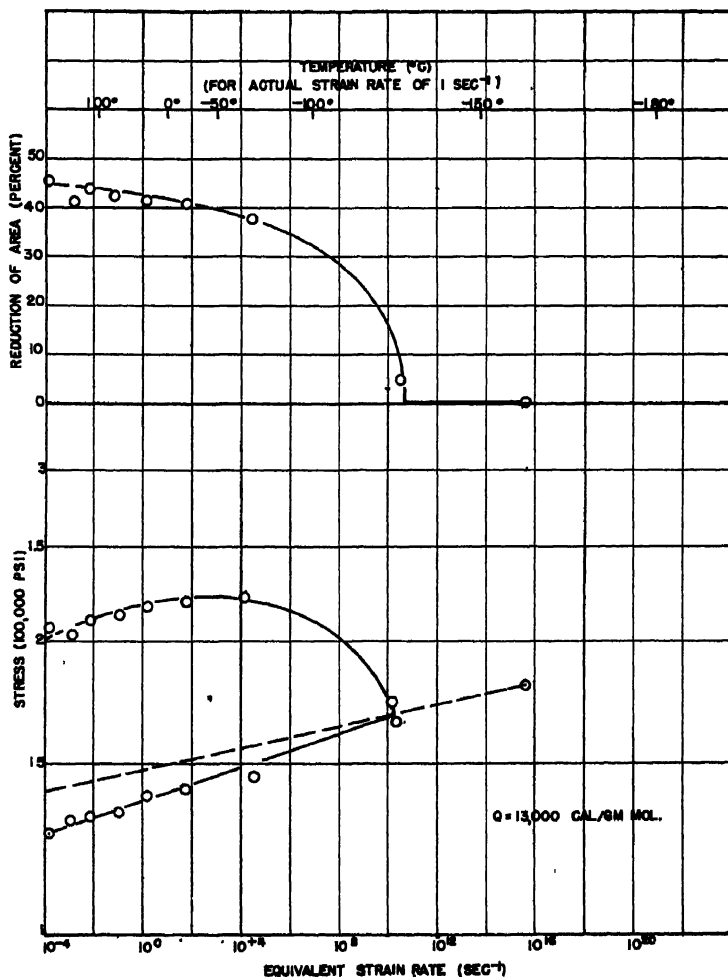


FIG. 9.—TENSILE PROPERTIES OF A PEARLITIC STEEL AS FUNCTION OF STRAIN RATE AND TEMPERATURE.

Yield strength, 130,000 lb. per sq. inch.

curves (*A*, *B*, *C*) rise and the strain-hardening modulus increases slightly. Brittle failure occurs when the elastic line *E* intersects the fracture strength of the undeformed metal *D*.^{*} As the strain rate is

type of fracture also changes from a ductile cup-cone type through transverse to the brittle or crystalline type. These various types of fractures are illustrated in Fig. 8.

This discussion has been limited to the effect of equivalent strain rate on the isothermal properties of the pearlitic steel,

^{*} The slope of the elastic line has been exaggerated for purposes of illustration.

since the technique utilized in this investigation imposes essentially isothermal conditions. The independent effect of the strain rate in changing the deformation from essentially isothermal to essentially adiabatic has been discussed in a previous paper.³ This second effect is particularly large at low temperatures, where the shape of the adiabatic stress-strain curves is radically different from that of the isothermal curves.

(under normal test conditions). As the strength of the steel is increased (by heat-treatment) the fracture strength increases less rapidly than the yield strength, therefore brittle failure should occur at a higher temperature. The significance of the small separation between the yield strength and fracture strength of the undeformed metal in relation to the brittle failure in impact is the subject of a later paper.⁷ Suffice it to say that in the notched-bar

TABLE 3.—*Tempered Martensite*
YIELD STRENGTH, 100,000 POUNDS PER SQUARE INCH

Deoxidation: Vanadium			Steelmaking: Electric Furnace					Heat-treatment: $\frac{5}{8}$ -in. Rounds. Water- quenched from 1625°F. Drawn for 3 Hr. at 1290°F.					
			Forming: Centrifugal Casting										
Tem- perature, Deg. C.	Strain Rate $\times 10^4$	Type of S-S Curves ^a	Yield Strength at Plastic Strain		Tensile Strength		Fracture Stress	Strain			E _p , ^c Lb per Sq. In.	R. A., Per Cent	Type of Fracture ^d
			of 0.001 ^b	of 0.01 or L.Y.P.	Load Orig. Area	Load Act. Area		to T. S.	to F. S.	at Y.P.E.			
20	2.2	R	97	104 0	115 1	134 5	200.0	0.112	0.770		100	54.8	C.P.
20	18	R	101	107.5	119.2	132.0	219 0	0.108	0.900		105	59.4	C.P.
20	84	R	104	110.0	122 3	131 0	220 5	0.095	0.860		110	58.1	C.P.
-14	18	D	105	112.0	125.1	140 0	217.0	0.115	0.780	0.01	110	54.0	C.P.
-65	2.2	D	116	121.0	138 3	169 5	241 0	0.202	0.830	0.01	115	56.4	Star
-70	84	D	118	125 0	139 0	162 0	222 0	0.151	0.656	0 01	115	48.1	Star
-130	18	D	135	135 0	145 8	170.0	232 5	0 150	0 745	0.02	115	52 5	Star
-170	84	D	150	150.0	156.9	179.0	245 0	0.130	0.656	0.02	120	48.1	Trans.
-190	18	D					265 0 ^e					42.0	Trans.

^a R, rounded—no drop in load at yield. D, drop in load at yield. All stresses 1000 lb. per sq. inch.

^b By the method employed. Difficult to determine accurately.

^c E_p is the slope of the strain-hardening curve.

^d See Fig. 12.

^e Other data not recorded.

The results of the experiments on the specimens that were air-cooled and tempered to 130,000 lb. per sq. in. yield strength are presented in Table 2 and as Fig. 9. The fracture strength of the undeformed metal has been obtained in the manner described above and is also plotted in Fig. 9. The brittle failure of this steel occurs at a lower equivalent strain rate (10^{10} sec.⁻¹) or at a higher temperature than that of the steel heat-treated to the lower strength. Brittle failure occurs at a lower equivalent strain rate (or higher temperature) primarily because of the smaller separation between the yield strength and fracture strength of the undeformed metal

impact test the separation of yield and fracture strength is decreased by virtue of the increased strain rate and the transverse constraint imposed by the notch. This decrease in separation between the yield and fracture strengths raises the temperature of brittle failure very nearly to room temperature. Small differences in the separation between the yield strength and the fracture strength of the undeformed metal will be reflected in rather large differences in the temperature at which brittle failure occurs. The less the separation, the higher will be the temperature of brittle failure and the greater the separation, the lower it will be.

Tempered Martensitic Steel

The results of the experiments at the two strength levels of this type of steel are presented in Tables 3 and 4 and in

quently becomes smaller. The logarithm of the yield and fracture strengths increases linearly with the logarithm of the equivalent strain rate to about 10^3 sec.^{-1} (or to

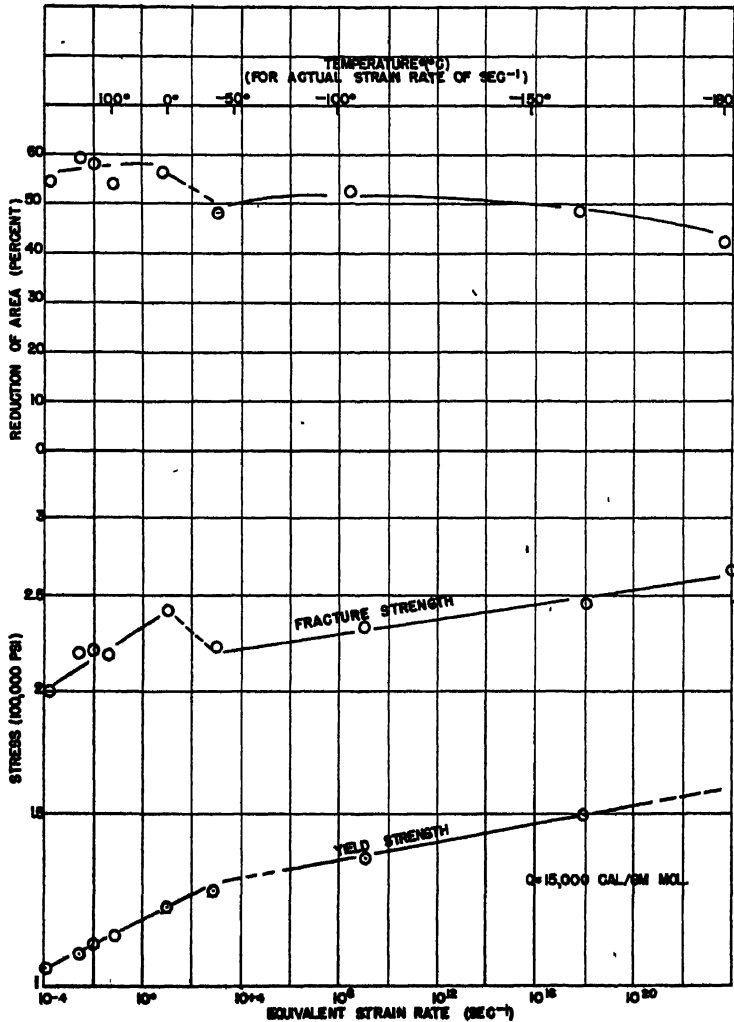


FIG. 10.—TENSILE PROPERTIES OF A TEMPERED MARTENSITIC STEEL AS FUNCTION OF STRAIN RATE AND OF TEMPERATURE.

Yield strength, 100,000 lb. per sq. inch.

Figs. 10 and 11. As the strength increases, the separation of the yield and fracture strengths under the normal test conditions ($10^{-4} \text{ sec.}^{-1}$) decreases and the ductility as measured by reduction of area conse-

about -70°C.). The fracture strength, however, rises more rapidly than the yield strength (at both strength levels) and the reduction of area increases slightly. At an equivalent strain rate of about 10^3 sec.^{-1}

the dependence of both yield and fracture strength on equivalent strain rate changes discontinuously. This change is such, however, that the yield and fracture strengths

both must change. A change in Q would of course introduce a change of coordinates of Figs. 10 and 11. This abrupt change is associated with a sudden change of type

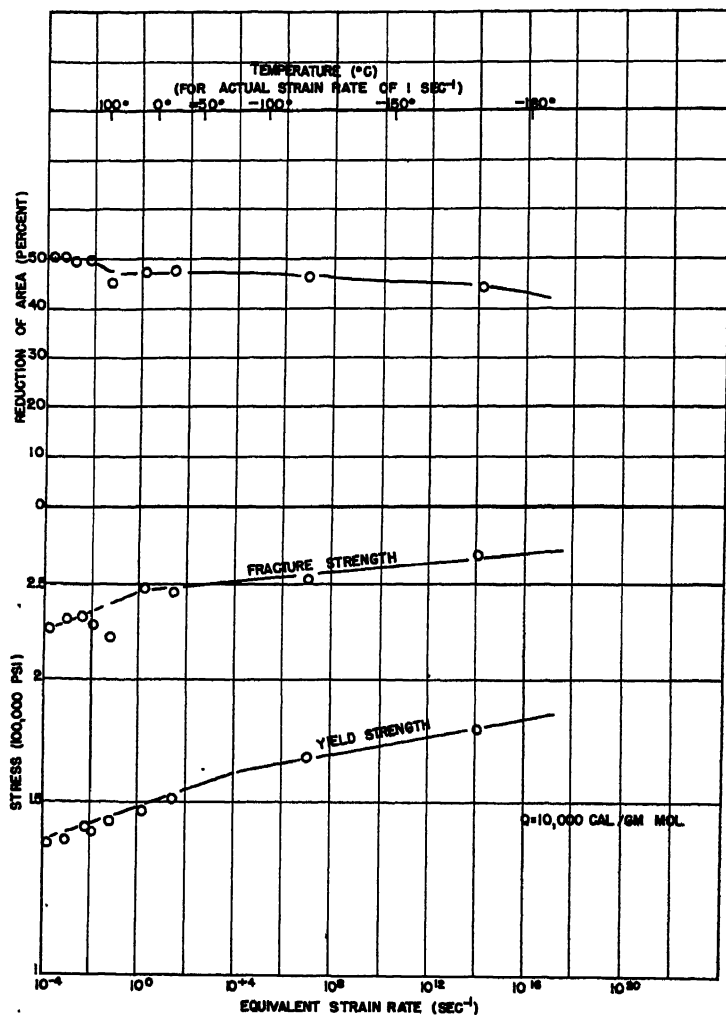


FIG. 11.—TENSILE PROPERTIES OF A TEMPERED MARTENSITIC STEEL AS FUNCTION OF STRAIN RATE AND OF TEMPERATURE.

Yield strength, 130,000 lb. per sq. inch.

continue to rise at very nearly the same relative rate, and therefore the ductility can at most change very slowly. This discontinuous change with increasing equivalent strain rate necessitates that r or Q or

of fracture, but the mechanism of the change is at present unexplained. The authors have arbitrarily assumed Q to be constant, in order to illustrate the general behavior.

The slight decrease in ductility at high equivalent strain rates is due primarily to the slight decrease in the separation of the yield and fracture strengths and to an

for fracture of this tempered martensitic steel. Because of the spheroidal nature of the carbides of this structure, deformation will not result in an orientation of

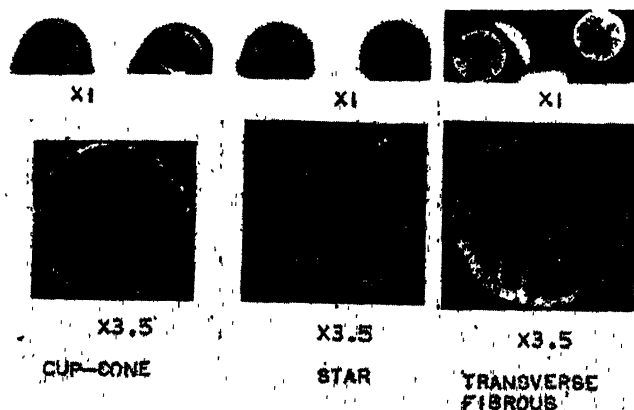


FIG. 12.—TYPES OF FRACTURES OF TEMPERED MARTENSITE STEEL AT VARIOUS TEMPERATURES OR STRAIN RATES.

increase in the strain-hardening modulus (slope of the linear portion of the flow curve). There is no evidence of any effect of prior deformation on the stress required

the carbide particles. Thus, the average dimension of the particles in a plane perpendicular to the applied stress does not change with deformation; therefore

TABLE 4.—*Tempered Martensite*
YIELD STRENGTH, 130,000 POUNDS PER SQUARE INCH

Deoxidation: Vanadium			Steelmaking: Electric Furnace				Heat-treatment: Water-quenched from 1265°F. Drawn for 3 Hr. at 1265°F. 5/8-in Rounds						
			Forming: Centrifugal Casting				Strain			E _s , Lb Per Sq. In.	R. A., Per Cent	Type of Fracture ^d	
Tem- perature, Deg. C.	Strain Rate × 10 ⁴	Type of S-S Curve ^a	Yield Strength at Plastic Strain		Tensile Strength		Fracture Stress						
			of 0.001 ^b	of 0.01 or L.Y.P. ^c	Load Orig. Area	Load Act. Area		to T. S.	to F. S.	at Y.P.E.			
20	2.2	R	131.0	136.3	145.0	168.0	226.5	0.145	0.708	R	100.0	50.8	C.P
20	18	R	133.0	138.0	146.0	164.5	230.4	0.125	0.706	R	110.0	50.8	C.P
20	84	R	135.0	142.0	148.8	167.0	232.7	0.110	0.656	R	120.0	49.4	C.P.
-12	2.2	R	134.0	140.0	147.0	161.5	228.0	0.080	0.690	R	110.0	49.9	C.P.
-12	84	R	137.0	144.0	150.3	166.0	221.0	0.095	0.660		110.0	45.1	C.P.
-70	7.2	?	142.0	147.0	160.0	189.0	248.0	0.160	0.628		110.0	47.2	C. Star
-70	84	?	146.0	151.0	163.0	192.0	246.0	0.170	0.648		110.0	47.7	C. Star
-140	84	D	167.0	167.0	176.4	197.0	253.0	0.110	0.620	0.25 app. 0.015 app.	110.0	46.1	C. Star
-180	84	D	179.0	179.0	184.0	211.0	268.0	0.110	0.584		110.0	44.4	C. Star

^a R, rounded—no drop in load at yield. D, drop in load at yield. All stresses 1000 lb. per sq. inch.

^b By the method employed. Difficult to determine accurately.

^c E_s is the slope of the strain-hardening curve.

^d See Fig. 12

the fracture strength should not depend upon the prior deformation.*

Even at high actual strain rates or very low temperatures, these steels should not break brittly. The type of fracture does, however, change as the equivalent strain rate increases (as temperature decreases). At about 10^2 sec.^{-1} , the fracture changes abruptly from a cup-cone to a star type, and as the equivalent strain rate is further increased the fracture transforms gradually to a transverse-fibrous type. These fractures are illustrated in Fig. 12.

CONCLUSIONS

1. The flow stress and fracture strength have been obtained over a wide range of temperature and of strain rate for both pearlitic and a tempered martensitic steel at two stress levels.

2. The effect of deformation upon fracture strength has been obtained for a pearlitic steel.

3. The observations indicate that deformation has a negligible effect upon the fracture strength of the tempered martensitic steel.

4. The anomalous effect of deformation upon the fracture strength of a pearlitic structure may be interpreted as due to a reorientation of the carbide lamellae.

5. The phenomenon of fracture is readily understood in terms of the concept of a flow stress and a stress at fracture first introduced by Ludwik.

6. In the yield-strength ranges of the steels examined, only the pearlitic steels were brittle at high strain rates and at low temperatures.

ACKNOWLEDGMENT

The authors would like to acknowledge the encouragement, constructive criticism, and inspiration they have received from

Colonel H. H. Zornig, Director of the Laboratory of Watertown Arsenal.

REFERENCES

1. P. Ludwik: Über die Bedeutung der Elastizitätsgrenze, Bruchdehnung und Kerkzähigkeit für den Konstrukteur. *Ztsch. Metallkunde* (1924) 16, 207.
- P. Ludwik and R. Scheu: Vergleichende Zug-, Druck, Dreh-, und Walzversuche. *Stahl und Eisen* (1925) 45, 373.
- P. Ludwik: Streckgrenze, Kalt- und Warmspannbarkeit. *Ztsch. ver. deut. Ing.* (1926) 70, 379.
2. C. Zener and J. H. Hollomon: Plastic Flow and Rupture of Metals. *Trans. Amer. Soc. Metals* (1943) 33, 163.
3. C. Zener and J. H. Hollomon: Effect of Strain Rate on Plastic Flow of Steel. *Int. Applied Physics* (1944) 15, 22.
4. W. Kuntze: For Survey and Bibliography see references in articles by D. J. McAdam, Jr. listed in ref 5.
5. D. J. McAdam Jr.: Technical Cohesive Strength of Metals. *Trans. Amer. Soc. Mech. Engrs.* (1941) 63, A-155.
- Technical Cohesive Strength and Yield Strength of Metals. *Trans. A.I.M.E.* (1942) 150, 311.
- 5a. D. J. McAdam Jr. and R. W. Clyne: The Theory of Impact Testing. *Proc. Amer. Soc. Test. Mat.* (1938) 38, pt. 2, 112.
6. G. Sachs: Report on Embrittlement of Steel Under Multiaxial Stress. Eng. Foundation, Welding Research Committee, New York.
- G. Sachs and J. Lubahn: Effects of Notching on Strained Metals. *The Iron Age* (1942) 150 (15), 31, 150 (16), 49.
7. J. H. Hollomon: The Notched-bar Impact Test. This volume, p. 298.

DISCUSSION

R. H. HEYER,* Middletown, Ohio.—Of the three important tests using notched samples, the notched-bar fatigue test and the notched tensile test are gaining in recognition and are being developed into useful tests, while little progress is being made in improvement of the notched-bar impact test.

It is possible that the notched tensile test may become more widely used than the notched-bar impact test because it measures notch brittleness under more favorable conditions and gives an answer in pounds per square inch average stress and percentage of reduction of area rather than in energy units, which are not readily interpreted and cannot be converted to sections of other sizes or shapes.

* The authors have not found it possible to measure the effect directly, as was done for the tempered pearlitic steel, since the tempered martensitic material did not break brittly at the lowest temperature of test.

* Research Laboratory, American Rolling Mill Company.

The notched tensile test also has its limitations in this respect and the conditions under which a cohesive strength limit are determined should always be stated. Present-day acceptance of these tests varies from the following statement of Hollomon and Zener, "... any deductions regarding fracture stress must be regarded with suspicion if based upon notched bars," to McAdam, who is extracting all possible nutriment from the notched tensile test, and, I believe, is making vitamin injections.

The principal criticisms of the notched tensile test are centered about the indeterminate state of stress in the test section and the devious extrapolations often applied to the data. For practical applications, it should not be necessary to attempt to determine a true cohesive limit by extrapolation to zero notch angle and zero area ratio.

In our experience, it has become apparent that much useful information can be gained by using a single notch angle and root radius at three or four notch depths. While it is too early to suggest standardization of any particular test procedure, the great advantage of such standardization should not be overlooked.

We are using a 60° notch, which has merit from the standpoint of machinability and has been the most generally used of all notch angles in reported investigations. The critical feature in preparing the sample is, of course, the root radius. We have not been successful consistently in producing sharp notches by Gensamer's file method, or in any other manner. Furthermore, it has become clear that a small root radius that relieves local stress concentration is advantageous. By lapping a high-speed tool bit to a sharp point, using metallographic polishing papers and then relieving the point slightly, steels up to 350 Brinell can be machined with a 60° notch having a root radius close to 0.001 in. The work is flooded with a good cutting oil during notching. The notch is then lapped, using a human hair and a thick paste of levigated alumina in liquid soap. Blond hairs can be selected at diameters between 0.0015 and 0.002 in. The lapping operation produces a smooth, polished notch with a root diameter of about

0.003 in. or a root radius of 0.0015 in. The contours of the tool bit and the notch are checked by shadow-picture methods at 50 times magnification using a metallurgical microscope.

We believe that the use of some form of lapped notch with a reproducible root radius would greatly improve the reliability of notched tensile tests and make it possible to compare results of all investigators.

J. H. HOLLOWON and C. ZENER (author's reply).—The elucidation of the philosophy of the notched-bar test would require more information and more space than is available at this time. No test should be performed solely for the sake of performing it. First, it must be determined what is to be measured, and, when this has been decided, the test should be chosen or designed that will measure the desired quantities. The quotation of Mr. Heyer from our paper should be carefully examined. It is significant that we stated that deductions regarding the *fracture stress* must be viewed with suspicion. The complexity of the stress distribution and the difficulty of obtaining an exact knowledge regarding the path of the deformation restrict the interpretation of the average yield stresses or average fracture stresses measured in notched-bar tests. Other quantities, such as the temperature of brittle fracture of the relative energy absorbed, may be semiquantitative or at least qualitatively interpreted.

It is believed that frequently the interpretation of the results of notched-bar tests is carried to an unreasonable extent. A discussion of the significance and interpretation of the notched-bar impact test is given by one of the authors beginning on page 298 of this volume. This presentation emphasizes that any such test must be interpreted in terms of the fundamental variables affecting the mechanical properties of metals. No other interpretation can be effective.

The suggestions regarding the production of very sharp notches are extremely interesting and should prove valuable to those interested in performing notched-bar tests.

The Notched-bar Impact Test

By J. H. HOLLOMON,* STUDENT ASSOCIATE A.I.M.E.

(New York Meeting, February 1944)

THE interpretation of notched-bar impact results has been a matter of controversy since the introduction of more or less standard tests by Fremont,¹ Charpy² and others at the turn of the century. Many investigators³⁻¹¹ have contributed to the understanding of the significance of such tests. Several symposiums^{12,13} have been held with the express purpose of discussing the significance and interpretation of the impact tests. It is not the purpose of this paper to review all these contributions to the development of the knowledge on this subject, but rather to present an interpretation of notched-bar impact tests that appears to be in agreement with the available published data.

Fundamentally, the interpretation discussed in this paper of the brittle failure of some steels in notched-bar impact test is similar to the qualitative analysis presented by Ludwik³ in the 1920's. Essentially, Ludwik stated that the function of the notch was to increase the tensile stress necessary for yielding, and that brittle failure occurred when the stress necessary

for yielding exceeded the normal stress required for fracture (with no plastic deformation). Ludwik, however, had no means of measuring this normal stress necessary for failure of a plastically* undeformed metal, therefore he could not extend his interpretation beyond the qualitative stage. Kuntze¹⁴ and recently McAdam¹⁵ attempted to determine the effect of deformation on the stress necessary for fracture by testing, in tension, specimens notched to various depths and angles. Because of the uncertainties in Kuntze's (and McAdam's) analysis of the stresses (which have been pointed out by Sachs¹⁶) and the inherent nonuniformity in the stress distribution in notched bars, the results of such investigations are difficult to interpret. A more direct method of measuring the effect of deformation on the fracture stress was suggested in previous papers¹⁷⁻¹⁸ and has been utilized in the present investigation.

The present paper concerns itself primarily with the behavior of notched impact specimens. The effects of strain rate, temperature, and stress distribution, which are discussed with reference to the impact specimen, apply just as well to the behavior of metal at the bases of notches in any engineering structure. All that is necessary is to determine the stress distribution in the structure at the base of the notches.

The statements or opinions in this article are those of the author and do not necessarily express the views of the Ordnance Department. Published by permission of the War Department. Manuscript received at the office of the Institute Oct. 7, 1943. Issued as T.P. 1667 in METALS TECHNOLOGY, April 1944

The description of the data upon which the interpretation presented in this paper is based is contained in a paper by J. H. Hollomon and Clarence Zener,¹⁸ which has not yet been published.

* Captain, Ordnance Department, U. S. Army, Watertown Arsenal, Watertown, Massachusetts.

¹ References are at the end of the paper.

* Throughout this paper "fracture strength of the undeformed metal" refers to a metal *plastically* undeformed or *plastically* deformed to a very small strain.

An impact specimen may be considered nothing more than a simple engineering structure.

The purpose of the present study is accomplished by correlating the results of

NOTCHED-BAR SPECIMENS

State of Stress

The distribution of stresses in notched bars has been discussed in some detail by

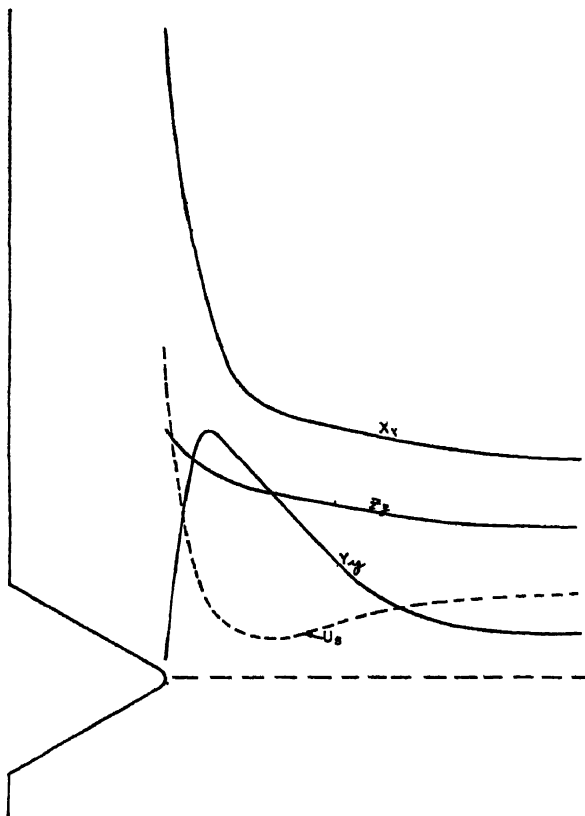


FIG. 1.—VARIATION OF STATE OF STRESS ACROSS NOTCHED CYLINDER IN TENSION. (After Gensamer⁵.)

X_x = longitudinal stress.

Y_y = radial stress.

Z_z = transverse (or circumferential) stress.

U_s = shear-strain energy.

the impact tests with those of tensile tests obtained at various low temperatures and high strain rates. Tensile results of two steels are used simply as examples to illustrate the effects of the variables of impact tests. Before correlation of these tensile and impact properties is possible, it is necessary, however, to review briefly the distribution of stresses at the bases of sharp notches.

Neuber¹⁹ (circular bar with hyperbolic notches), by Frocht²⁰ (circular bars with U-shaped notches), by Coker and Filon²¹ (square bars with V and keyhole notches), and by McAdam and Mebs.²² The state of stress below a notch in a cylindrical test bar under tensile stress is described schematically in Fig. 1. In this figure, X_x refers to the longitudinal tensile stress, which is maximum at the base of the notch; Z_z

refers to the circumferential (tangential) stress; and Y_r refers to the radial stress, which must necessarily be zero at the surface of the notch. The state of stress described in this figure for a cylindrical notched bar in tension is similar to that found just below the center of the notch in bending.⁵

According to the Von Mises viewpoint (p. 10 of ref. 24), yielding occurs when the shear strain energy is equal to a critical value. The shear-strain energy is given by the following relation:

$$U_s = [(X_s - Y_s)^2 + (Y_s - Z_s)^2 + (Z_s - X_s)^2] / 12G \quad [1]$$

where X_s , Y_s , and Z_s are the three principal stresses and G , the modulus of rigidity. The variations of shear-strain energy with depth below the notch is also represented schematically in curve U_s , Fig. 1. According to the Mohr viewpoint (p. 11 of ref. 24), yielding occurs when the maximum shearing stress reaches a critical value. The maximum shearing stress (one half the difference between maximum and minimum principal stresses) will vary with the depth below the notch in nearly the same fashion as the shear strain energy.

The Von Mises criterion for yielding is the more nearly correct for most metals, with the notable exception of steels that have a drop of load at yielding, which probably obey the Mohr hypothesis. Thus, in general, yielding will occur when the maximum shear-strain energy reaches a critical value. In the notched bar, this energy is a maximum at the very base of the notch, and falls off sharply just below the notch. It may be that this sharp gradient in shear-strain energy (or in maximum shearing stress) requires a higher critical value for yielding than would a uniform distribution of shear-strain energy (p. 4 of ref. 24). Since this effect has not been investigated and cannot be evaluated at this time, the study of the notched bar will

be confined to other factors, which can be discussed qualitatively at least.

The sharper or the deeper the notch, the greater will be all of the principal stresses just below the base of the notch, for a constant notch angle. The magnitude and the gradient of the shear strain energy (or maximum shear stress) will also increase as the principal stresses become more concentrated if the rest of the geometry and the applied load are constant. The quantitative effect of increasing the depth and radius of the notch on the concentration of the longitudinal tensile stress at the base of a V-notch in a Charpy test bar is presented as Fig. 2 (derived from the data of Coker and Filon²¹). The stress concentration factor b is defined as the ratio of the maximum longitudinal stress at the base of the notch to the average stress in the unnotched section. This relation between b and the sharpness of the notch may be applied to the case of bending to a good approximation, if the ratio of the depth of the notch to the height of the test bar is small.* As the notch becomes deeper, the notched area decreases and the average stress beneath the notch becomes greater. Thus even though the stress concentration factor as defined above increases as the notch is made deeper, the gradient in longitudinal stress beneath the notch may decrease.

As the ratio of the depth of the notch to its radius increases, the ratio of the maximum longitudinal stress to the average longitudinal stress increases. The elastic strain rate at the base of the notch is given by:

$$\dot{\epsilon} = b\dot{\epsilon}_0 \quad [2]$$

where ϵ is the elastic strain rate at the base of the notch, b the stress concentration

* It should be noted that the discussion of the stresses at the base of the notch are of a semiquantitative nature. The stress distribution will be affected by the elastic waves set up by the impact.

factor and $\dot{\epsilon}_0$ the elastic strain rate in the unnotched section.

Directly below and at the surface of the notch, the radial stress is zero, and the ex-

yielding for these two cases may be derived directly from Eqs. 3 and 4:

$$\left(\frac{X_{z_0}'}{X_z'}\right)^2 = 1 - \left(\frac{Z_s'}{X_z'}\right)^2 + \left(\frac{Z_s'}{X_z'}\right)^2 \quad [5]$$

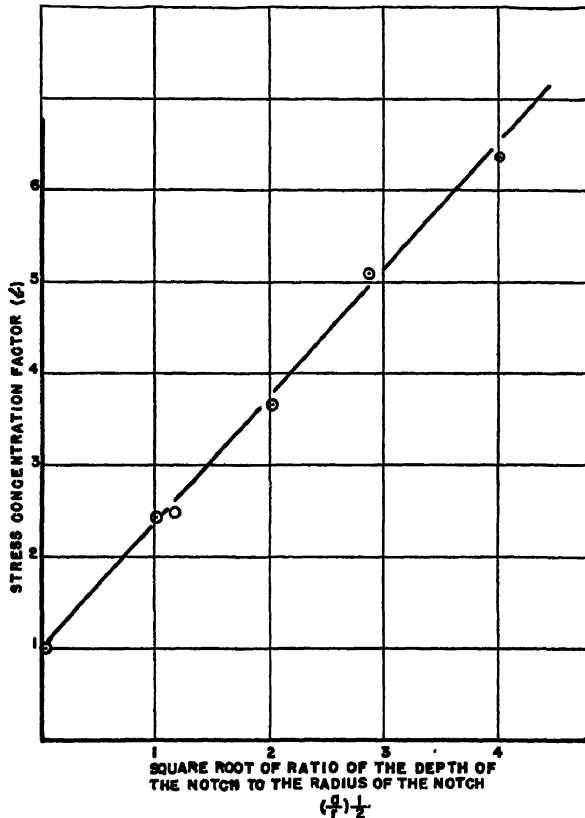


FIG. 2.—EFFECT OF NOTCH DEPTH AND SHARPNESS ON LONGITUDINAL TENSILE STRESS AT BASE OF NOTCH (FOR V-NOTCH CHARPY BAR). (After *Coker and Filon*.¹¹)

pression for the shear-strain energy reduces to:

$$U_s = [(X_s - Z_s)^2 + Z_s^2 + X_s^2]/12G \quad [3]$$

In the absence of the transverse stress (in the case of simple longitudinal tension) the shear-strain energy is given by:

$$U_s = 2X_{s_0}^2/12G \quad [4]$$

where X_{s_0} is the longitudinal tensile stress in the absence of other principal stresses.

Since yielding will occur for a given value of U_s , the relation between the stresses at

where the superscript ' refers to the stress at yielding. If the ratio of the radius of the notch to the bar width is sufficiently small so that the unstressed mass in the shoulder of the specimen completely prevents the material from the additional contraction, which should accompany the increase in longitudinal stress at the base of the notch, the transverse stress at the midwidth of the bar at the base of the notch will be given approximately by the Eq. 6 (see Appendix A for derivation):

$$Z_s = \sigma(b - r)\gamma \quad [6] \quad \text{about 5 (Fig. 2) and the increase in yield strength is nearly 11 per cent.}$$

where σ is Poisson's ratio; b , the stress-concentration factor, and γ the average

As the width of the bar increases, or the radius of the notch decreases, the restraint

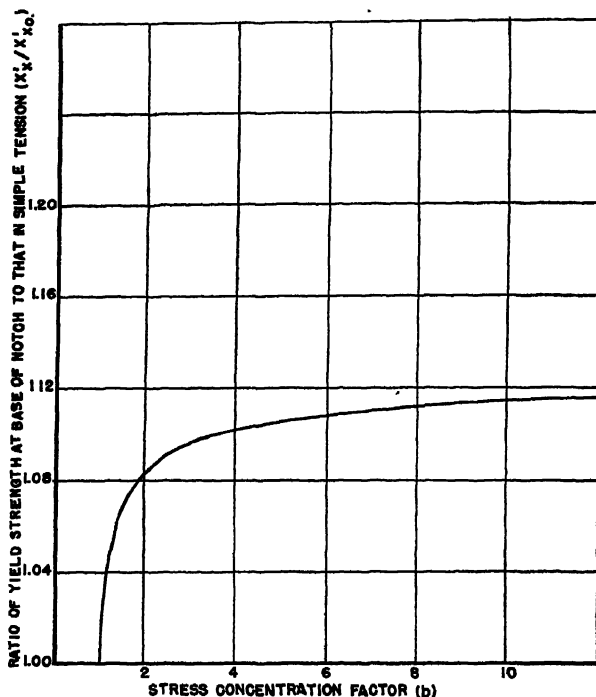


FIG. 3.—EFFECT OF STRESS CONCENTRATION FACTOR ON TENSILE STRESS NECESSARY FOR YIELDING.

longitudinal stress in the unnotched section. Combining Eqs. 5 and 6:

$$\left(\frac{X'_{s0}}{X'_s}\right) = 1 - \frac{\sigma(b-1)}{b} + \left(\frac{\sigma(b-1)}{b}\right)^2 \quad [7]$$

since

$$X_s = b\gamma$$

For the case of no lateral contraction, due to the concentration of the stress, the increase in yield strength due to the presence of this transverse stress is plotted in Fig. 3 as a function of the stress-concentration factor. For the standard²³ Charpy impact test specimen with a V-notch of 0.01 in. radius, the stress-concentration factor is

to transverse contraction, and thus, the transverse tensile stress, increases. The variation of the transverse stress at the base of the notch and at the center of the bar with this ratio is presented in Fig. 4 (see Appendix A for calculations). For values of the ratio of notch radius to bar width below about $\frac{1}{10}$, the transverse tensile stress is very nearly equal to its maximum value. At the surface of the bar on its sides, the transverse stress must necessarily be zero.

This discussion of the effect of the transverse stress tacitly assumes that the material does not have a deformation curvature during the elastic deformation, which would relieve the transverse stress. In notched-bar impact specimens, the inertia

of the material probably aids in reducing this curvature.

From these considerations, the primary effects of the notch in a square bar during bending may be summarized:

1. The longitudinal tensile stress at the base of the notch is increased. The concentration of this stress depends upon the ratio of the depth of the notch to its radius for a constant form of notch.

2. The elastic-strain rate at the base of the notch is greater than the strain rate in the unnotched section and is equal to the stress-concentration factor multiplied by this strain rate.

3. The notch introduces a sharp gradient in the shear-strain energy just below the notch.

4. Because of the presence of a transverse tensile stress, the longitudinal tensile stress necessary for yielding is increased. The magnitude of this increase will depend on both the stress-concentration factor and the ratio of notch radius to bar width. The maximum possible increase is about 12 per cent (Fig. 3). The effect on the transverse stress of changing the ratio of radius of notch to width of bar is very small except for the large values ($> \frac{1}{10}$) of the ratio.

Types of Test Specimens

There are certain minor differences in the various standard type impact-test specimens. The square Izod test bar with a V-notch placed slightly away from the middle of the length of the bar is used rather generally in Great Britain, and both the square and round bars are used to some extent in this country. In the testing of this type of specimen, the bar is clamped at one end and struck on the notch side at the other end. This method of loading produces an asymmetrical stress distribution at the base of the notch.²¹ This asymmetry will depend also upon the stresses set up by the clamp. Since, in the testing of ductile materials with this type of speci-

men, complete fracture of the specimen does not always occur, it is often difficult to compare the results of the impact tests.

In the United States, the standard Charpy test bar with a keyhole notch has been used more generally, since it is believed that more reproducible values of the impact energy are obtained. The Charpy specimen has the additional advantage of facilitating low-temperature tests. The Charpy test is performed by placing the test specimen loosely on a platform between two supports at its ends. The impact is accomplished by a pendulum striking on the side opposite the notch at the mid-length of the bar. In this method of testing, the asymmetry of the stress distribution inherent in the Izod test is avoided and fracture usually occurs even for the most ductile material. Since the standard keyhole-notch specimens are of such size that the maximum energy required to fracture very ductile steel specimens is only about 40 to 50 ft-lb., small differences between materials are sometimes difficult to determine. Furthermore, very little careful analysis of the stresses at the base of the keyhole notch as a function of the specimen geometry has been attempted.

Many investigators have modified the Charpy specimen by using a V-notch rather than a keyhole. This specimen has the advantage that the maximum spread between very ductile and brittle steels is of the order of magnitude of a 100 ft-lb.; and, it is believed that small differences in materials are therefore more readily distinguishable. Furthermore, more attention has been paid to the study of the variation of geometry of the test bar for this type of specimen and the effects of variables are more readily understandable.

Although this report concerns itself primarily with V-notch Charpy test specimens, it is believed that the interpretations apply in a general manner to any type of impact specimen.

RELATION BETWEEN TENSILE AND NOTCHED-BAR IMPACT PROPERTIES

in which

$$\dot{p} = \dot{\epsilon} p Q / RT$$

Since the notched-bar impact test is characterized by high strain rates at the

and S is some measure of the strength of the material; ϵ , the strain; $\dot{\epsilon}$, the strain

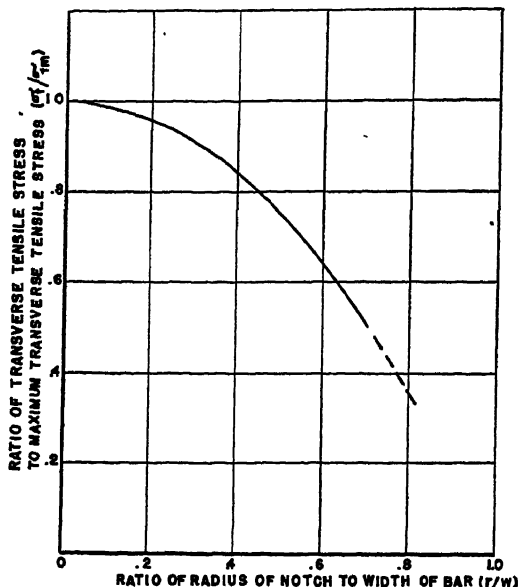


FIG. 4.—EFFECT OF VARYING NOTCH RADIUS AND BAR WIDTH ON TRANSVERSE STRESS AT BASE OF NOTCH.

base of the notch and often is performed at temperatures below room temperature, it is necessary to determine the effect of these variables on the normal tensile properties of at least some typical metals, in order to interpret the properties observed in notched-bar impact tests.

Physical Properties in Tension

By a technique (p. 26 of ref. 24), based upon the assumption of an equivalence between the effects of decreasing temperature and increasing strain rate on the mechanical properties of metals, the tensile properties of several typical steels have been determined at high (equivalent) strain rates. This technique assumes that the strength of metals is related to the temperature, strain rate, and strain in the following manner:

$$S = S_p(\epsilon) \quad [8]$$

rate; Q , a heat of activation characteristic of the material; R , the gas constant, and, T , the absolute temperature of testing. After determining the constant Q for a particular material, and for a given range of strain rate and temperature, the isothermal tensile properties at various rates of strain and at various temperatures may be determined by the equivalence. The properties of several steels have been obtained in this fashion as a function of equivalent strain rate.* Since the stress at a given strain is a function of \dot{p} , the properties of the material will be the same for any value of the strain rate and temperature at which \dot{p} is a constant. Thus, the

* The "equivalent strain rate" is defined as the strain rate that will produce at a given temperature (in this case, room temperature) the same properties that were measured at a small actual strain rate at some lower temperature.

effects of high strain rates may be obtained at room temperature for a given material by determining Q and then performing tensile tests at various low temperatures.

The effect of equivalent strain rate on the isothermal* tensile properties for these two sets of specimens are presented in Fig. 5

The fracture strength represented by

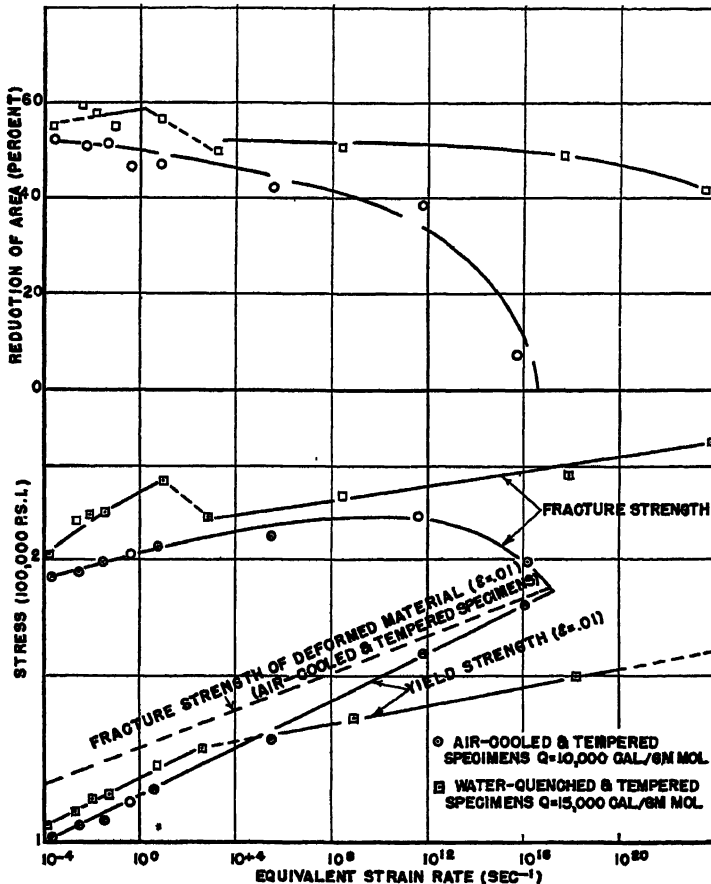


FIG. 5.—EFFECT OF EQUIVALENT STRAIN RATE ON TENSILE PROPERTIES OF TYPICAL STEEL.

The results of these experiments have been described elsewhere^{17,18} in detail, but the main features will be reviewed. Specimens from a Cr-Mo-V casting containing 0.25 per cent C. were heat-treated in two groups: the first was air-cooled from above the critical temperature and the second was water-quenched. Both sets of specimens were tempered to about the same yield strengths. All the tensile and impact data were obtained on these specimens.

solid lines in this figure are those measured after various amounts of plastic deformation. The stress required to fracture a metal may vary, however, with the amount of plastic deformation before fracture. Such an effect was suggested some years ago by Ludwik,⁹ Kuntze,¹⁴ and recently Mc-

* In discussing the general features of notched-bar impact tests, the isothermal tensile properties will suffice for most purposes even though the adiabatic stress-strain curves may be approximately calculated.

Adam,¹⁵ have attempted to measure the effect of deformation by testing tensile specimens notched to various depths and angles. This technique is uncertain because

tion, at -190°C ., and their fracture stresses were measured. By this method, the effect of prior deformation upon the fracture stress was obtained. The results are plotted

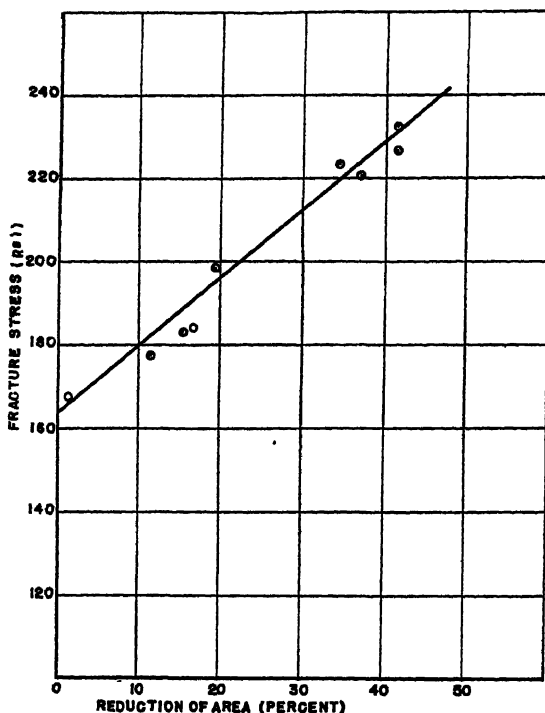


FIG. 6.—EFFECT OF PRIOR DEFORMATION ON FRACTURE STRESS AT -190°C . (AIR-COOLED STEEL).

of the difficulties in determining the stress in the plastic range at the bases of the sharp notches. In a previous paper,¹⁸ a more direct method for finding the effect of deformation was suggested and some preliminary results presented. This method, however, is applicable only to metals that in tension break brittly at some temperature. Specimens taken from the steel casting already described were heat-treated by air cooling followed by tempering to very nearly the same yield strength as the air-cooled set of specimens whose tensile properties are described in Fig. 5. These specimens were deformed plastically by various amounts at room temperature and then broken, with little further deforma-

tion, in Fig. 6. With increasing plastic deformation, the fracture stress increases.

If the assumption is made that the increase of fracture stress with deformation is independent of the temperature at which the deformation occurs, the fracture stress of the undeformed metal may be determined as a function of equivalent strain rate. For each value of equivalent strain rate, the reduction of area may be obtained from Fig. 5 and its effect in increasing the fracture stress determined from Fig. 6. The fracture strength of the undeformed metal has been determined as a function of equivalent strain rate by subtracting from the measured fracture stress, the increase in stress brought about

by deformation. The variation of the fracture strength of the undeformed steel obtained in this manner with the equivalent strain rate is plotted as the dashed line in Fig. 5. The logarithm of the fracture strength of the undeformed metal and the logarithm of the yield strength increase linearly as the logarithm of the equivalent strain rate increases. The fracture strength rises less rapidly than does the yield strength, and brittle failure occurs when the two straight lines intersect.

It is not possible, with the technique described above, to determine the effect of deformation on the fracture strength of the steel that does not break brittly in the tensile tests in the range of temperature employed. It is only possible to conclude that since this material did not break brittly in the range of temperature and strain rate investigated, the yield strength does not exceed the fracture strength of the undeformed steel. Furthermore, it may be inferred that since the decrease in deformation at high equivalent strain rates does not reflect itself in a decrease in fracture strength, deformation has little effect on the fracture strength.

Impact Properties of Air-cooled Steel

It is now possible to attempt a correlation of the tensile and impact properties of these typical steels. The first effect that must be considered in the notched-bar impact test is that of strain rate. For the case of the standard V-notch Charpy bar of 0.01-in. radius of notch, the average strain rate can be calculated from appendix B to be 120 sec.^{-1} .^{*} For the V-notch Charpy bar under consideration, the ratio of the depth of notch to its radius is 8, and from Fig. 2, the stress-concentration factor b is found to be approximately 5. The elastic strain rate at the base of the notch, therefore, is equal to about 600 sec.^{-1} , or $10^{2.8} \text{ sec.}^{-1}$ or approximately 10^3 sec.^{-1} . The effect of

temperature at a strain rate of 10^3 sec.^{-1} on the tensile properties of the air-cooled and tempered specimens has been derived from Fig. 4 by utilizing the equivalence of the effects of strain rate and temperature. The effect of decreasing the temperature at this strain rate on the fracture and yield strengths is illustrated by the dashed lines in Fig. 7. The solid line illustrates the variation of the fracture strength of the undeformed metal with decreasing temperature. At this strain rate, this steel should break brittly at -170°C . Therefore, this steel when deformed in simple longitudinal tension at a strain rate of 10^3 sec.^{-1} should be ductile at all temperatures above -170°C .

In a notched-bar impact bend test, however, the longitudinal tensile stress necessary for yielding is raised by an amount depending upon the magnitude of the transverse stress. As was noted in a previous section, the increase in longitudinal stress necessary for yielding (for the V-notch Charpy specimen) due to this effect is 11 per cent. The effect of this increase in yield strength upon the impact properties is illustrated in Fig. 7. (For the case of the standard V-notch Charpy impact test specimens, the ratio of radius of notch to width of bar is so small ($\frac{1}{40}$) that the transverse stress is very nearly equal to the maximum value consistent with the stress-concentration factor.)

For the case of the standard V-notch Charpy specimen, the yield strength will equal the fracture strength of the undeformed steel at about -40°C , and brittle failure will occur at that temperature. If the ratio of notch radius to bar width is made larger, the transverse constraint is less, and brittle failure will occur at a lower temperature.

It is now possible to describe in detail how the energy required to fracture notched-impact test specimens of this material will depend upon temperature. A schematic description of the impact

^{*} Often referred to as inch per inch per second.

properties of this type of steel in terms of the tensile stress-strain curves is presented as Fig. 8. Curve 1 represents the stress- of the fracture strength with strain. At the intersection of these curves, plastic deformation is terminated and failure results.

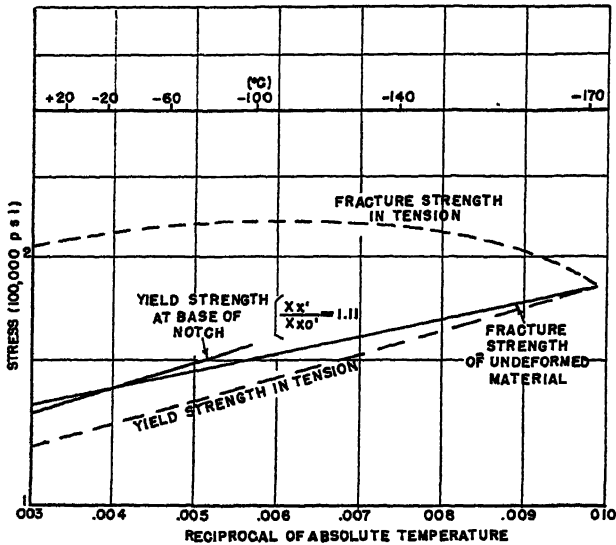


FIG. 7.—EFFECT OF DECREASING TEMPERATURE ON TENSILE PROPERTIES OF A TYPICAL STEEL AT STRAIN RATE OF 10^3 SEC.^{-1} (AIR-COOLED SPECIMENS).

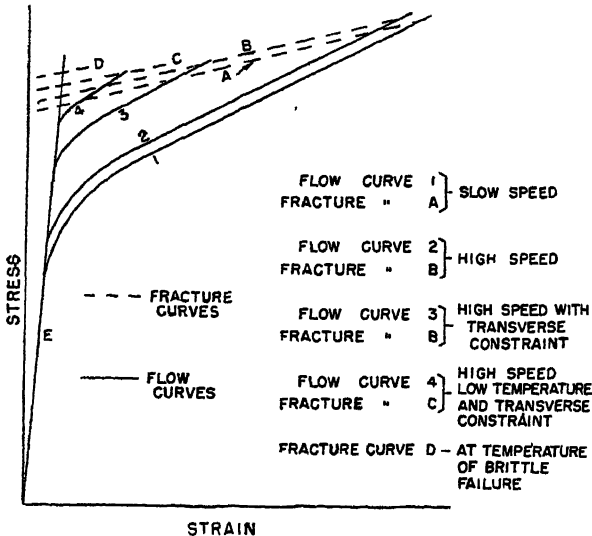


FIG. 8.—SCHEMATIC REPRESENTATION OF MECHANISM OF BRITTLE FAILURE OF TYPICAL STEEL (AIR-COOLED).

strain curve (or flow curve) obtained at ordinary testing speeds at room temperature and curve A describes the variation

As the strain rate is increased, both curves rise, the flow curve more rapidly than the fracture-strength curve. It has been shown¹⁷

that the plastic-flow curve shifts upward very nearly parallel to itself and for the purposes of this discussion it is assumed that the fracture-strength curve does also.

metal just below the notch may fail in a ductile manner with the formation of a crack. Since this crack may be very sharp, the material below this new notch may fail

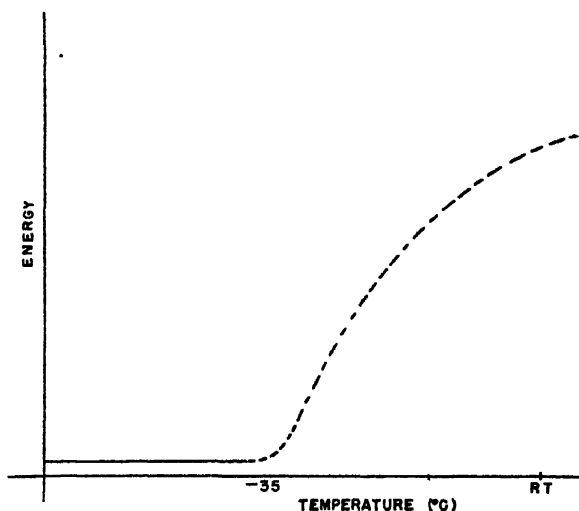


FIG. 9.—EFFECT OF TEMPERATURE ON NOTCHED-BAR IMPACT ENERGY (DERIVED).

The effect of the transverse stress in transferring from the tensile specimen to the notched specimen is to shift the entire flow curve upward,* thus decreasing the strain before fracture (intersection of curves 3 and B). As the temperature is decreased, the fracture-strength curve shifts upward more slowly than the flow curve and the amount of deformation before fracture decreases rapidly until the yield strength becomes equal to the fracture strength of the undeformed metal at the temperature of brittle failure.

This discussion in essence assumes that the fracture of the entire specimen is determined by the original notch. Above the temperature of brittle failure, however, the

brittleness (p. 148 of ref. 13) because of the increase in strain rate and transverse stress due to the sharper notch. This progressive increase in depth and sharpness of the notch will further contribute to the rapid decrease in impact energy, as the temperature is decreased to that at which the entire bar breaks brittly.

The schematic variation in impact energy for V-notch impact specimens as derived from Fig. 8 is presented as Fig. 9. As the temperature is decreased below room temperature for this air-cooled steel, the energy necessary for fracture decreases rapidly to about $-40^{\circ}\text{C}.$, at which temperature brittle failure occurs.

The variation of impact energy with temperature for steel specimens heat-treated in the same fashion as the air-cooled tensile specimens is presented in Fig. 10. The impact specimens were of the V-notch Charpy type having a 0.01-in. notch radius. The impact energy decreases sharply with decreasing temperature below

* It is assumed that the transverse stress has no effect on the fracture curve. This viewpoint is consistent with the data now available, even though there is at present no direct experimental evidence to confirm the assumption. The effect previously noted²⁴ of the transverse stress in reducing the fracture strength may now be explained by the decrease in deformation which accompanies the imposition of the transverse stress.

20°C. and becomes equal to zero (3 to 4 ft.-lb.)* at about -40°C. Below -40°C. the entire fracture was characterized by the so-called crystalline appearance. Above

transverse stress must necessarily be zero, the yield strength will be below the fracture strength. Since the bottom side of the specimen undergoes deformation as the

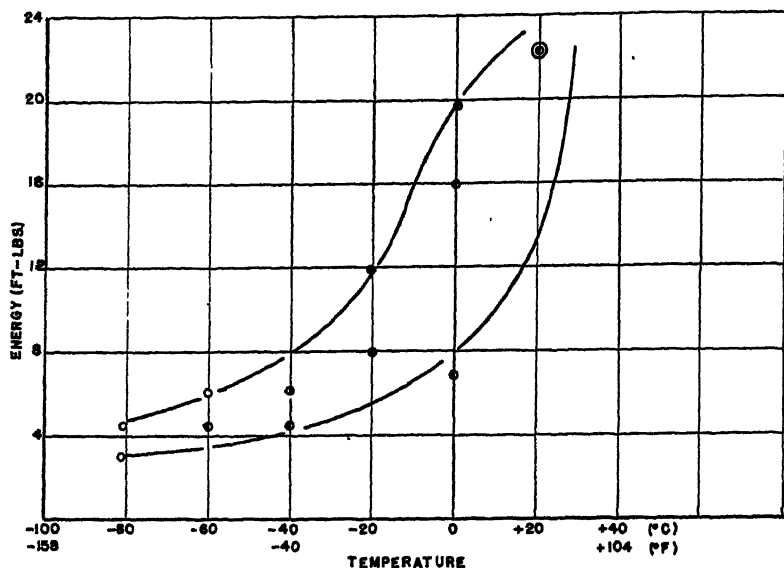


FIG. 10.—VARIATION OF IMPACT ENERGY WITH TEMPERATURE. SPECIMENS TREATED IN $\frac{5}{8}$ -INCH ROUNDS AIR-COOLED AND TEMPERED.

-40°C., a very small layer of material just below the notch evidenced some plastic deformation before fracture; but the major portion of the fracture was of the crystalline type.

For some steels that undergo a transition from ductile to brittle† type of fracture, transition-zone fractures are observed with an area in the center, which is characterized by crystalline (indicative of a nonductile fracture) appearance surrounded completely by material that has suffered deformation. Just above the temperature for complete brittle failure, the material just beneath the notch does not break brittly because its yield strength is below the fracture strength of the undeformed material. Since at the sides of the specimen the

specimen fractures, its fracture strength is raised and brittle failure is prevented until a lower temperature is reached. The very center breaks brittly because the strain rate and transverse stress, and consequently the yield strength, are raised by the formation of a sharp crack. Brittle failure of the entire bar does not occur until the temperature is reached at which the sharpness of the original notch is sufficient to raise the yield strength to the fracture strength of the undeformed metal. An exact discussion of the mechanism of failure at the base of the very sharp "natural" notch is extremely difficult. Some of the complexities have been pointed out previously.¹³

* Actually, it takes about 2 to 3 ft.-lb. to knock the specimen off the anvil.

† Brittle fracture herein is considered to mean that the specimen breaks with only the absorption of elastic energy.

Impact Properties of Water-quenched Steel

The effect of decreasing temperature on the tensile properties of water-quenched

and tempered steel at a strain rate of 10^3 sec.⁻¹ is plotted in Fig. 11. Since this material does not break brittly in the tensile test, it is not possible to determine the

fracture stress at or slightly below room temperature (at a strain rate of 10^3 sec.⁻¹) cannot at present be explained. Since a large amount of deformation occurs before

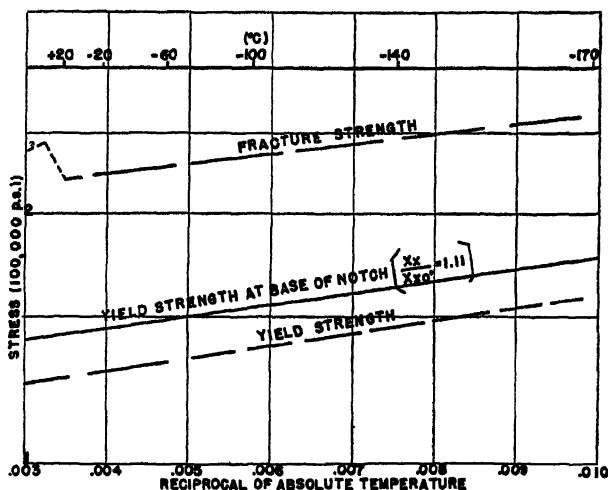


FIG. 11.—EFFECT OF DECREASING TEMPERATURE ON TENSILE PROPERTIES OF A TYPICAL STEEL AT STRAIN RATE OF 10^3 SEC.⁻¹ (WATER-QUENCHED AND TEMPERED SPECIMENS).

effect of deformation on the fracture strength; therefore it is impossible to determine the fracture strength of the undeformed material.

The solid line of Fig. 11 represents the variation with temperature of the longitudinal stress necessary for yielding at the base of the notch. On the assumption that there is little effect of deformation on the fracture stress (or even assuming the same effect of deformation as for the air-cooled steel) brittle failure will not occur for this material down to at least -170°C . at this strain rate. The difference between the yield and fracture stresses gives a measure of the amount of deformation* that will occur at each temperature. Assuming that the deformation is isothermal and, therefore, that Fig. 11 applies directly to the impact test, the variation of the impact energy will be given schematically by the full line of Fig. 12. The sudden decrease in

failure and the deformation is essentially adiabatic at the strain rates that occur in the Charpy test, the temperature of the material will rise during the deformation and the fracture-strength curve shown in Fig. 11 will be shifted toward lower temperatures. The extent of this shift can be calculated¹⁷ approximately. However, for the present purposes, it is sufficient that the sharp drop occurs at a somewhat lower temperature than would be predicted from the isothermal properties (dashed line of Fig. 12).

The actual Charpy-test results are presented in Fig. 13 for this material. The sharp drop occurs at about -40°C . and thereafter the energy decreases only slightly with decreasing temperature. (For other similar materials, it has been found that this very slight decrease continues to -190°C . No information has been obtained for lower temperatures.) The fact that brittle failure does not occur in the range of temperature investigated for this type

* This will also depend on the exact shape of the stress-strain curve.

of material lends credence to the assumption that the effect of deformation on the metals that do not break brittly at low

The notched-bar impact energy for metals that do not break brittly at low

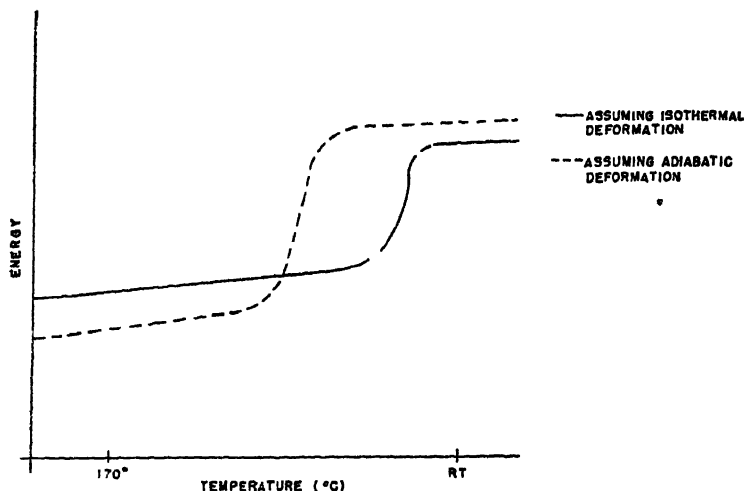


FIG. 12.—EFFECT OF DECREASING TEMPERATURE ON NOTCHED-BAR IMPACT ENERGY (DERIVED) (WATER-QUENCHED AND TEMPERED).

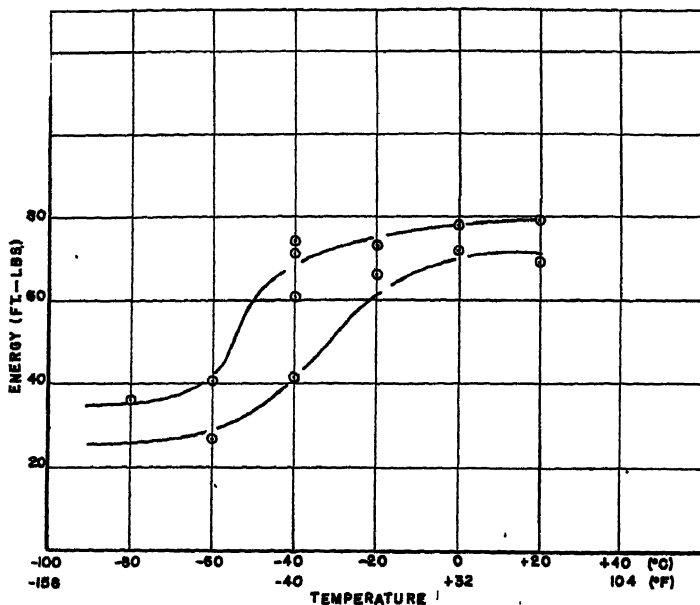


FIG. 13.—VARIATION OF IMPACT ENERGY WITH TEMPERATURE. SPECIMENS TREATED IN $\frac{5}{8}$ -INCH ROUNDS, WATER-QUENCHED AND TEMPERED.

fracture strength is small and that the separation between the yield and fracture strengths of the undeformed metal is large.

temperatures should decrease with temperature more rapidly than would be predicted from a consideration of the areas

under the tensile stress-strain curves at the significant temperatures and strain rates. This more rapid decrease in energy can be accounted for only if the volume of the metal suffering deformation decreases as the temperature is lowered. As has been indicated in the previous discussion concerning water-quenched steel, the ductility decreases slightly and the strength increases markedly as the temperature decreases. This decrease in strain before fracture will effect a decrease in the amount of metal below the notch that suffers deformation, and consequently a further reduction in the energy absorbed.

EFFECT OF VARIABLES OF IMPACT TEST

Radius of Notch

Changing the sharpness of the notch by varying its radius of curvature (while maintaining the rest of the geometry constant) changes both the strain rate and the transverse stress. If, however, the ratio of notch radius to bar width is less than about $\frac{1}{10}$ (Fig. 4) and the stress-concentration factor is above about 2.5 (Fig. 3), the principal effect of varying the radius will be to change the strain rate. If a/r becomes greater than $\frac{1}{10}$ or b less than 2.5, changing the notch radius will change the transverse stress and, consequently, the longitudinal stress necessary for yielding.

For a steel that breaks without deformation in an impact test, the relation between the strain rate and temperature at which brittle failure occurs will be given (see Eq. 8) by the following equation:

$$\dot{p}_B = \dot{e}_B e^{Q/RT_B} \quad [9]$$

where \dot{p}_B is a constant and the subscript B refers to brittle failure. Since the effects of strain rate and temperature are equivalent, fracture without deformation will occur at a combination of these two variables at which Eq. 9 is satisfied.

Combining Eqs. 9 and 2, the relation between the stress-concentration factor

and the temperature at which brittle failure occurs is found:

$$\dot{p}_B = \dot{e}_B e^{Q/RT_B} \quad [10]$$

Since the average strain rate depends only upon the speed of the impact and the size of the test bar, if these variables are kept constant the relation between the stress-concentration factor and the temperature at which brittle failure occurs may also be written as:

$$\ln \dot{p}_B = Q/RT_B + K \quad [11]$$

where K is a constant. Thus the logarithm of the stress-concentration factor will be a linear function of the reciprocal of the absolute temperature. This relation, however, will be valid only under the conditions of testing in which the variations necessary to produce changes in the stress-concentration factor do not also appreciably change the longitudinal stress required for yielding.

The effect of notch radius (for a constant depth of notch) has been investigated by Gagnebin and Armstrong.²⁵ These investigators measured the impact energy as a function of temperature for V-notch Charpy specimens having various radii of curvature at the bases of the notches. From these results for each radius of notch, the temperature at which brittle failure* occurs was determined and the value of the stress-concentration factor for each radius was obtained from Fig. 2. From these data, the logarithm of the stress-concentration factor is plotted in Fig. 14 as a function of the reciprocal of the absolute temperature of testing, for a plain carbon and a nickel steel. For stress-concentration factors above about 2.5 ($r/w < \frac{1}{10}$) the logarithm of the stress-concentration factor is approximately a linear function of the reciprocal of the absolute temperature, indicating that the principal effect of changing the radius is to change the strain rate at the base

* It was assumed arbitrarily when the impact energy had decreased to 40 ft.-lb. that brittle failure had occurred (any value of the energy would have sufficed.)

of the notch in accordance with Eq. 11. For stress-concentration factors below 2.5 ($r/w < 1/10$) the effect of decreasing the radius of the notch is very much greater. In this range, decreasing the radius of the notch will decrease the transverse stress* and the longitudinal stress necessary for yielding and, therefore, reduce the temperature of brittle failure.

The effects of varying the radius of the notch in impact bend tests can now be summarized:

1. If the ratio of radius of the notch to the width of the bar is below about $1/10$, and the stress-concentration factor is above about 2.5, the principal effect of varying the radius will be to change the rate of strain.

2. If the ratio of the radius of the notch is above about $1/10$, or the stress-concentration factor below 2.5, increasing the radius of the notch will decrease both the strain rate and the longitudinal stress necessary for yielding.

These results will apply to any type of impact test bar, even though the discussion was restricted to V-notch test bars.

Impact Velocity

If the geometry of the test specimen is kept constant, the elastic strain rate may be varied by changing the impact velocity. The effect of increasing the strain rate will be to bring the yield and fracture strengths closer together. If the material breaks brittly, the relation between the temperature and the velocity of impact for brittle failure may be derived directly. Since the average elastic strain rate is proportional to the velocity of impact (appendix B), Eq. 10 becomes:

$$K = V_B e^{Q/RT_B}$$

or

$$\ln V_B = -Q/RT_B + \ln K \quad [12]$$

* There are two separate effects, one brought about by the change in stress-concentration factor (Fig. 3) and the other through changes in constraint (Fig. 4).

where K is a constant, V_B the velocity of impact and T_B the absolute temperature at which brittle failure occurs. Thus for brittle failure the logarithm of the impact velocity should be a linear function of the reciprocal of the absolute temperature at which brittle failure occurs.

The results of experiments performed by Witman and Stepanoff⁸ are presented as Fig. 15 to illustrate this linear relationship. As the velocity of impact increases, the temperature at which brittle failure occurs rises in agreement with Eq. 12.

The effects of velocity of impact may be summarized:

1. Changing the velocity of impact changes the yield and fracture strengths and the difference between them. The exact dependence of the tensile properties on speed depends upon the type of metal.

2. If a metal breaks brittly, the relation between the impact velocity and temperature at which brittle failure occurs is given by Eq. 12.

Width of Bar

Varying the width of test bar, of course, will change the total volume of material affected by the deformation, and, therefore, the energy necessary for fracture. For a ratio of notch radius to bar width less than about $1/10$, the primary effect of increasing the test bar is to increase the mass of the specimen. For ratios of r/w greater than about $1/10$, increasing the width of the bar will decrease the transverse stress and concomitantly decrease the longitudinal stress necessary for yielding. The effect of varying the width of the impact specimen has been the subject of controversy since Moser¹⁰ first published his results, in which he showed that for a certain steel and a certain test bar geometry increasing the width of the test bar had the surprising effect of decreasing the energy necessary for fracture. The results of Moser's experiments are illustrated in Fig. 16. For slow tests, the energy neces-

sary for fracture increases uniformly with increasing width. For the "impact" tests, the energy increased to a width of about 2.5 cm. and then the impact energy de-

Fig. 7). As the width of the bar increases, the transverse stress and consequently the yield strength increases and brittle failure will occur at a higher and higher tempera-

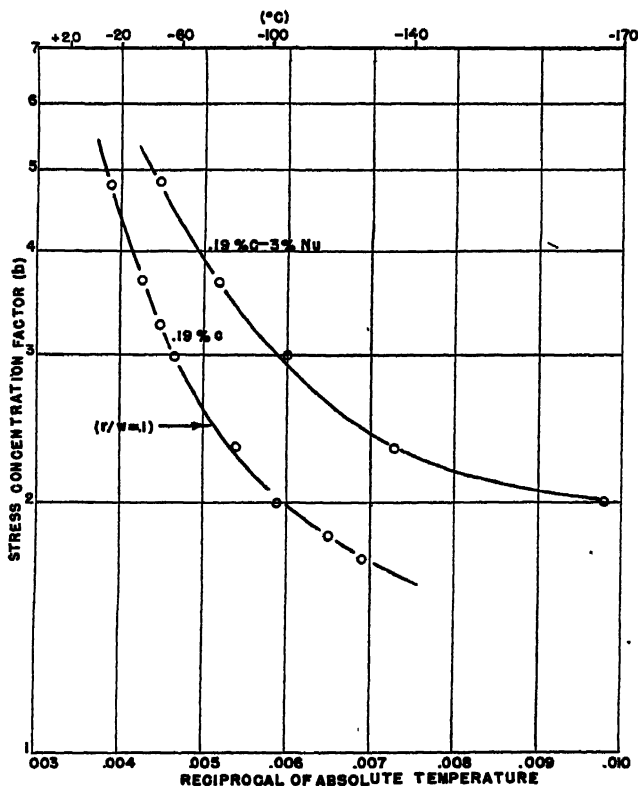


FIG. 14.—EFFECT OF CHANGING STRESS CONCENTRATION FACTOR (BY CHANGING RADIUS OF NOTCH) ON TEMPERATURE OF BRITTLE FAILURE. (From data of Armstrong and Gagnebin.²⁵)

creased sharply and the failure changed from the fibrous or ductile type to the crystalline or brittle type. For the smallest bar of Moser's experiments, the ratio of notch radius to bar width was $\frac{1}{4}$. (Keyhole notches of 0.25-cm. radius.) Increasing the width of the bar, therefore, increases the transverse stress. For a bar 1 cm. wide, the longitudinal stress necessary for yielding was not equal to its maximum value, for the transverse stress was less than its maximum. Brittle failure for this case would occur at a low temperature* (see

ture. Since the maximum increase that can be affected in the longitudinal stress necessary for yielding is about 12 per cent (for $b > 2.5$) if the separation of the yield strength and fracture strength of the undeformed steel for the geometry of the test bar and strain rate employed is less than 12 per cent of the yield stress, brittle failure will not occur at the temperature of test. For a steel to undergo a transition from ductile to brittle failure as the bar

occurs for a given geometry of test bar will vary, of course, with the steel. However, the results of Moser's experiments may be interpreted for the steel of Fig. 7.

* The temperature at which brittle failure

width is increased, it is necessary that the separation between the yield stress and fracture stress of the undeformed steel be less than 12 per cent. (If the stress-concentration factor is less than about 2.5, the

determining the effect of widening the test specimen, the temperature of the test should be so chosen that the specimen breaks ductilely, at least for the narrowest bar.

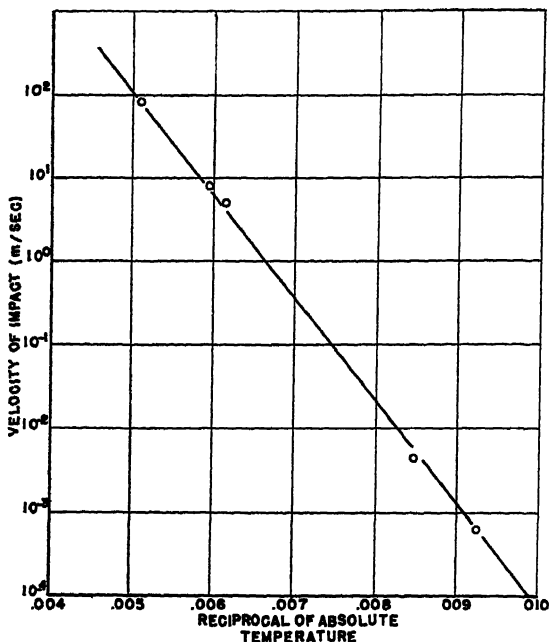


FIG. 15.—EFFECT OF IMPACT VELOCITY ON TEMPERATURE OF BRITTLE FAILURE, UNNOTCHED SPECIMENS. (After Wilman and Stepanoff.⁹)

separation may be less for brittle failure to occur.) The higher the strain rate, the less is this separation between the yield strength and the fracture strength of the undeformed metal. At slow speeds, this separation may be such that widening the bar will not induce brittle failure (Fig. 16).

If the ratio of r/w is less than about $\frac{1}{10}$, increasing the width of the bar should not appreciably change the temperature at which brittle failure occurs. The transition zone, however, may appear to shift to lower temperatures since the values of the energy for ductile or partially ductile failures will be increased by a more or less constant factor because of the increase in the volume of the material suffering deformation. Therefore it is necessary that in

For a test bar having a ratio of r/w greater than $\frac{1}{10}$, increasing the bar width will cause the temperature at which brittle failure occurs to shift to a higher and higher temperature. Such an effect was observed by Maurer and Mailander,²⁶ whose results are plotted as Fig. 17. In general, for values of the ratio of r/w in this range, the effect of increasing the width is simply to bring the yield and fracture strengths closer together.

The effects of bar width on the impact test may be summarized:

1. If the ratio of radius of notch to bar width is less than about $\frac{1}{10}$, changing the width of the bar should have little effect other than to increase the volume of the metal suffering deformation.

2. If the ratio of notch radius to bar width is greater than about $\frac{1}{10}$, changing the width of the bar will change the transverse stress and consequently vary the

depend entirely upon the difference between the yield and fracture strengths for the specific conditions of the test employed. The lower the temperature or the higher

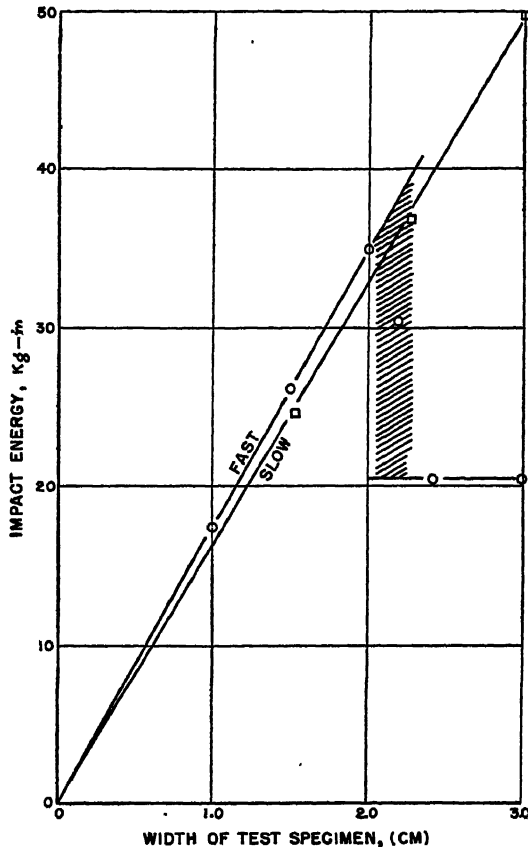


FIG. 16.—EFFECT OF WIDTH OF SPECIMEN ON IMPACT ENERGY AT TWO SPEEDS. (After Moser.¹⁰)

longitudinal tensile stress required for yielding, as well as changing the volume of metal suffering deformation.

3. If the separation between the yield strength in pure tension and fracture strength of the undeformed metal is greater than about 12 per cent under the conditions of the impact test (such as temperature and strain rate), brittle failure should not occur for a test specimen of any width. Whether or not brittle failure will occur for a specimen of a given width will

the strain rate, the less will be this separation and the more likely will be the possibility of brittle failure.

SIGNIFICANCE AND USE OF NOTCHED-BAR IMPACT RESULTS

Notched-bar impact results are in essence relative measures of the areas under stress-strain curves for particular test conditions. Such tests indicate the relative ability of metals to deform under the conditions of stress distribution, strain rate and tem-

perature that are imposed. More specifically, the test determines for a given set of conditions whether or not the yield strength is equal to the fracture strength.

yield and fracture strength for similar metals under the stress-strain curves of these materials only if the impact tests are performed under identical conditions. The

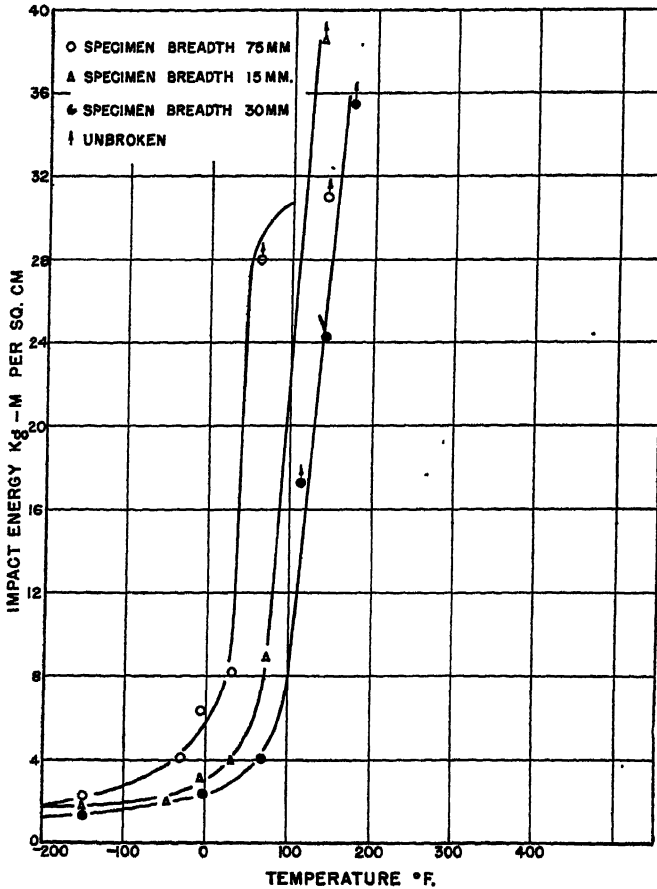


FIG. 17.—EFFECT OF WIDTH OF SPECIMEN ON TEMPERATURE OF BRITTLE FAILURE. (After Maurer and Mailander.¹⁰)

Since the amount of material suffering deformation is difficult to determine, the impact energy cannot be interpreted exactly at the present time in terms of tensile properties unless the material breaks brittly and the energy required for fracture is essentially zero. For materials that break ductilely, the values of the impact energies can be used to compare relative areas for the separation between

conditions under which the test is to be performed must be determined by the conditions of service to which the steel is to be subjected. If the designer of an engineering structure can predict the most unfavorable conditions the steel used will meet in service, it is then possible by the proper choice of impact specimen and test conditions to reproduce at least approximately the service conditions by notched-bar

impact tests. The various possible steels may be then compared on the basis of such impact tests and a choice of metal made. Often a designer must compromise by accepting a steel that he believes (or has sufficient experience to be certain) will perform the engineering function satisfactorily instead of demanding the most suitable steel.

For most engineering structures, it is expected that the restraint imposed by the geometry will be sufficient so that the transverse stress will reach its maximum value at the bases of notches and fillets (Fig. 4). For this reason, an impact specimen should be used in which the ratio of notch radius to bar width is less than $\frac{1}{10}$. If the restraint (or transverse stress) is expected to be less, the ratio of notch radius to bar width can be made greater than $\frac{1}{10}$. In designing an engineering structure, the designer attempts to maximize the radii of the notches and fillets. If notches are unavoidable, the designer should attempt to estimate the maximum depth and sharpness of the notches that might occur in a structure suffering shock loading and the maximum average strain rates and minimum temperatures to be expected. With certain general knowledge of the steels that are available, the designer may be in a position to choose the radius of notch of the specimen and the temperature at which the test should be performed. (The impact velocity is usually fixed by the available testing machines.) If it is not feasible to reproduce the strain rate by increasing the sharpness of the notch or the impact velocity, the temperature may be lowered below the minimum temperature expected by an amount necessary to approximate the required increase* in strain rate.

Tests should then be performed under these fixed conditions and the relative

acceptability of the steels determined. If a steel breaks brittly under these conditions, the structure is liable to failure with little absorption of energy. Some materials may require greater energy for fracture than others, and it is in this case that the designer must use his judgment. In most cases the results of standard impact tests may be used if it is realized that a metal that has a lower transition temperature than another for a given radius of notch may have a higher transition temperature for a sharper notch. If a steel does not break brittly even at very low temperatures when tested in impact with very sharp notches, it can be inferred that it is suitable for service in which the notches will be less sharp. If fine distinctions are to be made between steels for a particular service, it is necessary to attempt to reproduce the service conditions by an impact test and compare the steels by this test

SUMMARY

An interpretation of the brittle failure of some steels in notched-bar impact tests is presented. This interpretation is based upon the effects of the stress distribution present at the base of the notch and the effects of high rates of strain and low temperatures on the properties of several typical steels. Brittle failure is due primarily to the small separation between the yield strength and the fracture strength of the undeformed metal and to the increase in the longitudinal tensile stress necessary for yielding induced by the transverse constraint imposed by the notch.

Increasing the width of a notched-bar specimen, in general, will increase the volume of material suffering deformation and thereby increase the energy required for fracture. If the ratio of notch radius to bar width is less than about $\frac{1}{10}$, the primary effect of changing the width of the bar is to change the volume of material undergoing deformation. If, however, the ratio of the notch radius to bar width is greater

* The limited data now available indicate that for most steels a small change in temperature is equivalent to a large change in strain rate.

than about $\frac{1}{10}$, changes in the width of the bar will produce changes in the transverse constraint sufficient to affect appreciably the temperature of brittle failure, as well as change the volume of the material suffering deformation.

The strain rate at the base of the notch may be increased by changing the geometry of the test bar or increasing the velocity of the impact. Increasing the radius of curvature of the notch will serve primarily to decrease the strain rate, and vice versa, if the ratio of notch radius to bar width is less than $\frac{1}{10}$ and the stress concentration factor is greater than about 2.5. For conditions of geometry outside these limits, increasing the radius of the notch will also decrease the transverse stress, and vice versa.

Decreasing the temperature and raising the strain rate are equivalent in their effects and serve to decrease the separation between the yield strength and fracture strength of the undeformed metal. Some steels do not break brittly in the impact test, and these same materials maintain their ductility in simple tension to very low temperature or to very high strain rates.

The interpretation of the impact test presented in this paper and the relations between the variables of the test should aid the designer of engineering structures in choosing the conditions of the notched-bar test so that the value of the impact energy may become a relative measure of the suitability of the various steels for particular engineering applications.

APPENDIX A

CALCULATION OF TRANSVERSE STRESS AT BASE OF NOTCH

BY C. ZENER,* MEMBER A.I.M.E.

Outside of the immediate vicinity of notch, all stresses vanish except X_z , which

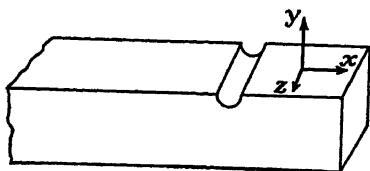


FIG. 18.

is constant. In order to calculate the stress Z_x at the base of the notch, a system of surface stresses Z_x is applied over the face of the plate in vicinity of the notch that will render the faces plane. It may then be shown that the stresses in the plate are independent of z . This conclusion is most readily arrived at by considering the plate

to be subdivided into an arbitrarily large number of thin slabs, all of which have the same distribution of surface stresses.

Let b represent the factor by which X_z has increased at the base of the notch. Y_y is zero, at this surface, and it is desired to find Z_x . The strain ϵ_{xx} is the strain associated with the uniaxial stress γ away from notch. The additional X_z stress $[(b-1)\gamma]$ is therefore associated with no further ϵ_{xx} . This condition leads to the equation:

$$0 = \frac{1}{E} (Z_x - \sigma(b-1)\gamma) \quad [1]$$

or

$$Z_x = \sigma(b-1)\gamma \quad [2]$$

We now relieve the surface stresses over the faces. This relief may be regarded as the addition of surface stresses of the same magnitude but of opposite sign. An approximate computation will now be made of the effect of these added surface tractions upon the stresses Z_x along notch

Denote by F the total force applied on a face:

$$F = \int Z_x dA \quad [2]$$

* Senior Physicist, Watertown Arsenal, Watertown, Massachusetts.

If the dimensions of the region over which F is applied are small compared with the width W of bar, the effect of F near the center of the bar will not be appreciably affected by the manner in which F is distributed.

The solution is given by Love²⁷ for the stresses produced in a medium of infinite extent by the application of singular forces. Let the force F be applied at the origin of coordinates in direction of z , and an opposite force be applied along axis of z at a point W away from origin. The stress Z_x midway between the two points is then:

$$\Delta Z_x = (2F/W^2)\alpha$$

where α is a factor very nearly equal to unity; namely, $(3/\pi)(\lambda + \frac{1}{2}M)/(\lambda + 2M)$. It is to be expected that the difference between the plate and the infinite medium will be a factor of 2, since each force in the case of the plate is effectively supported by only half the material as compared with the case of the infinite medium. Therefore, we have the approximation:

$$Z_x = 4F/W^2$$

It remains to obtain an estimate of F . The integral of Eq. 3 is equal to:

$$\int Z_x dA = C_1 r^2 (Z_x)_m$$

where C_1 is a numerical constant of the order of magnitude of unity, r is the radius of curvature of the notch, and $(Z_x)_m$ is the maximum value of Z_x ; namely, $\sigma(b-1)\gamma$. Therefore, at the base of the notch at the mid-point of the bar:

$$Z_x = \sigma(b-1)\gamma \{1 - C_1(4)(r/W)^2\}$$

An attempt at an estimate of C_1 was made by an exact computation for the case of a circular hole in a plate. In this particular case, C_1 is exactly zero. The only contribution to ΔZ_x then comes from the dipole distribution of the form, which will lead to a term $(r/w)^4$. This attempt in-

dicates that C_1 is small compared with unity. Fig. 4 of the text has been constructed with $4C_1$ set equal to unity.

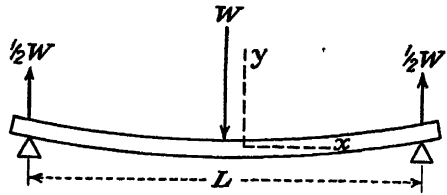


FIG. 19.

$y(x)$: displacement with respect to center of beam.

APPENDIX B

RELATION BETWEEN VELOCITY AND STRAIN RATE IN BENDING TEST

In an elastic beam, the curvature is directly proportional to the moment acting across a plane. Thus if y is the displacement, x the coordinate along the beam (see accompanying figure):

$$d^2y/dx^2 \sim M \quad [1]$$

From a consideration of the external forces acting upon the beam, it may be shown that M decreases linearly from a maximum at center to zero at the ends:

$$M(x) = M_0(1 - x/\frac{1}{2}L) \quad [2]$$

Therefore, upon combining Eqs. 1 and 2:

$$d^2y/dx^2 = y_0''(1 - x/\frac{1}{2}L) \quad [3]$$

Double integration of Eq. 3 gives for the displacement D of the center with respect to the end supports:

$$D = \frac{1}{12} y_0'' L^2 \quad [4]$$

The relation between the curvature and the maximum strain, ϵ_0 , is given by:

$$\epsilon_0 = a/R = ay_0'' \quad [5]$$

where R is the radius of the curvature at center and a is the distance from the center of the beam to the surface (a = radius for

circular beam, $\frac{1}{2}$ thickness for rectangular beam).

By combination of Eqs. 4 and 5 the following is obtained:

$$D = \frac{1}{2} \epsilon_0 L^2 / a$$

$$\text{or } \frac{dD}{dt} = \frac{L^2}{12a} \frac{d\epsilon_0}{dt}$$

$$\text{or } \frac{dD}{dt} = \frac{L^2}{6h} \cdot \frac{d\epsilon_0}{dt}$$

where h is the thickness of the bar.

REFERENCES

1. C. Fremont: A New Method of Testing of Metals. *Bull. Soc. d'Enc.* (1897) **96**, 1409.
2. G. Charpy. Note on the Testing of Metals by the Bending of a Notched Bar in Impact. *Bull. Soc. Ing. Civ.* (June 1901) **213**.
3. P. Ludwik: Über die Bedeutung der Elastizitätsgrenze, Bruchdehnung und Kerbzähigkeit für den Konstrukteur. *Ztsch. Metallkunde* (1924) **16**, 207.
P. Ludwik and R. Scheu: Vergleichende Zug-, Druck, Dreh-, und Walzversuche. *Stahl und Eisen* (1925) **45**, 373.
P. Ludwik: Streckgrenze, Kalt- und Warm-sprödigkeit. *Ztsch. Ver. deut. Ing.* (1926) **70**, 379.
4. K. Heindlhofer. The "Plasticity" of Iron at Low Temperatures. *Trans. A.I.M.E.* (1935) **116**, 232.
5. M. Gensamer: Strength of Metals under Combined Stresses. Cleveland, 1941.
6. S. L. Hoyt: Notched Bar Testing. *Metals and Alloys* (1936) **7**, 5, 39, 102, 140. Contains excellent bibliographic references.
7. D. J. McAdam, Jr. and R. W. Clyne: The Theory of Impact Testing. *Amer. Soc. Test. Mat.* (1938) **38**, pt. 2, 112.
8. F. F. Witman and V. A. Stepanoff: Influence of Deformation Speed on Cold Embrittlement of Steel. *Jnl. Tech. Physics*, U. S. S. R. (1939) **9**(12), 1070.
9. O. R. J. Lee: The Notched Bar Test. *Proc. Inst. of Mech. Engrs.* (1940) **143**, 114. Contains excellent bibliographic references.
10. M. Moser: Zur Gesetzmässigkeit der Kerbschlagprobe. *Kruppsche Monatshefte* (1921) **2**, 225.
M. Moser: Die Ergebnisse des Kerbschlagversuches. *Kruppsche Monatshefte* (1924) **5**, 48.
11. R. Mailander: Das Ähnlichkeitsgesetz bei Kerbschlagprobe. *Kruppsche Monatshefte* (1926) **7**, 217.
12. Symposium on Impact Testing. *Amer. Soc. Test. Mat.* (1938) **38**, pt. 2, 21.
13. Discussion on Notched-bar-impact Testing. *Trans. The Manchester Assn. Engrs.* (1937-1938)
14. W. Kuntze: For Survey and bibliography see references in articles by D. J. McAdam, Jr listed below. (1942) **150**, 311.
15. D. J. McAdam, Jr.: Technical Cohesive Strength of Metals. *Trans. Amer. Soc. Mech. Engrs.* (1941) **63**, A-155 and Technical Cohesive Strength and Yield Strength of Metals. *Trans. A.I.M.E.* (1942) **150**, 311.
16. G. Sachs: Report on Embrittlement of Steel Under Multiaxial Stress. Eng. Foundation, Welding Research Committee, New York.
G. Sachs and J. Lubahn: Effects of Notching on Strained Metals. *The Iron Age* (1942) **150**, (15), 31; (16), 49.
17. C. Zener and J. H. Hollomon: Effect of Temperature and Strain Rate on the Properties of Steel. Not yet published.
18. J. H. Hollomon and C. Zener: Conditions of Fracture of Steel. Presented as part of the Symposium on Cohesive Strength, A.I.M.E. Meeting in Chicago, Oct. 19, 1943.
19. H. Neuber: Exact Elastic Solutions Concerning the Notch Effect on Plates and Bodies of Rotational Symmetry. *Ztsch angew. Mathematik* (1933) **13**, 439.
20. M. M. Frocht: Factors of Stress Concentration Photoelastically Determined. *Jnl. Applied Mechanics* (1935) **2**, A-67.
21. E. G. Coker and L. N. G. Filon: Photoelasticity, 362, London, 1939.
22. Metals Handbook, 1939, 135.
23. D. J. McAdam, Jr. and R. W. Mebs: An Investigation of the Technical Cohesive Strength of Metals. *Metals Technology*, A.I.M.E. (Aug. 1943).
24. G. Zener and J. H. Hollomon: Plastic Flow and Rupture of Metals. *Pub. No. 9*, Amer. Soc. Metals (1943).
25. T. N. Armstrong and A. P. Gagnebin: Impact Properties of Some Low-alloy Nickel Steels. *Trans. Amer. Soc. Metals* (1940) **28**, 1.
26. E. Maurer and R. Mailander: Zur Frage der Blasprodigkeit. *Stahl und Eisen* (1925) **45**, 400.
27. A. E. H. Love. Mathematical Theory of Elasticity, Ed. 4, 185-196. Cambridge, 1934.

Excellent bibliographic references may also be found in:

Von F. Fettweis: Die Kerbschlagprobe Entwicklung und Kritik. *Archiv Eisenhüttenwesen* (1928-29) **2**, 625.

DISCUSSION

(F. G. Tammall presiding)

M. METZGER,* Harrison, N. J.—On Figs. 10 and 13, two lines are plotted. Do they represent two specimens of steel or does one represent adiabatic and the other isothermal deformation?

J. H. HOLLOWOM (author's reply).—The two lines in Figs. 10 and 13 were drawn simply to include all the data. Because of the spread

* Crucible Steel Company of America.

in impact data often observed, this method of plotting appears to be the most illustrative.

H. W. RUSSELL,* Columbus, Ohio.—In the field of low-temperature impact, there is a phenomenon that often occurs. In the Charpy test, it is frequently found that at some low temperature either ductile or brittle fractures will occur, but not intermediate values. The results are best represented as two overlapping curves. Such results are possibly best illustrated in the data published by Sergeson for the Joint High Temperature Committee in the A.S.T.M. in 1936.

J. H. HOLLOWOM.—There are many details of the behavior of steels when notched and broken in impact which could not be covered in the oral presentation, but most of them are discussed in the paper as printed. This phenomenon of a sharp transition from ductile to brittle failure is a case in point.

If one could break an infinitesimally small specimen at some temperature or rate of loading, the type of fracture would change from completely ductile to completely brittle. For an actual specimen, however, the nature of the deformation is such that the severity of the conditions of fracture progressively increases as the crack progresses across the specimen. Suppose, for example, that a specimen is being broken at a temperature slightly above that at which brittle failure would occur under the conditions of severity imposed by the original notch. The metal at the base of the notch will deform considerably before fracture. A sharp crack, however, will be formed and, at some point beneath this crack, the metal will break in a brittle fashion. Such fractures consist of a fibrous zone surrounding a crystalline or brittle zone and are referred to as transition fractures. Thus, it is possible to obtain intermediate values of impact energy in the range of transition from completely ductile to completely brittle fractures. The metal itself, however, does not behave in an intermediate fashion; it is either ductile or brittle. The interpretation of this sudden transition in terms of stress-strain curves is presented in the paper.

E. F. PONCELET,† Butler, Pa.—We have found that the amount of energy required to

produce brittle fracture in glass depends on the elastic properties of the striking solid. Is anything known about the behavior of steel in this respect?

J. H. HOLLOWOM.—I do not know of any information on this subject.

E. F. PONCELET.—Does it make much difference, or does it make little difference if you use a very hard impacting tool or a relatively soft one on steel?

J. H. HOLLOWOM.—The problem of the actual nature of the brittle fracture of steels has not been studied in any great detail. The primary metallurgical problem is to determine the factors that control the amount of plastic deformation that will precede fracture in structural materials. It is only necessary to know whether or not material fails brittly. The exact nature of this brittle failure is the subject of another type of investigation.

N. A. ZIEGLER,* Chicago, Ill.—All the theory and conclusions of this paper are based on relatively slow speeds, used in conventional impact testing. It is known, however, that with high-velocity impact the mechanism of fracturing is different. For example, with slow speed of impact, the specimen must be supported on some suitable device before it can be fractured; when the speed of impact increases beyond a certain value, a specimen can be fractured by its own inertia, without any support at all. I would be interested to know whether the conclusions of this paper apply to such conditions.

J. H. HOLLOWOM.—It is believed that the principles presented in this paper apply to fracture over the entire range of strain rates. At very high velocities of impact, other factors, such as the propagation of plastic deformation, may contribute to further complication. It is necessary, of course, in any interpretation of the notched-bar test to know approximately the strain rate at the base of the notch. When the specimens are broken, at very high velocities, a relatively exact estimate of the strain rate may not be possible.

F. G. TATNALL,† Eddystone, Pa.—Impact is one of the mystery men of physical testing.

* Battelle Memorial Institute.

† Preston Laboratories.

* Crane Company.

† Baldwin Locomotive Works.

A great many people have condemned the impact test as being vague and elusive. Captain Hollomon is doing much to bring it out into the open and make it a useful yardstick.

He says that the material above the notch has some tensile stress in it. It was my understanding generally that that region was practically unstressed longitudinally and hence was acting only as a lateral restraint. In other words, if an ordinary tensile test is made on an unnotched machined specimen, this test does not reproduce conditions in a welded ship plate, because when a ship plate is subjected to tensile load it cannot contract laterally in accordance with Poisson's ratio, being restrained by the surrounding material.

It looks to me as though the notched-bar impact tensile test is intended to reproduce the restraint suffered by a material when it is part of a structure.

I read a recent article by Dr. Krivobok, which concludes that until we study impact as a tensile test with lateral restraint we do not fully understand it.

For instance, Dr. MacGregor, at M.I.T., has said that the only real difference between static tensile test and a notched-bar impact tensile test is the notch. Is that right, Captain Hollomon?

J. H. HOLLOWON.—In order to answer Mr. Tatnall's questions, it is desirable to reword them:

1. What is the difference between the tensile test and the notched-bar impact test?

2. Is it correct that the only difference between these two tests is the principles of a transverse constraint?

These two questions present an opportunity for discussion of the mechanical testing of metals that may serve to clarify some of its aspects.

Only certain fundamental variables must be considered in determining the mechanical behavior of metals. Plastic flow and rupture are functions of the strain rate, temperature, stress distribution and prior history. The latter includes both the structure of the metal under consideration and the degree and effect of any prior deformation. These variables are inter-related. The effect of strain rate on, say, the yield strength of two metals may be different if their structures are different. In any attempt

to correlate the behavior of metals in different tests, the difference of the magnitude of these variables is of primary importance.

In comparing the tensile test with the notched-bar impact test, two of these variables are different. The material at the base of the notch is essentially constrained from the transverse contraction and a transverse tensile stress induced, and the strain rate at the base of the notch is greater than is usually employed in the tensile test. Furthermore, the notched-bar test is frequently conducted at temperatures other than room temperature. If the effect of these three variables on the stress required for plastic flow and the stress required for fracture are fully understood, it is possible to correlate the behavior of metals in these two types of tests.

In these two tests, the primary difference arises from the presence of a transverse stress, and it is the effect of this transverse stress on the plastic flow and fracture that is of fundamental importance to the understanding of the notched-bar impact test. The effect of the strain rate is relatively minor.

B. F. SHEPHERD,* Phillipsburg, N. J.—Just something in the nature of a general statement: The experts in mechanical testing appear to have the practice of defining structure by stating the method of quenching or tempering, which, after all, is a very vague way of stating the thing in which we are primarily interested; that is, metallographic structure. If the investigators would state the actual structure as quenched or quenched and tempered they would cover everything—quenching, medium and everything else. It would mean a little more than just to state that it is quenched and tempered or air-cooled. Quenching is, only a means of controlling the transformation rate, which, of course, produces the final structure.

J. H. HOLLOWON.—Mr. Shepherd's point is very well taken. The photomicrographs of the steels used for these experiments have been presented in another paper. The water-quenched and tempered specimens consist of tempered martensite, the air-cooled and tempered specimens consist of proeutectoid ferrite and pearlite (the carbides of which were slightly spheroidized during the tempering treatment).

* Ingersoll Rand Company.

E. F. PONCELET.—I should like to ask another question. I believe this paper relates only to fractures starting in the notch. That means that only what I would call very slow impact is considered. On fast enough impact the pressure wave has no time to generate the stress in the notch while the impact is in progress; and quite a different type of cracks and fractures develops. The stresses involved are given by the formula of Hertz. These fractures start on the compression side and form the "percussion cone." I do not know enough about when and how this type of fracture occurs and am interested in learning more about it. This type of fracture is entirely different from the type of impact fractures caused by what might be called slow impact. Are there any data about those things available?

J. H. HOLLOWOM.—The subject that Dr. Poncelet brings up is much too involved to discuss at this time. I should like to say that this phenomenon enters the problem for only extremely high velocities of impact and has little importance to the problem under discussion.

G. L. COX,* Watertown, Mass.—I want to emphasize one thing. We at the Arsenal have been studying the problem of the effect of high rates of loading on the properties of materials for some time, largely because most applications with which we are concerned deal with high strain rates.

In the middle 1930's, H. C. Mann built a variable-velocity impact machine to work on this problem. He observed some rather phenomenal things, as most of you know, as he raised the velocity. The order of velocity with the machine was considerably higher than that of the standard Charpy test; however, even then the machine was incapable of reaching velocities as high as are often encountered, as, for example, the attack of a projectile on a piece of armor.

We all know that if the temperature is lowered, steels may become brittle at the low temperatures. There is some evidence available in the fairly recent work of other investigators that increasing the strain rate also tends to

make a material more brittle. Maybe these two phenomena are all we know, and maybe not. We have turned this problem over to some of the research workers at Watertown Arsenal, and we think they have done some pretty good work. However, the accomplishments so far apparently are not complete and may be "full of holes." I was hoping to hear at this meeting some discussion as to the limitations of our thinking and that certain qualified people would express their thoughts in the matter to such an extent that we could be guided in our future efforts.

Somewhat as a premise to our thinking, we know that as the temperature is lowered the tensile properties of steel are raised. Also, if the strain rate is increased, the tensile strength, particularly yield, is increased.

Those two considerations may not be parallel. They may have only an incidental empirical relationship to each other. In fact, I have used the corollary that we can establish a relationship between the life of automobile tires and the speed at which the car is driven, and we can also establish a relationship between the life of these tires and the roughness of the road—but what is the relationship between the speed of the car and the roughness of the road?

If there is any relationship between speed of testing and lowering the temperature, certainly it is easier to lower the temperature than to increase the speed within the limits in which we are interested.

I hope that out of this research we may obtain a new concept of how to view the intrinsic behavior of a piece of metal when it is subjected to deformation at extremely high rates of loading.

J. H. HOLLOWOM.—The question Colonel Cox has introduced concerned us a great deal during the early stages of the research of which this paper is a partial report. There is considerable evidence, however, that the effects of strain rate and temperature when properly considered are equivalent. Carpenter and Robertson²⁷ suggested a qualitative relationship between the two variables several years ago. Dr. Zener and I attempted to determine whether or not this relationship was quanti-

*Lieutenant Colonel, Ordnance Department, Watertown Arsenal.

²⁷H. Carpenter and J. M. Robertson: *Metals*, 1, England, 1939, Oxford Univ. Press.

tative, and we believe that it is. The relationship between the effects of strain rate and temperature is similar to a relationship between the changes of pressure and volume in an ideal gas. The nature of the relationship between pressure, volume and temperature of an ideal gas permits an infinite number of combinations of pressure and volume for a given temperature. The pressure for a given temperature varies reciprocally with the volume. In parallel fashion, for a given yield strength, the logarithm of the strain rate varies with a reciprocal of the absolute temperature. There is, in an analogous fashion, an infinite number of possible combinations of strain rate and temperature, which will produce the same yield strength. The relation between the strain rate and temperature has been discussed in the paper. The exact nature of the dependence of the mechanical properties on temperature is not important to this relationship.

G. SACHS,* Cleveland, Ohio.—I would like to emphasize the fact, which Dr. Poncelet has pointed out, that all relations between temperature and speed can be valid only for speeds that are very slow in comparison with the propagation speed of elastic waves. At very high speeds, no simple relation between speed and impact energy can be expected.

J. H. HOLLOMON.—I should like to agree with Professor Sachs that this paper is concerned with speeds that are relatively slow compared with the speed of propagation of elastic waves in steel. However, it is believed that at least the qualitative relation between the effect of strain rate and temperature that has been proposed will be valid even at these higher rates of loading.

S. L. HOYT,† Columbus, Ohio.—The author gives an important and timely discussion of the mechanics of a notched bar. A major point is the discussion of the respective roles of triaxial stress and stress concentrations, and the relief of the latter by a small amount of deformation at the root of the notch. The latter agrees nicely with opinions expressed by engineers that if the metal at the notch can deform by 1 to 2 per cent, any stress concentration from geometry is eliminated.

It seems to the writer that therein is a major reason for testing notched bars statically, so that a full stress-strain diagram can be obtained. The relatively small amount of quantitative testing that has been done indicates that there are important differences in behavior, which show up directly or soon after bending starts, resulting either in an early crack of a brittle type or a late crack of a more ductile type. This suggests the desirability of separating the behavior during test into two steps, the first being the early elastic deformation and the second, subsequent plastic deformation.

During the former, the stress concentration is present and must be significant. It would appear to the writer that this stress concentration has an important bearing on the behavior, either (1) the opening of a crack, or (2) as the alternate behavior, the initiating of the plastic deformation which lowers the stress concentration.

During the second stage of the test an analysis of the situation would require a running summary which would integrate the effects of the now modified geometry and stress system, and the altered cohesive and flow strengths of the steel. This subdivision of the behavior of a notched bar appears to be sound and correct, possibly necessary to its proper understanding.

For notched-bar testing as commonly practiced, the above is probably not of much significance, since the bars usually break in a ductile fashion with high energy values. However, the test becomes truly revealing of notch sensitivity or notch toughness when the conditions are determined that show the change from ductile to brittle behavior, the "match" point discussed in reference.²⁹ The writer would like to see this point emphasized for notched-bar testing, since it seems important to ascertain the level of notch toughness in terms of notch geometry, temperature, and rate of strain, which limit ductile behavior. As a compromise or simplification, the double-width Charpy bar has been found to be useful by checking the steel under an additional degree of restraint, while the use of temperature as a variable is likewise helpful.

²⁹ S. L. Hoyt: Notched Bar Testing and Impact Testing. *Trans. A.S.T.M.* (1938) 38, II, 162.

* Case School of Applied Science.

† Battelle Memorial Institute.

J. H. HOLLOMON.—Dr. Hoyt emphasizes that the fracture of a notched bar in impact consists of two phases: (1) the behavior of the material at the base of the preformed notch and (2) the behavior of the material at the base of the continuously changing forming crack. To understand completely the nature of the notched-bar impact fractures, the conditions surrounding these two phases of fracture must be completely understood. The temperature at which completely brittle failure occurs, however, is controlled by the preformed

notch. Quantitative information concerning the transition from ductile to brittle failure, therefore, can be obtained without a knowledge of the exact nature of the crack that progresses across the specimen. It is the conditions surrounding this transition from ductile to brittle failure that are of the greatest importance. The author does not believe that much information can be gained from testing double-width Charpy bars which cannot be obtained directly from any given standard test bar.

Hardness Measurement as a Rapid Means for Determining Carbon Content of Carbon and Low-alloy Steels

By K. L. CLARK* AND NICHOLAS KOWALL*

(New York Meeting, February 1944)

MAXIMUM furnace efficiency and close control of final steel composition demand that the steel melter be able to follow closely the variations in the carbon content of the bath.

For many years, the fracture test has been used by melters for estimating carbon, because it requires only a very short time to pour a sample into a chill mold, cool it in water, break it with a sledge hammer, and observe the fracture. After long experience gained from the observation of such fractures, most melters are able to estimate the carbon content of steel with amazing accuracy, particularly in the lower carbon ranges.

Notwithstanding the utility of the fracture test, there has been widespread interest in other methods for rapid carbon determination to supplement it and to ensure against possible errors in human judgment. Several methods, based upon measurement of magnetic properties as functions of carbon content, have been described in the literature¹⁻⁶ and have been found to give reasonably reliable results in plant practice when scrap composition is known and controlled.

A difficulty encountered in the use of analyzers of the magnetic type is that alloying elements do change the relationship between carbon content and magnetic properties and it becomes necessary to

establish calibration curves for all the expected combinations of alloy residuals that are not oxidized in the bath. The work reported here is of an investigation of a method that is independent of alloying elements normally present in constructional steels, being based upon the relatively well-known fact that in plain carbon and low-alloy steels martensitic hardness is a function of carbon content alone.

WORK OF OTHER INVESTIGATORS

In 1938, Burns, Moore and Archer published a curve⁷ that showed that the hardness of martensite is a function of carbon from 0.10 to 0.50 per cent and is independent of grain size or alloy content, at least within the range found in constructional S.A.E. compositions. Some of the deeper hardening types investigated, however, contained carbon to a maximum of only 0.20 per cent.

Using this principle, Kern⁸ developed a method of rapid carbon determination for S.A.E. 43xx steels. His procedure consisted of chill-casting a test bar that was large enough to give a surface that could be prepared for Brinell indentations. The test piece was quenched immediately after solidification was complete and hardness readings were taken, so that the carbon content could be read from an experimentally determined curve giving the relationship between as-quenched hardness and carbon.

EXPERIMENTAL WORK

Although Kern's work had been done with a relatively deep-hardening steel, it

Published by permission of the Navy Department. Manuscript received at the office of the Institute Nov. 26, 1943. Issued as T.P. 1681 in METALS TECHNOLOGY, January, 1944.

* Division of Physical Metallurgy, U. S. Naval Research Laboratory, Anacostia Station, Washington, D. C.

¹ References are at the end of the paper.

appeared that, with certain modifications, the method could be made applicable to carbon steels and to the shallow-hardening alloy steels as well as the deeper hardening alloy types. In order to assure reasonably complete hardening in as many types of steel as possible, it was necessary to reduce the test piece to minimum dimensions compatible with ease of handling and accuracy of hardness measurement. A specimen having a diameter of $\frac{1}{4}$ in. was found suitable provided the Rockwell test was used to measure hardness.

The technique involved in sampling and testing is as follows: A sample is removed from the bath in a small, well-slugged spoon. The slag is skimmed off and the metal deoxidized with an excess of aluminum, to prevent porosity. The sample is then poured into a runner cup centered over the cavity of the chill mold shown in Fig. 1. Since solidification occurs very rapidly, the runner cup is knocked to one side immediately and the mold is sprung apart by means of beaker tongs welded to the mold halves (Fig. 2). The hot test piece (estimated to be at 2000°F.) is quenched in a pail of agitated ice water. A sample in the form of a short cylinder is taken from the thin section by making parallel transverse cuts, approximately $\frac{1}{4}$ in. apart, with a water-cooled abrasive cut-off wheel. The burrs are ground from the edges of the parallel faces and three or four Rockwell readings are taken midway between center and outside on one of the cut surfaces. The carbon content is then read from a curve of as-quenched hardness and carbon content previously determined by the combustion method. The entire procedure requires approximately two minutes.

Although the method is simple, certain precautions are necessary to ensure reliable results:

1. It is essential that the test piece be released rapidly from the mold into the quenching bath. Otherwise its temperature

may be lowered to a point where incomplete hardening will result from the quench.

2. During cutting, a stream of coolant must be directed upon the abrasive wheel

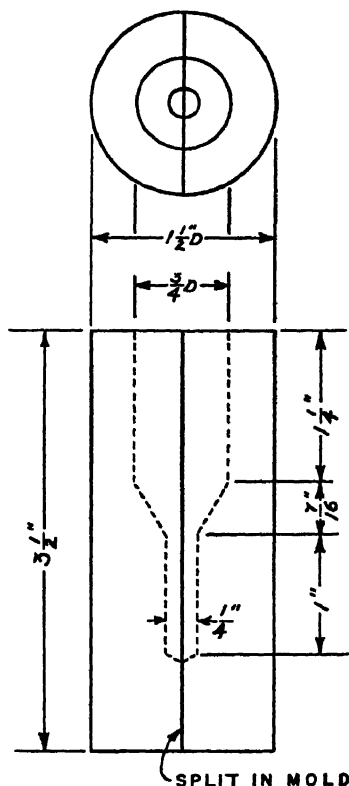


FIG. 1.—SPLIT CHILL MOLD.
Material $1\frac{1}{2}$ -inch round cold-rolled steel.

and the specimen, to prevent tempering. Submerged cutting is preferred.

3. Usual precautions regarding hardness testing must be observed. Of the conditions that may cause erroneous hardness readings, most act to cause low readings. It is advisable to take the highest Rockwell reading if variation occurs in any one sample. Frequent checks on the calibration of the machine should be made by means of standard hardness blocks.

Fig. 3 is a curve plotted from the data obtained by taking samples from more than 60 induction-furnace steel heats. Hardness

measurements were made in the manner described and, in each case, metal from the sampling spoon was analyzed for carbon by the combustion method to establish the

The size of specimen and conditions of quenching must be standardized in order that reproducible, quantitative results may be obtained. It is believed that the



FIG. 2.—MOLD ASSEMBLY AND TEST PIECE, $\frac{1}{4}$ NATURAL SIZE.

calibration. The steel compositions upon which this curve was based included carbon, medium manganese, medium manganese-molybdenum, copper, and various unclassified low-alloy steels (containing nickel to a maximum of about 0.50 per cent, chromium in varying quantities to about the same maximum, and combinations of the two with and without molybdenum). No attempt was made to segregate the steels into alloy types; all values were plotted on the same curve

DISCUSSION OF RESULTS

The points show very little scatter from the average curve. The mean deviation is less than 0.01 per cent carbon and only a few points fall beyond 0.02 per cent carbon within the range indicated.

For purposes of comparison, Kern's data were converted from Brinell to Rockwell C° and plotted on the same coordinates (Fig. 4). The spread between the two curves is due probably to the difference in section size of the test pieces and possibly to the variations that usually arise in converting hardness values from one scale to another. The hardness values obtained by Burns, Moore, and Archer, also shown in Fig. 4, are considerably higher than those obtained by quenching the cast test pieces.

$\frac{1}{4}$ -in. diameter specimen used in these experiments approaches the optimum size. The quenching practice employed appears satisfactory; it might be changed, however, to give different though reproducible values. In any case it is desirable to check the curve and technique carefully by laboratory control before attempting to adapt it to routine practice.

It is to be emphasized that the carbon content cannot be determined by this method for steels that contain alloying elements in quantities sufficient to cause appreciable amounts of austenite to be retained under the conditions of quench stipulated.

CONCLUSIONS

The method described is considered to be a satisfactory shop method for carbon control during melting of plain carbon and low-alloy steels, for several reasons:

1. Results are reproducible and sufficiently accurate.
2. Testing procedure is rapid.
3. Simplicity of the method makes it possible to train unskilled personnel readily.
4. The calibration of the hardness-testing equipment can be checked easily and quickly.

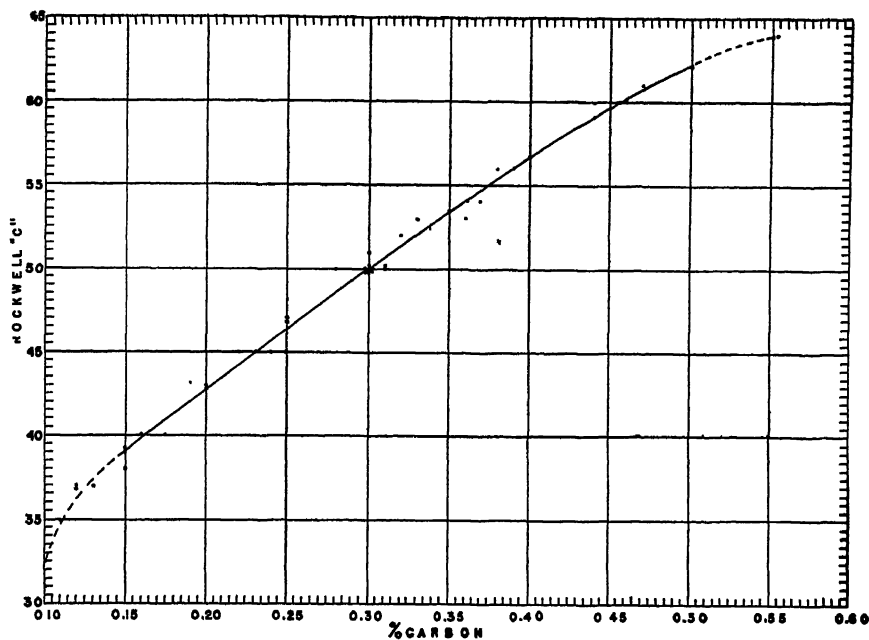
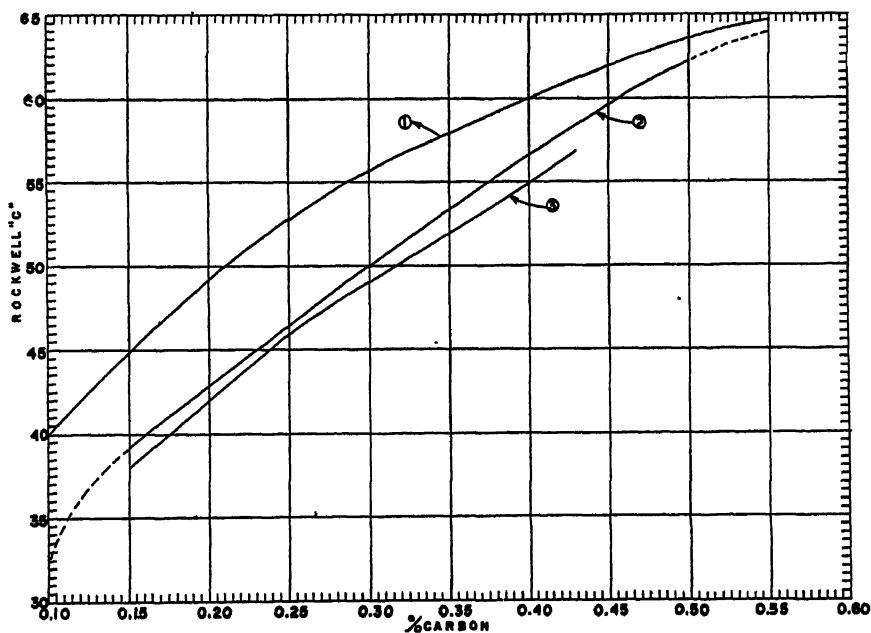


FIG. 3.—CARBON CONTENT VS. AS-QUENCHED HARDNESS.

FIG. 4.—COMPARISON CURVES. CARBON CONTENT VS. AS-QUENCHED HARDNESS.
Data from (1) Burns, Moore and Archer;⁷ (2) Naval Research Laboratory; (3) R. O. Kern.⁸

5. Alloying elements in the low-alloy steels do not affect the determination; in fact, it can be said that they are beneficial, since they increase hardenability.

ACKNOWLEDGMENT

Grateful acknowledgment is made to H. F. Taylor, for helpful suggestions in conducting the experiments and in preparation of the manuscript; also to the Navy Department for sponsoring the work and for permission to publish the results.

REFERENCES

1. C. J. G. Malmberg: A Magnetic Method for Determining Carbon in Steel and Its Application in Deoxidation Processes. *Jernkontorets Ann.* (1930) **114**, 508.
2. G. Soler: New Carbometer Control Speeds Production and Improves Quality. *Metal Progress* (1937) **31**, 159.
3. Rogers, Wentzel and Riott: A New Method for the Rapid Determination of Carbon in Samples of Plain Carbon Open Hearth Steel. *Trans. Amer. Soc. Metals* (1939) **27**, 175.
4. H. H. Blossjo: A Rapid Method for Determining Carbon in Plain Carbon Steels for Control Purposes. *Trans. Amer. Foundrymen's Assn.* (1939) **47**, 469.
5. H. K. Work and H. T. Clark: A New Instrument for the Magnetic Determination of Carbon in a Steel Bath. *Trans. A.I.M.E.* (1940) **140**, 475.
6. Rogers, Wentzel and Riott: Magnetic Methods for Determining Carbon in Steel. *Trans. Amer. Soc. Metals* (1941) **29**, 969.
7. Burns, Moore and Archer. Quantitative Hardenability. *Trans. Amer. Soc. Metals* (1938) **26**, 1.
8. R. O. Kern: Rapid Carbon Determination at Furnace of Remelted Alloy Steels. *Amer. Foundryman* (Sept. 1942) **4** (9) 8.
9. Metals Handbook (1939) 127. Amer. Soc. Metals, Cleveland, Ohio.

DISCUSSION

(F. B. Foley presiding)

N. C. FICK,* Columbus, Ohio.—We are in agreement with the authors that a rapid,

practical test such as they propose will be of considerable value to the steel melter who must follow closely the variations in carbon content of the bath. The authors obtained their specimens by use of a chill mold, and that sectioning was a necessary prerequisite to hardness testing. By using an aspirator bulb and length of glass tubing, we have been able to obtain a test specimen so uniform and smooth that satisfactory Rockwell readings can be taken directly on the surface.

The bulb is released at the moment the tube is dipped into the deoxidized metal and the unit is immediately quenched into an iced brine bath. Since a part of the glass remains on the specimen and serves as an insulator between the metal and the quenching bath, it is necessary to record as the maximum Rockwell hardness the highest readings obtained, which are found, of course, where the glass immediately broke away from the specimen when quenched. Cross-section hardness readings of specimens both as quenched from the glass tube and as reheated and quenched from 2000°F. were nearly identical to the surface hardness readings obtained during the original quench.

With reference to Fig 4, the hardness values have fallen between the curves of Burns, Moore and Archer and those of the Naval Research Laboratory. For a 0.32 carbon steel, Burns, Moore and Archer obtained a Rockwell C hardness of 56.5, Battelle 55, Naval Research Laboratory 51.5, R. O. Kern 50; for a 0.39 carbon steel, the values are 59.5, 58.5, 56, and 54, respectively.

—These observations have been made on a limited number of heats in the 0.30 to 0.40 per cent carbon range and no final conclusions with respect to possible extent of application can be reached until more data have been accumulated.

* Battelle Memorial Institute.

Fracture and Comminution of Brittle Solids

BY EUGENE F. PONCELET*

(New York Meeting, February 1944)

ABSTRACT

THIS paper attempts to analyze the phenomena involved in the fracture of brittle solids by simple compression.

Glass squares standing on edge, and compressed between two parallel steel jaws, developed jagged fractures, roughly parallel to the compression. Polarized light disclosed the presence of high local stress concentrations indicating poor contact all along the contact surfaces with the steel jaws. Teszar has shown that partial contact between the jaws and such a compressed solid causes tensile stresses in the free surfaces of the solid normal to the compression. Furthermore, Scoble has shown that in brittle solids fractures are caused by, and develop normally to, a sufficient tensile stress. It follows that such "partial-contact" cracks must be expected.

With optically flat jaws and specimens, no "partial-contact" cracks developed. Instead, very smooth cracks vertical to the compression appeared upon release of the pressure. Investigation showed that the friction with the rigid steel opposed the return of the glass to its original width, after creeping on the steel as compression built up, thus setting up tensile stresses in the glass surfaces. It was not found

possible to eliminate these "release" cracks.

Compressed to destruction, such specimens flew to dust. A Microflash photograph taken during the explosive disintegration revealed: (1) oblique parallel fragmentation cracks, 30° off the direction of the compression; (2) transverse forking fragmentation cracks, normal to the former; (3) release cracks parallel to the compression; (4) a disintegration cloud.

Given a distribution of submicroscopic cracks of random orientation throughout the glass, Griffith has shown the highest tensile stresses to be located at the tip of the cracks 30° off the direction of the compression. Although the preexistence of such cracks or flaws in unstressed glass is doubtful, they can be generated by the distorting forces set up by the compression itself.

Atoms, in a structure held together by Morse-type forces or bonds, have under tension both a stable and an unstable state of equilibrium. The difference in energy level between these two states is a function of the tension, and this difference must be borrowed from the thermal energy level of the bonds to reach the unstable state and result in a broken bond. As the fraction of the bonds having at any instant a sufficient thermal energy level is a known function of that level, it is possible to determine, in function of the prevailing tension, the fraction of the bonds that are broken.

Upon breaking of the bond uniting two atoms at the tip of an advancing crack, the two atoms accelerate away from each other, causing in the solid propagation of a

Manuscript received at the office of the Institute Nov. 1, 1943. Issued as T.P. 1684 in METALS TECHNOLOGY, April 1944 and in MINING TECHNOLOGY, May 1944.

* Special Advanced Fellow of the Belgian-American Educational Foundation, Massachusetts Institute of Technology, Cambridge, Massachusetts.

longitudinal pressure pulse normal to the crack plane on each side of the crack, and of a transverse pulse in the crack plane.

Upon reaching the next bond ahead of the crack front, the transverse pulse raises the stress at that bond to the crack-tip tension. Were this crack-tip tension sufficient to break every bond as it is met, the crack front would advance at transverse wave velocity; as not all of them are broken, the average crack velocity is proportionately less. The crack velocity is consequently a function of the broken-bond frequency and consequently of the crack-tip tension.

This crack velocity is essentially unstable and it accelerates or decelerates with such rapidity that a crack usually appears either moving at top velocity or standing still. This top velocity corresponds to such high stresses at the crack tip that broken bonds also appear in the vicinity of the tip obliquely to the crack plane, and open up deviating cracks. When viewed on edge, such cracks appear as forking-cracks. This phenomenon causes a diversion of energy from the crack front in different directions, thus effectively holding the crack-tip stresses—and with them the crack velocities—below a top ceiling.

The parallel longitudinal pressure pulses emanating from an advancing crack reflect at a free boundary as parallel tension pulses and as transverse pulses of the same direction but of lesser velocity. It so happens

that the reflected pulses from any first crack in the compressed specimen oriented 30° off the compression are the only ones that could possibly have set off the oblique fragmentation cracks; also the transverse fragmentation cracks observed.

The kick-back of energy, released in the shape of pressure pulses by the rupture of a bond at the tip of an advancing crack front, is the same on both sides of the crack. The concentration of pulse energy in the two fragments resulting from the crack is consequently inversely proportional to the volume of these fragments. It happens that the stress carried by their reflected pulses, required to produce further cracks in the fragments, is proportional to this pulse-energy concentration. The larger fragments, therefore, have less tendency than the smaller fragments to fracture further, and then eventually form residual particles unable to split further, while the smaller fragments repeat the process. These smaller fragments continue splitting up and throwing off residual particles of smaller and smaller size until the whole solid is reduced to a collection of residual particles, having a definite size distribution.

The large amount of energy stored in the compressed specimen produced such high energy concentrations in all the fragments that residual particles were not formed before a very small size was reached and consequently appeared as a disintegration cloud.

The Influence of Various Elements upon the Position of the Eutectoid in the Iron-carbon (Carbide) System

BY CARL L. SHAPIRO* AND JEROME STRAUSS,* MEMBERS A.I.M.E.

(Chicago Meeting, October 1943)

THIS is a critical examination of the theory that *the amount of carbon necessary to form the iron-carbon (carbide) eutectoid is lowered by the addition of any carbide-forming element*. Although this theory has been built up over a long period of years, it appears, in the light of recent published investigations upon the ternary constitutional diagrams of iron with carbon and other alloying elements, to be no longer tenable. A survey of these new results, summarized below, shows that (as is known) some metals lower the carbon content of the iron-carbon (carbide) eutectoid, whereas others raise it, but (as not heretofore clearly set forth) some first move the eutectoid in one direction and then, at higher concentrations, shift it in the opposite direction. Moreover, these differences in behavior exist even among the common alloying metals classed as carbide formers.

PART I

INFLUENCE OF BODY-CENTERED CUBIC ELEMENTS

The effects of the various body-centered cubic metals (chromium, tungsten, molybdenum, vanadium, columbium and tantalum) are reviewed individually.

Manuscript received at the office of the Institute July 2, 1943. Issued as T.P. 1646 in METALS TECHNOLOGY, December 1943.

* Vanadium Corporation of America, New York, N. Y.

¹ References are at the end of the paper.

Iron-carbon-chromium System.—In the monograph on Alloys of Iron and Chromium, Kinzel and Crafts¹ concluded that the carbon content of the eutectoid is lowered by increasing the chromium content. The quantitative influence of chromium on the eutectoid point of iron-carbon alloys was shown by Monypenny² (Fig. 1) and no data have been forthcoming to refute his findings.

Iron-carbon-tungsten System.—Gregg,³ in the monograph on Alloys of Iron and Tungsten, accepted the data showing that tungsten decreases the amount of carbon required to form the eutectoid. The influence of tungsten on the eutectoid percentage of carbon as determined by Oberhoffer and Daeves⁴ is shown in Fig. 2; these results have received general approval.

Iron-carbon-molybdenum System.—In the monograph on Alloys of Iron and Molybdenum, Gregg⁵ reviewed the work of Guillet,⁶ Swinden,⁷ and Reed,⁸ all showing that molybdenum lowered the carbon content of the eutectoid, whereas Takei⁹ contradicted this conclusion. Svetchnikoff and Alferova,¹⁰ a little later, showed that large additions of molybdenum shift the eutectoid to the right. These last-named investigators found that molybdenum, up to 1.2 per cent, shifts the pearlite point and the point of maximum solubility of cementite in the gamma phase only slightly in the direction of lower carbon content; on the other hand, increasing amounts of molyb-

denum above 1.2 per cent first results in a double carbide and then abruptly moves the pearlite and maximum cementite solubility points to higher carbon content; when

changes with the amount of the element present; viz., (1) small amounts of molybdenum dissolve in the ferrite and decrease the amount of carbon necessary to form

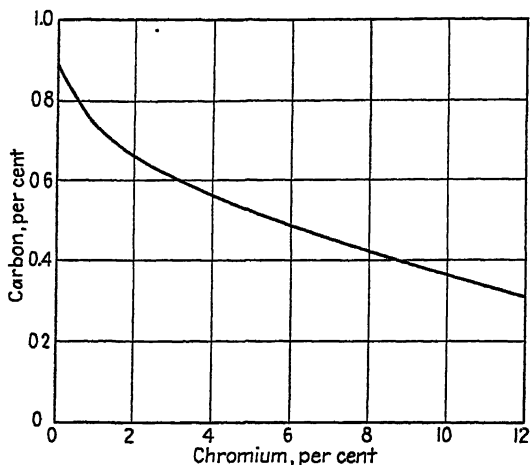


FIG. 1.—INFLUENCE OF CHROMIUM ON THE EUTECTOID POINT. (*Monypenny*.³)

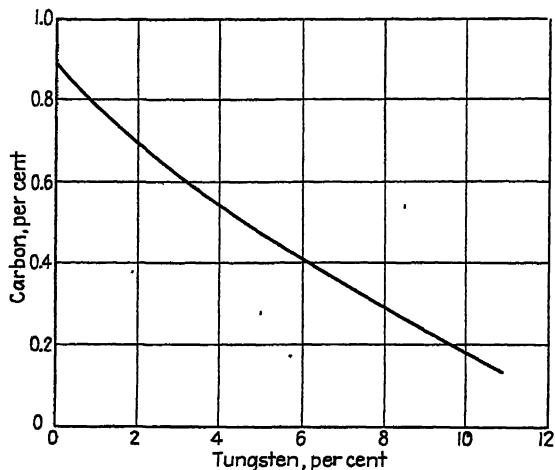


FIG. 2.—INFLUENCE OF TUNGSTEN ON THE EUTECTOID POINT. (*Oberhoffer and Davies*.⁴)

the molybdenum content has reached 10 per cent, the eutectoid point is at 1.32 per cent carbon, with its cementite limit as 1.83 per cent carbon.

Thus, a summary of the effect of molybdenum upon the eutectoid position seems to indicate a directional behavior that

the eutectoid composition; (2) when a certain molybdenum content is added to iron-carbon alloys, a double molybdenum carbide is formed and the carbon content of the eutectoid from that concentration upward must be increased in order to compensate for carbon loss due to carbide

formation, so that the eutectoid position is shifted toward higher carbon content with increasing proportions of molybdenum.

*Iron-carbon-vanadium System.**—Al-

Iron-carbon-tantalum System.—Gender and Harrison²⁰ recently investigated the effect of tantalum upon iron-carbon alloys. Although no ternary equilibrium diagram

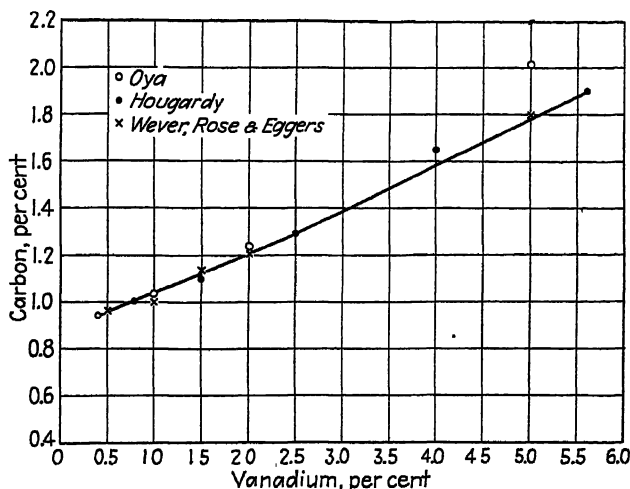


FIG. 3.—INFLUENCE OF VANADIUM ON THE EUTECTOID COMPOSITION.

though Reed,⁸ Guillet,¹¹ Portevin,¹² Giesen¹³ and Arnold and Read¹⁴ claimed that the amount of carbon required to produce the eutectoid structure is lowered by vanadium, the recent researches of Oya,¹⁵ Vogel and Martin,¹⁶ Hougardy¹⁷ and Wever, Rose and Eggers¹⁸ show the contrary; namely, that vanadium increases the amount of carbon required to form the eutectoid percentage instead of lowering it. This is indicated in Fig. 3, which is compiled from the ternary equilibrium diagrams of the four last mentioned investigations.

Iron-carbon-columbium (Niobium) System.—The iron-carbon-columbium ternary system has been recently investigated by Eggers and Peters.¹⁹ The effects of 0.2 to about 2.0 per cent columbium upon the iron-carbon (carbide) eutectoid are shown in Fig. 4. Eggers and Peters' results indicate that columbium shifts the eutectoid point to the right or higher carbon concentrations.

was constructed and columbium existed as an impurity in the tantalum, their results reveal definite indications. They stated that tantalum very markedly reduces the proportion of pearlite present and, if sufficient tantalum is added, a hypereutectoid steel (containing 1.20 per cent carbon) will appear to be structurally similar to an ordinary 0.60 per cent carbon hypoeutectoid steel; only 2.2 per cent tantalum is necessary to effect this change. High percentages of tantalum, such as 18 per cent, will, according to these authors, remove all pearlite present even in a hypereutectoid steel of 1.20 per cent carbon.

These results indicate that tantalum very effectively combines with carbon and shifts the eutectoid to higher carbon concentrations.

Summary.—Consideration of all available data thus shows definitely that the theory that all body-centered cubic carbide-forming elements shift the eutectoid point to lower carbon contents is not valid. The only body-centered cubic carbide-forming

* Abstracted from the forthcoming monograph, "The Alloys of Iron and Vanadium."

elements that shift the eutectoid to the left are chromium and tungsten, whereas vanadium, columbium and tantalum definitely move it to the right, toward increas-

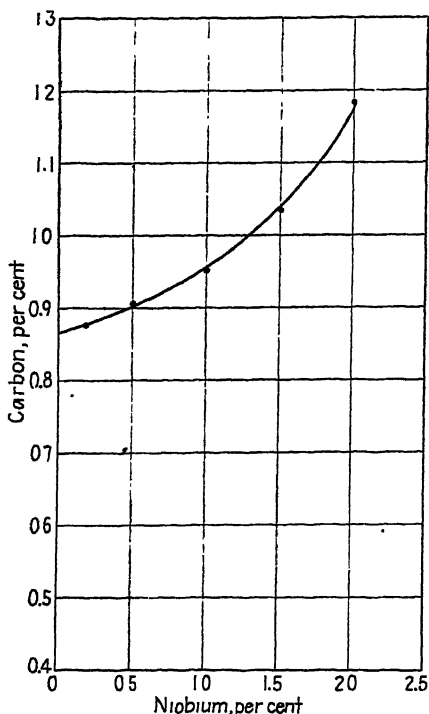
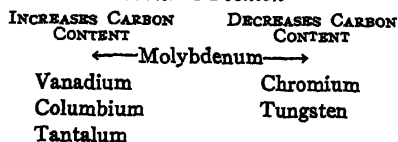


FIG. 4.—INFLUENCE OF COLUMBIUM ON THE EUTECTOID POINT. (Eggers and Peters.¹⁰)

ing carbon content. Molybdenum can be classified as an intermediate element, since small proportions shift the eutectoid to the left and large amounts move the eutectoid composition to the right.

These conclusions are illustrated by the following diagram:

Effect of Body-centered Cubic Elements upon the Eutectoid Position



PART II

INFLUENCE OF OTHER ALLOYING ELEMENTS

In part I of this critique, the influence of the body-centered cubic metals upon the eutectoid position was discussed. This section summarizes the existing information on the effects of other common alloying elements upon the eutectoid position. The results, in part I, are taken from the latest published ternary constitutional diagrams.

Iron-carbon-aluminum System.—Löhberg and Schmidt²¹ summarized all the existing work upon the iron-carbon-aluminum constitutional diagram prior to their investigation of this system. Although many points are in doubt, all investigators seem to agree that increasing percentages of aluminum shift the eutectoid position toward higher carbon contents.

Iron-carbon-beryllium System.—Gajew and Ssokolow²² investigated the iron-rich section of the iron-carbon-beryllium system. Their results, approximated in Fig. 5 from their diagrams, reveal that beryllium moves the eutectoid position to the right.

Iron-carbon-cobalt System.—Vogel and Sundermann²³ studied the ternary system of iron-carbon-cobalt. The effect of cobalt upon the position of the iron-carbon (carbide) eutectoid is shown in Fig. 6, which was approximated from their data on this system. These results disclose that increasing amounts of cobalt shift the eutectoid position to the left, or in the direction of decreasing carbon content.

Iron-carbon-copper System.—Although the iron-carbon-copper ternary constitutional diagram is imperfectly surveyed, the results as recorded by Gregg and Daniloff²⁴ indicate that the effect of copper upon the eutectoid position is to shift it toward lower carbon contents.

Iron-carbon-manganese System.—Bain, Davenport and Waring²⁵ determined the influence of manganese upon the eutectoid

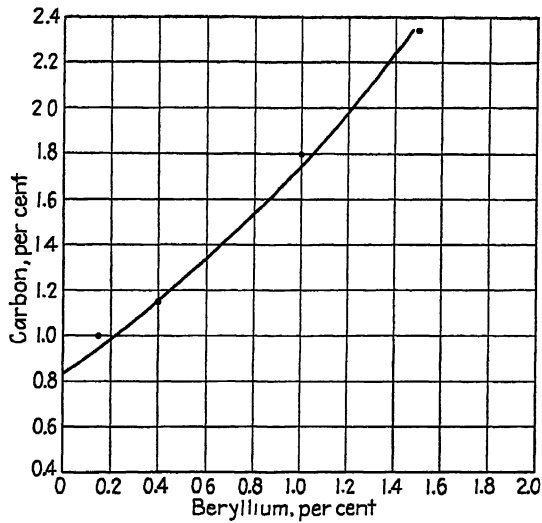


FIG. 5.—INFLUENCE OF BERYLLIUM UPON THE EUTECTOID POSITION. (*Gujew and Ssoklow.*²²)

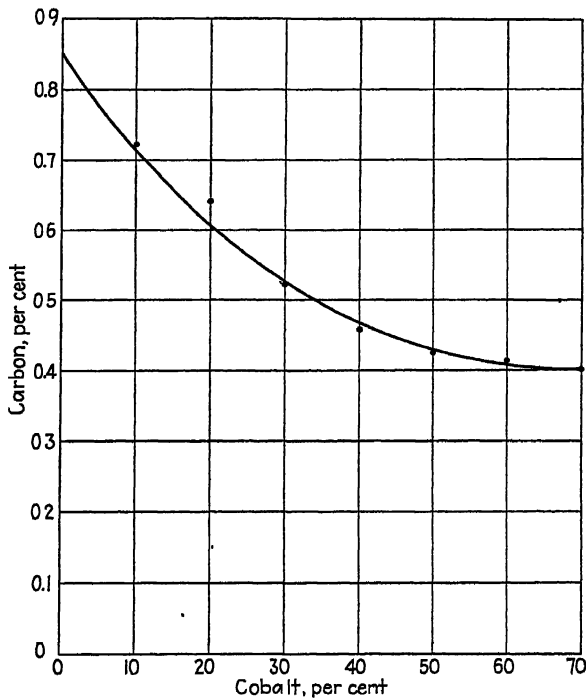


FIG. 6.—APPROXIMATE EFFECT OF COBALT ON THE EUTECTOID POSITION. (*Vogel and Sundermann.*²³)

position. Their data, reproduced as Fig. 7, indicate that increasing percentages of manganese progressively lower the iron-carbon (carbide) eutectoid composition.

lowers the carbon content of the eutectoid (Fig. 9).

Iron-carbon-titanium System.—Tofaute and Buttinghaus²⁸ studied the iron-rich

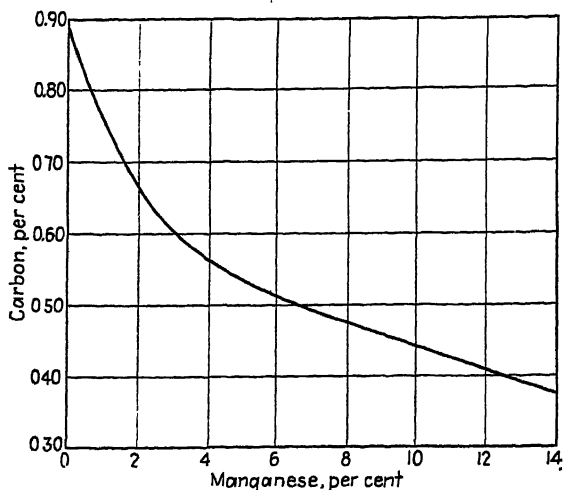


FIG. 7.—CARBON CONTENT OF EUTECTOID AS A FUNCTION OF MANGANESE CONTENT. (Bain, Davenport and Waring.²⁵)

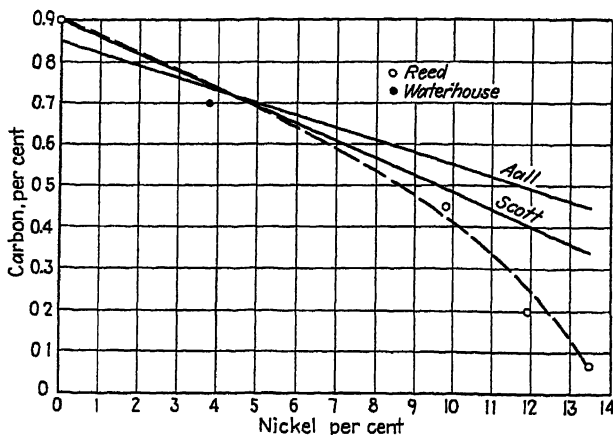


FIG. 8.—VARIATION WITH NICKEL CONTENT OF THE LINE OF TWOFOLD SATURATION ORIGINATING IN THE IRON-CARBON EUTECTOID. (Marsh.²⁶)

Iron-carbon-nickel System.—Marsh²⁶ has summarized the existing information on the iron-carbon-nickel constitutional diagram. According to Fig. 8, nickel decreases the carbon content of the iron-carbon (carbide) eutectoid.

Iron-carbon-silicon System.—Greiner, Marsh and Stoughton²⁷ show that silicon

section of the ternary iron-carbon-titanium constitutional diagram. Their equilibrium results are approximated in Fig. 10 and indicate that titanium increases the carbon content of the eutectoid.

Iron-carbon-zirconium System.—Vogel and Löhberg²⁹ investigated the iron-carbon-zirconium ternary system. Fig. 11, which is

approximated from Vogel and Löhberg's data, shows that the carbon content of the alloying elements, other than the body-

Summary.—The influence of various alloying elements, other than the body-

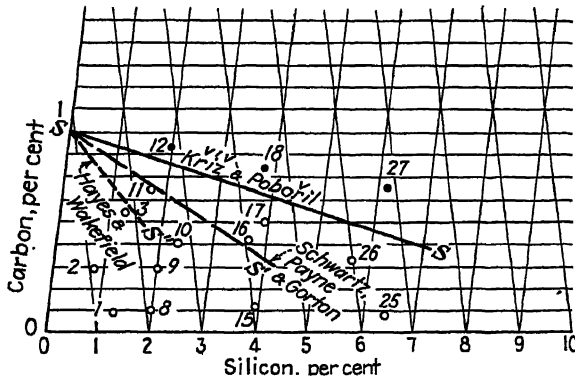


FIG. 9.—EFFECT OF SILICON ON EUTECTOID POINT. (Greiner, Marsh and Stoughton²⁷)

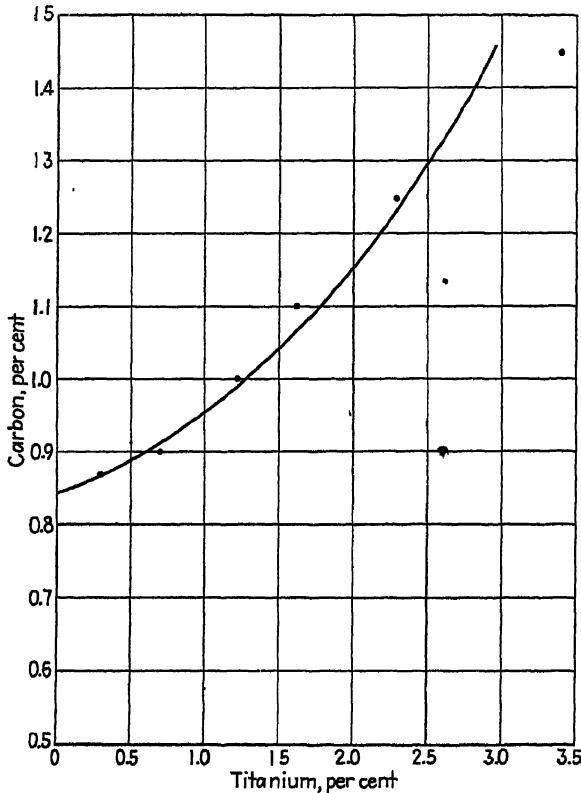


FIG. 10.—INFLUENCE OF TITANIUM UPON THE EUTECTOID POSITION. (Tofaute and Buttinghaus.²⁸)

iron-carbon (carbide) eutectoid increases progressively with zirconium.

centered cubic metals, upon the position of the iron-carbon (carbide) eutectoid has

been briefly set forth in the foregoing. These effects are summarized in Table 1.

TABLE 1.—*Effect of Some Alloying Elements upon the Eutectoid Position*

INCREASES CARBON CONTENT	DECREASES CARBON CONTENT
Aluminum	Cobalt
Beryllium	Copper
Titanium	Manganese
Zirconium	Nickel
	Silicon

PART III

A PROPOSED THEORY TO EXPLAIN THE INFLUENCE OF VARIOUS ELEMENTS UPON THE EUTECTOID POSITION

Since no adequate explanation could be advanced in support of the earlier theory,

TABLE 2.—*Effect of Various Alloying Elements upon the Carbon Content of the Iron-carbon (Carbide) Eutectoid*

Moves Eutectoid to Right	Moves Eutectoid to Left	Moves Eutectoid to Left then Right
Aluminum Beryllium Columbium Tantalum Titanium Vanadium Zirconium	Chromium Cobalt Copper Manganese Nickel Silicon Tungsten	Molybdenum .

one is now presented which explains the mechanism by which various elements alter the eutectoid position. As a basis for this explanation, the published effects of the

various elements upon the position of the iron-carbon (carbide) eutectoid, which were discussed in parts I and II, are compiled in Table 2. Inasmuch as the majority of the elements listed in Table 2 are known carbide formers, the ternary constitutional diagrams of all of these elements were surveyed for carbide formations. The results obtained are given in Table 3. Since this table shows that some of the elements that move the eutectoid to the left are non-carbide-forming while the remainder in this group (middle column, Table 3) are carbide formers, the ternary equilibrium diagrams of these elements were again examined.

The ternary iron-carbon-chromium constitutional diagrams by Tofaute, Sponheuer and Bennek,³⁰ and Tofaute, Kuttner and Buttinghaus³¹ show that, at rather high chromium contents, a peritecto-eutectoid* reaction replaces the eutectoid reaction. The effect of increasing chromium content upon the position of the peritecto-eutectoid reaction is shown in Fig. 12, which is compiled from their ternary sectional diagrams. These results disclose a linear relationship between carbide formation and peritecto-eutectoid position, as was previously shown in Fig. 3, presenting the influence of vanadium upon the eutectoid position. Con-

* For a description of the sense in which the authors have employed this term, see appendix A.

TABLE 3.—*Initial Classification of Alloying Elements Based upon Reported Effects on the Eutectoid*

Moves Eutectoid to Right	Carbides	Moves Eutectoid to Left	Carbides	Moves Eutectoid to Left then Right	Carbides
Aluminum..... Beryllium..... Columbium..... Tantalum..... Titanium..... Vanadium..... Zirconium.....	(Al ₄ C ₃) (Be ₃ C) (Cb ₃ C ₂)(CbC) TaC TiC (V ₄ C ₃), (VC) ZrC	Chromium..... Cobalt..... Copper..... Manganese..... Nickel..... Silicon..... Tungsten.....	((Fe, Cr) ₇ C ₃), ((Fe, Cr) ₃ C)* none none ((Fe, Mn) ₃ C), ((Mn, Fe) ₃ C), (Mn, Fe) ₇ C [†] ((Fe, Ni) ₃ C)* none (?) [‡] ((Fe, W) ₃ C), (WC)*	Molybdenum...	(ω), (θ)′

* Composition of carbides varies with chromium concentrations.

† Composition of carbides varies with Mn concentrations (Wells³²).

‡ Waterhouse.³³

* Composition of complex compound undetermined.

† Decomposition product of either or both tungsten-bearing cementite and the ternary compound ((Fe, W)₃C) (Gregg³).

ω = double carbides of Fe and Mo; θ = Mo₃C, which is capable of dissolving Fe and Mo (Gregg³).

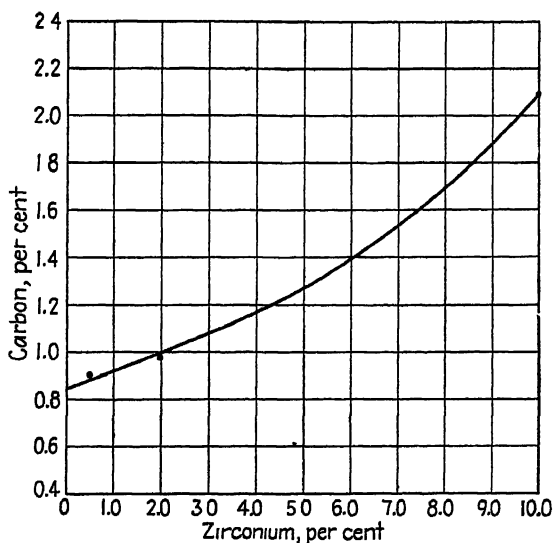
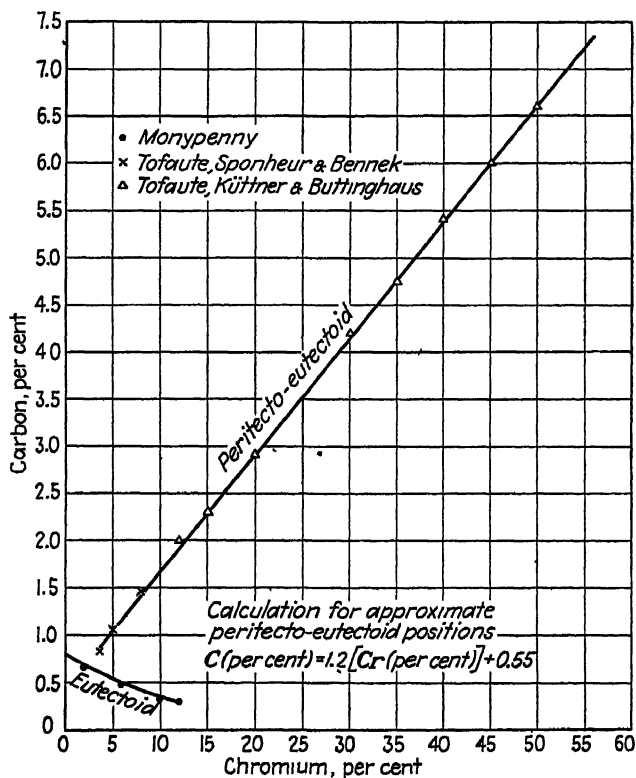
FIG. 11.—INFLUENCE OF ZIRCONIUM UPON THE EUTECTOID POSITION. (Vogel and Löhberg.³⁰)

FIG. 12.—INFLUENCE OF CHROMIUM UPON THE EUTECTOID AND PERITECTO-EUTECTOID POSITIONS.

sequently, it may be stated that in the ternary iron-carbon-chromium system chromium first lowers the carbon content of the eutectoid and, after forming definite

The ternary constitutional diagrams, including manganese, nickel and other metals with iron and carbon, respectively, are also very incomplete. If it is assumed

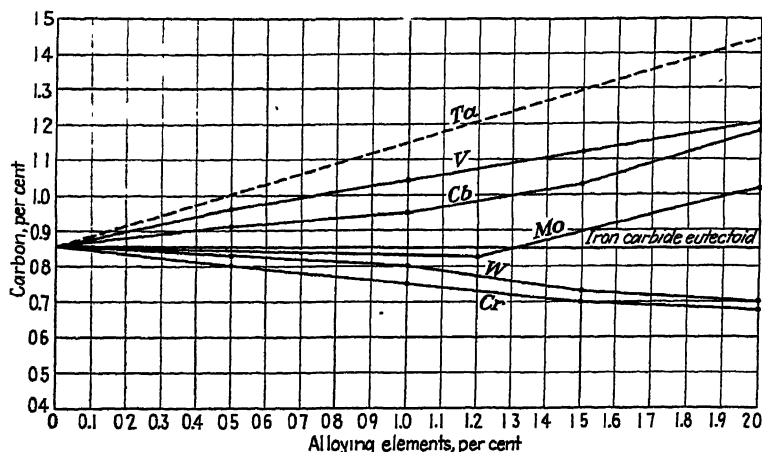


FIG. 13.—EFFECT OF BODY-CENTERED-CUBIC ELEMENTS ON EUTECTOID COMPOSITION.

carbides, the eutectoid reaction becomes a peritecto-eutectoid reaction and is moved linearly to higher carbon contents with increasing chromium content.

Since the incomplete iron-carbon-tungsten ternary diagram does not offer definite data to plot the peritecto-eutectoid reaction that exists within this system, some pertinent summaries of Takeda's work³² by Gregg³ are presented below to illustrate the possible similarity of the behavior to that in the iron-carbon-chromium system:

The A_{2-3} curve—i.e., the intersection of the A_2 and A_3 surfaces—is raised with the increased tungsten content up to 1335°C. (peritecto-eutectic point) at 12 per cent tungsten, 0.33 per cent carbon. The carbon content in this eutectoid composition decreases with the addition of tungsten and becomes 0.2 per cent at 4 to 5 per cent tungsten, beyond which it increases.

The range consisting of the alpha, delta and eta phases exists in temperature ranges below 735°C. (1355°F.) at which a peritecto-eutectoid reaction, $\gamma + \eta \rightleftharpoons \alpha + \theta$, takes place. This composition range shifts toward the higher carbon side as the tungsten content increases.

that definite carbides exist within these systems, peritecto-eutectoid reactions must occur and the positions of these reactions must be moved linearly toward higher carbon content with increased alloying.

Table 4 reclassifies the various elements based upon these assumptions plus the limited data available. According to these and Fig. 13, there are four classes of elements:

Class I. Elements that progressively increase the carbon content of the eutectoid composition and widen the ferrite field.

Class II. Elements that progressively decrease the carbon content of eutectoid composition and narrow the ferrite field.

Class III. Elements that, up to a certain concentration, first decrease the carbon content of the eutectoid composition and narrow the ferrite field and, beyond this concentration, raise the carbon content of the eutectoid composition and enlarge the ferrite field.

Class IV. Elements that, up to a certain concentration, first raise the carbon content of the eutectoid composition and enlarge the ferrite field, and, beyond this concen-

tration, lower the eutectoid composition and restrict the ferrite field.

Elements of class I are strong carbide formers and appear to have a greater

carbon, Fig. 14 presents the calculated eutectoid composition of a carbon steel containing various amounts of vanadium without taking into consideration the very

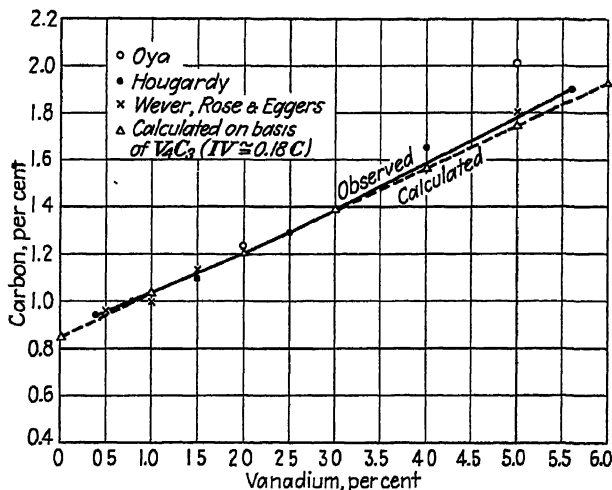


FIG. 14.—INFLUENCE OF VANADIUM ON EUTECTOID COMPOSITION.

affinity for carbon than does iron. Consequently, these elements will first combine with the amount of carbon required to fulfill the composition of their respective carbides before iron can form cementite. As a result of this primary carbide formation, the amount of carbon remaining to form cementite or pearlite is reduced and, for any constant carbon content, the increase in ferrite or decrease in cementite is almost proportional to the amount of alloying element. In other words, in order to produce a eutectoid steel containing any element of class I, the carbon content of plain carbon steel must be increased by exactly the same amount that the element requires to form its respective carbide or carbides. This additional amount of carbon can be easily calculated if the composition of the carbide or carbides and the solubility of the class I element in ferrite* is known.

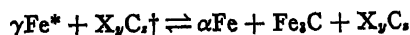
As a specific instance, if it is assumed that the eutectoid is at 0.85 per cent

slight solubility of vanadium or vanadium carbide in iron.

Any great deviation between the observed and calculated eutectoid lines of class I elements indicates the presence of another carbide richer or poorer in carbon content, depending upon whether the calculated carbon percentage of the eutectoid is higher or lower than the observed results. Class I elements do not enter into true eutectoid reactions, but rather peritecto-eutectoid reactions. As soon as any element of class I forms a definite carbide, which exists in equilibrium with austenite above the γ \rightarrow α transformation temperature, the eutectoid reaction



becomes peritecto-eutectoid



Elements of class II possess a greater affinity for iron than for carbon. These

* By this is meant, not the solubility in the absence of carbon but the solubility of the carbide of the element at the eutectoid temperature.

* Solid solution of carbon, with or without the alloying element, in austenite.

† Compound of alloying element and carbon with or without iron.

elements of class II form varying solid solutions with iron and carbon and do not form any definite carbides with carbon alone or with iron and carbon. If class II elements formed carbides of any description, they would automatically in some composition range undergo a peritecto-eutectoid reaction which would tend to shift the eutectoid (peritecto-eutectoid) to the right and thereby they would be classified as class III elements instead of class II. Whether or not such a reaction would shift the position of the eutectoid (peritecto-eutectoid) to a higher carbon content than that of the iron-carbon (carbide) eutectoid is inconsequential in this discussion.

Elements of class III partake of the behavior of classes II and I in this order. These elements, according to their constitutional diagrams, first restrict the solubility of carbon in gamma iron and, on subsequent cooling below the temperature of initial alpha-iron formation, the carbon content of the iron-carbon (carbide) eutectoid is not proportional to the amount of alloying element but decreases asymmetrically in relation to the alloying element content. This latter observation is illustrated in the various diagrams presented (Figs. 1, 2 and 7), which show the effect of alloying upon the eutectoid position. The reason for this decrease in percentage of alloying element per per cent carbon may lie in the formation of double carbides, which vary in their content of iron, carbon and alloying element. The carbide compositions first formed are rich in iron and poor in alloying element and, as the percentage of alloying element increases, the carbides become proportionately richer in alloying element until the double carbide of iron, carbon and alloying element either disappears to form an iron-free carbide (alloying element plus carbon) or a low-iron, high-alloying-element carbide.

Elements of class IV theoretically should first respond as class I and then as class II. The mechanism is the same as that of

class III, but in reverse. Although this type of reaction does not seem to occur in any of the ternary constitutional diagrams of iron and carbon with a third element, it seems possible that such a reaction may conceivably occur in other types (non-ferrous) of ternary diagrams where compounds apparently have decreasing and increasing solubility ranges.*

This explanation of the increase or decrease in the carbon content of the iron-carbon (carbide) eutectoid by alloying encompasses all alloying elements in steel regardless of their lattice structure. The effects, as distinguishing the several classes, are shown graphically in Fig. 15. Whenever two or more elements of the various classes are alloyed, the sum total of their effects cannot usually be deduced by combining their individual influences, but most likely will be in the direction of the stronger element or in the direction of the element that is present in the greatest concentration. It may also be possible that, when elements of various classes are employed together, their individual influences may be severely altered so that jointly they may respond in an entirely different manner.

Conclusion

From the evidence submitted in parts I and II of this paper, it is quite apparent that the alloying elements influence the iron-carbon (carbide) eutectoid in such manner as to classify them as follows:

Class I. Elements that increase the carbon content of the iron-carbon (carbide) eutectoid. These elements form definite carbides and the carbon content of the eutectoid (peritecto-eutectoid) increases almost proportionally to the amount of carbon required by these elements to fulfill their structural formulas.

* As indicated, no such condition is known in iron-rich systems of iron, carbon and third elements. The possibility of a condition of this type, however, may be present on the alloy-rich side of such a system or (as noted) in nonferrous systems.

Class II. Elements that decrease the carbon content of the iron-carbon (carbide) eutectoid. These elements form varying solid solutions with iron and do not form any definite carbide directly with carbon or with iron and carbon.

Class III. Elements that first decrease and then increase the carbon content of the iron-carbon (carbide) eutectoid. These elements first form varying solid solutions or varying compounds with iron or iron and carbon and, at certain alloying concentrations, form rather definite carbides and undergo peritecto-eutectoid reactions; hence the decrease and subsequent increase of the carbon content of the eutectoid.

PART IV

FURTHER THEORETICAL CONSIDERATIONS

In parts I and II of this paper, the effects of various elements upon the carbon content of the eutectoid position were summarized. From the results of this survey, a theory was presented in part III which explains the data reported in parts I and II. However, the authors do not feel that their theory is complete because some parts of the various constitutional diagrams have never been investigated. Consequently, although their presented theory is in accord with the reported results, they believe that this theory must be slightly modified to include the following suggested probabilities.

The basis of these suggestions is that the ternary constitutional diagrams of class I elements (Table 4) are incomplete in the lowest ranges of alloy content. The

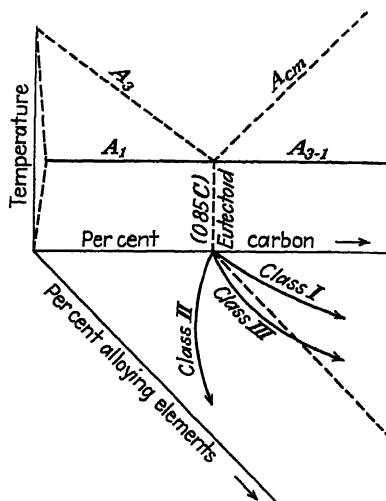


FIG. 15.—EFFECT OF VARIOUS CLASSES OF ALLOYING ELEMENTS ON THE EUTECTOID POSITION.

diagrams show that the various elements of class I form definite iron-free carbides as soon as any appreciable amount of the alloying element is added. This results in replacing the eutectoid ($\gamma\text{Fe} \rightleftharpoons \alpha\text{Fe} + \text{Fe}_3\text{C}$) by a peritecto-eutectoid reaction ($\gamma\text{Fe} + \text{X}_y\text{C}_z \rightleftharpoons \alpha\text{Fe} + \text{Fe}_3\text{C} + \text{X}_y\text{C}_z$) with a consequent linear increase in carbon content

TABLE 4.—*Later Classification of Alloying Elements Based upon Assumptions and Unconfirmed Predictions of Their Effects on the Eutectoid*

Class I	Carbides	Class II	Carbides	Class III	Carbides
Aluminum.....	(Al ₄ C ₃)	Cobalt.....	None	Molybdenum.	(ω), (θ) ^b
Beryllium.....	(Be ₂ C)	Copper.....	None	Chromium....	(Fe, Cr) ₇ C ₃ , (Fe, Cr) ₃ C ^c
Columbium....	(Cb ₃ C ₄) (CbC)	Silicon.....	None(?) ^d	Tungsten.....	(Fe, W) ₃ C, (WC) ^d
Tantalum.....	(TaC)			Manganese...	(Fe, Mn) ₃ C, ((Mn, Fe) ₃ C), ((Mn, Fe) ₇ C ₃) ^e
Titanium.....	(TiC)			Nickel.....	((Fe, Ni) ₃ C) ^f
Vanadium.....	(V ₄ C ₃), (VC)				
Zirconium.....	(ZrC)				

^a Composition of complex compound undetermined.

^b ω = double carbides of Fe and Mo; θ = Mo₃C, which is capable of dissolving Fe and Mo (Gregg^g).

^c Composition of carbides varies with chromium concentrations.

^d Decomposition product of either or both tungsten-bearing cementite and the ternary compound ((Fe, W)₃C) (Gregg^g).

^e Composition of carbides varies with Mn concentration (Wells^h).

^f Waterhouse.²⁴

of the eutectoid (peritecto-eutectoid) What the authors suggest is that at low alloying concentrations of perhaps less than about 0.2 per cent or, in some instances, much

carbides are present, to replace the eutectoid by a peritecto-eutectoid and shift the carbon content of the reaction linearly to the right in direct proportion to the carbon

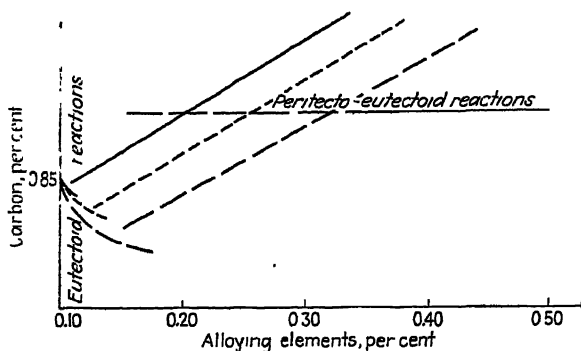


FIG. 16a.

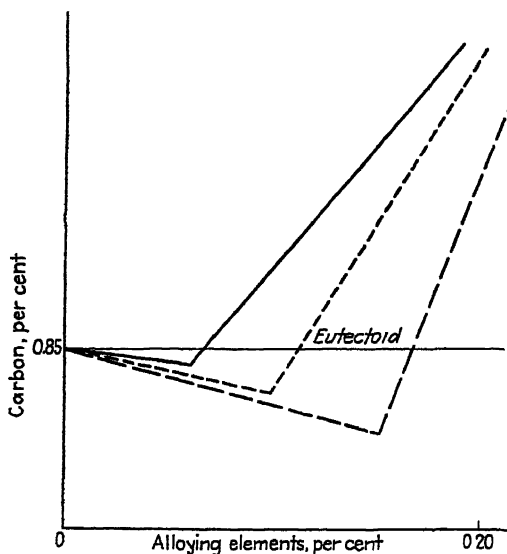


FIG. 16b.

less than even 0.1 per cent, these elements may be found to form a eutectoid with extremely limited solubility and, when larger amounts are added, the excess carbide gives rise to a peritecto-eutectoid reaction. The result of the limited solubility and formation of a eutectoid would be to lower slightly the carbon content of the eutectoid and, as soon as any excess

necessary to replace the carbon converted into these carbides. This has been previously shown for chromium and molybdenum, respectively. A generalization is graphically shown in Fig. 16.

Fig. 16a shows the suggested formation of eutectoid and peritecto-eutectoid reactions that are identical in general form with those of the ternary iron-carbon-

chromium constitutional diagram (Fig. 12). The percentages of alloy required to replace the eutectoid by a peritecto-eutectoid reaction could be extremely small (less than 0.2 per cent, even as little as 0.005 per cent). In the iron-carbon-chromium ternary diagram (Fig. 12) the actual value is high (close to 3 per cent). Another comparison may be made (between Fig. 16*b* and Fig. 13); typical results have been already reported in the ternary iron-carbon-molybdenum system in which the effect of molybdenum per unit of alloying is not so marked as are the effects produced by the potent elements of class I.

In summation, the authors suggest that extremely small amounts of class I elements, which form definite iron-free carbides, first lower the carbon content of the eutectoid and, as soon as definite insoluble carbides are formed, the carbon content of the eutectoid (peritecto-eutectoid) is moved linearly to the right. This suggestion would automatically transfer elements of class I to class III (Table 4). However, some differentiation must be made between class I elements, which form iron-free carbides, and class III elements, which form iron-containing carbides. The future must decide, however, whether class I elements should be grouped as the authors have done in Table 4 or placed in class III, which would be then subdivided into class III*a*, elements forming iron-free carbides, and class III*b*, elements forming iron-containing carbides. The distinction would, of course, be drawn not solely on this basis of carbide type but on the results in respect to the general magnitude of the alloy addition necessary to effect the shifting in the direction of eutectoid movement.

CONCLUSION

In conclusion, it should be emphasized that it was the hope of the authors in preparing this paper that it might lead those who may now or in the future have time and facilities available to undertake addi-

tional experimental work on these ternary systems. Such efforts should ultimately lead to accumulation of data on the basis of which an understanding of these phenomena could result that would represent an advance beyond the present conceptions, which, while useful, need to be supplemented in order that we may have a more precise understanding of what may have seemed to some to be simple reactions, but which are believed to be more complex than has been generally accepted.

APPENDIX A

While in the process of writing this paper, the question of nomenclature became paramount. This was especially true in describing a normal eutectoid reaction (see Appendix B for definitions) which contained in equilibrium a compound (carbide). After much consideration, the term "peritecto-eutectoid reaction" was adopted because of its previous usage and its similarity to a "peritectic reaction" (see Appendix B).

In order to simplify the term "peritecto-eutectoid" or "peritecto-eutectoid reaction," the authors define it broadly in the manner in which they have applied it throughout the preceding text.

In the binary constitutional diagram of iron and carbon (carbide), at approximately 0.83 per cent carbon, austenite transforms into two phases (ferrite and lamellar cementite). This reaction was called a "eutectoid reaction" by Howe (see Appendix B) and the resultant product was termed "pearlite." When an alloying element is added to the binary system of iron and carbon (carbide), the reactions in this ternary iron-carbon-alloying element system may or may not be similar to those in the binary iron-carbon (carbide) system, depending upon the following conditions:

1. If the amount of alloying element is completely soluble in austenite, no apparent change should occur in the eutectoid

reaction beyond a change in eutectoid composition, transformation rates, transformation temperature, etc.

2. If the amount of alloying element is greater than that soluble in austenite or the alloying element has a greater affinity for carbon than for iron, or vice versa, the alloying element will form a compound with carbon (with or without iron). As a result, the iron-carbon (carbide) eutectoid actually no longer exists, since it is a phenomenon resulting (on cooling) in only two phases ($\gamma\text{Fe} \rightleftharpoons \alpha\text{Fe} + \text{Fe}_3\text{C}$), and is replaced by a transformation reaction that yields three phases— γFe (solid solution) + compound (carbide with or without iron) $\rightleftharpoons \alpha\text{Fe} + \text{Fe}_3\text{C} + \text{compound}$ (with or without iron)—when cooled under equilibrium conditions. Therefore, in order to distinguish this ternary iron-carbon-alloying element reaction from the binary iron-carbon (carbide) eutectoid reaction, the authors called it a “peritecto-eutectoid” reaction, since it has been previously so described (see Appendix B).

Another subject presented by the authors for discussion is the question of eutectoid and peritecto-eutectoid transformation temperatures. In the binary iron-carbon (carbide) system, the eutectoid reaction occurs at approximately 723°C . (1333°F .), or over a temperature range that is extremely narrow. However, in a ternary system of iron and carbon with an alloying element that forms a compound, the peritecto-eutectoid transformation extends over an appreciable temperature range, since the alloy compound precipitates preceding or during the austenite transformation. Consequently, the transformation temperature range extends over a wide temperature interval instead of an extremely narrow one, as in the iron-carbon (carbide) system. This has been recorded by the authors for the ternary iron-carbon-vanadium system (see forthcoming “Alloys of Iron and Vanadium” Monograph). B. Kjerrman [*Trans. Amer. Soc. Metals* (1926)

9, 430-451] also reported similar effects in plain carbon steels, caused by the presence of phosphorus, silicon and manganese.

APPENDIX B

DEFINITIONS OF EUTECTOID

Thus a steel of 0.90 per cent carbon* consists of pearlite alone . . . is called “eutectoid.”

* In the case of pure carbon steel the eutectoid carbon content is about 0.90 per cent. But the carbon content of the eutectoid may prove to be affected by the presence of other elements, that carbon content with which pearlite alone, without either additional ferrite or cementite, is formed in the transformation. Steel which thus consists of pearlite alone should be called eutectoid, even if, because of the presence of manganese, or other penetrating elements, its carbon content should vary from 0.9 per cent.

H. M. Howe: *The Metallography of Steel and Cast Iron*. New York, 1916. McGraw-Hill Book Co. 641 pp.

Steel made up exclusively of pearlite is now quite universally called “eutectoid” steel, after Howe, the name suggesting the great resemblance between pearlite and eutectic alloys, while at the same time clearly indicating that pearlite is not a true eutectic alloy.

A. Sauveur: *The Metallography and Heat-Treatment of Iron and Steel*. The University Press, Cambridge, Mass., 1935. 531 pp.

At the point *S*, where the solubility curve of ferrite intersects the solubility curve of cementite, the solid solution (austenite) is saturated with respect to both ferrite and cementite, and both of these phases are precipitated at constant temperature with a considerable evolution of heat, as an intimate mixture which, from its analogy to a eutectic is termed the *eutectoid*.

Z. Jeffries and R. S. Archer: *The Science of Metals*. New York, 1924. McGraw-Hill Book Co. 460 pp.

We need merely to substitute the word “solid solution” for the words “liquid solution” or “melt” in the diagram for the eutectic and we have instead of the simple eutectic reaction the exact case of austenite (solid solution) decomposition in steel to form pearlite, called “eutectoid” to distinguish it from the liquid reaction.

G. E. Doan: *The Principles of Physical Metallurgy*. New York, 1935. McGraw-Hill Book Co. 332 pp.

For the eutectoid mixture which does not arise in the liquid state (in freezing) but is due to a transformation, Howe has proposed the name *eutectoid*.

E. Heyn and M. Grossmann: *Physical Metallurgy*. New York, 1925. John Wiley & Son. 440 pp.

When the alloy has all the characteristics of the eutectic mixture which separates from a liquid solid and, since the separation takes place from a *solid* solution, the name eutectoid is commonly given to it.

R. S. Williams and V. O. Homerberg: *Principles of Metallography*. New York, 1928. McGraw-Hill Book Co. 259 pp.

DEFINITIONS OF PERITECTIC

The temperature at which this reaction takes place is called the peritectic temperature, and the reaction itself is referred to as the peritectic reaction. When this reaction occurs, there are different solid phases in equilibrium with the melt above and below the peritectic temperature. During the peritectic reaction there are three phases (two solids and one liquid) in equilibrium, so that the temperature must remain constant until at least one of the phases disappears.

Z. Jeffries and R. S. Archer: *The Science of Metals*. New York, 1924. McGraw-Hill Book Co. 460 pp.

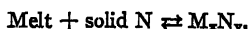
Group III, Alloys Whose Two Component Metals Exhibit Unlimited Intersolubility in the Liquid State, a Partial Solubility in the Solid State, and the Curves of Primary Solidification Intersect a Transition Point Which Correspond to the Temperature of the Peritectic Reaction. Like the alloys of Group I and II, those here show complete liquid solubility; like the alloys of Group IIb, they show partial solid solubility. Differing, however, from any case of Group II, the curves of the liquids of this series of alloys intersect, not at a minimum, but at a transition point, in temperature somewhat between the melting points of the two metals. The temperature of intersection corresponds to that of a reversible chemical reaction, called the peritectic reaction. This reaction, on cooling, occurs between the

solid phase already formed (the properitectic phase) and the residual melt, to form a new solid phase, either another solid solution, or an intermetallic compound; from these two possibilities arise the two subdivisions of the group.

When the Product of the Peritectic Reaction is a solid solution, the reaction may be expressed as follows:



When the product of the peritectic reaction is an intermetallic compound, the reaction may be expressed as follows:



L. K. Van Wert: *An Introduction to Physical Metallurgy*. McGraw-Hill Book Co. 272 pp. New York, 1936.

PREVIOUS USAGE OF THE TERM "PERITECTO-EUTECTOID"

The determination of the nature of the non-variant reaction in the γ -phase of vanadium steels depends on whether the A_1 point of carbon steel is raised or lowered on the addition of vanadium. If the A_1 point is raised on the addition of vanadium, the non-variant reaction should be peritecto-eutectoid, and if lowered, it should be ternary-eutectoid.

According to the results obtained the A_1 point of carbon steel is raised about 10°C . with 0.2 per cent vanadium and 15°C . with 0.5 per cent vanadium, remaining constant on further increasing the vanadium. From this fact, it is considered that the non-variant reaction in the γ -phase is a peritecto-eutectoid reaction.

M. Ôya: *Metallographic Investigation of Vanadium Steels*. *Sci. Repts. Tôhoku Imperial Univ.* (1930) 19, 331-365.

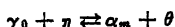
The curved surfaces of $\text{S}_1\text{P}_1\text{P}_2$ and $\text{S}_1\text{S}_2\text{P}_2$ (hatched in Fig. 6) are the solubility surfaces of $\epsilon(\text{V}_4\text{C}_3)$ and Fe_3C , respectively, in the solid solution, and point p_1 (Figs. 5, 6 and 7), show the composition of the α solid solution in equilibrium with the γ phase O at the peritecto-eutectoid point.

M. Ôya: *On the Equilibrium of the Iron-Vanadium-Carbon System*. *Sci. Repts. Tôhoku Imperial Univ.* (1930) 19, 449-473.

The range consisting of alpha, delta and eta phases exists in temperature ranges below

735°C., at which a peritecto-eutectoid reaction, $\gamma + \eta \rightleftharpoons \alpha + \theta$ takes place. This composition range shifts towards the higher carbon side as the tungsten content increases.

Point O is a peritecto-eutectoid point at which an invariant reaction



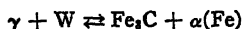
takes place; this reaction will be denoted by A_2 . Its composition lies at about 1 per cent tungsten, 0.9 per cent carbon, and its temperature is 2° to 3°C. higher than that of the A_1 point in the plain carbon steel.

Other references were also made by Takeda to peritecto-eutectoid reactions.

S. Takeda: Metallographic Investigation of the Ternary Alloys of the Iron-Tungsten-Carbon System. Introduction and Part I: On the Carbides in Tungsten Steels. Part II: Transformation and Constitution of Tungsten Steels. Part III: The Equilibrium Diagram of the Iron-Tungsten-Carbon System. *Tech. Repts.* Tohoku Imperial Univ., Sendai. (1930) 9, 483-514, 627-664; (1931) 10, 42-92.

J. L. Gregg: Alloys of Iron and Tungsten. New York, 1934. McGraw-Hill Book Co. 511 pp.

γ -(Fe)-phase is decomposed by the peritecto-eutectoid reaction:



Takesi Takei: On the Equilibrium Diagram of the Iron-Molybdenum-Carbon System. *Kinokuni no Kenkyu* (1932) 9, 97-124; 142-173.

J. L. Gregg: Alloys of Iron and Molybdenum. New York, 1932. McGraw-Hill Book Co. 507 pp.

REFERENCES

1. A. B. Kinzel and W. Craft: Alloys of Iron and Chromium, 1. New York, 1937. McGraw-Hill Book Co.
2. J. H. G. Monypenny: The Structure of Some Chromium Steels. *Jnl. Iron and Steel Inst.* (1920) 101, 493-525.
3. J. L. Gregg: Alloys of Iron and Tungsten. New York, 1934. McGraw-Hill Book Co.
4. P. Oberhoffer and K. Daevs: Notes on the So-called Double-carbide-bearing Chromium and Tungsten Steels. *Stahl und Eisen* (1920) 40, 1515-1516.
5. K. Daevs: Solubility Limits for Carbon in Ternary Steels, I.—The System Tungsten-iron-carbon. *Ztsch. anorg. Chem.* (1921) 118, 67-74.
6. J. L. Gregg: Alloys of Iron and Molybdenum. New York, 1932. McGraw-Hill Book Co.
7. L. Guillet: Comparison of the Properties and Classifications of the Ternary Steels. *Rev. de Met., Mem.* (1905) 2, 350-367. *Tr., Stahl und Eisen* (1905) 25, 1439-1444.
8. T. Swinden: Carbon-Molybdenum Steels. *Iron and Steel Inst., Carnegie Schol. Mem.* (1911) 3, 66-124.
9. E. L. Reed: Influence of Special Elements on the Carbon Contents of the Iron-Carbon Eutectoid. *Trans. Amer. Soc. Steel Treat.* (1932) 20, 115-174.
10. T. Takei: On the Equilibrium Diagram of the Fe-Mo-C Systems. *Kinokuni no Kenkyu* (1932) 9, 97-124, 142-173.
11. B. N. Svetschnikoff and N. S. Alferova: *Theoretical and Practical Metallurgy, Russia* (in Russian) (1936) 4, 72.
12. L. Guillet: New Investigations of Ternary and Quaternary Vanadium Steels. *Rev. de Met., Mem.* (1907) 4, 775-783.
13. A. M. Portevin: Contribution to the Study of the Special Ternary Steels. *Iron and Steel Inst., Carnegie Schol. Mem.* (1909) 1, 230-364.
14. W. Giesen: Special Steels in Theory and Practice. *Iron and Steel Inst., Carnegie Schol. Mem.* (1909) 1, 1-59.
15. J. O. Arnold and A. A. Reed: The Chemical and Mechanical Relations of Iron, Vanadium and Carbon. *Jnl. Iron and Steel Inst.* (1912) 85, 215-227.
16. M. Oya: Metallographic Investigations of Vanadium Steels. *Sci. Repts. Tohoku Imperial Univ.* (1930) 18, 331-364; also Equilibrium Diagram of Iron-vanadium-carbon System. *Sci. Repts. Tohoku Imperial Univ.* (1930) 18, 449-472.
17. R. Vogel and E. Martin: On the Ternary System iron-carbon-vanadium. *Archiv Eisenhüttenwesen* (1931) 4, 487-495.
18. H. Hougardy: Contribution to the Knowledge of the Iron-carbon Vanadium Systems. *Archiv Eisenhüttenwesen* (1931) 4, 497-503.
19. F. Wever, A. Rose and H. Eggers: Contribution to the Knowledge of the Iron-rich Section of the Ternary Iron-carbon-vanadium System. *Mitt. K. W. I. Eisenforsch.* (1936) 18, 230-246.
20. H. Eggers and W. Peters: The Iron Corner of the Iron-niobium-carbon Diagram below 1050°C. *Mitt. K. W. I. Eisenforsch.* (1938) 20, 205-211.
21. R. Gender, and R. Harrison: Tantalum-iron Alloys and Tantalum Steels. *Jnl. Iron and Steel Inst.* (1936) 134, 173-210.
22. K. Lohberg and W. Schmidt: The Iron Section of the Iron-aluminum-carbon System. *Archiv Eisenhüttenwesen* (1937-38) 11, 607-614.
23. I. S. Gajew and R. S. Sokolow: Alloys of the System Iron-carbon-beryllium. *Metallurg* (in Russian) (1937) 6, 11-20.
24. R. Vogel and Sundermann: The System Iron-cobalt-carbon. *Archiv Eisenhüttenwesen* (1932-33) 6, 35-38.
25. J. L. Gregg and B. N. Daniloff: Alloys of Iron and Copper. New York, 1934. McGraw-Hill Book Co.
26. E. C. Bain, E. S. Davenport and W. S. N. Waring: The Equilibrium Diagram of Iron-manganese-carbon Alloys of Commercial Purity. *Trans. Inst. Met. Engrs.* (1932) 100, 228-256.

26. J. S. Marsh: Alloys of Iron and Nickel 1. New York, 1938. McGraw-Hill Book Co.
27. E. S. Greiner, J. S. Marsh and B. Stoughton: Alloys of Iron and Silicon. New York, 1933. McGraw-Hill Book Co.
28. W. Tofaute and A. Buttinghaus: The Iron Section of the Iron-titanium-carbon System. *Archiv Eisenhüttenwesen* (1938-39) 2, 33-36.
29. R. Vogel and K. Lohberg: The System Fe-Fe₃C-ZrC-Fe₃Zr. *Archiv Eisenhüttenwesen* (1933-34) 7, 473-478.
30. W. Tofaute, A. Sponheuer and H. Bennek: Transformation, Hardening and Tempering Phenomena in Steels with up to 1% C and up to 12% Cr. *Archiv Eisenhüttenwesen* (1934-35) 8, 499-506.
31. W. Tofaute, A. Kuttner and A. Buttinghaus: The Iron-chromium-chromium Carbide Cr₇Cr—Cementite System. *Archiv Eisenhüttenwesen* (1936) 9, 606-616.
32. S. Takeda: Metallographic Investigation of the Ternary Alloys of the Iron-tungsten-carbon System. Introduction and Part I: On the Carbides in Tungsten Steels. Part II: Transformation and Constitution of Tungsten Steels. Part III: The Equilibrium Diagram of the Fe-W-C System. *Tech. Repts.* Tohoku Imperial Univ., Sendai (1930) 9, 483-514, 627-664; (1931) 10, 42-92.
33. C. Wells: Constitution of Iron-Manganese-Carbon Alloys. *Metals Handbook* (1939) 409-414. Amer. Soc. for Metals.
34. G. B. Waterhouse: The Influence of Nickel and Carbon on Iron. *Jnl. Iron and Steel Inst.* (1905) 68, 376-407.

DISCUSSION

(Carl M. Loeb, Jr., presiding)

L. D. JAFFE,* Cambridge, Mass.—This paper contains a useful presentation of the existing data, and brings out the often neglected fact that addition of an alloying element may change the nature of the eutectoid reaction. The authors' theory of the mechanism by which various elements alter the "eutectoid" position, and the resulting predictions of the effects of the several elements, is an interesting contribution.

* Laboratory of Physical Metallurgy, Harvard University.

One point in appendix A, however, does not seem to be wholly clear. It is stated that the peritecto-eutectoid transformation,



extends over an appreciable temperature range. This statement is difficult to reconcile with the phase rule, which indicates that in a three-component system at an arbitrary (atmospheric) pressure four phases can exist in equilibrium only at one temperature and with one composition of each phase. Does "appreciable" temperature range perhaps refer to a "pro-peritecto-eutectoid" austenite "compound" or austenite-cementite reaction, analogous to the pro-eutectoid austenite-cementite reaction in the iron-carbon binary system, rather than to the "peritecto-eutectoid" reaction itself?

C. L. SHAPIRO and J. STRAUSS.—Mr. Jaffe's pertinent question has been answered in part by himself and is explained in paragraphs 1 and 2 of Appendix A. As stated in paragraph 1: if the alloying element is completely soluble in austenite, the allotropic transformation (ternary eutectoid) reaction behaves simply like an austenite-cementite (proeutectoid austenite-cementite) reaction that occurs normally in the iron-carbon (carbide) binary system. However, as stated in paragraph 2 of Appendix A, if an alloy carbide compound is formed and dissolved in austenite, the binary eutectoid reaction becomes peritecto-eutectoid and the gamma-alpha transformation becomes a "pro-peritecto-eutectoid" austenite—"alloy compound" reaction, as Mr. Jaffe describes it, instead of a pro-eutectoid austenite-cementite reaction. On cooling from the peritecto-eutectoid transformation temperature range (since the reaction occurs over a temperature range and does not take place at a single constant temperature) cementite is precipitated from the alpha-iron solid solution and the final aggregate at room temperature becomes ferrite (alpha iron) plus cementite plus the carbide alloy compound.

Orientation in Low-carbon Deep-drawing Steel

BY JAMES K. STANLEY*

(Chicago Meeting, October 1943)

PREFERRED orientation, particularly in irons and low-carbon steel, is a phenomenon that is both of considerable importance and theoretical interest. At times it is a liability and at other times an asset. In deep-drawing operations, preferred orientation is extremely undesirable because it necessitates trimming operations and increases scrap loss. Furthermore, oriented metals are likely to crack more easily than randomly oriented material because the forming of symmetrical and unsymmetrical shapes out of preferentially oriented metals and alloys increases the probability of rupture in regions of high stress, owing to differential ductility.¹ In the electrical industry, on the other hand, preferentially oriented silicon irons are in demand for transformer application because of the improved magnetic permeabilities in the rolling direction.² This phenomenon of preferred orientation in soft magnetic materials has been responsible for the tremendous improvement in transformer design and construction in recent years.

Directional properties in metals have received a great deal of attention in the metallurgical literature,³⁻⁹ in which much of the information reported about orientation has been obtained by conventional methods, mechanical properties and X-rays. A wealth of data has been obtained and often at a great expenditure of time. The

recent introduction of the magnetic torque measurements on ferromagnetic materials provides a very simple and rapid method of evaluating orientation. The judicious use of the method can supply important information, but it should be borne in mind that such studies must be supplemented by X-rays, optical methods,¹⁰ and etch and pressure figures¹¹ to get a rational understanding of the orientation phenomena.

No claims are made that the magnetic torque of evaluating orientation will reveal the behavior of the metal in deep drawing. For this purpose the accepted tests for deep-drawing quality must be used. For a good drawing stock, which must have low impurities, desirable grain size, ductility, strength, hardness, good surface, random orientation, and good recrystallization behavior, it cannot be expected that any simple test will be satisfactory for appraising all the factors. The only factor on which the magnetic method can be used is orientation, which is, of course, of considerable importance. When directionality can cause a 10 to 15 per cent change in tensile strength and a 100 to 300 per cent change in tear length,¹² it goes without saying that a reliable as well as rapid method for detecting these changes would be desirable.

There are certain inherent advantages in testing orientation by the torque method: The method is rapid with the proper type of equipment; no elaborate preparation of specimens is required—it is only necessary to punch or machine a 1-in. disk of the sheet material and insert it into the testing device.

Manuscript received at the office of the Institute May 5, 1943. Issued as T.P. 1635 in METALS TECHNOLOGY, September 1943.

* Research Engineer, Research Laboratories, Westinghouse Electric and Manufacturing Co., East Pittsburgh, Pa.

¹ References are at the end of the paper.

The method will not contribute much to the solution of deformation processes and textures or even recrystallization textures but it is a convenient tool for following

If, however, a mechanical torque is applied to the disk to prevent its rotation, and if the magnetic torque is plotted for various angular positions, the angle be-

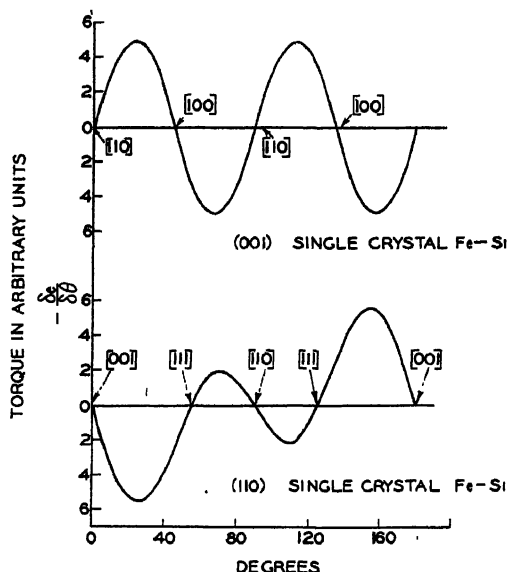


FIG. 1.—MAGNETIC TORQUE CURVES OBTAINED ON INDICATED PLANES IN IRON-SILICON ALLOYS.

changes in orientation due to rolling and heat-treating.

MAGNETIC TORQUE MEASUREMENTS AS AN INDEX OF ORIENTATION

It is fairly well known that single crystals of ferromagnetic materials have directions of easy magnetization as well as directions of difficult magnetization¹³⁻²⁰. In a polycrystalline material it is possible—by choice of rolling and annealing conditions—to get individual crystals to align themselves in such manner as to obtain preferred orientations, in which case it is also possible to have easy and difficult directions of magnetization.²¹⁻²⁴ If a disk of a single crystal or an oriented polycrystalline material is mounted in a strong magnetic field, the field will tend to rotate the disk so as to bring one of the easy directions of magnetization into the direction of the field (see Appendix).

tween the field and the direction of magnetization, the shape of the curve obtained will depend upon the kind of orientation present in the disks.* If random orientation exists in a polycrystalline metal there will be no variation; if the orientation of a disk is well developed the type of curve may approach that of a single crystal. This is shown in Fig. 1.

Experimentally there are several ways of determining these torque curves. A torsion instrument¹³ can be used in which the restoring torque is obtained by twisting the wire supporting the disk and acting as its axis. Another method is that of using an analytical balance with the disk mounted at the center of the balance bar, the axis of the disk passing along the knife edge.²⁵ The amount of weights required to bring

* No attempt will be made here to discuss the curves in terms of anisotropy constants. For discussion see Tarasov and Bitter.²⁵

the balance to equilibrium is a measure of the restoring torque. Still another method is that developed by Dr. S. Siegel, of the Westinghouse Research Laboratories, in which a change in flux in a disk rotating in a magnetic field activates a fluxmeter, which operates an automatic recording device, thereby drawing the torque curve.

The maximum amplitude of the torque curve is then a function of the degree of preferred orientation (see Appendix). If the amplitude is measured in some arbitrary units and divided by the thickness of the material, an index of the orientation can be obtained. While the torque method does not offer any solution as to the nature of the orientation present, in terms of planes and directions, it does afford a very rapid way of determining the degree of orientation of the predominant crystallographic structure once the basic orientation has been established.

SCOPE OF PRESENT INVESTIGATION

While a logical sequence of exposition of orientation phenomenon would consist of hot-rolling, cold-rolling, and recrystallization orientations, it was found advisable to treat the development of cold-rolling and recrystallization orientations before the hot-rolling orientation, because the torque studies were very informative about the first two but not about the latter.

The paper reports and discusses the phenomenon of orientation in low-carbon steel under the following sections:

1. *Cold-rolling Orientation*.—Changes in orientation were observed on the steel that had received two preliminary treatments (to study their effect) before the material was cold-rolled.

a. A portion of the deep-drawing stock, which had been received in a cold-finished condition, was recrystallized for 10 hr. at 700°C. before cold-rolling in order to remove all evidence of cold-work.

b. Another portion of the stock was

heated to 980° and 1000°C. above the critical temperature, and was furnace-cooled through the transformation to remove previous orientations before it was cold-rolled.

c. Some as-received material also was cold-rolled without any treatment whatever.

2. *Recrystallization Orientation*.—The development of the recrystallized orientation by annealing the cold-rolled material mentioned in section 1 was studied after annealing for various times at different temperatures.

a. The cold-worked material that had received a preliminary anneal at 700°C., and which subsequently was cold-rolled various amounts, was recrystallized at 600° and 850°C. Samples were furnace-cooled at approximately 5° per minute.

b. The cold-worked material that first had been heated above the A_3 also was cold-rolled and then recrystallized at 600° and 850°C.

c. The as-received material that had been only cold-rolled was recrystallized at 600°C.

3. *Destruction of Orientation by Cooling from above the Critical*.

4. *Hot-rolling Orientation*.

5. *Appendix: Theory of Method Used for Measurement of Magnetic Torque*.

GENERAL PROCEDURE OF ROLLING, HEATING AND ANNEALING

Cold-rolling was carried out on a four-high mill, using working rolls of 2-in. diameter. It was done carefully by using light reductions—about 5 per cent per pass—to prevent overheating.

For hot-rolling, the material was reduced on a two-high mill with rolls of 5-in. diameter.

Annealing, for heating through the critical range and for recrystallization, was carried out in a dry hydrogen atmosphere with a minus 60 to minus 70°C. dew point, in which state the gas may be considered a

neutral atmosphere. The bright surfaces caused by the anneal made ideal surfaces for rolling and punching dies for torque testing.

For hot-rolling the strips were heated in an electric air-muffle furnace.

Cold-rolling Orientation

Material Recrystallized at 700°C. before Cold-rolling.—The material used for this test was a cold-finished deep-drawing steel 0.061 in. thick, of the following composition: Carbon, 0.05 per cent; manganese, 0.35; phosphorus, 0.012; sulphur, 0.031; silicon, 0.01.

Prior to rolling, this strip was recrystallized 10 hr. at 700°C. It was then reduced various amounts on the four-high mill, after which 1-in. disks were punched for magnetic testing.

In Fig. 2 are the torque curves observed in this cold-rolled strip. Type I was obtained for reduction up to about 30 per cent and type II above 50 per cent. In the region from 30 to 50 per cent, type II is superimposed on type I, giving rather complex torque curves.

Curves of type I,* probably mixtures of the recrystallization orientation and the cold-rolling orientation (type II), do not show any variation in torque amplitude with increasing cold-work. In the region 30 to 50 per cent reduction, the curves are not amenable to study because of their complexity. Curves of type II, however, can be analyzed because they show a variation of amplitude with cold-working.

* The origin of this type of torque curve is somewhat obscure but it may be explained as a combination of the {110} and {001} planes because if single-crystal planes of 3.25 per cent silicon iron (110) and {001} are used for torque curves and combined in different amounts, curves similar to that of type I are obtained. If the recrystallization texture, resulting from heating the cold finished strip, is assumed to be essentially that of {110} planes in the rolling plane or if the hot-rolling orientation is of the same kind, and if the cold-rolling orientation is largely of {001} planes, a combination of the two can lead to a torque curve of type I.

In analyzing the data, a convenient procedure is to plot the degree of orientation $\frac{a}{t}$ against the $\log_{10} \frac{t}{t_0}$ where t is the final

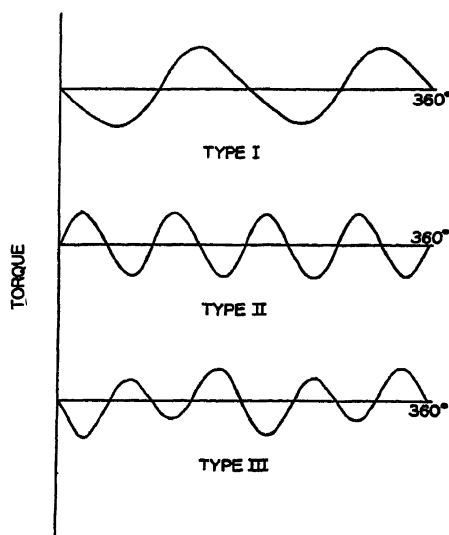


FIG. 2.—TYPICAL MAGNETIC TORQUE DIAGRAMS OBTAINED ON ROLLING AND ANNEALING LOW-CARBON STEEL.

thickness, t , the initial thickness, and a the maximum amplitude of the torque curve (Fig. 3). The data plot as straight lines and the value of such plots will become even more apparent in the discussion of the recrystallization orientation.

Orientation Developed in Materials Furnace-cooled from 980° and 1000°C. before Cold-rolling.—The low-carbon steel used was supposed to be a hot-rolled product finished by cold-rolling. It was decided that heating this material above the critical temperature might remove evidences of any hot-work and cold-work.

A sample of the steel was heated to 980°C. in dry hydrogen and cooled in the furnace. The amplitude of the torque curves was very small, and for practical purposes it could be considered randomly oriented. After this treatment the strip was cold-rolled, punched, and tested. The data are reported in Fig. 3.

The experiment was repeated by heating some other material to 1000°C., rolling, punching, and testing. These data are also plotted in Fig. 3. While the curves are

it is probable that the (100) planes become more parallel to the plane of the sheet and that the perfection in parallelism continues with increasing reductions and is

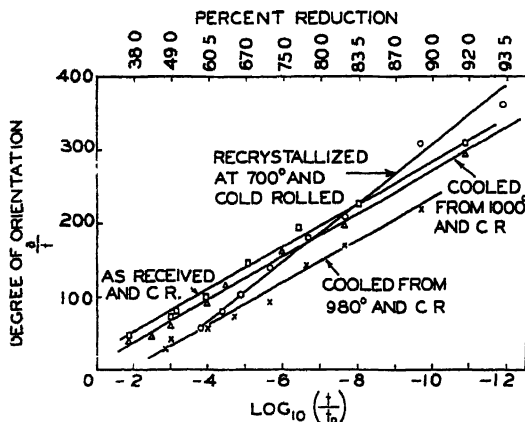


FIG. 3.—CHANGE IN COLD-ROLLED ORIENTATION WITH REDUCTION.

similar, they do not coincide; the reason for this is unknown.

Orientation Developed in Cold-rolling As-received Material.—The low-carbon steel in the as-received condition has a magnetic torque curve of type I, Fig. 2, and remains in the initial as-received orientation up to about 30 per cent reduction. Beyond 30 per cent, the cold-rolled orientation appears (type II, Fig. 2) and the amount of the cold-rolling orientation increases with increasing cold-work (Fig. 3).

Orientation Developed in Low-carbon Steel by Cold-rolling

Numerous investigations²⁸⁻³³ have been carried out on cold-rolled iron and steel and there is satisfactory agreement that the texture is chiefly one in which the [110] directions of the grains lie along the rolling direction and that the (100) planes lie in the plane of the rolled sheet. Deviations from the ideal positions occur, of course, both as to directions about the rolling direction as an axis and of the planes with respect to the plane of the sheet. With severe cold-work, above 50 per cent,

also undoubtedly favored by the thinning of the sheet. Simultaneously the deviation of the [110] from the direction of rolling also decreases with cold-work. This would explain the increase in the degree of orientation with increasing deformation, as in Fig. 3. These observations are in accord with Post³⁴ and McLachlan and Davey.³⁵

A single crystal of 3.25 per cent silicon iron* of the (001) plane gives identical torque curves (see Fig. 1) with those obtained for low-carbon steel by severe working.

Recrystallization Orientation

Orientation of Material Annealed and Cold-rolled, then Reannealed at 600° and 850°C.—A sample of the cold-finished, low-carbon, deep-drawing steel was annealed 10 hr. at 700°C. in dry hydrogen to remove all traces of the finishing rolling. Cold-rolling was carried out from 0.061 to 0.003 in. in steps of about 5 per cent reduction. After the rolling and punching of two similar sets

* Single crystals of iron large enough for torque testing are difficult to make because of the transformation. It is comparatively easy to make large crystals of silicon iron.

of the disks, one set was annealed 25 hr. at 600° and the other 25 hr. at 850°C., after which the disks were tested.

The degree of orientation as a function of

the 850°C. anneal also are shown in Fig. 6. At this temperature the degree of preferred orientation is increased by continued annealing and probably will continue to

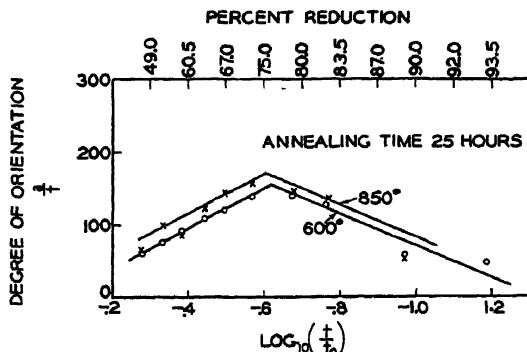


FIG. 4.—CHANGE IN ORIENTATION OF COLD-WORKED MATERIAL ON RECRYSTALLIZATION.

the initial and final thickness is shown for both temperatures in Fig. 4. The diagram indicates that at a certain deformation a maximum in the degree of orientation is reached. This critical deformation is in the range of cold-working specified in claims of cited patents.²

Fig. 4 also indicates that higher temperatures, as long as they are below the A_3 , are more favorable to the enhancement of preferred orientation than are low temperatures.

Deformations up to 45 per cent gave complex torque curves on recrystallization and therefore were not used.

Orientation of Material Furnace-cooled from 1000°C., Cold-rolled, Then Reannealed at 600° and 850°C.—After cold-rolling, one set of the material was recrystallized for various periods (1 hr., 25 hr. and 50 hr.) at 600° and another set (1 hr., 10 hr., 25 hr. and 50 hr.) at 850°C. The change in degree of orientation with reduction on annealing at 600°C. after cold-work is shown in Fig. 5, which shows that prolonged annealing at this temperature does not result in any change in the orientation; i.e., there is neither an increase nor a decrease in the amount of preferred orientation. Curves for

improve with time as long as there is grain growth (coalescence).

Orientation in As-received Material Cold-rolled and Then Annealed at 600°C.—This material had been cold-rolled various amounts after being received and was then annealed 11 hr. at 600°C. to recrystallize it. The maximum in the degree of orientation appears to be about the same as for material that had been recrystallized before the cold-working. The curve obtained on recrystallization is similar to the 600°C. curve of Fig. 4.

Orientation in Recrystallized Low-carbon Steel

The form of the torque curves obtained in the recrystallized material are of two types. Up to about 30 per cent reduction the form of the torque curves is of type I (Fig. 2), which has been considered as a mixture of the hot-rolled and cold-rolled orientations. From 30 per cent reduction to about 50 per cent the orientation is somewhat complicated by the appearance of the recrystallized orientation in the material. Beyond 50 per cent reduction the form of the torque curve is of type III (Fig. 2), corresponding to an orientation having a

(110) plane in the rolling plane and a [001] direction parallel to the direction of rolling; i.e., the same type of torque curve obtained

In another series of tests the following was observed on as-received material that had been furnace-cooled from 1000°C.

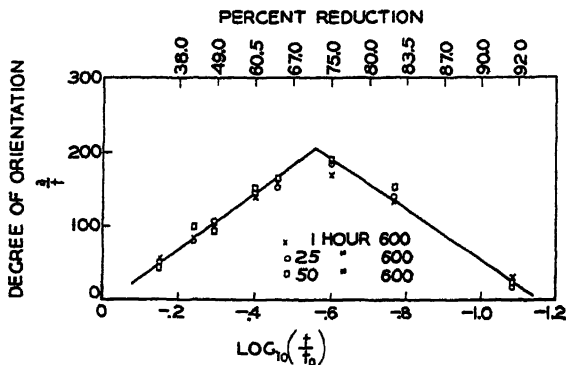


FIG. 5.—CHANGE IN ORIENTATION OF COLD-WORKED MATERIAL ON RECRYSTALLIZATION AT 600°C

for a (110) single-crystal disk as shown in Fig. 1.

Destruction of Orientation by Cooling from above the Critical

It would seem, since transformations proceed by well-defined crystallographic mechanisms, that such lattice changes might generate new preferred orientations. However, since distortion accompanies these allotropic changes, the nature of orientations formed may be so numerous that all traces of the primary preferred orientation would probably be erased. This seems to be true, but Tammann¹¹ found, in electrolytic iron, that a preferred orientation is partly retained on normalizing. To get further data on this point samples of steel were used that had been cold-rolled various amounts, annealed at 600° to recrystallize them, and then heated to 950° and furnace-cooled. It was found that a trace of some complex orientation persisted in samples that had been originally cold-rolled less than 15 per cent but for samples that had been cold-rolled more than that amount and annealed before cooling through the critical, all traces of the recrystallization orientation disappeared.

Three different treatments were given this furnace-cooled material:

1. A series of samples was reduced to various gauges from 0.060 (0 per cent reduction) to 0.005 (92 per cent) by cold-rolling.
2. A second series was similarly prepared and annealed 50 hr. at 600°C.
3. A third series was similarly prepared and annealed 50 hr. at 850°C.

All three lots of material were then heated above the critical (1000°C.) and cooled in the furnace. In all cases where the strip had been cold-worked 40 per cent or more, with or without recrystallization before heating above and cooling through the critical, complete removal of orientation was obtained.

It would seem then that in series 1, a preliminary cold-work of 40 per cent or more is a prerequisite for obtaining complete random orientation in low-carbon deep-drawing steel on cooling the material through the transformation. In series 2 and 3, in which the material was recrystallized after cold-working, random orientation upon transformation results only in a previously well-developed recrystallization orientation, which occurs when a material is cold-worked about 40 per cent or more

by rolling followed by annealing. In the material cold-rolled less than 40 per cent as well as in the material recrystallized at 600° and 850° after deformation up to 40

passes are too severe orientation can be retained even though the strip is above A_1 . Hot-rolling near the A_1 always produces preferred orientation.

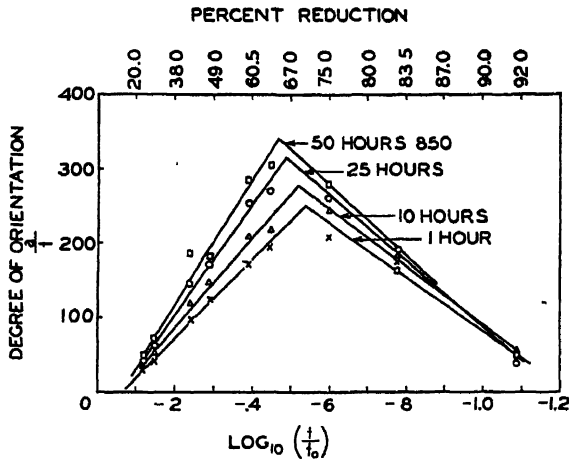


FIG. 6.—CHANGE IN ORIENTATION OF COLD-WORKED MATERIAL ON RECRYSTALLIZATION AT 850°C.

per cent, some complex residual orientation remained after cooling through the critical range. The amplitude of these residual complex curves was quite small and for practical purposes the orientation can be considered virtually eliminated.

It was also found, as might be expected, that pure iron (0.006 per cent C) behaves similarly to the low-carbon steel.

Hot-rolling Orientation

Very little is known about hot-rolling orientation as compared with our knowledge of cold-rolling orientation, because hot-rolling orientations are not so pronounced and apparently do not lead to deep-drawing difficulties as does cold-processed strip. Hot-rolling is considered here as rolling at or above red heat, say 600°C.

Goss²² says that low-carbon steel strip may or may not retain an oriented structure on hot-rolling below the A_3 depending on the amount of rolling. Rolling above the A_3 results in random orientation because of the transformation, but if the finishing

For hot-rolling experiments some hot-rolled steel of heavier gauge (0.133 in.) of a composition similar to the first material, was obtained.

In these experiments, the strip was heated to the desired temperature in an air muffle furnace and immediately given one pass on a 5-in. diameter mill. After this single pass, the strip was cooled, samples cut and the strip reheated and given an additional pass, and so on. This rolling was done in the "alternate" sense; the first time one end was introduced into the rolls, identified by pointing the strip, and on the next reduction the opposite end entered the rolls.

The torque curves obtained by hot-rolling at 950°C. and cooling through the transformation are extremely complicated and a different orientation appears at each reduction. Since each torque curve is different from each succeeding one, it indicates that different planes become parallel to the rolling plane after each reduction. Since the torque curves are not similar to some of the single-crystal torque curves, it

is impossible to say what the orientation is in kind and degree.

Material rolled identically as above but in the "single" sense—i.e., the same end of the strip always entered the rolls—gave virtually the same complex torque curves.

Torque curves were also obtained on hot-rolling the same steel at 800°C. It was found that there exists a degree of similarity in the curves but not sufficient to warrant any definite conclusion as to the orientation. About all that can be said about the hot-rolling orientation formed at 800° is that it is less complicated than the one formed at 950°C.

Although the torque method of study of orientation in hot-rolling is not very informative, it can be said that hot-rolling does produce preferred orientations but these are rather complex, probably because numerous planes can orient readily in the rolling plane, particularly $\{211\}$ and $\{100\}$, and to a lesser degree $\{110\}$, $\{111\}$, $\{123\}$, and $\{310\}$.

SUMMARY

The development of orientation in cold-rolling of low-carbon deep-drawing steel has been followed by the magnetic torque method. A linear relationship was found between the degree of orientation and the logarithm of the ratio of the final to the initial thickness. When the steel strip was cold-rolled in the as-received, recrystallized, and normalized (furnace-cooled through the transformation) states, all materials showed this linear relationship on cold-working.

The change in degree of orientation on recrystallization of the cold-worked material was also studied. A maximum in the degree of preferred orientation is found in the region 65 to 75 per cent reduction, when the cold-rolled strip was subsequently recrystallized at 600° and 850°C. Prolonged annealing (up to 50 hr.) at 600°C. does not result in any improvement

but prolonged annealing at 850°C. increases the degree of orientation.

That preferred orientation, either in the cold-rolled or the recrystallized material, can be destroyed by heating the materials above the critical range is known, but complete random orientation does not occur unless the material has been cold-worked a minimum of 40 per cent or has a recrystallized preferred orientation.

The magnetic torque method does not add any new knowledge on the nature of hot-rolling orientations other than to indicate that complex orientations are produced.

APPENDIX

The work done in magnetizing a cubic crystal to saturation along a direction determined by the direction cosines α_1 , α_2 , α_3 , with respect to cubic axes is

$$E = K_0 + K_1(\alpha_1^2\alpha_2^2 + \alpha_1^2\alpha_3^2 + \alpha_2^2\alpha_3^2) + K_2(\alpha_1^2\alpha_2^2\alpha_3^2) + \dots [1]$$

where K_1 and K_2 are anisotropy coefficients and the Eq. 1 defines them.

If a thin single crystal, or an oriented polycrystalline disk, is placed in a strong magnet field, a torque about the axis perpendicular to the plane of the disk acts upon it. The torque arises because the magnetization vector J is not parallel to the applied field H . A torque of magnitude $H \times J = HJ_n$ acts on the disk, where J_n is the component of magnetization normal to H .

If the disk is uniformly magnetized to its saturation intensity J_s , the torque acting on the disk due to its anisotropy is

$$T = - \frac{\delta E}{\delta \theta}$$

or, taking the derivative of Eq. 1,

$$T = -2K_1 \sum_{1,2} (A_n \sin 2n\theta + B_n \cos 2n\theta) + 2K_2 \sum_{1,2,3} (C_n \sin 2n\theta + D_n \cos 2n\theta)$$

where A_n , B_n , C_n , D_n , are functions of the orientation angles.

For a simple case, for (001) plane, the torque on a crystal disk about the (001) axis normal to the disk is

$$T = -\frac{K_1}{2} \sin 4\theta$$

where θ is the angle between [010] direction and the magnetization vector J .

For a (110) plane the torque becomes

$$T = -\frac{K_1}{8} (2 \sin 2\theta + 3 \sin 4\theta) - \frac{K_2}{64} (\sin 2\theta + 4 \sin 4\theta - 3 \sin 6\theta)$$

where θ is measured from the [001] direction in the disk to J .

In our investigation a specimen of 1 in. diameter was mounted on a shaft and driven at rate of 1 r.p.m. Two coils of about 2000 turns each, as half shells, cover the disks but do not turn with the specimen. This assembly is put between the poles of an electromagnet operated by storage batteries. All determinations reported here were taken at 2250 oersteds (10 amp. in our coil).

In measuring J_n the plane of the coils is initially fixed parallel to H so that none of the flux due to H links the coils. The coils are a part of the fluxmeter circuit. The variations in J_n with the angular position of the disk in the magnet field are measured by the flux-meter circuit.

A permanent record is obtained by driving the disk in synchronism with a paper-covered drum, so that the angular position on the drum is related to that of the disk. A photocell arrangement on a movable carriage with a pen attached follows the reflections from the mirror of the flux-meter, so that a torque curve is obtained.

REFERENCES

1. J. D. Jevons: *Met. Ind.* (London) (1939) 54, 35.
2. U. S. Patents 2287466; 1965559, and 2158065.
3. W. Boos and E. Schmid: *Ztsch. Tech. Phys.* (1931) 12, 71.

4. F. Wever: *Trans. A.I.M.E.* (1931) 93, 51.
5. K. Kaiser: *Ztsch. Metallkunde* (1927) 19, 435.
6. W. H. Bassett and T. C. Bradley: *Trans. A.I.M.E.* (1933) 104, 181.
7. J. T. Norton: Amer. Soc. Test. Mat. Symposium on Radiography and X-rays (1936) 318.
8. N. P. Goss: *Trans. Amer. Soc. Metals* (1941) 29, 20.
9. E. W. Palmer and C. S. Smith: *Trans. A.I.M.E.* (1942) 147, 164.
10. C. S. Barrett and L. H. Levenson: *Trans. A.I.M.E.* (1940) 137, 76.
11. G. Tammann: *Jnl. Inst. Metals* (1930) 64, 29.
12. J. D. Jevons: *Met. Ind.* (London) (1936) 48(20) 563; (22) 607, 619.
13. H. J. Williams and R. M. Bozorth: *Phys. Rev.* (1939) [ii] 55(7), 673.
14. H. Schlechtweg: *Ann. Physik* (1936) [5] 27(7), 573.
15. R. M. Bozorth: *Phys. Rev.* (1936) [iii] 50(11), 1076.
16. J. D. Kleis: *Phys. Rev.* (1936) [iii] 50(12), 1178.
17. R. M. Bozorth and L. W. McKeehan: *Phys. Rev.* (1937) [ii] 51(3), 216.
18. R. G. Puty: *Phys. Rev.* (1936) [iii] 50(12), 1173.
19. L. W. McKeehan: *Phys. Rev.* (1937) [ii] 51(2), 136.
20. J. H. Van Vleck: *Phys. Rev.* (1937) [ii] 52(2), 1178.
21. L. P. Tarasov: *Trans. A.I.M.E.* (1939) 135, 353.
22. L. P. Tarasov: *Phys. Rev.* (1939) 56, 1231.
23. N. P. Goss: *Trans. Amer. Soc. Metals* (1935) 23, 511.
24. N. S. Akulov and N. Bruchatov: *Ann. Physik* (1932) 15.
25. L. P. Tarasov and F. Bitter: *Phys. Rev.* (1937) 52, 353.
26. Z. Jeffries: *Trans. A.I.M.E.* (1924) 70, 303.
27. S. T. Konobejewski: *Ztsch. Phys.* (1926) 39, 415.
28. F. Wever: *Mitt. K. W. Inst. Eisenforsch.* (1923) 5, 69.
29. F. Wever: *Ztsch. Physik* (1924) 28, 69.
30. G. Kurdsumow and G. Sachs: *Ztsch. Phys.* (1930) 62, 592.
31. M. Gensamer and R. F. Mehl: *Trans. A.I.M.E.* (1936) 120, 277.
32. N. P. Goss: *Trans. Amer. Soc. Metals* (1936) 24, 967.
33. H. V. Gough: New Int. Assn. Test. Mat., First Communications Group A (1930) 133.
34. C. B. Post: *Trans. Amer. Soc. Metals* (1936) 24, 679.
35. D. L. McLachlon and W. P. Davey: *Trans. Amer. Soc. Metals* (1937) 25, 1084.

DISCUSSION

(Anson Hayes presiding)

L. P. TARASOV,* Worcester, Mass.—The results described in this paper are very similar to those obtained by the writer²¹ several

* Research Laboratories, Norton Company.

years ago when investigating the orientation behavior of a low-carbon silicon steel containing 3 per cent Si. Unfortunately, even though the experimental methods in the two cases were basically the same, different methods of expressing and plotting the data have obscured this similarity.

Mr. Stanley has confined himself to the maximum amplitude of the torque curve while the writer dealt with this curve in terms of amplitudes of the two principal sinusoidal components. If T is the torque and θ the angle measured from the rolling direction, the torque curve is given accurately enough for orientation work by $T = A_1 \sin 2\theta + A_2 \sin 4\theta$. Changes in the maximum amplitude of the torque curve and in the magnitude of A_2 , disregarding its sign, correspond very closely to each other when A_2 is large compared with A_1 or when these two coefficients remain in the same ratio. In orientation studies like the present one, however, A_1 and A_2 vary independently of each other and the two may be of nearly the same size, with the result that the maximum amplitude and A_2 do not change in the same manner.

An advantage of the maximum amplitude is that it can be obtained easily by direct measurement whereas the coefficients A_1 and A_2 require a little calculation after measurements are made at certain selected angles. In routine work on specimens having a well-defined torque curve, the maximum amplitude is as satisfactory a criterion as any other. However, when the torque curves change in a complicated manner, as the author found for his hot-rolled specimens, there is a distinct advantage to expressing the results in terms of A_1 and A_2 . Then a seemingly discontinuous change in the type of the torque curve will often be seen to be merely the result of the rapid passage of one of the coefficients through zero. A further advantage of these coefficients is that all the results of a given experiment can be plotted on a single graph, regardless of how the type of the torque curve happens to change.

In calling the maximum amplitude the degree of orientation, there is a danger that the latter term may be misinterpreted by the average reader not familiar with magnetic torque studies. This term is really an abbreviation for "apparent degree of orientation as detected by the magnetic torque method." A

low torque curve for polycrystalline material may mean either that the texture is very random, or that the texture is predominantly one with an orientation giving a low torque, or that two or more textures are present, which individually would give high torque curves but which are so oriented that their torques are oppositely directed and hence cancel out. To avoid the implication that the amplitude of the torque is related only to the degree of perfection of the texture, it might be preferable to replace "degree of orientation" by a more noncommittal term, such as "orientation factor."

In order to compare the writer's data on silicon steel with those presented in this paper on deep-drawing steel, it is best to transform the A_1 and A_2 values for the former into maximum amplitudes. When this is done, it is found that cold-rolled silicon steel follows a linear relationship, similar to those shown in Fig. 3. Inasmuch as his data are expressed in arbitrary units, it is not possible to decide which steel has the greater rate of increase in orientation factor as the percentage reduction increases. It is true that the orientation factor starts out higher for silicon steel, since in this case the straight line when extended slightly crosses the vertical axis before reaching the horizontal one, while the opposite is true for the deep-drawing steel. Whether the orientation factor for the silicon steel continues to be higher than the other at greater reductions can be determined only if Mr. Stanley recalculates his data from arbitrary units of torque into absolute ones.

It would be of considerable value to have such a comparison available because the two steels in question differ essentially only in their silicon content. Were the data expressed in absolute units, or, better yet, in terms of the anisotropy constant K_1 , it would be possible to see just how the addition of 3 per cent Si affects both the cold-rolling and the recrystallization textures. If other steels are later studied in this manner, further comparisons would be feasible.

When the data for recrystallized silicon steel are recalculated and plotted on the same basis as Fig. 4, exactly the same sort of a curve results. The intersection of the two straight-line portions of the curve for silicon steel recrystallized at 850°C. comes between 65 and

70 per cent reduction, just as for the deep-drawing steel. However, a higher minimum recrystallizing temperature is required for

the resulting texture is fairly stable; and to diminish the effect of time at the recrystallizing temperature.

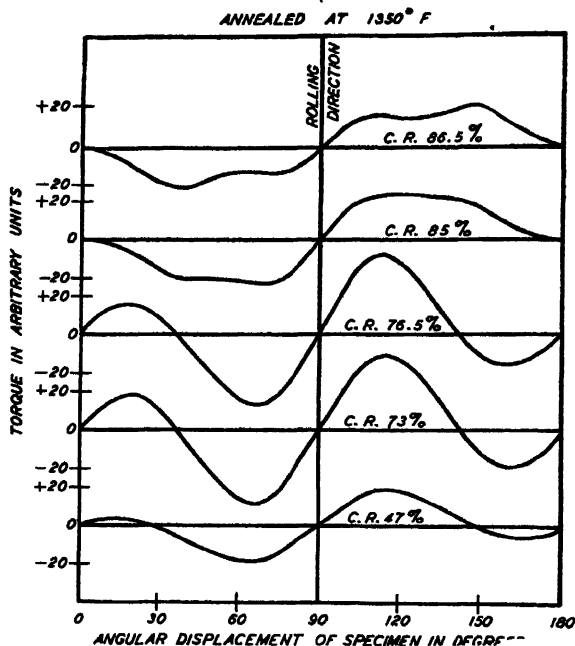


FIG. 7.—INFLUENCE OF COLD REDUCTION ON DIRECTIONALITY OF STRIP STEEL ANNEALED AT 1350°F.

silicon steel in order to obtain substantially the same torque curves that are obtained at higher temperatures. For deep-drawing steel, 600°C. is clearly high enough, while for the silicon steel it was necessary to go to at least 700°C., and even higher for reductions that were less than 80 per cent. No significant change in the torque curves of silicon steel was observed when the time was changed from 1 to 24 hr., provided the temperature was not too close to the lower limit for recrystallization. This contrasts with the behavior of the deep-drawing steel when recrystallized at 850°C., for its orientation factor increased with increasing time.

To summarize, the effects of adding 3 per cent Si on the recrystallization texture are to leave unchanged the percentage reduction at which the highest recrystallized orientation factor is obtained; to raise considerably the recrystallization temperature above which

G. H. ENZIAN,* Pittsburgh, Pa.—The subject studied by the author is an important one and one which, in all probability, will assume increasing importance in future manufacture of sheet and strip steel for deep drawing and pressing. Most of our present knowledge of preferred orientation and directional properties has been gained from slow, tedious, and rather complicated X-ray studies, which are not at present adaptable to production and control work. Mr. Stanley has presented a readily understandable approach to a study of directionality in strip steel and has described a test method that could easily be incorporated into metallurgical control laboratories as well as being applicable to research on the subject.

The paper is of especial interest to us because we have been studying the subject, also using magnetic torque tests, over a period covering

* Research and Development Division, Jones and Laughlin Steel Corporation.

the past three or four years. Information accumulated in this time in general substantiates the results published in this paper. As

orientation, as expressed by Mr. Stanley, a maximum was probably attained between 76.5 and 85 per cent reduction.

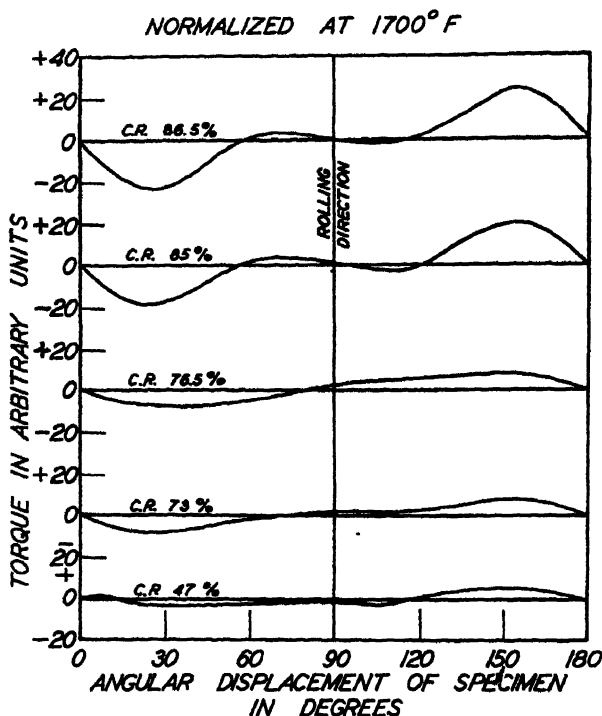


FIG. 8.—INFLUENCE OF COLD REDUCTION ON DIRECTIONALITY OF STRIP STEEL NORMALIZED AT 1700°F.

manufacturers of strip steel, we have been primarily interested in practical applications for the information furnished by studies of magnetic anisotropy, and have used the test to advantage in several instances.

Our studies have shown that the amount of cold reduction is extremely important in the consideration of factors influencing directional properties in strip steel. For example, samples of low-carbon rimmed steel were obtained after cold-reducing various amounts from 47 to 86.5 per cent. Specimens from each cold reduction were annealed at 1350°F. and the magnetic torque curves resulting from this treatment are shown in Fig. 7. A rather complex type curve, possibly the result of superimposition of the rolling and recrystallization textures, was formed at the higher cold reductions, but in terms of the degree of

Similar cold-reduced samples were normalized by air cooling after heating to 1700°F., and it was found that the resulting torque curves were quite different from those obtained on the annealed material. It is generally assumed that normalizing removes all effect of prior cold-work, but, as can be seen in Fig. 8, this was not found to be true when severe cold reductions were used. Material cold-reduced 47 per cent, 73 per cent, and 76.5 per cent, normalized at 1700°F., evidently has such a low degree of preferred orientation that the magnetic torque curves obtained were erratic and quite complex. At 85 and 86.5 per cent reduction, however, magnetic torque curves obtained after normalizing had a characteristic sinusoidal shape and appreciable amplitude; attempts to lower the directionality of these samples by normalizing

at temperatures up to 2015°F. were not successful.

It is interesting to note that in terms of the maximum amplitude of the torque curve, the

tion in box-annealing cycles can do little to change conditions. Normalizing cold reduced material is expensive and is detrimental to surface quality, and therefore this practice is

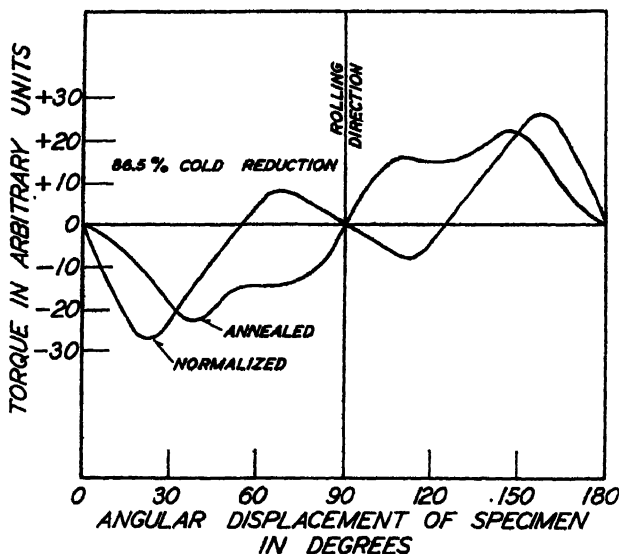


Fig. 9.—COMPARISON OF DIRECTIONALITY OF ANNEALED AND NORMALIZED STRIP STEEL COLD-REDUCED 86.5 PER CENT.

material cold-reduced 86.5 per cent apparently had slightly more pronounced preferred orientation after normalizing than after annealing; a comparison of the torque curves for each heat-treatment is shown in Fig. 9.

Additional studies on heat-treatment of cold-reduced strip steel showed that the degree of orientation remaining after box annealing is not subject to a great deal of control by variation of the annealing temperature. Samples with varying degrees of cold reduction were tested after annealing at temperatures ranging from 750° to 1550°F. It was found that annealing temperatures higher than that necessary for recrystallization had no appreciable effect on the orientation established at the minimum recrystallization temperature. For all degrees of cold reduction studied, the magnetic torque curves obtained after annealing at 1550°F. were essentially the same as those obtained at 1050°F.

It is evident from these results that the directional properties of cold-reduced strip steel are fixed after cold-rolling and that varia-

not usually a practical means of producing low directionality. Since variations in annealing cycles can do little to change the conditions in so far as directionality is concerned, in order to control the orientation of the finished product necessary corrective measures must be taken at some earlier step in the processing of the steel. It is probable that in many cases changing the amount of cold reduction will give a satisfactory product, but in order to predict in what direction a change should be made, the effect of cold reduction on the orientation of the final product must be fully understood.

Since changing the amount of cold reduction necessarily changes the hot band gauge for any particular application, the effect of variations in hot-rolling practice should also be known. It has been shown in Fig. 1 that the degree of orientation of cold-reduced steel is influenced by the extent of preferred orientations before cold-rolling. Hot rolling produces preferred orientation, and it is probable that variations in hot-rolling practice will result

in variations in the hot-rolled texture. The rate of cooling after hot-rolling may also affect the directionality of the hot-rolled material, and thus influence the orientation of the fin-

and seems to be the result of superimposition of the 45° ear curve and the 90° ear curve.

There are, of course, other instances where magnetic torque testing can be used to prac-

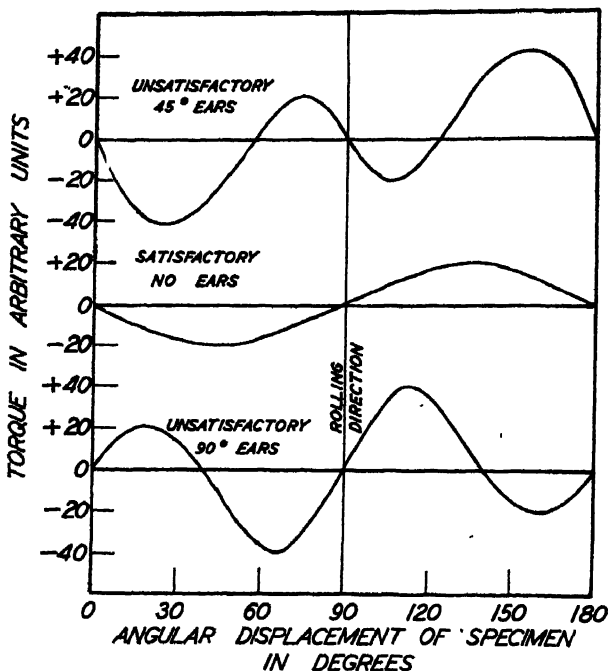


FIG. 10.—RELATIONSHIP BETWEEN MAGNETIC TORQUE CHARACTERISTICS AND "EARING" IN DEEP-DRAWN CUPS.

ished strip. The effect of these and other processing variables are not known and more information would be welcome.

A recent application for the magnetic torque test has been in a study of "earring" in drawing small cups from cold-reduced strip steel. Samples of steel were obtained, which, on cupping, produced ears at 45° to the rolling direction, ears at 90° to the rolling direction, and also material that did not form ears. Typical torque curves for these three types of material are shown in Fig. 10. The upper torque curve and 45° ears were associated with low reductions in cold-rolling; that is, about 30 or 35 per cent. The lower torque curve and the 90° ears were encountered at cold reductions over about 50 or 55 per cent. Satisfactory material, obtained at intermediate cold reductions, generally had torque characteristics shown in the middle curve of Fig. 4

tical advantage. The subject of directional properties is a large one and one that needs considerable study. With the practical approach to a study of directionality offered by the magnetic torque test, it is hoped that the full significance of this fundamental property of sheet and strip steel will be more universally recognized and that further study will be encouraged.

W. M. SAUNDERS, JR.,* Providence, R. I.—This paper should be of great value to the producer of strip steel for deep drawing, and the author is to be congratulated on publicizing the magnetic torque balance, a fairly recent new tool for the metallurgist. He has also furnished quantitative figures for degree of

* With Walter M. Saunders, Analytical and Consulting Chemist.

orientation, which have previously been described in a qualitative way.

About five years ago, using the magnetic torque balance constructed by Dr. L. P. Tarasov in Professor Bitter's laboratory at Massachusetts Institute of Technology, some unpublished research⁸⁷ disclosed that earing of low-carbon steel, a phenomenon due to directional properties, could be predicted by torque measurements on the strip before cupping. Whenever a torque curve like that shown as type II in Fig. 2 was found in a certain strip, ears at 45° to the rolling direction resulted when the strip was cupped. A torque curve like type III existed in all strip that drew with 90° ears. Freedom from ears was always obtained when random orientations from normalizing were indicated by torque measurements, and also with strip showing a curve like type I. Correlation of type of ears, either 45°, 90° or none, with torque curves on many samples from commercial cold-rolled strip, as supplied in the annealed state ready for deep drawing, seldom revealed a curve like type I. For the very few where such a curve was found, no ears formed on cupping, but attempts to duplicate reductions, annealing times, and temperatures, on subsequent heats of steel were unsuccessful in obtaining consistently a curve like type I. Almost invariably commercial cold-rolled strip from several sources of supply showed a recrystallization orientation like type III. Likewise type II, the cold-rolled structure, was never encountered except experimentally.

In view of the large number of samples that showed a recrystallization structure, obtained by cold-rolling in the range of 50 to 80 per cent, and subsequently annealing at 1150° to 1325°F. (621° to 718°C.), it does not appear probable that the type I curve will be present in many commercial steels. It would be surprising, therefore, if other heats of steel than the one Mr. Stanley used should give a torque curve like type I when annealed at 700°C., following commercial practice. In fact, the research referred to definitely established that a torque curve like type II resulted from recrystallizing at low temperatures of around 1000°F. (538°C.) and type III represented

the texture when recrystallizing at 1100°F. (593°C.) when the same annealing time was given. The change from the cold-rolled to recrystallization orientation takes place at a critical time and temperature, which was found to vary with different heats of steel, all cold-rolled commercially with the same cold reductions. Such a phenomenon must account for the extraordinary case where ear-free strip is produced, when annealing time and temperature happened to result in hitting the critical point where the cold-rolled and recrystallization orientations canceled each other in their effect on ear formation.

Normalizing definitely eliminates ears, and it was also found that no ears resulted from strip cold-reduced 50 per cent, normalized, and then cold-reduced 30 per cent more. Such a treatment gave a torque curve like type I, and is confirmed by Mr. Stanley's work.

An interesting corollary of this work is that a simple cupping press may be used instead of the magnetic torque equipment. As previously mentioned, if 45° ears are found on cups, an orientation like type II is indicated, and with 90° ears, type III must be present. With no ears, either type I is present, which is not common in strip produced commercially, or the strip has been normalized.

S. SIEGEL,* East Pittsburgh, Pa.—The author's paper is an interesting application to other problems of a method that has been used principally for studying preferred orientations in materials of interest for magnetic purposes, such as electrical sheet iron.

As he points out, in a case as general as that which is the subject of the paper, little information can be obtained from the use of the magnetic torque method alone. This situation arises from the fact that there are many more unknowns than the number of independent data. In the expression for the torque per unit volume

$$T = -2K_1 \sum_{i,2} (A_n \sin 2n\theta + B_n \cos 2n\theta) + 2K_2 \sum_{i,2,3} (C_n \sin 2n\theta + D_n \cos 2n\theta) \quad [A]$$

there are in all 10 constants, $A_n \dots D_n$. However, the relative magnitudes of K_1 and

⁸⁷ W. M. Saunders, Jr.: Earing of Low-carbon Steel. Doctor's Thesis, M. I. T., 1939.

* Magnetic Department, Westinghouse Electric and Manufacturing Company.

K_2 in iron are such that the effect of K_2 on an experimental torque curve is small, which reduces the number of constants to only four, $A_{1,2}$, $B_{1,2}$. In addition, the symmetry of the rolling process requires that the rolling direction be a direction of symmetry, and that the rolling plane be a plane of symmetry. This requirement removes the possibility of having any appreciable cosine terms if the grain size is small enough so that the disk is a representative sample. Hence any experimental torque curve can yield at most two constants, A_1 and A_2 .

In a polycrystalline sample, with no other knowledge of orientations available, each orientation present really requires three pieces of data to determine it completely; for example, its rolling plane, rolling direction, and the relative population of this orientation type. When many types of orientation may be present in a single sample, the large amount of data required for a complete analysis is apparent. In the X-ray method of determining pole figures, each film gives some information, but many pictures, at various angles to the rolling plane, must be taken to get a complete story. In the magnetic method, the torque curve on a disk from the sheet gives only one "picture," and by the nature of the method it is difficult to prepare samples cut from inclined planes.

There are simple examples, however, in which the torque curve can give quantitative information by itself or in conjunction with other simple measurements. Thus curves of type II do indicate that the principal orientation present is $(100)[\bar{1}\bar{1}0]$ and it is possible to determine the fraction of the material so oriented and the fraction randomly oriented. Similarly, in well-developed recrystallized orientations in Fe-Si sheets, the torque curves indicate that the principal orientation is $(110)[001]$, and when the constants A_1 and A_2 are combined with data for the permeability, at 10 oersteds, in the rolling direction, it is possible to determine the spread of orientation present around the principal $(110)[001]$ orientation. In such cases magnetic measurements alone give fairly complete information on orientations present.

It may be worth while to point out that the torque per unit volume, given by Eq. A, is the asymptotic value attained for a very large

applied field. In finite fields the torque depends on the true field in the specimen, which is the applied field minus the demagnetizing field.

All of the data reported by the author were taken at an applied field of 2250 oersteds. The data are taken on disks that vary in thickness from 0.060 to 0.006 in., over this range of thickness the demagnetizing field varies from 940 to 100, and the true field in the disk from 1300 to 2150. With this variation in true field there would be a variation in torque per unit volume, for disks of identical orientation distribution but varying thickness, of the order of 15 per cent. The curves of Fig. 3, therefore, should have a concave curvature upward, the points for the large thickness being raised by about 15 per cent. While the linearity of these curves should thus not be taken too seriously, the data do, of course, indicate a monotonic rise of orientation with cold-work.

For the same reason the maxima in Figs. 4, 5, and 6 may require a slight shift to the right, by at most a few per cent in reduction of thickness.

J. K. STANLEY (author's reply).—The author appreciates Mr. Tarasov's statement that the use of the maximum amplitude is a convenient measure of torque diagrams showing changes in orientation but that it is not as rigorous an expression of such changes as the more tedious determination of the coefficients A_1 and A_2 . The author's paper was intended primarily to show how information obtained from magnetic torque curves could be used in a simple manner to give useful information about changes going on in steel with various metallurgical treatments. Such information accurately expressed in the equations as mentioned by Mr. Tarasov is harder to interpret especially to the uninitiated so that the full benefit of the torque analysis would not be obtained.

Mr. Tarasov makes a suggestion that perhaps "orientation factor" might be a more noncommittal term to use for "degree of orientation." It appears immaterial whether one talks about "orientation factor" or "degree of orientation" as long as the readers understand that it is an abbreviation, as Mr. Tarasov says, for "apparent degree of orientation as detected by the magnetic torque method."

The data on silicon iron presented by Mr. Tarasov is similar to the experience on silicon iron at Westinghouse. Mr. Tarasov finds no significant change in torque diagrams in his silicon iron by annealing it 1 to 24 hr. Our experience shows that little change can be expected in 3.25 per cent silicon iron even at 100 hr. at 700° and 800° but changes do take place at 900°C and higher, with increasing rapidity the higher the temperature.

Mr. Tarasov discusses silicon steel but apparently he has in mind a commercial magnetic silicon iron, since steel is defined as an alloy of iron, carbon, and manganese. High-grade magnetic materials usually contain extremely small amounts of carbon and manganese compared with the true silicon steels used for engineering purposes.

The discussion offered by Messrs. G. H. Enzian and W. M. Saunders, Jr. is appreciated because of their familiarity with strip steel manufacture.

Mr. Enzian shows that normalizing a cold-reduced low-carbon rimming steel from 925° and also from 1100°C. does not eliminate the preferred orientation. The author, on the basis of his work, would think that normalizing would eliminate the orientation, inasmuch as cold-worked steel, and steel with a good recrystallization texture, when heated to 1000°C. and furnace-cooled does have random orientation. Perhaps the differences between furnace cooling and normalizing are respon-

sible for this discrepancy. W. M. Saunders, Jr. implies just the opposite, by his statements that "normalizing definitely eliminates ears . . ." and "freedom from ears was always obtained when random orientations from normalizing were indicated by torque measurements . . ."

Mr. Enzian says that annealing the cold-rolled strip from the lowest temperature required for recrystallization (565° to 845°C.) showed the magnetic torque curves to be essentially the same. He fails to give the annealing times, which may have something to do with the fact that no differences were noted, which is not in accordance with the author's findings.

A statement is made by Mr. Enzian with respect to possibility that the hot-rolling orientations existing before rolling are important in determining the degree of orientation. This observation is corroborated by the author's observations on silicon irons, where a correlation was found between the hot-rolling orientation and the subsequent recrystallization orientation.

The discussions of Messrs. Enzian and Saunders on the relationship of earing, due to preferred orientation, in deep drawing show how the torque method can be used in practical problems.

The limitations of the torque method as used, discussed by Dr. Siegel, should be borne in mind by those contemplating the use of such instruments.

Recrystallization and Twin Relationships in Silicon Ferrite

By C. G. DUNN,* MEMBER A.I.M.E.

(New York Meeting, February 1944)

MANY investigations have been made concerning the nature of plastic deformation and recrystallization of metals either in the form of polycrystalline materials or in the form of single crystals. However, similar work on strip materials composed of large grains as thick as the strip and having a high degree of preferred crystal orientation has not been carried out extensively. Such materials are ideal not only for studying changes in single crystals under conditions where neighboring grains exert their influences but also for obtaining the complete change in orientation of a grain or group of grains during the course of plastic deformation and subsequent recrystallization.

It is well known that first-order twins in the form of Neumann bands may be produced during the plastic deformation of ferrite crystals, particularly silicon ferrite crystals.¹⁻³ Furthermore, it is believed that high-stress regions exist in the vicinity of these bands^{4a} and it has been said that these banded regions would be active in recrystallization processes.⁵ Evidence to that effect in silicon ferrite had already been presented with photomicrographs showing recrystallization among Neumann bands during the early stages of recrystallization.^{5,6} Similar evidence has been published for nonferrous metals.⁵

Merging of fine parallel deformation bands during annealing to form twin bands

of ordinary appearance in alpha brass has been offered not only as evidence of an active role being played by mechanical twins but also as evidence that such twins existed prior to recrystallization.⁵ Proof that such new structures are actually first-order twins, or even twins at all, must be considered inadequate except for those cases where X-ray or optical data have been obtained to confirm the necessary orientation relationship.^{7,8} A. B. Greninger has obtained excellent illustrations of annealing twins in alpha iron.⁹ Since his material was previously deformed by sharp hammering, a process that generally induces Neumann bands, the existence of twins following annealing might suggest that they grew from mechanical twins. In connection with transformation twins in alpha iron, Greninger reported that grains containing three twin orientations occurred rarely and none occurred with three sets of well-developed bands.⁹

The work at the Pittsfield Works Laboratory on silicon ferrite in the form of large-grained strip steel deformed a small amount and annealed to partially recrystallize the grains indicates that the deformation and recrystallization processes that lead to annealing twins involve more complex processes than the formation of Neumann bands and the growth of such bands. Some groups of annealing twins are obtained which contain not only three well-developed twin structures, but also contain more than one order of twins. It is also shown, in one case, that an interrelated group of twins did not arise within one single parent grain and, furthermore, orientations of grains in the group

Manuscript received at the office of the Institute Nov. 22, 1943. Issued as T.P. 1691 in METALS TECHNOLOGY, February 1944.

* Research Physicist, Pittsfield Works Laboratory, General Electric Co., Pittsfield, Massachusetts.

¹ References are at the end of the paper.

are not consistent with growth of Neumann bands within the original deformed grains.

Although the present work is part of a program aimed at establishing a mechanism of recrystallization in silicon ferrite, it is not possible at this time to do more than speculate on the origin of the new orientations obtained during recrystallization except for the orientations in twin groups that are thought to arise by a secondary nucleation process. It is, therefore, the object of this paper to present some groups of twins that have been obtained during our work on plastic deformation and recrystallization of strip steel and to discuss, on the basis of our present information, the relationship these groups may have with the original material.

PREPARATION OF SPECIMENS AND EXPERIMENTAL PROCEDURE

The material used in the present investigation was produced by the Allegheny-Ludlum Steel Corporation by cold-rolling processes that develop a high degree of preferred crystal orientation in the final annealed silicon-steel strip.¹⁰⁻¹² This material, 0.008 in. thick, contained: 3.45 per cent Si; 0.008 C; 0.008 P; 0.020 S; 0.075 Mn; 0.031 Al and 0.072 Cu.

To illustrate results on twin relationships obtained in this laboratory, most of the data will be those on two specimens designated RW₂ and RW₃; other specimens will be referred to in the section on results and interpretations only for points of special interest. Specimen RW₂ was photographed after being very lightly etched with dilute nitric acid to develop the grain structure. Fig. 1 shows a portion of the original 6 by 2-in. specimen.

Transmission Laue diffraction patterns were then obtained on about 60 grains in several areas of this specimen, in order to determine the orientations of the grains. Orientations were determined with the aid of a Wulff net after certain reflection spots in the diffraction patterns had been



FIG. 1.—SPECIMEN RW₂, SHOWING GRAIN APPEARANCE OF HIGH ORIENTATION SILICON-STEEL STRIP. $\times 3.6$.

FIG. 2.—SPECIMEN RW₂, SHOWING EXTENT OF RECRYSTALLIZATION THAT OCCURRED DURING 900°C ANNEAL. SAME AREA AS SHOWN IN FIG. 1. $\times 3$.

FIG. 3.—SPECIMEN RW₃, SHOWING GROUP OF RECRYSTALLIZED GRAINS AMONG OLD ONES AFTER 900°C ANNEAL. $\times 3.5$. Original magnifications given. Reduced about one third in reproduction.

identified, using standard diffraction patterns for various orientations of the body-centered cubic lattice.^{13*} Except for the cold-rolling schedule, no data

Photographs were taken of the recrystallized areas (Figs. 2 and 3).

Recrystallized and unrecrystallized grains were then X-rayed to obtain their orienta-

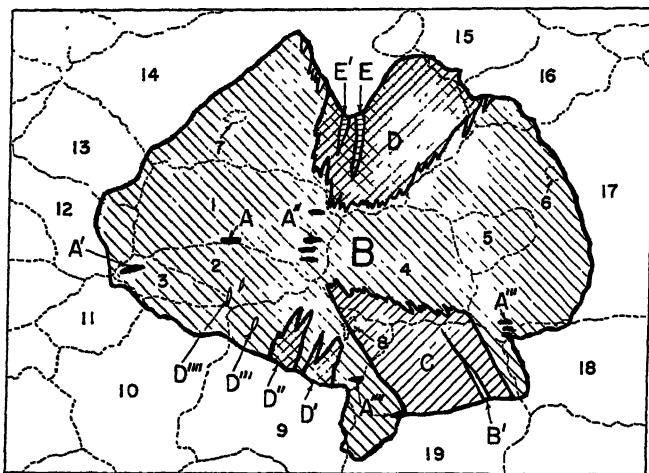


FIG. 4.—OLD AND NEW GRAINS IN SPECIMEN RW2.

Old and new grain boundaries are given by broken and solid lines, respectively. Numbers refer to old grains; letters to new grains.

prior to recrystallization were taken for specimen RW3. Cold-rolling was carried out on a mill having 8-in diameter rolls in an x direction, which coincided with the original roll direction used in the production of the strip steel. Schedules were as follows: RW2 reduced 2.5 per cent in thickness in six passes; RW3 reduced 2.5 per cent in one pass. X-ray data were obtained on specimen RW2 to note the effect of the cold-work. Both specimens were then annealed by raising the temperature uniformly from 500° to 900°C. in 20 hr., the aim being to obtain early stages of recrystallization. An atmosphere of pure, dry hydrogen was used during this anneal. Both specimens were lightly etched with dilute nitric acid, to reveal areas where recrystallization had occurred.

tions and the condition or shape of their respective Laue diffraction spots. Orientations of the new grains were determined in the manner described above except that, instead of using a Wulff net, the orientations of the cube poles were calculated directly from the positions of two or three diffraction spots on each film.

Since recrystallization appeared to be incomplete, heat-treatments at higher temperatures were given to both these specimens, to see whether the new grains would grow at the expense of the old ones and what sort of recovery of the old grains would occur. The first treatment was an 1175°C. 2-hr. anneal in pure, dry hydrogen. Specimen RW3 was then annealed again for 2 hr. at 1300°C.

Following the 1175°C. anneal, measurements were made of the directions of grain-boundary lines in the surface of specimen RW2 and also in the surfaces formed by cutting through the recryst-

* There is a general mix-up of positive and negative numbers in these standard Laue-graphs and there are several errors in the indexing of diffraction spots according to form of plane involved.

tallized grains in the x direction.¹⁴ These angle measurements were rather qualitative, because the grain boundaries did not form good straight lines. Nevertheless,

or the $\{100\}$ poles of the crystal lattice. Although two directions of this type are sufficient to determine the orientation of a grain, three are given so that the data may

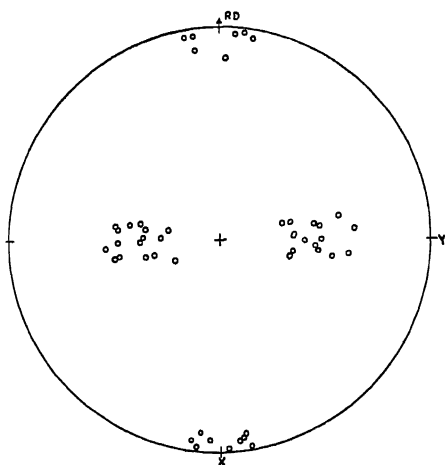


FIG. 5.— $\{100\}$ POLES OF OLD GRAINS OF SPECIMEN RW2 PLOTTED ON A WULFF NET USING DATA OF TABLE 1.

they indicated the presence of $\{112\}$ composition planes.

EXPERIMENTAL RESULTS

Fig. 1 shows typical grain structures of the material before cold-rolling. Fig. 2 shows the same area of this specimen following partial recrystallization in an anneal that reached 900°C . The exact change in grain structure is shown schematically in Fig. 4 by a superposition of initial and final grain structures. Old grains are designated by numbers, new grains by letters. Prime marks on a letter serve to identify grains in a group of common orientation. For example, grains A' and A''' have the same orientation as grain A . Such common orientations were established optically and by X-ray diffraction methods. Data on orientations therefore are listed only according to letters and numbers.

Grain-orientation data are given in terms of the three cube-edge directions

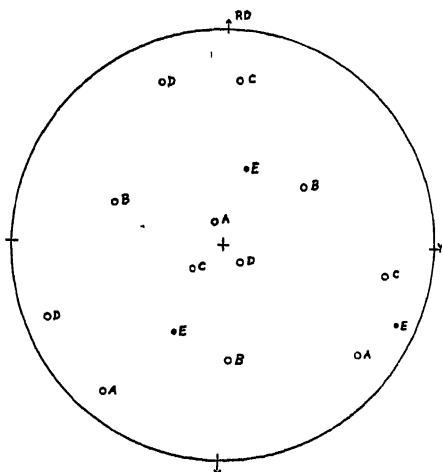


FIG. 6.— $\{100\}$ POLES OF NEW GRAINS OF SPECIMEN RW2 PLOTTED ON A WULFF NET USING DATA OF TABLE 2.

be plotted directly on a stereographic net. Rectangular coordinate directions X , Y , Z coincide with rolling direction, cross-rolling direction and the normal to the surface of a sample, respectively. Consequently, Wulff-net coordinates θ and ϕ are equivalent to the angle variables used in the following transformation equations from X , Y , Z coordinates to r , θ , ϕ coordinates, with r fixed as the radius of the reference sphere (also radius of the Wulff net).

$$\begin{aligned} X &= r \cos \theta \\ Y &= r \sin \theta \cos \phi \\ Z &= r \sin \theta \sin \phi \end{aligned}$$

(This gives $\theta = 0$ when $X = r$; and $\phi = 0$ when $Y = r \sin \theta$ and $Z = 0$.)

Data on the orientations of old grains in specimen RW2 are given in Table 1. They are plotted in stereographic projection form as shown in Fig. 5. The orientations were determined either before or after recrystallization. For example, X-ray

data on grains 1, 2, 3, 4, 7 and others were taken before heat-treating, and on grains such as No. 17, which were partially

TABLE 1.—Orientations of Grains Prior to Recrystallization, Specimen RW2
WULF NET COORDINATES GIVE POSITIONS OF {100} POLES

Grain No.	Orientation		Grain No.	Orientation		Grain No.	Orientation	
	θ	ϕ		θ	ϕ		θ	ϕ
1	8 0	32 0	8	No Data		15	172 5	160 0
	98 0	57 0					92 5	51 0
	86 5	146 5					83 0	140 5
2	9 0	35 0	9	5 5	128 0	16	9 0	152 0
	99 5	31 0		90 2	39 0		87 0	41 5
	91 0	121 0		95 5	128 5		98 0	131 0
3	11 0	10 0	10	169 5	14 0	17	174 5	25 0
	98 2	53 5		82 0	53 0		85 0	40 5
	82 5	142 5		96 5	142 0		91 0	130 0
4	7 0	167 0	11	170 0	138 0	18	170 0	165 0
	84 5	27 5		94 5	25 0		96 0	39 5
	95 0	117 0		80 0	114 0		82 0	128 5
5	No data		12	6 5	32 0	19	2 5	0 0
				97 0	42 5		92 0	51 0
				89 0	132 0		87 5	140 5
6	No Data		13	170 0	78 0			
				83 0	34 0			
				83 0	124 5			
7	172 0	10 0	14	8 0	138 0			
	84 5	52 0		89 7	46 0			
	95 0	141 0		97 0	136 0			

TABLE 2.—Orientations of Recrystallized Grains and Their Calculated Four First-order {112} Type Twins, Specimen RW₂

WULFF NET COORDINATES GIVE POSITIONS OF {100} POLES

Crystal	Observed Crystal		Twin 1		Twin 2		Twin 3		Twin 4	
	θ	ϕ	θ	ϕ	θ	ϕ	θ	ϕ	θ	ϕ
A	53.8 102.6	13.7 94.2	33.1 117.7	80.7 45.1	59.6 87.1	71.8 103.5	90.6 109.6	47.2 140.6	142.9 101.3	127.4 21.9
B	39.1 33.8	168.2 83.5	106.3 52.9	143.9 15.3	149.3 80.2	78.5 14.2	80.0 156.1	137.1 148.5	55.3 58.7	103.9 143.5
C	117.0 107.3	46.1 145.2	103.1 39.8	95.4 169.5	165.1 78.0	66.2 106.3	67.3 81.0	172.8 78.7	141.5 69.3	102.1 40.4
D	80.8 164.7	13.6 72.2	33.7 118.0	81.0 46.7	116.8 35.4	76.8 30.8	122.3 128.3	121.4 0.6	41.5 131.9	146.0 154.5
E	77.1 155.0	105.7 149.8	105.7 33.4	145.0 83.1	68.1 48.4	155.5 118.7	55.4 86.6	57.9 126.8	94.2 82.0	60.4 30.1
F	67.0 81.4	172.4 78.7	117.7 107.1	45.8 145.2	66.8 129.5	6.2 75.6	144.4 55.1	41.8 34.4	24.0 111.9	138.7 116.7
G	48.0 67.0	118.8 6.3	154.7 66.6	149.2 172.9	86.3 91.4	52.0 141.9	112.6 23.6	22.4 38.7	117.1 60.2	132.9 60.0
H	129.1	76.1	81.0	78.9	174.9	32.2	96.0	114.9	137.5	8.8
I	Not observed		33.8	83.5	70.8	91.7	96.4	81.0	21.5	26.5
J	Orientation of twin 4 of B taken		117.0	46.1	138.0	24.0	9.0	139.0	93.3	108.4
K	Not observed		107.3	145.2	125.8	167.5	98.4	172.0	111.9	16.5
L	Orientation of twin 2 of F taken		7.0	12.0	58.7	143.5	32.0	54.0	25.0	110.2
M			86.0	139.5	141.5	102.1	118.8	81.2	90.3	21.6
N			95.5	50.0	69.3	40.4	77.2	165.0	115.0	112.0
O	2.5 87.5 92.0	0.0 140.5 51.0					Not calculated			

recrystallized, after the first anneal. Unfortunately, recrystallization had proceeded too far to obtain the orientations of grains 5, 6, and 8, which previously were

Data on the orientation of new grains or structures of specimen RW2 are given in Table 2 and plotted in Fig. 6. To facilitate the analysis of these grains,

the orientations of all first-order $\{112\}$ type twins of grains *A*, *B*, *C*, *D* and *E* were calculated and the results listed in Table 2.

Fig. 3 shows the appearance of specimen RW₃ after partial recrystallization. Fig. 7

Table 4. Fig. 9 is the pole-figure plot of these observed grains.

RESULTS AND INTERPRETATIONS

Angles of variation between cube poles of observed grains and those calculated to

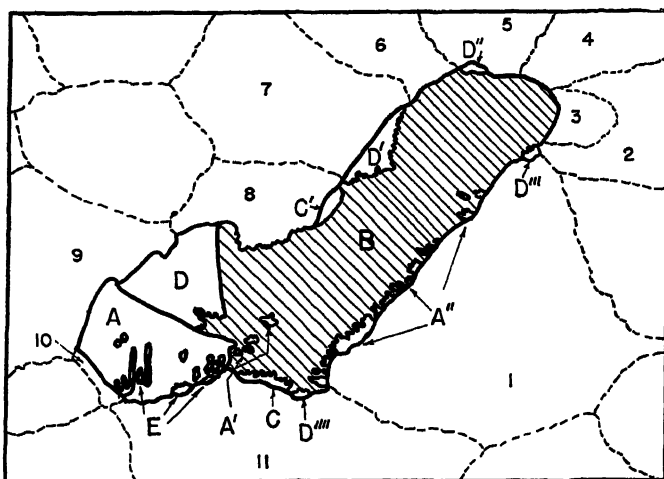


FIG. 7.—DIAGRAM OF NEW GRAINS SURROUNDED BY OLD ONES IN SPECIMEN RW₃. Boundaries of old and new grains are given by broken and solid lines, respectively. Numbers refer to old grains; letters to new grains.

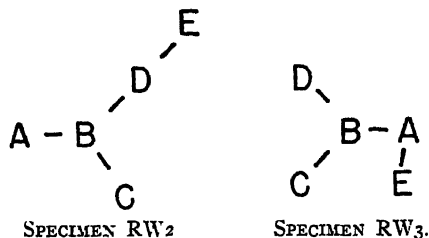
TABLE 3.—Orientation of Old Grain Material, Specimen RW₃
WULFF NET COORDINATES GIVE POSITIONS OF $\{100\}$ POLES

Grain No.	Orientation		Grain No.	Orientation		Grain No.	Orientation	
	θ	ϕ		ϕ	θ		θ	ϕ
1	16 5	171 0	5	6 5	20.0	9	166 5	10 0
	80 5	44 5		96 5	31.5		79 0	49.0
	103 0	132.0		88 5	121 5		98 0	137 0
2	0 0	0 0	6	170.5	9 0	10	7 5	40 0
	90 0	45 0		81 5	38 5		97 0	36 5
	90 0	135 0		94.5	128 0		90 5	126 5
3	170 5	25 0	7	4 0	102 0	11	12 0	11 0
	80 5	30 5		97 5	39 0		100.5	39 0
	90 0	120 5		93.0	129 0		85 0	128.0
4	173 0	65.0	8	12 0	143 0			
	83 5	37.0		84 0	26 0			
	86 0	127 5		100 0	115.0			

shows the extent of this recrystallization, old grains as before being designated by numbers and new grains by letters. Orientations of old grains immediately surrounding the new are given in Table 3 and in stereographic form in Fig. 8. Orientations of new grains and their respective calculated twins are given in

satisfy the twin relationship are given in Table 5. These angles were obtained in the standard way with the aid of a Wulff net and they average somewhat less than a degree for the two groups of grains. This close agreement, within our limits of error, indicates that twin relationships exist throughout the entire

group of new grains in each of these samples. The exact orientation relationships are shown schematically as follows, the hyphen standing for $\{112\}$ twin:



If grains or particles were being represented, a more complex diagram would be required to include everything in each group.

may be concluded that these groups are composed of $\{112\}$ twins.

On the other hand, no first-order $\{112\}$ twin relationships were found between old and new grains in spite of the fact that data for specimen RW2 include three new orientations within areas originally occupied by grains 19, 14 and 9, two orientations within each of six grains such as No. 1, and one orientation in each of the remaining seven grains. Although twin 3 of A in RW2 has an orientation that would fall within the area of spots shown in Fig. 5, it does not agree well with any of the observed old grains. A somewhat similar statement applies for twin 3 of A of specimen RW3, except that

TABLE 4.—Orientations of Recrystallized Grains and Their Calculated Four First-order $\{112\}$ Type Twins, Specimen RW3

WULFF NET COORDINATES GIVE POSITIONS OF $\{100\}$ POLES

Grain	Observed Crystal		Twin 1		Twin 2		Twin 3		Twin 4	
	θ	ϕ	θ	ϕ	θ	ϕ	θ	ϕ	θ	ϕ
E	47 5	139 9	154 7	165 0	160 3	42 3	84 6	71 5	117 0	151 5
	65 6	25 1	112 2	13 0	21 6	57 5	91 5	101 3	58 7	79 7
	127 6	95 2	79 6	98 5	95 3	134 3	174 7	56 8	135 7	29 5
A	155 3	165 5	47 7	139 3	53 4	53 5	111 3	135 6	32 1	103 7
	112 5	12 5	65 7	25 2	143 2	61.5	23 4	162 2	107 1	164.1
	80 1	98 2	128 0	94 6	86 1	146.4	80 4	49 3	116 1	65 5
B	153 9	53 7	154 1	165 0	106 9	102 7	39 8	158 6	133 7	135 8
	142 3	61 0	111 6	12 5	19 6	122 3	128 4	172 1	98 7	37 2
	86 8	146 8	86 6	98 8	84 5	14 1	96 6	76 9	45 9	119 2
C	106 5	102 5	53 2	53 7	116 6	51 6	124 6	152 9	79 1	62 4
	17 4	121 4	142 7	61 9	37 9	1 8	132 3	24 0	61 1	158 5
	84 9	14.1	86 1	146 6	65 4	128 3	61.5	84 7	148 9	134 0
D	39 4	158 9	52 8	53 4	85 1	29 5	103 1	124 8	138 3	104 3
	128 5	171 3	142 7	61 3	165 1	100 2	26 5	63 0	97 9	5 2
	96 1	76 4	86 2	146 4	76 2	120 7	112 3	29 3	49 2	88 5

These diagrams show that B has three first-order twins, A, C and D, and one second-order twin, E. E in the group for specimen RW2 may be called a third-order twin of A or C.

The orientation relationships for these groups may be visualized with the aid of the pole figures shown in Figs. 6 and 9. In the section on experimental procedure, qualitative data on the composition planes were reported as $\{112\}$ for RW2, and since it is well known that twins in alpha iron have $\{112\}$ composition planes, it

in this case the orientation of this twin would fall slightly out of the area of spots shown in Fig. 8. In any event, there are other orientations, such as B, C and D, which cannot be obtained from the original structure through a first-order $\{112\}$ twin transformation.

It might be of interest to consider the possibility of relationships involving twins of higher order. For example, some interesting data on change in orientation have been obtained in a sample pulled 8 per cent in tension and annealed at

900°C. Partial recrystallization of the sample occurred entirely within an old grain among Neumann bands which

a small angle of variation. This is based on the fact that old and new grains had a common $\{110\}$ plane within error of analysis and a measured angle of 28°

TABLE 5.—Data from Tables 2 and 3 Rearranged to Show Twin Relationships, Specimens RW2 and RW3

Crystal	Observed		Twin	Calculated		Angle of Variation, Deg.
	θ	ϕ		θ	ϕ	
SPECIMEN RW ₂						
A	53 8	13 7	B-Twin 1	52 9	15.3	2
	102 6	94 2		103 1	95 4	1
B	39 1	168 2		39 8	169 5	1
	33 8	83 5	A-Twin 1	33 1	80 7	1½
	117 0	46 1		117 7	45 1	1
B	107 3	145 2		106 3	143 9	2
	33 8	83 5	C-Twin 1	33 7	81 0	1
	117 0	46 1		118 0	46 7	1
	107 3	145 2		105 7	145 0	1½
B	33 8	83 5	D-Twin 1	33 4	83 1	1½
	117 0	46 1		117 7	45 8	1
	107 3	145 2		107 7	145 2	¾
C	80 8	13 6	B-Twin 2	80 2	14 2	1
	164 7	72 2		165 1	66 2	1½
	77 1	105 7		78 0	106 3	1
D	155 0	149 8	B-Twin 3	156 1	148 5	1
	67 0	172 4		67 3	172 8	½
	81 4	78 7		81 0	78 7	½
D	155 0	149 8	E-Twin 1	154 7	149 2	1
	67 0	172 4		66 6	172 9	1
	81 4	78 7		81 0	78 9	½
E	48 0	118 8	D-Twin 2	48 4	118 7	½
	67 0	6 3		66 8	6 2	½
	129 1	76 1		129 5	75 6	1
19	2 5	0 0	G-Twin 1	7 0	12 0	4½
	87 5	140 5		86 0	139 5	2
	92 0	51 0		95 5	50 0	4
SPECIMEN RW ₃						
A	155 3	165 5	B-Twin 1	154 1	165 0	1½
	112 5	12 5		111 6	12 5	1
	80 1	98 2		80 6	98 8	1
A	155 3	165 5	E-Twin 1	154 7	165 0	¾
	112 5	12 5		112 2	13 0	½
	80 1	98 2		79 6	98 5	½
B	53 9	53 7	A-Twin 2	53 4	53 5	½
	142 3	61 0		143 2	61 5	½
	86 8	146 8		86 1	146 4	¾
B	53 9	53 7	C-Twin 1	53 2	53 7	1½
	142 3	61 0		142 7	61 9	¾
	86 8	146 8		86 1	146 6	½
B	53 9	53 7	D-Twin 1	52 8	53 4	1
	142 3	61 0		142 7	61 3	¾
	86 8	146 8		86 2	146 4	½
C	106 5	102 5	B-Twin 2	106 9	102 7	½
	17 4	121 4		19 0	122 3	2
	84 9	14 1		84 5	14 1	½
D	39 4	158 9	B-Twin 3	39 8	158 6	½
	128 5	171 3		128 4	172 1	1
	96 1	76 4		96 0	76 9	1
E	47 5	139 9	A-Twin 1	47 7	139 3	½
	65 6	25 1		65 7	25 2	½
	127 6	95 2		128 0	94 6	¾

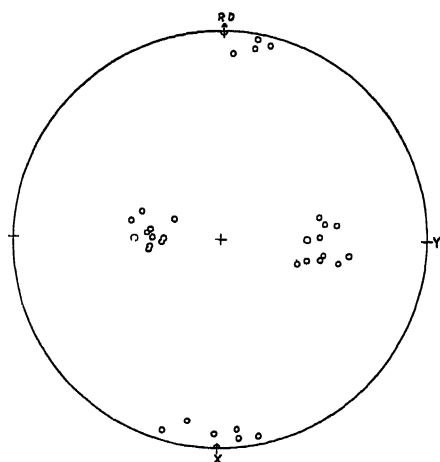


FIG. 8.— $\{100\}$ POLES OF OLD GRAINS OF SPECIMEN RW3 PLOTTED ON A WULFF NET USING DATA OF TABLE 3.

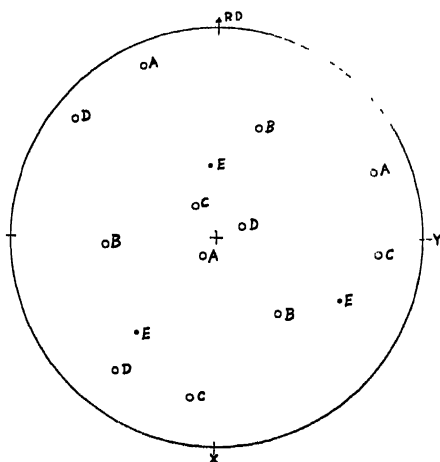


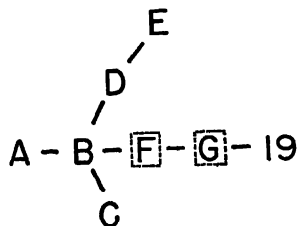
FIG. 9.— $\{100\}$ POLES OF NEW GRAINS OF SPECIMEN RW3 PLOTTED ON A WULFF NET USING DATA OF TABLE 4.

were formed in the deformation process. Relationship of new orientation to old was that of a third-order twin except for

corresponding to a rotation of the lattice about a $\langle 110 \rangle$ direction normal to the common $\{110\}$ plane (in a third-order twin of this type the angle would be

$31^{\circ}36'$).† The $3\frac{1}{2}^{\circ}$ difference can be accounted for in terms of the range of orientation of the deformed old grain. Some changes in orientation that occurred during recrystallization in specimens RW₃ and RW₂ according to Figs. 5, 6, 8 and 9 are consistent with high-order twin transformations. To illustrate this, consider an orientation B^* having threefold symmetry ($[111]$ direction along the Z -axis) with a $[\bar{1}10]$ direction along the Y -axis; this orientation being very near B of RW₂. The four twin orientations of B^* (A^* , C^* , D^* and F^*) would be similar to A , C , D and B of RW₂, respectively, except that B would have to be rotated 180° about the Z -axis. F^* would have the $[111]$ direction along the Z -axis and the $[\bar{1}10]$ direction along the negative Y -axis. Starting with B^* and F^* and restricting the number of axes of rotation ($\langle 110 \rangle$ type) to two, it is possible to derive six second or third-order twin orientations, which fall within the observed areas shown in Fig. 5. On the basis of close similarity of our groups to this one, it might be reasonable to think that second or third-order twin relationships existed between the old and some of the new orientations of specimens RW₂ and RW₃. However, a real twin relationship would require agreement in terms of individual grains of the old material. Our samples are incomplete in this respect, since grains 5, 6 and 8 in RW₂ were not observed, and some old grains in RW₃ may have completely disappeared during recrystallization. Nevertheless, it is interesting to note a relationship that was found in specimen RW₂, involving old grain No. 19. Table 2 gives data on the orientation of twins showing that the orientation of grain B is near that of a third-order twin of grain No. 19. For simplicity in describing the series, the twins and their orientations

are designated as follows: F , twin 4 of B ; G , twin 2 of F ; No. 19, near twin 1 of G . The orientation of grain 19 differs from twin 1 of G by a maximum variation of $4\frac{1}{2}^{\circ}$ (see Table 5). Although a deviation of this amount may be partly due to a spread in orientation of the deformed grains (about 3° according to asterism of Laue spots and about $4\frac{1}{2}^{\circ}$ in regions containing Neumann bands as shown by our X-ray studies of these bands), there is disagreement beyond the errors of analysis in the $\{110\}$ plane, which grains B and No. 19 should have in common. The disagreement, however, may arise from distortion of the old grain in some way. The relationship of the new grains to the old in specimen RW₂ according to this picture is shown schematically as follows:



Missing twins F and G (see Table 2) permit linkage with old grain No. 19.

It is interesting to speculate about the relationship between old and new grains in terms of a mechanism of recrystallization involving nucleation according to twin relationships or by growth of second or third-order $\{112\}$ deformation twins. Such deformation twins might develop within Neumann bands or at the intersection points of certain Neumann bands during plastic deformation. These bands may be present in various ways in the deformed grains of our samples. Fig. 10 gives an illustrative example showing intersecting Neumann bands for strip steel of the type used in these experiments. This specimen was cold-reduced 4 per cent in one pass and given a macroetch with

† Slip in a $[11\bar{1}]$ direction in a $\{112\}$ plane will rotate the lattice $109^{\circ}28'$ or $70^{\circ}32'$ about a $[\bar{1}10]$ direction for each stage of twinning.

dilute nitric acid, to accentuate the banded structure that was plainly visible in the surface of the rolled sample. Although second-order twins have not been observed

orientation. Fig. 11 gives a similar case for a large new grain containing 12 twins of common orientation. Comparing the large grain with unrecrystallized grains

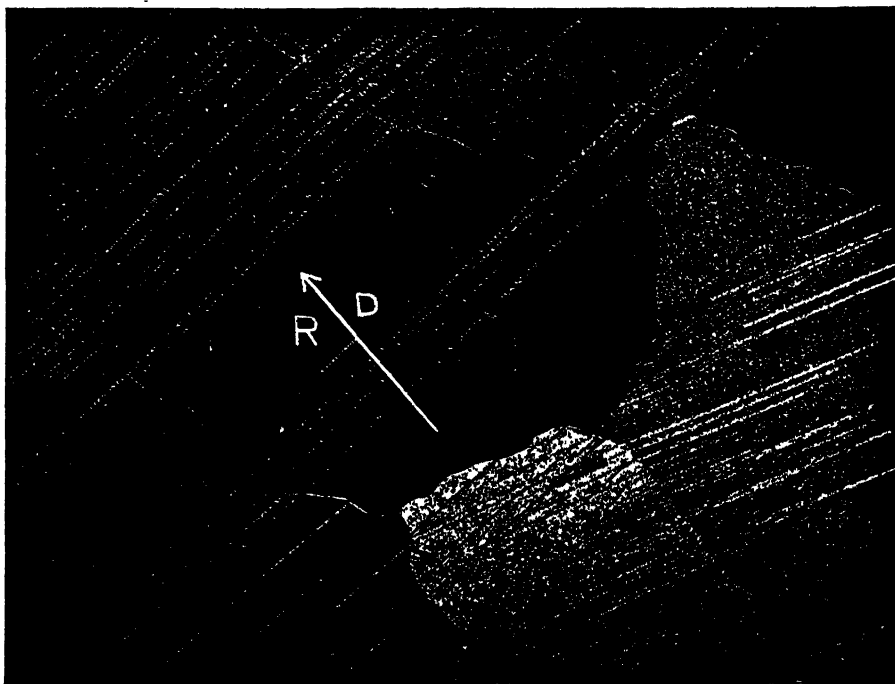


FIG. 10.—ILLUSTRATIVE EXAMPLE OF NEUMANN BANDS PRODUCED IN SILICON-STEEL STRIP BY 4 PER CENT REDUCTION IN THICKNESS. MACROETCH USING NITRIC ACID. $\times 9$.

as yet, it is known that they form in metals such as antimony¹⁶ and zinc.⁵ It is also known that Neumann bands sometimes play a role in recrystallization of silicon ferrite,⁶ and this was brought out in connection with our samples pulled in tension. We might, therefore, speculate on the possibility that our new orientations began through growth of suitable twins, probably second or third-order, formed during the plastic deformation process.

However, a speculation such as this would not be enough to account for all the orientations obtained during recrystallization. For instance, there are widely separated grains or particles such as A , A' , and A''' in RW₂ which have a common

in the adjacent upper left portion of the photograph, it appears likely that the island grains formed in widely separated grains of the original material. These new grains or particles of common orientation are not easy to account for except on the basis of some sort of dependent or secondary nucleation arising during growth of a new grain and because of this growth. For example, referring again to specimen RW₂, analysis shows that the nearest first-order twin of A to the orientations of grains 1 and 3, grains in which particles of orientation A form, is 10° to 13° off in terms of directions of cube poles. Conversely, no first-order twin of grains 1 and 3 would fit within 10° as a first-order

twin of grain *B*. Nevertheless, such first-order twins in the form of Neumann bands might play a role in the nucleation of material of orientation *A* through

at the expense of old grains in contact with the large new grain than to suppose that they formed in an independent manner through a fortuitous growth of



FIG. 11.—SAMPLE OF STRIP STEEL COLD-ROLLED 2.5 PER CENT AND ANNEALED FOR 2 HOURS AT 1175°C., TIME UP TO TEMPERATURE BEING 4 HOURS ETCHED WITH NITRIC ACID. $\times 2$.

recovery and adjustments that are brought about by the growth of grain *B*. The orientation of *D* in grains 9 and 14, however, could not reasonably arise through adjustments of Neumann bands, but perhaps could arise through adjustments of 10° to 14° in second-order twins.

Mathewson, referring primarily to work on single crystals of brass, said:

It is believed that many and perhaps most of the new orientations formed during recrystallization of these face-centered cubic metals are due to complex twinning resulting in strained boundaries which permit growth and readjustment in various forms.⁸

It seems more reasonable to suppose that the separated grains of common orientation in specimen RW₂ and the sample illustrated in Fig. 11 developed

grains of common orientation or by a second partial recrystallization of the large new grain. The original orientations differ too much from grain to grain to permit separate growth of new grains having a common orientation, and a lattice free of strain (a large recrystallized grain) seems an unlikely place for further recrystallization.

If we should attempt to describe the growth of a group such as that developed in specimen RW₂, we would be uncertain as to which orientation appeared first on recrystallization and uncertain as to where it started. However, on the basis of the relationship suggested on page 9, we might suppose that it started within grain No. 19, perhaps near the boundary formed with grain 4, through nucleation of a grain of orientation *B* or *C* or *A* (all

three grew within grain No. 19). Furthermore, it is fairly easy to imagine a heterogeneous growth process that would generate the entire group shown in Fig. 4 if secondary nucleation produces grains such as those of the *D* series. For example, if *B* nucleates *C* in grain 19, *C* nucleates *B* in grain 4, and *B* in turn nucleates *A* in grain 1 and *D* in grain 14. *D* in turn would then nucleate *E* in grain 14 and *E* would be a second-order twin of *B*. Furthermore, it is worth pointing out that the isolated grains in the upper part of grain *B* that are in contact with old grain No. 14 have the orientation of grain *D*. The appearance of these grains indicates that they might join and become part of grain *D* if further growth could be induced. In any case, the serrated edges of grain *D* appear to have formed from separate nucleation off grain *B* during the growth process. It is also interesting to note that grains of orientation *A* and *E* do not appear to grow very well. Since they have orientations somewhat near first-order twins of the old grains, the structure difference between old and new grains may be insufficient to induce rapid growth, especially if a composition plane of the $\{112\}$ type should tend to form. Barrett says⁴⁶ that the shifting of atoms from the strained matrix to the new grain may proceed slowly if the new grain has the orientation of the matrix and most rapidly if the orientation differs in a certain way. A similar statement may apply to twinned orientations. In any case, growth should be more rapid near Neumann bands because our observations indicate greater strain or change in orientation of the deformed grain near these bands.

Several effects were found upon annealing specimens RW₂ and RW₃ at high temperatures. Although grain *B* in RW₂ did grow some at the expense of grains 11 and 12, there was very little growth of the new grains. This was also true of RW₃ annealed at 1300°C. Interesting

results on recovery of old grains were found as shown in Fig. 12. Up to 1175°C. the results are very similar to those obtained by Collins and Mathewson¹⁸ on recrystallization of aluminum single crystals. Referring to the series shown in Fig. 12, changes in the structure of grains can be followed. The sharp Laue diffraction spots shown in Figs. 12*b* and 12*d* indicate that grains of the starting and recrystallized materials are undeformed single crystals. Fig. 12*c*, however, showing considerable asterism of a fairly uniform type, at least indicates an over-all state of distortion in the deformed grain. (Distortions due to internal stresses cannot be evaluated from the Lauegraph.) When such a grain is annealed and recovery processes occur instead of recrystallization, it is known that internal stresses are relieved or partially relieved. Figs. 12*e* and 12*f* give the appearance of the Laue reflections after recovery at 900° and 1175°C., respectively. The asterism is now non-uniform, and this may be interpreted in terms of the development of a macromosaic structure within the grain. Fig. 12*g* shows that recovery has proceeded a long way toward a perfect single crystal in a grain annealed at 1300°C. However, the reflection spot is still nonuniform, and this may mean that the grain has a rather coarse mosaic structure.

Because of the role played by strain in recrystallization phenomena, it seems evident that recovery of the type encountered in our work would oppose recrystallization processes. Such a view is in agreement with those expressed on recovery in aluminum.¹⁸ Furthermore, our results show that recovery inhibits the growth process in recrystallization because high-temperature anneals do not promote growth to any significant degree. In this connection, it is of considerable significance that recovery at high temperature was more predominant than recrystallization in specimen RW₃. Another in-

teresting aspect of recovery was noted in the sample illustrated in Fig. 11. Some unrecrystallized grains produced Laue diffraction spots similar to the one shown

1300°C. anneal. Furthermore, A' , most of A'' , D'' , D''' and C were absorbed by B . Growth of B also removed the serrated edges of the residue of A'' and of D' .

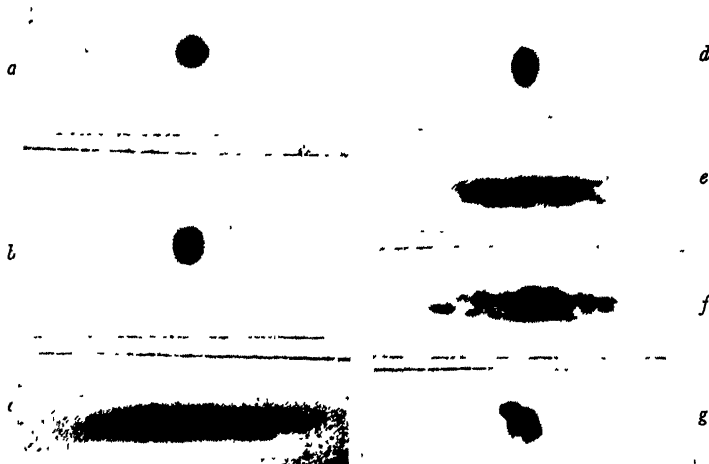


FIG. 12—SINGLE LAUE REFLECTIONS FROM OLD AND NEW GRAINS AFTER VARIOUS TREATMENTS
X 4.

Reflection spots are taken from similar regions of ordinary Lauegrams obtained with 45-kv. radiation, the radial direction between the images of undeviated and reflected beams being horizontal.

- a. Spot from undeviated beam.
- b. Grain before treatment
- c. Grain after 2.5 per cent reduction by rolling.
- d. New or recrystallized grain after 900° anneal.
- e. Residue of partially consumed old grain adjacent to new grain after 900° anneal.
- f. Residue of partially consumed old grain adjacent to new grain after 1175° anneal.
- g. Residue of partially consumed old grain adjacent to new grain after 1300° anneal.

in Fig. 12f in two kinds of regions as follows: (1) area containing lines of Neumann-band origin; (2) area free from Neumann-band appearance. Furthermore, the Lauegrams were essentially the same with no extra reflection spots from the area containing traces of old Neumann bands. This indicates that the recovery process has removed all or most of the Neumann-band structure.

Another significant change took place during the high-temperature anneals. Structures such as A'' (Fig. 4) in RW₂ were absorbed by grain B in the 1175° anneal. All of E in grain A of specimen RW₃ (Fig. 7) was absorbed by A during the

This shows that the twin boundaries were not stable. McKeehan,⁸ however, showed that twin boundaries were stable in ferrite annealed for 3 hr. at 700°C. We can account for the difference in results on the basis of higher atomic mobility made possible by the high temperatures we used.

Since these fine twin structures tend to disappear through absorption at high temperature, we believe that they did not form from recrystallized grains and that early stages of recrystallization should be used in general to observe them.

Some of our present work is concerned with a search for second or third-order

twins in deformed grains of silicon ferrite and especially in areas where Neumann bands intersect. Information on recrystallization and the role played by mechanical twins is being obtained.

SUMMARY

1. It has been shown that recrystallization of plastically deformed silicon ferrite can produce complex groups of grains or particles twin-related through more than one order or generation of twins.

2. Relationships between old and new grain orientations are considered on the basis of first, second and third-order twins. A speculation is made that certain grains among the new ones may be derived through growth of high-order mechanical twins formed in the old grains by plastic deformation.

3. Complicated groups of recrystallized grains are shown, which have many isolated particles of common orientation and which are first-order twins of the separating matrix. To account for them and the origin of the entire group, some sort of secondary nucleation seems necessary. It has been suggested, therefore, that a grain can nucleate a twin orientation during its growth and this twin can nucleate another twin either of higher or lower order.

4. It has been shown that recovery of old grains plays a significant role in the recrystallization process. Recovery not only inhibits growth of the nucleated grains but continues to operate even after growth of new grains has stopped. Such recovery can proceed far enough to closely approximate the original structure prior to deformation. Furthermore, Neumann bands within deformed grains appear to be absorbed during recovery of a grain in the neighborhood of 1200°C.

5. Twins in the form of small grains or particles within a large recrystallized grain do not have stable boundaries at

high temperatures. The large grain in such a group usually absorbs the small particles. In other cases twin boundaries are changed by growth of one grain at the expense of the other.

ACKNOWLEDGMENT

The writer wishes to acknowledge the encouraging interest shown by Mr. A. McK. Gifford, Director of the Pittsfield Works' Laboratory, and Mr. W. Morrill, head of the Magnetic Section, in the experimental work and the preparation of the present paper.

He is indebted to Dr. M. Kronberg for diffraction patterns, for illustrations used in the paper, and for valuable discussions during the course of the work.

Aid in the numerical calculations was given by Miss Jane Marshall.

Finally, the author wishes to express his appreciation to those who have contributed in various ways either in the experimental work or in the preparation of this paper.

REFERENCES

1. O. Mugge: Über neuere Strukturflächen an den Krystallen der gediegenen Metalle. *Jahrb. für Mineral.* (1899) 2, 55.
2. H. M. Howe: The Metallography of Steel and Cast Iron. New York, 1916. McGraw-Hill Book Co.
3. C. H. Mathewson and G. H. Edmunds. The Neumann Bands in Ferrite. *Trans. A.I.M.E.* (1928) 80, 311-333. Iron and Steel Division.
4. C. S. Barrett: Structure of Metals; (a) 317, (b) 421. New York, 1943. McGraw-Hill Book Co.
5. C. H. Mathewson: Twinning in Metals. *Trans. A.I.M.E.* (1928) 78, 7-54.
6. V. N. Krivobok: A Photomicrographic Study of the Process of Recrystallization in Certain Cold-worked Metals. A.I.M.E. Pamphlet 1557 (1926).
7. C. F. Elam: Banded Structure in Aluminum and Copper. *Nature* (1927) 120, 259.
8. L. W. McKeehan: Twinning in Ferrite. *Trans. A.I.M.E.* (1928) 78, 453-459. Discussion by C. F. Elam.
9. A. B. Greninger. Transformation Twinning in Alpha Iron. *Trans. A.I.M.E.* (1936) 120, 293-308.
10. N. P. Goss: New Development in Electrical Strip Steel Characterized by Fine Grain Structure Approaching the Properties of a Single Crystal. *Trans. Amer. Soc. Metals.* (1935) 23, 511. U. S. Patent 1965559.

11. R. M. Bozorth: The Orientations of Crystals in Silicon Iron. *Trans. Amer. Soc. Metals* (1935) **23**, 1107.
12. J. T. Burwell: Crystal Orientation in Silicon-iron Sheet. *Trans. A.I.M.E.* (1940) **140**, 353.
13. Masaichi Majima, Kōgakuhakushi, and Sakuchi Togino: The Radiograph of a Crystal having the Body-centered Cubic Lattice. *Sci. Paper I.P.C.R. Tokyo*, (1927) **7**, (126), 259.
14. A. J. Phillips: Twinning in Copper and Brass. *Trans. A.I.M.E.* (1928) **78**, 429-444.
15. H. J. Gough and H. L. Cox: *Proc. Roy. Soc. London* (1930) **A-127**, 431; *Jnl. Inst. Metals* (1932) **48**, 227.
16. J. A. Collins and C. H. Mathewson: Recrystallization of Aluminum Single Crystals. *Trans. A.I.M.E.* (1940) **137**, 150-169.

Precipitation and Reversion of Graphite in Low-carbon Low-alloy Steel in the Temperature Range 900° to 1300°F.

By G. V. SMITH,* JUNIOR MEMBER A.I.M.E., R. F. MILLER,* MEMBER, AND C. O. TARR,* JUNIOR MEMBER

(New York Meeting, February 1944)

METALLURGISTS have long recognized that the Fe_3C type of carbide is not a stable phase in steel and that, given sufficient time, it will decompose with formation of graphite, at least at temperatures below about 2050°F.¹ This slow graphitization has never been of much concern to users of hypoeutectoid steels, for in such steels it occurs only during prolonged exposure at elevated temperature. In 1935, Kinzel and Moore² reported complete graphitization of the carbide of a 0.15 per cent carbon steel that had been in service for about 26,000 hr. at a temperature of about 1100° to 1200°F. In discussing this paper, both Mathews and Sauveur reported graphitization of slightly hypereutectoid steels. In an extensive investigation of graphitization of high-purity iron-carbon alloys, Wells¹ produced graphite at 700°C. (1290°F.) in an alloy containing as little as 0.13 per cent carbon, and showed that graphite may precipitate either directly from austenite or from decomposition of Fe_3C , also that the rate of graphitization tends to increase with increase of temperature, at least up to a certain point, and with the presence of graphite nuclei.

Jenkins, Mellor and Jenkinson,³ studying the structural changes in carbon steels

ranging from 0.17 to 1.14 per cent carbon during stress-rupture tests at elevated temperature, observed graphite in an aluminum-killed 0.40 per cent carbon steel after fracture in 4340 hr. under a stress of 17,900 lb. per sq. in. at 840°F. and in many of the steels after stress-rupture test at 1200°F. Unstressed samples of 0.60, 0.86 and 1.14 per cent carbon steels graphitized almost completely in 360 hr. at 1200°F., while samples of 0.90 and 1.10 per cent carbon steels were somewhat graphitized, and steels containing 0.24, 0.40 and 0.57 per cent carbon showed no sign of graphite. Their results indicate that graphite precipitates the more readily the higher the carbon content, though this tendency is influenced to some extent by deoxidation practice, and that graphitization is accelerated by plastic deformation.

In a recent study of the graphitization of 0.4 and 0.6 per cent carbon steel strip, made by M. A. Hughes,⁴ it was found that at 1200°F. graphite appeared after 72 hr. in aluminum-killed but not in silicon-killed steel, and that the rate of graphitization was increased by slow cooling from 1600°F. and by cold-working prior to annealing.

In creep tests of normalized 0.15 per cent carbon steel killed with 2.5 lb. of aluminum per ton, at the U. S. Steel Corporation laboratory at Kearny, spheroidization and some graphitization were found after 3000 hr. at 1000°F. under a stress as low as 1500 lb. per sq. inch.

Manuscript received at the office of the Institute Nov. 30, 1943. Issued as T.P. 1695 in METALS TECHNOLOGY, June 1944.

* Research Laboratory, U. S. Steel Corporation of Delaware, Kearny, New Jersey.

¹ References are at the end of the paper.

GRAPHITIZATION OF LOW-CARBON LOW-ALLOY STEEL

No examples of graphitization of low-carbon low-alloy steel appear to have been reported in the literature; but two instances of graphitization of carbon-molybdenum steel have been noted here. In the first of these instances, a specimen of 0.15 per cent carbon, 0.50 per cent molybdenum steel, made to fine-grain practice, which had been normalized at 1650°F. and tempered at 1300°F., was tested in creep at 1100°F. under a stress of 3500 lb. per sq. in. for 13,000 hr.; it was then overloaded to 7500 lb. per sq. in. and failed after about 1000 hr., showing a moderate amount of graphite in the severely deformed metal near the fracture. In the second instance, a small amount of graphite was found in a normalized specimen of the same type of steel after 5000 hr at 1000°F. under a stress of 15,000 lb. per sq. inch.

Though somewhat beyond the scope of this paper because of the high carbon content of the materials, the extensive investigations by Austin and co-workers⁵⁻⁸ should be mentioned. These workers succeeded in graphitizing high-purity and commercial steels containing up to 0.5 per cent of Cr, Mn, Ni, Cu or Si, and found that the rate of graphitization appears to go through a maximum in an intermediate temperature zone (1000° to 1200°F.). This maximum rate is due presumably to a change in the balance, at higher temperature, between the tendency toward increased reaction rate and the increasing stability of the carbide.

Recently there was a failure at a generating station, which has been traced to graphitization near a weld in a carbon-molybdenum steam pipe. This fracture occurred suddenly around the whole periphery of the wall of an aluminum-killed, carbon-molybdenum steam pipe 12¾ in. o.d. by 1¼ in. wall, at a distance of approximately ¼ in. from the border of the fusion zone of a weld by which it was joined

to the main steam header of the boiler. The reported welding conditions involved a 400°F. preheat and a subsequent stress-relief treatment of 3 hr. at 1200°F. The pipe had been in service at a steam temperature and pressure of 935°F. and 1300 lb. per sq. in., respectively, for 5½ years. Metallographic examination revealed a profuse amount of graphite, disposed in network fashion around the Widmanstätten areas, in a narrow region on both sides of the fracture; this network of graphite, which in many places was continuous, provided an easy path for fracture and clearly was the reason for failure. The zone of graphitization occurred near the lower limit of the "heat-affected" zone of the base metal in a region that, from metallographic examination, apparently reached a temperature of 1300° to 1350°F., i.e., the lower critical temperature, A_1 ; further, the width of the graphite zone was so narrow that the path of fracture closely conformed to this isothermal line of the individual weld passes. In the unaffected base metal of the pipe, there were occasional graphite nodules, though these, because they were scattered, are of no concern.

EXPERIMENTAL PROCEDURE

In studying the effect of temperature on the structural stability of low-carbon low-alloy steels, several experiments were made in an attempt to produce graphite in carbon-molybdenum steel by holding it just below the A_1 temperature. We reasoned that if graphite could grow to an appreciable size in 5 years at 935°F., or in 5000 hr. at 1000°F., it should appear in much shorter time at 1300°F. One series of tests involved holding, either under stress or not, at temperatures up to the A_1 and for times up to 250 hr., samples of aluminum-killed carbon-molybdenum steel in which a temperature gradient had been produced while the sample was either stressed or unstressed. Spheroidization and agglomeration of the carbide occurred, but

no graphite was observed. In a second study, not concerned primarily with graphitization, samples of silicon-killed carbon-molybdenum steel were held for periods up to 1000 hr. at temperatures of 1000°, 1100°, or 1200°F., and up to 500 hr. at 1300°F. Spheroidization and agglomeration of the carbide again occurred,* but no graphite was found.

Since the experiments of Jenkins, Mellor and Jenkinson³ indicate that graphitization is accelerated by plastic deformation, stress-rupture specimens of aluminum-killed carbon-molybdenum steel from a previous investigation⁹ were carefully re-examined. These specimens had been tested at 1100°F. in the pearlitic and in the spheroidized conditions, and showed fracture times up to 2000 hr.; but again there was no evidence of graphitization.

DISCUSSION OF RESULTS

It now appears that the seemingly anomalous behavior of carbon-molybdenum steel, which graphitizes slowly at 900° to 1100°F. but not at all at 1300°F., is associated with a change in composition and stability of the carbide. In steel containing carbide-forming elements such as molybdenum, the carbide may be not of the Fe_3C type, which is known to be unstable with respect to graphite, but of the iron-molybdenum-carbide type. Moreover, carbides of different composition may exist at different temperatures, or after different times at constant temperature; and at some temperatures more than one carbide type may coexist. Little information is available concerning the stability of such types of carbide with respect to graphite, though it seems certain that they are less unstable than Fe_3C , and may be completely stable.

Crafts and Offenhauer^{10,11} recently in-

vestigated the nature of the carbides in low chromium-molybdenum steels, and found that on quenching and then tempering such steel at a temperature below the range 500° to 550°C. (930° to 1020°F.), the carbide then present is the Fe_3C type, but at higher tempering temperature is some alloy carbide. The type of alloy carbide, as determined by X-ray diffraction, is, in intermediate chromium steels, Cr_7C_3 , in higher chromium steels, Cr_4C , and in molybdenum steels, Mo_2C . All of these types were found in a series of chromium-molybdenum steels. They also observed that chromium carbide formed in chromium steels when austenite transformed in the pearlite range. The type of carbide that forms in the molybdenum and chromium-molybdenum steels on transforming to pearlite was not studied, but probably it is an alloy carbide.

These conclusions suggest the reason for the absence of graphitization in a carbon-molybdenum steel even when held for a long time just below the A_1 temperature. At such a temperature, according to the data cited above, the prevailing carbide may be of the Mo_2C type, which, with respect to graphite, is presumably more stable than Fe_3C , and may even be completely stable. On the other hand, during long-time exposure in the temperature range 900° to 1000°F., graphite may form because the prevailing carbide is then Fe_3C , which is unstable and decomposes slowly. The possibility should also be borne in mind that insufficient mobility of molybdenum atoms may inhibit the formation of Mo_2C at the lower temperature, the carbon then combining with the ubiquitous iron; this may be true either for quenched and tempered steels, as Crafts and Offenhauer observed, or on transformation during continuous cooling, the lack in this latter case being of time rather than just of atomic mobility. If, on the other hand, Mo_2C were the carbide initially present, it might be metastable below 1000° to 1100°F.

* Preliminary results of a similar study of an aluminum-killed steel indicate that the rate of spheroidization is appreciably greater than for silicon-killed steel.



FIGS. 1-6.—STRUCTURAL CHANGES OF GRAPHITIZED AND UNGRAPHITIZED CARBON-MOLYBDENUM STEEL ON HOLDING AT 1300°F. PICRAL ETCH. $\times 750$.

Fig. 1. Carbon-molybdenum steel as graphitized by $5\frac{1}{2}$ years at 935°F.

Fig. 2. Nongraphitized material adjacent to that of Fig. 1.

Fig. 3. Same material as Fig. 1 after one week at 1300°F.

Fig. 4. Same material as Fig. 2 after one week at 1300°F.

Fig. 5. Same material as Fig. 1 after $2\frac{1}{2}$ weeks at 1300°F.

with respect to either Fe_3C or graphite, the end result being the same in either case.

The validity of this general hypothesis can be proved if samples of the same carbon-molybdenum steel, held at 1000° and 1300°F . for a long period, show graphite forming slowly at the lower temperature but not at all at the higher. The time required for this experiment is undesirably long, however, and the fact that there were available specimens of the steel from the failed pipe mentioned earlier, which had already graphitized, suggested a much quicker method—namely, to see whether this graphite would disappear on holding at 1300°F . Consequently, a specimen of carbon-molybdenum steel containing graphite that had formed during several years service at 925°F . was heated to 1300°F . (A_1 being about 1330°F .) for several weeks, protected from oxidation and decarburization by sealing in vacuo in a silica bomb. As noted earlier, only a very narrow section of the sample contained graphite, this section being adjacent to a weld and having reached, during welding, a temperature of approximately 1300° to 1400°F . On holding at 1300°F . the graphite gradually disappeared and was replaced by carbide, as shown by comparison of Fig. 1, representative of the initial material, with Figs. 3 and 5 for the same material after 7 and 18 days, respectively, at 1300°F . Holding at 1300°F . for an additional 3 weeks did not cause any great change in amount of graphite beyond that in Fig. 5. The excess of carbon in this formerly graphitized part of the steel may, as pointed out below, account for the slowing down of the rate of reversion of the graphite because of depletion of the molybdenum needed to form the alloy carbide. In any event, at this temperature, the stable phase is clearly not graphite but a carbide, presumably of the Mo_2C type; and this may well be true also for other steels containing one or more carbide-forming elements.

The accompanying change in the Wid-

manstätten structure of adjacent non-graphitized metal is shown in Figs. 2, 4 and 6. It may be noted that there is obviously a greater amount of carbide in the degrephitized region than in the adjoining ungraphitized region. This is readily explainable by the considerations that graphite, besides being the stable phase, is less soluble in ferrite than is carbide, and forms by diffusion of carbon through the ferrite solid solution to the graphite nucleus and there precipitating. Conceivably, then, graphitization in a limited region could bring about, in time, the substantial depletion of carbide within an entire specimen. Attention may also be called to the size of the carbide particles developed on reversion of the graphite as compared with that brought about by agglomeration of pre-existing smaller particles. This formation of relatively large particles is to be attributed, presumably, to the strong driving force that urges the carbon atoms out of graphite into solution in the ferrite, combined with the difficulty of forming new carbide nuclei. On the other hand, the only force tending to cause agglomeration of the small particles is that exerted by surface tension.

It is to be noted that in forming Mo_2C , one part by weight of carbon (atomic weight 12) ties up 16 parts by weight of molybdenum (atomic weight 96). Thus, in a steel with 0.15 per cent C and 0.50 per cent Mo, there will be excess carbon if all the carbide is Mo_2C and all the molybdenum is present in that form. However, Crafts and Offenbauer,¹¹ by chemical analysis of electrolytically extracted carbides, found that at 1200°F , Mo_2C can dissolve about 20 per cent of its weight of iron, on which basis the amount of the Mo_2C type carbide would be greater than if the carbide contained only molybdenum and carbon. On the other hand, some molybdenum, though probably a small amount, may exist in solution in ferrite. Evidently there is need for more systematic study of the nature and range of stability

of the several types of carbide that may form in steels, and of the partition of alloying elements between carbide and matrix. Such an investigation has already been started by Bowman, Parke and Herzig.¹²

REFERENCES

1. C. Wells: Graphitization of High Purity Iron Carbon Alloys. *Trans. Amer. Soc. Metals* (1938) 26, 289-357.
2. A. B. Kinzel and R. W. Moore: Graphite in Low-carbon Steel. *Trans. A.I.M.E.* (1935) 116, 318-329.
3. C. H. M. Jenkins, G. A. Mellor and E. A. Jenkinson: Investigation of the Behavior of Metals under Deformation at High Temperature. *Jnl. Iron and Steel Inst.* (1942) 145, 51.
4. M. A. Hughes, Carnegie-Illinois Steel Corporation, Ohio Works, Youngstown, Ohio, private communication.
5. C. R. Austin and B. S. Norris: Effect of Tempering Quenched Hyper-eutectoid Steels on Physical Properties and Microstructure. *Trans. Amer. Soc. Metals* (1938) 26, 788-845.
6. C. R. Austin and B. S. Norris: Temperature-gradient Studies of Tempering Reactions of Quenched Hyper-eutectoid Steels. *Trans. A.I.M.E.* (1938) 131, 349-371.
7. C. R. Austin and M. C. Fetzner: Effects of Composition and Steelmaking Practice on Graphitization below the A₁ of Eighteen 1 Per Cent Carbon Steels. *Trans. A.I.M.E.* (1941) 145, 213-224.
8. C. R. Austin and B. S. Norris: Effects of Small Amounts of Alloying Elements on Graphitization of Pure Hyper-eutectoid Steels. *Trans. Amer. Soc. Metals* (1942) 30, 425-454.
9. R. F. Miller, G. V. Smith and G. L. Kehl: Influence of Strain Rate on Strength and Type of Failure of Carbon-Molybdenum Steel at 850°, 1000° and 1100°F. *Amer. Soc. Metals Preprint* 24 (1942).
10. W. Crafts and C. M. Offenhauer: Carbides in Low-chromium Steels. *Trans. A.I.M.E.* (1942) 150, 275-287.
11. W. Crafts and C. M. Offenhauer: Carbides in Low Chromium-molybdenum Steels. *Trans. A.I.M.E.* (1943) 154, 361.
12. F. E. Bowman, R. M. Parke and A. J. Herzig: The Alpha Iron Lattice Parameter as Affected by Molybdenum, and an Introduction to the Problem of the Partition of Molybdenum in Steel. *Trans. Amer. Soc. Metals* (1943) 31, 487.

DISCUSSION

(F. M. Walters, Jr., presiding)

F. B. FOLEY,* Philadelphia, Pa.—In developing a theory to account for graphitization, the effect of elements such as silicon, nickel

and aluminum must be taken into account. It would be short sighted to base any such theory on only the type of carbide present, to the exclusion of these elements, which are soluble in the ferrite and which do not normally enter into chemical combination with carbon at the temperatures under consideration. These elements, nevertheless, are well known to promote graphitization. Not only must the carbide, which decomposes to form the graphite, be taken into account but the ferrite matrix as well.

In regard to the molybdenum-bearing steel in question the authors cite authority for the existence of the carbide Fe₃C in the temperature range where graphitization has occurred. It is, they say, at a higher temperature that the carbide Mo₂C forms. If this be so, the composition of the ferritic phase is also undergoing a change for, if the molybdenum be not combined with carbon in the lower temperature range it is in solution in the ferrite, where it may act, as would other known graphitizers, which are all ferrite soluble, to promote graphitization.

There is abundant evidence in the literature of the formation of Fe₃C in a carburizing environment at temperatures well below the critical. Byrom¹³ records the complete conversion of a 3/16-in. steel plate of C 0.15, Mn 0.27, Si tr., S 0.05, P 0.03 to carbide of iron of C 0.60, Mn 0.25, Si tr., S 0.55, P 0.03 over a period of several years at a temperature not exceeding 932°F. (500°C.) in blast-furnace gases. Similar results were obtained with Armco iron and with thin strips of electrolytic iron, which carburized in a matter of a couple of weeks. The ferrite in these cases was relatively free of graphitizers. The evidence seems to be that in the absence of graphitizers in solution in the ferrite, carbide of iron is probably in stable equilibrium with ferrite at temperatures below Ac. Byrom's work showed that no carbide was formed in electrolytic iron at 752°F. (400°C.).

In the case in question may it be that the carbide at 935°F. is Fe₃C with the molybdenum in solution in the ferrite, and that the action of the molybdenum in attempting to get into the carbide, which it is said to succeed in

* Superintendent, Research Department, The Midvale Company.

¹³ Byrom: *Jnl. Iron and Steel Inst.* (1915) 92, 106.

doing at somewhat higher temperatures, causes the carbide to dissociate, with the resultant precipitation of carbon in elemental form?

The temperature of graphitization in the case reported by Kinzel and Moore was never clearly stated and, from the description of the cracking process given by Moore, could have been as high as 1228°F. (663°C.), the Ae point of the steel in question. Wells found that "traces of graphite may have been formed" in C 0.13 and there was "slight evidence of traces of graphite" in C 0.28 steel heated at 1292°F. (700°C.) for 150 hr. This is not at all surprising when it is realized that the beginning of the Ac reaction may be well below this temperature.

Although the matter was not recorded in the literature at the time, I found the bottom plates of a petroleum coking still embrittled by the formation of a layer of iron carbide on the face in contact with the layer of coke within the still. The bottoms of such stills were of low-carbon plate, which hardly attained the temperature of incandescence.

The reaction involving the state of carbon in steel below the critical temperature can apparently proceed either toward the formation of graphite or carbide, depending on temperature and the composition of the solid and gaseous phases involved. The direction in which the reaction proceeds is not determined by the state of one of the variables alone.

G. V. SMITH (author's reply).—Though the authors did not attempt (or intend) to develop any theory to account for the effect of added elements upon graphitization it is, of course, interesting to have Mr. Foley's comments on this matter.

There are two subdivisions into which the subject of graphitization can logically be divided; namely, thermodynamic stability and rate of formation. Whether, in a particular instance, carbide or graphite is the stable phase depends, as Mr. Foley has pointed out, on the composition and nature of all the constituents or phases (at equilibrium) present; that is, when it is said that a carbide in a

particular steel is stable, it is meant, of course, that it is stable in equilibrium with ferrite (or austenite), not that it is stable in the free state (as if it were removed from the iron solid solution matrix) Whether an added element acts to increase or decrease the stability of carbide can be measured or calculated in principle at least according to the usual procedures of the chemical thermodynamicist.

The question of rate of graphitization is a much more difficult thing to settle, for we know a great deal less about this than about stability. All that the authors can do is to emphasize that an apparent stability of carbide in a steel may be only the result of a slow rate of reversion to graphite, and conversely, that the accelerating effect of certain elements upon graphitization may result not from an increase in the thermodynamic instability of the carbide, but rather from an effect upon the rate of solution of the carbide or of subsequent diffusion, or on the ease of nucleation and growth of graphite.

The question of the temperature limits for the stability of Fe_3C has received a great deal of attention over a number of years, and the evidence is overwhelming that at least for temperatures below some 2000°F., Fe_3C is unstable with respect to graphite even in the absence of "graphitizers." This is in contradiction to Mr. Foley's conclusion in his third paragraph. May we point out that the fact that Fe_3C will form during the carburizing of steel, low-metalloid iron or electrolytic iron, does not mean that it is a stable phase? Metastable or unstable phases frequently occur, particularly in solid state reactions; the iron-carbon system is an important and outstanding example.

Finally, a minor point, but we cannot accept Mr. Foley's statements that the "Ae" point of the Kinzel and Moore steel was as low as 663°C., nor that in Wells' pure iron-carbon alloys the beginning of the "Ac" reaction may be well below the temperature of 700°C. In both cases transformation on heating cannot occur below the eutectoid temperature, which for these alloys is in the neighborhood of 720°C.

The Bainite Reaction in Hypoeutectoid Steels

BY E. P. Klier* AND TAYLOR LYMAN,† JUNIOR MEMBERS A.I.M.E.

(New York Meeting, February 1944)

THE structures formed when austenite is quenched to subcritical temperatures and allowed to transform isothermally have been the subject of intensive study since the work of Davenport and Bain.¹ Isothermal transformation diagrams summarizing the results of many of these studies have become widely familiar to metallurgists.

Of particular interest to metallographers are the dark-etching, acicular products of transformation formed by isothermal reaction below the temperature of maximum velocity of the austenite to pearlite reaction. These products, the bainite structures, can be formed in a wide variety of steels. However, the constitution of bainite is not well understood and divergent views have been expressed as to its mode of formation.

In this investigation a combination of dilatometric, microscopic and X-ray methods has been brought to bear upon the problem in the hope of some elucidation of the bainite reaction as it occurs in hypoeutectoid steels.

MECHANISM OF BAINITE FORMATION

Davenport and Bain¹ considered the mechanism of bainite formation to consist of two steps—an allotropic transformation followed by precipitation of carbide. The separation in time of the two processes was considered to be very slight in the upper

temperature range and very marked at temperatures just above the martensite range. This concept has been restated by Vilella, Guellich and Bain² in the form of a definition of the acicular mode of transformation as:

The successive, abrupt formation of flat plates of supersaturated ferrite along certain crystallographic planes of the austenite grains; this supersaturated ferrite begins at once to reject carbide *particles*, (not lamellae), at a rate depending upon temperature. In effect, this is the *acicular mode* of transformation, even though the temperature be such as to limit the actual life of the quasi-martensite to millionths of a second.

The investigation of isothermal decomposition of austenite in certain alloy steels (notably those containing chromium or molybdenum) has revealed that there may be a range of temperatures between the pearlite and bainite reactions in which the austenite decomposes at a relatively low rate.³⁻⁶ Further, it is characteristic that in the second region of fast reaction the decomposition of the austenite is incomplete by one reaction but goes to completion by a second reaction. These observations led Wever⁷ to a description of the bainite reaction as follows:

1. The reaction takes place by initial precipitation of a martensitic intermediate structure.
2. In the upper temperature range this structure readily decomposes into ferrite and cementite. In the lower range carbon separates in an unknown form
3. In the upper temperature range the precipitated carbide nucleates the precipitation

Manuscript received at the office of the Institute Dec. 1, 1943. Issued as T.P. 1696 in METALS TECHNOLOGY, June 1944.

* Instructor in Metallurgy, The Pennsylvania State College, State College, Pa.

† Instructor in Metallurgy, University of Notre Dame, Notre Dame, Indiana.

¹ References are at the end of the paper.

of carbide from the remaining austenite [during the second reaction]. In the lower range carbide no longer exerts a nucleating effect on the austenite.

Griffiths, Pfeil and Allen⁸ have given a comprehensive survey of the literature prior to 1939. From the information then available these authors drew idealized curves for reaction rate vs. temperature for several possible cases. They further suggested that the decomposition of austenite may occur by the overlapping of the pearlite and intermediate (bainite) reactions, apparently interpreting the in-

EXPERIMENTAL PROCEDURE

Alloys

It has been shown by Wever and Mathieu¹² that the character of the austenite to bainite reaction changes considerably in degree if not in kind in the iron-manganese-carbon system as the carbon content of low-manganese alloys is increased to bring the steels into the hyper-eutectoid range. Owing in part to this fact, the steels considered in the present investigation have been restricted to hypoeutectoid compositions of low or medium alloy content.

TABLE I.—*Compositions of Steels Investigated*

Steel	Composition, Per Cent							
	C	Mn	Si	Cr	Ni	Mo	Cu	U
3 % Cr. . .	0.38	0.20	0.18	2.98				
1 % Cr. . .	0.44	0.77	0.28	0.98	0.18			
1 % Cr 0.4 % Mo . .	0.42	0.72		0.99	0.05	0.42		
0.2 % Uranium. . .	0.54	0.66						0.2
4 % Ni. . .	0.50	0.73		0.04	3.92			
1.7 % Mn . .	0.39	1.67			<0.10			
1 % Cu. . .	0.32	0.64			<0.10		1.14	
0.22 % C 0.5 % Mn . .	0.22	0.51	0.02					
0.36 % C 0.7 % Mn . .	0.36	0.73	0.07					
0.47 % C 0.8 % Mn . .	0.47	0.80	0.30					

intermediate reaction in the same light as did Wever.

Mehl^{9,10} has postulated that bainite forms by a process of nucleation and growth in which ferrite is the nucleating phase as distinguished from pearlite nucleated by cementite.

Greninger and Troiano¹¹ studied the isothermal decomposition of hypereutectoid austenite and advanced the proposal that austempering products are formed as aggregates, not as single-phase particles.

There is an evident need for new experimental data in order that the mechanism of the austenite to bainite transformation may be established. An examination of alloyed austenites containing various elements in solution is desirable in order that conclusions regarding the generality of phenomena may be arrived at.

The analyses of the steels used are given in Table I. The 3 per cent Cr steel was supplied by the Carpenter Steel Co. in bar form. The 1 per cent Cu steel was available in the form of an ingot weighing about 20 lb. All other alloys are commercial steels received as hot-rolled bars. The 1 per cent Cu steel was forged at 1000°C. (1832°F.), quenched and tempered before the specimens were cut. Specimens of the other steels were cut from the rolled bars. A brief study (see page 17) was made of the 4 per cent Ni steel after a bar had been heated for 14 hr. at 1300°C. (2372°F.) to promote homogeneity.

Dilatometric Method

The dilatometer used was a modification of the type used by Davenport and Bain. Dilatometer specimens were $\frac{1}{16}$ to $\frac{1}{32}$ in.

thick, the distance between notch centers being 1 in. except for the uranium steel, for which an internotch distance of $\frac{3}{4}$ in. was used. Except for the 3 per cent Cr and 1 per cent Cr steels, which were austenitized at 1200°C. for 20 and 15 min., respectively, specimens spot-welded to iron wires were austenitized for 3 min. at 1100°C. (2012°F.) in a vertical tube furnace with purified nitrogen atmosphere. Specimens of 1 per cent Cr steel from a different heat, having a composition almost exactly the same as those austenitized at 1200°C., were austenitized for 3 min. at 1100°C. (2192°F.), and the bainite region of the isothermal transformation diagram determined was found to be almost exactly the same as that for the 1 per cent Cr steel reported here. Specimens were transferred from austenitizing furnace to dilatometer by means of the attached wires. The time elapsing between removal from the austenitizing furnace and immersion in the stirred lead bath was 5 to 8 sec. The temperature of the lead bath was controlled to $\pm 2^\circ\text{C}$. below about 550°C. (1022°F.). At the higher temperatures the control was $\pm 5^\circ\text{C}$. The dial gauge used was graduated in 0.0001 in. and was read to one fourth of a scale division.

Microscopic Examination

Microscopic examination of the alloy steels was carried out on specimens approximately $\frac{1}{4}$ by $\frac{1}{4}$ by $\frac{1}{8}$ in. Specimens of the plain carbon steels were "slivers" $\frac{1}{8}$ by $\frac{1}{8}$ by $\frac{1}{8}$ in. These slivers were austenitized for 1 to 1½ min. at 1100°C. (2012°F.). A few slivers were held at 1100°C. for 3 minutes.

X-ray Methods

Constituents were identified by means of Debye patterns obtained using the K-radiations from chromium and cobalt. Slivers (size given above) were carefully ground on emery paper and etched after heat-treatment, before being placed in the cameras.

When it was desired to check the presence or absence of carbides, slivers were sometimes etched electrolytically in a 5 per cent aqueous solution of hydrochloric acid.

GRAPHICAL PRESENTATION OF RESULTS

The results for seven of the steels studied are reported in graphical form on time-temperature coordinates. For the most part, the lines appearing on these isothermal transformation diagrams have their usual meanings, and it has been considered unnecessary to label the lines indicating the beginning of austenite decomposition and the beginning and end of the pearlite reaction. The lines marked "End of bainite formation" should not be interpreted as meaning, necessarily, that 100 per cent of the austenite has transformed. This point will be discussed as the results are presented.

Ae₁ and Ae₃ temperatures are approximate only, as are the Ar'' temperatures, with the exception of the 3 per cent Cr and 1 per cent Cr steels. The upper limit of the martensite range has been determined by the microscopic method for these two steels.

RESULTS

Steel with 3 Per Cent Chromium

Since the decomposition of austenite in the 3 per cent Cr steel has been studied more thoroughly than in any of the other steels reported, the transformation characteristics will be considered in detail. Microscopic and dilatometric data are summarized in the isothermal transformation diagram given in Fig. 1.

Above approximately 700°C. (1292°F.) decomposition of austenite begins with precipitation of ferrite. The amount of ferrite formed before the start of the pearlite reaction is a function of the temperature, being a maximum at Ae₁ and decreasing to zero at about 690°C. (1274°F.). Between 690° and about 590°C.,

it is not possible to distinguish a separate ferrite precipitation. At 550°C. ferrite is again precipitated before the pearlite reaction sets in.

and below yields the temperature of minimum rate as about 520°C. Below 520°C. the austenite has not been completely transformed, although specimens

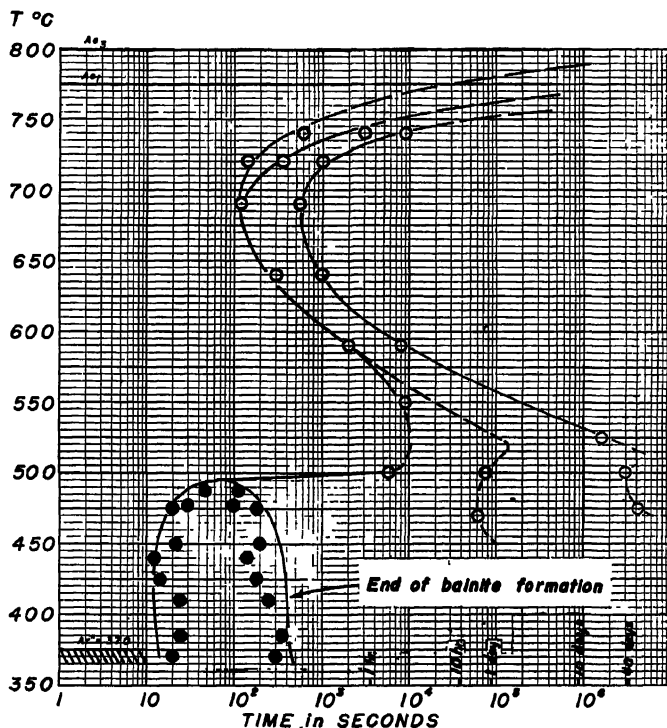


FIG. 1.—ISOTHERMAL TRANSFORMATION DIAGRAM FOR 3 PER CENT CHROMIUM STEEL.

Open circles, points determined metallographically.

Filled circles, 0.5 per cent and 99.5 per cent extension in dilatometer.

C, 0.38 per cent; Mn, 0.20; Cr, 2.98. Austenitized at 1200°C. Grain size, 2-3.

At 500°C. ferrite precipitation starts after approximately 6000 sec. at temperature. This precipitation continues at a very low rate. A second reaction sets in at about 75,000 sec. The two reactions proceed together very slowly, complete transformation of the austenite requiring more than 35 days. A representative photomicrograph is shown in Fig. 2.

Near 520°C. (968°F.) a region of minimum reaction rate for both ferrite and pearlite reactions is indicated. The start of the "pearlite" reaction has been accurately determined at 500° and 470°C. and extension of the curves from above

showing more than 90 per cent decomposition were obtained at 500° and 475°C. The curve for the end of the second reaction has been drawn in conformity with these observations.

Below 500°C. austenite decomposition proceeds in a different fashion. Transformation begins in less than 30 sec. at all temperatures from 490° to 370°C. and, as is most clearly shown by dilatometric data, appears to stop in less than 5 min. When the transformation stops there remains austenite, which is undecomposed. The reaction of the last traces of this austenite requires more than 40 days at

475°C., while at temperatures below this the time for complete reaction becomes so great as to preclude determination.

bainite reaction—is a function of the temperature. At 490°C. less than 10 per cent of the austenite decomposes by the



FIG. 2.—3 PER CENT CHROMIUM STEEL QUENCHED FROM 1200°C. TO 500°C AND HELD FOR 8 DAYS, $3\frac{1}{2}$ HOURS
Original magnification 500; reduced $\frac{1}{4}$ in reproduction. Etched in Nital.
Ferrite, second reaction product (dark) and unreacted matrix (white).

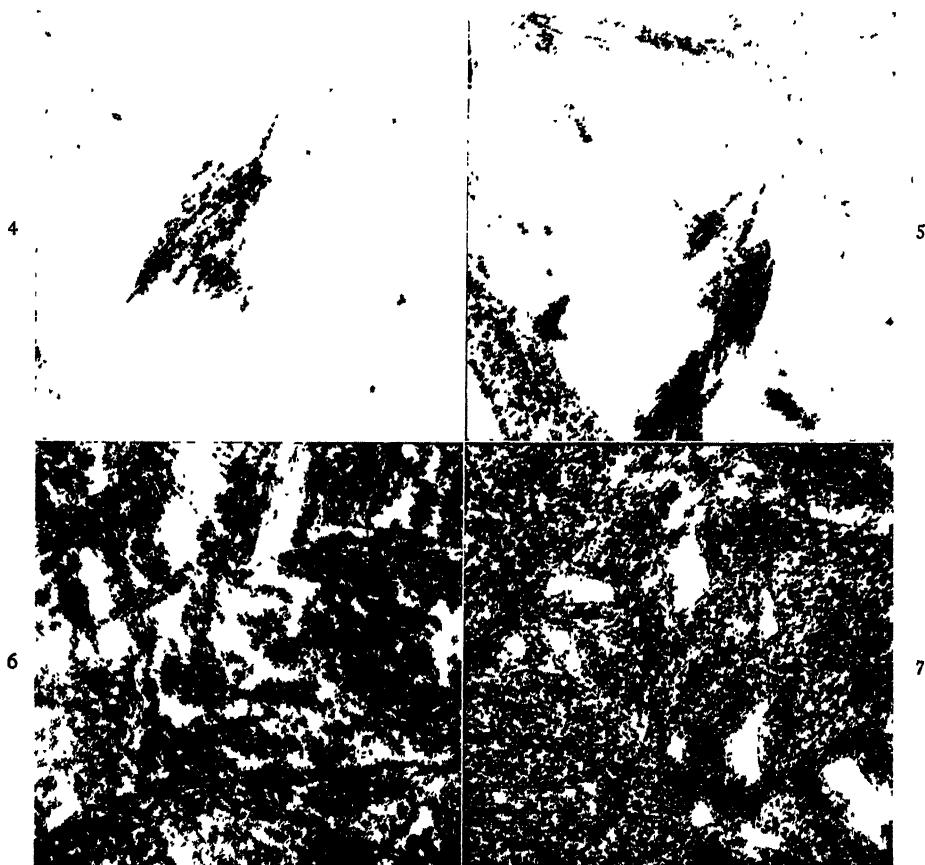
FIG. 3.—3 PER CENT CHROMIUM STEEL QUENCHED FROM 1200°C. TO 460°C. AND HELD FOR 18 DAYS
Original magnification 500; reduced $\frac{1}{4}$ in reproduction. Etched in Nital.
Bainite, second reaction product (dark) and unreacted matrix (white).

The amount of transformation that takes place by the first reaction—the

bainite reaction while at 450°C. the degree of completion is about 80 per cent in less

than 5 min. Even after $15\frac{1}{2}$ hr., no further transformation is evident. Figs. 4 to 7 are illustrative of the decomposition progress at 450°C .

servable dilatometrically and the total extension increases rapidly with decreasing temperature. While the degree of completion is not directly proportional to the



FIGS. 4-7.—3 PER CENT CHROMIUM STEEL QUENCHED FROM 1200°C . TO 450°C . AND HELD FOR TIMES INDICATED. $\times 500$. ETCHED IN NITAL.

Fig. 4. 20 seconds.
Fig. 5. 1 minute.

Fig. 6. 15 minutes
Fig. 7. $15\frac{1}{2}$ hours.

The temperature dependence of the degree of completion of the bainite reaction in this steel is made evident from a consideration of the total extensions of the dilatometer specimens during the reaction. These total extensions are plotted against the reaction temperature in Fig. 8. At about 490°C . the reaction takes place in an amount just great enough to be ob-

total extension at a given temperature, for reasons that have been discussed by Wever and Jellinghaus⁴ and Allen, Pfeil and Griffiths,¹³ the curve of Fig. 8 indicates that there is an important temperature dependence. At no temperature investigated did complete transformation of the austenite take place by the bainite reaction. Figs. 9 to 12 show that the rate

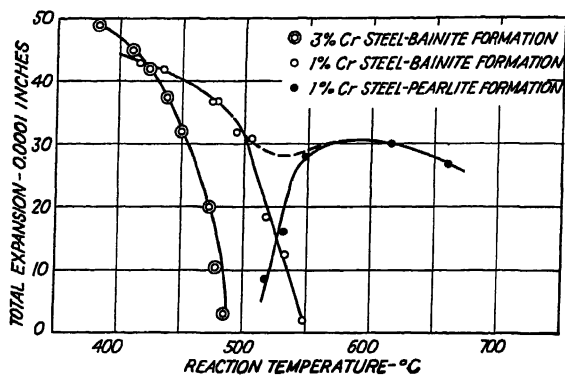
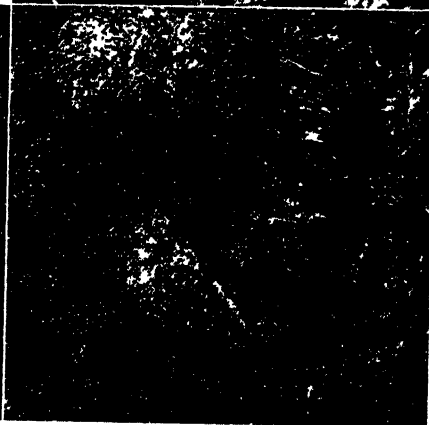
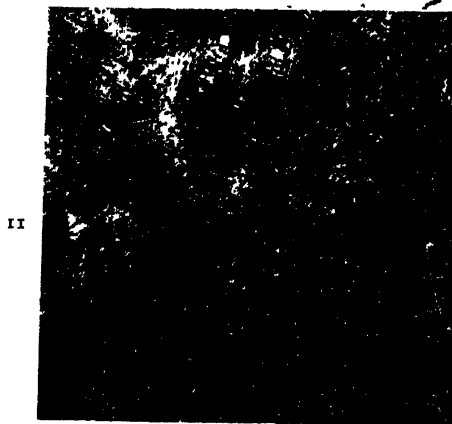


FIG. 8.—DEPENDENCE OF TOTAL EXPANSION OF DILATOMETER SPECIMENS UPON REACTION TEMPERATURE DURING ISOTHERMAL DECOMPOSITION. All specimens 1 inch between notch centers.



FIGS. 9-12.—3 PER CENT CHROMIUM STEEL QUENCHED FROM 1200°C. TO 350°C. AND HELD FOR TIMES INDICATED. $\times 200$. ETCHED IN NITAL.

Fig. 9. 1 minute.

Fig. 10. 2 minutes.

Fig. 11. 4 minutes.

Fig. 12. 29 minutes.

during the first 4 min. is comparatively high and that after 29 min. at 350°C. there is austenite still untransformed.

Debye patterns obtained from sliver

present at room temperature. Austenite lines are not present after a direct quench from above A_{e3} to room temperature. The X-ray data relating to gamma retention

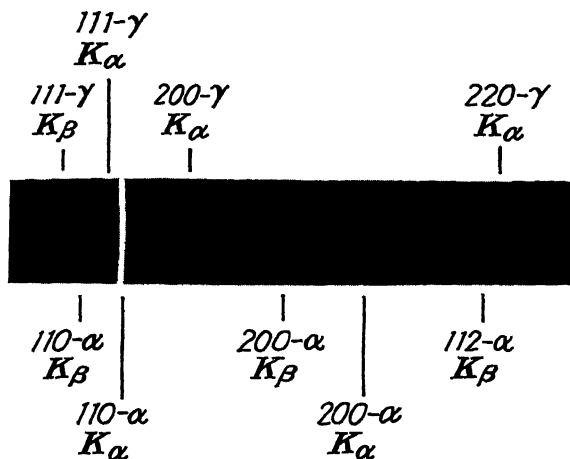


FIG. 13.—DEBYE PATTERN OBTAINED FROM 3 PER CENT CHROMIUM STEEL SLIVER TRANSFORMED AT 450°C. FOR 6 MINUTES. Unfiltered chromium radiation.

specimens transformed to completion of the bainite reaction at temperatures from 475° to 350°C. show that austenite is

TABLE 2.—Phase Identification Obtained with the 3 Per Cent Chromium Steel after Transformation in the Bainite Region

Transformation Temperature		Time at Temperature	Structure and X-ray Line Intensity
Deg. C.	Deg. F.		
475	887	90 sec.	Very weak gamma
475	887	180 sec.	Medium gamma
475	887	23 hr.	Tetragonal split, diffuse
450	842	90 sec.	Weak gamma
450	842	180 sec.	Strong gamma
450	842	360 sec.	Very strong gamma
450	842	1 hr.	Medium gamma
450	842	15 hr.	Very weak gamma + tetragonal split
450	842	26 hr.	Tetragonal split
405	761	30 sec.	Weak gamma
405	761	60 sec.	Very weak gamma
405	761	180 sec.	Gamma (?)
405	761	300 sec.	Very weak gamma
350	662	60 sec.	Very weak gamma
350	662	120 sec.	Very weak gamma

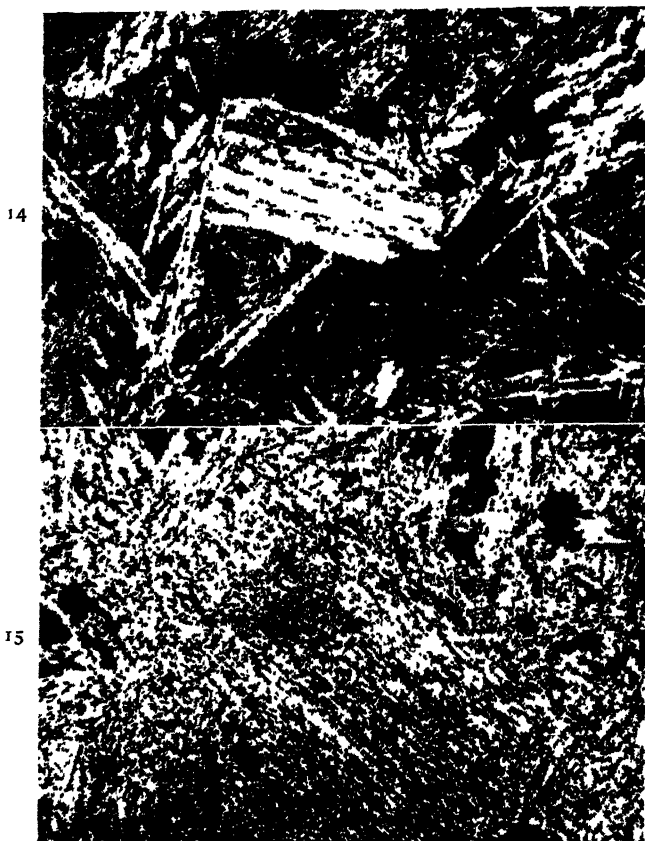
are summarized in Table 2, and a representative X-ray pattern is reproduced in Fig. 13. At 475°C., about 20 per cent of the austenite transforms by the bainite reaction and gamma lines in the X-ray pattern are quite distinct. Of greatest importance is the location of this austenite in the microstructure.

In an effort to find the austenite, numerous specimens were transformed isothermally, water-quenched and then tempered. Figs. 14 and 15 show representative tempered structures. The complete darkening of the matrix after tempering indicates that the matrix austenite present at 475°C., after the bainite reaction ends, transforms to martensite on cooling to room temperature. This eliminates the possibility of sufficient gamma in the matrix remaining untransformed to give the pattern. That the gamma remains after tempering has been shown for a sliver of the 3 per cent Cr steel held at 450°C. for 6 min., water-

cooled and tempered at 475°C. for 30 min. The gamma lines, though distinct after this treatment, were much less so than before final tempering.

lowered so that considerable austenite remains at room temperature.

The first possibility can be eliminated by consideration of the tempered structure.



FIGS. 14 AND 15.—3 PER CENT CHROMIUM STEEL PARTIALLY TRANSFORMED IN THE BAINITE REGION, QUENCHED AND TEMPERED.

Original magnification 500; reduced $\frac{3}{4}$ in reproduction.

Picral etch. Dark-etching background indicates that matrix was martensite after first quench to room temperature.

Fig. 14. Quenched from 1200°C. to 475°C., held for 4 minutes, quenched to room temperature, tempered at 750°C. for 15 seconds and quenched.

Fig. 15. Quenched from 1200°C. to 450°C., held for 3 hours, quenched to room temperature, tempered at 450°C. for 45 minutes and quenched.

Two possibilities logically present themselves as accounting for this retained austenite: (1) austenite of unchanged carbon content is "stabilized"; (2) austenite immediately surrounding the precipitate is enriched to such a degree that Ar'' is

If the austenite were retained by a stabilization process it would be logical to expect some of it to be situated in the parts of the specimen that at transformation temperature contained the greatest amounts of austenite. It is evident from

Fig. 15 that there is no appreciable amount of austenite present in the darkened matrix.

There is other evidence that the austenite retained is enriched:

1. On holding at constant temperature the gamma patterns gradually become weaker. Although at 475°C. (887°F.) the second reaction does not begin until approximately 20 hr. has elapsed, gamma is no longer evident in the X-ray patterns after approximately 1 hr. As the intensity of the gamma lines decreases a tetragonal split appears, which is still present after 23 hours.

2. Gamma lines were most intense after 6 min. at 450°C. (842°F.). They are retained, although weak, through 15 hr. at temperature.

3. At temperatures below 450°C. the intensity of the gamma lines rapidly diminishes, regardless of the degree of decomposition that has taken place. At 350°C. (662°F.) the bainite reaction goes nearly to completion, yet in all patterns taken gamma was discernible only with great difficulty.

Table 3 contains X-ray data obtained from specimens decomposed at 500°C. (932°F.). The following facts are emphasized.

TABLE 3.—*Martensite Axial Ratios after Isothermal Decomposition of Austenite in 3 Per Cent Chromium Steel at 500°C.*

TIME AT TEMPERATURE	c/a
5 hr.	*
17 5 hr.	*
26 hr.	1.022
41.5 hr.	1.021
48.5 hr.	1.021
55.5 hr.	1.020
67.5 hr.	1.019
120 hr.	*
13 days	*

* Diffuse alpha lines.

The formation of ferrite, which starts after 100 min. at temperature, and the diffusion of carbon occur in such a manner that after 26 hr. an enriched austenite is obtained, which, during water-quenching to room temperature, forms martensite

with an axial ratio of 1.02. This tetragonality is maintained until approximately 70 hr., after which it is gradually reduced so that after 120 hr. at temperature no tetragonal split is observed. Sharp alpha lines, however, are not obtained after 13 days at temperature.

Since, according to the results of Honda and Nishiyama,¹⁴ who used techniques very similar to those employed in the present work, a tetragonality of 1.02 for a plain carbon martensite corresponds to a carbon content of 0.5 to 0.6 per cent, it might appear that an enrichment of the austenite to eutectoid composition had taken place after 26 hr. at 500°C. However, the position of the eutectoid composition in the Fe-Cr-C system is not known accurately enough to allow this conclusion to be drawn and, since the decreasing axial ratio does not correspond to a large reduction in the amount of austenite transforming to martensite on cooling, a different explanation must be found.

In connection with these observations, two considerations regarding the movement of carbon at temperatures within the bainite range are important:

1. During the relatively short period of the bainite transformation carbon movement is very rapid, in order to produce the local enrichment that has already been indicated.

2. At the end of the bainite reaction a condition is reached in which the velocity of carbon movement is smaller by orders of magnitude than that at the start of the reaction, the lower rate being probably of the order of magnitude of the rate of diffusion under the simple influence of a concentration gradient at this temperature. Consistent with this supposition are the fact that the bainite reaction does not continue to the point where all the austenite is transformed and the fact that the undecomposed portion does not react except after a long delay.

It seems evident that the tetragonal split observed during transformation at 500°C. is due not to an enrichment of the austenite matrix to eutectoid composition but rather to an enrichment of the austenite immediately surrounding the precipitate. This carbon in enriched regions slowly diffuses into the surrounding austenite and the tetragonal split disappears. The matrix austenite may then be at eutectoid composition. The decomposition then proceeds by the formation and growth of ferrite and carbon-rich masses at the expense of the austenite.

Crafts and Offenauer¹⁶ have studied the carbide structure in a 2.6 per cent Cr, 0.4 per cent C steel as a function of the temperature at which it formed during the decomposition of martensite. A change in the carbide structure slightly above 500°C. was observed by these investigators. As will be shown later, such a change in the carbide can have no effect on the bainite transformation but may well play an important role in the course of the second transformation. For this reason a study of the carbides formed during isothermal decomposition of the 3 per cent Cr steel was undertaken, the results of which are summarized in Table 4.

Between 600°C. (1112°F.) and about 500°C. (932°F.) no carbide structure is sufficiently well formed to give a good pattern. However, a very good carbide pattern was obtained after 3 min. at 450°C. (842°F.). The pattern indicated the presence of Fe_3C . After 15.5 hr. at 450°C. this structure was unchanged. The rate at which the bainite transformation takes place would seem to preclude the possible diffusion of chromium from the precipitating volumes. Since enriched austenite exists within the volumes occupied by the first transformation product and remains undecomposed for hours (Table 2), it seems necessary to assume that the Fe_3C is formed within the volumes depleted in carbon during transformation. The dark-

etching appearance of bainite is consistent with this view. Thus the carbide formed is characteristic of a 3 per cent Cr, low-carbon (considerably less than 0.4 per cent C) steel. As a consequence the carbide structures formed during the bainite reaction cannot be expected to throw light on the transition temperature for a carbide formed from a 3 per cent Cr, 0.4 per cent C martensite.

TABLE 4.—Carbide Identification Obtained with the 3 Per Cent Chromium Steel after Isothermal Decomposition at Various Temperatures

Transformation Temperature		Time at Temperature	Structure and X-ray Line Intensity
Deg. C	Deg. F		
750	1382	2.25 hr	Weak Fe_3C plus Cr_7C_3
720	1328	1080 sec.	Weak Fe_3C
650	1202	900 sec.	Very weak Fe_3C
600	1112	1.75 hr.	Fe_3C (?)
450	842	90 sec.	Fe_3C (?)
450	842	180 sec.	Medium Fe_3C
450	842	15.5 hr.	Strong Fe_3C

The fact that good Fe_3C lines may be obtained from bainite formed at 450°C., 50°C. below the carbide transition temperature, whereas, at 600°C. the carbide structure is identified only with considerable difficulty does not then detract from the contention that the carbide transition temperature is in the neighborhood of 500°C.

The consequences of such carbide transition will be evident not in the bainite reaction which gives rise to a transitional structure based on the body-centered cubic form of iron, but rather in the second reaction which results in the formation of both ferrite and carbide.

The rate of transformation by the second reaction must increase with decreasing temperature just below the transition temperature on theoretical grounds. As has been explained, the line representing the end of austenite decomposition at temperatures below 600°C. cannot be

considered to be determined accurately. However, the experimental data are definite in indicating that the initial rate of the second reaction is greater at 470°C. than at 500°C., and that the period of induction is shorter at 470°C.

From the preceding discussion, it appears possible to describe the isothermal decomposition of austenite in the bainite region as follows:

1. In restricted volumes, carbon atoms move in such a way as to yield austenite regions of alternate high-carbon and low-carbon concentration.

2. The low-carbon austenite transforms by a martensite-like process into a super-saturated ferrite.

3. The supersaturated ferrite formed begins at once to decompose, precipitating an iron carbide in a ferrite matrix to form the dark-etching, acicular product that has become known as bainite.

4. The enriched austenite decomposes or by diffusion loses a part of the dissolved carbon.

5. The austenite that has not taken part in the bainite transformation, that is, the unreacted matrix, decomposes by a mechanism which is to be distinguished from the mechanism of the austenite to bainite reaction. It is possible that at certain temperature levels the decomposition of the matrix austenite will precede the decomposition of the enriched austenite.

*Steel with 1 Per Cent Chromium and
0.4 Per Cent Molybdenum and Steel
with 1 Per Cent Chromium*

The isothermal transformation diagrams for the 1 per cent Cr, 0.4 Mo and the 1 per cent Cr steels are given in Figs. 16 and 17, respectively. The upper portion of Fig. 16 has been drawn in dashed lines on the basis of microscopic examination of specimens transformed at three temperatures. Previously published diagrams^{16,17} for S.A.E. steels of the 1 per cent Cr, 0.2 per cent Mo type are in agreement on the facts that

ferrite precipitation precedes pearlite formation at all temperatures above the bainite region and that the pearlite reaction is considerably retarded by the addition of molybdenum.

The diagram for the 1 per cent Cr steel shows an almost continuous merging of the proeutectoid ferrite and bainite reactions. The pearlite reaction appears to undergo no discontinuity with temperature change such as has been shown for the 3 per cent Cr steel to be due to carbide transition. According to the data of Crafts and Offen-hauer,¹⁸ Fe₃C is formed at all temperatures below Ae₁ in a 1 per cent Cr, 0.4 per cent C steel.

It may be noted that the ferrite separation process in the 1 per cent Cr 0.4 per cent Mo steel just above the bainite range is qualitatively similar to the corresponding process in the 3 per cent Cr steel, although in the latter there is a carbide transition in this temperature range while in the 1 per cent Cr, 0.4 per cent Mo steel the data of Crafts and Offenauer¹⁸ indicate that there is no change in carbide structure with temperature. This further substantiates the conclusion already reached that carbide transition will not influence the course of the bainite reaction.

It is evident from dilatometric, X-ray and microscopic data that the mode of transformation of these steels in the bainite region is the same as in the 3 per cent Cr steel. In each of these steels the amount of transformation of austenite to bainite was found to be dependent on temperature. Thus the lines on the transformation diagrams marked "End of bainite formation" do not indicate that all of the austenite has transformed. In Fig. 8 the total extensions of dilatometer specimens are plotted against reaction temperature for the 1 per cent Cr steel to illustrate this fact. It is evident that there is a temperature region for this steel in which two reactions have been separated by the dilatometric method.

For both steels it was possible to retain enriched austenite at room temperature after transformation of austenite to bainite. Observations at different temperatures

steel. Ar'' was determined by the microscopic method for both steels. As was pointed out by Klier and Troiano,¹⁹ the Ar'' temperatures for 1 per cent Cr and

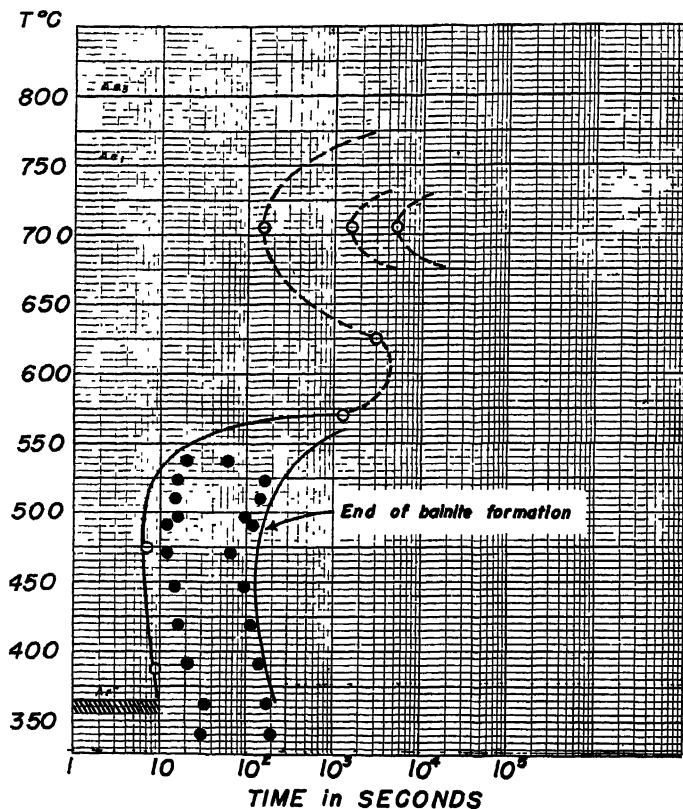


FIG 16.—ISOTHERMAL TRANSFORMATION DIAGRAM FOR 1 PER CENT CHROMIUM, 0.4 PER CENT MOLYBDENUM STEEL.

Open circles, points determined metallographically

Filled circles, 2.5 per cent and 97.5 per cent extension in dilatometer.

C, 0.42 per cent; Mn, 0.72; Cr, 0.99; Mo, 0.42. Austenitized at 1100°C. Grain size, 3-4.

within the bainite region indicated that the degree of enrichment is a function of temperature of transformation. The X-ray work was carried only far enough to establish qualitative similarity to the results obtained in the 3 per cent Cr steel, which was investigated in considerable detail.

It may be noted that the Ar'' temperature for the 1 per cent Cr steel is about 30°C. lower than that for the 3 per cent Cr

3 per cent Cr steels of identical carbon and manganese contents should be nearly the same; therefore it is probable that the considerable difference in the manganese contents of the two steels accounts for the lower Ar'' temperature of the 1 per cent Cr steel investigated here.

Steel with 0.2 Per Cent Uranium

The transformation diagram for a 0.2 per cent uranium steel is presented in

Fig. 18. In general, the characteristics of bainite formation observed in steels already described have been confirmed in this steel. However, the pearlite and bainite trans-

formation of bainite or proeutectoid ferrite (the two reactions merge at about 600°C.) precedes the formation of pearlite

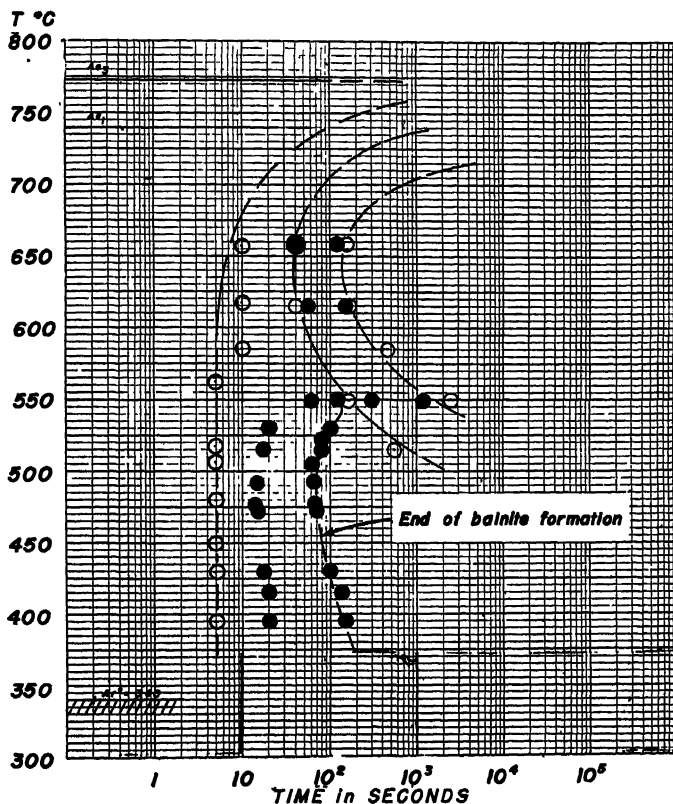


FIG. 17.—ISOTHERMAL TRANSFORMATION DIAGRAM FOR 1 PER CENT CHROMIUM STEEL
Open circles, points determined metallographically.
Filled circles, 2.5 and 97.5 per cent extension in dilatometer.
C, 0.44 per cent; Mn, 0.77; Cr, 0.98 Austenitized at 1200°C. Grain size, 2

formations overlap to such a degree between 550° and 500°C. (1022° and 932°F.) that separation of the two is not possible using the dilatometric method. The curves for the beginning of pearlite and end of bainite formation in this region are drawn on the basis of microscopic observations and are intended to show that above 520°C. (968°F.) bainite formation is only partly completed before the pearlite reaction begins. A dilation-time curve obtained at 558°C. (1036°F.) showed

at all temperatures. The amount of precipitation occurring before the start of the pearlite reaction varies with temperature, being a minimum at about 625°C.

Steel with 4 Per Cent Nickel

Investigations carried out on a 4 per cent Ni steel have shown that there is a range of temperatures in which decomposition of austenite takes place with both bainite and pearlite formation.

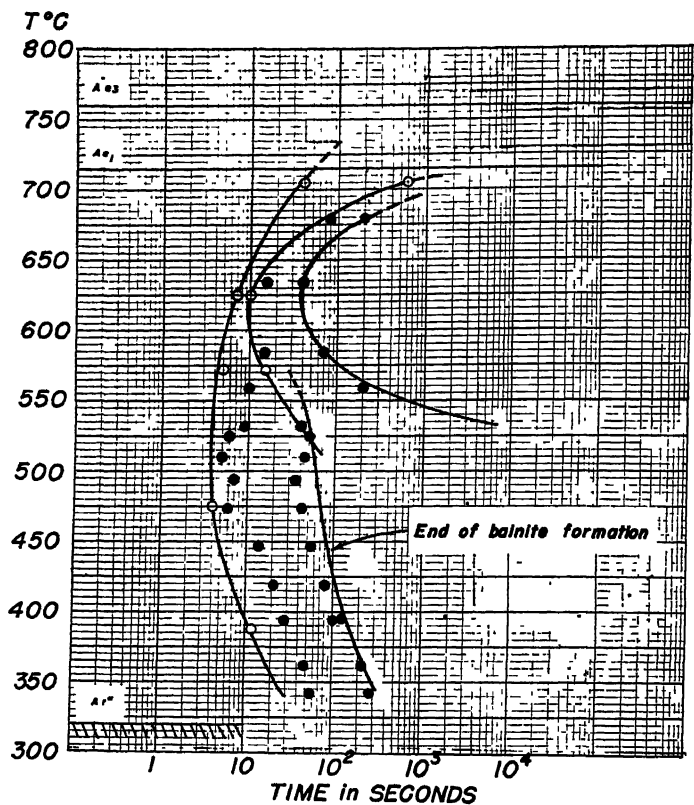


FIG 18.—ISOTHERMAL TRANSFORMATION DIAGRAM FOR 0.2 PER CENT URANIUM STEEL
 Open circles, points determined metallographically.
 Filled circles, 2.5 and 97.5 per cent extension in dilatometer.
 C, 0.54 per cent; Mn, 0.60; U, 0.2. Austenitized at 1100°C. Grain size, 5.

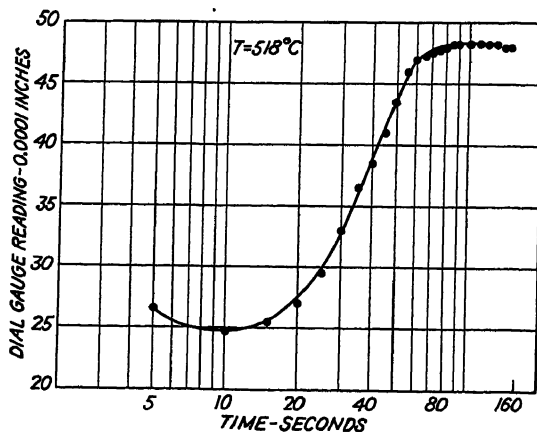


FIG. 19.—DILATION VS. TIME CURVE OBTAINED DURING ISOTHERMAL TRANSFORMATION OF 4 PER CENT NICKEL STEEL AT 518°C

Dilation vs. time curves obtained gave no indication that two reactions were proceeding together at temperatures in the neighborhood of 500°C. (932°F.). Fig. 19

considerably better than in the range where two reactions are occurring.

The photomicrographs of Figs. 21-24 illustrate the progress of the two reactions

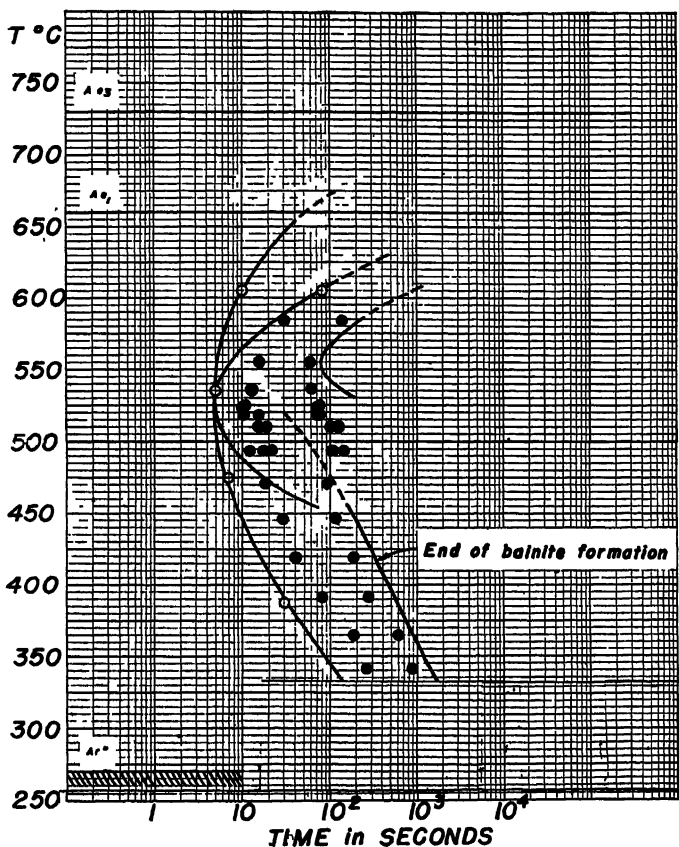


FIG. 20.—ISOTHERMAL TRANSFORMATION DIAGRAM FOR 4 PER CENT NICKEL STEEL. Open circles, points determined metallographically. Filled circles, 2.5 and 97.5 per cent extension in dilatometer. C, 0.50 per cent; Mn, 0.73; Ni, 3.92 Austenitized at 1100°C. Grain size, 3-4.

is a typical dilatometric curve. Microscopic observation of partially reacted specimens quenched from temperatures between 450° and 540°C. have been used to place the positions of the lines in this region of the isothermal transformation diagram (Fig. 20). The plotted dilatometric points in this region show a considerable scatter. In the lower temperature region reproducibility of beginning and end of dilation has been observed to be

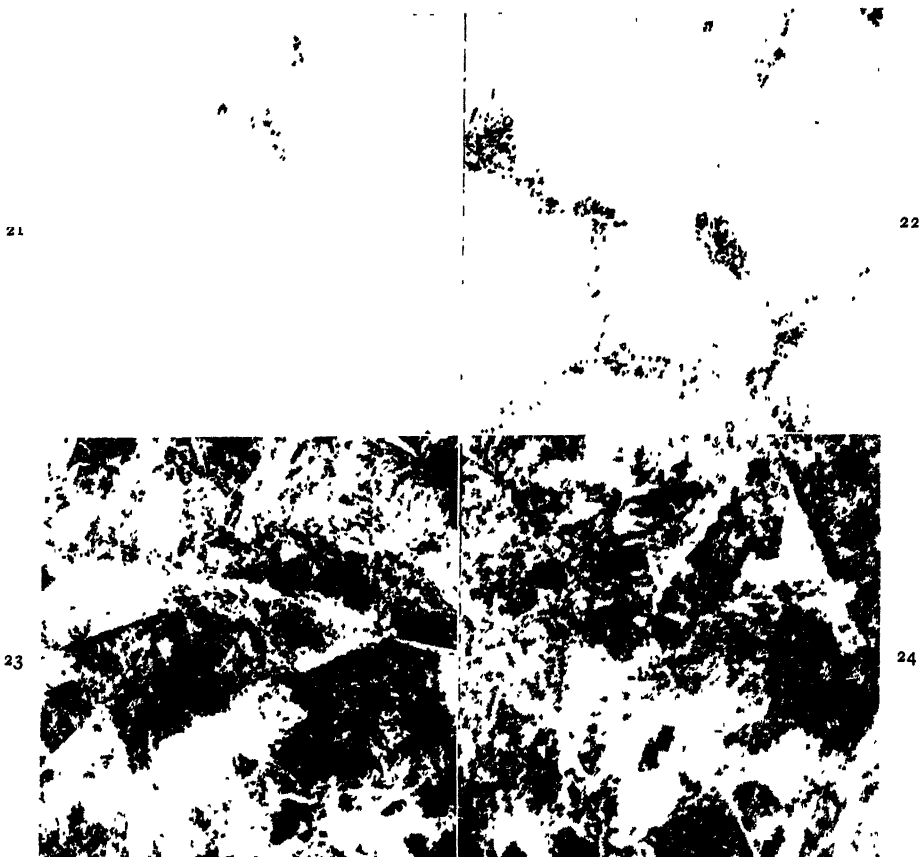
at 518°C. (964°F.), the temperature at which the dilation vs. time of Fig. 19 was obtained. After 240 sec. at 518°C., transformation is not complete.

At 525°C. (977°F.) transformation is predominantly by the pearlite mechanism. Below 475°C. (887°F.) the bainite reaction assumes the major role. No nodular structures of easy recognition occur below about 460°C. (860°F.)

The presence of austenite in partially reacted slivers quenched from the range 475° to 525°C. cannot be interpreted as evidence of enrichment, since austenite

transformation characteristics except that corresponding stages of transformation were reached in shorter times.

The occurrence of an overlapping of the



FIGS. 21-24.—4 PER CENT NICKEL STEEL QUENCHED FROM 1100°C. TO 518°C. AND HELD FOR TIMES INDICATED. $\times 500$. ETCHED WITH PICRAL.

Fig. 21. 10 seconds.

Fig. 22. 20 seconds.

Fig. 23. 120 seconds.

Fig. 24. 240 seconds.

can be retained in this steel on a direct quench from above A_{e_3} .

In order to determine the effect of homogenization on the transformation characteristics, a bar of this steel was heated at 1300°C. (2372°F.) for 14 hr. A brief metallographic study of the homogenized material was restricted to the temperature range 475° to 525°C. and showed that there was no change in the

two reaction mechanisms in this 4 per cent Ni steel is not entirely unexpected in view of the results of Lange and Mathieu²⁰ on steels of somewhat higher nickel contents.

Steels with 1 Per Cent Copper and 1.7 Per Cent Manganese

The transformation diagrams for the 1 per cent Cu and 1.7 per cent Mn steels are given in Figs. 25 and 26, respectively.

Metallographic study showed that the progress of transformation in both steels was similar in all important respects to that observed in the 4 per cent Ni steel.

Plain Carbon Steels

Three hypoeutectoid plain carbon steels have been investigated. Transformation rates are very high in these steels—com-

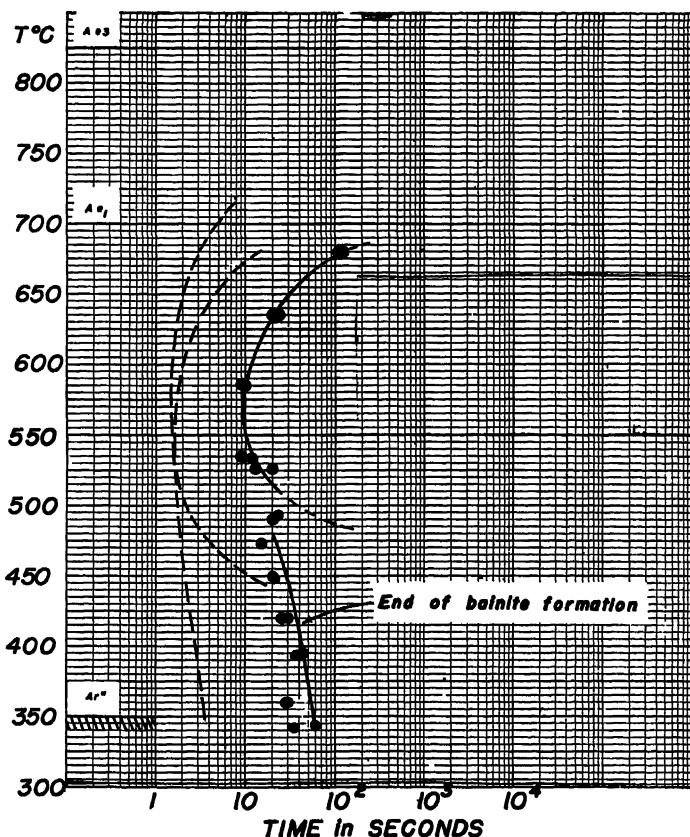


FIG. 25.—ISOTHERMAL TRANSFORMATION DIAGRAM FOR 1 PER CENT COPPER STEEL. Plotted points represent 97.5 per cent extension of dilatometer specimens. C, 0.32 per cent; Mn, 0.64; Cu, 1.14. Austenitized at 1100°C. Grain size, 4-5.

Having established this similarity, it was deemed unnecessary to attempt to place the boundaries with precision and the diagrams for these two steels are to be regarded as approximate only. The degree of completion of the bainite reaction increases with decreasing temperature and the overlapping of bainite and pearlite reactions extends over a range of about 50° to 75°C. in both cases.

plete decomposition occurred in 3 sec. at 570° to 600°C. (1058° to 1112°F.) in the 0.36 per cent C, 0.7 per cent Mn steel—and if the isothermal method of study is to be used specimens must be very small. Accordingly, sliver specimens only were used. These slivers were examined microscopically before X-ray analysis. The accuracy of measurement of time at

temperature was not great enough to allow transformation diagrams to be drawn.

Pertinent results obtained with the 0.36 per cent C, 0.7 per cent Mn steel are as follows:

conclusion that the most probable location of this austenite is that indicated by arrows in Fig 28. This places the austenite in contact with the carbon-poor ferrite and permits the conclusion, already con-

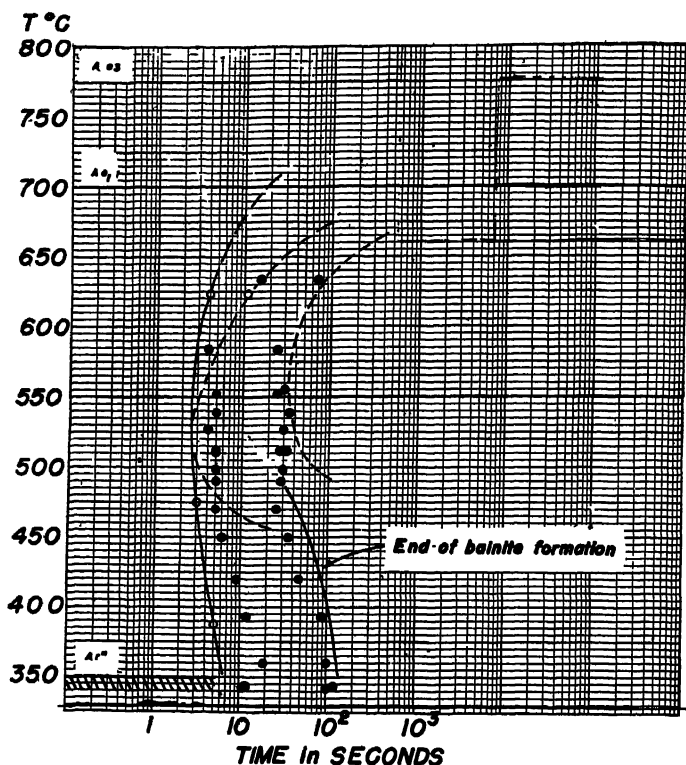


FIG. 26.—ISOTHERMAL TRANSFORMATION DIAGRAM FOR 1.7 PER CENT MANGANESE STEEL.

Open circles, points determined metallographically.

Filled circles, 2.5 and 97.5 per cent extension in dilatometer.

C, 0.39 per cent; Mn, 1.67. Austenitized at 1100°C. Grain size, 3-4.

1. A specimen held for less than one second at 620°C. contained ferrite plus pearlite that was not fully resolved with an objective of numerical aperture 1.30.

2. After one second at 570°C., decomposition was about 30 per cent. The structure is shown at two magnifications in Figs 27 and 28. An X-ray pattern obtained from this specimen showed that austenite was present at room temperature. Consideration of the morphological and etching characteristics have led to the

considered in some detail for the 3 per cent Cr steel, that austenite is present at room temperature as a result of carbon enrichment.

3. Near 500°C. (932°F.) the course of transformation during the first 2 sec. at temperature was difficult to follow. The first product to form isothermally has etching characteristics almost identical with the martensite formed during subsequent quenching to room temperature. The size and shape of this product are

roughly comparable with the size and shape of martensite "needles." After 3 sec. at 505°C. both acicular and nodular transformation products are present in considerable amount. The acicular product has become dark-etching and may be designated bainite. After 5 sec. at 406°C. decomposition is about 50 per cent, as shown in Figs. 29 and 30.*

4. At 450°C. the reaction has just started in 2 sec., as shown in Fig. 31. Holding for 3 sec. gives the structure of Fig. 32. X-ray patterns from the latter structure show the presence of lines that could be Fe_3C lines. Figs. 31 and 32 illustrate the transient character of the product first formed at 450°C. in this steel. Once formed, an additional second at temperature is sufficient to cause considerable decomposition and change materially the etching characteristics. That the structures are not the result of etching technique is shown by a consideration of the matrix structure. In both Figs. 31 and 32 the martensite matrix is revealed to about the same degree.

Austenite lines, though weak, have been positively identified on the X-ray patterns obtained from specimens held for short times at temperatures between 500° and 570°C. No positive evidence of austenite in specimens partially reacted at 450°C. has been obtained.

It seems possible to describe the transformation kinetics for this steel as follows:

1. During decomposition at temperatures between 620° and 570°C. the ferrite reaction remains distinct from the pearlite reaction, although at certain temperatures the two reactions may proceed simultaneously.

2. At about 570°C. the ferrite reaction merges into the bainite reaction. Decomposition at temperatures between 570° and 500°C. takes place with the formation of both bainite and pearlite.

3. At 450°C. decomposition appears to go to completion by the bainite reaction.

A 0.22 per cent C, 0.5 per cent Mn steel and a 0.47 per cent C, 0.8 per cent Mn steel were examined to determine whether there were any important differences in the transformation characteristics of the three plain carbon steels. The results indicated a general similarity. Austenite lines were easily obtained from the 0.47 per cent C steel. A Debye pattern from a sliver of the 0.22 per cent C steel held for 1 sec. at 523°C. showed very faint austenite lines.

A photomicrograph of the 0.47 per cent C steel held 6 sec. at 518°C. shows both nodular and acicular products (Fig. 33). The appearance of new needles in the matrix and the branching of needles is illustrated. It has been observed in several of the steels studied that the bainite reaction proceeds in this fashion as well as by the apparent extension of platelike volumes in two dimensions.

It seems possible to define the bainite reaction for these hypoeutectoid plain carbon steels in the same terms that have been used to characterize the reaction in the alloy steels. The differences are considered to be differences in degree only.

DISCUSSION OF RESULTS

The isothermal transformation diagrams determined in the course of this work have been presented in the approximate order of increasing similarity to the results for plain carbon steels. Transformation within a single austenite crystal by two reaction mechanisms at some, perhaps all, temperatures within the bainite range is considered to be a characteristic feature of isothermal austenite decomposition in hypoeutectoid steels. These two reaction mechanisms may

* Diffraction patterns obtained from this specimen and from specimens held for short times at 543° and 516°C. contained lines that do not correspond to lines from ferrite, austenite, or Fe_3C . Reproducibility of these results has not been good. It is tentatively suggested that decomposition to form Fe_3C takes place through a transition phase at some temperatures.

be widely separated in time or they may overlap to such an extent that it is difficult reaction sets in within a few seconds after the beginning of the bainite reaction. Thus,



FIGS. 27 AND 28.—STEEL SLIVER (0.36 PER CENT CARBON, 0.7 MANGANESE) QUENCHED FROM 1100° TO 570°C., HELD FOR 1 SECOND AND QUENCHED TO ROOM TEMPERATURE.

X-ray pattern showed that austenite was present in this specimen after the quench to room temperature.

Fig. 27, $\times 1000$; Fig. 28, $\times 2500$. Etched in dilute Picral.

Arrows indicate probable locations of austenite.

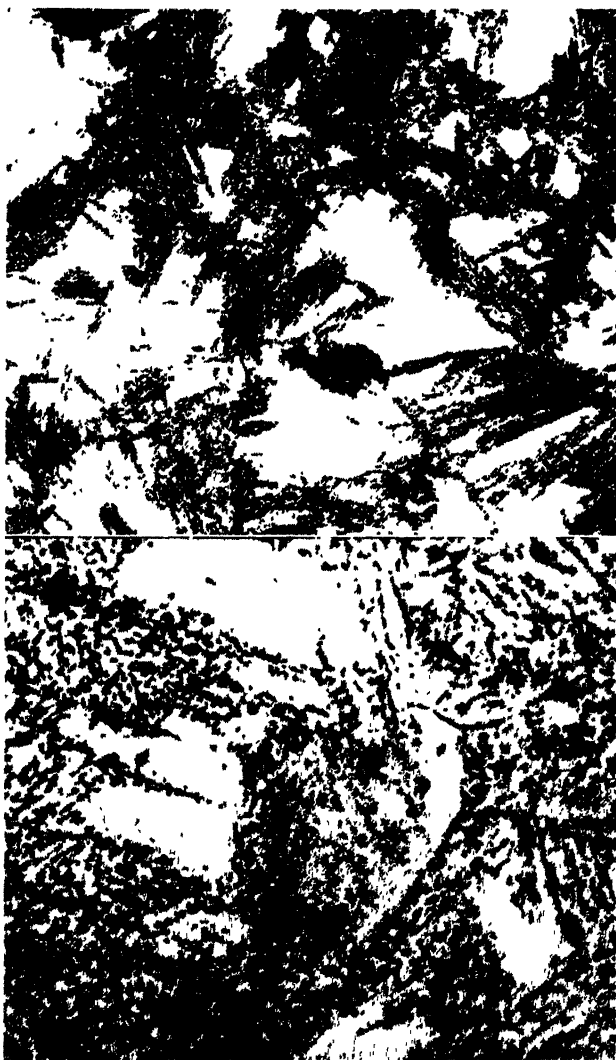
Original magnifications given; reduced $\frac{1}{4}$ in reproduction.

to detect when the first reaction ends. In the 3 per cent Cr steel separation is a maximum. In the plain carbon steels the second

alloying additions to steel may be considered from the point of view of their relative effectiveness in separating the two

reactious at temperatures below about 550°C. (1022°F.) No broad generalizations

tion of the bainite reaction is a function of temperature. The results reported here



29

30

FIGS. 29 AND 30.—STEEL SLIVER (0.36 PER CENT CARBON, 0.7 MANGANESE) QUENCHED FROM 1100° TO 496°C., HELD FOR 5 SECONDS AND QUENCHED TO ROOM TEMPERATURE.

Both acicular and nodular products are present.

Fig. 29, $\times 500$; Fig. 30, $\times 2500$. Etched in dilute Picral.

Original magnifications given; reduced $\frac{1}{4}$ in reproduction.

or thoroughgoing comparisons of alloying additions on this basis are yet possible.

It has been known for more than a decade that, in certain steels, the degree of comple-

indicate that this is a general phenomenon in hypoeutectoid steels. This temperature dependence of the degree of completion, most strikingly illustrated in the 3 per cent

Cr and 1 per cent Cr steels of this investigation cannot be adequately represented on an isothermal transformation diagram. A direct consequence of this characteristic

it evident that this is not true in general. Of great importance, when the end of austenite decomposition is represented on the isothermal transformation diagram, is



FIGS. 31 AND 32 — STEEL SLIVER (0.36 PER CENT CARBON, 0.7 MANGANESE) QUENCHED FROM 1100° TO 450°C. AND HELD FOR THE TIMES INDICATED. $\times 2500$. ETCHED IN DILUTE PICRAL. Original magnification given; reduced $\frac{1}{4}$ in reproduction.

Fig. 31, 2 seconds. This illustrates the product first formed during the bainite reaction in this steel.

Fig. 32, 3 seconds.

feature of the bainite reaction is that the complete disappearance of austenite after isothermal decomposition in the bainite range may require a time considerably longer than has usually been recognized. There seems to be little doubt that austenite decomposition may be complete in relatively short times at temperatures somewhat above Ar'' for some steels; e.g., the 4 per cent Ni and 1.7 per cent Mn steels of this investigation. Yet, the results for the 3 per cent Cr steel, where incomplete reaction by bainite formation was observed at all temperatures down to and including 350°C. (Ar'' is 370°C. for this steel) make

the experimental method used and the criterion adopted for determination of this line. In the present work the end of austenite decomposition has not been represented except for the 3 per cent Cr steel, and the end of bainite formation has been shown on the basis of dilatometric evidence. Again, it is pointed out that in certain steels the end of bainite formation does undoubtedly correspond to the end of austenite decomposition for a range of temperatures immediately above Ar'' .

It seems evident that the bainite reaction begins only after some carbon movement has taken place in the matrix.

When first formed, the product is supersaturated. The etching effects obtained may be considered satisfactory evidence of this fact. Still to be determined is the rela-

on cooling may account for some of the inferior physical properties, particularly in notched-bar tests, which have been reported by Döpfer and Wiester,²¹ Payson



FIG. 33.—STEEL SLIVER (0.47 PER CENT CARBON, 0.8 MANGANESE) QUENCHED FROM 1100°C. TO 518°C. AND HELD FOR 6 SECONDS.
Original magnification 1000; reduced $\frac{1}{6}$ in reproduction. Etched in dilute Picral.

tionship between the degree of supersaturation of the product and the degree of completion the bainite reaction may attain at a given temperature.

A description of the transformation of austenite in the bainite region has been given (p. 405), based on detailed study of the 3 per cent Cr steel. The experimental results for the other steels studied lead to the conclusion that this description applies to hypoeutectoid steels in general. The existence of carbon-enriched austenite dispersed throughout the bainite transformation product is considered to be a phenomenon of general importance. That this austenite may remain undecomposed for a considerable time at some temperatures has been shown for the 3 per cent Cr steel. It is suggested that the presence at room temperature of carbon-enriched austenite or of martensite formed from it

and Hodapp,²² and Griffiths, Pfeil and Allen⁸ for certain alloy steels transformed isothermally in the bainite range.

The mechanism of bainite formation presented involves very rapid carbon movement in local regions followed by a lattice transformation in carbon-poor volumes. The size of the product when first formed is antithetical to the concept of a nucleus. Large nuclei can be expected to form only at temperatures very near to the equilibrium transformation temperature and only after long delay.

Once started, bainite formation proceeds in large part by the appearance of new volumes of this product and by the branching of previously formed volumes. There seems to be little tendency for growth in the usual sense of accretion. Thus nucleation and grain-growth concepts cannot be expected to assist in building up a theory of bainite

formation. An adequate theory of this reaction must explain the temperature dependence of the degree of completion of the reaction and must account for the rapid movement of carbon in local regions at temperatures where diffusion in the ordinary sense is comparatively slow.

SUMMARY

1. Isothermal decomposition of austenite has been studied in hypoeutectoid steels containing chromium, chromium and molybdenum, uranium, nickel, manganese and copper in solution. Plain carbon steels of carbon contents 0.22, 0.36 and 0.47 per cent have been studied also. The isothermal transformation diagrams for the alloy steels have been presented in the approximate order of decreasing separation in time of the bainite and pearlite reactions.

2. The following mechanism of bainite formation in hypoeutectoid steels is proposed:

- a. In restricted volumes rapid carbon movement takes place in such a way as to yield austenite regions of alternate high and low carbon concentration.
- b. The low-carbon austenite transforms at the reaction temperature into a supersaturated ferrite by a martensite-like lattice rearrangement. The degree of supersaturation of the product is a function of temperature.
- c. This supersaturated ferrite begins at once to decompose, precipitating an iron carbide in a ferrite matrix to form the dark-etching, acicular product known as bainite.

3. The degree of completion of the bainite reaction is a function of the transformation temperature, the degree of completion increasing rapidly with decreasing temperature. Matrix austenite undecomposed during bainite formation transforms by another mechanism on continued holding at the reaction temperature.

4. Austenite enriched in carbon during bainite formation, in virtue of its high carbon content, can be retained at room temperature. The decomposition of this enriched austenite on holding at the transformation temperature may precede or follow the decomposition of the unreacted matrix austenite depending upon the temperature and the chemical compositions of the two austenites.

5. It is suggested that the presence at room temperature of carbon-enriched austenite or of martensite formed from it on cooling may account for some of the inferior physical properties that have been reported for certain alloy steels transformed isothermally in the bainite region.

6. It is concluded that concepts of nucleation and grain growth cannot assist in the formulation of a theory of the bainite reaction.

ACKNOWLEDGMENTS

The experimental work reported here was carried out in the metallurgy laboratories of the University of Notre Dame. It is a pleasure to acknowledge the helpful assistance of the director of the laboratories, Dr. A. R. Troiano. The results for one of the steels reported here have been the subject matter of a thesis under his direction. Dr. E. G. Mahin, head of the Department of Metallurgy, University of Notre Dame, has been helpful in many ways. The authors are grateful to Mr. F. J. Shortsleeve also, for his assistance in carrying out a considerable part of the experimental work.

REFERENCES

1. E. S. Davenport and E. C. Bain: Trans. formation of Austenite at Constant Subcritical Temperatures. *Trans. A.I.M.E.* (1930) 90, 117.
2. J. R. Vuella, G. E. Guellich and E. C. Bain: On Naming the Aggregate Constituents in Steel. *Trans. Amer. Soc. Metals* (1936) 24, 225.
3. F. Wever and H. Lange: Zur Umwandlungskinetik des Austenits—I. Magnetische Untersuchungen des Austenitzersalles. *Mitt. K.-W.-I. Eisenforschung* (1932) 14, 71.

4. F. Wever and W. Jellinghaus: Zur Umwandlungskinetik des Austenits—II. Dilatometrische Untersuchungen des Austenitfallens. *Mitt. K-W-I. Eisenforschung* (1932) **14**, 85.
5. F. Wever and W. Jellinghaus: Widerstandsmessungen zur Umwandlungskinetik des Austenits. *Mitt. K-W-I. Eisenforschung* (1933) **15**, 167.
6. E. S. Davenport: Isothermal Transformation in Steels. *Trans. Amer. Soc. Metals* (1939) **27**, 837.
7. F. Wever: Ueber die Umwandlungen bei der Stahlhartung. *Zisch. Metallkunde* (1932) **24**, 270.
8. W. T. Griffiths, L. B. Pfeil and N. P. Allen: The Intermediate Transformation in Alloy Steels. Second Report Alloy Steels Research Committee, Iron and Steel Inst. (1939) Sec. XII, 343.
9. R. F. Mehl: The Physics of Hardenability. Hardenability of Alloy Steels. Amer. Soc. Metals (1938).
10. G. V. Smith and R. F. Mehl: Lattice Relationships in Decomposition of Austenite to Pearlite, Bainite, and Martensite. *Trans. A.I.M.E.* (1942) **150**, 211.
11. A. B. Greninger and A. R. Troiano: Crystallography of Austenite Decomposition. *Trans. A.I.M.E.* (1940) **140**, 307.
12. F. Wever and K. Mathieu: Ueber die Umwandlungen der Manganstähle. *Mitt. K-W-I. Eisenforschung* (1940) **22**, 9.
13. N. P. Allen, L. B. Pfeil and W. T. Griffiths: Determination of the Transformation Characteristics of Alloy Steels. Second Report Alloy Steels Research Committee, Iron and Steel Inst. (1939) Sec. XIII, 369.
14. K. Honda and Z. Nishiyama: The Nature of the Tetragonal and Cubic Martensites. *Sci. Repts. Sendai* (1932) [I] **21**, 299.
15. W. Crafts and C. M. Offenbauer: Carbides in Low-chromium Steel. *Trans. A.I.M.E.* (1942) **150**, 275.
16. R. M. Parke and A. J. Herzig: Hardenability of Molybdenum S.A.E. Steels. *Metals and Alloys* (1940) **11**, 6.
17. E. S. Davenport, R. A. Grange and R. J. Hafsten: Influence of Austenite Grain Size upon Isothermal Transformation Behavior of S.A.E. 4140 Steel. *Trans. A.I.M.E.* (1941) **145**, 301.
18. W. Crafts and C. M. Offenbauer: Carbides in Low Chromium-molybdenum Steels. *Trans. A.I.M.E.* (1943) **154**, 361.
19. E. P. Klier and A. R. Troiano: Discussion of paper by H. H. Chiswick and A. B. Greninger. Amer. Soc. Metals, Preprint No. 12 (1943).
20. H. Lange and K. Mathieu: Ueber den Ablauf der Austenitumwandlung im unterkühlten Zustand bei Eisen-Nickel-Kohlenstoff-Legierungen. *Mitt. K-W-I. Eisenforschung* (1938) **20**, 125.
21. H. Dopfer and H. J. Wiester: Der Einfluss der Legierungselemente auf die Umwandlungen des Austenits und die Festigkeitseigenschaften legierter Stähle bei gestufter Vergütung. *Archiv Eisenhüttenwesen* (1935) **8**, 541.
22. P. Payson and W. Hodapp: Austempering of S.A.E. Alloy Steels Not Always Advantageous. *Metal Progress* (1939) **35**, 118.

DISCUSSION

(Walter Crafts presiding)

G. V. SMITH,* Kearny, N. J.—The writer has found this paper very interesting and worth while and, with respect to the postulated mechanism of the bainite reaction, quite thought provoking. It is felt that the experimental evidence deduced in support of the hypothesis that in the formation of bainite in hypoeutectoid steels "rapid carbon movement takes place in such a way as to yield austenite regions of alternate high and low carbon concentration" and that "the low-carbon austenite transforms at the reaction temperature into a supersaturated ferrite by a martensitelike rearrangement" is not incontrovertible. This is particularly true when the authors also state that "the size of the product when first formed is antithetical to the concept of a nucleus" and that "there seems to be little tendency for growth in the usual sense of accretion."

On their face, then, the postulations appear to involve at least two physical improbabilities, and this suggests careful consideration of the experimental evidence. The two apparent physical improbabilities are: (1) that the required diffusion of carbon could take place in such a short time, and (2) that the required depletion and enrichment of carbon could occur along crystallographic planes throughout such tremendous atomic distances as apparently are contemplated.

The finding by X-ray diffraction methods of austenite in samples reacted to bainite is extremely interesting, but the writer finds it less easy than the authors to dismiss the first suggested possibility for the austenite retention; namely, that austenite of unchanged carbon content is "stabilized." It does not seem logical to the writer that some of the austenite necessarily must be situated "in the parts of the specimen that at transformation temperature contained the greatest amounts of austenite," but rather that all of the austenite could be emplaced between the plates of bainite. This latter possibility could occur, for example, because of the local stress conditions arising from the volume expansion accompanying the transformation. The ques-

* U. S. Steel Corporation, Research Laboratory.

tion might be asked: Why does the amount of bainite formed depend upon the reaction temperature, increasing with decreased temperature? Might not the question of state of stress be the reason in part for this dependency? I believe this sort of explanation was originally put forth by Carpenter and Robertson* to explain the dependency of the amount of martensite on the temperature.

The "other evidence that the austenite retained is enriched" has to do with the intensity of the gamma diffraction lines and the occurrence of a tetragonal split. The evidence regarding the intensities seems rather uncertain, and it would appear that the effects observed would occur whether or not the austenite were enriched, i.e., the observations fit the possibility of a "stabilized" austenite as well as an enriched austenite, the intensity being solely dependent, for practical purposes, on the amount of austenite. The postulation that carbon diffuses from the enriched austenite areas to the large volumes of austenite appears to be extremely unlikely in the time available.

With regard to the "tetragonal split," there are several questions. Why was not a "tetragonal split" observed in all samples only partially reacted, as, for example, that of Fig. 13? I assume that by "tetragonal split" the authors mean the splitting of, say, the $\{110\}$ diffraction line of body-centered cubic ferrite into two lines, owing to the distortion to the tetragonal lattice. How did the authors distinguish between the martensite resulting from the assumed enriched austenite and that from the remainder of the sample? Since the samples of Tables 2 and 3 were not reacted to completion, there should be martensite with a "tetragonal split" and axial ratio corresponding to the nominal carbon content and, which might be difficult to distinguish, owing to line diffuseness, from martensite of slightly higher carbon content. Do the authors feel that the change of axial ratio in Table 3 from 1.002 to 1.019 is outside their experimental error, and do they have any explanation of why, if real, the change should occur so slowly up to 67.5 hr. and then disappear entirely before 120 hr.? Incidentally, it does not seem perti-

nent to use the data of Table 3 to argue with respect to the bainite reaction, since at 500°C. the reaction product according to Fig. 1 is "ferrite," not bainite.

To the writer, the greatest difficulty in the hypothesis is that mentioned earlier; namely, that of the necessary prearrangement of atoms in the austenite lattice having to occur on such a vast scale in order that the bainite platelets may spring full-formed from the matrix lattice. This is, of course, exactly what occurs during the formation of the initial nuclei in all reaction processes that involve growth, but, it is to be emphasized, on a much reduced scale, the nuclei forming in submicroscopic size. There appear to be two general mechanisms by which solid-state reactions occur; (1) by a growth process involving diffusion and (2), by a shearing process not involving diffusion. What the authors apparently contemplate is a combination of the two, which to this reader is difficult to accept either on theoretical grounds or on the basis of the experimental evidence presented. Rather, the concepts attributed by the authors to Bain and to Wever are thought to be more nearly correct.

C. M. OFFENHAUER,* Niagara Falls, N. Y.—The authors are to be congratulated on their investigation of the bainite reaction. The photomicrographs illustrating the various structures are very fine examples of metallographic technique.

Several points might be clarified by further information. It is stated that austenite may be enriched by the bainite reaction to such an extent that the A_r'' temperature is depressed below room temperature. This amount of enrichment would imply that:

- 1 The bainite structure contains less carbon and probably less chromium than the parent austenite because a considerable alloy content would be necessary to account for the persistence of the austenite.

- 2 The volumetric proportion of transformation of the low-carbon, low-alloy structure would have to be fairly large to account for any but the most microscopically local enrichment

* H. Carpenter and J. M. Robertson *Metals* 2, 881. London, 1939, Oxford Univ. Press.

* Research Metallurgist, Union Carbide and Carbon Research Laboratories.

The composition of the bainite has not been shown to be low in carbon or low in chromium. The photomicrographs indicate the possibility of a low-carbon structure, at least near the beginning of the reaction, and perhaps this same type of reaction continues until the beginning of the second reaction. Studies of the bainite reaction made at the Union Carbide and Carbon Research Laboratories have indicated that the initial bainite in a chromium steel appears to consist of acicular ferrite containing a relatively small proportion of carbides near the middle of the needle. It would seem justifiable, then, to assume that the original bainite formed is relatively low in carbon. We should like to ask the authors if they have any reason to believe that the reaction product is also low in chromium, or whether they consider that enrichment of the austenite by chromium is necessary for the retention of austenite.

It is implied in Table 2 and on page 40 that the retained austenite gradually increases to a maximum for the 6-min. isothermal treatment at 450°C, and then decreases. We should like to know the relative amounts of transformation that represent maximum retention of austenite and if this fraction of transformation represents the maximum austenite retention at other temperatures.

E. P. Klier (author's reply).—The discussions by Mr. Offenbauer and Dr. Smith deal particularly with the X-ray data obtained for the 3 per cent Cr steel. Especially is this true with respect to the data from which it has been argued that the austenite retained at room temperature has been enriched with carbon. Before proceeding with the presentation of some additional data that further clarify this point, it is desirable to consider briefly the role of carbon in developing the tetragonal martensite structure.

The data of Honda and Nishiyama,¹⁴ in particular, show that freshly formed martensite possesses a body-centered tetragonal crystal structure. The tetragonality of this structure, however, is measurable only for carbon contents between about 0.55 and 1.8 per cent. In this range the tetragonality or axial ratio c/a increases linearly with carbon content.

A specimen of the 3 per cent Cr, 0.38 per cent C steel quenched to room temperature

does not contain martensite of a measurable tetragonality, therefore the appearance of a measurable tetragonality for martensite formed in this steel must necessarily mean that this martensite formed from an austenite containing considerably more than 0.38 per cent carbon.

The accuracy with which the ratio c/a can be reproduced allows this value to be stated to three real numbers. Thus in Table 3 the thousandths place is subject to some uncertainty, although the consistency of the values might be considered as arguing for the near correctness of the fourth real number. In terms of carbon content, however, this fourth number is of little significance; i.e., the martensite formed after transforming 26 hr. has the same carbon content as the specimen transformed 67.5 hours.

In Table 5 are presented data indicating the products obtained during the initial stages of bainite formation.

TABLE 5.—Phase Identification for Initial Stages of Bainite Formation

Steel	Transformation Temperature		Time at Temperature	Structure
	Deg. C.	Deg. F.		
3 per cent Cr	475	887	90 sec	γ + tet. split(?)
3 per cent Cr	475	887	180 sec	γ + tet. split
3 per cent Cr	475	887	23 hr.	tet. split + (γ)?
1 per cent Cr, 0-40 per cent Mo.	515	959	90 sec.	γ + tet. split
1 per cent Cr	550	1022	120 sec	tet. split
1 per cent Cr	515	959	45 sec.	γ + tet. split
1 per cent Cr	505	941	320 sec	γ + tet. split

For the 3 per cent Cr steel the doublet lines are weak, as would be expected from the slight precipitation (cf. Fig. 14). The $(111)\gamma$; $(110)\alpha$ and $((101)\alpha + (011)\alpha)$ lines are clearly distinguishable after transformation for 3 min. at 475°C. (887°F.), however. This tetragonal structure was not observed for like times at 450°C. (842°F.), the austenite lines becoming evident without the appearance of the tetragonal structure.

The data presented for steel 1 per cent Cr show better the alterations in the transformation phenomena on lowering the temperature of transformation. The differences between the

mechanisms of ferrite and bainite formation are matters of degree and are not generic differences. It is unfortunate that in the paper other differences are inferred

The data above show conclusively that adjustments in carbon concentration do take place during the course of the bainite reaction. That this carbon adjustment is on the scale previously indicated necessarily follows. It must be concluded that Dr. Smith's objections to the proposed mechanism of bainite formation are not valid.

In answer to Mr. Offenhauer, it is doubtful whether chromium diffusion takes place during bainite formation in the 3 per cent Cr steel. That chromium is not necessary for austenite retention is evident from the results for steels containing no chromium

For a given reaction temperature, austenite retention at room temperature appears to be a maximum at the virtual end of bainite formation, while the bainite present at this point varies as a function of the reaction temperature

CONTENTS

Institute of Metals Division, Volume 156, Transactions A.I.M.E., 1944.

Institute of Metals Division Lecture

Some Problems in Organizing Industrial Research By W. M. PEIRCE. (<i>Metals Technology</i> , April 1944).	17
--	----

Physical Metallurgy

Microradiography—a New Metallurgical Tool. By S. E. MADDIGAN and B. R. ZIMMERMAN. (<i>Metals Technology</i> , Feb. 1944) (With discussion).	33
Metallography with the Electron Microscope. By CHARLES S. BARRETT. (<i>Metals Technology</i> , Sept. 1943) (With discussion).	62
Application of Electron Microscope to Study of Aluminum Alloys. By F. KELLER and A. H. GEISLER. (<i>Metals Technology</i> , April 1944) (With discussion).	82
Orientations in Diffusion Layers By SHUELING WOO, CHARLES S. BARRETT and ROBERT F. MEHL. (<i>Metals Technology</i> , June 1944) (With discussion).	100
Factors Affecting Rates of Work-hardening in Primary Substitutional Solid Solutions. By J. H. FRYE, JR., and C. P. SUN. (<i>Metals Technology</i> , April 1944) (With discussion).	111

Copper and Copper-rich Alloys

Effect of Grain Size and Bar Diameter on Creep Rate of Copper at 200°C. By E. R. PARKER and C. F. RIISNESS. (<i>Metals Technology</i> , Feb. 1944) (With discussion).	117
Effect of Cooling Rate and Minor Constituents on the Rupture Properties of Copper at 200°C. By D. L. MARTIN and E. R. PARKER. (<i>Metals Technology</i> , Dec. 1943) (With discussion).	126
High-speed Tensile Impact Tests on Single-crystal and Polycrystalline Bars of Copper. By E. R. PARKER and E. A. SMITH. (<i>Metals Technology</i> , April 1944).	142
Solubility of Hydrogen in Molten Copper-tin Alloys. By MICHAEL B. BEVER and CARL F. FLOE. (<i>Metals Technology</i> , April 1944) (With discussion).	149
Preferred Orientation in Annealed 70-30 Brass Wire. By H. L. BURGHOFF and J. S. PORTER. (<i>Metals Technology</i> , April 1944) (With discussion).	160
Structure of Copper-zinc Alloys Oxidized at Elevated Temperatures. By F. N. RHINES and B. J. NELSON. (<i>Metals Technology</i> , Sept. 1943).	171
Grain Growth and Recrystallization of 70-30 Cartridge Brass. By R. S. FRENCH. (<i>Metals Technology</i> , Feb. 1944) (With discussion).	195
Stress-corrosion Cracking of 70-30 Brass by Amines. By H. ROSENTHAL and A. L. JAMIESON. (<i>Metals Technology</i> , Feb. 1944) (With discussion).	212
Physical Properties of a 65-Cu, 10-Mn, 25-Zn Alloy. By J. R. LONG and T. R. GRAHAM. (<i>Metals Technology</i> , June 1944) (With discussion).	222

Miscellaneous Alloys

The Constitution of the Lead-antimony and Lead-antimony-silver Systems. By B. BLUMENTHAL. (<i>Metals Technology</i> , Sept. 1943) (With discussion).	240
Constitution of the System Indium-zinc. By F. N. RHINES and A. H. GROBE. (<i>Metals Technology</i> , Feb. 1944) (With discussion).	253

Liquidus Determinations in Zinc-rich Alloys (Zn-Fe; Zn-Cu; Zn-Mn). By GERALD EDMUNDS. (<i>Metals Technology</i> , June 1944) (With discussion)	263
Rolled Zinc-titanium Alloys. By E. A. ANDERSON, E. J. BOYLE and P. W. RAMSEY. (<i>Metals Technology</i> , Feb. 1944) (With discussion)	278
The Structure of Anodic Oxide Coatings. By J. D. EDWARDS and F. KELLER. (<i>Metals Technology</i> , April 1944) (With discussion)	288
The Present Status of Electrolytic Manganese and Its Alloys. By R. S. DEAN. (<i>Metals Technology</i> , June 1944) (With discussion).	301

Symposium on Practical Aspects of Diffusion

Preface. By ROBERT F. MEHL. (<i>Metals Technology</i> , Jan. 1944)	325
The Influence of Gas-metal Diffusion in Fabricating Processes By FREDERICK N RHINES. (<i>Metals Technology</i> , Jan. 1944) (With discussion)	335
The Degassing of Metals. By F. J. NORTON and A. L. MARSHALL. (<i>Metals Technology</i> , Jan. 1944) (With discussion)	351
Diffusion in Relation to Changes in Microstructure. By MARIE L. V. GAYLER. (<i>Metals Technology</i> , Jan. 1944) (With discussion)	372
Diffusion in Alclad 24S-T Sheet. By F. KELLER and R. H. BROWN. (<i>Metals Technology</i> , Jan. 1944) (With discussion)	377
Diffusion of Indium in Bearings. By A. A. SMITH, JR. (<i>Metals Technology</i> , Jan. 1944) (With discussion).	387
Diffusion in Chromizing. By I. R. KRAMER.	393

INDEX

(NOTE. In this index the names of authors of papers and discussions and of men referred to are printed in SMALL CAPITALS, and the titles of papers in *italics*.)

A

- Adirondack region: iron-ore enterprises, 51
- Aging: low-carbon steel: causes, 229
 - yield-point elongation eliminated by treatment of steel in wet hydrogen, 207
- ALLISON, F. H. JR.: *Discussion on Variables Affecting the Results of Notched-bar Impact Tests on Steels*, 280
- Annealing. in wet hydrogen: factors influencing effectiveness of treatment, 220
 - to eliminate yield-point elongation in steel, 211

B

- BARRETT, R. L. AND McCAUGHEY, W. J.: *The Role of Basic Slags in the Elimination of Phosphorus from Steel*, 87, discussion, 96
- Bessemer steel: killed. manufacture, 107
 - properties, 107
 - uniformity of inherent grain size, 124
 - properties: comparison with those of open-hearth steel, 112
- Bothlehem Steel Co.: selection of blast-furnace refractories, 55
- Birmingham district. iron ores: brown: concentration, 53
 - type, 52
 - red: concentration, 51
 - type, 53
 - shipments, 53
- Blast-furnace operation: effect of washing Pittsburgh coking coals, 67
- Blast-furnace refractories: comparison, 57
 - disintegration: amount carbon necessary, 63
 - selection: factors affecting choice, 55
- BOCK, W. K. AND SCHWARTZ, H. A.: *Tensile Properties of Medium-carbon Low-alloy Cast Steels*, 250
- Boron: deoxidizing power in liquid steel: compared with those of other elements, 98
- BREDIG, M. A.: *Discussion on The Role of Basic Slags in the Elimination of Phosphorus from Steel*, 95
- BROPHY, G. R. AND MILLER, A. J.: *Discussion on Effect of Some Elements on Hardenability of Steel*, 150

C

- Carnegie Institute of Technology: study of aging and the yield point in steel, 207
- Carrie blast furnaces: effect of washing Pittsburgh coking coals, 67

- Case School of Applied Science: study of role of basic slags in elimination of phosphorus from steel, 87
- Cast iron: gray: mechanical properties: effect of graphite, 23
 - useful functions of graphite, 36
- Cast steel: medium-carbon low-alloy: normalized and/or quenched: impact resistance, 262
 - line of strength vs. elongation: calculation from chemical composition, 250
 - yield point or yield strength: determined by heat-treatment, 259
- CHRISTENSON, A. L.: *Discussion on The Effect of Quenching Temperature on the Results of the End-quench Hardenability Test*, 136
- CHRISTENSON, A. L. AND JACKSON, C. E.: *The Effect of Quenching Temperature on the Results of the End-quench Hardenability Test*, 125; discussion, 137
- Clairton by-product coke plant and coal washer, 67
- CLARK, K. L. AND KOWALL, N.: *Hardness Measurement as a Rapid Means for Determining Carbon Content of Carbon and Low-alloy Steels*, 328
- Coal washing: Pittsburgh coking coal: effect on blast-furnace operation, 67
- Coke: blast-furnace: effect of washing Pittsburgh coals, 67
- Coking coals: washing: Pittsburgh: effect on blast-furnace operation, 67
- COMSTOCK, G. F.: *Discussions: on Aging and the Yield Point in Steel*, 242, 243
 - on Effect of Some Elements on Hardenability of Steel, 148
- Concentration: iron ores: United States, 38
- COUNSELMAN, T. B.: *Concentration of Iron Ores in the United States*, 38
- COY, G. L.: *Discussions: on The Notched-bar Impact Test*, 325
 - on Variables Affecting the Results of Notched-bar Impact Tests on Steels, 281
- CRAFTS, W.: *Discussions: on Effect of Some Elements on Hardenability of Steel*, 152
 - on The Effect of Quenching Temperature on the Results of the End-quench Hardenability Test, 136
- CRAFTS, W. AND LAMONT, J. L.: *Effect of Some Elements on Hardenability*, 157
- CRAMER, R. E.: *Discussion on Influence of Hydrogen on Mechanical Properties of Some Low-carbon Manganese-iron Alloys and on Hadfield Manganese Steel*, 201

D

- DAVENPORT, E. S. AND RICKETT, R. L.: *Discussion on Effect of Several Variables on the Hardenability of High-carbon Steels*, 179
- DEVRIES, G.: *Discussion on The Effect of Quenching Temperature on the Results of the End-quench Hardenability Test*, 137
- DUNN, C. G.: *Recrystallization and Twin Relationships in Silicon Ferrite*, 372

E

- EMERICK, H. B.: *Discussion on The Manufacture and Properties of Killed Bessemer Steel*, 123
- ENZIAN, G. H.: *Discussion on Orientation in Low-carbon Deep-drawing Steel*, 365
- EPSTEIN, S.: *Discussion on Aging and the Yield Point in Steel*, 243
- Eutectoid. definitions, 350

F

- FEILD, A. L.: *Discussion on The Relative Deoxidizing Power of Boron in Liquid Steel and the Elimination of Boron in the Open-hearth Process*, 102
- FICK, N. C.: *Discussion on Hardness Measurement as a Rapid Means for Determining Carbon Content of Carbon and Low-alloy Steels*, 332
- FOLEY, F. B.: *Discussion on Precipitation and Reversion of Graphite in Low-carbon Low-alloy Steel in the Temperature Range 900° to 1300° F.*, 392
- Fracture: of brittle solids by compression. glass, 333
of steel conditions, 283

G

- General Electric Co. study of influence of hydrogen on mechanical properties of some low-carbon manganese-iron alloys and on Hadfield manganese steel, 183
study of recrystallization and twin relationships in silicon ferrite, 372
- GENSAMER, M.: *Discussion on Variables Affecting the Results of Notched-bar Impact Tests on Steels*, 281
- GENSAMER, M. AND LOW, J. R. JR.: *Aging and the Yield Point in Steel*, 207; discussion, 243 et seq.
- Glass fracture and comminution by compression, 333
- Goss, N. P.: *Discussion on Influence of Hydrogen on Mechanical Properties of Some Low-carbon Manganese-iron Alloys and on Hadfield Manganese Steel*, 203
- Graphite in steel. See Steel
- GURRY, R. W.: *The Relative Deoxidizing Power of Boron in Liquid Steel and the Elimination of Boron in the Open-hearth Process*, 98; discussion, 105

H

- Hadfield manganese steel mechanical properties: influence of hydrogen, 183, 195

- HAFNER, R. H., KRAMER, I. R. AND TOLEMAN, S. L.: *Effect of Sixteen Alloying Elements on Hardenability of Steel*, 138
- Hardenability metals end-quench test: cooling rates effect of quenching temperature, 125
steel. effect of alloying elements, 138, 157
- Hardness measurements. steel for determining carbon content, 328
- HAYES, A.: *Discussion on Aging and the Yield Point in Steel*, 243, 244
- Heavy-media separation iron ore Mesabi Range, 44
- HEYER, R. H.: *Discussion on Conditions of Fracture of Steel*, 296
- HOLLOMON, J. H.: *The Notched-bar Impact Test*, 298; discussion, 322 et seq.
Discussion on Variables Affecting the Results of Notched-bar Impact Tests on Steels, 280
- HOLLOMON, J. H. AND ZENER, C.: *Conditions of Fracture of Steel*, 283; discussion, 297
- Howe lecture: twenty-first gray iron—steel plus graphite, 13
- HOYT, S. L.: *Discussion on The Notched-bar Impact Test*, 326
- Hydrogen wet treatment to eliminate yield-point elongation in steel, 207

I

- Impact tests notched-bar. See Notched-bar.
- Iron-carbon alloys eutectoid definitions, 350
eutectoid position influence of carbide-forming elements aluminum, 338
beryllium, 338
brief bibliography, 352
chromium, 335
cobalt, 338
columbium, 337
copper, 338
manganese, 338
molybdenum, 335
nickel, 340
nomenclature, 349
silicon, 340
tantalum, 337
theory proposed as explanation, 342
titanium, 340
tungsten, 335
vanadium, 337
zirconium, 340
- Iron cast. See Cast Iron.
- gray steel plus graphite, 13
- Iron mines Adirondack region, 51
- Iron ore: Birmingham district. See Birmingham.
concentration. United States, 38
Lake Superior district: reserves, 1941, 40
Mesabi Range: classes, 40
concentration methods, 41
sintering. Mesabi Range, 48

J

- JACKSON, C. E.: *Discussion on The Effect of Quenching Temperature on the Results of the End-quench Hardenability Test*, 136

- JACKSON, C. E. AND CHRISTENSON, A. L.: *The Effect of Quenching Temperature on the Results of the End-quench Hardenability Test*, 125; discussion, 137
- JACKSON, C. E., PUGACZ, M. A. AND MCKENNA, F. S.: *Variables Affecting the Results of Notched-bar Impact Tests on Steels*, 263
- JAFFE, L. D.: *Discussion on Influence of Various Elements upon the Position of the Eutectoid in the Iron-carbon (Carbide) System*, 353
- Jigging. iron ore: Mesabi Range, 42
- JUNGE, C. H.: *Discussion on Effect of Some Elements on Hardenability of Steel*, 153

K

- KLIER, E. P.: *Discussion on The Bainite Reaction in Hypoeutectoid Steels*, 421
- KLIER, E. P. AND LYMAN, T.: *The Bainite Reaction in Hypoeutectoid Steels*, 394
- KOWALL, N. AND CLARK, K. L.: *Hardness Measurement as a Rapid Means for Determining Carbon Content of Carbon and Low-alloy Steels*, 328
- KRAMER, I. R.: *Discussion on Effect of Some Elements on Hardenability of Steel*, 153
- KRAMER, I. R., HAFNER, R. H. AND TOLEMAN, S. L.: *Effect of Sixteen Alloying Elements on Hardenability of Steel*, 138
- KRANER, H. M. AND SNYDER, E. B.: *The Selection of Blast-furnace Refractories*, 55
- KELLEY, F. C.: *Discussion on Influence of Hydrogen on Mechanical Properties of Some Low-carbon Manganese-iron Alloys and on Hadfield Manganese Steel*, 201
- KING, C. D.: *The Washing of Pittsburgh Coking Coals and Results Obtained on Blast Furnaces*, 67

L

- LAMONT, J. L. AND CRAFTS, W.: *Effect of Some Elements on Hardenability*, 157
- LEITER, R. W. E. AND WINLOCK, J.: *Discussion on Aging and the Yield Point in Steel*, 245
- LOEB, C. M. JR.: *Discussion on Effect of Some Elements on Hardenability of Steel*, 148
- LOW, J. R. JR., AND GENSAMER, M.: *Aging and the Yield Point in Steel*, 207; discussion, 243 et seq.
- LYMAN, T. AND KLIER, E. P.: *The Bainite Reaction in Hypoeutectoid Steels*, 394

M

- MACKENZIE, J. T.: *Gray Iron—Steel Plus Graphite*, 13
- Magnetic torque method: limitations, 369
- study of earing in small cups from cold-reduced strip steel, 368
- testing orientation in low-carbon deep-drawing steel, 354
- theory, 362
- Magnetites: eastern: concentration, 51
- reserves, 50
- Manganese-iron alloys: high-carbon. *See* Hadfield Manganese Steels.
- low-carbon: mechanical properties: influence of hydrogen, 183

- MARSHALL, R. H., ROWLAND, E. S. AND WELCHNER, J.: *Effect of Several Variables on the Hardenability of High-carbon Steels*, 168; discussion, 182
- MCCAUGHEY, W. J. AND BARRETT, R. L.: *The Role of Basic Slags in the Elimination of Phosphorus from Steel*, 87; discussion, 96
- MCKENNA, F. S.: *Discussion on Variables Affecting the Results of Notched-bar Impact Tests on Steels*, 279, 280
- MCKENNA, F. S., JACKSON, C. E. AND PUGACZ, M. A.: *Variables Affecting the Results of Notched-bar Impact Tests on Steels*, 263
- MQUAID, H. W.: *Discussion on The Effect of Quenching Temperature on the Results of the End-quench Hardenability Test*, 136
- Mesabi Range iron ore classes, 40
- concentration, 41
- sintering, 48
- METZGER, M.: *Discussion on The Notched-bar Impact Test*, 322
- MILLER, A. J. AND BROPHY, G. R.: *Discussion on Effect of Some Elements on Hardenability of Steel*, 150
- MILLER, R. F., SMITH, G. V. AND TARR, C. O.: *Precipitation and Reversion of Graphite in Low-carbon Low-alloy Steel in the Temperature Range 900° to 1300°F.*, 387
- Models. graphite flakes, 15
- MOORE, G. A.: *Discussion on Influence of Hydrogen on Mechanical Properties of Some Low-carbon Manganese-iron Alloys and on Hadfield Manganese Steel*, 203

N

- National Malleable and Steel Castings Co.: study of tensile properties of medium-carbon low-alloy cast steels, 250
- National Tube Co.: study of manufacture and properties of killed bessemer steel, 107
- Naval Research Laboratory. hardness measurement as a rapid means for determining carbon content of carbon and low-alloy steels, 330
- study of effect of quenching temperature on results of the end-quench hardenability test, 125
- study of effect of sixteen alloying elements on hardenability of steel, 138
- study of variables affecting the results of notched-bar impact tests on steels, 263
- New York. iron mines, 51
- Notched-bar impact tests: brief bibliography, 322
- difference from tensile tests, 324
- on steel: air-cooled steel, 307
- calculation of transverse stress at base of notch, 320
- conditions of fracture, 283
- relation to tensile properties, 298, 304
- reproducibility of notch conditions, 280
- significance and use of results, 317
- state of stress of specimens, 299
- stress at base of notch. transverse: calculation, 320
- throwing of broken specimen: energy loss, 279, 281

- Notched-bar impact tests: types of specimens, 303
 variables affecting breadth of specimen, 263, 266, 280, 314
 radius of notch, 263, 267, 280, 313
 resistance to deformation of specimen, 263, 274
 shape of notch, 263, 268, 279
 speed of test, 263, 272, 314, 323, 325
 temperature of test, 263, 269, 279
 water-quenched steel, 310
 preparation of notch: importance, 281
 Notre Dame University: study of the bainite reaction in hypoeutectoid steels, 394
- O
- OFFENHAUER, C. M.: *Discussion on The Bainite Reaction in Hypoeutectoid Steels*, 420
 Ohio State University: study of role of basic slags in elimination of phosphorus from steel, 87
 Open-hearth practice: elimination of boron, 98
 Open-hearth steel: properties: comparison with those of bessemer steel, 112
 Orientation in low-carbon deep-drawing steel testing by magnetic torque method, 354
- P
- Peritectic: definition, 351
 Peritectic-eutectoid reaction: definitions, 349, 351, 353
 Phosphorus: elimination from steel. *See* Steel.
 Pig iron: production: effect of washing Pittsburgh coking coals for blast-furnace use, 67
 PONCELET, E. F.: *Fracture and Comminution of Brittle Solids* (Abstract), 333
Discussion on The Notched-bar Impact Test, 323, 325
 PUGACZ, M. A., JACKSON, C. E. AND MCKENNA, F. S.: *Variables Affecting the Results of Notched-bar Impact Tests on Steels*, 263
- Q
- Quenching temperature: effect on cooling rates in end-quench hardenability test, 125
- R
- Refractories: blast-furnace. *See* Blast-furnace Refractories.
 RICKETT, R. L. AND DAVENPORT, E. S.: *Discussion on Effect of Several Variables on the Hardenability of High-carbon Steels*, 179
 ROWLAND, E. S., WELCHNER, J. AND MARSHALL, R. H.: *Effect of Several Variables on the Hardenability of High-carbon Steels*, 168; *discussion*, 182
 RUSSELL, H. W.: *Discussion on The Notched-bar Impact Test*, 323
- S
- SACHS, G.: *Discussion on The Notched-bar Impact Test*, 326
 SAUNDERS, W. M. JR.: *Discussion on Orientation in Low-carbon Deep-drawing Steel*, 368
 SCHWARZ, H. A. AND BOCK, W. K.: *Tensile Properties of Medium-carbon Low-alloy Cast Steels*, 250
 SCOTT, H.: *Discussion on Variables Affecting the Results of Notched-bar Impact Tests on Steels*, 281
 SHAPIRO, C. L. AND STRAUSS, J.: *Influence of Various Elements upon the Position of the Eutectoid in the Iron-carbon (Carbide) System*, 335; *discussion*, 353
 SHEPHERD, B. F.: *Discussion on The Notched-bar Impact Test*, 324
 SIEGEL, S.: *Discussion on Orientation in Low-carbon Deep-drawing Steel*, 369
 Silicon ferrite recrystallization: twin relationships, 372
 SIMS, C. E.: *Discussion on The Manufacture and Properties of Killed Bessemer Steel*, 123
 Sintering: iron ore: Mesabi Range, 48
 Slag: basic: role in elimination of phosphorus from steel, 87
 SMITH, E. C.: *Discussion on The Manufacture and Properties of Killed Bessemer Steel*, 123
 SMITH, G. V.: *Discussions: on Precipitation and Reversion of Graphite in Low-carbon Low-alloy Steel in the Temperature Range 900° to 1300°F.*, 393
on The Bainite Reaction in Hypoeutectoid Steels, 419
 SMITH, G. V., MILLER, R. F. AND TARR, C. O.: *Precipitation and Reversion of Graphite in Low-carbon Low-alloy Steel in the Temperature Range 900° to 1300°F.*, 387
 SNYDER, E. B. AND KRANER, H. M.: *The Selection of Blast-furnace Refractories*, 55
 SOSMAN, R. B.: *Discussion on The Manufacture and Properties of Killed Bessemer Steel*, 123
 SOUTHARD, J. C.: *Discussion on The Relative Deoxidizing Power of Boron in Liquid Steel and the Elimination of Boron in the Open-hearth Process*, 102
 STANLEY, J. K.: *Orientation in Low-carbon Deep-drawing Steel*, 354, *discussion*, 370
 Steel (*see also* Iron-carbon Alloys):
 bending test: relation between velocity and strain rate, 321
 bessemer. *See* Bessemer
 carbon content: determined by hardness measurements, 328
 cast. *See* Cast Steel.
 earing: cold-reduced strip: magnetic torque study, 368
 eutectoid: definitions, 350
 fracture: conditions, 283
 graphite: formation: mechanism, 14
 models of flakes, 15
 rosettes, 15
 whorls, 15
 hardenability: effect of alloying elements:
 aluminum, 138, 157
 antimony, 138
 arsenic, 138
 beryllium, 138
 boron, 157
 chromium, 138, 157
 cobalt, 138

- Steel: hardenability: effect of alloy elements. columbium, 138
copper, 138
germanium, 138
manganese, 138, 157
molybdenum, 138, 157
nickel, 138, 157
silicon, 138, 157
tellurium, 138
tin, 138
titanium, 138, 157
vanadium, 157
zirconium, 157
effect of variables high-carbon steels, 168
time, temperature and prior structure, 168
end-quench curves explanation of "shelf" or "hump," 179
hydrogen purification: review of literature, 239
hypoeutectoid: bainite formation mechanism, 394
bainite reaction, 394
brief bibliography, 418
liquid: boron as deoxidizer, 98
deoxidation application of thermodynamics, 105
deoxidation mechanism, 105
equilibrium between oxygen and other elements, 110
low-carbon: strain-aging and yield point. causes, 229
low-carbon deep-drawing orientation. testing by magnetic torque method, 354
low-carbon low-alloy. graphite. precipitation and reversion in temperature range 900° to 1300°F, 387
manganese Hadfield: mechanical properties influence of hydrogen, 183
notched-bar impact tests. See Notched-bar.
open-hearth: boron elimination, 98
peritectic: definitions, 351
peritecto-eutectoid reaction: definitions, 349, 351, 353
phosphorus. elimination: role of basic slags, 87
plus graphite equals gray iron, 13
properties: relation to composition, 123
silicon ferrite: recrystallization and twin relationships, 372
strain-aging and yield point: elimination: by addition of titanium, 242
elimination: by treatment in wet hydrogen, 207
review of literature, 238
STOUT, R. D.: *Discussion on The Effect of Quenching Temperature on the Results of the End-quench Hardenability Test*, 136
STRAUSS, J. AND SHAPIRO, C. L.: *Influence of Various Elements upon the Position of the Eutectoid in the Iron-carbon (Carbide) System*, 335; discussion, 353
- T
- Taconite: Mesabi Range: grades, 41
unaltered. concentration, 49
Tailing re-treatment: iron ore: Mesabi Range, 47
- TARASOV, L. P. *Discussion on Orientation in Low-carbon Deep-drawing Steel*, 363
TARR, C. O., SMITH, G. V. AND MILLER, R. F.: *Precipitation and Reversion of Graphite in Low-carbon Low-alloy Steel in the Temperature Range 900° to 1300°F*, 387
TATNALL, F. G.: *Discussions: on The Notched-bar Impact Test*, 323
on Variables Affecting the Results of Notched-bar Impact Tests on Steels, 279, 281
Timken Roller Bearing Co. study of effect of several variables on the hardenability of high-carbon steels, 168
TISDALE, N. F. *Discussion on The Relative Deoxidizing Power of Boron in Liquid Steel and the Elimination of Boron in the Open-hearth Process*, 103
Titanium use in steel to eliminate strain-aging and yield point elongation, 242
TOLEMAN, S. L., KRAMER, I. R. AND HAFNER, R. H.: *Effect of Sixteen Alloying Elements on Hardenability of Steel*, 138
- U
- UHLIG, H. H. *Influence of Hydrogen on Mechanical Properties of Some Low-carbon Manganese-iron Alloys and on Hadfield Manganese Steel*, 183; discussion, 204
Union Carbide and Carbon Research Laboratories: study of effect of some elements on hardenability, 157
U S Steel Corporation: study of deoxidizing power of boron in liquid steel and elimination of boron in open-hearth process, 98
study of precipitation and reversion of graphite in low-carbon low-alloy steel in temperature range 900° to 1300°F., 387
washing of Pittsburgh coking coal and results obtained on blast furnaces, 67
- V
- Vanadium Corporation of America: study of the influence of various elements upon the position of the eutectoid in the iron-carbon (carbide) system, 335
- W
- WALTERS, F. M. JR.: *Discussion on Variables Affecting the Results of Notched-bar Impact Tests on Steels*, 281
Washing iron ore: Mesabi Range, 41
Watertown Arsenal. study of conditions of fracture of steel, 283
study of the notched-bar impact test, 298
WELCHNER, J., ROWLAND, E. S. AND MARSHALL, R. H.: *Effect of Several Variables on the Hardenability of High-carbon Steels*, 168; discussion, 182
Westinghouse Electric and Manufacturing Co.: study of orientation in low-carbon deep-drawing steel, 354
WINLOCK, J. AND LEITER, R. W. E.: *Discussion on Aging and the Yield Point in Steel*, 245

- WRIGHT, E. C.: *The Manufacture and Properties of Killed Bessemer Steel*, 107, discussion, 124
- Z
- ZAPFFE, C. A. Discussions: on Aging and the Yield Point in Steel, 244
on The Relative Deoxidizing Power of Boron in Liquid Steel and the Elimination of Boron in the Open-hearth Process, 104
- ZENER, C. AND HOLLOMON, J. H.: *Conditions of Fracture of Steel*, 283; discussion, 297
- ZIEGLER, N. A. Discussions: on Tensile Properties of Medium-carbon Low-alloy Cast Steels, 262
on The Notched-bar Impact Test, 323
on Variables Affecting the Results of Notched-bar Impact Tests on Steels, 280

